Northeastern University
Chemistry Building
Library

MOLECULAR ASSOCIATION

To Professor R. S. Mulliken

MOLECULAR ASSOCIATION

Including Molecular Complexes

VOLUME 2

Edited by

R. FOSTER

Chemistry Department

University of Dundee

1979

ACADEMIC PRESS

LONDON NEW YORK SAN FRANCISCO

A Subsidiary of Harcourt Brace Jovanovich, Publishers

461
M63
v.2

ACADEMIC PRESS INC. (LONDON) LTD.
24/28 Oval Road,
London NW1

United States Edition published by
ACADEMIC PRESS INC.
111 Fifth Avenue,
New York, New York 10003

Copyright © 1979 by
ACADEMIC PRESS INC. (LONDON) LTD.

All Rights Reserved
No part of this book may be reproduced in any form by photostat, microfilm, or any other means, without written permission from the publishers

British Library Cataloguing in Publication Data
Molecular association.
Vol. 2
1. Molecular association
1. Foster, Roy, *b. 1928*
539'.6 QD461 62-22124

ISBN 0-12-262702-4

PRINTED IN GREAT BRITAIN BY
PAGE BROS. (NORWICH) LTD., MILE CROSS LANE, NORWICH

Contributors

R. ARNDT, *Institut für Physikalische Chemie, Technische Universität, Hans Sommer Strasse 10, D3300 Braunschweig, West Germany.*

R. J. LAUB, *Department of Chemistry, University College of Swansea, Swansea SA2 8PP, U.K. (Present address: Department of Chemistry, Ohio State University, Columbus, Ohio 43210, U.S.A.)*

A. LEDWITH, *Donnan Laboratories, University of Liverpool, Liverpool L69 3BX, U.K.*

NOBORU MATAGA, *Department of Chemistry, Faculty of Engineering Science, Osaka University, Toyonaka, Osaka, Japan.*

M. OTTOLENGHI, *Department of Physical Chemistry, The Hebrew University, Jerusalem, Israel.*

J. M. PEARSON, *Xerox Corporation, Webster Research Laboratories, Webster, N.Y. 14580, U.S.A.*

R. L. STRONG, *Department of Chemistry, Rensselaer Polytechnic Institute, Troy, New York 12181, U.S.A.*

M. TAMRES, *Department of Chemistry, University of Michigan, Ann Arbor, Michigan 48109, U.S.A.*

S. R. TURNER, *Xerox Corporation, Webster Research Laboratories, Webster, N.Y. 14580, U.S.A.*

C. A. WELLINGTON, *Department of Chemistry, University College of Swansea, Swansea SA2 8PP, U.K.*

J. YARWOOD, *Department of Chemistry, University of Durham, Durham City DH1 3LE, U.K.*

Robert S. Mulliken

In many areas of science the boundaries of sub-disciplines are not sharp. Categorization in the realm of molecular complexes is particularly daunting. Robert Mulliken brought order to our understanding of a large area of this field by producing a simple valence-bond description for the interaction between molecules of a species which is relatively electron-donating and molecules of a second species which is relatively electron-accepting. He was thereby able to account for the electronic absorption spectra which characterize many such complexes. Robert Mulliken's first publication of this idea was a "note added in proof" to a paper published in 1950 in *The Journal of the American Chemical Society*. This was followed two years later by comprehensive treatments of systems now usually termed "electron-donor–acceptor (EDA) complexes". There had been valuable theoretical and experimental contributions from earlier workers and, indeed, it was Professor J. H. Hildebrand's experiments with iodine solutions which had led to Mulliken's original proposition. But the publications of Robert Mulliken were the watershed. There was an immediate acceleration of interest, and nearly three decades later we still see the direct chain-branching effect of this work, not only in the field of molecular complexation as such, but also in its implication in photochemical and biochemical processes, and in solution and solid-state properties. This great surge of interest has also led to remarkable advances in the study of a variety of electron-transfer systems.

The development of the original model over the intervening years is well described in the monograph written by Robert Mulliken and W. B. Person (Molecular Complexes: A Lecture and Reprint Volume, 1969).

It is in appreciation of his key contribution that this volume of essays is dedicated to Professor Mulliken.

Roy Foster

Preface to Volume 2

This book follows the pattern of the first volume, where the general intention of the series is described in the Preface. To summarize briefly, we are concerned with the interactions between various chemical species (ionic or uncharged) in which the binding between the components is normally weaker than a covalent bond. The components may be of the same or, as is more usual, of different species. Such interactions include those often described as "molecular complexes". However, explicit limits defining this term are difficult to set, and in any case we should not wish to be bound by them. For example, we would want to include diffuse types of association of indefinite stoichiometry, such as molecular clustering. The contributions are intended to provide critical essays rather than exhaustive reviews of current literature with little or no comment.

It is often said that the most interesting and productive areas of science are at the interfaces of the various disciplines. The study of molecular associations is a good example of this statement. The application of techniques such as infrared and Raman band-shape analysis and intensity measurements (Chapter 4) and gas–liquid chromatography (Chapter 3) can provide new insights into the processes involved, as well as a deeper appreciation of the physical methods themselves.

One boundary in the study of molecular association is the limit of detection of complexes. This problem, which is involved in experimental studies of so-called "contact charge transfer", is discussed in Chapter 5.

In another direction, the study of complexes which involve component species in excited states (exciplexes) has developed as a large and important area of study. In the first volume of this series, the involvement of exciplexes in photochemical reactions was discussed. In the present volume the photophysical aspects of exciplexes are considered (Chapter 1).

Some of the most important applications of electron-donor–acceptor complexes have arisen through their electrical properties. The behaviour of polymer-coating complexes of this type and their present and future application in processes such as electrophotography (Xerography), photoelectric devices and power sources are the subject of Chapter 2.

I should like to thank the contributors and the publishers for their patience and understanding during the production of this volume, and I am especially grateful to Dr E. T. Stewart and to Dr A. Nechvatal for their generous assistance in the final stages.

Dundee, January 1979 *Roy Foster*

Acknowledgements

Grateful acknowledgements are due to the following for permission to use published data. The first number in each of the following sets indicates the chapter. References to the authors concerned are made in the text.

Akademische Verlagsgesellschaft (*Zeitschrift für Physikalische Chemie, N. F.*): Figs 1.4, 1.8.

The American Chemical Society (*Journal of the American Chemical Society*): Figs 1.10, 3.12, 3.13, 5.3, 5.6, 5.15, 5.17, 5.19, 5.24, 5.25, Tables 3.XVII, 3.XVIII; (*Journal of Physical Chemistry*): Figs 1.6, 5.8, 5.9, 5.10, 5.11, 5.12, 5.13, 5.14, 5.18, 5.20; (*Analytical Chemistry*): Figs 3.16, 3.17, 3.18, Tables 3.X, 3.XV.

The American Institute of Physics (*Journal of Chemical Physics*): Figs 1.2, 1.7, 4.10, 4.11, 4.14; (*Journal of Applied Physics*): Figs 2.8, 2.9, 2.10, 2.11, 2.12, 2.15, 2.16.

The Chemical Society (*Journal of the Chemical Society*): Figs 3.5, 3.6, 3.7, 3.8, 3.9, 3.10, 4.12(a), 4.13(a), 5.4, 5.5, 5.7, 5.23.

The Chemical Society of Japan (*Bulletin of The Chemical Society of Japan*): Figs 1.3, 1.9.

Deutsche Gesellschaft für Lichtforschung (Progress in Photobiology, Proceedings of the 6th International Congress); Fig. 5.21.

Elsevier Scientific Publishing Company (*Journal of Chromatography*): Figs. 3.21, 3.22, Tables 3.II, 3.XII, 3.XIII, 3.XXI.

National Research Council of Canada (*Canadian Journal of Chemistry*): Fig. 5.22.

North Holland Publishing Company (*Chemical Physics*): Fig. 4.7; (*Chemical Physics Letters*): Figs 1.11(a), 1.13, 5.16.

Oliver and Boyd (Fluctuation Relaxation and Resonance in Magnetic Systems, ed. D. Ter Haar): Figs 4.5 and 4.6.

Plenum Publishing Corporation (Spectroscopy and Structure of Molecular Complexes, ed. J. Yarwood): Fig. 4.2.

Schulz Verlag, Hans Ferdinand (Proceedings of the 5th International Conference on Raman Spectroscopy): Fig. 4.15.

Taylor and Francis (Proceedings of the International Conference on Amorphous and Crystalline Semiconductors); Fig. 2.14.

Wiley and Sons and Wiley-Interscience (*J. Polymer Science, Polymer Letters*): Fig. 2.17; (Physico-Chemical Applications of Gas Chromatography, by R. J. Laub and R. L. Pecsok): Tables 3.I, 3.III, 3.XX. (Molecular Complexes: A Lecture and Reprint Volume by R. S. Mulliken and W. G. Person): Fig. 5.1.

CONTENTS

Contributors v
Robert S. Mulliken: an appreciation vii
Preface ix
Acknowledgements xi

Chapter 1. Photophysical Aspects of Exciplexes
NOBORU MATAGA and MICHAEL OTTOLENGHI

I. Introduction 2
A. Definitions and characteristic examples 2
B. Electronic and geometrical structures of exciplexes 4
C. Exciplex generation pathways 8
II. Inter- and Intra-molecular Exciplex Formation Processes . . . 8
A. The kinetics of exciplex generation and decay 8
B. Electron transfer and solvent relaxation 14
C. Formation of exciplexes by radical-ion recombination . . . 20
D. Formation of exciplexes by exciting ground-state molecular aggregates 24
E. Short-lived (non-fluorescent) exciplexes 26
III. Electronic and Geometrical Structures of Exciplexes 31
A. Absorption spectra of inter- and intra-molecular heteroexcimers, and of excited electron-donor–acceptor (EDA) complexes . . . 31
B. Geometrical structures as derived from the fluorescence of some intramolecular exciplexes 35
C. Solvent effects in exciplex systems 39
IV. Primary General Processes in Exciplexes 55
A. Ionic dissociation 55
B. Intersystem crossing (ISC) 65
References 71

Chapter 2. The Nature and Applications of Charge-transfer Phenomena in Polymers and Related Systems
J. M. PEARSON, S. R. TURNER and A. LEDWITH

I. Introduction 80
II. Formation of Higher Order Complexes 85
III. Orientation and Conformation Effects in Electron-donor–acceptor Complexes 89
IV. Multiple Charge-transfer Transitions 93

V. Charge-transfer Complexes of Polymers 99
A. Polymers as donor molecules 100
B. The polymer chain effect on complex formation 103
C. Polymers as acceptor molecules 106
D. Polymeric intramolecular charge-transfer complexes . . . 110
VI. Electrical Properties 114
A. Experimental techniques 118
B. Donor polymers with small molecule acceptors 123
C. Acceptor polymers with small molecule donors 149
D. Intramolecular polymeric complexes 153
E. Charge-transfer complexes in polymeric binders 157
F. Polyacetylene complexes 158
G. Present and future applications 158
VII. Conclusions 162
References 163

Chapter 3. Study of Complexation Phenomena by Gas–Liquid Chromatography

R. J. Laub and C. A. Wellington

I. Introduction: Physicochemical Applications of Gas–Liquid Chromatography 172
A. The chromatographic method: advantages and limitations . 173
B. Retention equations 173
C. Instrumentation 175
D. Sources of error 179
E. Accuracy of gas–liquid chromatographic data 184
II. Gas–Liquid Chromatographic Studies of Complexation Phenomena . 184
A. Evidence of complexation 186
B. Quantitative assessment of complexation phenomena . . . 187
C. Comparison of glc data with those of other techniques . . . 202
III. Recent Developments 206
A. Concentration effects in non-ionic solvent–additive systems . . 207
B. Solvent effects 208
C. Diachoric solutions hypothesis 209
D. Microscopic partition (MP) theory of solutions 230
IV. Practical Consequences of MP Theory 237
A. The Laub–Purnell window diagram procedure 239
B. Extension to multi-component stationary phases 249
C. Extension to solute mixtures of initially unknown content . . 250
D. Use with relative retention data 251
E. Application to gas–solid and gas–liquid–solid chromatography . 253
F. Application to liquid chromatography. 253
G. Application to other system variables 254
References 256

Chapter 4. The Study of Intermolecular Interactions in the Liquid Phase Using Infrared and Raman Band Shapes and Intensities
J. YARWOOD and R. ARNDT

I. Introduction 267
II. Background Theory 272
A. Introduction 272
B. Reorientational motions 275
C. Vibrational relaxation 285
III. Examples of the Determination of Intermolecular Forces using Infrared and Raman Spectroscopy 296
A. Simple liquids 296
B. Associated liquids 312
References 325

Chapter 5. Contact Charge-transfer Spectra
MILTON TAMRES and ROBERT L. STRONG

I. Introduction 332
II. Theory of EDA Complexes 333
A. Ground-state stability 333
B. Absorption spectra 336
C. Solvent effects 338
III. Thermodynamic Properties from CT Spectra 339
A. Equilibrium constant 340
B. Internal energy change 349
IV. Operational Criteria for Contacts 351
A. Internal energy change 352
B. Equilibrium constant 352
C. Wavefunction coefficient ratios 353
D. Viscosity and phase-change effects 354
V. Selection of Data for Contacts 357
VI. Molecular Halogen Acceptors 359
A. With alkanes 360
B. With cyclopropanes 365
C. With aromatic hydrocarbons 366
D. With alkenes 366
E. With alkyl halides 368
F. With halogen donors 378
G. With other donors 378
VII. Transient Halogen Atom Acceptors 379
A. Halogen atom recombination 380

B. Charge-transfer spectra of halogen atoms 386
C. Vapour-phase halogen atom charge-transfer spectra . . . 393
D. Alkyl halide–halogen atom charge-transfer spectra . . . 393
VIII. Molecular Oxygen Acceptor. 397
IX. Highest Valency Halides, Oxides and Oxyhalide Acceptors . . . 416
X. Substituted Methane Acceptors 421
XI. π*-Acceptors 432
XII. Miscellaneous 442
References 446

Author Index 457

Subject Index 484

1 Photophysical Aspects of Exciplexes

NOBORU MATAGA

Department of Chemistry, Faculty of Engineering Science, Osaka University, Toyonaka, Osaka, Japan

MICHAEL OTTOLENGHI

Department of Physical Chemistry, The Hebrew University, Jerusalem, Israel

I. Introduction 2
A. Definitions and characteristic examples 2
B. Electronic and geometrical structures of exciplexes . . . 4
C. Exciplex generation pathways 8
II. Inter- and Intra-molecular Exciplex Formation Processes . . . 8
A. The kinetics of exciplex generation and decay 8
B. Electron transfer and solvent relaxation 14
1. Time-dependent exciplex spectroscopy 14
2. Kinetic and thermodynamic aspects of electron transfer in polar solvents 16
C. Formation of exciplexes by radical-ion recombination . . . 20
D. Formation of exciplexes by exciting ground-state molecular aggregates 24
E. Short-lived (non-fluorescent) exciplexes 26
III. Electronic and Geometrical Structures of Exciplexes 31
A. Absorption spectra of inter- and intra-molecular heteroexcimers, and of excited electron–donor–acceptor (EDA) complexes . . . 31
B. Geometrical structures as derived from the fluorescence of some intramolecular exciplexes 35
1. Excimers 35
2. Heteroexcimers 37
C. Solvent effects in exciplex systems 39
1. Theoretical predictions 39
2. Analysis of experimental solvent effects 43
IV. Primary General Processes in Exciplexes 55
A. Ionic dissociation 55
1. Exciplexes 56
2. Excited EDA complexes 59
3. Role of solvation relaxation 60

B. Intersystem crossing (ISC) 65
1. Exciplexes in non-polar solutions 65
2. Exciplexes in polar solutions 67
References 71

I. INTRODUCTION

A. Definitions and Characteristic Examples

The term "exciplex" is now familiar, describing atomic or molecular aggregates that are unstable in the ground state but are stable under electronic excitation. In the case of organic molecules, such an aggregate was first identified by Förster and Kasper[1] for pyrene in solution. The fluorescence quantum yield of the pyrene monomer decreases as the concentration increases, and a new red-shifted fluorescence band arises, lacking any vibrational structure. No corresponding changes in the ground-state absorption spectrum are observed. The concentration dependence of both fluorescence bands indicates that the red-shifted band is due to a dimer, formed by the interaction between excited- and ground-state monomers. Such an excited

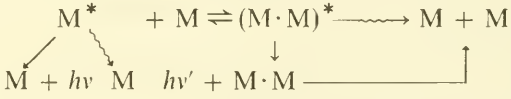

(1)

aggregate formed between identical atoms or molecules is termed "excimer".† Excimer formation has now been observed for a multitude of aromatic hydrocarbons and their derivatives in fluid solutions. Excimers are also known in crystals and in low-temperature rigid solvents. In such cases the ground-state molecules are already present as parallel pairs (or assume geometries favourable for excimer formation), and the final excimer configuration is achieved only after light absorption, being associated with further geometrical rearrangements of the two molecules. In addition to intermolecular excimers, intramolecular excimer formation has also been observed for composite molecules where two or more aromatic groups are linked together by a flexible $-(CH_2)_n-$ chain of varying length, or for cyclophanes where the two groups are more rigidly connected by two $-(CH_2)_n-$ chains. The study of such intramolecular systems provides valuable information for the elucidation of the structure of excimers.

In the present article, no detailed discussion of excimers will be given except for a few intramolecular systems. For comprehensive treatments we refer to specific review articles.[3–7]

† The term "excimer" was first introduced by Stevens and Hutton.[2]

Excimer-type emission from an exciplex composed of quite dissimilar molecules was first observed by Leonhardt and Weller following the quenching of excited perylene by ground-state *N,N*-dimethylaniline.[8] This short-lived 1:1 aggregate was termed "heteroexcimer"† or "exciplex".‡ Contrary to the excimer case, heteroexcimers possess a polar structure (A^-D^+), where A denotes the electron acceptor and D the donor. Transient aggregates of dissimilar molecules are not limited to 1:1 complexes. Triple excited complexes of the type ($D_2^+A^-$) have been observed for naphthalene (D) and 1,4-dicyanobenzene (A),[11] as well as for benzene (and its methyl derivatives) (D) and 1,2,4,5-tetracyanobenzene (TCNB) (A).[12] In the latter case, a ground-state 1:1 EDA (electron-donor–acceptor) complex generates upon excitation of the triple complex, which may thus be termed an exciplex.[13]

In a somewhat broader sense, the excited states of some hydrogen-bonded complexes may also be termed exciplexes. In systems such as naphthol–triethylamine[14] photoinduced proton-transfer generates a fluorescence band associated with a polar ion-pair state.

Although frequently treated separately, excited states of EDA complexes generated by direct (charge-transfer) excitation of stable ground-state aggregates have many features in common with heteroexcimers or exciplexes. In fact, there is no sharp dividing line between the two excited species, which differ only in the degree of their ground-state stability. In the present work the behaviour of excited EDA complexes will be discussed to some extent in relation to exciplexes. We refer to recent reviews for detailed discussions of excited EDA complexes.[13, 15]

As in the excimer case, heteroexcimer formation has been observed both in fluid solutions and in rigid low-temperature solvents.[9] Intramolecular heteroexcimers have also been reported for composite systems where the electron donor and acceptor groups are linked by $-(CH_2)_n-$ chains of various lengths. Such systems have provided important information related to the charge-transfer (CT) mechanism, to the dynamics of intramolecular heteroexcimer formation and to the geometrical structure of heteroexcimers.[17–22] Other intramolecular donor–acceptor systems, like the arylaminonaphthalenesulphonates have also been studied.[23]

It is the purpose of the present chapter to discuss recent advances in the photophysics of exciplexes. Special attention is paid to the application of fast pulsed excitation methods to the study of electronic structures and of

† The term "heteroexcimer" was introduced by Mataga *et al.*[9]

‡ The term "exciplex" was first used by Walker *et al.*[10] for interpreting the effects of polar solvents on the fluorescence spectra of indole. However, well-defined "exciplex" formation between the excited indole and the polar solvent molecules is still doubtful. At present, the term "exciplex" is usually generally used, covering both excimers and heteroexcimers. Some authors prefer a more restricted definition, using the term "exciplex" as one equivalent to "heteroexcimer".

basic primary processes such as solvation, intersystem crossing and ionic dissociation and recombination phenomena. The reader is referred to the account of Beens and Weller for a theoretically oriented discussion of excited states of EDA complexes,[13] and to the comprehensive review by Davidson on charge-transfer exciplexes as intermediates in photochemical reactions.[24]

B. Electronic and Geometrical Structures of Exciplexes

In general, the electronic states of a composite system may be expressed by the superposition of several configurations:

$$\Psi \approx C_1\Phi(M_1^*M_2) + C_2\Phi(M_1M_2^*) + C_3\Phi(M_1^-M_2^+) + C_4\Phi(M_1^+M_2^-) + C_5\Phi(M_1M_2) \qquad (2)$$

For the exciplexes C_5 is usually negligible, but it plays an important role in EDA complexes, accounting for their stability in the ground state. In the case of excimers, $|C_1| = |C_2|$ and $|C_3| = |C_4|$. Originally, exciton resonance interaction, i.e. the first two terms in equation (2), was assumed in order to account for the stability of the excimer.[1] Ferguson[25] interpreted the excimer electronic structure in terms of a charge-transfer structure, i.e. by an equal weight superposition of the third and fourth terms in equation (2).

Subsequent quantum chemical treatments,[26] though inevitably approximate, led to the conclusion that both exciton-resonance and charge-transfer interactions must be assumed to account for the stability of the excimer state and for the large red-shift of its fluorescence spectrum. Therefore, the excimer state may be expressed by the following type of wavefunction:

$$\psi_{exc} \approx a\{\Phi(M^*M) \pm \Phi(MM^*)\} + b\{\Phi(M^-M^+) \pm \Phi(M^+M^-)\}. \qquad (3)$$

In the above theoretical calculations, a more or less symmetrical sandwich structure of the excimer was assumed. Hirayama's observation (the "$n = 3$ rule"), postulating that excimer formation in the diphenylalkane

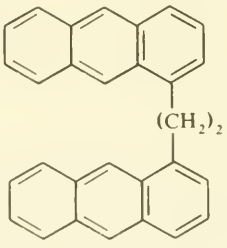

(1)

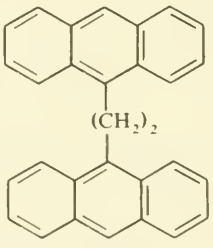

(2)

series occurs only when $n = 3$, seems to support this assumption.[27a] The study carried out by Chandross[27b] on dinaphthylalkanes does not seem to contradict the above assumption, although in this case the excimer emission was observed not only with $n = 3$ but also with $n = 4$. On the other hand, it has been confirmed[28] that 1,1′- as well as 9,9′-(anthracene)—$(CH_2)_2$—(anthracene) [1,2-di-(1-anthryl)ethane (**1**) and 1,2-di-(9-anthryl)-ethane (**2**)] show two kinds of excimer fluorescence bands. One (type-1) is observed in fluid solutions at room temperature, while the other (type-2) is generated by exciting the photodecomposition product of the intramolecular photodimer in a rigid solvent at 77 K. The type-1 fluorescence band is quite similar to that observed by exciting the photodecomposition product of the intermolecular photodimer in a rigid matrix at low temperatures. On the other hand, the intramolecular excimer fluorescence band observed in a rigid solvent at low temperature (type-2) is considerably red-shifted (by ~ 70 nm) compared with that (type-1) observed in solution at room temperature. The type-2 excimer seems to be close in structure to the symmetrical sandwich, while only one benzene ring appears to overlap in the case of the type-1 excimer (see Fig. 1). The fact that the fluorescence of the type-2 excimer cannot be observed at room temperature may be ascribed to the competing rapid photodimerization reaction. Thus, a symmetrical sandwich structure

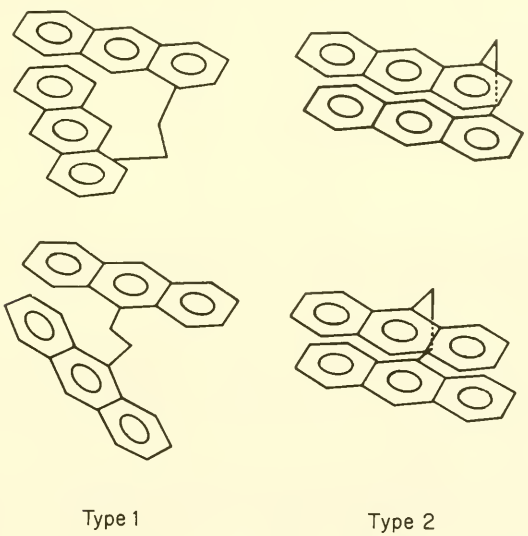

FIG. 1. Two kinds of excimer structure (type-1 and type-2) suggested for 1,2-di-(1-anthryl)ethane (upper) and 1,2-di-(9-anthryl)ethane (lower).

is by no means a necessary condition for the excimer fluorescence. An identical conclusion has been obtained by Zachariasse and Kühnle[27c] from a study of a series of α,ω-di(pyrenyl)alkanes, Pyr—$(CH_2)_n$—Pyr with $n = 2$–16.

Studies of solvent polarity effects on the corresponding fluorescence spectra[29] have indicated that the electronic structures of typical heteroexcimers, as well as those of some excited EDA complexes, are substantially polar, that is the third or fourth term in equation (2) may be dominant relative to the other terms. The energy E_{he} (above the separated ground-state components) of a heteroexcimer exhibiting such a pronounced charge-transfer character may be thus approximated in terms of the ionization potential of the donor (I), the electron affinity of the acceptor (EA), the Coulomb interaction energy between the ions (C) and the heteroexcimer solvation energy, ΔH_S:

$$E_{he} = I - EA - C - \Delta H_S \tag{4}$$

The heteroexcimer emission frequency $h\nu'$ will be obtained by subtracting the ground-state Franck–Condon destabilization energy U from E_{he}. In the same solvent, ΔH_S may be approximately constant throughout a series of heteroexcimers. If in such a series C and U may also be approximated as constants, $h\nu'$ will be proportional to $(I - EA)$. Since I and EA are correspondingly proportional to the oxidation potential of the donor (E^{ox}) and to the reduction potential of the acceptor (E^{red}), $h\nu'$ is also expected to be proportional to $(E^{ox} - E^{red})$. Such approximate proportionality relations have been observed for some series of heteroexcimers.[30, 31] The energy E_{he} can be obtained by subtracting the dissociation enthalpy ΔH_d of the excited complex from the fluorescence energy $h\nu$ of the component that is excited in the heteroexcimer formation reaction:

$$E_{he} = h\nu - \Delta H_d. \tag{5}$$

A linear relationship between $(E^{ox} - E^{red})$ and E_{he} of equation (5), covering about sixty heteroexcimer systems in aliphatic hydrocarbon solvents, has been confirmed.[32]

A relatively new tool for the elucidation of the electronic structure of heteroexcimers and excited EDA complexes is the measurement of their excited singlet–singlet ($S_n \leftarrow S_1$) absorption spectra by means of laser flash spectroscopy. Such studies on excited EDA systems were first carried out for several TCNB complexes. Potashnik and Ottolenghi[33] measured the $S_n \leftarrow S_1$ spectra of such complexes using a pulsed nitrogen laser for excitation. Masuhara and Mataga[34, 35] developed a method of laser flash spectroscopy which is especially suitable for EDA systems. Owing to the high laser excitation density, a relatively high population of the complex fluorescent

state may be achieved, leading to a substantial self-absorption of its (CT) fluorescence. Owing to its broad spectral distribution, the emission band can be used as monitoring source for the $S_n \leftarrow S_1$ absorption. Using this method, excited singlet absorption spectra of a series of TCNB complexes were recorded. Similar measurements were performed by Nagakura and coworkers[36] using a dye laser as the monitoring beam. All such experiments yielded spectra that could be well approximated by the superimposed absorption bands of the TCNB anion and of the donor cation, directly demonstrating the highly polar nature of the fluorescent state. More complex spectra have been reported for a series of characteristic heteroexcimers.[37, 38] The nature of such spectra will be discussed below in some detail.

As in the excimer case, intramolecular systems in which the electron donor and acceptor are linked by methylene chains were examined in order to elucidate the geometric requirements for charge-transfer and exciplex generation processes. Chandross and Thomas[17] investigated the intramolecular heteroexcimer formed between naphthalene and aliphatic amines. Since the heteroexcimer was generated for both α- and β-derivatives with $n = 2$, it was concluded that the process is not associated with very rigid geometrical restrictions. Studies on intramolecular heteroexcimers between aromatic hydrocarbons and aromatic amines were first reported by Okada *et al.* and Ide *et al.*[18] Investigation of the (anthracene)—$(CH_2)_n$—(*N*,*N*-dimethylaniline) (**3**) (sometimes 1,1′-linked) and (pyrene)—$(CH_2)_n$—(*N*,*N*-dimethylaniline) (**4**) systems clearly indicates the invalidity of the "$n = 3$

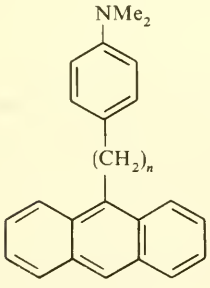

(3)

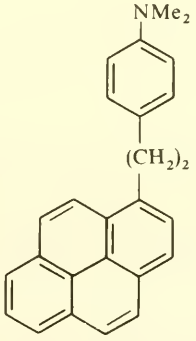

(4)

rule" since the heteroexcimer fluorescence is observed not only with $n = 3$ but also with the $n = 2$ and $n = 1$ derivatives. Another example of an intramolecular heteroexcimer was reported by Itoh *et al.* [19] for the system (9,10-dicyanoanthracene)—$(CH_2)_3$—(naphthalene).

C. Exciplex Generation Pathways

The best-known and commonly investigated pathway leading to exciplex generation involves the interaction between ground-state and (singlet) excited molecules. In typical intermolecular systems the process is diffusion controlled, exhibiting a time-dependent rate constant,[39] as most clearly demonstrated by picosecond excitation studies.[40] Investigations[20,21,41] of related intramolecular systems, such as (**3**), $n = 3$, (**4**), $n = 3$, (**3**), $n = 2$, and (**4**), $n = 2$, where exciplex generation is accompanied by geometrical changes from extended to folded forms, indicate that the rates of exciplex formation are determined by rotations about CH_2—CH_2 bonds.

Alternative routes leading to exciplexes involve chemiluminescent[42] or electrochemiluminescent[43] radical-ion recombination processes. In these cases exciplexes are generated via two principal mechanisms:

(i) As primary products of radical-ion recombination:

$$^2A^- + {}^2D^+ \rightarrow {}^1(A^-D^+)^*$$

and

$$^2A^- + {}^2A^+ \rightarrow {}^1(AA)^*$$

(ii) Via bimolecular annihilation of triplets formed from radical-ion recombination:

$$^2A^- + {}^2D^+ \rightarrow \left\{ \begin{matrix} {}^3A^* + D^* \\ A + {}^3D^* \end{matrix} \right\} \qquad {}^3A^* + {}^3D^* \rightarrow {}^1(A^-D^+)^*$$

$$^2A^- + {}^2A^+ \rightarrow {}^3A^* + A \qquad {}^3A^* + {}^3A^* \rightarrow {}^1(A \cdot A)^*$$

A detailed discussion of heteroexcimer formation and decomposition processes is presented in the following section. No separate treatment of excimers will be given since in most respects they may be treated analogously, being regarded as a special exciplex case.

II. INTER- AND INTRA-MOLECULAR EXCIPLEX FORMATION PROCESSES

A. The Kinetics of Exciplex Generation and Decay

A general scheme, accounting for the variety of processes associated with exciplex formation (by optical excitation) and decay, may be represented

as follows:[45]

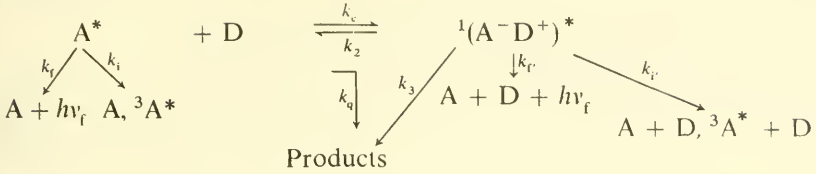

(6)

On the basis of this scheme, assuming an exciting pulse that is shorter than the decay time of A* and $^1(A^-D^+)^*$, the time dependence of fluorescence intensities in the system may be shown[45] to be described by the following expressions:

$$I(t) = \{Ck_f/(\beta - \alpha)\}\{(\beta - \mu)\exp(-\alpha t) + (\mu - \alpha)\exp(-\beta t)\}$$
$$I'(t) = \{Ck_f k_c[D]/(\beta - \alpha)\}\{\exp(-\alpha t) - \exp(-\beta t)\} \tag{7}$$

$$\left.\begin{matrix}\alpha \\ \beta\end{matrix}\right\} = \tfrac{1}{2}(\mu + \nu) \mp \sqrt{(\nu - \mu)^2 + 4k_c k_2[D]} \tag{8}$$

$$\mu = k_f + k_i + k_1[D] = (1/\tau) + k_1[D], k_1 = (k_q + k_c)$$

$$\nu = k_f' + k_i' + k_2 + k_3 = (1/\tau') + k_2 + k_3$$

$I(t)$ represents the fluorescence decay curve of A*, $I'(t)$ reflects the exciplex fluorescence rise and decay processes, while C is the concentration of A* at $t = 0$.

The actual (observed) decay curves are distorted by both instrument response function and exciting source (lamp) profile so that:

$$I(t)_{obs} = \int_0^t I(t - t')I_L(t')\,dt'$$
$$I'(t)_{obs} = \int_0^t I'(t - t')I_L(t')\,dt' \tag{9}$$

where $I_L(t)$ is the source profile distorted by the detection system.[39,46] Although the agreement between the above model and the observed fluorescence decay profiles is not always quantitative, approximate values of rate constants have been obtained with it for a variety of systems.[4,5,39,47] In principle, from the temperature dependence of these rate constants, the activation energies of the corresponding processes can be determined, from which exciplex binding energies can be obtained. However, actual evaluations of such thermodynamic quantities were mainly made by measuring the temperature dependence of excimer fluorescence quantum yields.[4,7] For example, from the reaction scheme (6) the following equation can be

derived:[48]

$$\frac{\eta}{\eta'} = \left(\frac{k_f}{k_f'[D]}\right)\frac{(k_f' + k_f')}{k_c^0}\exp\left(\frac{E_c}{RT}\right) + \left(\frac{k_2^0}{k_c^0}\right)\exp\left\{-\frac{(E_2 - E_c}{RT}\right\} + \left(\frac{k_3^0}{k_c^0}\right)\exp\left\{-\frac{(E_3 - E_c)}{RT}\right\} \quad (10)$$

where η and η' are the fluorescence quantum yields of A* and of the exciplex, respectively, and the various rate constants are expressed as:

$$k_c = k_c^0 \exp(-E_c/RT), k_2 = k_2^0 \exp(-E_2/RT), \text{ and } k_3 = k_3^0 \exp(-E_3/RT).$$

Detailed studies of fluorescence decay kinetics and thermodynamic quantities related to exciplex formation were made for several heteroexcimers involving aromatic hydrocarbon–amine systems such as perylene–DMA,[49] anthracene–DMA,[50] pyrene–DMA,[51,52] pyrene–DEA,[53,45] pyrene–tri-n-butylamine,[45,48] anthracene–DEA,[53] perylene–DEA,[53] and biphenyl–DEA,[53] where DMA = *N*,*N*-dimethylaniline and DEA = *N*,*N*-diethylaniline.

Since the formation of typical excimers and heteroeximers is a rapid diffusion-controlled reaction, any accurate treatment should consider the rate constant of exciplex formation, k_c, as a time-dependent parameter. The effect may best be visualized as previously described by Noyes.[54] At $t = 0$, the reactants A* and D are randomly distributed, but as time proceeds those distributions in which an A* is near a D are preferentially depleted. This produces a spatially non-uniform distribution of D around A* molecules. It is the resulting flux of D from the more concentrated regions of the liquid towards A* that determines the rate at which A* molecules will react. Since the molecular concentration gradients are time-dependent, also the rate constant for the reaction will change with time. A solution of the corresponding diffusion equation leads to the following expression for the rate, $\phi(t)$, of reaction between A* and D.

$$\phi(t) = \frac{4\pi\rho D'C}{1 + 4\pi\rho D'/k}\left[1 + \frac{k}{4\pi\rho D'}e^{X^2}\operatorname{erfc} X\right] \quad (11)$$

where $X = \left[\sqrt{(D't)}/\rho\right](1 + k/4\pi\rho D')$, ρ is the molecular diameter of the reacting molecules, D' is the sum of their diffusion coefficients, C is the concentration of the quencher at a large distance from A* (i.e. the mean concentration of D in the solution), t is the time after the creation of A*, and k is an elementary time-independent bimolecular rate constant. [$k = \Phi/C_\rho$, where C_ρ is the concentration of D molecules in coordination with A*, i.e. those at an intermolecular distance ρ from A*. The measured

bimolecular rate constant, $k_c = \Phi(t)/C$, is identical to k only when $k \ll 4\pi\rho D'$, i.e. for reactions that are far below the diffusion-controlled limit.]

A direct experimental study of the time dependence of a diffusion-controlled rate constant was first carried out by Ware and coworkers who applied fast fluorescence decay measurements to the quenching of excited naphthalene by CBr_4.[55] In exciplex systems, an accurate analysis of fluorescence decay curves in the nanosecond range involves the solution of coupled differential equations based on a reaction scheme such as (6), including a time-dependent rate constant $k_c(t)$. Numerical solutions of such a problem have been obtained for the anthracene–DMA system in a non-polar solvent.[50]

A clear, direct, way of observing transient effects in diffusion-controlled kinetics involves the application of mode-locked laser excitation, followed by ultrafast absorbance measurements with picosecond time resolution. Such experiments were first carried out by Eisenthal and coworkers[40, 56] in exciplex systems where the formation of the heteroexcimer product can most conveniently be followed by its characteristic absorption in the visible. Chuang and Eisenthal[56] measured the formation process of the anthracene–DEA heteroexcimer in hexane by exciting anthracene with the second harmonic of a picosecond pulse from a mode-locked ruby laser, and monitoring the absorption of the excited complex with the fundamental 6943 Å frequency. The general scheme for heteroexcimer formation was expressed by:

$$\begin{array}{ccccc} A^* & + & D & \xrightarrow{\Phi(t)} & {}^1(A^-D^+)^* \xrightarrow{k_f} A + D \\ {\scriptstyle h\nu}\uparrow & & \downarrow{\scriptstyle k_A} & & \\ A & & & & \end{array} \qquad (12)$$

where $\Phi(t)$ is the time-dependent rate function of exciplex formation and k_A and k_f are the corresponding unimolecular decay rate constants of A^* and ${}^1(A^-D^+)^*$. The concentrations of A^* and ${}^1(A^-D^+)^*$ [$n_A(t)$ and $n_c(t)$, respectively] can be obtained by solving the following equations:

$$\begin{aligned} dn_A(t)/dt &= [k_A + \Phi(t)]n_A(t) \\ dn_c(t)/dt &= \Phi(t)n_A(t) - k_f n_c(t). \end{aligned} \qquad (13)$$

Since, under the prevailing experimental conditions ([D] = 0·2–8 M), k_A and k_f are negligibly small in comparison with $\Phi(t)$, $n_c(t)$ can be approximated by:

$$n_c(t) = n_A(0)[1 - \exp(-\int_0^t \phi(t')\,dt')]. \qquad (14)$$

The observed rise curves of the heteroexcimer can be well simulated by using equation (11) for the rate function $\phi(t)$ (see Fig. 2), leading to the con-

clusion that electron transfer in this system occurs at an intermolecular distance ρ of 8 Å with an elementary rate constant $k \approx 10^{11}\,\mathrm{mol}^{-1}\,\mathrm{s}^{-1}$. In systems containing 3M DEA, or in the neat DEA liquid, the formation of the heteroexcimer follows an exponential time dependence characteristic of a bimolecular process with the rate constant $10^{11}\,\mathrm{mol}^{-1}\,\mathrm{s}^{-1}$. At these high

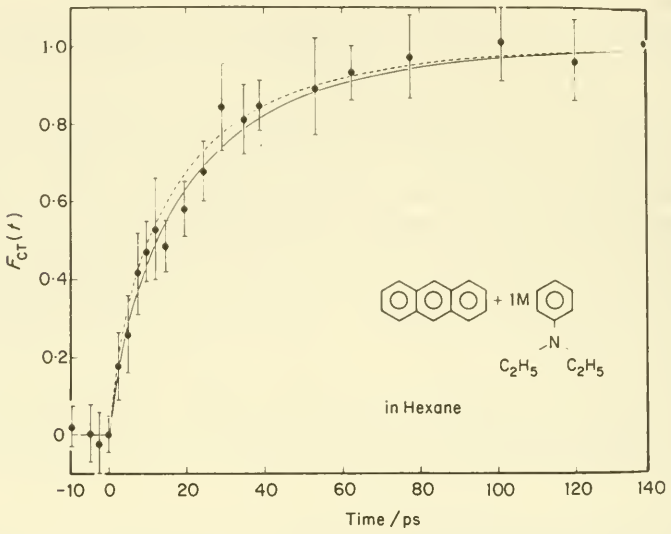

FIG. 2. Rise curve of the heteroexcimer absorption in the anthracene–DEA(1 M)–hexane system as observed by picosecond laser photolysis. The solid curve is calculated using equation (14) with $\rho = 8$ Å and $k = 11 \times 10^{10}\,\mathrm{l\,mol}^{-1}\,\mathrm{s}^{-1}$. $F_{CT}(t) = n_C(t)\,n_A(0)$. [Reproduced with permission from T. J. Chuang and K. B. Eisenthal, *J. Chem. Phys.*, **62**, 2213 (1975).]

DEA concentrations, it appears that translational motions contained in the diffusion treatment are not important. The circumstances are somewhat different in the case of intramolecular heteroexcimers such as (**3**) and (**4**) examined in order to elucidate the geometrical requirements associated with exciplex formation. It was found that the process is considerably affected by the presence of the methylene chain between the electron donor and acceptor moieties.[21,41,57] Since the distance between the two groups in (**3**), $n = 3$, is approximately 4 Å, the rate expected for CT complex formation in view of the results obtained for the intermolecular system is of the order of $10^{11}\,\mathrm{s}^{-1}$. Picosecond laser experiments in hexane solutions for (**3**), $n = 3$,[41] show that the complex generation function is given by the expression:

$$F(t) = 1 - \exp(-ft) \tag{15}$$

with $f \approx 1{\cdot}1 \times 10^9\,s^{-1}$ at room temperature. The process is therefore considerably slower than the intermolecular case. This is attributed to the effect of the methylene bonds on the relative rotational motion of the donor and the acceptor groups, which is mainly associated with hindered rotations about the CH_2—CH_2 bonds, requiring activation energies of the order of 12–16 kJ mol^{-1} (3–4 kcal mol^{-1}). This interpretation is confirmed by temperature dependence effects on fluorescence yields, which give activation energies for the formation of intramolecular exciplexes. The values obtained in non-polar solutions for (9,10-dicyanoanthracene)—$(CH_2)_3$—(naphthalene)[19] and dinaphthylpropanes[27b] are of the order of 12–16 kJ mol^{-1}.

Intramolecular heteroexcimer formation for (**4**), $n = 3$, was studied by analysing the fluorescence rise and decay curves obtained by pulsed nitrogen laser excitation.[21,57] In decalin, which is more viscous, the formation process is slower than in hexane. In this system the rise and decay of the exciplex fluorescence at room temperature can be reproduced by equation (16), with $\alpha^{-1} = 90$ ns and $\beta^{-1} = 8$ ns.

$$I(t) = C[\exp(-\alpha t) - \exp(-\beta t)]. \tag{16}$$

Again, the rate constant for exciplex formation is smaller than the elementary rate constant of the intermolecular case, also exhibiting a marked temperature dependence ($\beta^{-1} = 25$ ns at $-10°$, compared with 58 ns at $-50°$C). It is interesting that, as shown in Fig. 3, the rise time of the (**4**), $n = 3$, heteroexcimer fluorescence in both butan-2-ol and pentan-1-ol at room temperature is very short (below the 2 ns rise time of the exciting pulse).[21,57] Since both solvents are more viscous than decalin, this result clearly indicates the importance of the solvent polarity in the electron transfer process. Presumably, orientational fluctuations of surrounding solvent dipoles, as well as a restricted approach of the two moieties, may induce electron transfer (forming a loose-structure CT state) without requiring the sandwich configuration that characterizes the fluorescence in a non-polar solvent. Alternatively, the ground-state (**4**), $n = 3$, molecule may assume a folded configuration in alcoholic solvents accounting for the higher rates of exciplex generation. In considerably more viscous solutions at low temperatures, exciplex formation is slowed down even in the above polar solvents, though the temperature effect is not as remarkable as in non-polar solvents.

Analogous behaviour of a solvent-induced appearance of a fluorescence band, similar to those of the above intramolecular heteroexcimers, was observed for 9,9′-bianthryl[58a] as well as for *p*-dimethylaminobenzonitrile (**11**)[58b–62] (see discussion below). The formation time of the heteroexcimer-like fluorescent state of 9,9′-bianthryl in acetone solution has been confirmed to be shorter than 500 ps.[63] Presumably, the process involves intramolecular

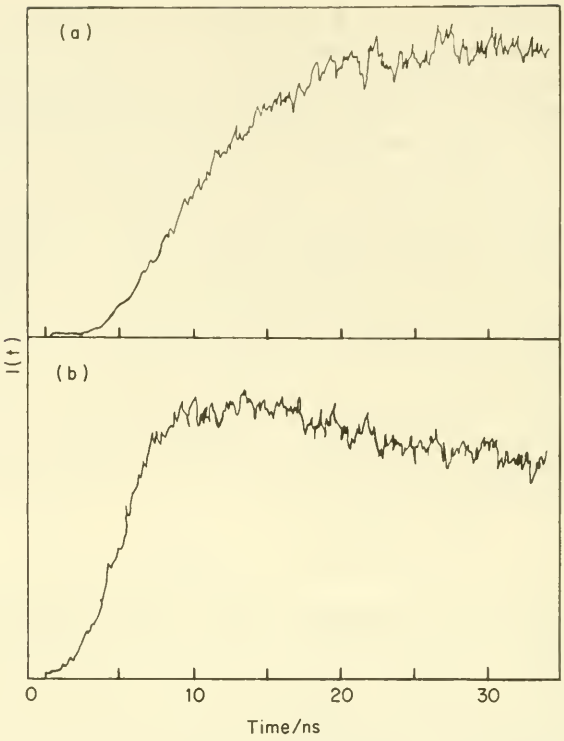

FIG. 3. Fluorescence rise and decay curves of the heteroexcimer (**4**), $n = 3$, in decalin (a) and in pentan-1-ol (b). [Reproduced with permission from T. Okada, T. Saito and N. Mataga, *Bull. Chem. Soc. Japan*, **50**, 331 (1977).]

charge-transfer controlled by a reorientation of the surrounding solvent molecules with a postulated formation time of 1–10 ps.

B. Electron Transfer and Solvent Relaxation

1. Time-dependent Exciplex Spectroscopy

The processes generating a polar exciplex are intimately connected with solvent-reorganization phenomena. After electron transfer, occurring for example in the anthracene–DEA system at an intermolecular distance of ~ 8 Å,[56] further approach of the two ions will take place, followed by a solvent-relaxation process. In the following sections (cf. Sections III.A, C) we shall see that the main solvent effects on the spectra of polar exciplexes are due to the solvent's static dielectric properties being associated with an environmental reorientation which leads to solvation (stabilization) of the

polar excited state. Thus, if the polar complex excited state is prepared in a polar solvent from a relatively non-polar pair, both emission and absorption spectra are expected to evolve with time, reflecting the dynamics of solvation of the excited state. This process will be essentially undetectable by conventional excitation methods in ordinary solvents at room temperature when the relaxation time (τ_r) is much shorter than the lifetime of the emitting state (τ_f). In such a case emission essentially occurs only from totally solvated complexes. However, at low temperatures and high viscosities, solvent relaxation is slowed down and, when $\tau_r \geqslant \tau_f$, a substantial fraction of the emission will take place from partially relaxed exciplex–solvent configurations. This leads to a time-dependent fluorescence spectrum, as theoretically predicted[64a] and experimentally observed[64b] for the general case of polar molecular excited states.

In exciplex systems the above effects may be easily observed in cases such as EDA complexes in which the polar fluorescent state is formed from a relatively non-polar ground state by the very act of light absorption within the complex CT band. Following preliminary observations of temperature-induced fluorescence shifts,[65a] Egawa *et al.*[65b] investigated the TCNB–toluene EDA complex in toluene as solvent at 147 K. Using pulsed N_2 laser excitation, they observed a time-dependent red shift of the fluorescence in the 1–100 ns range, directly reflecting the solvent reorientation process. This relaxation, from the Franck–Condon excited state to the equilibrium fluorescent state, is associated with an extraordinarily large Stokes shift. Its value, which at room temperature is *ca.* 12 000 cm^{-1}, seems to be too large for the solvation of a single dipolar species. In fact, although reorientation is certainly involved, subsequent studies based on $S_n \leftarrow S_1$ spectral measurements[12] have indicated that 1:2 ($A^- D_2^+$) exciplex formation does contribute substantially to the observed Stokes shift at elevated temperatures.

In the case of exciplexes populated by diffusional quenching, the direct observation of solvent relaxation is complicated by the fact that τ_r is usually shorter than the bimolecular (rate determining) quenching reaction which leads from, for example, $^1A^*$ to $^1(A^- D^+)^*$. Nevertheless, Nakashima *et al.*[48] found suitable experimental conditions for the observation of solvent relaxation in such systems. Time-resolved spectra for pyrene (acceptor) in highly viscous supercooled tri-n-butylamine (TBA, donor) at 156 K (see Fig. 4) showed that within the first 20 ns the maximum of the exciplex emission band undergoes a red shift accompanied by a simultaneous increase in intensity (from a non-zero initial value). The first effect is attributed to some specific (AD) pairs having an initial geometrical configuration leading to very fast formation of the exciplex. A solvent reorientation occurs subsequently, leading to the time-dependent red shift of the fluorescence. The

time-dependent increase in intensity is attributed to a rearrangement of solvent–solute configurations that lacked the initial geometry required for the immediate formation of the exciplex. This rearrangement occurs in the same time range as for solvent relaxation around the newly formed dipole. To some extent, heteroexcimers formed between donor–acceptor

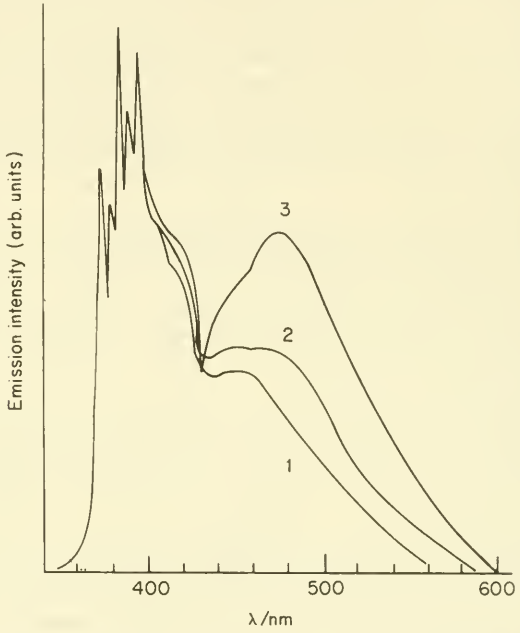

FIG. 4. Time-resolved fluorescence spectra in the pyrene–TBA two-component system at 156 K. Time delays from the origin of the exciting pulse are: (1) 1·5 ns; (2) 4·5 ns; (3) 20 ns. The spectra normalized at the monomer band. [Taken from N. Nakashima, F. Ushio, N. Mataga and C. Yamamaka, *Z. Phys. Chem.* (N.F.), **79**, 150 (1972)].

pairs with favourable relative geometries were observed in rigid low-temperature glasses. However, in such cases no solvent relaxation did occur during the excited state lifetime. Similar results were obtained for the pyrene–triethylamine system.[48]

2. Kinetic and Thermodynamic Aspects of Electron Transfer in Polar Solvents

As previously pointed out, charge-transfer fluorescence quenching in solvents of low and medium polarity leads to the generation of fluorescent exciplexes, the main role of the solvent being that of stabilizing the excited state. In highly polar solvents, electron transfer, directly producing a ground-state solvent-shared ion-pair, effectively competes with exciplex generation (cf. Section IV.A). The following brief outline of some principal features of

electron-transfer reactions associated with fluorescence quenching in solution is based on the detailed background as available for typical electron-transfer reactions (e.g. electron transfer between metal complexes in solution, non-homogeneous electrode processes). Common mechanisms different from those characteristic of, for example, bond rupture reactions, may prevail in a variety of purely electron-transfer processes.[66a]

Since electron-transfer in an activated complex may be rapid compared with nuclear motions, non-equilibrium systems will first be formed followed by relaxation with respect to the nuclear configuration of both reactants and surrounding solvent molecules. Systematic investigations of electron-transfer reactions have been performed with systems involving aromatic hydrocarbons (as fluorescers) and various electron donors and acceptors such as amine and cyano-compounds (as quenchers) in acetonitrile solutions.[67,68] Rehm and Weller analysed their results by means of a scheme originally suggested by Marcus:[66b]

$$M^* + Q \underset{k_{-1}}{\overset{k_1}{\rightleftharpoons}} M^* \cdots Q \underset{k_{-2}}{\overset{k_2}{\rightleftharpoons}} {}^2M^{\mp} \cdots {}^2Q^{\pm} \overset{k_3}{\rightarrow} M \cdots Q \tag{17}$$

where k_3 includes all possible deactivation paths of the solvent-shared ion-pair ($^2M^{\mp} \cdots {}^2Q^{\pm}$), mainly the back transfer of an electron leading to the neutral ground-state ($M \cdots Q$). Such a scheme leads to the following expression for the overall rate-constant of fluorescence quenching:

$$k = \frac{k_1}{1 + k_{-1}/k_2 + (k_{-1}/k_3)(k_{-2}/k_2)}. \tag{18}$$

Substituting $k_2 = k_{20} \exp(-\Delta G^*/RT)$ and $(k_{-2}/k_2) = K^{-1} = \exp(\Delta G^0/RT)$, equation (19) is finally obtained:

$$k = \frac{k_1}{1 + (k_{-1}/k_{20}) \exp(\Delta G^*/RT) + (k_{-1}/k_3) \exp(\Delta G^0/RT)} \tag{19}$$

ΔG^* is the free energy of activation, i.e. the free energy needed to obtain an overall nuclear configuration (especially in relation to the surrounding solvent molecules) where the free energies of ($M^* \cdots Q$) and ($^2M^{\mp} \cdots {}^2Q^{\pm}$) are equal. The free energy difference, ΔG^0, between the relaxed states of ($M^* \cdots Q$) and ($^2M^{\mp} \cdots {}^2Q^{\pm}$) can be calculated by means of equation (20):

$$\Delta G^0 = E^{ox} - E^{red} - e^2/\epsilon' a - \Delta E_{00} \tag{20}$$

where E^{ox} and E^{red} are the oxidation potential of donor and the reduction potential of acceptor, respectively. $e^2/\epsilon' a$ is the Coulomb interaction energy

between the two radical ions at the encounter distance a in the solvent of dielectric constant ϵ',† and ΔE_{00} is the electronic excitation energy of the fluorescer.

The experimental results for numerous acceptor–donor pairs indicate that, when $\Delta G^0 \lesssim -40\,\text{kJ mol}^{-1}$ $(-10\,\text{kcal mol}^{-1})$, k is approximately constant *ca.* $10^{10}\,\text{l mol}^{-1}\,\text{s}^{-1}$. In other words, for such large negative ΔG^0 values the reaction is essentially diffusion-controlled, i.e. $\Delta G^* \approx 0$. However, for $\Delta G^0 > -40\,\text{kJ mol}^{-1}$, an activation free energy is necessary for the reaction to occur. The accumulated data indicate that the quenching rate constant k can be reproduced satisfactorily by equations (21) and (22):

$$k = \frac{2{\cdot}0 \times 10^{10}}{1 + 0{\cdot}25\{\exp(\Delta G^*/RT) + \exp(\Delta G^0/RT)\}}\ \text{l mol}^{-1}\,\text{s}^{-1} \tag{21}$$

$$\Delta G^* = \Delta G^0/2 + \{(\Delta G^0/2)^2 + (\Delta G_0^*)^2\}^{1/2} \tag{22}$$

where ΔG_0^* is the value of ΔG^* when $\Delta G^0 = 0$, and is equal to $10\,\text{kJ mol}^{-1}$. It should be mentioned that (22) is a purely empirical relation with no sound theoretical basis. Marcus gave an expression for ΔG^* based on his theory of non-equilibrium polarization in the activated intermediate state:

$$\Delta G^* = \Delta G_0^*(1 + \Delta G^0/4\Delta G_0^*)^2. \tag{23}$$

Although this equation agrees very well with the observed results when $\Delta G^0 > -60\,\text{kJ mol}^{-1}$; it shows strong deviations for more negative ΔG^0 values, a discrepancy that was not clearly understood.[67] Efrima and Bixon[66c] have explained such effects, still within the framework of Marcus's theory, by taking into account possible vibrational excitations which accompany the electron transfer. Possible mechanisms of intermolecular electron transfer in the excited state were discussed[68] by analogy with Förster's classification of excitation transfer mechanisms.

Assuming an adiabatic electron transfer in the activated complex, the following condition should be satisfied:[67]

$$4|\beta|/h \gtrsim n \tag{24}$$

where n is the transfer frequency which brings the system from $(M^* \cdots Q)$ to $(M^{\pm} \cdots Q^{\mp})$ in the activated state, and β is the matrix element of the electronic interaction between these two configurations. Since the frequency of the electron transfer is close to the rate of the solvent relaxation which follows the electron-transfer act, $n = 10^{12}$–$10^{11}\,\text{s}^{-1}$. These values of n

† Dielectric constant is symbolized by ϵ' in this and other chapters to differentiate it from ϵ which is used to represent optical molar absorption coefficient (extinction coefficient).

correspond to $|\beta| = 10^{-3}$–10^{-4} eV, which is smaller than the thermal energy at room temperature, and indicate that no specific orientation between the reactants in the activated state is necessary for the electron transfer to occur. This seems to be in agreement with the fact that the intramolecular heteroexcimer formation in (**4**) and (**3**) can be observed not only with $n = 3$

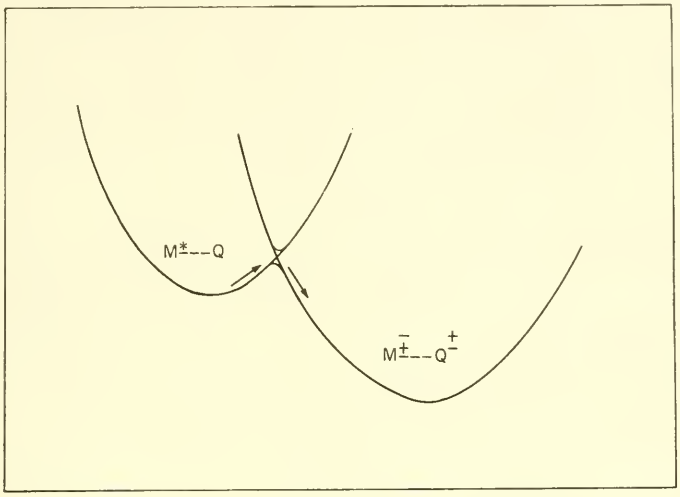

FIG. 5. Configuration coordinate diagram for the electron-transfer process.

but also with $n = 2$ and 1 in polar solvents.[18,20,21,22b] However, it appears to contradict the conclusion derived from the picosecond laser studies in the anthracene–DEA system, that a definite orientation of the reactants is required for the electron transfer to occur even in acetonitrile solutions.[56]

Since the free energy difference between the ion-pair state ($M^{\mp} \cdots Q^{\pm}$) and the neutral ground-state ($M \cdots Q$) is large, the activation free-energy for this process may be negligible. Therefore:

$$k_3 = k_{30} \exp(-\Delta G_3^*/RT) \approx k_{30} \tag{25}$$

so the value of k_{30} might be approximately equal to the rate of the solvent relaxation.[67] Thus, immediately after electron transfer in the encounter complex, dissociation to the separated ions and deactivation to the neutral (ground or triplet) state will be competing with each other. However, since there are cases in which k_{30} is considerably lower than the rate constants for ionic dissociation or triplet generation, the above statement does not appear to be of general validity.

C. Formation of Exciplexes by Radical-ion Recombination

As described in detail in the subsequent sections radical ions formed in CT quenching processes (either directly or from dissociation of the fluorescent exciplex) may recombine to give the neutral ground-states or the triplet states of A or D. Subsequent triplet–triplet annihilation processes may produce excited singlets and then exciplexes by reacting with appropriate ground-state partners. Alternatively, exciplexes may be formed as direct products of radical-ion recombination or triplet–triplet annihilation. All these paths, generating fluorescent exciplexes, are also available when radical ions are produced chemically or electrochemically (rather than photochemically). In fact, exciplex fluorescence caused by radical-ion recombination reactions is observed when mixing solutions of chemically produced cation and anion radicals[42,69] as well as in electrochemiluminescence experiments[43,44,71] in which radical ions are produced by electrode reactions.

Weller and Zachariasse[42,69] have studied in detail the chemiluminescence caused by the radical-ion recombination in ethereal solutions of a variety of systems. Characteristic behaviour patterns may be classified as follows.

I. Anions (A^-) of aromatic hydrocarbons(A) with the cation (D^+) from TMPD (*N*,*N*,*N'*,*N'*-tetramethyl-*p*-phenylenediamine) [A: (1) chrysene; (2) anthracene; (3) perylene; (4) tetracene; (5) pyrene; (6) 9,10-dimethylanthracene; (7) pentacene; (8) biphenyl; (9) naphthalene; (10) phenanthrene; (11) triphenylene; (12) *N*-ethylcarbazole]. In cases (1) and (4), the chemiluminescent species following the radical recombination reaction is exclusively $^1A^*$, while both monomer and excimer ($^1A_2^*$) fluorescence are observed in the experiments associated with systems (5) and (6). No emission is observed in case (7). The phenomena may be rationalized by assuming that, for both (1) and (7), $^3A^*$ can be produced by radical-ion recombination: $A_S^- + D_S^+ \rightarrow {}^3A^* + D$, while the formation of $^3D^*$ is energetically impossible. Triplet–triplet (T–T) annihilation leads to $^1A^*$ in cases (1) and (4) ($^3A^* + {}^3A^* \rightarrow {}^1A^* + A$), and to the excimer for (5) and (6) ($^3A^* + {}^3A^* \rightarrow {}^1A_2^*$). Since in case (7) $2\Delta E(^3A^*) < \Delta E(^1A^*)$, the formation of $^1A^*$ by T–T annihilation is impossible. In cases (8) and (12), the chemiluminescence spectra are due to the superimposed fluorescence of $^1A^*$,$^1D^*$ as well as to that of heteroexcimer $^1(A^-D^+)^*$. Since in such systems $\Delta G(A_S^- \cdots D_S^+) \geqslant \Delta E(^3A^*)$, $\Delta E(^3D^*)$, both $^3A^*$ and $^3D^*$ can be produced by ion recombination, with $^1A^*$ and $^1D^*$ being formed by subsequent T–T annihilations of each triplet species, respectively. In parallel, the heteroexcimer is produced by the mixed T–T annihilation reaction: $^3A^* + {}^3D^* \rightarrow {}^1(A^-D^+)^*$. Thus, in all the above systems, the formation of triplet states by radical-ion recombination, followed by T–T annihilation leading to the fluorescent state, accounts

for the observed chemiluminescence spectra. The chemiluminescence yields in these cases are relatively low (*ca.* 10^{-5}–10^{-4} einstein mol^{-1}), but considerably higher values (*ca.* 10^{-2} einstein mol^{-1}) are observed when using tri-*p*-substituted triphenylamines as D.

II. Anions (A^-) of aromatic hydrocarbons (A) with the cation (D^+) from TPTA (tri-*p*-tolylamine) [A: (1) pyrene; (2) anthracene; (3) 9-methylanthracene; (4) 9,10-dimethylanthracene; (5) 1-cyanoanthracene]. In all these systems, the fluorescence of both $^1A^*$ and the heteroexcimer can be observed. However, in contrast with the system of class I, the heteroexcimers are now formed directly via radical-ion recombination, the generation of $^1A^*$ being accounted for by the partial dissociation of the heteroexcimer:

$$A_s^- + D_s^+ \rightarrow {}^1(A^-D^+)^* \rightarrow {}^1A^* + D \qquad (26)$$

(In the above systems the generation of $^1D^*$ by a reaction analogous to (26) is energetically impossible.) Such direct heteroexcimer formation is associated with relatively high chemiluminescence yields.

It should be pointed out that cases exist in which heteroexcimers cannot be produced photochemically via the conventional $^1A^* + D$ or $^1D^* + A$ quenching reactions. In such systems chemiluminescent or electrochemiluminescent paths to radical ions may still provide efficient routes to exciplexes. For example, the non-planar (helical) molecule 3,4-benzophenanthrene does not form a heteroexcimer with DMA in cyclohexane, probably because of steric hindrance. However, exciplex formation can be observed following the recombination of the 3,4-benzophenanthrene radical anion with the tri-(*p*-dimethylaminophenyl)amine cation in THF. Another example involves benzophenone exciplexes where, owing to the very rapid intersystem crossing (~ 10 ps), heteroexcimer formation via the reaction of the short-lived excited singlet with aromatic amines is impossible, so no heteroexcimer fluorescence is observed using photoexcitation. However, such an emission may be produced via the radical-ion recombination reaction between the benzophenone anion and the tri-(*p*-dimethylaminophenyl)amine cation.

Exciplex formation mechanisms from electrogenerated radical ions are similar to those discussed above for chemiluminescent systems. Chandross and his coworkers[70] first suggested the formation of excimers by the recombination of radical ions:

$$A_s^- + A_s^+ \rightarrow {}^1(A \cdot A)^*.$$

Extensive studies of electrochemical luminescence involving exciplexes have been performed mainly by Bard and coworkers[43,44] in systems involving radical-ions such as benzophenone$^{\cdot-}$, naphthalene$^{\cdot-}$, tri-*p*-tolylamine$^{\cdot+}$ and *N*,*N*,*N*′,*N*′-tetramethyl-*p*-phenylenediamine$^{\cdot+}$. An interesting feature of many

of these systems is the possibility of observing heteroexcimer emission in a highly polar solvent such as acetonitrile for which no exciplex emission is usually observable in most of the systems that have been investigated using optical excitation. Actually, most electrochemiluminescence studies make use of solutions that are more polar and of higher ionic strength, relative to those involved in chemiluminescent systems. They have, however, the advantage of covering a wide spectrum of (D and A) molecules and solvents, not being limited to the very stable reactant system (i.e. ethereal solutions of A_s^- and D_s^+) required in chemiluminescence studies. Of special importance is the effect of external magnetic fields on the emission from electrochemiluminescent systems. The effect has been successfully used to uncover the participation of triplet species in the light producing process.[43, 44, 71] Thus, the magnetic field affects the rate of reactions involving triplet–triplet annihilation (or quenching of triplets by paramagnetic species) but not those leading to exciplexes directly via electron transfer.

The mechanism of exciplex formation via radical-ion recombination is closely related to the effects of solvent polarity on the excimer emission of some intramolecular systems. For example, it has been confirmed that the excimer fluorescence of both 1,2-di-(1-anthryl)ethane (**1**) and 1,2-di-(9-anthryl)ethane (**2**) markedly depends on the solvent polarity. As the solvent dielectric constant increases, the yield of the monomer fluorescence (Φ_M) decreases, while that of the excimer (Φ_D) increases.[28] A quantitative analysis of the effect was derived from the dependence of Φ_M, Φ_D and (Φ_D/Φ_M) on the solvent polarity parameter $\Delta f = \{(\epsilon' - 1)/(2\epsilon' + 1) - (n^2 - 1)/(2n^2 + 1)\}$, where ϵ' and n are the dielectric constant and refractive index of the solvent (see below). In the region where $\Delta f < 0{\cdot}29$, Φ_M of (**2**) decreases while Φ_D increases with increasing solvent polarity. The effect is interpreted in terms of excimer generation via the intramolecular recombination of a polar (bi-ion-radical) state. In the region where $\Delta f > 0{\cdot}29$, the sum $\Phi_t = \Phi_D + \Phi_M$ decreases considerably. The phenomenon, which is similar to the behaviour of 9,9′-bianthryl,[58a] appears to be in keeping with the familiar behaviour of exciplexes showing fluorescence quenching in polar solvents (e.g. the arylaminonaphthalene sulphonates.[23] Somewhat different behaviour is encountered in the case of (**1**) for which Φ_t does not decrease (while Φ_D increases with a decrease of Φ_M) even in the highly polar region. This behaviour is explainable by assuming two paths for excimer formation: (1) intramolecular association of the excited- and ground-state counterparts; (2) creation of the solvent-induced biradical CT state, in competition with direct excimer formation, followed by the reverse intramolecular charge-transfer to yield the excimer. The latter process is, in this case, highly competitive with the quenching reaction which is the dominant one for 9,9′-bianthryl and (**2**) in polar solvents.

Using the formula:

$$\Delta G(A^+ \cdots A^-) = E_{1/2}(A/A^+) - E_{1/2}(A^-/A) - e^2/\epsilon' a \qquad (27)$$

where $E_{1/2}(A/A^+) = 0{\cdot}96$ V and $E_{1/2}(A^-/A) = 1{\cdot}99$ V are the oxidation and reduction potentials of anthracene, both versus SCE, and assuming separation of $a = 4$ Å between the two moieties, the energy of the CT state in acetonitrile was estimated as $\Delta G(A^+ \cdots A^-) = 2{\cdot}82$ eV. Thus, the CT state seems to be situated just below the lowest excited singlet state of the monomer, accounting for its generation following light absorption by one of the two monomeric ground-state moieties.

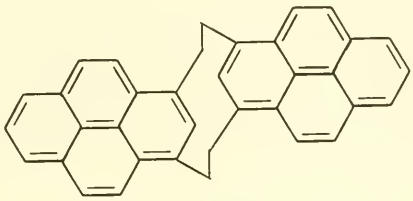

(5)

A similar phenomenon has been observed in the case of meta-pyrenophane (**5**).[72] The absorption spectrum of (**5**) is solvent-independent, closely corresponding to that of pyrene. In a non-polar solvent such as methylcyclohexane, (**5**) shows a pyrene-like fluorescence ($\lambda_{max} \sim 390$ nm, and $\tau_{1/2} \sim 150$ ns), attributable to the lowest locally-excited state. On the other hand, in polar solvents such as acetonitrile, a broad structureless fluorescence band with a solvent-independent emission maximum ($\lambda_{max} \sim 475$ nm) is observed along with the monomer emission. The assignment of the broad band to an intramolecular excimer fluorescence formed via a polar CT intermediate, thus implying a substantial reorientation of solvent dipoles, is consistent with the fact that the corresponding emission cannot be observed in rigid media at 77 K, even in acetonitrile as solvent. As in the cases of the dianthrylethanes (**1**) and (**2**), the yield of the fluorescence from the locally excited state (Φ_M) decreases, while that of the excimer (Φ_D) increases at high solvent polarities at room temperature. These results indicate that the molecule, characterized by an extended ground-state configuration (which is maintained in the initially formed locally-excited state), transforms into the folded excimer state in polar solutions. The process, which is presumed to occur in the polar CT intermediate, represents the intramolecular analogue of direct exciplex generation via radical-ion recombination in the previously discussed intermolecular systems. It is most likely associated with a transannular coulombic interaction in the CT state which is sufficiently strong to

overcome the considerable barrier between *anti* and *syn* forms. A kinetic

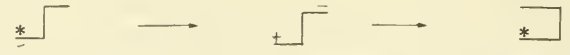

(28)

analysis shows that the constant observed for the rate of excimer formation from the locally excited state (of the order of 10^6–10^7 s^{-1}) increases with increasing solvent polarity.

D. Formation of Exciplexes by Exciting Ground-state Molecular Aggregates

In addition to the paths previously discussed, in which exciplexes are formed by encounter collisions in fluid solutions, excimer and heteroexcimer emission have also been generated by exciting ground-state molecular aggregates. For example, a fluorescence attributable to the excimers of naphthalene, pyrene and perylene is observed in a low-temperature (77 K) rigid cyclohexane matrix where no diffusional encounters may take place during the lifetime of the (monomer) excited state. Special attention was devoted to the excimer fluorescence of anthracene, which cannot be observed in fluid solution owing to the efficient photodimerization reaction. However, as first observed by Chandross,[73] excitation of the photodecomposition products of dianthracene in rigid organic matrices at low temperatures (77 K or 22 K) leads to excimer fluorescence. Similarly, also heteroexcimer emissions have been reported in a low-temperature cyclohexane matrix.[9]

The ground-state aggregate leading upon excitation to the exciplex fluorescent state was detected for pyrene, in a 77 K cyclohexane matrix, by recording the fluorescence excitation spectrum. The excitation spectrum of the excimer fluorescence was distinctly different from that of the monomer fluorescence. The latter closely coincided with the absorption spectrum of pyrene in a liquid solution, while the former seems to correspond to a red-shifted and somewhat broadened ^1L_a band of monomer.[74a] Similar studies have been carried out for the perylene–DMA and pyrene–DEA heteroexcimer systems. The absorption spectra of these systems in a low-temperature cyclohexane matrix are broadened and red-shifted compared with the monomer band, coinciding with the excitation spectra of the observed heteroexcimer fluorescence.[74b] It should be noted that, rather than by lowering the temperature, loose ground-state complexes leading to CT exciplex emission may be produced by using highly concentrated solutions of the components. This has been verified for the pyrene–DMA system, characterized by an association constant of $\sim 0{\cdot}2$ l mol^{-1} in hexane at room temperature.[76] Furthermore, by raising the temperature of such solutions,

enhancement of the long-wavelength side of the pyrene absorption band is observed, which seems to be attributable to a collisional interaction between the electron donor and the acceptor.[74b]

The formation of loose ground-state molecular complexes leading to CT emission was also observed in intramolecular systems. Thus, 1-(1-anthryl)-3-(4-*N*,*N*-dimethylaminophenyl)propane forms an intramolecular complex in a methylcyclohexane–isopentane supercooled liquid mixture at low temperatures whose absorption spectrum matches the excitation spectrum of the observed CT fluorescence.[74b] Another example is provided by the studies of Itoh and coworkers on the effects of temperature on the fluorescence of the intramolecular exciplex system (9,10-dicyanoanthracene)—$(CH_2)_3$—(naphthalene), as well as on the corresponding intermolecular systems of 9,10-dicyanoanthracene and alkylnaphthalenes.[19,75] In agreement with the previously discussed aromatic hydrocarbon–amine systems, direct excitation of the complex aggregate formed at low temperatures leads to a fluorescent complex state that is indistinguishable from the exciplex generated by the usual collisional quenching at higher temperatures.

The exact nature of the molecular interaction in the loose ground-state complexes described above is essentially undefined. In the symmetric systems, van der Waals forces probably prevail. In the asymmetric aggregates it is likely that CT interactions (including collision-induced weak CT interactions, as those leading to the so-called "contact" CT complexes) may contribute to the ground-state binding energy. This contribution is however quite small and the transition responsible for light absorption in these systems is essentially to a locally excited (though perturbed) monomer state. It is in this respect that the above aggregates are different from the well-known EDA complexes. In the latter case the excited complex state is produced by the very act of light absorption within a predominantly charge-transfer band, in a process involving only limited geometrical changes. In the former, charge transfer occurs after population of a locally excited monomer state. Thus, although both lead to CT complex emission, the two combinations are different in the nature of their ground-state as well as in that of their optical transitions. It is for this reason that the "loose" aggregates have been separately discussed.

Finally, we should mention the existence of definite geometrical requirements for the formation of loose complexes which lead to CT emission upon excitation. Thus, even in pure DMA as solvent, no anthracene–DMA exciplex fluorescence can be observed at 77 K.[30] In the two-component systems pyrene–DMA and pyrene–DEA at 77 K, the excited complex is generated but only to a limited extent,[48] in a way similar to the case of pyrene–DEA in a rigid low-temperature cyclohexane matrix. It is thus

evident that only specific ground-state aggregate pairs of suitable geometrical configuration may lead to the fluorescent complex state. Other geometries, though possibly suitable for ground-state aggregation, will only lead to monomer fluorescence, no reorientational motion during the lifetime of the excited state being possible in the rigid medium. The fact that, in fluid polar solvents, excited hetero-complexes are formed in the cases of (**3**) and (**4**), not only with $n = 3$ but also with $n = 2$ and $n = 1$, does not contradict the above conclusions in relation to reorientational motion. Thus, in the latter cases, solvation appears to stabilize exciplex structures that are unstable in low-temperature rigid media. Direct evidence for the occurrence of such orientational rearrangements at elevated temperatures was obtained by applying picosecond laser excitation methods to (two-component) anthracene–DEA solutions at 25°C.[56] Using 7 ps pulses for exciting and probing, it was shown that the exciplex is generated with a time lag of about 40 ps. This was ascribed to partial reorientation of the donor and the acceptor, necessary for electron transfer.

E. Short-lived (Non-fluorescent) Exciplexes

According to the somewhat restricted definition given in the beginning of the present article, the term exciplex is reserved for atomic or molecular aggregates that are unstable in the ground state but are stable in an electronic excited state. "Instability" implies that the ground-state potential energy surface is repulsive or dissociative, the aggregates undergoing a very rapid separation process. On the other hand, the "stability" of the exciplex state implies a lifetime that is relatively long, so that, for example, emission is observed in all cases except those in which the radiative transition probability is extremely small. In fact, the preceding discussions were mostly devoted to fluorescent exciplex systems. It is obvious, however, that if the exciplex state is rapidly deactivated by some efficient radiationless process, no emission will be observed. Nevertheless, such short-lived excited states may still be termed exciplexes if the basic requirements for their electronic wavefunctions (i.e. CT character for heteroexcimers and CT and resonance interactions for excimers) are satisfied. This wider definition extends the discussion not only to short-lived exciplexes in polar solutions, where deactivation is due to ionic dissociation (these are treated in some detail in the present chapter), but also to a large number of systems in which the exciplex deactivation is due to specific chemical reactions. Such systems have been reviewed extensively by Davidson.[24] It is likely that the development of picosecond spectroscopy will lead to direct observation of such species whose existence is now being postulated only on the basis of indirect evidence. However, since there is a lack of direct information concerning,

for example, the absorption and emission spectra, and consequently very little is known concerning the physical aspects of such systems, they will remain out of the main scope of the present review. In the following sections we shall limit ourselves to brief remarks on a few non-fluorescent systems. Some are relevant to those discussed in detail in the present work (i.e. aromatic hydrocarbon–primary amine and aromatic hydrocarbon– secondary amine). Others are of interest since they do not lead to net chemical changes but are essential for rationalizing fluorescence quenching experiments.

As for the previously discussed tertiary amines (DEA, DMA, etc.), the fluorescence of aromatic hydrocarbons is also quenched by the corresponding primary and secondary derivatives. In such cases, however, the reaction (which appears to be charge-transfer in nature) does not lead to the characteristic heteroexcimer fluorescence as in the case of tertiary amines.[9, 20a, 77] It seems likely that charge-transfer interactions in the encounter complex, followed by some efficient radiationless processes, play an important role in the case of quenching by amines with a free N—H group. Since the effect is specific to the existence of such a group, a possible mechanism for this quenching process may involve charge transfer followed by a rapid proton transfer, the net process being the transfer of a hydrogen atom[20a, 77] followed by recombinations yielding species such as DAH, HAAH.[78]

$$\begin{array}{l} A^* + HD \xrightarrow{k_q} (A^- \cdot HD^+)^* \xrightarrow{k_r} (\dot{A}H \cdot \dot{D}) \xrightarrow{k_d} \dot{A}H + \dot{D} \longrightarrow \\ \quad h\nu \uparrow \qquad\qquad\qquad\qquad\qquad\qquad\qquad\qquad\qquad\qquad \\ A + HD \longleftarrow \quad k_i + k_r \qquad\qquad\qquad\quad \hookrightarrow \text{DAH, HAAH, etc.} \end{array} \tag{29}$$

Assuming that k_f and k_i in systems such as pyrene–*N*-methylaniline or pyrene–*N*-ethylaniline are close to their values in, for example, the pyrene–DMA heteroexcimer, the lifetime of the pyrene–*N*-methylaniline or pyrene–*N*-ethylaniline heteroexcimer in non-polar solvents may be estimated using the relation:

$$\Phi_f = k_f/(k_f + k_i + k_r) = k_f\tau \lesssim 10^{-4} \tag{30}$$

where Φ_f is the heteroexcimer fluorescence yield, and the limit of 10^{-4} is set by the sensitivity of the detection systems. The value thus obtained is $\tau \lesssim 60$ ps, predicting that in this system the detection of the transient heteroexcimer state is attainable using the currently available methods of picosecond spectroscopy. The mechanism represented by the scheme (29) is in keeping with the formation of the pyrene semiquinone radical as well as the amino radical, both products being detected by means of pulsed photochemical experiments with nanosecond and microsecond time resolution.[77] Fluorescence quenching by primary and secondary amines

is also observed in polar solvents. In a solvent such as acetonitrile electron transfer is accompanied not only by proton transfer but also by ionic dissociation, as was confirmed by laser flash photolysis for pyrene quenched by aniline.[77] In such a system the generation of the solvent-shared ion-pair may efficiently compete not only with the formation of the exciplex (see below) but also with its decay via proton transfer. Phenomena similar to those described above have also been observed in the case of the hydrogen-atom transfer reaction between excited benzophenone and amines.[79, 80a]

Although some hydrogen-bonded complexes, such as the β-naphthol–triethylamine ($\beta OH \cdot NR_3$) system, show "exciplex" fluorescence from the ion-pair state $(\beta O^- \cdot HNR_3^+)^*$ produced by proton transfer in the excited state, such a fluorescence is completely quenched when pyridine (NX) is used as the proton acceptor for some proton donors such as naphthols, naphthylamines and carbazole.[5, 80b] Energetic considerations[67b] and flash photolysis studies[81] indicate that hydrogen-atom transfer in the excited state (leading to e.g. $\beta O + HNX$) plays an important role in quenching the fluorescence of these systems. The details of this process are still unclear. A likely suggested mechanism[82] involves a primary proton-transfer step in the excited state, leading to $(\beta O^{-*} \cdots HNX^+)$, followed by electron transfer to form the singlet biradical-pair ($\beta O \cdot HNX$). The cycle will be completed by back-electron and proton transfer reactions in the ground state. The latter point may account for the fact that no transient radical absorption bands were detected in the pulsed laser photolysis of a system such as carbazole–pyridine.[83]

An even broader definition of exciplexes would lead to the discussion of ultrashort-lived species such as encounter complexes and excited electronic states which very rapidly interconvert to dissociation products. An almost classical example involves the quenching of aromatic fluorescence by molecular oxygen.[84, 85] The main deactivation process, involving the generation of aromatic triplet states,[86–88] is schematically represented by:

$$^1M^* + {}^3O_2 \rightarrow {}^3(M \cdot O_2)^* \rightarrow {}^3M^* + {}^3O_2.$$

Tsubomura and Mulliken[86] have suggested that in the intermediate complex $^3(M \cdot O_2)^*$ a transition takes place from a locally-excited aromatic singlet to the CT triplet state. Evidence for a CT intermediate is based on the detection of ionic dissociation products ($^2M^+ + {}^2O_2^-$) in polar solvents[88] and on correlations with quenching rate constants.[89] Whatever should be the detailed path, out of a variety of possible coupling schemes,[90] it is evident that ultrashort-lived CT exciplexes are involved in the O_2 (and possibly NO) quenching reactions of excited singlet states of aromatic molecules. In contrast to these considerations, the lack of heavy-atom

effects indicates that triplet CT states are not involved in the deactivation of the singlet CT states of 6-*N*-arylaminonaphthalene-2-sulphonates.[23]

In relation to the above ultrashort-lived exciplex intermediates involving molecular oxygen, it is worthwhile mentioning the case of a fairly stable non-fluorescent complex formed between excited DPPD (*N*,*N*-diphenyl-*p*-phenylenediamine) and oxygen.[91] The species, exhibiting an absorption similar to that of the $DPPD^+$ radical cation and a lifetime of ~ 50 ns, has apparently a contact ion-pair structure. In polar solvents it undergoes dissociation to the corresponding ion-radicals.

Considerable attention has been paid to the rate of ultrashort-lived CT (exciplex) states in the quenching of excited singlet and triplet states of organic molecules by simple diamagnetic inorganic ions (X^-). Linschitz and coworkers were the first to suggest an important role of intermediate charge-transfer states for both singlets and triplets.[92] However, in contrast to the case of, for example, the photoreduction of carbonyl triplets by amines, where the role of CT states is well established,[79,93] the picture for both triplet and singlet quenching by diamagnetic ions is not completely clear. Watkins, who showed that the fluorescence quenching process leads to triplet states, argued against both CT and external heavy-atom mechanisms.[94] He pointed out, however, the role of some kind of coupling with CT states in the case of singlet quenching, excluding it in the triplet deactivation process. Some unambiguous results in this respect have been obtained by Treinin and Hayon.[95] Examining a series of aromatic carbonyls, dyes and pyrazine (M*), they obtained a "titration curve" (Fig. 6) relating the triplet quenching rate constant to the energy different $E_{CT} - E_{M^*}$ where E_{CT} is the estimated energy of the $(M^- \cdot X)^*$ complex in its excited charge-transfer state ($X^- = I^-, N_3^-, Br^-$, etc.). Although exhibiting some systematic deviations, similar behaviour also characterizes the singlet quenching rate-constants. The authors conclude that the quenching of both singlets and triplets by anions follows similar routes, the proximity of a CT level providing a most efficient path. The nature of the CT (exciplex) intermediate is related to the fact that no indication of a net electron-transfer reaction is observed for either triplets[95] or singlets.[94] Since electron transfer appears to be thermodynamically feasible, kinetic barriers (associated with solvent and complex configurational reorientation) inhibiting a complete electron-transfer followed by dissociation are invoked.[95] The term exciplex for the excited $(M^-X)^*$ species in the above system thus refers to an encounter complex, non-relaxed in relation to both solvent and intrinsic geometries, which has enough CT character to undergo fast intersystem crossing but not enough to make full charge-transfer a fast competitive process.[95,96] [Only $^1M^* + X^- \rightarrow {}^3M^* + X^-$ and $^3M^* + X^- \rightarrow M + X^-$, but not $^1M^*$ (or $^3M^*$) $+ X^- \rightarrow M^- + X$, are observed.]

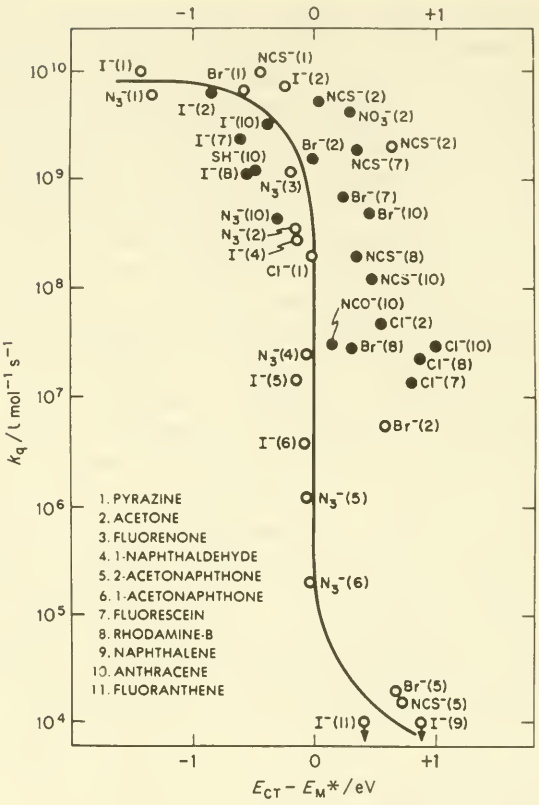

FIG. 6. Relations between rate constant (k_q) for quenching of excited [singlet S_1 (●) and triplet T_1 (○)] organic molecules (M*) by inorganic ions, and estimated proximity ($E_{CT} - E_{M^*}$) of non-fluorescent CT exciplex state. [Reproduced with permission from A. Treinin and E. Hayon, *J. Phys. Chem.*, **98**, 3884 (1976).]

In conclusion, the above examples demonstrate the extremes to which the concept of the exciplex may be extended. Exciplex lifetimes in the range from picoseconds and nanoseconds to microseconds (for triplet exciplexes) are determined by the rates of emission and of dissociative and other radiationless processes. These are in turn controlled by the shape of the exciplex potential energy surface, by its binding energy, and also by environmental properties such as temperature and solvent. The question of which systems should be termed exciplexes is thus a matter of definition. It is probable that the term will undergo considerable amplification, especially with respect to short-lived non-fluorescent intermediates.

III. ELECTRONIC AND GEOMETRICAL STRUCTURES OF EXCIPLEXES

In the Introduction we outlined the general features of the electronic and geometrical structure of exciplexes. In the following section (III.B) we pay special attention to some intramolecular systems where fluorescence data have provided important information on the geometry of the excited state. A special discussion (Section III.A) is also devoted to the absorption spectra of exciplexes, which are complementary to fluorescence measurements but in some respects provide more direct information on the nature of the excited state. Finally, in Section III.C, solvent effects are discussed in view of their role in determining the electronic structure and decay modes of the excited complex. This section includes further discussion and information on systems that have already been introduced in Sections III.A and III.B.

A. Absorption Spectra of Inter- and Intra-molecular Heteroexcimers, and of Excited Electron–donor–acceptor (EDA) Complexes

As pointed out in the Introduction, absorption spectra of fluorescent CT states may be obtained by applying pulsed laser excitation methods. The spectra of the excited EDA complexes involving TCNB and pyromellitic dianhydride (PMDA) as acceptors, with methyl-substituted benzenes and naphthalene as donors, were recorded in fluid dilute solutions at room temperature as well as in rigid media at 77 K and in (room temperature) poly-methyl methacrylate.[33–35] In all cases the absorption spectra could be approximated by superpositions of bands due to the acceptor anion-radical with those due to the donor cation-radical. The $S_n \leftarrow S_1$ spectra of systems containing acceptors (TCNB, PMDA, *p*-dicyanobenzene) in liquid donors (benzene, toluene, mesitylene and α-methylnaphthalene) at room temperature could be reproduced by a superposition of the bands of the acceptor anion and of the donor dimer cation (D_2^+).[12] Such observations constitute direct evidence for the charge-transfer nature of the fluorescent state of such complexes. The polar "contact ion-pair" structures $^1(A^-D^+)^*$ and $^1(A^-D_2^+)^*$ prevail in the two systems, respectively, exhibiting two types of absorption transitions:

(a) $^1(A^-D^+)^* \xrightarrow{h\nu} {}^1(A^-D^{+*})$ localized excitation within D^+

$^1(A^-D_2^+)^* \xrightarrow{h\nu} {}^1(A^-D_2^{+*})$ localized excitation within D_2^+

(b) $^1(A^-D^+)^* \xrightarrow{h\nu} {}^1(A^{-*}D^+)$
$^1(A^-D_2^+)^* \xrightarrow{h\nu} {}^1(A^{-*}D_2^+)$ localized excitations within A^-.

Early calculations on the Franck–Condon excited state (i.e. assuming a configuration identical to that of the equilibrium ground-state) of a complex such as TCNB–toluene predicted an almost equal contribution of CT [i.e. $^1(A^-D^+)^*$] and locally excited (i.e. A*D) structures to the wavefunction of the excited complex.[96] To account for the observed $S_n \leftarrow S_1$ spectra of the complex (indicative of an essentially pure CT state), a theoretical study was performed[97] assuming the following geometrical configurations:

(a)	$R_x = 1{\cdot}20$ Å	$R_y = 0{\cdot}695$ Å	$R_z = 3{\cdot}40$ Å
(b)	$R_x = 1{\cdot}20$ Å	$R_y = 0$	$R_z \geqslant 3{\cdot}40$ Å
(c)	$R_x = R_y = 0$		$R_z = 3{\cdot}40$ Å

in which R_x and R_y represent the coordinates of the centre of one of the two benzene rings, taking the centre of the other as the origin of the co-ordinates. R_z denotes the interplanar distance between the two rings, assumed to be parallel.

The results of the calculations clearly indicate a CT character in the S_1 state of almost 100 per cent in the case of model (c). However, neither the intermolecular configuration of model (a) (which appears to be close to that of the ground-state complex[96]) nor that of model (b) (both assuming $R_z = 3{\cdot}40$ Å) accounts for the observed CT character of the S_1 state. Although model (b) does yield an essentially pure CT state if large R_z values are assumed, it would not account for the actual structure of the excited state as it would then be energetically unfavourable owing to a smaller Coulombic attraction than that of model (c). The theoretical analysis is thus indicative of a relaxation process, from the (ground-state) geometry of a less polar excited Franck–Condon state (a) to that (c) of the highly polar relaxed fluorescent state. Similar conclusions were derived by interpreting experimental fluorescence radiative transition probabilities on the basis of the electronic structure of the S_1 state.[98] When the excited complex is generated in pure donor solvents, the relaxation reaction is also associated with the formation of the D_2^+ species. In such a case, however, the exact sequence of geometrical changes, involving the relative donor–acceptor geometry and the donor aggregation step, is still unclear.

The question arises as to what extent does the (a) → (c) structural change take place in low-temperature rigid matrices. In this respect it is worthwhile mentioning that the $S_n \leftarrow S_1$ spectrum of the TCNB–toluene complex at 4·2 K in poly-methyl methacrylate) is quite close to that of the TCNB anion. On the basis of the previous discussion this would suggest that the (a) → (c) structural relaxation occurs in the above medium even at 4·2 K. It should be

pointed out, however, that such a conclusion is based on the assumption[96] that the ground-state geometry, and thus that of the Franck–Condon excited state, is close to that of model (a). Although this has actually been proved for TCNB–hexamethylbenzene on the basis of an X-ray analysis in the crystalline state,[99] in rigid matrices and in liquid solutions the structure of the ground-state complex may be closer to that of model (c). In such a case an almost pure CT state will be generated by the very act of excitation without implying further structural changes.

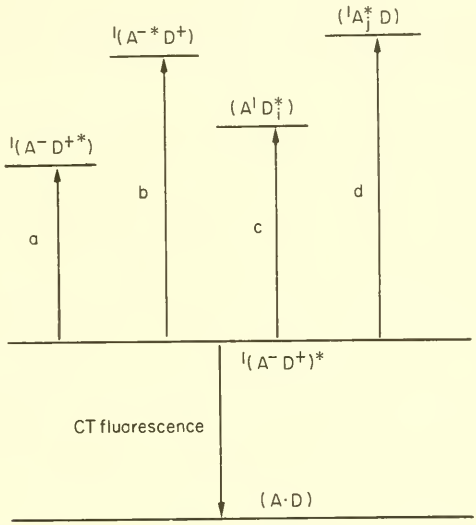

FIG. 7. Possible types of transition in the absorption spectra of heteroexcimers. [Taken from R. Potashnik, C. R. Goldschmidt, M. Ottolenghi and A. Weller, *J. Chem. Phys.*, **55**, 5344 (1971).]

Generally speaking, reverse CT transitions such as (c) and (d) should arise in the absorption spectra of exciplexes, in addition to those [(a) and (b)] localized in the ions (see Fig. 7).

(c) $$^1(D^+A^-)^* \xrightarrow{h\nu} (A\,^1D_i^*)$$

(d) $$^1(D^+A^-)^* \xrightarrow{h\nu} (^1A_i^*D).$$

$^1D_i^*$ and $^1A_i^*$ represent the ith singlet state (S_i) of D and A respectively. The relative intensity of such transitions should depend on the extent of

mixing between the corresponding locally excited (AD_i^* and DA_i^*) and CT configurations. Absorption bands which might be ascribed to transitions of types (c) and (d) have been observed in the spectra of some typical exciplexes.[16, 37, 100] For example, in the case of the pyrene–DEA heteroexcimer, absorption bands additional to those attributed to the localized ionic transitions (a) and (b) were observed in the neighbourhood of 900, 600 and 450 nm. Such bands were assigned to the following back-CT transitions [(c) or (d)]: $^1(A^-D^+)^* \xrightarrow{h\nu} {}^1(A_3^*D)$, $^1(A_4^*D)$ and $^1(A_5^*D)$, respectively.

It should be noted that the absorption bands assigned to the back-CT transitions are of considerable intensities (some of these bands are more intense than those of the ions). Since the intensity of a transition such as, for example, (c) increases with the amount of D^* character in the fluorescent exciplex state (the transition moment for a pure CT state being negligibly small), this would imply a non-pure CT configuration for the above exciplex systems. However, the bands of the ions are quite intense, with maxima that are very close to those of the corresponding ground-state radical-ions.

The absorption spectra of triplet EDA complexes which are locally excited in nature are essentially identical to those of the corresponding triplets of the free partners.[101] However, an analysis similar to that presented above for the fluorescent (CT) singlet state should also be applicable to triplet states of exciplexes which are of a predominantly CT character. This has been confirmed by Nagakura and coworkers who measured the $T_i \leftarrow T_1$ spectra of several TCNB complexes, carrying out a detailed calculation of all triplet-state energies and percentage CT character.[102] Since the topic has been reviewed in some detail[15] we shall limit ourselves to recalling the case of the TCNB–hexamethylbenzene complex whose T_1 state is predominantly CT in nature. A band around 7×10^3 cm^{-1} was assigned to the transition from T_1 to the T_3 state, for which a 44 per cent CT character was calculated. This band may thus be approximated as an essentially "back-CT transition" of type (d), i.e. $^3(D^+A^-)^* \xrightarrow{h\nu} (^3A^* \cdot D)$. Two additional bands around 13×10^3 and 18×10^3 cm^{-1} are of a similar character. On the other hand, an intense band around 23×10^3 cm^{-1} was identified as due to transitions to two almost pure CT triplets (T_8, T_9). It thus reflects local excitations within the $TCNB^-$ anion of the type (b) discussed above for the singlet manifold.

Triplet exciplexes have also been reported by Whitten and coworkers following the reaction of triplet metalloporphyrins or anthracene with acceptors such as quinones and nitro-aromatics.[103] Such species have absorption spectra similar, but not identical, to those of the substrate triplets. Although the reaction is associated with ionic dissociation in polar media, the above identity was interpreted in terms of a low CT character in the excited state.

B. Geometrical Structures as Derived from the Fluorescence of Some Intramolecular Exciplexes

The above discussion has pointed out the difficulty of elucidating the detailed structure of an intermolecular exciplex on a purely experimental basis. It appears, however, that useful information may be obtained in this respect from the study of model systems in which the exciplex generating groups are connected by methylene chains. Several recent investigations on such systems will be discussed below for both heteroexcimers and symmetric excimers. Although beyond the scope of the present review the excimers are here included in view of the analogies with the corresponding heteroexcimer systems.

1. Excimers

The so-called $n = 3$ rule for excimer formation in systems represented by the structure Ar—$(CH_2)_n$—Ar, was first put forward by Hirayama for diphenylalkanes[27a] and subsequently confirmed by Chandross for dinaphthylakanes.[27b] The $n = 3$ restriction for excimer formation suggests a unique symmetrical sandwich structure as supported by ordinary theoretical calculations. As a general rule, however, this model appears to be correct only as a first approximation. Thus, studies as discussed below were performed for anthracenophanes,[104] dipyrenylalkanes[27c] and dianthrylethanes,[28, 104] clearly indicating the existence of several possible excimer configurations. Intramolecular interaction may also occur between radicals, as shown[105] in the case of 4-carbomethoxypyridinyls connected at the nitrogen by a $n = 4$ or $n = 3$ methylene chain (**6**).

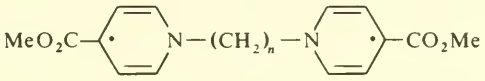

(**6**)

Emission spectra of the anthracenophanes (**7**)–(**10**) have been measured. In a rigid solution at 77 K, *syn*-[2.2](1,4)anthracenophane (**7**) shows a broad excimer emission peaking at 630 nm (τ 62 ns). On the other hand, the fluorescence band of *anti*-[2.2](1,4)anthracenophane (**10**), showing a vibrational structure and a lifetime which is much shorter than that of (**7**), does not seem to arise from an excimer species. Still different behaviour is exhibited by [2.2](1,4)(9,10)anthracenophane (**8**). This molecule shows a broad excimer band in a rigid solvent at 77 K, but differing from that of (**7**) in both emission maximum (570 nm) and lifetime (150 ns). For both (**7**) and (**8**), the excimer fluorescence intensity at room temperature is much weaker

(7)

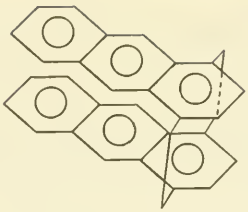

(8)

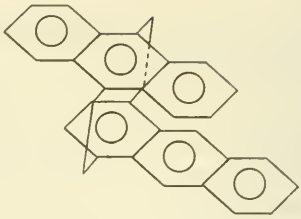

(9)

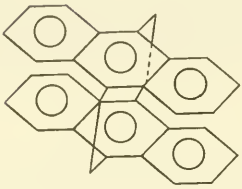

(10)

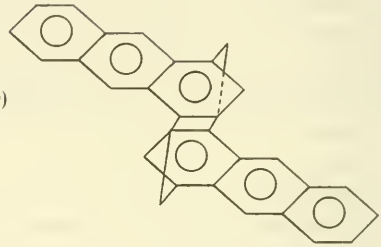

than at 77 K, a phenomenon attributable to the enhancement of the intramolecular photodimerization reaction in the case of (**8**), and both photodimerization and *syn* → *anti* isomerization in the case of (**7**). No excimer emission is observed for [2.2](9,10)anthracenophane (**9**), which is also probably due to the very effective intramolecular photodimerization. It is thus evident that at least two different exciplex emissions, associated with two distinct geometrical arrangements, are possible for the anthracene excimer system.

As pointed out in the Introduction (I.B.) (see Fig. 1) each of the two $n = 2$ systems, 1,2-di-(1-anthryl)ethane (**1**) and 1,2-di-(9-anthryl)ethane (**2**), also forms two kinds of intramolecular excimer (type-1 and type-2), differing in the relative orientation of the anthracene rings. The wavelengths of the above excimer fluorescence band maxima are in the order (**7**) > (**8**) > (**1**) (type-2), (**2**) (type-2) > (**1**) (type-1), (**2**) (type-1). Thus, the red shift seems to increase with increasing overlap between the two anthracene rings. The overlap may play an important role in stabilizing the excimer state and destabilizing the Franck–Condon ground-state.

Similar conclusions have been derived for the α,ω-di-(1-pyrenyl)alkanes [Pyr—$(CH_2)_n$—Pyr, $n = 2$–16, 22] series.[27c] The intramolecular excimer emission is strongest for $n = 3$ (in accordance with the $n = 3$ rule), it is essentially absent for $n = 7$ and $n = 8$, and it increases until $n = 11$, remaining more or less constant for larger n. In keeping with this, the emission energy is the same for $n = 3$ and $n = 10$–16, 22 but is considerably higher for $n = 2, 4, 5, 6, 8, 9$ (see Fig. 8). The constant low energy value is attributed to the parallel symmetrical sandwich structure, while a reduced

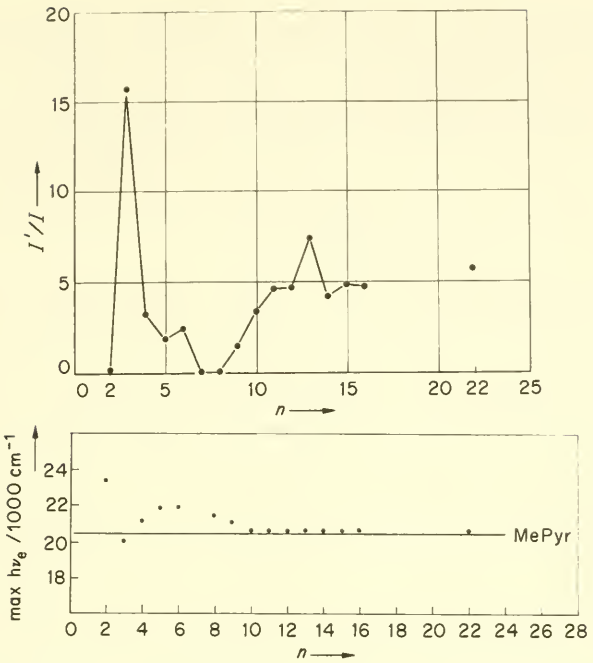

FIG. 8. Ratio of intramolecular excimer (I') and monomer (I) emission intensities (top), and energy of excimer emission (bottom), as function of n in α,ω-di-(1-pyrenyl)alkanes, Pyr—$(CH_2)_n$—Pyr. [Reproduced with permission from K. Zachariasse and W. Kühnle, *Z. Phys. Chem.* (N.F.), **101**, 267 (1976).]

overlap between the pyrene moieties is responsible for the blue shift in the $4 < n < 9$ and $n = 2$ compounds, where the length of the $-(CH_2)_n-$ chain prevents the formation of the parallel sandwich.

2. Heteroexcimers

Intramolecular heteroexcimer formation in systems where the electron donor and acceptor are linked via methylene chains was first studied by Chandross[17] for various naphthylalkylamines. It was observed that not only (**11**), $n = 3$, and (**12**), $n = 3$, but also (**11**), $n = 2$, and (**12**), $n = 2$ (for which close geometrical overlap between the nitrogen atom and a ring

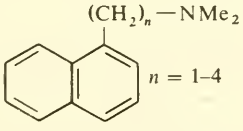

(**11**)

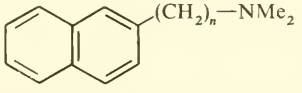

(**12**)

carbon atom, such as C_1, C_2 or C_9 is considerably inhibited) show heteroexcimer fluorescence spectra similar to those of the naphthalene–triethylamine intermolecular heteroexcimer.[106, 107] It therefore appears that the geometrical requirements for exciplex interaction in the above systems are not extremely critical. However, the fact that the heteroexcimer fluorescence in compounds with $n = 2$ appears at energies considerably higher than those of compounds with $n = 3$ is indicative of a reduced donor–acceptor interaction in the geometrically inhibited system.

Indications on the invalidity of the $n = 3$ rule, and on the absence of serious geometrical restrictions for intramolecular exciplex formation, were also reported[18, 20–22] for the systems p-$(CH_3)_2N—C_6H_4-(CH_2)_n-$(1-pyrenyl) and p-$(CH_3)_2N—C_6H_4—(CH_2)_n—$(9-anthryl), with $n = 1, 2, 3$ [(**4**), $n = 1, 2, 3$, and (**3**), $n = 1, 2, 3$]. The absorption spectra of all the above molecules are not indicative of any ground-state interactions. However, as pointed out in the Introduction (I.B), although in non-polar solvents the fluorescence spectra of (**3**), $n = 1, 2$, and (**4**), $n = 1$, are only due to localized excited states within the anthracene or pyrene parts, heteroexcimer emissions are observed (along with the locally excited fluorescence) in the cases of (**4**), $n = 2, 3$, and (**3**), $n = 3$. This result implies a stronger interaction between the two moieties in the CT heteroexcimer state in the case of (**4**), $n = 2, 3$, and (**3**), $n = 3$, as compared with (**3**), $n = 1, 2$, and (**4**), $n = 1$. The former may assume sandwich-type configurations favouring larger Coulomb interactions than those of the sterically inhibited $n = 1$ systems. Again, the observed blue shift of the band maximum in (**4**), $n = 2$, relative to (**4**), $n = 3$, shows that the Coulomb interaction energy in (**4**), $n = 2$, is smaller than that in the low-strain (**4**), $n = 3$, system. Moreover, since the electron affinities of anthracene and pyrene are very close, the observation that (**4**), $n = 2$, shows a heteroexcimer fluorescence while (**3**), $n = 2$, does not, indicates a geometrical structure in (**4**), $n = 2$, that favours Coulomb interactions more than in (**3**), $n = 2$. It is worthwhile noting that even the sterically inhibited (**3**), $n = 1, 2$, and (**4**), $n = 1$, do show heteroexcimer fluorescence in polar solvents, indicating that the plane parallel sandwich structure is not an essential requirement for heteroexcimer formation. The appearance of the heteroexcimer emission of these molecules in polar systems is apparently due to pronounced stabilization of the CT exciplex state by solvation. The effect is explained by steric restrictions, imposing a donor–acceptor distance that is considerably larger than that of the parent sandwich-type heteroexcimers [e.g. (**3**), $n = 3$, (**4**), $n = 3$]. Accordingly, the intramolecular Coulomb interaction will be smaller for (**3**), $n = 1, 2$, and (**4**), $n = 1$, but the resulting high dipole moment will lead to a marked stabilization of the CT state in polar solvents (see discussion below on solvent effects).

As discussed in Section II.A the processes of heteroexcimer formation for

(**3**), $n = 3$, and (**4**), $n = 2$, 3, in non-polar solvents are considerably slower than those of the corresponding intermolecular systems. This clearly indicates that in these cases the formation process is affected by hindered rotations about the CH_2—CH_2 bonds. Thus, the intramolecular CT fluorescence state seems to be formed from the locally excited state by changes in the geometrical structure as indicated in (31).

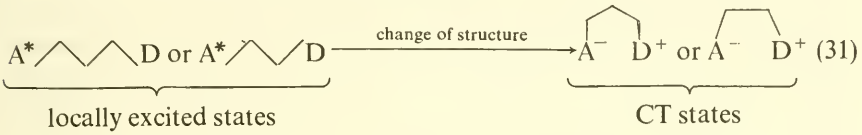

(31)

where the structures in the four formulae (from left to right) represent the methylene chains of (**3**),(**4**), $n = 3$, or (**3**),(**4**), $n = 2$, and (**3**),(**4**), $n = 3$, or (**3**),(**4**), $n = 2$, respectively.

In contrast to these cases, no pronounced changes in geometry appear to be involved in the (**3**), $n = 1$, and (**4**), $n = 1$, heteroexcimer formation processes. Thus, in solvents that are sufficiently polar to make the energies of the locally excited and the heteroexcimer state nearly equal, the heteroexcimer formation and decomposition processes are fast enough for an equilibrium to be established between the two states during the $\sim 10^{-8}$ s excited-state lifetime of both (**3**), $n = 1$, and (**4**), $n = 1$.[21, 57]

As discussed in Section II.A, the intramolecular heteroexcimer formation process in polar solvents seems to differ from the low polarity path in that electron transfer may take place without assuming the sandwich-type structure. Detailed studies[57] on the fluorescence kinetics of (**4**), $n = 3$, suggest the population of several kinds of heteroexcimer, differing in lifetime and geometrical structure (but not in energy). At relatively high temperatures, an equilibrium is established between the various species, leading to a single exponential decay. However, at low temperatures, the species are not easily interconvertible during the excited-state lifetime, resulting in a multiple component decay curve. Time-resolved absorption spectra for (**4**), $n = 3$, excited in low-temperature propan-2-ol, have shown that the absorption corresponding to a short-lived fluorescent species is very close to the superposition of the absorption bands of the pyrene anion and the DMA cation. The spectrum of a longer-lived component is, however, quite broad, being similar to that observed in the same solvent at room temperature.[57]

C. Solvent Effects in Exciplex Systems

1. Theoretical Predictions

Essentially all measurable properties of polar exciplexes, such as emission and absorption spectra, fluorescence lifetimes and quantum yields, rates and

enthalpies of formation, as well as intersystem crossing and ionic photodissociation yields, are markedly solvent dependent. A rationalization of experimental phenomena implies an understanding of the interactions between a polar solute and its solvent environment. Thus, before presenting and discussing the details of the available data, we shall briefly review the theoretical background and its implications to polar exciplexes.

The available theoretical analysis of intermolecular interactions in solution,[108] accounting for both dispersion and usual electronic forces, is based on the treatments of Ooshika,[109] McRae,[110] Longuet-Higgins and Pople[111] and Liptay.[112] Solvation is considered as a perturbation and is treated according to second-order perturbation theory. The arising interaction terms are usually calculated adopting Onsager's reaction field model[113] which treats the system as a rigid dipole of moment μ at the centre of a spherical cavity of radius a immersed in a homogeneous (solvent) continuum with dielectric constant ϵ' and refractive index n. The solvent acts on the solute molecule as an effective electric field, the reaction field F, arising from the orientation and inductive polarizations of the dielectric continuum by the solute dipole. The best available experimental test for the theory is a comparison with observed solvent effects on fluorescence and absorption frequencies ($\Delta\tilde{\nu}_f$ and $\Delta\tilde{\nu}_a$). We shall therefore focus our attention on these parameters which are always calculated under the restrictions imposed by the Franck–Condon principle, i.e. by assuming that absorption transitions take place from a ground equilibrium state to an excited state in which the molecular configurations of solute and solvent are identical to those of the ground-state system. In emission (at room temperature and normal viscosities) the transition is from an equilibrated fluorescent state with energy E_{ex} to a ground state of identical nuclear configuration with energy E_g. Based on the above treatments which yielded equations for $\Delta\tilde{\nu}_f$ and $\Delta\tilde{\nu}_a$, Lippert[114] and Mataga and coworkers[115,116] obtained a more practical expression for the wavenumber difference $\Delta\tilde{\nu}_a - \Delta\tilde{\nu}_f$ in which the major contribution comes from the term:

$$\Delta\tilde{\nu}_a - \Delta\tilde{\nu}_f \approx \frac{2}{hc}\frac{(\mu_{ex} - \mu_g)^2}{a^3}\left[\frac{\epsilon' - 1}{2\epsilon' + 1} - \frac{n^2 - 1}{2n^2 + 1}\right] \tag{32}$$

with other terms, accounting for dispersion (polarizability) and solvent dipole–induced solute dipole interactions, being relatively small. μ_{ex} and μ_g are correspondingly the dipole moments of the excited and ground states.

As described by Beens,[117] identical conclusions, i.e. equation (32), are a direct consequence of Onsager's reaction field model when the solvent perturbation is carried out only to first order, in other words, when solvent effects on the exciplex electronic structure are *a priori* omitted. The treatment

is based on the (somewhat simplified) expression for the reaction field, arising from both orientation and inductive polarizations of the solvent dielectric due to the solute's dipole:[113]

$$\boldsymbol{F} = \boldsymbol{\mu} f_{\epsilon'} \qquad \text{where } f_{\epsilon'} \equiv \frac{2}{a^3}\left(\frac{\epsilon' - 1}{\epsilon' + 2}\right). \tag{33}$$

The reaction field ($\boldsymbol{F}_{\text{ind}}$) due solely to the inductive polarization is given by a similar expression, with ϵ' replaced by the square of the refractive index n (optical dielectric constant):

$$\boldsymbol{F}_{\text{ind}} = \boldsymbol{\mu} f_n \qquad \text{where } f_n \equiv \frac{2}{a^3}\left(\frac{n^2 - 1}{2n^2 + 1}\right). \tag{34}$$

Thus, the effective field due to the orientation polarization, i.e. the contribution of the permanent solvent dipoles, is:

$$\boldsymbol{F}_{\text{or}} = \boldsymbol{F} - \boldsymbol{F}_{\text{ind}} = \boldsymbol{\mu}(f_{\epsilon'} - f_n). \tag{35}$$

Based on the above expressions it is possible to evaluate the difference between the ground-state energy of the molecule $E_g = \langle \Psi_g | \mathscr{H}^0 + \mathscr{H}'_g | \Psi_g \rangle$ and that in the Franck–Condon (FC) excited state $E_{ex}^{FC} = \langle \Psi_{ex} | \mathscr{H}^0 + \mathscr{H}'_{ex} | \Psi_{ex} \rangle$. $\mathscr{H}$ is the Hamiltonian in the gas phase, and $\mathscr{H}'_g$ and $\mathscr{H}'_{ex}$ represent the corresponding perturbations given by $\mathscr{H}'_g = \boldsymbol{\mu}_{op} \cdot \boldsymbol{F}_g$ and $\mathscr{H}'_{ex} = -\boldsymbol{\mu}_{op} \cdot \boldsymbol{F}_{ex}$. $\boldsymbol{\mu}_{op} \equiv \boldsymbol{\mu}_g$ and $\boldsymbol{\mu}_{ex}$ are the corresponding electric dipole-moment operators, and $\boldsymbol{F}_g$ and $\boldsymbol{F}_{ex}$ represent the reaction fields in each of the states. After accounting for the increase in the solvent polarization energy during the transition, the expression:

$$hc\tilde{\nu}_a = E_{ex}^0 - E_g^0 - \mu_{ex}\mu_g(f_{\epsilon'} - f_n) - \tfrac{1}{2}\mu_{ex}^2 f_n + \mu_g^2(f_{\epsilon'} - \tfrac{1}{2}f_n) \tag{36}$$

is obtained[117] for the absorption transition frequency. Analogously, the emission frequency from the solvation equilibrated fluorescence state to the Franck–Condon ground state is:

$$hc\tilde{\nu}_f = E_{ex}^0 - E_g^0 + \mu_{ex}\mu_g(f_{\epsilon'} - f_n) + \tfrac{1}{2}\mu_g^2 f_n - \mu_{ex}^2(f_{\epsilon'} - \tfrac{1}{2}f_n) \tag{37}$$

with E_{ex}^0 and E_g^0 denoting the corresponding gas-phase energies. It can be seen that equation (32) is readily obtained by subtracting equation (37) from equation (36).

In the case of molecular complexes which are stable only in the excited state, $\tilde{\nu}_{abs}$ is not available experimentally and use is only made of expression (36) which, if $|\boldsymbol{\mu}_g| \ll |\boldsymbol{\mu}_{ex}|$, assumes the form:

$$\tilde{\nu}_f = \tilde{\nu}_f^0 - (\mu_{ex}^2/hc)(f_{\epsilon'} - \tfrac{1}{2}f_n). \tag{38}$$

The applicability of the above simplified model to polar exciplexes, and thus the validity of expression (38), was first questioned by Mataga and his coworkers[118] who argued that the exciplex dipole moment μ_{ex} cannot be treated as a solvent-independent parameter. In other words, the exciplex electronic structure (i.e. wavefunction) should be affected by the medium, so that in polar solvents solvation of the exciplex will oppose the electronic delocalization between A and D, leading to an increased polar character (dipole moment). A similar approach has been suggested to account for solvent effects on the spectra of merocyanine dyes, interpreted in terms of an increased contribution of intramolecular zwitterionic forms to the wavefunction in polar solvents.[119]

Based on the above ideas, theoretical treatments of solvent polarity effects on the electronic structure of polar exciplexes have been developed[117, 120, 20a, 22b] in which the role of the solvent is essentially that of affecting the energy difference between the zero order (A^-D^+) state and the various non-polar states (locally excited and ground no-bond state), and consequently the eigenfunctions and eigenvalues associated with an exciplex wavefunction such as:

$$\Psi = \Sigma C_i \Psi_i = C_1 \Psi(A^-D^+) + C_2 \Psi(AD) + C_3 \Psi(A^*D) + C_4 \Psi(AD^*) + \ldots \tag{39}$$

The emission wavenumber $\tilde{\nu}_f$ is determined by the energy difference $(E_{ex} - E_g^{FC})$ which depends on μ_{ex} and thus on Ψ via $\mu_{ex} = \langle \Psi | \boldsymbol{\mu}_{op} | \Psi \rangle$. It is therefore evident that solvent effects on $\tilde{\nu}_f$ should be related to the solvent dependence of all C_i and thus of μ_{ex}.

An expression [equation (40)] relating the variation in $\tilde{\nu}_f$ due to small variations in the solvent parameters f'_ϵ ($f'_\epsilon \equiv \frac{1}{2}a^3 f_\epsilon$) and f'_n ($f'_n \equiv \frac{1}{2}a^3 f_n$) has been obtained by Beens and Weller[13] for an exciplex case in which only C_1 and C_4 (or C_3) are not negligible:

$$\delta(hc\tilde{\nu}_f) = -\frac{2\mu^2}{a^3}\delta(f'_\epsilon - \tfrac{1}{2}f'_n) - (f'_\epsilon - f'_n)\frac{d(\mu^2/a^3)}{df'_\epsilon}\delta f'_\epsilon \tag{40}$$

If μ^2 is solvent independent (e.g. when $C_1^2 \approx 1$), as also in the complex geometry (a^3), then a plot of $\tilde{\nu}_c$ against $(f'_\epsilon - \frac{1}{2}f'_n)$ should be linear, in agreement with the simplified equation (38). Deviations from linearity, i.e. curvatures in these plots, should correspond to a solvent dependence of μ^2/a^3.

Mataga and coworkers[22b] have explicitly expressed [cf. equation (41)] the wavenumber of the exciplex fluorescence in terms of the coefficients C_1 and C'_1 of $\Psi(A^-D^+)$ in the lowest excited and ground state wavefunctions correspondingly:

$$hc\tilde{\nu}_f = E_1 - E_0 + \tfrac{1}{2}(C_1^4 + C'^4_1)\mu_0^2 f_n + C_1^2 C'^2_1 \mu_0^2 (f_\epsilon - f_n) \tag{41}$$

E_0 and E_1 are the lowest and second lowest eigenvalues of the secular equations obtained by applying the variation principle to the system described by equation (39), and μ_0 is the dipole moment of the pure CT (A^-D^+) state [$\mu_0 = \langle\Psi(A^-D^+)|\boldsymbol{\mu}_{op}|\Psi(A^-D^+)\rangle$]. Expression (41) is obtained after adding to E_1 and E_0 the polarization energy of the solvent. Solution of the secular equation expresses E_1, E_0 and C_i in terms of the Hamiltonian matrix elements which, if only three states [(A^-D^+), (A*D), (AD] are involved, assume the form:

$$\langle\Psi(A^-D^+)|\mathscr{H}|\Psi(A^-D^+)\rangle = \langle\Psi(A^-D^+)|\mathscr{H}_0|\Psi(A^-D^+)\rangle + \langle\Psi(A^-D^+)|\mathscr{H}'|\Psi(A^-D^+)\rangle = E_c - \langle\Psi(A^-D^+)|\boldsymbol{\mu}_{op}.\boldsymbol{F}|\Psi(A^-D^+)\rangle = E_c - C_1^2\mu_0 f_{\epsilon'} \tag{42}$$

$$\langle\Psi(A^-D^+)|\mathscr{H}|\Psi(A^*D)\rangle \approx \langle\Psi(A^-D^+)|\mathscr{H}^0(A^*D)\rangle \equiv \alpha \tag{43}$$

$$\langle\Psi(A^-D^+)|\mathscr{H}|\Psi(AD)\rangle \approx \langle\Psi(A^-D^+)|\mathscr{H}^0|\Psi(AD)\rangle \equiv \beta \tag{44}$$

$$\langle\Psi(A^*D)|\mathscr{H}|\Psi(A^*D)\rangle \approx \langle\Psi(A^*D)|\mathscr{H}^0|\Psi(A^*D)\rangle \equiv E_e \tag{45}$$

$$\langle\Psi(AD)|\mathscr{H}|\Psi(AD)\rangle \approx \langle\Psi(AD)|\mathscr{H}^0|\Psi(AD)\rangle \equiv E_g. \tag{46}$$

In the application of the variation principle it should be recalled that the Hamiltonian matrix elements in solution depend on $\mathscr{H}'$ and thus on $\boldsymbol{F}$ and $\boldsymbol{\mu}$. Since $\boldsymbol{\mu}$ depends on the actual wavefunction it is seen that iterative, self-consistent field, calculations should be carried out for obtaining the correct eigenvalues and eigenfunctions of the system.

2. Analysis of Experimental Solvent Effects

Emission frequencies. In the case of EDA complexes CT transitions may be observed both in absorption and in emission. However, for weak complexes (Mulliken "outer" complexes), in which C_1' is small, $\mu_g \approx 0$, so according to equation (36) $\tilde{\nu}_a$ will be essentially independent of the solvent dielectric constant, in agreement with experiment. Since these systems are usually very poor fluorescers in fluid solutions at room temperature, essentially all available quantitative data on spectroscopic solvent effects are obtained from fluorescence data of inter- or intra-molecular exciplexes with a repulsive ground state. Such solvent effects were first reported by Mataga and coworkers[118] in the case of the pyrene–*N*,*N*-dimethylaniline (DMA) exciplex. The data were plotted against the solvent parameter ($f_{\epsilon'}' - \frac{1}{2}f_n'$) and yielded a fairly straight line at relatively low polarities, leading [using equation (38) and assuming $a = 4$–5 Å] to the value $\mu \approx 10$ D for the exciplex dipole moment. Substantial deviations from linearity at high polarities were qualitatively attributed to the inadequacy of equation (38) owing to a considerable increase of the dipole moment induced by solvent interaction.

Experimental correlations between the above solvent parameter and the emission frequency have been obtained by Weller and coworkers[121, 122] for several other exciplex systems such as anthracene–*N*,*N*-diethylaniline (DEA), biphenyl–DEA, pyrene–DEA. Because of considerable scattering of points in the plots of $\tilde{\nu}_f$ versus $(f'_\epsilon - \frac{1}{2}f'_n)$ (attributed to specific solvent–solute interactions), curvatures corresponding to solvent-induced variations of μ^2/a^3 [second term in equation (40)] could not be detected. However, reliable relative values of μ^2/a^3 were obtained by plotting the $\tilde{\nu}_f$ values of two different complexes in a variety of solvents against each other.[122] This procedure, which leads to straight lines with relatively little scatter, is assumed to cancel specific interactions that are not contained in the solvent parameter $(f'_\epsilon - \frac{1}{2}f'_n)$.

A substantial problem associated with the quantitative interpretation of the experimental data arises from the fact that the evaluation of μ requires a knowledge of a and vice versa. According to Lippert,[114] a should be somewhat greater than the corresponding dimension of the complex, but it cannot accurately and independently be estimated. Since, for most of the investigated exciplexes, the variations in μ^2/a^3 matched the expected variations in the complex dimensions, it was concluded[122] that the excited states involved correspond to an essentially pure CT state ($C_1 \approx 1$). Assuming a distance of 3–3·5 Å between the charges, it was found that this state is characterized by a dipole moment of $\mu_0 \approx 12{\cdot}5$ D. Using this number, a value of $a = 5{\cdot}5$ Å was obtained for e.g. the anthracene–DEA exciplex. One exception was found in the case of the hexamethylbenzene–biphenyl exciplex, for which the observed $\tilde{\nu}_f$ and the estimated radius ($a = 4{\cdot}8$ Å) lead to $\mu_{ex} = 6{\cdot}37$ D. This implies that the excited state is not of pure CT nature, so the coefficients of locally-excited structures in equation (39) are not negligible. Since $\mu_{ex} = \langle\Psi|\mu_{op}|\Psi\rangle \approx C_1^2\langle|\Psi(A^-D^+)|\mu_{op}|\Psi(A^-D^-)\rangle = C_1^2\mu_0$, the above data lead to the value $C_1 \approx 0{\cdot}7$. In spite of the approximations associated with the model that yields equation (38), it is thus evident that solvent effects on $\tilde{\nu}_f$ may provide important basic information on the exciplex electronic structure.

Solvent effects on $\tilde{\nu}_f$, interpretable in terms of environmental effects on the exciplex electronic structures, have been obtained by Mataga and coworkers who investigated[20, 21, 18a, 22b] the intramolecular systems (**3**), $n = 0$, 1, 2, 3, and (**4**), $n = 1$, 2, 3, as well as the intermolecular exciplex 1-cyanonaphthalene–naphthalene. Three different classes of behaviour are observed. The plots of $\tilde{\nu}_f$ versus $(2f'_\epsilon - f'_n)$ for the molecules (**3**), $n = 1$, 2, and (**4**), $n = 1$, are linear in the high polarity region, exhibiting a sharp break around $(2f'_\epsilon - f'_n) \approx 0{\cdot}35$, below which $\tilde{\nu}_f$ is solvent-independent and matches the emission of the isolated anthracene or pyrene moieties (e.g. Fig. 9). The data are interpreted in terms of a solvation-induced reversal

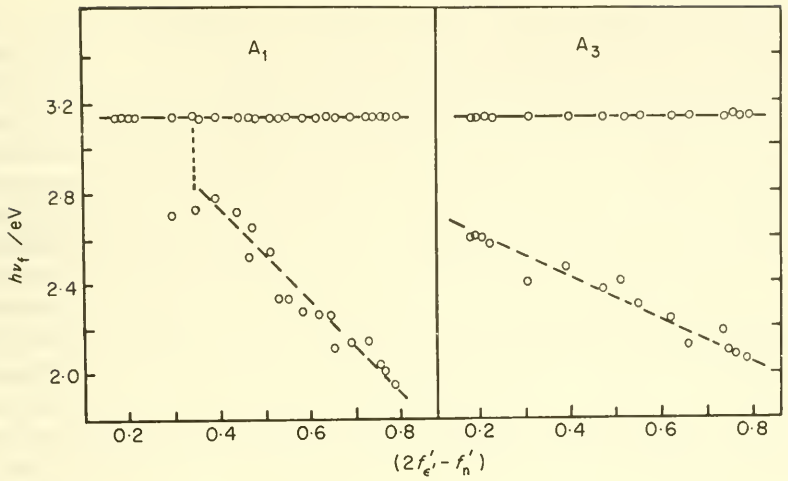

FIG. 9. Relations between $h\nu_f$ and $(2f'_{\epsilon'} - f'_n)$ observed for (**3**), $n = 1$, and (**3**), $n = 3$). The top parallel lines represent the emission of anthracene. [Reproduced with permission from S. Masaki, T. Okada, N. Mataga, Y. Sakata and S. Misumi, *Bull. Chem. Soc. Japan*, **49**, 1277 (1976).]

of the two non-interacting energy levels. In polar solvents the pure CT state lies below the locally excited S_1 state of the hydrocarbon which is the lowest state in a non-polar environment. Using the μ^2/a^3 value obtained from the slope of a linear region such as shown in Fig. 9, and applying the simple dielectric continuum model for calculating the energy of the CT state, they obtained satisfactory agreement between the observed break in the curve and the value of $(2f'_{\epsilon'} - f_n)$ for which the two states become iso-energetic.

This picture was also found to be consistent with an analysis according to equation (41), expressing E_1, E_0, C_1 and C'_1 in terms of the matrix elements of the corresponding secular equation. The solvent-induced shifts of the fluorescence of e.g. (**3**), $n = 1$, could be best reproduced with $\beta = 0$ and $\alpha = 0{\cdot}05$ eV, implying very small interactions between the CT and other states so that, in the polar region above $(2f'_{\epsilon'} - f'_n) \approx 0{\cdot}33$, $C_1 \approx 1$ independently of the solvent. The plots of $\tilde{\nu}_f$ versus $(2f'_{\epsilon'} - f'_n)$ for (**3**), $n = 3$, and (**4**) $n = 3$, exhibit fairly linear behaviour over the whole polarity range, so only negligible solvent-induced changes in their electronic structure seem to occur. In these cases the CT states are very polar and, owing to strong Coulomb interactions between the two moieties, they lie lower than the locally-excited state even in non-polar solvents. These conclusions were consistent with an analysis of the $\tilde{\nu}_f$ data according to equation (41) and equations (42)–(46), yielding for (**3**), $n = 3$, a very small α and a negligible β,

with a solvent-independent C_1^2. In contrast to this, the plots for (**3**), $n = 0$, and (**4**), $n = 2$, and 1-cyanonaphthalene–naphthalene belong to a third class of behaviour. They show clear deviations from linearity (representable by a continuous curve or by the superposition of two lines with different slopes), thus reflecting a solvent-induced change of the exciplex electronic structure. In the case of (**3**), $n = 0$, an analysis according to equation (41) and equations (42)–(46) leads to substantial values for α and β ($\alpha = 0{\cdot}4$ eV, $\beta = 0{\cdot}3$ eV) indicating that the CT state interacts strongly with the locally-excited and ground states. Since C_1^2 is less than 1, it may be subject to solvent effects. In keeping with this, the calculated value for C_1^2 shows a gradual increase with increasing solvent polarity, reaching a value of $\sim 0{\cdot}9$ in acetonitrile. The comparison of such conclusions with experimental data is complicated, however, by complex solvent effects on the fluorescence lifetime and yield of (**3**), $n = 0$, indicating the existence of a dual luminescence arising from two emitting states of considerably different structure (see discussion below).

Okada and his coworkers[18a, 22b] used data discussed above for drawing conclusions about the geometrical restrictions prevailing during intramolecular CT complexation in the excited state. In the cases of (**3**), $n = 1, 2$, they pointed out that, because of a large separation between donor and acceptor groups, the stabilization energy of the CT state due to the Coulomb force between the pair may be smaller than in the cases of ordinary intermolecular exciplexes. However, since their dipole moments in the CT state are much larger ($\mu \approx 26$ D) than those of ordinary exciplexes, the solvation in a polar solvent may be very effective in stabilizing the CT state. In the case of (**3**), $n = 3$, since its CT fluorescence and dipole moment (~ 15 D) are similar to those of the corresponding intermolecular exciplex, they concluded that the geometrical restrictions for heteroexcimer formation are not very critical, i.e. the two rings do not necessarily have to overlap or to be parallel in the exciplex state.

A theoretical analysis[20a] of the intermolecular 1-cyanonaphthalene–naphthalene system was carried out by considering a wavefunction with four configurations: $\Psi = C_1\Psi(A^-D^+) + C_2\Psi(A^+D^-) + C_3\Psi(A^*D) + C_4\Psi(AD^*)$. Iterative calculations show considerable interaction between locally excited and CT states, indicating a strong solvent effect on the amount of CT character of the exciplex state.

Solvent effects have provided valuable tools for investigating the excited states of various intramolecular CT systems lacking the degree of flexibility necessary to obtain substantial overlap between donor and acceptor moieties, as available for e.g. (**3**), $n = 2, 3$, (**4**), $n = 2, 3$. As an example of such systems, molecules (**3**), $n = 0$, 1, and (**4**) $n = 1$, were quoted; here the geometrical changes associated with the formation of their fluorescent CT states are limited. In a molecule such as (**3**), $n = 0$, even a partial geometrical overlap

between the anthracene and aniline moieties is not allowed. The emitting system is thus an example of an intramolecular CT state to which the applicability of the term exciplex may seem questionable. Obviously there appears to be no discontinuity in the gradual transition from sandwich-type inter- and intra-molecular exciplexes to simple highly polar excited molecular states, e.g. from (**3**), $n = 3$, to (**3**), $n = 0$, via (**3**) $n = 2$, and (**3**), $n = 1$. In the subsequent sections we shall discuss some examples of the latter systems which, as in the case of (**3**), $n = 0$, contain well-defined donor and acceptor groups. The discussion is by no means a complete survey of the numerous quotable examples. The molecules discussed have been chosen on the basis of the considerable attention that they attracted and also in view of their relevance to the general field of exciplex chemistry.

p-*N*,*N*-Dimethylaminobenzonitrile (**13**) exhibits anomalous fluorescence in polar solvents, consisting of two bands (a) around 23 000 cm^{-1} and (b) around 29 000 cm^{-1}. In rigid glasses or hydrocarbon solvents only the (b)-band is observed. Lippert and his coworkers[123] interpreted this solvent dependence in terms of two emitting electronic states in the same manifold [a less polar (^1L_b) and a strongly polar (^1L_a)], invoking an inversion of states during the (polar) solvent orientational relaxation. An alternative explanation of the same phenomenon suggested an excimer as responsible for the (a)-band.[124] Both interpretations of this well-known example of anomalous fluorescence were found to be incorrect by Rotkiewicz *et al.*[60] Thus fluorescence polarization data were found inconsistent with the first model (both bands have the same polarization, in contrast to what is expected for ^1L_b and ^1L_a states), while the lack of concentration effects [60, 59b] ruled out the excimer interpretation. The alternative model advanced by Rotkiewicz and his coworkers[60] assigned the double emission to two states, differing in the orientation of the dimethylamino group with respect to the benzene ring. A perpendicular conformation, highly polar owing to charge transfer from the nitrogen lone-pair to a π^* orbital on the —C≡N, is responsible for the (a)-band. Accordingly the (b)-band is ascribed to a planar conformation which is less polar owing to charge distribution over the entire conjugated system.

A different approach has been presented by Kosower and Dodiuk[125] who plotted the emission energies against the solvent polarity parameter $E_T(30)$.† Two correlation lines were found for the high energy emission (b). A high-slope line was assigned to fluorescence from a highly polar perpendicular structure, identical to that suggested by Rotkiewicz *et al.* for the (a)-band. The low-slope line was ascribed to the planar configuration. Thus, the previous model was adopted for interpreting the high energy emission

† For a definition of $E_T(30)$, see p. 51.

in terms of two conformers of different polarities. On the other hand, the low energy (a)-band was assigned to the fluorescent state of a molecule to which a proton has been added, as supported by deuterium isotope effects in two solvents. In addition to these three states, an emission, attributed to a dimer, was also identified.[125] The main difficulty with the above assignments involves the observation that the low energy fluorescence is quite intense in dry aprotic polar solvents such as acetonitrile[125, 126] and dimethylformamide.[126] Moreover, the recently reported observation[126] that (**14**) and (**15**) (both forced to the perpendicular geometry) exhibit only the low energy (a)-band, while the planar (**16**) molecule shows only the high energy emission, is consistent with the original assignment of Rotkiewicz *et al.*, although it still cannot explain the deuterium isotope effect. Struve *et al.*[61, 127, 128] reported a 20–40 ps rise time for the low energy conformer (A*), as compared with 7–20 ps for the high energy species (B*). These numbers reflect the relaxation processes associated with each of the two emitting states. Fluorescence quenching studies[129] using high O_2 pressures have shown that A* is generated from B*. In acetonitrile the $B^* \rightarrow A^*$ process occurs with a lifetime of 11 ps. Since the solvent reorientation correlation time is only ~ 1 ps it was concluded that the relaxation is not controlled exclusively by solvent reorientation but mostly by the internal rotation kinetics of the dialkylamino group.

Dual luminescence was also observed[130, 131] in the case of the previously discussed [9-(4-dimethylanilino)anthracene] molecule (**3**), $n = 0$. Its fluorescence exhibits a fast high-energy component attributed to a state F*, followed by a slower decay of a lower energy state S*. The fluorescence from S* exhibits a rise time that matches the decay of F*,[130] indicating that F* is a precursor of S*. However, the exact nature of the geometry change associated with the transition from F* to S* is not clear. A study of various derivatives similar to those, (**13**)–(**16**), previously reported for (**13**) indicates that in this case the change is not associated with the orientation of the dimethylamino group.[130]

Kosower and coworkers[132, 23a] have investigated the photophysics of the 6-*N*-arylaminonaphthalene-2-sulphonate system, one of a group often

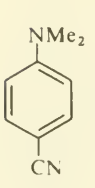

(13)

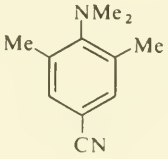

(14)

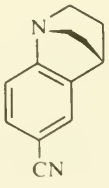

(15)

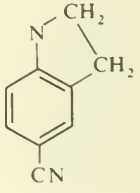

(16)

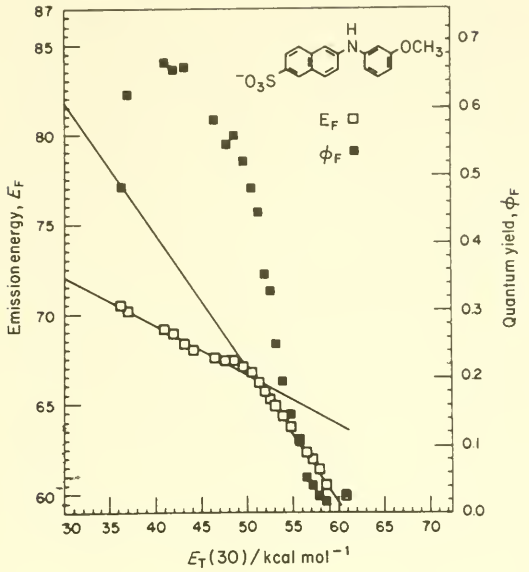

FIG. 10. Use of the empirical solvent parameter $E_T(30)$ for the identification of two emitting states in 6-*N*-arylamino naphthalene-2-sulphonates. [Reproduced with permission from E. M. Kosower, H. Dodiuk, K. Tanizawa, M. Ottolenghi and N. Orbach, *J. Amer. Chem. Soc.*, **98**, 2167 (1975).]

employed as fluorescence probes in biological systems. Fluorescence emission energies and quantum yields, plotted against $E_T(30)$, the empirical solvent polarity parameter (see below), reveal two slopes, the higher sensitivity to solvent being exhibited in the more polar solvent[132] (Fig. 10). The slopes are interpreted in terms of two emitting states, a locally-excited naphthalene-centred state $S_{1,\,np}$ in less polar solvents, and a charge-transfer state $S_{1,\,CT}$ in polar solvents:

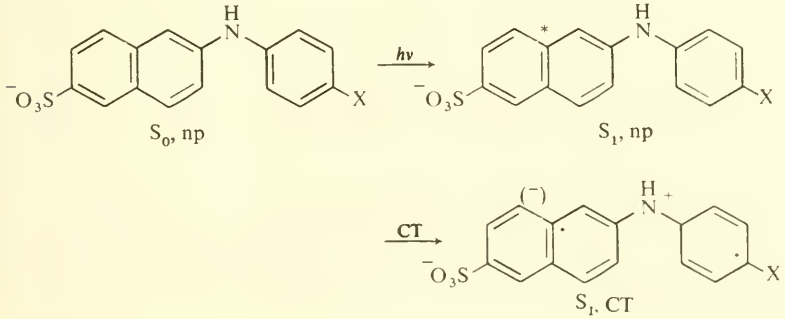

(47)

The striking discovery of a strong quenching of fluorescence in highly polar solvents, which called attention to the arylaminonaphthalene sulphonates in the first place,[133] can thus be seen as a property of the CT state. The formation of the charge-transfer state can be inhibited in highly viscous solvents like glycerol, in which the lifetime of the $S_{1,np}$ state becomes shorter than the rate at which the $S_{1,CT}$ state is formed, so only fluorescence from the former state is observed.[23a] The general nature of the quenching mechanism is shown by two types of experiment. Laser pulse excitation of a number of arylaminonaphthalenesulphonate derivatives reveals that the yield of triplet state falls off sharply as solvent polarity is increased, precluding any significant role for the triplet state in the quenching found in polar solvents. Further, quenching is greatly diminished (factor of 3 or more) in moderate viscosity, high-polarity, solvents like ethane-1,2-diol, indicating that quenching is also a charge-transfer process.[23a] The character of the two states, $S_{1,np}$ and $S_{1,CT}$, has been confirmed by substituent effects, the former being relatively insensitive to the aryl substituent with respect to both formation (absorption) and emission, and the latter highly sensitive to the electron-donating or -withdrawing character of substituents. The simplified scheme (48) illustrates the important processes.

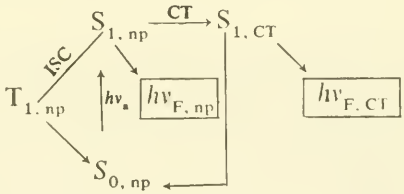

(48)

An approach to the analysis of solvent polarity effects in CT systems, which does not make use of theoretical models (as outlined in Section III.C.1), has been used by Kosower and coworkers who have advocated the applicability of empirical solvent polarity parameters, like $E_T(30)$ and Z, in the evaluation of fluorescence emissions. The basic idea is to use a well-understood reference process to establish expectations for a series of solvents, and is discussed in detail in Kosower's book.[134] Both parameters are based on the charge-transfer absorption bands of pyridinium derivatives. The Z-value, introduced by Kosower in 1958,[135] is based on the charge-transfer band for 1-ethyl-4-carbomethoxypyridinium iodide [equation (49a)], and its character has been demonstrated directly by Kosower and Lindqvist using flash-photolysis.[136]

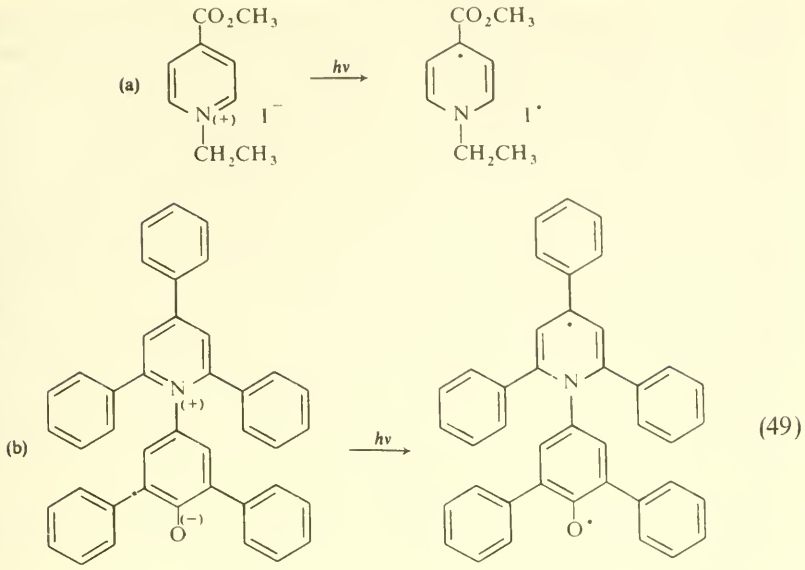

(49)

The $E_T(30)$-value[137] is based on the charge-transfer band of pyridinium phenol betaine [equation (49b)] and represents an intramolecular CT transition. It has been recommended[134] that data for the process under investigation (e.g. an exciplex emission) be compared with an appropriate model process. Thus, for an intramolecular exciplex, one would use $E_T(30)$-values, while for an intermolecular exciplex the Z-value should be more useful. Both parameters reflect the sum of the interactions of a charge-transfer state with a solvent, and provide a fast and reliable index of whether or not an unknown process behaves in a parallel fashion. Furthermore, since the parameters, especially Z-value, may be further analysed through a division of the changes in parameters between ground and excited states,[139] a reasonably quantitative idea of the thermodynamic states for exciplexes can be obtained. At present the question as to which of the two approaches, i.e. the theoretical approximation (41) or the empirical $E_T(30)$ or Z-value scales, should be preferred is still a matter of considerable controversy. Application of both procedures to a variety of systems may help to clarify this question.

Attention has also been drawn to the symmetrical 9,9′-bianthryl molecule whose fluorescence was found by Schneider and Lippert to exhibit a considerable red shift at higher solvent polarities.[58a] Here, too, the picture seems to be one in which an asymmetrical CT state is stabilized by the solvent,

relative to the non-polar (locally excited) symmetrical one that prevails in non-polar solvents. It appears, however, that in this case the solvent not only affects the energy of the CT state but is essentially responsible for its existence by inducing asymmetry via solvation of the two oppositely charged anthracene moieties. When Lippert's data for 9,9′-bianthryl were examined with the use of $E_T(30)$, three emitting states could be identified.[132]

As discussed in Section II.C, interesting examples of solvent effects which seem to be closely related to that of 9,9′-bianthryl have been found for 1,2-dianthrylethanes, (anthracene)—$(CH_2)_2$—(anthracene) [1,2-di-(1-anthryl)-ethane (**1**), 1,2-di-(9-anthryl)ethane (**2**)] and metapyrenophane (**5**).[72] These compounds exhibit an intramolecular excimer fluorescence which is enhanced in polar solvents, where it is accompanied by suppression of the monomer fluorescence band. This result indicates the creation of the solvent-induced CT state, e.g. A^-—$(CH_2)_2$—A^+, which undergoes excimer formation in competition with quenching and (CT) fluorescence. This interpretation is supported by energetic considerations.[72, 28]

Solvent effects on the emission of intramolecular exciplexes, which cannot be explained by bulk solvent effects such as described above, have been reported by Chandross.[138, 62] It was found that the fluorescence maxima of systems such as *N*,*N*-dimethyl-3-(1-naphthyl)propylamine, the anthracene derivative (**3**), $n = 0$, discussed above, and 4-dimethylaminobenzonitrile (**11**), are all markedly red-shifted by the addition of small quantities of polar molecules (e.g. propionitrile or *N*,*N*-dimethylformamide) which essentially do not alter the overall dielectric properties of the (non-polar) solvent employed. The observations are interpreted by assuming stoichiometric (usually 1:1) complex formation between the exciplex and the small dipolar molecules. Such specific interactions, according to which one or two dipolar molecules may sometimes be sufficient to change the nature of the emitting state from locally excited to CT, are attributed to dipole–dipole and polarization forces. It was suggested[62, 138] that the same effect (rather than charge-transfer between excited solute and solvents) is also responsible for e.g. complexation of excited indoles with dioxan or acetonitrile, for which the term exciplex was coined.[10] In any event, the suggested existence of specific interactions between exciplexes and single (polar) solvent molecules calls for caution when attempting to account for solvent effects by the bulk (continuum) model as outlined above.

The absorption spectrum. An independent insight into the electronic structure of exciplexes can be obtained from absorption (rather than emission) spectroscopy. As previously reported, exciplex absorption spectra in non-polar solvents have been interpreted[37] in terms of a superposition of localized excitations within ionic moieties and of reverse CT transitions of

locally excited states of A or D. Recently, the transient absorbance change in the nanosecond range was recorded for the pyrene(P)–DEA system in a variety of solvents.[38, 139] An analysis of the results, including the effect of dissolved oxygen, which may either quench the exciplex or react with the pyrene negative ion ($^2P_S^-$), permitted a discrimination between the exciplex and the free ions, based on kinetic rather than spectroscopic considerations.[139] It was found that the absorption spectrum of the exciplex varies continuously with the solvent polarity, so in polar solvents it becomes indistinguishable from that of the separately solvated ions, $^2P_S^-$ and $^2DEA_S^+$. Essentially identical results were obtained for a variety of other characteristic exciplexes[100] (e.g. see Fig. 11). Likely explanations for such solvent effects may be: (a) The results directly reflect the increased contribution of

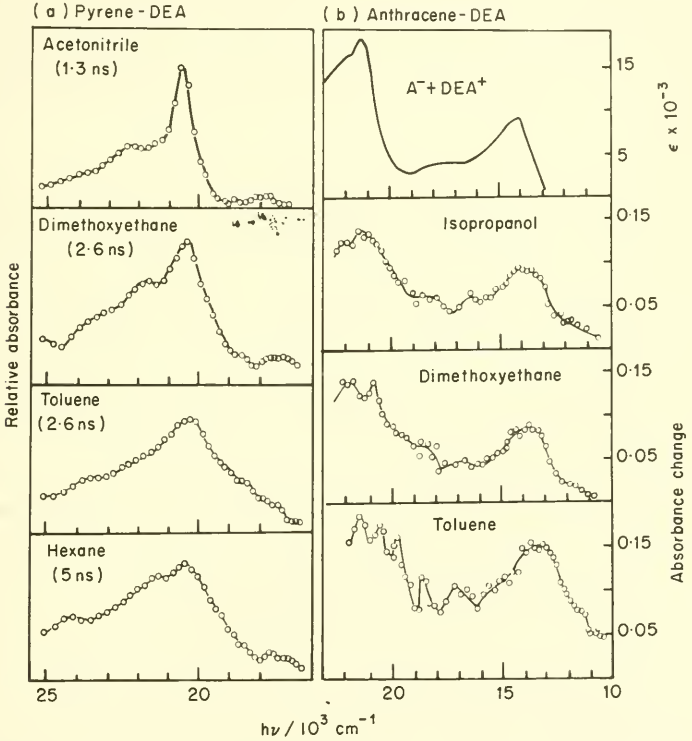

FIG. 11. Absorption spectra of heteroexcimers in solvents of different polarities: (a) For pyrene–DEA as obtained using picosecond laser photolysis. Time values marked are delays between exciting and monitoring pulses. [Taken from H. Fujiwara, N. Nakashima and N. Mataga, *Chem. Phys. Lett.*, **47**, 185 (1977).] (b) For anthracene–DEA, obtained ~15 ns from the origin of an 8 ns exciting pulse. [Reproduced with permission from N. Orbach, Ph.D. Thesis, Hebrew University, Jerusalem (1977).]

the CT structure to the exciplex wavefunction upon increasing the solvent polarity. The diminishing contribution of the locally excited states at higher polarities weakens the reverse CT transitions, with an accompanying gain in the extinction coefficients of the localized transitions within P_S^- and DEA_S^+.[139] (b) Alternatively, it may be assumed that the exciplex is close in electronic structure to a contact ion-pair even in non-polar solvents. The observed solvent effect would then be accounted for by assuming that the absorption bands of the ions are modified (e.g. broadened) in non-polar solvents owing to the strong field of the corresponding counter-ion. In a moderately polar solvent, the donor–acceptor distance in the exciplex may increase owing to solvation, leading to an exciplex spectrum closer to that of the free ions. (c) A third effect, whose importance for the interpretation of the above spectra may not be negligible, is associated with the possibility that, at medium solvent polarities, a fast equilibrium may be established between the exciplex and the solvent-shared ion-pair. The transient absorption spectrum (exhibiting the same lifetime of the exciplex fluorescence) may in such cases reflect the superposition of the spectra of both exciplex and ion-pair.

As we have previously pointed out, curvatures in the plots of $\tilde{\nu}_f$ versus $(f'_{\epsilon'} - \frac{1}{2}f'_n)$ for polar intermolecular exciplexes, reflecting solvent effects on the wavefunction and dipole moment, have not been observed. This is probably due to the fact that, since the corresponding exciplexes are effectively polar (i.e. $C_1^2 \approx 1$), the solvent-induced variations in C_1^2 and thus in μ_{ex} are relatively small and are therefore subject to masking by scattering due to specific solvent effects. However, if one accounts for the solvent polarity effects on the exciplex absorption in terms of the first explanation (a), it would appear that the probabilities of the various exciplex transitions are sensitive to small changes in the C_i values even when $C_1^2 \approx 1$. Thus, excited singlet–singlet spectroscopy may provide unique insights into the nature of the CT excited state which are unattainable via luminescence parameters such as $\tilde{\nu}_f$.

Excited $S_n \leftarrow S_1$ spectra have also been recorded for some of the previously discussed intramolecular systems. The spectra of (**4**), $n = 2, 3$, are markedly solvent dependent. In a polar solvent such as pentan-1-ol they are very close to the superimposed absorptions of the $(pyrene)^-$ and DMA^+ ions.[21, 57] A somewhat broader nature of the (**4**), $n = 3$, absorption is probably indicative of interactions due to its sandwich structure which are absent in the case of (**4**), $n = 2$. Owing to steric inhibitions the latter molecule is probably characterized by an exciplex that is very close to a solvated ion-pair. Though somehow disagreeing on the details, both Okada and his coworkers[18a, 22a] and Asher and Ottolenghi[131] report for (**3**), $n = 0$, a marked solvent polarity effect on the absorption of S^*, which is indicative of changes in its electronic

structure induced by the polar environment. In highly viscous polar solutions at low temperatures, where solvent relaxation cannot take place during the lifetime of the excited state, the $S_n \leftarrow S_1$ spectrum is very close to that observed at room temperature in a non-polar solvent such as n-hexane.[131] Similar conclusions apply to 9,9′-bianthryl for which the spectrum in non-polar solvents resembles that of anthracene, while in polar media it is similar to the superimposed spectra of the anthracene anion and cation.[63] In the case of anthracene derivatives, the main $S_n \leftarrow S_1$ band (~ 810 nm) appears to characterize the non-polar ($S_{1,np}$) state. That corresponding to the $S_{1,CT}$ state has not yet been unambiguously identified.[139]

A few comments are finally appropriate as to time-resolved absorption (rather than emission) spectra of exciplexes or excited EDA complexes. Such observations may yield information, complementary to emission data, on the solvation (and structural reorganization) dynamics of the excited state; for example dipole annihilation transitions of types (c) and (d) [but not (a) and (b)] are expected to exhibit a time dependent energy shift. The relative intensities of various (locally excited within A*, D*, A^-, D^+ and CT) transitions will also change during the solvent and structural relaxation processes. Experimentally, such observations are likely only for intramolecular exciplexes (or excited EDA complexes) where the excited state is prepared by the very act of light absorption. (In intermolecular exciplexes the relatively slow bimolecular diffusional formation process is experimentally superimposed on the subsequent relaxation phenomena, interfering with their detection.) In fact, as discussed in Section III.6, nanosecond time-resolved absorption spectra of the (**4**), $n = 3$, heteroexcimer in propan-2-ol, measured in a low-temperature viscous medium, clearly reflect changes due to a structural relaxation, most probably from an extended to a sandwich geometry.[57] Thus, immediately after the excitation, the spectrum is similar to the superposition of the sharp ion-bands. As time proceeds, it changes to a broader one which also characterizes the same system at room temperature. Analogous changes in the transient spectrum of (**4**), $n = 3$, can be observed also at room temperature by means of picosecond laser photolysis.[140]

IV. PRIMARY GENERAL PROCESSES IN EXCIPLEXES

A. Ionic Dissociation

Owing to their polar nature, dissociation to the corresponding radical-ion products is the most general process undergone by heteroexcimers and excited EDA complexes in polar media. Although these have many features in

common, the discussion will be separated, dealing first with exciplexes (mainly in relation to fluorescence quenching phenomena) and subsequently with excited EDA complexes. Ionic photodissociation in exciplexes covers topics of fundamental importance to a broad range of chemical and biochemical systems such as mechanistic organic photochemistry, electrochemistry and photosynthesis. It also opens important prospects concerning the direct observations of the dynamics of ionic dissociation and recombination processes. These have been out of the range of the classical studies which mostly dealt with equilibrium (thermodynamic) properties.

1. Exciplexes

In addition to the previously discussed effects on the absorption and emission frequencies, increasing the solvent polarity in polar exciplex systems such as anthracene–DEA and pyrene–DMA is also associated with a remarkable reduction of both fluorescence intensity and lifetime.[118, 122, 141, 142] Ultimately, in highly polar solvents such as methanol or acetonitrile the fluorescence is extremely weak and, as shown by early flash photolysis experiments,[142b] the quenching process is accompanied by the formation of the corresponding donor and acceptor radical-ions.

Early attempts to present a detailed mechanism for the radical ion generation process were based on the observation that (for the two previously mentioned exciplexes) the fluorescence yield (ϕ_f) decreases more rapidly with increasing solvent polarity than does the corresponding fluorescence lifetime (τ_f)[118b, 122] (see Fig. 12). To understand two different approaches to this problem let us consider the expression:

$$\phi_f = \phi_f^0 k_f/(k_f + k_d) = \phi_f^0 k_f \tau_f$$

in which ϕ_f^0 is the yield of exciplex generation in a CT quenching process such as ($^1A^* + D$), while k_f and k_d are correspondingly the radiative and non-radiative rate constants to the ground state.

Mataga and coworkers[118] attributed the above discrepancy to solvent effects on the exciplex electronic structure as previously discussed. Their argument is based on the assumption that, for an exciplex described by the wavefunction $\Psi = C_1\Psi(A^-D^+) + C_2\Psi(AD)^*$ [where $(AD)^*$ denotes locally excited structures of either A or D], the main contribution to the emissive probability arises from dipole moments of local transitions such as $\langle {}^1\Psi(A^*)|\boldsymbol{\mu}_{op}|{}^1\Psi(A)\rangle$. In other words, the emissive transition probability (k_f) will depend on C_2^2 and is therefore expected to decrease at high solvent polarities. An additional solvent effect leading to the same trend was postulated in relation to the matrix element $\langle\Psi(AD)|\boldsymbol{\mu}_{op}|\Psi(A^-D^+)\rangle$ which also contributes to the exciplex emissive probability. As previously discussed, solvation may affect the intermolecular distance within the exciplex and thus

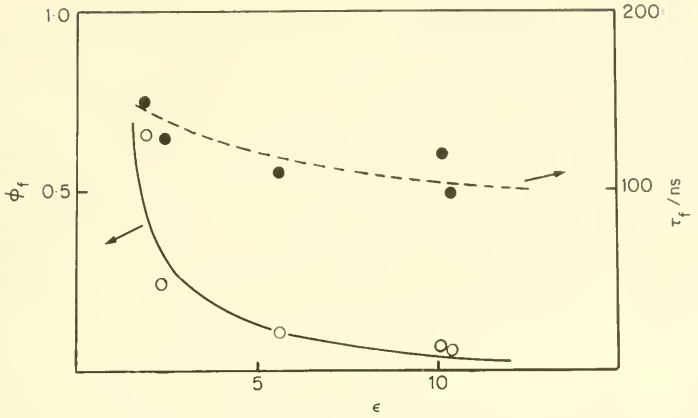

FIG. 12. Effect of solvent polarity (static dielectric constant ϵ') on the fluorescence yield (ϕ_f) and the fluorescence liftime (τ_f) of the pyrene–DMA heteroexcimer. [See N. Mataga, T. Okada and N. Yamamoto, *Chem. Phys. Lett.*, **1**, 119 (1967).]

the above matrix element which is sensitive to this parameter. On the other hand, since the energy gap between the relevant states is reduced, and since the rate of ionic dissociation (k_i) is enhanced by polarity, the decay paths represented by $k_d = k_i + k_r$ (where k_r is the rate constant for the radiationless transition to the ground state) will increase in solvents with high dielectric constants. Thus, Mataga and his coworkers assumed a solvent-independent value $\phi_f^0 = 1$, attributing the drop in ϕ_f/τ_f to such changes in k_f and k_d.[118] According to this model, ionic dissociation takes place exclusively from the thermalized exciplex in competition with fluorescence and radiationless deactivation.

Weller and coworkers[142] explained the polarity dependence of ϕ_f/τ_f by invoking solvent effects, not only on k_i but also on ϕ_f^0, due to competition between ion-pair and fluorescent exciplex formation in the encounter complex $^1A^* \cdots D$. They formulated the scheme (50)

$$\begin{array}{l} {}^1A^* + D \rightarrow {}^1A^* \cdots D \overset{k_c}{\nearrow} {}^1(A^-D^+)^* \xrightarrow{k_d + k_f} A + D \\ \qquad\qquad\qquad\qquad\qquad\quad \Big\downarrow k_i \\ \qquad\qquad\qquad\qquad\quad \underset{k_i'}{\searrow} ({}^2A_S^- \cdots {}^2D_S^+) \xrightarrow{k_s} {}^2A_S^- + {}^2D_S^+ \end{array} \qquad (50)$$

according to which the exciplex yield $\phi_f^0 = k_c/(k_c + k_i')$ decreases at high polarities owing to an increase in the ratio k_i'/k_c, thus leading to a solvent dependence of the parameter ϕ_f/τ_f. According to this model the ionic dissociation products are formed in two competitive routes, one via, and the other circumventing, the thermalized fluorescent exciplex.

Based on the above scheme, and assuming that k_d and k_f are solvent independent, experimental data were used to calculate the ratio k_i'/k_c as a function of the solvent polarity.[122, 142a] The observed increase in this ratio with increasing polarity was rationalized in terms of the influence of solvent polarity on the free energies of the excited complex (ΔG_c) and the solvent-shared ion-pair (ΔG_i) which were theoretically estimated using the previously discussed solvent-continuum models. At low ϵ' values, where $\Delta G_i > \Delta G_c$, $k_c > k_i'$, the situation being reversed at high polarities. This simplified approach does not take into account solvent effects on k_f as well as possible solvent effects on intersystem crossing rates in the exciplex (see below), both of which may affect k_d leading to erroneous estimates of k_i'/k_c.

At present it is difficult to account quantitatively for the solvent effects on ϕ_f and τ_f in terms of either or both of the above approaches. Theoretical considerations indicate that, though the observed dependence of the radiative transition probability (evaluated from the ratio ϕ_f/τ_f) on the solvent polarity shows the same trend as that calculated on the basis of Mataga's approach. i.e. solvent effects on C_2^2 and on $\langle \Psi(AD)|\mu_{op}|\Psi(A^-D^+)\rangle$, there still exists a large discrepancy between the two curves.[117] On the other hand, the previously reported[139] solvent effects on the absorption of the pyrene–DEA exciplex accompanying the solvent-induced drop in ϕ_f and τ_f may be indicative of a marked change in the exciplex electronic structure, i.e. on the magnitude of e.g. C_2^2. It is thus likely that a polarity-induced drop in k_f contributes significantly to the decrease in ϕ_f/τ_f as suggested by Mataga and coworkers.

In spite of the difficulties associated with obtaining an unambiguous confirmation of the above scheme on the basis of solvent effects on the parameter ϕ_f/τ_f, direct experimental evidence in its favour has been provided by the laser photoconductivity studies of Mataga and coworkers.[143] Working with pyrene or anthracene quenched by DMA in pyridine ($\phi = 12{\cdot}3$), they observed that most of the photocurrent is present immediately after the laser pulse, in agreement with the direct generation of $(^2A_S^- \cdots {}^2D_S^+)$ from $^1A^* \cdots D$. However, a small fraction grows in slowly at a rate matching the decay of the exciplex fluorescence, thus confirming the thermal dissociation of $^1(A^-D^+)^*$ to the ion pair. Evidence in favour of two such paths has been obtained from the study of temperature effects on the yields of radical ions in the above system.[144]

It is worthwhile mentioning at this point that in polar solvents it is still impossible to discriminate experimentally, by absorption spectroscopy, between four physically distinguishable polar species present in intermolecular CT systems, i.e. between the fluorescent exciplex $^1(A^-D^+)^*$, the solvent-shared ion-pair $(^2A_S^- \cdots {}^2D_S^+)$, the separated ions still correlated geometrically in a diffusive photochemical cage $\{^2A_S^- \cdots {}^2D_S^+\}$ (see discussion

below), and the separated ions $^2A_S^-$ and $^2D_S^+$, homogeneously distributed in the bulk of the solution. Thus, fast transient absorbance changes, exhibiting spectra identical to those of $^2A_S^-$ and $^2D_S^+$ observed in viscous and low-temperature alcoholic solutions, were initially attributed to geminate recombination within the photochemical cage $\{^2A_S^- \cdots {}^2D_S^+\}$.[145] It was suggested later,[139] on the basis of selective O_2 quenching experiments, that such fast decay processes should actually be attributed to the fluorescent exciplex $^1(A^-D^+)^*$, exhibiting the same absorption as that of the superimposed ions (see Section III.C.2). The ionic recombination reactions in the above species will be discussed in some detail below, in relation to intersystem crossing phenomena in exciplexes.

In a non-polar solvent such as *n*-hexane ($\epsilon' = 1{\cdot}89$), the free energy of a characteristic dissociated ion-radical state, such as ($pyrene_S^- \cdots DMA_S^+$), is of the order of 5 eV.[143] Since this value is well above the energy of most of the ultraviolet laser or continuous sources employed ($\lambda_{exc.} \geqslant 300$ nm), no monophotonic ionization processes are possible in this energy range. However, it has been shown that the consecutive absorption of two quanta, via:

$$D \xrightarrow{h\nu_1} {}^1D^* \xrightarrow{A} {}^1(D^+A^-)^* \xrightarrow{h\nu_2} D_S^+ + A_S^-$$

accounts for the photoconductivity of exciplex systems such as TMPD–naphthalene and TMPD–biphenyl.[146]

2. Excited EDA Complexes

The ionic photodissociation of excited EDA complexes has been mainly investigated by applying pulsed laser excitation with optical (absorption) or electrical (conductivity) detection in the nanosecond range. The attention of most groups has centred on the electronic nature of the dissociating excited state (e.g. triplet versus singlet mechanisms) as well as on the degree of complex and solvent relaxation (e.g. Franck–Condon versus thermalized states). Other aspects have been the dissociation of primarily formed ion-pairs and the geminate recombination of radicals within the so-called "solvent cage". The discussion of the latter topic will be postponed to Section IV.B which deals with triplet generation paths.

The first direct observation of the dissociation dynamics of an excited EDA complex was carried out using flash photolysis for the pyromellitic dianhydride(PMDA)–mesitylene systems in a mixed ether–isopentane solvent at 152 K.[147] Excitation in the CT band of the complex generates a CT triplet state whose decay, followed via its phosphorescence intensity, matched the growing-in of the ions absorbance. Thus, in this case the triplet undergoes a spontaneous thermal ionic dissociation process:

$$(DA) \xrightarrow{h\nu} {}^1(D^+A^-)^* \xrightarrow{ISC} {}^3(D^+A^-)^* \rightarrow D^+ + A^-$$

Similar observations, proving that photo-induced ionization occurs via a triplet state of the complex, were carried out by Achiba and Kimura in the cases of the PMDA–dioxan, PMDA–ether and PMDA–tetrahydrofuran CT complexes.[148] On the other hand, PMDA complexes in acetonitrile photodissociate via the CT singlet state.[140, 149] A triplet mechanism also prevails for the tetracyanoethylene–ether (or acetonitrile) complexes.[148b, c] Ionic photodissociation phenomena in EDA complexes have also been investigated in relation to ionic polymerization mechanisms.[150, 151] From data on the photopolymerization of the TCNB(or PMDA)–α-methylstyrene complex induced by CT band excitation, Irie *et al.*[150] presented evidence in favour of a CT triplet intermediate. However, a contribution of direct dissociation from the CT singlet state was also reported in this system.[150] Another example of a mixed singlet–triplet mechanism is associated with the PMDA–naphthalene derivative complexes,[152] where the triplet dissociation rate was found sensitive to the solvent polarity. A biphotonic dissociation mechanism, similar to the one suggested for singlet heteroexcimers,[146] has been reported for a variety of acceptors (TCNB, PMDA, TCPA)–ether complexes in rigid glasses at 77 K.[153] The formation of stable radical-ions even in rigid media, where diffusional separation is essentially impossible, was rationalized in terms of an irreversible reaction of the D^+ counter-ion with a neighbouring solvent molecule. Similar observations were reported by Irie *et al.*[154] for PMDA–benzene derivative complexes in rigid glasses at 77 K. The data are interpreted in terms of the formation of ion-pairs, exhibiting internal electrostatic interactions, which are stable to diffusive recombination annihilation.

Several factors have been pointed out as controlling the degree of ionization from either triplet or singlet states (e.g. solvent polarity, degree of CT character, excited-state lifetime). However, no clear general prediction or classification can yet be made concerning the applicability of either mechanism to specific systems.

3. Role of Solvation Relaxation

Mataga and coworkers have devoted considerable attention to the discrimination between photodissociation from fully thermalized exciplex states, and paths involving systems that are non-relaxed with respect to intrinsic and solvent parameters. Information relevant to this problem was derived for singlet states by means of nanosecond laser excitation accompanied by measurements of both transient absorption spectra and transient photocurrents. We previously reported the cases of pyrene and anthracene DMA systems in pyridine where the rise time of the photocurrent, due to the free dissociated ions, could be accounted for by a slow dissociation process from the relaxed exciplex state $^1(A^- D^+)$ while a fast component was indica-

tive of direct ionization from the encounter complex $^1A^* \cdots D$. The latter mechanism is supposed to involve a short-lived exciplex $^1(A^- \cdots D^+)$, non-relaxed mainly with respect to solvation, in which competition takes place between solvent (and intrinsic) geometrical relaxation to $^1(A^-D^+)^*$ and ionic dissociation to the solvent-shared, or geminate, ion-pair $(A_S^- \cdots D_S^+)$.

A similar fast rise in the photocurrent was observed in the TCNB–benzene complex, where a CT state is created by the very act of light absorption. Investigations of this system in 1,2-dichloroethane as solvent have shown that the rise curve of the photocurrent does not follow the equation $\int_0^t p(t')\{1 - \exp[-(t' - t)/\tau]\}\, dt'$, but can be reproduced by $\int_0^t p(t')\, dt'$, where $p(t')$ and τ represent respectively the shape of the (~ 15 ns) exciting laser pulse and the lifetime of the CT fluorescent state.[148] On the basis of this observation it was concluded that relaxation to the fluorescent state (as directly observable by time-resolved fluorescence studies[65b]) and ionic dissociation are competitive processes within the non-relaxed FC state. It should be recalled (cf. Section III.B.1) that, in the TCNB–benzene two-component system, relaxation not only involves the orientational motion of the surrounding solvent, but also the generation of a 1:2 exciplex, $(A^-D_2^+)^*$.[12] Since a 1:2 exciplex may also be formed in 1,2-dichloroethane as solvent, the ionic dissociating state might well be the (relaxed) excited singlet state of the 1:1 complex, whose lifetime is considerably shorter than that of the fluorescing 1:1 exciplex.

The suggested efficient (picosecond) ionic dissociation in non-relaxed states, versus the inefficient (slower than $\sim 10^{-7}$ s) reaction in the thermalized exciplexes, is still unaccounted for in terms of a detailed physical model. It appears that the effect cannot be explained by a higher CT character in the Franck–Condon state (see the relevant discussion in Section III.A). It is possible that excess of thermal energy may still be available in the solvated fluorescent state which will lead to separation before deactivation to the potential minimum in the $^1(A^-D^+)^*$ exciplex. Thus, solvation, thermal deactivation, and ionic separation may constitute a highly complex scheme of events which follow the initial electron-transfer step. In view of the previously reported biphotonic ionization phenomena, detailed (light intensity) effects should be studied in all EDA excitation experiments in order to rule out a biphotonic mechanism with the relaxed fluorescent state as the photoactive intermediate.

The role of solvent relaxation in the process of ionic dissociation has also been discussed in relation to triplet complexes. Of special interest is the extensively investigated triplet benzophenone quenched by amines.[79, 93] Cohen *et al.*[155] and Davidson and coworkers[156] suggested that the photoreduction of the benzophenone triplet $^3(BP)^*$ by amines (AH) proceeds via CT complex formation followed by proton transfer. The BP^- and AH^+

species have subsequently been observed by laser photolysis, confirming the competition between ionic dissociation and hydrogen abstraction in the ^{3}(BP)*–DEA system[80a] Arimitsu *et al.* investigated the quenching reaction by pulsed laser photolysis for different amines in a variety of solvents.[80a] They confirmed that ionic dissociation takes place only when the final ionic state is lower in energy than the triplet BP state. However, the quantum yield for the ion production is determined by the balance between dissociation and proton (or H atom) transfer. For AH = DEA and DMT = (*N*,*N*-dimethyl-*p*-toluidine), they suggest the scheme:

$$^3(\mathrm{BP})^* + \mathrm{AH} \rightarrow (^3(\mathrm{BP})^* \cdots \mathrm{AH}) \xrightarrow{(a)} {}^3(\mathrm{BP}^- \cdots \mathrm{AH}^+)^{\#} \quad \begin{matrix} \xrightarrow{(b)} \mathrm{BP}_S^- + \mathrm{AH}_S^+ \\ \xrightarrow{(c)} \mathrm{BPH}^{\cdot} + \mathrm{A}^{\cdot} \end{matrix} \qquad (51)$$

$^3(\mathrm{BP}^- \cdots \mathrm{AH}^+)^{\#}$ is an encounter collisional complex of high CT character which is non-relaxed with respect to solvent orientation. In this primary species, solvation and separation to the free BP_S^- and AH_S^+ ions (b) competes with proton transfer yielding the ketyl and benzophenone radicals (c). In other systems (involving e.g. triethylamine, aniline, *p*-toluidine as donors) direct hydrogen-atom transfer (d) competing with the generation (a), rather than with the decay (b) of $^3(\mathrm{BP}^- \cdots \mathrm{AH}^+)$, has been suggested[157] as a likely alternative path leading to the neutral radicals.[80]

Masuhara *et al.*[144] presented an analysis of the dependence of the yield (ϕ) of the ions formed (via the fast mechanism, see above) in the TCNB–toluene and pyrene–DMA systems on the solvent polarity. They obtained agreement with the expression:

$$\log(1/\phi) = p/\epsilon' + q \qquad (52)$$

where ϵ' is the static dielectric constant of the solvent, and p and q are constants. This behaviour was found to be derivable from Onsager's ion recombination model extended by Mozumder[158] which is based on the expression:

$$\phi = \alpha \exp(r_c/r_0)$$

with

$$r_c = e^2/\epsilon' kT \text{ (Onsager's length).} \qquad (53)$$

The model assumes that a fraction α (independent of the solvent polarity) in the dissociative state is converted into a geminate ion-pair with an initial separation r_0. Such pairs undergo further diffusional separation which, in

competition with geminate (cage) recombination, will lead to the final fraction of free ions. Another theoretical approach, which yields agreement with the experiments, is based on the application of the Horiuchi–Polanyi relation[159] ($\Delta E = \alpha \Delta F_{ion}$, $0 < \alpha < 1$) between the activation energy ΔE of the unimolecular ionic dissociation rate constant, and the free energy difference ΔF between the initial (excited CT singlet state, non-relaxed with respect to solvation) and final (separated solvated ions) states. Such agreements are in keeping with the assumption that the ions produced originate in a non-relaxed dissociative CT state possessing an excess energy that determines the initial separation r_0 from which thermal diffusion initiates. On the other hand, the experimental values of the fast component of the photocurrent were clearly inconsistent with Eigen's expression[160] for the rate of dissociation of an ion pair with an initial separation a:

$$k_{diss} = \frac{4\pi(D_A^- + D_D^+)e^2}{\epsilon' kT\Delta V} \frac{1}{\exp(e^2/\epsilon' kTa) - 1}. \tag{54}$$

The expression, in which D_A^- and D_D^+ are the corresponding diffusion coefficients, e is the electronic charge and $\Delta V = 4\pi Na^2/3$ is the volume of the dissociative exciplex, is based on the theory of reaction rates.[161] The latter is derived from phenomenological laws of macroscopic processes in which the ion-pair association and dissociation are determined by Fick's law (including electrostatic interactions) and which obviously cannot account for the postulated initial non-thermalized state. The above conclusions were derived from experiments on a single system (e.g. pyrene–DMA) in a series of solvents. When a set of different EDA complexes were submitted to pulsed photoconductivity measurements in the same solvent, the yield of free ions (ϕ) exhibited a specific dependence on the particular system, with no general correlation between ϕ and the free-energy change of the ionic photodissociation process.[162] The phenomena were attributed to reactions in the non-relaxed CT state $^1(A^- \cdots D^+)^\#$ (e.g. deactivation to the ground state and ISC), depending on specific chemical properties of the donor and acceptor moieties.

Very recently, the absolute values of the ionic photodissociation yields of the above systems were re-examined mainly in acetonitrile solutions.[163] Previous values for some systems, especially for TCNB–toluene, were found to be too low. Similar results were reported for TCNB–benzene systems.[164] Nevertheless, the dependence of the yield on the solvent polarity can be well expressed by (52) based on Onsager's ion recombination model for all systems examined.

The question arises as to the feasibility of directly observing the dynamics of the ionic separation or recombination processes, either in the ion pair or in the "cage" correlated state. In the latter, the interionic distance in the

pair is relatively high (up to 50–100 Å), so electrostatic interactions are negligible. However, the ions are still geometrically correlated and may undergo geminate recombination due to an almost random diffusional motion.[158] An initial fast absorbance decay for pyrene quenched by DEA in low-temperature viscous polar media was initially attributed[145] to a cage recombination of the ions. Subsequently, from an oxygen quenching analysis, the fast decaying component was identified as due to the fluorescent exciplex state exhibiting an absorption spectrum identical to that of the ions.[139] It appears, however, that in propan-2-ol below -60 C the ionic absorbance cannot be solely accounted for by the free dissociated ions ($A_S^- + D_S^+$) or the fluorescent exciplex $^1(D^+A^-)^*$. There exists a third, fast absorbance decay arising from a non-fluorescent species whose spectrum is identical, within the limits of experimental accuracy, to that of the free ions or the exciplex.[100] The species responsible for this decay was identified as a geminate pair. However, since under the prevailing experimental conditions the ion-pair lifetime as estimated using Eigen's equation, as well as the lifetime of a geminate pair in a photochemical cage, were both of the same order of magnitude (that of the observed decay), a clear assignment of the pair was not made. It is probable that both physical phenomena, ion-pair and cage recombination, contribute to this ionic decay.

A photocurrent rise in the nanosecond range, attributed to the dissociation of the solvated ion-pair into the free ions, was reported by Hino *et al.* in the case of the pyrene–*p*-dicyanobenzene EDA complex.[165] In a solvent such as dichloromethane the photocurrent rises exponentially with rate constant $1{\cdot}3 \times 10^7\ s^{-1}$ which is lower than the reciprocal lifetime of the (instantaneously formed) fluorescent exciplex state ($1/\tau_f \approx 3{\cdot}5 \times 10^7\ s^{-1}$). The discrepancy between the two numbers, which is even higher in solvents such as dichloroethane or pyridine, led to the assignment of the photocurrent rise to the dissociation of a solvated ion-pair. The observed rise time rate constants were compared to those calculated using Eigen's equation, assuming an encounter distance of $a = 7$ Å. The calculated k_{diss} and experimental (k_c) values agreed within a factor of $\sim 2{\cdot}5$. On this basis [neglecting the contribution of the ion-pair recombination rate (k_r) to the ion-pair lifetime, which is equal to $(k_r + k_{diss})^{-1}$] it was concluded that in this system the diffusional separation process starts from a classical solvated ion-pair. The situation is thus different from that prevailing in the pyrene–DMA system where diffusional motion, in e.g. dichloromethane, was estimated to start at $r_0 = 24{\cdot}7$ Å.[144] To summarize, in spite of the complexity of the effects observed in a variety of systems, it appears that pulsed photolysis in exciplex systems provides a powerful tool for the direct experimental observation of geminate reactions of ion pairs and caged ions, as well as for the corresponding tests of the related theoretical treatments.

B. Intersystem Crossing (ISC)

The triplet states generated from CT excitation of EDA complexes have been extensively investigated via their phosphorescence emission. The subject has been thoroughly reviewed by Nagakura,[15] along with the corresponding theoretical calculations (including spin alignment phenomena) esr spectra, and T → T absorption. The accumulated information has led to a comprehensive, self-consistent picture, especially in relation to the excited state wavefunction; the degree of CT character, ranging in a series of complexes from purely locally excited triplets to highly polar structures, can be estimated by means of the phosphorescence spectra and the zero-field splitting constant parameter ($D^* = [3/4(h\nu)^2 - 3g\beta B_{min})^2]^{1/2}$), as well as by the T → T absorption spectra. The latter have provided valuable information in relation to the CT character of higher triplet states of TCNB complexes.

Another problem which has attracted considerable attention but which is still poorly understood concerns the ISC mechanism, both from the complexes S_1 (CT) state to T_1, as well as from T_1 to S_0. It has long been recognized that ISC to the triplet state is enhanced by CT interactions in the fluorescent complex.[90] A correlation has also been obtained between the CT character (as determined by the D* values) with both radiative and non-radiative decay constants ($T_1 \rightarrow S_0$) of TCNB complexes in the triplet state.[15, 166] It should be pointed out, however, that the exact scheme responsible for the enhancement of spin–orbit coupling in EDA complexes[90, 167] is still unclear. Since the problem has been recently discussed[168] it will not be considered in the present review. In the following sections we shall focus our attention mostly on ISC mechanisms in heteroexcimers, a problem that has aroused much controversy in the past. For the sake of clarity the discussion will be separated, dealing first with exciplexes in non-polar solvents and subsequently in relatively polar solutions.

1. Exciplexes in Non-polar Solutions

As early as 1963 Leonhardt and Weller reported the production of triplet states following the CT fluorescence quenching (of perylene by DMA) in methylcyclohexane.[8] It was subsequently shown by laser photolysis that the process is a general one and quite efficient for a whole series of heteroexcimers.[16] The ISC mechanism responsible for triplet production in heteroexcimers was investigated by following the change in absorbance following a short (~ 10 ns) laser pulse.[169–171, 145] In a few cases in hexane or toluene [^{1}(TMPD)* + naphthalene; ^{1}(anthracene)* + DMA; ^{1}(TMPD)* + biphenyl] a growing-in at the wavelength of the corresponding characteristic triplet absorption was observed, establishing the occurrence of the process:

$$^1A^* + D \,(\text{or } ^1D^* + A) \rightarrow {}^1(A^-D^+)^* \xrightarrow{ISC} {}^3A^* + D. \qquad (55)$$

It is thus evident that the above ISC process in exciplexes takes place "classically', i.e. via a mechanism governed by spin–orbit interactions which competes with other radiative and non-radiative decay modes of the thermalized fluorescent state $^1(A^-D^+)^*$.

In other systems [e.g. ^{1}(anthracene)* + DEA; ^{1}(pyrene)* + DEA; ^{1}(pyrene)* + DMA; ^{1}DEA* + biphenyl; ^{1}DEA* + naphthalene, all in methylcyclohexane or toluene] which are also characterized by high $^3A^*$ yields, experiments using nanosecond excitation revealed only a very weak or a negligible absorbance growing-in attributed to a triplet generation process via reaction (55).[145, 170] To account for the initial absorbance present ~15 ns after the pulse, it was suggested[16, 145, 170] that, in addition to the "slow" ISC via reaction (55), a "fast" process, preceding the generation of the relaxed exciplex, should take place. The same explanation (favoured over that assuming an accidental similarity between the spectra of the triplet and the exciplex[171]) was also invoked to account for ISC in excited TCNB–EDA complexes at low temperatures.[172a] Such conclusions have been questioned by Nishimura *et al.*[172b] who applied picosecond excitation methods to the anthracene–DEA and pyrene–DEA systems. A detailed analysis of the results indicated that practically all the anthracene and pyrene triplets evolve via process (55), matching the exciplex fluorescence decay. It therefore appears that at present no definite general conclusions, for all the above systems, can be drawn with respect to the occurence of fast ISC from non-relaxed CT states.

Systems bearing on the problem of "fast" ISC mechanisms are those involving primary or secondary amine donors as quenchers of the fluorescence of an aromatic acceptor. It is well known that in such cases (e.g. with D = aniline, *N*-methylaniline and naphthylamines) a fluorescence corresponding to that characterizing the corresponding tertiary amine exciplexes (with D = DMA, DEA etc.) is almost negligible.[9, 30] Instead, initially so the previously discussed triplet benzophenone system, the quenching of the aromatic donor fluorescence in polar and non-polar solvents has been shown to be accompanied by the generation of the neutral radicals ȦH and Ḋ′ (using the notation D = D′H).[20a, 77, 173] As previously suggested by Yang and coworkers,[174] the mechanism appears to be one in which the primary generation of a CT exciplex is followed by a rapid proton transfer and then by separation to the neutral radicals:[77, 173, 140a]

$$^1A^* + (D'H) \rightarrow {}^1(A^-(D'H)^+)^* \rightarrow {}^1(AH{-}D')^* \rightarrow \dot{A}H + \dot{D}'.$$

Relevant to the question of ISC is the observation that the fluorescence quenching in two of the above systems (pyrene–aniline[77] and pyrene–*p*-toluidine[173]) in n-hexane or acetonitrile, is associated with a high yield

for formation of the pyrene triplet state $^3A^*$. In view of their presence at the end of the ~10 ns laser pulse,[77,173] such triplets cannot originate from any homogeneous radical recombination reaction. Moreover, in both n-hexane systems, $^3A^*$ yields comparable to those observed for pyrene–DEA have been reported.[77,175] Such a fact would be essentially inconsistent with the "slow" ISC path, since (for e.g. pyrene–*p*-toluidine in n-hexane) both exciplex yield and lifetime are smaller by a factor of ~100 relative to those of the pyrene–DEA (n-hexane) system.[173] ISC according to (55) would thus imply an ISC rate in $^1(A^-(D'H)^+)^*$ that is higher by the same factor relative to that characterizing the $^1(A^-DEA^+)^*$ exciplex. Since this is highly improbable, it is again necessary to invoke "fast" ISC phenomena, either from non-relaxed exciplex states (as discussed above) or via geminate radical recombination reaction as discussed below for polar solvents.

An additional triplet generation path, which is quite efficient in various non-polar systems, is associated with the quenching of exciplex fluorescence by molecular oxygen.[170] Two main processes are involved with the essentially diffusion-controlled O_2 quenching process:

$$\text{I. } {}^1(D^+A^-)^* + O_2 \rightarrow D + A + O_2$$

$$\text{II. } {}^1(D^+A^-)^* + O_2 \rightarrow {}^3A^* + D + O_2 \,(\text{or: } {}^3D^* + A + O_2)$$

Process I predominates in systems such as TMPD–biphenyl and TMPD–anthracene, while ISC via II predominates in the anthracene–DEA (or DMA) and pyrene–DMA systems. In other cases the two reactions may have comparable efficiencies. The detailed mechanisms of the two reactions are not well understood. Phenomenologically, II is similar to the well-known general case of fluorescence quenching by molecular oxygen, which is known to be associated with triplet-formation. In the exciplex case, short-lived non-fluorescent intermediates such as $^1(M^+O^-_2)^*$ or $^1(A{\cdot}D{\cdot}O_2)^*$ have been suggested in order to account for the oxygen quenching phenomena.[170]

2. Exciplexes in Polar Solutions

The CT quenching of fluorescence in polar solvents, in relation to which ionic dissociation phenomena were previously discussed, was also observed to be associated with the production of triplet states (either $^3D^*$ or $^3A^*$).[8,176,177] On the basis of the corresponding reaction observed in chemiluminescent systems (see above), and since triplet states are observed only when the triplet energy is below that of the (paired or dissociated) ions,[178,179] it was concluded[179] that the recombination reaction:

$$A^-_S + D^+_S \rightarrow {}^3A^* + D \,(\text{or } {}^3D^* + A) \qquad (56)$$

quantitatively accounts for the observed triplets. (The early suggestion,[178] that the recombination leading to the triplet state occurs within the solvent-shared ion-pair, was subsequently rejected[179] in favour of the above homogeneous reaction.) A direct observation of the latter process was first reported by Orbach, Potashnik and Ottolenghi[180] who followed, by laser photolysis, the decay of the ions and the simultaneous growing-in of the pyrene triplet state in the pyrene–DEA (methanol or acetonitrile) system. In keeping with the suggested scheme, it was also found[180] that the generation of the pyrene triplet could be inhibited by scavenging the $^2(\text{pyrene})_S^-$ ion with TCNB, a process leading to $(\text{TCNB})_S^-$, which subsequently regenerates the original ground-state system, via:

$$^2(\text{TCNB})_S^- + {}^2(\text{DEA})_S^+ \rightarrow \text{TCNB} + \text{DEA}.$$

The uniqueness of reaction (56), as the only source of triplet states following CT fluorescence quenching in polar solutions, was first questioned by Goldschmidt, Potashnik and Ottolenghi[169] who pointed out that considerable triplet absorption was present at the end of a short laser pulse, when no substantial contribution from homogeneous bimolecular recombination processes could be expected. This conclusion was subsequently rejected by Schomburg, Staerk and Weller[181] who confirmed the occurrence of reaction (56), establishing its second-order character, but failed to observe any initial triplet contribution other than that attributable to such homogeneous ("slow") ionic annihilation. However, in variance with this objection, the existence of a "fast" ISC path in polar solvents was subsequently re-confirmed by a detailed analysis[145] of the initial absorbance changes following pulsed excitation for a variety of exciplex systems in polar solutions. The problems encountered are similar to those described above in the case of non-polar solvents. However, instead of separating the time-dependent contributions of $^3A^*$ and $^1(A^-D^+)^*$, one faces the problem of separating the absorbance of $^3A^*$ (or $^3D^*$) from that of the radical ions $^2D_S^+$ and $^3A_S^-$. In contrast to non-polar solutions, where no quantitative independent information on the exciplex absorption spectrum is available, the spectra of $^2D_S^+$ and $^2A_S^-$ are available from a variety of sources. By appropriate subtraction for the spectra of the ions, it was shown that triplet states, other than those generated via reaction (56), are present at the end of the exciting laser pulse for a variety of systems (e.g. pyrene–DEA in acetonitrile or methanol, anthracene–DEA in acetonitrile, naphthalene–DEA in acetonitrile).[145,170] Moreover, $^3A^*$ was observed by means of picosecond laser photolysis in the time scale of 600 ps to 5 ns for the anthracene–DEA–acetonitrile system.[20b]

The establishment of the above "fast" or "prompt" triplet generation path in highly polar solvents such as methanol or acetonitrile raised questions

as to the detailed mechanism accounting for such processes. Initially it was suggested[169, 170, 180] that ISC was occurring from exciplex states which are non-relaxed with respect to vibrational energy and solvent structure. However, extension of the quenching experiments to low temperature and viscous solvents has led to a different approach, according to which two alternative mechanisms were suggested:[145, 139]

(a) ISC in a short-lived, but completely relaxed, exciplex proceeds via a reaction that is essentially identical to that (55) suggested for exciplexes in non-polar solvents (see above).

(b) In polar solution geminate radical ion-pairs will be produced (either classical closely interacting pairs, or caged radicals correlated by their random diffusive motion). Such pairs, formed in an initially singlet configuration, may undergo a transition to an overall triplet configuration, followed by recombination leading to $^3A^*$ or $^3D^*$:

$$A + D \xrightarrow{h\nu} {}^1A^* + D \rightarrow \{{}^2A_S^-(\uparrow)\cdots{}^2D^+(\downarrow)\} \rightarrow \{{}^2A_S^-(\uparrow)\cdots{}^2D^+(\uparrow)\} \rightarrow {}^3A^* + D$$

Although originally unfavoured in polar solvents,[145] mechanism (a) was later shown[139] to be the main contributor to the "fast" triplet generation in a system such as pyrene–DEA, even in a relatively polar medium such as amyl alcohol (pentan-1-ol) ($\epsilon' = 13{\cdot}9$) or propan-2-ol ($\epsilon' = 18{\cdot}3$). Thus, the ^{3}pyrene* growing-in process was actually observed to match the ^{1}(pyrene–DEA^+)* exciplex decay (Fig. 13). (The latter was originally misinterpreted

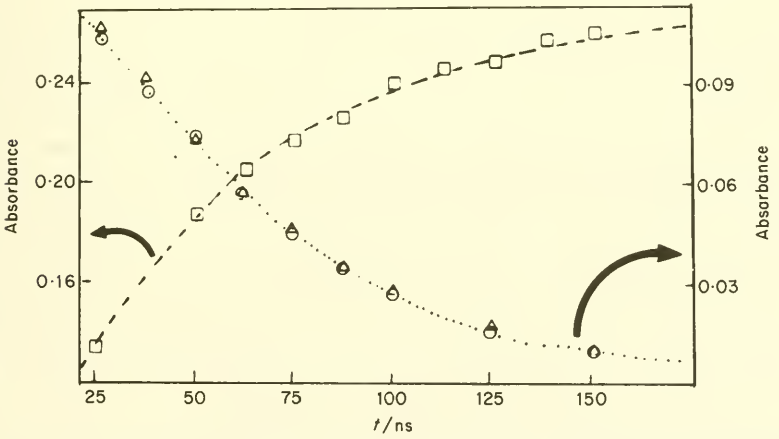

FIG. 13. Decay of the ^{1}(pyrene $^-DEA^+$)* exciplex fluorescence (△, arb. units) or absorbance (○) and the matching growing-in of the ^{3}pyrene* absorbance (□), as observed in isopropanol using pulsed laser excitation. [Reproduced with permission from N. Orbach and M. Ottolenghi, *Chem. Phys. Lett.*, **35**, 175 (1975).]

as the decay of the pyrene$_S^-$ $\cdots$ DEA$_S^+$ geminate pair.[145]) The question arose, however, as to the mechanism of the "fast" triplet generation in highly polar solvents such as methanol ($\epsilon' = 32$) or acetonitrile ($\epsilon' = 37$). In these solvents the exciplex fluorescence intensity (both yield and lifetime) is reduced by a factor of more than 30 relative to propan-2-ol, but the prompt triplet yield remains essentially unchanged.[139] Although mechanism (a) seemed unlikely to account for such observations (an unreasonable increase, by a factor of about 100, in the rate of ISC in the thermalized exciplex in methanol or acetonitrile, relative to propan-2-ol, would have been implied), a discrimination between paths (a) and (b) in highly polar solvents was impossible on the basis of the originally available data.

Closer examinations of the details of mechanism (b) have subsequently shown that it does play an important role in the generation of triplet states in highly polar exciplex systems. The treatment is based essentially on the approach of Brocklehurst in relation to the problem of spin correlation in the geminate recombination of radiolytically produced radical ions in hydrocarbons.[182] The loss of spin correlation in geminate radical ion-pairs was originally considered (both in the present exciplex system[145] and in the radiolysis experiments[183]) in terms of spin-relaxation times (T_1 and T_2 in the terminology of esr). It was, however, recognized that T_1 (of the order of microseconds) and T_2 are too slow to account for the observed fast (nanosecond) triplet generation process. As first pointed out by Kaptein[184] and Adrian[185] in relation to the radical-pair model[186] for CIDNP (chemically induced nuclear-spin polarization) and CIDEP (chemically induced electron-spin polarization), much faster changes in spin correlation may take place (in the nanosecond range) due to a coherent process resulting from the isotropic hyperfine interaction with hydrogen nuclei. The hyperfine coupling induces transitions between the degenerate S_0 and T_0, T_1, T_{-1} spin states of the radical pair. An external magnetic field effect is expected, due to lifting of the degeneracy between S_0 and $T_{\pm 1}$. On the basis of the radical-pair CIDNP model, Brocklehurst has presented a theory describing the rate at which triplet pairs are produced (or the time-dependent probability of recovering the singlet) from an initially produced singlet system.[182] The theory confirms the short time-scale (10^{-9}–10^{-8} s) of the above events and predicts: (a) a reduction of the triplet yield upon deuteration of A and D; (b) an enhancement of the singlet yield and a reduction of the triplet yield by an external magnetic field; (c) that partly deuterated compounds should show an oscillatory triplet/singlet time-dependent ratio.

The existence of the expected magnetic field effect for radical pairs in hydrocarbons has been confirmed by pulse radiolysis experiments.[187] As to exciplex systems, substantial deuteration effects have been observed on

the fast triplet yields for ^{1}pyrene* quenched by DEA in highly polar solvents.[100] In acetonitrile and methanol the yields obtained with deuterated pyrene ($C_{16}D_{10}$) were lower by 15 per cent and 20 per cent respectively, relative to those measured for $C_{16}H_{10}$. No deuteration effects were observed in propan-2-ol where the pyrene triplet is generated via reaction (a).

Since no deuteration effects (or completely different ones) are expected on the spin relaxation parameter T_1 (and T_2), the results clearly support triplet generation via scheme (b) with the isotropic hyperfine interaction mechanism. This conclusion is in keeping with the study of Michel-Beyerle and coworkers[188] and Schulten *et al.*[189] who reported external magnetic field effects on the yield of fast triplet generation following the quenching of pyrene fluorescence by DEA,[188] as well as by 3,5-dimethoxy-*N*,*N*-dimethylaniline, in methanol.[189] The experimental data agreed with a theoretical model for the hyperfine coupling interactions[189] as outlined above. Thus, at variance with the original findings of Schomburg *et al.*,[181] such studies have unambiguously confirmed the existence of the fast ISC path in polar solutions as postulated by Orbach and Ottolenghi,[145] favouring the geminate radical recombination path over the early suggestion invoking highly efficient spin–orbit coupling in non-relaxed states.

Acknowledgement

The authors are grateful to Prof. E. M. Kosower for many valuable comments and discussions.

REFERENCES

1. Th. Förster and K. Kasper, *Z. Phys. Chem.* (N.F.), **1**, 19 (1954); *Ber. Bunsenges. Phys. Chem.*, **59**, 977 (1955).
2. B. Stevens and E. Hutton, *Nature*, **186**, 1045 (1960).
3. Th. Förster, *Angew. Chem. Int. Ed. Engl.*, **8**, 333 (1969); "The Exciplex" (ed. M. Gordon and W. R. Ware), Academic Press, New York (1975), p. 1.
4. J. B. Birks, "Photophysics of Aromatic Molecules", Wiley-Interscience, New York (1970).
5. N. Mataga and T. Kubota, "Molecular Interactions and Electronic Spectra", Marcel Dekker, New York (1970).
6. W. Klöpffer, "Organic Molecular Photophysics", Vol. I (ed. J. B. Birks), Wiley-Interscience, New York (1973), p. 357.
7. J. B. Birks, in "The Exciplex" (ed. M. Gordon and W. R. Ware), Academic Press, New York (1975), p. 39; *Rep. Prog. Phys.*, **38**, 903 (1975).
8. H. Leonhardt and A. Weller, *Ber. Bunsenges. Phys. Chem.*, **67**, 791 (1963).
9. N. Mataga, T. Okada and H. Oohari, *Bull. Chem. Soc. Japan*, **39**, 2563 (1966).
10. M. S. Walker, T. W. Bednar and R. Lumry, *J. Chem. Phys.*, **45**, 3455 (1966); *ibid.*, **47**, 1020 (1967).

11. H. Beens and A. Weller, *Chem. Phys. Lett.*, **2**, 140 (1968).
12. N. Tsujino, H. Masuhara and N. Mataga, *Chem. Phys. Lett.*, **21**, 301 (1973); H. Masuhara and N. Mataga, *ibid.*, **22**, 305 (1973).
13. H. Beens and A. Weller, in "Organic Molecular Photophysics", Vol. II (ed. J. B. Birks), Wiley-Interscience, New York (1975), p. 159.
14. N. Mataga and Y. Kaifu, *J. Chem. Phys.*, **36**, 2804 (1962); *Mol. Phys.*, **7**, 137 (1963); N. Mataga, Y. Kawasaki and Y. Torihashi, *Theoret. Chim. Acta*, **2**, 168 (1964); H. Beens, K. H. Grellmann, M. Gurr and A. Weller, *Discuss. Farad. Soc.*, **39**, 183 (1965); A. Matsuzaki, K. Matsuzaki, K. Yoshihara and S. Nagakura, *Bull. Chem. Soc. Japan*, **47**, 1152 (1974).
15. S. Nagakura, "Excited States", Vol. 2 (ed. E. C. Lim), Academic Press, New York, (1975), p. 321.
16. M. Ottolenghi, *Accounts Chem. Research*, **6**, 153 (1973).
17. E. A. Chandross and H. T. Thomas, *Chem. Phys. Lett.*, **6**, 393 (1971).
18. (a) T. Okada, T. Fujita, M. Kubota, S. Masaki, N. Mataga, R. Ide, Y. Sakata and S. Misumi, *Chem. Phys. Lett.*, **14**, 563 (1972). (b) R. Ide, Y. Sakata, S. Misumi, T. Okada and N. Mataga, *Chem. Commun.*, 1009, 1972.
19. M. Itoh, T. Mimura, H. Usui and T. Okamoto, *J.* Amer. Chem. Soc., **95**, 4388 (1973); M. Itoh, T. Mimura and T. Okamoto, *Bull. Chem. Soc. Japan*, **47**, 1078 (1974); T. Mimura, M. Itoh and T. Okamoto, *ibid.*, **48**, 1941 (1975).
20. (a) N. Mataga, "The Exciplex" (ed. M. Gordon and W. R. Ware), Academic Press, New York (1975), p. 113. (b) N. Mataga and N. Nakashima, *Spectroscopy Lett.* **8**, 275 (1975).
21. N. Mataga, T. Okada, H. Masuhara, N. Nakashima, Y. Sakata and S. Misumi, *J. Luminescence*, **12/13**, 159 (1976).
22. (a) T. Okada, T. Fujita and N. Mataga, *Z. Phys. Chem.* (N.F.), **101**, 57 (1976). (b) S. Masaki, T. Okada, N. Mataga, Y. Sakata and S. Misumi, *Bull. Chem. Soc. Japan*, **49**, 1277 (1976).
23. (a) E. M. Kosower, H. Dodiuk, K. Tanizawa, M. Ottolenghi and N. Orbach, *J. Amer. Chem. Soc.*, **98**, 2167 (1975). (b) H. Dodiuk and E. M. Kosower, *J. Amer. Soc.*, **99**, 859 (1977).
24. R. S. Davidson, in "Molecular Complexes", Vol. 2 (ed. R. Foster), Elek Science, London; Crane Russak, New York (1974), p. 215.
25. J. Ferguson, *J. Chem. Phys.*, **28**, (1958).
26. (a) J. N. Murrell and T. Tanaka, *Mol. Phys.*, **7**, 363 (1964). (b) T. Azumi, A. T. Armstrong and S. P. McGlynn, *J. Chem. Phys.*, **41**, 3838 (1964).
27. (a) F. Hirayama, *J. Chem. Phys.*, **42**, 3163 (1965). (b) E. A. Chandross and C. J. Dempster, *J. Amer. Chem. Soc.*, **92**, 3586 (1970). (c) K. Zachariasse and W. Kühnle, *Z. Phys. Chem.* (N.F.), **101**, 267 (1976).
28. T. Hayashi, T. Suzuki, N. Mataga, Y. Sakata and S. Misumi, *Chem. Phys. Lett.*, **38**, 599 (1976); *J. Phys. Chem.*, **81**, 420 (1977).
29. (a) N. Mataga, T. Okada and N. Yamamoto, *Bull. Chem. Soc. Japan*, **39**, 2562 (1966). (b) H. Beens, H. Knibbe and A. Weller, *J. Chem. Phys.*, **47**, 1183 (1967).
30. N. Mataga and K. Ezumi, *Bull. Chem. Soc. Japan*, **40**, 1355 (1967).
31. D. Rehm and A. Weller, *Z. Phys. Chem.* (N.F.), **69**, 183 (1970).
32. A. Weller, in "The Exciplex" (ed. M. Gordon and W. R. Ware), Academic Press, New York (1975), p. 23.
33. R. Potashnik and M. Ottolenghi, *Chem. Phys. Lett.*, **6**, 525 (1970).
34. H. Masuhara and N. Mataga, *Chem. Phys. Lett.*, **6**, 608 (1970); *Bull. Chem. Soc. Japan*, **45**, 43 (1972).

35. H. Masuhara, N. Tsujino and N. Mataga, *Bull. Chem. Soc. Japan*, **46**, 1088 (1973).
36. T. Kobayashi, S. Matsumoto and S. Nagakura, *Chem. Lett.* (Japan), 235 (1974).
37. R. Potashnik, C. R. Goldschmidt, M. Ottolenghi and A. Weller, *J. Chem. Phys.*, **55**, 5344 (1971).
38. H. Fujiwara, N. Nakashima and N. Mataga, *Chem. Phys. Lett.*, **47**, 185 (1977).
39. W. R. Ware, *Pure and Applied Chem.*, **41**, 635 (1975).
40. K. B. Eisenthal, *Accounts Chem. Research*, **8**, 118 (1975).
41. T. J. Chuang, R. J. Cox and K. B. Eisenthal, *J. Amer. Chem. Soc.*, **96**, 6828 (1974).
42. K. Zachariasse, in "The Exciplex" (ed. M. Gordon and W. R. Ware), Academic Press, New York (1975), p. 275.
43. A. J. Bard and S. M. Park, "The Exciplex" (ed. M. Gordon and W. R. Ware), Academic Press, New York (1975), p. 305.
44. A. J. Bard and L. R. Faulkner, in "Creation and Detection of the Excited State" (ed. W. R. Ware), Vol. 3, Marcel Dekker, New York (1976).
45. N. Nakashima, N. Mataga and C. Yamanaka, *Internat. J. Chem. Kinetics*, **5**, 833 (1973).
46. W. R. Ware, in "Creation and Detection of the Excited State", Vol. IA (ed. A. Lamola), Marcel Dekker, New York (1971), p. 213.
47. J. B. Birks, "Organic Molecular Photophysics", Vol. II (ed. J. B. Birks), Wiley-Interscience, New York (1973), p. 409.
48. N. Nakashima, F. Ushio, N. Mataga and C. Yamanaka, *Z. Phys. Chem.* (N.F.). **79**, 150 (1972).
49. W. R. Ware and H. P. Richter, *J. Chem. Phys.*, **48**, 1595 (1968).
50. M. H. Hui and W. R. Ware, *J. Amer. Chem. Soc.*, **98**, 4718 (1976).
51. T. Okada, H. Matsui, H. Oohari, H. Matsumoto and N. Mataga, *J. Chem. Phys.*, **49**, 4717 (1968).
52. K. Yoshihara, T. Kasuya, A. Inoue and S. Nagakura, *Chem. Phys. Lett.*, **9**, 469 (1971).
53. H. Knibbe, D. Rehm and A. Weller, *Ber. Bunsenges. Phys. Chem.*, **73**, 839 (1969).
54. R. M. Noyes, "Progress in Reaction Kinetics", Vol. I (ed. G. Porter), Pergamon, New York (1961), p. 129.
55. T. L. Nemzek and W. R. Ware, *J. Chem. Phys.*, **62**, 477 (1975).
56. T. J. Chuang and K. B. Eisenthal, *J. Chem. Phys.*, **62**, 2213 (1975).
57. T. Okada, T. Saito and N. Mataga, *Bull. Chem. Soc. Japan*, **50**, 331 (1977).
58. (a) F. Schneider and E. Lippert, *Ber. Bunsenges. Phys. Chem.*, **72**, 1155 (1968); *ibid.*, **74**, 624 (1970). (b) E. Lippert, W. Lüder and H. Boos, in "Advances in Molecular Spectroscopy", Pergamon Press (1962), p. 443.
59. (a) N. Nakashima, H. Inoue, N. Mataga and C. Yamanaka, *Bull. Chem. Soc. Japan*, **46**, 2288 (1973). (b) N. Nakashima and N. Mataga, *Bull. Chem. Soc. Japan*, **46**, 3016 (1973).
60. K. Rotkiewicz, K. H. Grellmann and Z. R. Grabowski, *Chem. Phys. Lett.*, **19**, 315 (1973).
61. W. S. Struve, P. M. Rentzepis and J. Jortner, *J. Chem. Phys.*, **59**, 5014 (1973).
62. E. A. Chandross, in "The Exciplex" (ed. M. Gordon and W. R. Ware), Academic Press, New York (1975), p. 187.
63. N. Nakashima, M. Murakawa and N. Mataga, *Bull. Chem. Soc. Japan*, **49**, 854 (1976).
64. (a) N. G. Bakshiev, Y. T. Muzerenko and I. V. Piterskaya, *Opt. Spectrosc.* (USSR), **21**, 307 (1966). (b) W. R. Ware, P. Chow and S. K. Lee, *Chem. Phys. Lett.*, **2**, 356

(1968); W. R. Ware, S. K. Lee, G. J. Brant and P. P. Chow, *J. Chem. Phys.*, **54**, 4729 (1971).
65. (a) N. Mataga and Y. Murata, *J. Amer. Chem. Soc.*, **91**, 3144 (1969). (b) K. Egawa, N. Nakashima, N. Mataga and C. Yamanaka, *Chem. Phys. Lett.*, **8**, 108 (1971); *Bull. Chem. Soc. Japan*, **44**, 3287 (1971).
66. (a) R. A. Marcus, *Ann. Rev. Phys. Chem.*, **15**, 155 (1964). (b) R. A. Marcus, *J. Chem. Phys.*, **24**, 966 (1956). (c) S. Efrima and M. Bixon, *Chem. Phys. Lett.*, **25**, 34 (1974).
67. (a) D. Rehm and A. Weller, *Ber. Bunsenges. Phys. Chem.*, **73**, 834 (1969). (b) D. Rehm and A. Weller, *Israel J. Chem.*, **8**, 259 (1970).
68. N. Mataga and O. Tanimoto, *Theoret. Chim. Acta*, **5**, 111 (1969); T. Okada, H. Oohari and N. Mataga, *Bull. Chem. Soc. Japan*, **43**, 2750 (1970).
69. (a) A. Weller and K. Zachariasse, *J. Chem. Phys.*, **46**, 4984 (1967). (b) A. Weller and K. Zachariasse, in "Molecular Luminescence" (ed. E. C. Lim), Benjamin, New York (1969), p. 895. (c) A. Weller and K. Zachariasse, *Chem. Phys. Lett.*, **10**, 197 (1971). (d) A. Weller and K. Zachariasse, *ibid.*, **10**, 424 (1971). (e) A. Weller and K. Zachariasse, *ibid.*, **10**, 590 (1971). (f) K. Zachariasse, Thesis, Free University, Amsterdam (1972).
70. E. A. Chandross, J. W. Longworth and R. E. Visco, *J. Amer. Chem. Soc.*, **87**, 3259 (1965); E. A. Chandross, *Trans. N.Y. Acad. Sci.*, Ser. 2, **31**, 571 (1969).
71. H. Tachikawa and A. J. Bard, *Chem. Phys. Lett.*, **26**, 568 (1974); C. P. Keszthetlyi and A. J. Bard, *ibid.*, **24**, 300 (1974).
72. T. Hayashi, N. Mataga, Y. Sakata and S. Misumi, *Chem. Phys. Lett.*, **41**, 325 (1976); T. Hayashi, N. Mataga, T. Umemoto, Y. Sakata and S. Misumi, *J. Phys. Chem.*, **43**, 4175 (1965).
73. E. A. Chandross, *J. Chem. Phys.*, **81**, 424 (1977).
74. (a) N. Mataga, Y. Torihashi and Y. Ota, *Chem. Phys. Lett.*, **1**, 385 (1967). (b) T. Okada, and N. Mataga, *Bull. Chem. Soc. Japan*, **49**, 2190 (1976).
75. M. Itoh and T. Mimura, *Chem. Phys. Lett.*, **24**, 551 (1974); M. Itoh, *ibid.*, **26**, 505 (1974).
76. K. Yoshihara, K. Futamura and S. Nagakura, *Chem. Lett.* (Japan), 1243 (1972).
77. T. Okada, T. Mori and N. Mataga, *Bull. Chem. Soc. Japan*, **49**, 3398 (1976).
78. V. R. Rao, S. Vaidyanathan, U. Menon and V. Ramakrishnan, *Indian J. Chem.* **11**, 237 (1973); *Z. Physik. Chem.* (N.F.) **85**, 130 (1973).
79. S. G. Cohen, A. Parola and G. H. Parsons, Jr., *Chem. Rev.*, **73**, 141 (1973).
80. (a) S. Arimitsu and H. Masuhara, *Chem. Phys. Lett.*, **22**, 543 (1973); S. Arimitsu, H. Masuhara, N. Mataga and H. Tsubomura, *J. Phys. Chem.* **79**, 1255 (1975). (b) N. Mataga, F. Tanaka and M. Kato, *Acta Phys. Polon.*, **34**, 733 (1968).
81. K. Kikuchi, H. Watari and M. Koizumi, *Bull. Chem. Soc. Japan*, **46**, 749 (1973); S. Yamamoto, K. Kikuchi and H. Kokubun, *Chem. Lett.* (Japan), 65 (1976); *J. Photochem.*, **5**, 469 (1976).
82. E. M. Kosower, personal communication.
83. H. Masuhara, Y. Tohgo and N. Mataga, *Chem. Lett.* (Japan), 59 (1975).
84. J. B. Birks, "Photophysics of Aromatic Molecules", Wiley-Interscience, New York (1970, p. 492.
85. J. B. Birks, in "Organic Molecular Photophysics", Vol. 2 (ed. J. B. Birks and S. P. McGlynn), John Wiley, London, New York (1975), pp. 545-554.
86. H. Tsubomura and R. S. Mulliken, *J. Amer. Chem. Soc.*, **82**, 2411 (1960).
87. B. Stevens and B. E. Algar, *Chem. Phys. Lett.*, **1**, 58, 219 (1976).
88. R. Potashnik, C. R. Goldschmidt and M. Ottolenghi, *Chem. Phys. Lett.*, **9**, 424 (1971).
89. T. Brewer, *J. Amer. Chem. Soc.*, **93**, 775 (1971).

90. S. P. McGlynn, T. Azumi and M. Kinoshita, in "Molecular Spectroscopy of the Triplet State", Prentice Hall (1969), pp. 284–325.
91. Y. Taniguchi, A. Mioshi, N. Mataga, H. Shizuka and T. Morita, *Chem. Phys. Lett.*,**15**, 223 (1972).
92. H. Linschitz and L. Pekkarinen, *J. Amer. Chem. Soc.*, **82**, 2411 (1960); C. Steel H. Linschitz, *J. Phys. Chem.*, **66**, 2577 (1962).
93. J. B. Guttenplan and S. G. Cohen, *Tetrahedron Lett.*, **22**, 2163 (1972).
94. A. R. Watkins, *J. Phys. Chem.*, **77**, 1207 (1973); *ibid.*, **78**, 1885 (1974); *ibid.*, **78**, 2555 (1974).
95. A. Treinin and E. Hayon, *J. Phys. Chem.*, **98**, 3884 (1976).
96. S. Iwata, J. Tanaka and S. Nagakura, *J. Amer. Chem. Soc.*, **88**, 894 (1966).
97. H. Masuhara and N. Mataga, *Z. Phys. Chem.* (N.F.), **80**, 113 (1972).
98. T. Kobayashi, K. Yoshihara and S. Nagakura, *Bull. Chem. Soc. Japan*, **44**, 2603 (1971).
99. N. Niimura, Y. Ohashi and Y. Saito, *Bull. Chem. Soc. Japan*, **41**, 1815 (1968).
100. N. Orbach, Ph.D. Thesis, Hebrew University, Jerusalem (1977).
101. K. B. Eisenthal, *J. Chem. Phys.*, **46**, 3268 (1967); G. Briegleb, H. Schuster and W. Herre, *Chem. Phys.Lett.*, **4**, 53 (1969); Z. Teitelbaum, R. Potashnik and M. Ottolenghi, *Mol. Photochem.*, **3**, 107 (1971).
102. S. Matsumoto, S. Nagakura, S. Iwata and J. Nakamura, *Mol. Phys.* **26**, 1465 (1973).
103. J. K. Roy and D. G. Whitten, *J. Amer. Chem. Soc.*, **93**, 7093 (1971); J. K. Roy, F. A. Carroll and D. G. Whitten, *ibid.*, **96**, 6349 (1974); D. G. Whitten, J. K. Roy and F. A. Carroll, in "The Exciplex" (ed. M. Gordon and W. R. Ware), Academic Press, New York (1975), p. 247.
104. T. Hayashi, N. Mataga, Y. Sakata, S. Misumi, M. Morita and J. Tanaka, *J. Amer. Chem. Soc.*, **98**, 5910 (1976).
105. M. Itoh and E. M. Kosower, *J. Amer. Chem. Soc.*, **90**, 1843 (1968).
106. M. G. Kuzmin and L. N. Geseva, *Chem. Phys. Lett.*, **3**, 71 (1969).
107. A. Nakajima, *Bull. Chem. Soc. Japan.*, **42**, 3409 (1969).
108. For a review on the theory of solvent effects on electronic spectra, see Ref. 5, Ch. 8, pp. 371–410.
109. Y. Ooshika, *J. Phys. Soc. Japan*, **9**, 594 (1954).
110. E. G. McRae, *J. Phys. Chem.*, **61**, 562 (1957).
111. H. C. Longuet-Higgins and J. A. Pople, *J. Chem. Phys.*, **27**, 192 (1957).
112. W. Liptay, *Z. Naturforsch.*, **20a**, 1441 (1965).
113. L. Onsager, *J. Amer. Chem. Soc.*, **58**, 1486 (1936).
114. E. Lippert, *Z. Naturforsch.*, **10a**, 541 (1955); *Z. Elektrochem.*, **61**, 962 (1957).
115. N. Mataga, Y. Kaifu and M. Koizumi, *Bull. Chem. Soc. Japan*, **28**, 690 (1955).
116. N. Mataga, Y. Kaifu and M. Koizumi, *Bull. Chem. Soc. Japan*, **29**, 465 (1956).
117. H. Beens, Ph.D. Thesis, Free University of Amsterdam, Amsterdam (1969).
118. (a) N. Mataga, T. Okada and N. Yamamoto, *Bull. Chem. Soc. Japan*, **39**, 2562 (1966); (b) *Idem*, *Chem. Phys. Lett.*, **1**, 119 (1967).
119. H. Suzuki, in "Electronic Absorption Spectra and Geometry of Organic Molecules", Academic Press, New York (1967), p. 366.
120. S. Yomosa, *J. Phys. Soc. Japan*, **35**, 1738 (1973).
121. H. Beens, H. Knibbe and A. Weller, *J. Chem. Phys.*, **47**, 1183 (1967).
122. H. Knibbe, Ph.D. Thesis, Free University of Amsterdam, Amsterdam (1969).
123. E. Lippert, W. Luder and H. Boos, in "Advances in Molecular Spectroscopy" (ed. Mangini), Pergamon Press, Oxford (1962), p. 443.
124. O. S. Khalil, R. H. Hofeldt and S. P. McGlynn, *Chem. Phys. Lett.*, **17**, 479 (1972).

125. E. M. Kosower and H. Dodiuk, *J. Amer. Chem. Soc.*, **98**, 924 (1976).
126. K. Rotkiewicz, Z. R., Grabowski, A. Krowczynski and W. Kuhnle, *J. Luminescence*, **12/13**, 877 (1976); K. Rotkiewicz, contribution at the International Congress on Photobiology, Rome, August 1976.
127. W. Struve and P. M. Rentzepis, *J. Chem. Phys.*, **60**, 1532 (1974).
128. W. S. Struve and P. M. Rentzepis, *Chem. Phys. Lett.*, **29**, 23 (1974).
129. K. Rotkiewicz, Z. R. Grabowski and J. Jasny, *Chem. Phys. Lett.*, **34**, 55 (1975).
130. A. Siemlarczuk, Z. R. Grabowski and A. Krowczynski, to be published.
131. M. Asher and M. Ottolenghi, to be published.
132. E. M. Kosower and K. Tanizawa, *Chem. Phys. Lett.*, **16**, 419 (1972).
133. G. Weber and D. J. R. Laurence, *Biochem. J.*, **56**, xxxi (1954).
134. E. M. Kosower, "An Introduction to Physical Organic Chemistry", J. Wiley and Sons, New York (1968).
135. E. M. Kosower, *J. Amer. Chem. Soc.*, **80**, 3253 (1958).
136. E. M. Kosower and L. Lindqvist, *Tetrahedron Letters*, 4481 (1965).
137. Chr. Reichardt, "Lösungsmittel-Effekte in der Organische Chemie,', Verlag Chemie, Akinheim, Germany (1969).
138. E. A. Chandross and H. T. Thomas, *Chem. Phys. Lett.*, **9**, 397 (1971).
139. N. Orbach and M. Ottolenghi, *Chem. Phys. Lett.*, **35**, 175 (1975).
140. (a) N. Mataga, M. Migita and T. Nishimura, *J. Mol. Structure*, **47**, 199 (1978); (b) M. Migita, M. Kawai, N. Mataga, Y. Sakata and S. Misumi, *Chem. Phys. Lett.*, **53**, 67 (1978).
141. K. Kaneta and M. Koizumi, *Bull. Chem. Soc. Japan*, **40**, 2254 (1967); S. Murata, H. Kokubun and M. Koizumi, *Z. Phys. Chem.* (N.F.), **70**, 47 (1970).
142. (a) A. Knibbe, K. Rollig, F. P. Schafer and A. Weller, *J. Chem. Phys.*, **47**, 1184 (1964). (b) H. Knibbe, D. Rehm and A. Weller, *Ber. Bunsenges. Phys. Chem.*, **72**, 257 (1968). (c) D. Rehm and A. Weller, *ibid.*, **73**, 834 (1969)..
143. Y. Taniguchi, Y. Nishima and N. Mataga, *Bull. Chem. Soc. Japan*, **45**, 764 (1972); Y. Taniguchi and N. Mataga, *Chem. Phys. Lett.*, **13**, 596 (1972).
144. H. Masuhara, T. Hino and N. Mataga, *J. Phys. Chem.*, **79**, 994 (1975).
145. N. Orbach and M. Ottolenghi, in "The Exciplex" (International Exciplex Conference, London, Ontario, 1974) (ed. M. Gordon and W. R. Ware), Academic Press, New York (1975), pp. 75–106.
146. A. Alchalal, M. Tamir and M. Ottolenghi, *J. Phys. Chem.*, **76**, 2229 (1972).
147. R. Potashnik, C. R. Goldschmidt and M. Ottolenghi, *J. Phys. Chem.*, **73**, 3170 (1969).
148. (a) Y. Achiba and K. Kimura, *Chem. Phys. Lett.*, **19**, 45 (1973). (b) K. Kimura, Y. Achiba and S. Katsumata, *J. Phys. Chem.*, **77**, 2520 (1973). (c) Y. Achiba, S. Katsumata and K. Kimura, *Bull. Chem. Soc. Japan*, **45**, 1272 (1972).
149. H. Masuhara, M. Shimada and N. Mataga, *Bull. Chem. Soc. Japan*, **44**, 3310 (1971); M. Shimada, H. Masuhara and N. Mataga, *Chem. Phys. Lett.*, **22**, 1 (1972); *Bull. Chem. Soc. Japan*, **46**, 1903 (1973).
150. M. Irie, S. Tomimoto and K. Hayashi, *J. Phys. Chem.*, **76**, 1419 (1972); M. Irie, H. Masuhara, K. Hayashi and N. Mataga, *ibid.*, **78**, 341 (1974).
151. Y. Shirota, K. Kawai, N. Yamamoto, K. Tada, T. Shida, H. Mikawa and H. Tsubomura, *Bull. Chem. Soc. Japan*, **45**, 2683 (1972); Y. Taniguchi, Y. Nishima and N. Mataga, *Chem. Lett.* (Japan), 221 (1972); *Bull. Chem. Soc. Japan*, **46**, 1646 (1973); K. Tada, Y. Shirota and H. Mikawa, *Macromolecules*, **6**, 9 (1973); S. Tomimoto and K. Kayashi, *J. Polymer Sci.*, **11**, 1859 (1973).
152. Y. Achiba and K. Kimura, *Bull. Res. Inst. Appl. Electricity* (Japan), **26**, 114 (1974).

153. Y. Achiba and K. Kimura, *Chem. Phys. Lett.*, **36**, 65 (1975); Proceedings of the 1975 International Conference on Luminescence. *J. Luminescence*, **12/13**, 871 (1976).
154. M. Irie, Y. Yamamoto and K. Hayashi, *J. Phys. Chem.*, **79**, 699 (1975).
155. S. G. Cohen and H. M. Chao, *J. Amer. Chem. Soc.*, **90**, 165 (1968); S. G. Cohen and J. I. Cohen, *J. Phys. Chem.*, **72**, 3782 (1968).
156. R. F. Bartholomew, R. S. Davidson, P. F. Lambeth, J. F. McKellar and P. H. Turner, *J. Chem. Soc. Perkin Trans. II*, 577 (1972).
157. J. B. Guttenplan and S. G. Cohen, *J. Amer. Chem. Soc.*, **94**, 4040 (1972); R. W. Yip, R. O. Loufty, Y. L. Chow and L. K. Magdzinski, *Can. J. Chem.*, **50**, 3426 (1972).
158. A. Mozumder, *J. Chem. Phys.*, **48**, 1659 (1968); *ibid.*, **50**, 3153, 3162 (1969); in "Advances in Radiation Chemistry", Vol. 1 (ed. M. Burton and J. L. Magee), Wiley Interscience, New York (1969), p. 83.
159. S. Glasstone, K. J. Laidler and H. Eyring, "The Theory of Rate Processes", McGraw-Hill, New York (1941), p. 145.
160. M. Eigen, *Z. Phys. Chem.* (N.F.), **1**, 176 (1954).
161. I. Amdur and G. Hammes, "Chemical Kinetics Principles and Selected Topics", McGraw-Hill, New York (1966).
162. T. Hino, H. Akazawa, H. Masuhara and N. Mataga, *J. Phys. Chem.*, **80**, 33 (1976).
163. H. Masuhara and N. Mataga, to be published.
164. B. B. Craig and M. A. J. Rodgers, *J. Chem. Soc. Faraday Trans. II*, **72**, 1259 (1976).
165. T. Hino, H. Masuhara and N. Mataga, *Bull. Chem. Soc. Japan*, **49**, 394 (1976).
166. T. Kobayashi and S. Nagakura, *Bull. Chem. Soc. Japan*, **45**, 987 (1972).
167. N. Christodonleas and S. P. McGlynn, *J. Chem. Phys.*, **40**, 166 (1964); M. Chowdhury and L. Goodman, *J. Amer. Chem. Soc.*, **86**, 2777 (1964).
168. T. Azumi, *Chem. Phys. Lett.*, **19**, 580 (1973).
169. C. R. Goldschmidt, R. Potashnik and M. Ottolenghi, *J. Phys. Chem.*, **75**, 1025 (1971).
170. N. Orbach, J. Novros and M. Ottolenghi, *J. Phys. Chem.*, **77**, 2831 (1973).
171. E. J. Land, J. T. Richards and J. K. Thomas, *J. Phys. Chem.*, **76**, 3805 (1972).
172. (a) N. Tsujino, H. Masuhara and N. Mataga, *Chem. Phys. Lett.*, **15**, 357 (1972). (b) T. Nishimura, N. Naskashima, and N. Mataga, *ibid.*, **46**, 334 (1977).
173. F. Nolting, A. H. Weller and K. A. Zachariasse, Abstract, VIth IUPAC Symposium on Photochemistry, Aix-en-Provence, France, July 1976.
174. N. C. Yang and J. Libman, *J. Amer. Chem. Soc.*, **95**, 5783 (1973).
175. K. A. Zachariasse, personal communication.
176. H. Knibbe, D. Rehm and A. Weller, *Ber. Bunsenges. Phys. Chem.*, **67**, 791 (1963).
177. Y. Nakato, N. Yamamoto and H. Tsubomura, *Bull. Chem. Soc. Japan*, **40**, 2480 (1967).
178. H. Grellmann, A. R. Watkins and A. Weller, *J. Luminescence*, **1/2**, 678 (1970).
179. H. Grellman, A. R. Watkins and A. Weller, *J. Phys. Chem.*, **76**, 469 (1972).
180. N. Orbach, R. Potashnik and M. Ottolenghi, *J. Phys. Chem.*, **76**, 1133 (1972).
181. H. Schomburg, H. Staerk and A. Weller, *Chem. Phys. Lett.*, **21**, 433 (1973); *ibid.*, **22**, 1 (1973).
182. B. Brocklehurst, *Chem. Phys. Lett.*, **28**, 357 (1974); *J. Chem. Soc. Faraday Trans. II*, **72**, 1869 (1976).
183. B. Brocklehurst, *Nature*, **221**, 921 (1969).
184. K. Kaptein, *J. Amer. Chem. Soc.*, **94**, 6251 (1972).

185. F. J. Adrian, *J. Chem. Phys.*, **54**, 3912, 3918 (1971); **57**, 5107 (1972).
186. R. G. Lawler and H. R. Ward, in "Determination of Organic Structures by Physical Methods", Vol. 5 (ed. F. C. Nachod J. J. Zuckerman), Academic Press, New York (1973), p. 99; R. G. Lowler, *Accounts Chem. Res.*, **5**, 25 (1972).
187. B. Brocklehurst, R. S. Dixon, E. M. Gardy, V. J. Lopata, M. J. Quinn, A. Singh and F. P. Sargent, *Chem. Phys. Lett.*, **28**, 361 (1974).
188. R. Haberkorn and M. E. Michel-Beyerle, *Z. Naturforsch.*, **31a**, 499 (1976); M. E. Michel-Beyerle, R. Haberkorn, W. Bube, E. Steffons, H. Schröder, H. J. Neusser, E. W. Schlag and H. Seidlith, *Chem. Phys.*, **17**, 139 (1976).
189. K. Schulten, H. Staerk, A. Weller, H. J. Werner and B. Nickel, Th. Förster Memorial Issue, *Z. Phys. Chem.* (N.F.), **101**, 37 (1976).

2 The Nature and Applications of Charge-transfer Phenomena in Polymers and Related Systems

J. M. Pearson and S. R. Turner

Xerox Corporation, Webster Research Laboratories, Webster, N.Y. 14580, U.S.A.

A. Ledwith

Donnan Laboratories, University of Liverpool, Liverpool L69 3BX, U.K.

I. Introduction 80
II. Formation of Higher Order Complexes 85
III. Orientation and Conformation Effects in Electron-Donor–acceptor Complexes 89
IV. Multiple Charge-transfer Transitions 93
V. Charge-transfer Complexes of Polymers 99
A. Polymers as donor molecules 100
B. The polymer chain effect on complex formation 103
C. Polymers as acceptor molecules 106
D. Polymeric intramolecular charge-transfer complexes . . . 110
VI. Electrical Properties 114
A. Experimental techniques 118
1. Dember technique 118
2. Hall technique 119
3. Thermoelectric effect; Seebeck technique 119
4. Xerographic technique 119
5. Transient photocurrent technique 122
B. Donor polymers with small molecule acceptors 123
1. Poly-(N-vinylcarbazole) (PVK) systems 123
2. Other donor polymers 135
3. Ionenes and related materials 138
4. Ferrocene-containing polymers 142
5. Tetrathiafulvalene (TTF) and related materials . . . 144
C. Acceptor polymers with small molecule donors 149
D. Intramolecular polymeric complexes 153
E. Charge-transfer complexes in polymeric binders 157
F. Polyacetylene complexes 158

G. Present and future applications 158
1. Electrophotography 159
2. Photoelectric devices 160
3. Power sources 161
VII. Conclusions 162
References 163

I. INTRODUCTION

Charge-transfer (CT) transitions between organic molecules are well characterized and, in the simplified general case, correlate with promotion of an electron in the highest energy occupied molecular orbital (HOMO) of one component (referred to henceforth as the donor) and the lowest energy unoccupied molecular orbital (LUMO) of the other component (referred to as the acceptor). According to this notation, electron-donor molecules would possess relatively low ionization potentials and electron-acceptors would have relatively high electron affinities.

Following the stimulating predictions of Mulliken,[1] it was soon realized that, for a given acceptor, the energy of the CT transitions with a series of donors would decrease with decreasing ionization potentials of the donors. Similarly, for a given donor, CT transition energies decrease with increasing electron affinities of a series of acceptor molecules.

Initially the Mulliken explanation for charge-transfer electronic transitions was thought to imply a substantial degree of so-called charge-transfer binding energy between the two components. However, later work showed clearly that, despite the occurrence of well established CT transitions, the actual contribution of charge transfer to ground-state association of donor and acceptor is generally small. Full discussion of the origins and theories of charge-transfer spectra and related problems is available in several recent texts[2–5] and will not be discussed further except where they relate to specific problems involving polymers.

Typical electron-donor molecules include amines, ethers and sulphur compounds, and typical electron-acceptor molecules are halogen, nitro- and cyano-substituted compounds, and quinones. Aromatic molecules may be either donor or acceptor components, and ethylenic or aromatic conjugation of any substituent greatly increases its donor or acceptor capability.

Electron-donor–acceptor (EDA) complex formation is a widespread phenomenon between molecules having the properties listed above, although internuclear separation is relatively long (3–4 Å) and enthalpies of association relatively low (10–30 kJ mol^{-1}, 3–8 kcal mol^{-1}). It follows that association constants for EDA complex formation may be very small, and details of the potential errors involved in their estimation have been fully discussed.[2]

Despite the uncertainties concerning the nature and magnitude of the bonding in ground-state charge-transfer complexes, most are readily characterized by the appearance of a new electronic transition, whose energy can be readily determined, and hence there is little uncertainty about the energy separation between the ground and excited states of any given charge-transfer complex.

There are many types of CT phenomena but for the purposes of this article we shall consider only those in which the bonding and the electronic transitions occur inter-chromophorically, i.e. across space between donor and acceptor units. In some cases it is possible to have both donor and acceptor units chemically bonded at different parts of a single molecule thereby giving rise to intramolecular interaction. However, for this case also, it is assumed that the two components are coincidentally held together in a common region of space by the nature of the molecular fragment to which they are attached, and that there is no conjugative bonding between donor and acceptor units. In some very important special cases to be discussed later (e.g. paracyclophanes) it is possible to design the molecular framework in such a way that both donor and acceptor are rigidly held at some fixed intermolecular separation.

The inter-chromophoric nature of CT transitions is readily seen from the simple molecular orbital diagram which serves also to indicate the possibilities of transitions between the several highest energy filled orbitals of the donor to the single lowest energy unfilled orbital of the acceptor, and from the single highest energy filled orbital of the donor to the several lowest energy unfilled orbitals of the acceptor.

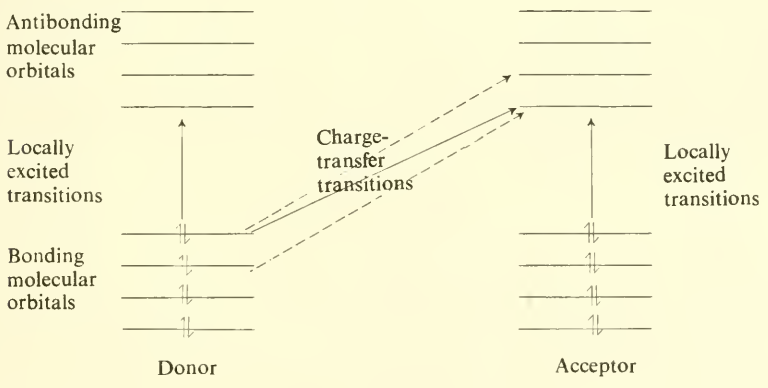

Another general feature of charge-transfer interaction is the possibility of complete electron-transfer from donor to acceptor with formation of a pair

of thermally equilibrated ion-radicals, e.g.

$$D + A \overset{K}{\rightleftharpoons} \underset{\text{CT complex (ground state)}}{[D, A]} \xrightarrow[(\epsilon)]{h\nu} \underset{\text{CT complex (excited state)}}{[D^{+\bullet}, A^{-\bullet}]^*} \rightarrow \underset{\text{ion radicals}}{D^{+\bullet}, A^{-\bullet}}$$

Formation of a pair of ion radicals from the excited state of a CT complex will depend on the nature of D and A, the medium in which the process takes place, and the temperature; it should not be assumed that excitation of a CT complex automatically leads to a pair of ion radicals. In many cases the latter arise via involvement of locally excited states of D or A and also via higher excited states of the D,A complex. These complications have been reviewed by Ottolenghi,[6] and chemical reactions arising via excitation of CT complexes in polymer-based systems have been surveyed by Hyde and Ledwith.[7]

Of particular relevance to the present discussion is the more recent characterization of exciplex formation by Weller and his associates.[8] An exciplex is formed by interaction of one excited molecule with another molecule in its ground state. In contrast to the usual donor–acceptor complexes, the two components are thought to interact repulsively when both are in ground states. Binding in the exciplex arises mainly from charge transfer between the two units, much as is envisaged for the excited states of CT complexes, and it is customary to denote exciplex formation as a donor–acceptor interaction. It should be noted however that exciplexes involve collisional interaction between a locally excited component and a ground-state component and, since most molecules in their excited states are simultaneously better donors and acceptors than in their ground states, the range of molecules participating in exciplex formation will be very much greater than for ground-state EDA complexes. Interrelationships between excited states of EDA complexes and exciplexes are indicated by Scheme 1, and a recent book[9] gives details of the scope and value of exciplex interactions.

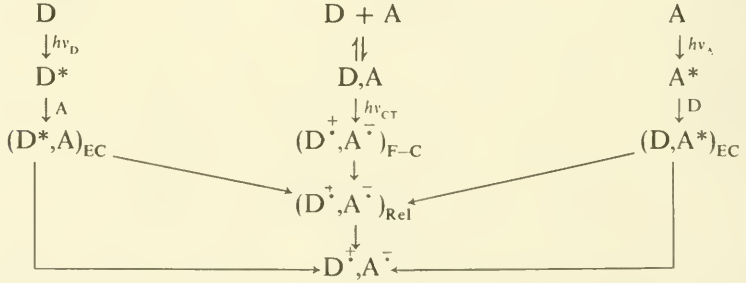

Scheme 1

Any distinction between collisional encounter complexes (denoted by EC) and exciplexes is indicated in Scheme 1 by the potential interconversions of the two possible EC complexes to a pair of ion radicals $[(D^{+}, A^{-})_{Rel}]$ having a solvation shell considerably relaxed from the Franck–Condon state $[(D^{+}, A^{-})_{F-C}]$ formed on direct excitation of a ground-state CT complex between the same components. Either of the encounter complexes, or the solvent-relaxed exciplex, could be responsible for formation of the solvent-equilibrated pair of ion radicals leading to ultimate photochemistry in the system. Reversion to the neutral starting components will be an important competing process at any stage of the equilibria indicated and, although the diagram uses a common donor D and acceptor A for both CT complexation and exciplex formation, there is no requirement for ground-state association prior to EC or exciplex formation.

As in the case of charge-transfer transitions, exciplex interaction may involve components that are independently bonded to a particular molecular framework but nevertheless interact in a through-space manner. Since exciplex formation is a special form of excited state quenching, luminescence studies afford a highly convenient experimental probe for charge-transfer phenomena in such systems, especially where the exciplex is itself a luminescing species.

Exciplexes are often referred to as hetero-excimers by analogy with the well established tendency of aromatic molecules to form emitting species—termed excimers—by collisional interaction of a ground-state molecule with a corresponding excited-state molecule (singlet or triplet). The general features of excimer formation are well documented in the review books edited by Birks,[10,11] and there is a recent survey of the importance of excimer interactions in polymers by Somersall and Guillet.[12]

Studies of luminescence from excimers and exciplexes have provided invaluable information regarding the effects of temperature, solvent, steric bulk of substituents, and molecular orientation on through-space interchromophoric interactions, and have thus provided both a stimulus and a partial rationale for an understanding of the closely related charge-transfer phenomena present in ground-state complexes.

We have already noted that the two general properties arising from CT effects in ground-state complexes are (i) occurrence of new spectroscopic transitions, thus greatly increasing the wavelength sensitivity, and (ii) the possible formation of a pair of ion radicals from neutral components. Obviously these two effects are interrelated and both will presumably play a role in any applications of CT complexes. The search for new organic photoconducting,[13] semiconducting and superconducting[14,15] systems continues unabated and provides considerable motivation for a better understanding of the nature of CT complexes, especially where polymeric

components are involved. One advantage of using polymer-based components lies in the enhanced material properties of given donor–acceptor combinations although other factors may be important (see later discussion). Most polymer based donor–acceptor combinations rely on the incorporation, by chemical bonding to the polymer backbone, of one or more of the well established organic molecules known to possess donor or acceptor capability. The general types of molecular structure that may be employed are well known, and recent reviews[16,17] have given compilations of donor and acceptor polymers based on the common donor and acceptor units. Detailed structures and properties of important polymeric electron–donor–acceptor systems are given later in the appropriate sections of this review.

Several interesting new acceptor and donor molecules have emerged recently which have stimulated research in the areas of CT complexes and electrical conductivity. Some examples of these are the polyquinocycloalkanes[18] (**1**)–(**5**), tetrathiafulvalene[19] (**6**) and its alkyl,[20] aryl[20] and selenium[21] homologues, *p*-phenylenebistetrathialfulvalene[22] (**7**), $\Delta^{4,4'}$-bithiopyran[23] (**8**), tetracyanoquinoquinazolinoquinazoline[24] (**9**) and 2,4-bisdicyanomethylene-1,3-dithietan[25] (**10**). Several of these compounds form

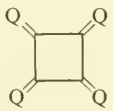

(1)

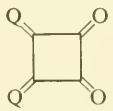

(2)

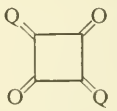

(3)

(4)

(5)

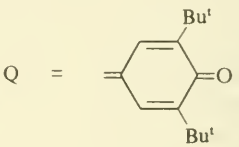

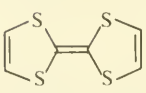

(6)

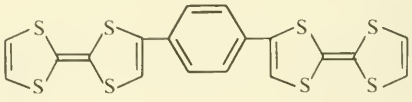

(7)

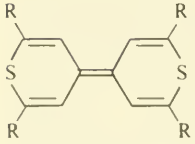

(8)

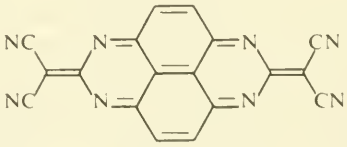

(9)

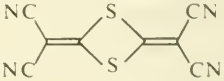

(10)

complexes that exhibit high electrical conductivity, and it seems reasonable to anticipate their incorporation into polymer-based systems in the near future. The limited information about polymeric derivatives at present available is discussed in a later section.

Before discussing the details of particular polymeric donor–acceptor combinations and their applications, it is pertinent to define those features of complex formation, additional to the more general questions relating to the nature and magnitude of the binding forces, that are likely to be of special significance with polymer molecules as donor or acceptor components. These will be considered under the headings of (a) formation of higher order complexes, (b) relative orientations or conformations of donor and acceptor components within a given complex, and (c) the existence and origins of multiple CT transitions for a given complex. Points raised under (a)–(c) have also to be considered for interactions between low molecular weight donors and acceptors but, with the exception of intramolecular complexes, there have been comparatively few attempts at any real understanding. It is of interest to make comparisons between polymeric and low molecular weight analogues, and the conformational restrictions imposed by polymer chains demand closer consideration of the phenomena associated with (a)–(c).

II. FORMATION OF HIGHER ORDER COMPLEXES

In the majority of EDA complexes it is assumed that 1:1 stoichiometry of the donor–acceptor pair prevails. Certainly the commonly used methods (e.g. Benesi–Hildebrand, Scatchard) for evaluating association constants are based on this assumption, and it is reasonable that 1:1 association is the most important. In principle, however, there are no reasons to rule out complexes of higher order, e.g. $(D)_nA$, $(A)_nD$, but the probability of their existence becomes progressively less likely as the order increases, i.e. $n > 2$. Indeed, given the very weak bonding forces in the 1:1 donor–acceptor adducts, it is difficult to conceive how higher order complexes could substantially enhance the stability of the adduct. Evidence for higher order EDA complexes comes mainly from spectroscopic (i.e. ultraviolet-visible and nmr) studies of intermolecular association where deviations from the assumed (e.g. Benesi–Hildebrand) correlation of absorbance with concentration are evident. Higher order complexes are frequently indicated by analysis of crystalline adducts, and the recently characterized 1:1 and 3:1 complexes of perylene with tetracyanoquinodimethane (TCNQ) are a good example.[26] Complexes of D_2A stoichiometry have been suggested[27] for the system hexamethylbenzene (donor) and 1,3,5-trinitrobenzene (acceptor),

and for several other systems where $[D]_0 \gg [A]_0$. In the formation of these ground-state higher order complexes it is important to consider whether the complex will have the configuration DAD or DDA (or the equivalent ADA or AAD).

The literature contains evidence supporting both the symmetrical, DAD, and the unsymmetrical, DDA, structures. Based on estimated ground-state dipole moments of termolecular complexes, Foster and coworkers[27] have suggested that the DAD structure is favoured. This assignment was supported by a more recent study[28] comparing complex formation between *N,N,N',N'*-tetramethyl-*p*-phenylenediamine with *p*-dinitrobenzene and 2,7-dinitro-1,6-methano[10]annulene. In the annulene system steric hindrance precludes the approach of a donor molecule on one side, and indeed only 1:1 complexes were formed under conditions where the related *p*-dinitrobenzene formed both 1:1 and 2:1 complexes. This was taken as evidence for a 2:1 complex in which the acceptor molecule is sandwiched between two donors, i.e. DAD. However, the use of *p*-dinitrobenzene as a model for the annulene creates uncertainty as to the real meaning of these results.

Absorption and emission studies on a series of three-layered cyclophane molecules tends to suggest that the unsymmetrical DDA structure is the more stable configuration. Misumi and coworkers[29] synthesized by a very elegant method the cyclophanes (**11**)–(**13**) where the donor and acceptor moieties are frozen in the appropriate array.

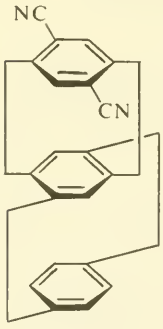

(11)

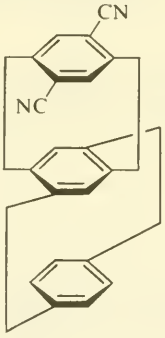

(12)

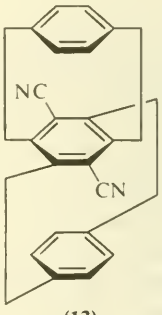

(13)

The fluorescence emission of structures (**11**) and (**12**) shows a stronger influence of solvent polarity (and hence a greater charge-transfer contribution) than the symmetrical DAD configuration in (**13**).[30] The increased π basicity of cyclophanes with increasing number of layers is now well established, suggesting that in polymeric systems with related interchromophoric order or high degrees of segmental freedom a similar apparent enhancement of donor (or acceptor) capability might be observed.

Supporting evidence for the enhanced degree of charge exchange in the DDA configuration comes from spectroscopic analysis of the cyclophanes (**14**) and (**15**) in which the acceptor component is a tropylium ion.[31] In dichloromethane (**14**) gives a CT band centred on 354 nm which extends almost to 500 nm and is particularly relevant in indicating the effect of distance on the complexing capacity of a weak donor such as a dialkylbenzene.

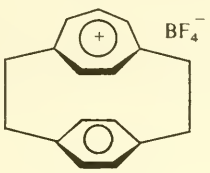

(14)

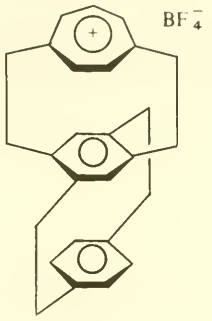

(15)

The absorption maximum of (**15**) (434 nm in dichloromethane) is at a much longer wavelength than that of (**14**), indicative of greater stabilization of the CT state of the DDA complex. Similarly the azulenophane (**16**) gives CT transitions with the acceptors 1,3,5-trinitrobenzene and tetracyanoethylene that are red-shifted by approximately 100 nm from those of the 2,6-dimethylazulene model compound.[32]

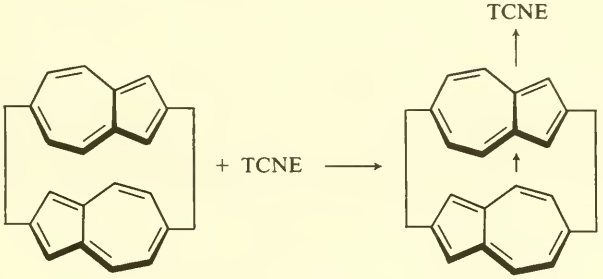

(16)

There are further examples of non-cyclophane systems that support the unsymmetrical DDA assignment. Excited state termolecular complexes have been invoked by several authors to account for the emission spectra of a number of D,A combinations where $[D]_0 \gg [A]_0$. Weller,[33] Mataga,[34] Itoh[35] and their coworkers suggested termolecular excited state complexes (exciplexes), (DDA)*, in the alkylnaphthalene–1,4-dicyanobenzene and

alkylbenzene–1,2,4,5-tetracyanobenzene systems. The termolecular complexes fluoresce at longer wavelengths than the more conventional (DA)* complexes. Their formation can occur from the exciplex, (DA)* + D ⇌ (DDA)*, or from the excimer, (DD)* + A ⇌ (DDA)*, depending on the relative concentration of D. Mimura and Itoh[36] also reported an intramolecular triple complex formed in the 1,3-dinaphthylpropane($\alpha\beta$ and $\beta\beta$)–1,4-dicyanobenzene system. In this case fluorescence emission from the termolecular complex was at 490 nm compared with that from the intramolecular excimer at 400 nm and from the exciplex at 420 nm. Formation of the termolecular complex from the exciplex was postulated. In this system the (DAD)* structure is highly improbable from steric considerations.

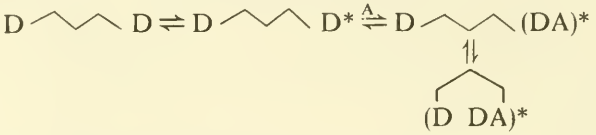

A recent theoretical analysis[37] of the triple exciplex in the naphthalene–1,4-dicyanobenzene system suggests that the (DDA)* array is more stable than (DAD)*. The sharing of the positive charge between two donor molecules, $D^{\delta+} \cdots DA^{\delta-}$, stabilizes the termolecular excited state complex. This is somewhat akin to the self-association stabilization of ion radical species with the neutral parent molecule, e.g. $(A,A)^{\mp}$[38] and $(D,D)^{+}$.[39]

For polymeric forms of donor and acceptor molecules the question of higher order complexes is especially important, owing to the obvious possibility for utilizing nearest neighbour pendant groups. In a polymeric environment the condition favouring multiple complexes, i.e. pendant D_0 (or A_0) $\gg$ A_0 (or D_0), is built into the system. Already it has been well established[10, 12] that neighbouring pendant aromatic moieties in a wide range of polymers give rise to efficient excimer emission. Association of a suitable acceptor molecule with the units of an excimer-forming site would provide the basis for formation of a DDA complex. The formation of DAD type complexes between appropriately oriented molecules seems equally probable:

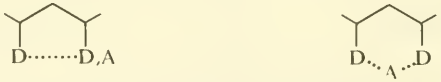

At present there is no clear evidence to distinguish between these, or even higher order, possibilities. From the model system studies, the D_nA types seem more favoured. However, it is clear that, in polymeric solutions and in the polymeric solid state, association of this nature will be greatly influenced by the conformational freedom within a given polymer backbone as well as the precise structure (and configuration) of the pendant interacting units.

III. ORIENTATION AND CONFORMATIONAL EFFECTS IN ELECTRON-DONOR–ACCEPTOR COMPLEXES

Formation of excimers between aromatic molecules requires a completely eclipsed sandwich conformation of the two participating units.[40] In contrast, exciplex interactions have far less stringent geometrical requirements[41,42] and sometimes occur[43,44] with equal facility for quite different relative conformations of the donor and acceptor components. Solvent may also play an important role in controlling orientation within an exciplex.[45,46]

X-ray crystallographic studies of EDA complexes[47] show clearly the existence of preferred molecular orientations that are quite removed from completely eclipsed sandwich-like structures, but it is still uncertain how much these may be taken to represent preferred conformations in solution or in amorphous polymer films. An extreme case, recently reported,[48] shows that the CT transitions exhibited by the crystalline complex between 4,4′-dinitrobiphenyl and benzidine arise even though the long axes of the donor and acceptor are perpendicular to each other.

The most important information concerning conformational effects in CT phenomena arises from detailed studies of intramolecular donor–acceptor complexes. Many systems have been synthesized in support of these investigations and six typical examples are indicated here. The value

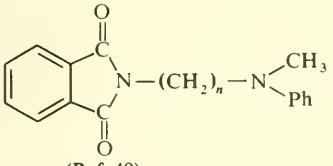

(Ref. 49)

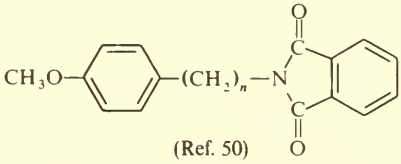

(Ref. 50)

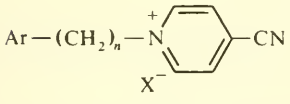

(Ref. 51)

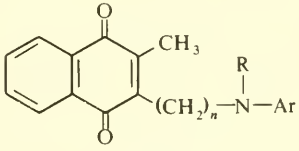

(Ref. 52)

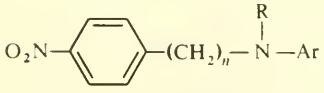

(Ref. 53)

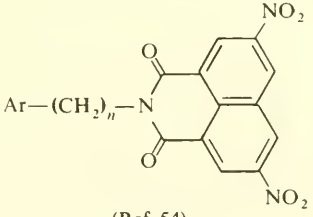

(Ref. 54)

of n leading to maximum CT absorption varies from system to system but this generally takes place at $n = 3$. However, it is important to note that, in all the systems investigated, strong CT interaction is observed for the molecules where $n = 1$. When $n = 1$ it is not possible for the donor and acceptor components to adopt anything remotely like a sandwich configuration, and hence it must be concluded that CT spectra may arise in cases where there is relatively little overlap of donor HOMO and acceptor LUMO orbitals. A further general feature of the systems shown is that CT interaction falls off dramatically as the value of n becomes greater than 3. Apparently, for association to occur in these intramolecular systems, the energy gained by the interaction of the groups must overcome the energy requirement for making the polymethylene chain adopt a particular conformation. Following this line of reasoning, the results of Sisido *et al.*[55] are particularly interesting. These authors synthesized a series of polysarcosines (**17**) having terminal *p*-

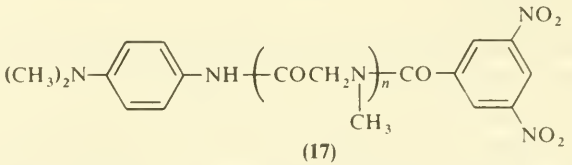

(**17**)

dimethylaminoanilido and 3,5-dinitrobenzoyl groups. The polymers (n varied between 6 and 25) when dissolved in chloroform exhibited a distinct absorption band around 455 nm, attributed mainly to intramolecular CT interactions. Calculations based on absorption (extinction) coefficients derived for low molecular weight model compounds showed that, at infinite dilution, the fraction of polymers forming intrachain complexes was 0·15 for $n = 6$ and decreased to 0·03 for $n = 25$. These values are almost 20–100 times larger than those estimated from Monte Carlo calculations and indicate that cyclized conformations of polysarcosine chains are greatly stabilized by the formation of intrachain complexes.

Perhaps the most striking demonstration of orientation effects on CT spectra is provided by the work of Staab and collaborators[56, 57] who have reported the synthesis of closely related cyclophane donor–acceptor pairs such as (**18**)–(**20**). For the three series of compounds, the eclipsed cyclophane

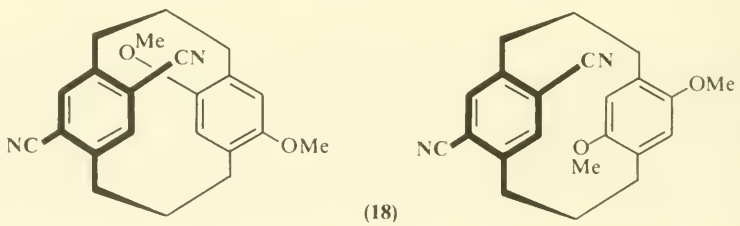

(**18**)

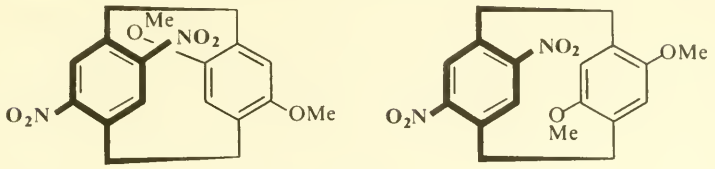

(19)

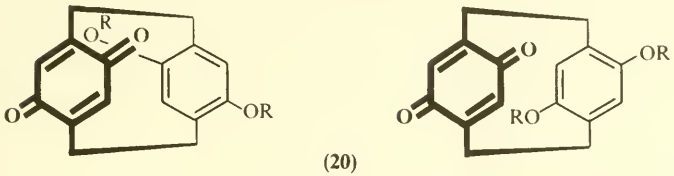

(20)

partner exhibited a much higher intensity CT band than the corresponding non-eclipsed molecule although values of the CT λ_{max} were very similar for both eclipsed and non-eclipsed pairs. These results are in accordance with the early prediction by Mulliken that overlap of donor HOMO and acceptor LUMO would allow maximum intensity in the CT transition. For the *para*-disubstituted aromatic units involved in the cyclophanes studied by Staab, nodal planes of the HOMO and LUMO orbitals run along the line joining the *para* positions, and hence maximum overlap of HOMO and LUMO occurs when the cyclophanes have eclipsed arrangements of donor and acceptor units.

Whilst the results of Staab and other workers referred to in the preceding paragraphs demonstrate dramatically the effects of donor–acceptor orientation on the intensities of CT transitions, it is clear nevertheless that non-sandwich arrangements of donor and acceptor may yield significant CT interaction. This point is further emphasized by the properties of compound (**21**) which exhibits[58] a broad CT absorption band (300–450 nm) in acetonitrile or dichloromethane not found in the absorption spectrum of either alkylated tropylium ions or alkylated benzenes.

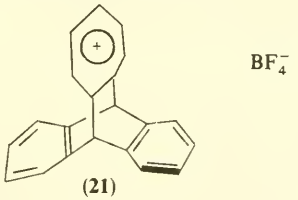

(21)

For simple intermolecular combinations of donor and acceptor molecules the question of orientation is much less well resolved. The most useful information comes from studies of the effects of solvent polarity on the

fluorescence of EDA complexes. Prochorow[59,60] showed that radiationless processes in excited EDA complexes of pyromellitic dianhydride and alkylated benzenes are mainly determined by the extent of interaction with surrounding solvent molecules. Related results for a corresponding intramolecular cyclophane system (**22**) were obtained by De Boer and coworkers[61] but it is not yet clear whether the interactions of excited EDA complexes with solvent involve mainly effects on the relative distance between the two components or effects on relative orientation of the donor and acceptor components.

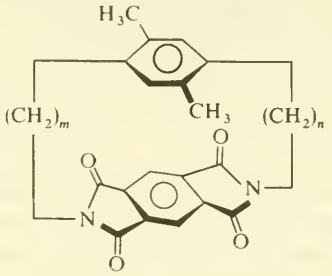

(**22**) $m = 3, n = 8$

(**23**) $m = n = 6$

It is significant that in the symmetrical cyclophane (**23**), $m = n = 6$, the CT absorption is much weaker than in the unsymmetrical homologue ($m = 3$, $n = 8$). This difference apparently corresponds to a difference in donor–acceptor orientation with the symmetrical molecule having a weaker transition probability in the axis joining the two planar aromatic groups. This point is of general relevance in connection with the symmetry requirements of multiple CT transitions and is discussed more fully in the following section.

Staab and Herz[62] have pointed out that [3,3]paracyclophanes such as (**24**) and (**25**) provide better models than [2,2]cyclophanes for intermolecular EDA complexes because of the increased nuclear separation (~3·2 Å), and that orientation effects on the intensities of CT bands are even more pronounced for the [3,3]paracyclophanes.

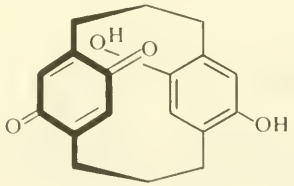

(**24**)

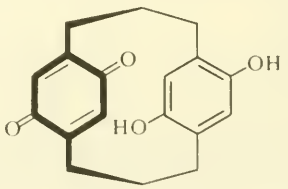

(**25**)

IV. MULTIPLE CHARGE-TRANSFER TRANSITIONS

The possibility that two distinguishable CT bands could originate from different relative orientations of donor and acceptor was first recognized by Orgel[63] in relation to the complexes of chloranil with substituted benzenes. Complexes of tetracyanoethylene (TCNE) with aromatic donors constitute the best-known[2] class exhibiting multiple CT transitions, and the most recent work[64–66] confirms that the two CT bands involve different excited states originating in the highest energy occupied molecular orbital, HOMO (1), and second highest energy molecular orbital, HOMO(2), of the alkylated benzene. According to Mulliken's maximum overlap principle, stabilization of the CT complexes is greatest when the nodal planes of donor and acceptor coincide. Thus for mono- and *para*-di-substituted benzenes, which can have nodes in the *xz* and *yz* planes, the two orientations (X) and (Y) would have allowed transitions from HOMO(2) and HOMO(1) respectively to the

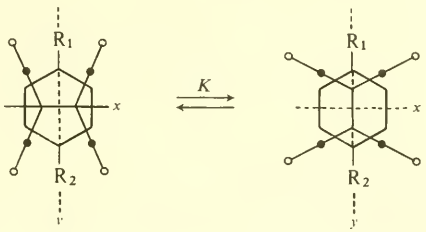

(X) (Y)

lowest unoccupied orbital (LUMO) of TCNE. For the special cases indicated it appears that the two orientations (X) and (Y) give rise to CT transitions of approximately equal intensities and, whilst (Y) is preferred for many mono-substituted benzenes, the energy differences between (X) and (Y) are less than 4 kJ mol^{-1} (1 kcal mol^{-1}).[64] It has been suggested[2] that, even if isomers such as (X) and (Y) exist, they could be taken to represent extreme conformer structures in which the relative rotation of one molecule with respect to its partner readily occurs. This would imply that the intensities of each CT band would be equal given that they have approximately equivalent oscillator strengths. However, it is clear from several different studies[64,67–69] that the two CT bands are not always present with equal intensities, and therefore it must be concluded that steric factors and perhaps exchange repulsion interactions are important in determining the geometry of CT complexes.

Apart from the detailed studies of complexes of TCNE there are comparatively few reports of the characterization of multiple CT transitions, and that of Sakurai and Kira[70] is noteworthy for its attempt to define a method

of resolving CT spectra into meaningful bands, in this case skewed Gaussian curves.

As will become apparent later, carbazole-containing polymers have been the most intensively studied as components of CT complexes, and carbazoles give rise to highly asymmetric CT spectra with a large number of acceptor molecules including TCNE, chloranil and 2,4,7-trinitrofluorenone. Klöpffer[71] was the first to recognize that the unsymmetrical CT spectra of carbazole compounds arise from the first two ionization levels, i.e. HOMO(1) and HOMO(2), of the carbazole ring system. More recently Marsh and coworkers[72] have made a detailed study of the origins of multiple CT transitions in complexes of chloranil with a wide variety of carbazole derivatives including several polymers. Nodal surfaces for the carbazole ring system and for chloranil are indicated in Fig. 1.

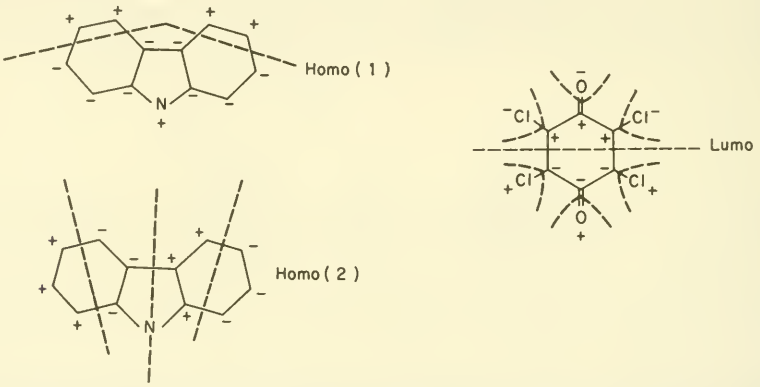

FIG. 1. Signs of orbital coefficients obtained from simple HMO treatment for the highest occupied molecular orbital [HOMO(1)] and second-highest occupied molecular orbital [HOMO(2)] for carbazole and the lowest empty molecular orbital (LUMO) for chloranil. Dashed lines indicate nodal surfaces.[72]

Two distinct conformations for a carbazole–chloranil complex are drawn in Fig. 2. The complexes are sandwich-like structures having parallel molecular planes and differ by a rotation around the z-axis (normal to the x–y plane) and a translation in the x–y plane. These two conformations are representative of the symmetry properties of all other possible parallel structures for this donor–acceptor pair. The conformation shown in Fig. 2A has a plane of reflection (σ_{xz}) which is lacking in the conformation shown in Fig. 2B. The group theoretical designation for the conformation in Fig. 2A is C_{1h}; the other conformation contains only an identity element and is designated C_1. In the limit of weak coupling between donor and acceptor molecules, the most probable contribution to the CT transition intensity

involves charge displacement in the z direction. In order to examine which transitions have an allowed z component (see Fig. 2) the symmetry properties of the x,y,z components of the dipole-moment operator and the orbitals of interest were derived, and these indicate clearly that the HOMO(2) → LUMO CT transitions in the C_{1h} conformation contain no z component and are not expected to contribute appreciably to the observed spectrum. Thus totally

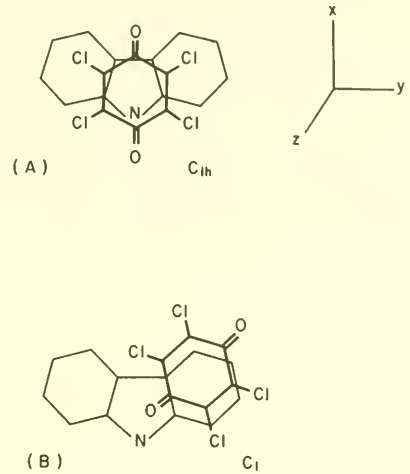

FIG. 2. Conformations for carbazole–chloranil complex; z axis out of the plane of the paper, x and y axes in the plane of the paper. Symmetric complex (C_{1h} point group) drawn in A; unsymmetric complex (C_1 point group) drawn in B.[72]

symmetric overlap of chloranil and carbazole derivatives would lead only to a CT band corresponding to transitions from the HOMO(1) level in the carbazole derivatives to the lowest empty molecular orbital in the acceptor. In the C_1 conformation both transitions from HOMO(1) and HOMO(2) are mixed, polarized with the z component, and may contribute to the observed spectrum.

These considerations are based on the symmetries of the donor and acceptor orbitals involved in the CT transitions which can be obtained via a simple HMO calculation. The use of semiempirical molecular orbital methods for the calculation of the orientation dependence of CT stabilization in molecular complexes is complicated by the assumptions inherent in the method of calculation, as well as the neglect of dispersion forces and solvation effects. Nevertheless Marsh and coworkers[72] performed PPP calculations in which an HMO basis was used for the SCF refinement. In this calculation the interplanar distance was allowed to vary between 3 and 6 Å, and for each distance several interplanar orientations were considered. The relative

CT stabilization energy as a function of the geometry of the complex was maximized for non-symmetrical conformations similar to that indicated in Fig. 2B. For this minimum energy conformation of a carbazole–chloranil pair, as we have just noted, CT transitions involving the first and second highest occupied molecular orbitals would be expected. On this basis it is to be expected that all carbazole derivatives form complexes with chloranil having a molecular orientation similar to Fig. 2B.

The early conclusion by Klöpffer[71] that CT transitions of carbazole derivatives arise from HOMO(1) and HOMO(2) donor levels is amply confirmed by the data cited by Marsh and coworkers.[72] Thus for *N*-ethylcarbazole the CT spectrum with chloranil as acceptor consists of two bands with λ_{max} 15222 and 19114 cm^{-1} respectively, corresponding to an energy separation of 0·47 eV. Ionization energies of HOMO(1) and HOMO(2) for *N*-ethylcarbazole obtained by photoelectron spectroscopy are 7·36 and 7·82 eV respectively.[73] The energy difference (0·46 eV) corresponds closely to that estimated via the CT spectrum. All *N*-alkylcarbazoles give rise to similar multiple CT transitions with many acceptor molecules but it is highly significant that for the *N*-acetylcarbazole–chloranil combination[72] there is only one CT band centred at 20857 cm^{-1}. In *N*-acetylcarbazole the highest occupied MO is substantially stabilized on account of the resonance effect of the acetyl substituent on the nitrogen lone-pair electrons, and in consequence the first and second ionization energies are not resolvable by photoelectron spectroscopy (ionization energy of HOMO(1) ≈ ionization energy of HOMO(2) ≈ 8·0 eV). This correspondence between the ionization energies and CT spectra provides convincing evidence for the origins of the CT bands in complexes of carbazole derivatives, although it is not yet clear whether the two CT bands arise within a single orientation of donor with respect to acceptor or from two distinct donor–acceptor conformations. Either explanation is possible but the analysis outlined above suggests that, unlike the case of TCNE–alkylbenzenes, carbazoles may exhibit multiple CT spectra from a single conformation or from a mixture of two different conformations.

Additional information as to the origins of CT bands in complexes of

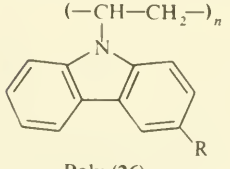

Poly-(26)

$R = -\overset{*}{C}H(CH_3)C_2H_5$

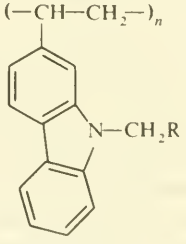

Poly-(27)

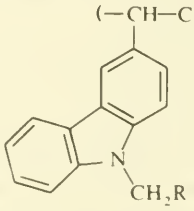

Poly-(28)

carbazoles is provided in a unique way by the studies of Chiellini, Solaro and Ledwith[74] who synthesized the optically active polymers and model compounds (**26**)–(**29**).

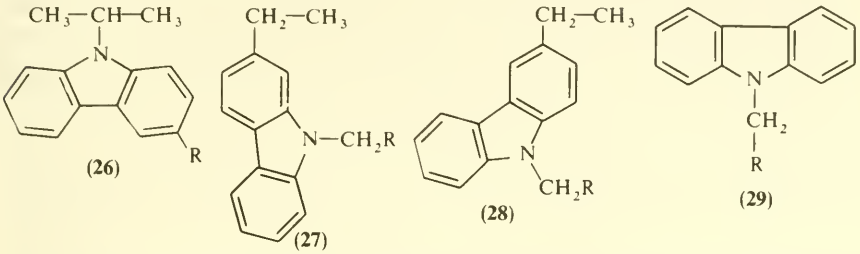

All polymers and low molecular weight analogues give rise to broad CT spectra with chloranil, having apparent λ_{max} in the region 530–580 nm and a distinct shoulder around 700 nm (Figs. 3 and 4).

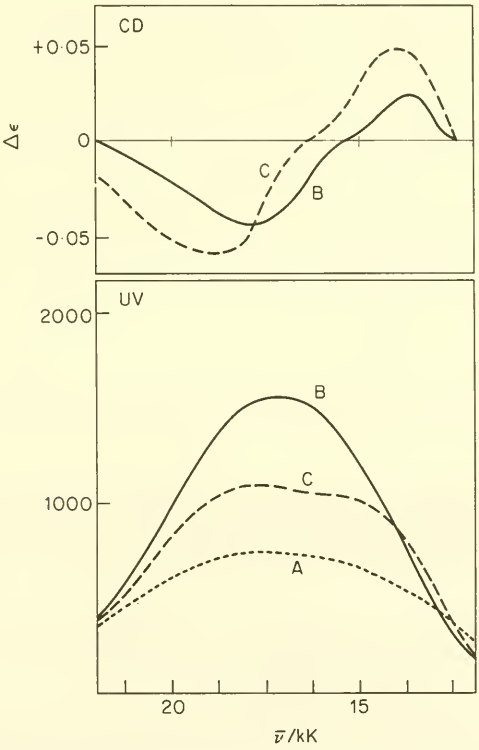

FIG. 3. UV and CD spectra of CT complexes of optically active poly(vinylcarbazole) derivatives with chloranil in dichloromethane at 37°C.[74] (A) poly-[(*S*)-3-s-butyl-9-vinylcarbazole], poly-(**26**); (B) poly-[(*S*)-9-(2-methylbutyl)-2-vinylcarbazole], poly-(**27**); (C) poly-[(*S*)-9-(2-methylbutyl)-3-vinylcarbazole], poly-(**28**).

Circular dichroism measurements provide unequivocal evidence for the existence of two distinct CT transitions in poly-(**27**), poly-(**28**) and the model compounds (**27**)–(**29**) but significantly the CT transitions of poly-(**26**) and (**26**), in which the chiral group is not attached directly to the nitrogen, are not optically active. The two CT transitions in carbazole–chloranil complexes, which are thought to arise via the HOMO(1) and HOMO(2) orbitals of

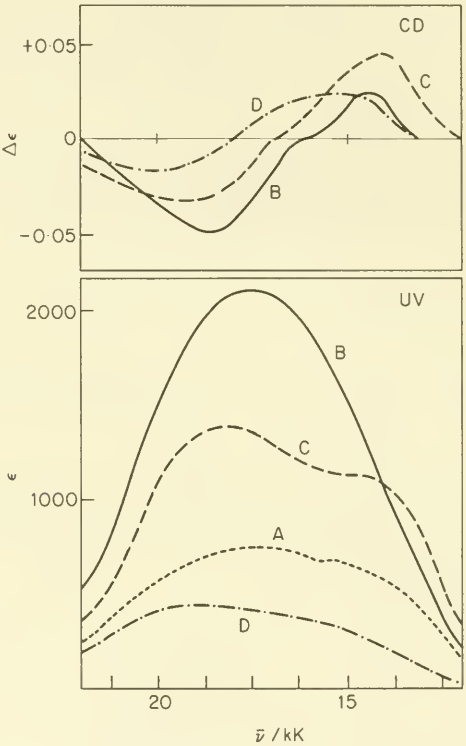

FIG. 4. UV and CD spectra of CT complexes of optically active carbazole derivatives with chloranil in dichloromethane at 37°C.[74] (A) (*S*)-3-s-butyl-9-isopropylcarbazole (**26**); (B) (*S*)-2-ethyl-9-(2-methylbutyl)carbazole (**27**); (C) (*S*)-3-ethyl-9-(2-methylbutyl)carbazole (**28**); (D) (*S*)-9-(2-methylbutyl)carbazole (**29**).

carbazole, are characterized by dichroic absorption bands having always positive and negative signs respectively, and this allows for unambiguous resolution of the CT absorption spectra.

Appropriate data for the peak positions in the CD spectra indicate close agreement between the CD peak separations and the corresponding energy differences for the two lowest energy ($^1L_a \leftarrow {}^1A$, $^1L_b \leftarrow {}^1A$) transitions in the carbazoles.

Assuming that the relative rotational strengths of the two CT transitions do not vary significantly for any one carbazole structural type, results for the simple *N*-alkylcarbazole (**29**) indicate that the higher energy of the two transitions is less intense than the lower energy CT transition as suggested by Landman *et al.*[72] on the basis of the two possible chloranil–carbazole conformations indicated in Fig. 2.

According to this analysis, stereochemical constraints will increasingly favour conformation B as one of the carbazole benzene rings and the nitrogen positions are substituted. Increasing conformer population of type B would have the effect of increasing the relative contribution of the higher energy CT transition.

A related analysis, based on transition-moment symmetries, has been used by Vogler, Ege and Staab[75] to account for the relative intensities of multiple intramolecular CT transitions in [2,2]paracyclophane analogues of the quinone–hydroquinone complex.

Multiplicity of transitions in CT spectra of carbazole complexes has also been extensively detailed by Okamoto *et al.*[76] These authors resolved the experimental CT spectra into two components of which the higher energy transition, i.e. that from HOMO(2), was most intense, in contrast to Landman *et al.*[72] who, for identical spectra, preferred a band resolution indicating the lowest energy transition, i.e. that from HOMO(1), as most intense. At present it is not possible to decide which method of band resolution is correct but the different interpretations serve to illustrate the futility of attempts to compare values of K and ϵ for complexes of carbazoles with various acceptors. This point will be discussed further in the following section.

V. CHARGE-TRANSFER COMPLEXES OF POLYMERS

Charge-transfer complexes formed from polymers are more complex than their low molecular weight models. Polymer chains are subject to conformational perturbations arising from the individual polymer backbones which introduce orientation and concentration effects absent in simple molecular systems. Such effects may result in an increased population of sites comprising more than one donor or acceptor unit and formation of higher order complexes. In studies of complex formation in dilute solutions these phenomena will be largely controlled by the actual donor–acceptor pair and by the polymer–solvent interactions which influence chain conformation. In the amorphous solid state (e.g. polymer films) these factors will be further complicated by any micro or macro phase separation in the polymer morphology.

It follows therefore that, whilst determinations of K and ϵ for dilute

solutions of polymeric donors or acceptors will be subject to all the errors and uncertainties normally encountered in such measurements, similar determinations in the amorphous polymeric state might be completely meaningless. Comparatively few determinations of association constants (K) and absorption (extinction) coefficients (ϵ) have been reported for polymeric CT complexes, and most of these relate to polymers containing carbazole units as donor species. We have already seen that complexes of carbazoles are complicated by overlapping CT transitions and, since this has seldom been taken into account in the Benesi–Hildebrand and similar procedures employed, values of the product $K\epsilon$ are probably the only significant parameters to be drawn from such studies. Even then the values of $K\epsilon$ can only be taken to represent an approximation to the extent of CT complex formation but it seems reasonable to make comparisons between polymeric donors (say) and their low molecular weight models on the basis of overall values of $K\epsilon$ rather than the possibly misleading individual values of K and ϵ. A comprehensive list of CT complexes involving polymeric components was given in an earlier review[16] and will not be reported in this survey. Instead emphasis will be given to those few systems where appropriate model compounds have been studied alongside their polymeric counterparts, and to relatively new complexes derived from polymeric components.

A. Polymers as Donor Molecules

Charge-transfer complexes of poly-(*N*-vinylcarbazole) (PVK) have been most studied of all polymeric CT complexes because of their potential applications in electrophotography (see later sections) and, whilst there can be no ambiguity as to the strong electron-donor character of carbazole units in polymeric environments, quantitative studies involving Benesi–Hildebrand and similar methods are generally unreliable because of a failure to make the necessary band resolution, as described in the preceding section. There is obvious value in establishing whether any given polymeric donor (or acceptor) is better or worse than its low molecular weight model compound in forming a particular complex, and determinations of K and ϵ offer a means of quantifying these effects. It is a great pity therefore that, for many publications[77–80] giving details of CT complexes of polymers containing carbazole groups, it is not possible to make the desired conclusions with any certainty. One fact that does emerge from these studies[76,79] is that poly-(*N*-vinylcarbazole) consistently forms CT complexes with a wide variety of acceptors in which derived values of K and of $K\epsilon$ are *lower* than those for the model compounds *N*-ethylcarbazole and *N*-isopropylcarbazole. For all other polymeric CT complexes, where the evidence is reliable, there is no clear distinction between the polymer and its model compounds. In many cases both polymer and

model give rise to similar values of $K\epsilon$, and in some cases the polymer yields higher values of $K\epsilon$ for particular acceptor molecules. It seems reasonable to assume that the uniquely lower values of K and $K\epsilon$ for poly-(*N*-vinylcarbazole) arise because of the high degree of steric interference to intermolecular association caused by the bulky carbazole groups directly bonded to the polymer backbone.

These effects are lost when the carbazole group is not attached directly to the polymer backbone[78–80] as illustrated (Table I) by complexes of a series of carbazole-containing polymers.[81]

TABLE I. Charge-transfer complexes[a] of carbazole-containing polymers with chloranil in dichloromethane at 25°C

R in 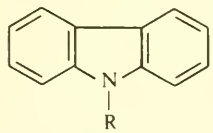	$K\epsilon/l^2\ mol^{-2}\ cm^{-1}$
$-C_2H_5$	1880
$-CH_2OCOC(CH_3)-CH_2-$	1526
$-CH_2CH_2OCOC(CH_3)-CH_2-$	2130
$-CH_2COO(CH_2)_2OCOC(CH_3)-CH_2-$	1481
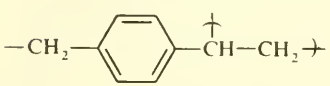	1407
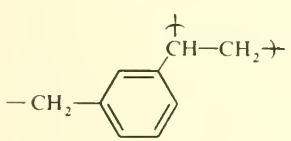	1393
$-CH(-)-CH_2-$ (PVK)	680

[a]Except for PVK, band shapes and values of λ_{max} were very similar to those for simple *N*-alkylcarbazoles (Fig. 4).

Additional and convincing evidence for steric effects in CT complexes of poly-(*N*-vinylcarbazole) is provided by the quite different relative intensities of the two CT transitions for complexes of the polymer and its simple *N*-alkylcarbazole models with chloranil.[72, 76]

The more usual case, in which a polymer appears to be a better donor than its model counterpart, is illustrated by recent results of Schulz and Geissler[82] who studied complexes formed between various acceptors and donor poly-

TABLE II. Charge-transfer complexes of poly(vinyl alcohol) acetals[82]

Donor	Acceptor	λ_{CT}/nm	$K\epsilon/l^2\,mol^{-2}\,cm^{-1}$
Fluorene-2-aldehyde trimethylene acetal	TCNQ	568	3581
Polymeric fluorene-2-aldehyde acetal (68–76% acetal formation)	TCNQ	554	23 235
Naphthalene-1-aldehyde trimethylene acetal	TCNE	532	1550
Polymeric naphthalene-1-aldehyde acetal (80% acetal formation)	TCNE	533	1740
Naphthalene-2-aldehyde trimethylene acetal	TCNQ	530	2597
Polymeric naphthalene-2-aldehyde acetal (71% acetal formation)	TCNQ	537	1949

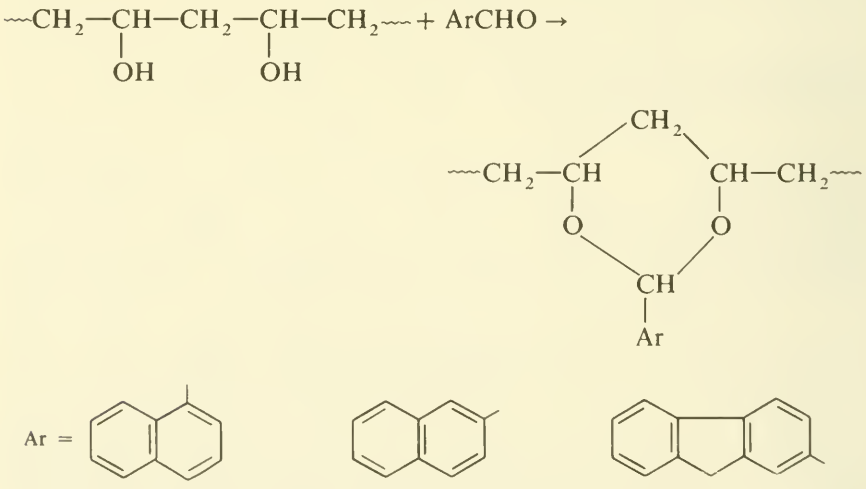

mer obtained by extensive acetal formation on poly(vinyl alcohol) with naphthalene-1- and -2-aldehydes and fluorene-2-aldehyde (Table II).

These data of Schulz and Geissler[82] confirm earlier conclusions of Litt and Summers[83] in respect of complexes derived from polymeric analogues of *N*-methylphenothiazine (**30**) and 4-(methylthio)anisole (**31**).

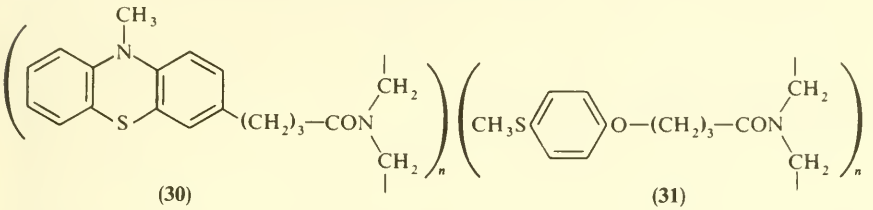

(**30**) (**31**)

Here again the polymers exhibited apparent values of association constants many times greater than those of model compounds although the choice of model (*N*-methylphenothiazine) was not really appropriate to the ring-alkylated phenothiazine polymer. However, independent work by Ledwith and Smith[84] has confirmed that poly(*N*-ethyl-2-vinylphenothiazine) ($K\epsilon$ 1249) appears to be a "better" donor than its model, *N*-ethyl-2-ethylphenothiazine ($K\epsilon$ 932), towards chloranil as acceptor in dichloromethane at room temperature.

Tazuke and collaborators[85] have reported a fairly extensive comparison of donor properties of polymers and appropriate model compounds, and their results illustrate the rather special potential uncertainties arising from estimations of K and ϵ in such systems. In particular these authors found that values of K and ϵ varied according to whether the donor (polymer) or small molecule acceptor was in excess, and this must render meaningless all but the most carefully designed comparisons. Nevertheless important conclusions drawn by Tazuke *et al.*[85] are: (i) the intrinsic donor strength of a group bound to a polymer will not be identical to that of an isolated donor group, the perturbation of adjacent donor groups apparently enhancing the donor strength, and (ii) the possibility of higher order complex formation may contribute to the fact that $K_{D \gg A} \neq K_{D \ll A}$. Thus there may be a special polymer chain effect on complexation by polymeric donors and acceptors, and it is pertinent to consider this possibility in the light of the foregoing discussion of general features of CT complexes.

B. The Polymer Chain Effect on Complex Formation

It is self-evident from the nature of polymer molecules that certain chain conformations will permit formation of higher order complexes, e.g.

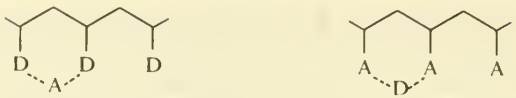

What is not clear is whether the polymeric chain effect would favour symmetrical complexation of, for example, A by two D units (DAD) or unsymmetrical association as in DDA or AAD. Conformational possibilities available to the main polymer backbone could, in principle, assist in the formation of either DAD or DDA types of complex, and it would be useful to be able to distinguish between these two types.

Earlier in this survey we showed how, for the special cases of structurally rigid cyclophanes, stabilization of CT states arises more easily in DDA than in DAD combinations. For polymers, the conformational degrees of freedom are not nearly so restricted as in cyclophanes but, by analogy, it is reasonable to assume greater stabilization of CT complexes by in-chain DDA conformational arrangements.

Irrespective of whether the complex has a DDA or a DAD arrangement, association constants would be expected to provide a quantitative indication of the extent of higher order complex formation, but the existing data suggest that, for currently available methods of determing K and ϵ, it is not useful to make such conclusions. However, there is little uncertainty in determining λ_{max} for CT complexes, and these in turn provide a reliable guide to the ionization energies and electron affinities of donor and acceptor components respectively. It follows therefore that comparison of λ_{max} values for polymeric donors (and acceptors) with those for corresponding model compounds should permit a distinction between possible DDA and DAD types of association since only the former would involve the additional stabilization factor observed for CT states of cyclophanes. In other words, CT complexes of polymeric donors in which DDA association occurs should be characterized by values of λ_{max} at longer wavelengths (lower energies) than those for corresponding complexes of low molecular weight models.

This assumption is supported by the results of Okamoto *et al.*[76] for complexes of carbazole-containing polymers with a number of acceptor molecules, and is entirely consistent with the previously noted conclusions of Tazuke *et al.*[85] for a wider range of polymeric donor types. However, interpretation of the CT spectra of carbazole compounds is complicated by the necessity for a band resolution procedure, as previously outlined, and experimental information from donor–acceptor systems free from such experimental difficulties is desirable. Polymeric donors and model compounds recently synthesized by Ledwith and Smith[84] provide some support. The phenothiazine (**32**) and methoxybiphenyl (**33**) polymers both exhibit λ_{max} at longer wavelengths than the corresponding model compounds.

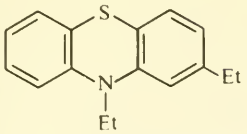

λ(TNF) = 578 nm

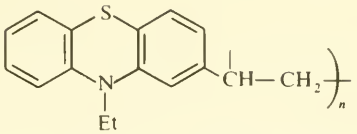

λ(TNF) = 590 nm

(32)

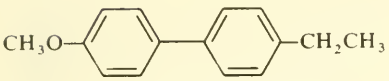

λ(chloranil) = 544 nm

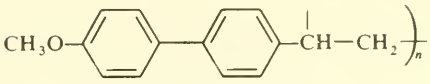

λ(chloranil) = 564 nm

(33)

The result for the phenothiazine polymer is also supported by the data of Gebus and Knoesel[86] who showed that, whereas poly-(2-vinylphenothiazine) formed a complex with tetrachlorophthalic anhydride in dioxan with λ_{max} 540 nm, random copolymers of the same monomer with methyl methacrylate gave comparable spectra with λ_{max} 525 nm. In this case the random copolymers may be taken as good models for the low molecular weight, isolated, counterpart.

Additional evidence for a polymer chain effect has recently been supplied by Iwatsuki and Inukai[87] who synthesized homopolymers of 1-(9-anthryl)-ethyl methacrylate (**34**) and its model counterpart 1-(9-anthryl)ethyl pivalate (**35**). The polymer (**34**) gave a CT complex with chloranil in chloroform solution with λ_{max} 645 nm, whereas the model compound (**35**) gave a similar

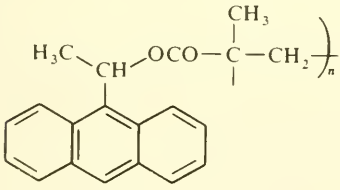

(34)

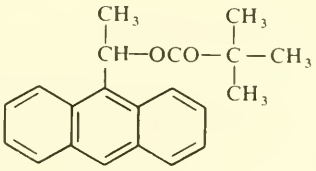

(35)

CT complex at λ_{max} 634 nm. It is significant that copolymers of 1-(9-anthryl)ethyl methacrylate and styrene gave CT spectra with chloranil which exhibited λ_{max} varying from 645 nm for the pure homopolymer to 634 nm, the same as for the model compound. Similar behaviour had been noted[78, 88] for other types of copolymer containing donor units and is to be expected if a real polymer chain effect operates.

It must be emphasized that any polymer chain effect of the kind under

discussion will be greatly influenced by polymer chain conformation which, in turn, will be influenced by both solvent and temperature. Taken with the more obvious variations due to acceptor (and donor) molecular structures, these effects will ensure that the magnitude of differences in λ_{max} for polymers and model compound complexes will vary greatly from system to system. As an example, we may refer again to the optically active models and polymers derived from carbazoles and described in the preceding section (**26**)–(**29**). It may be assumed that identification of peak positions in circular dichroism spectra of CT complexes of these materials (Figs. 3 and 4) is a reliable estimate of the energies of CT transitions for comparable polymer–model compound pairs, and the results reported by Chiellini, Solaro and Ledwith[74] may therefore be taken as unambiguous evidence of a polymer chain effect for the particular systems investigated. Thus for poly-[(*S*)-9-(2-methylbutyl)-2-vinylcarbazole], poly-(**27**), and its model (**27**), λ_{max} for the circular dichroism spectra of CT complexes with chloranil in dichloromethane at 37°C were 560, 730 and 540, 690 nm respectively. Similarly λ_{max} for the circular dichroism spectra of CT complexes of poly-[(*S*)-9-(2-methylbutyl)-3-vinylcarbazole], poly-(**28**), and its model (**28**) with chloranil were 530, 715 and 520, 710 nm respectively. These data help to resolve the ambiguity arising from overlapping CT bands in complexes of carbazole derivatives and support the conclusions of Okamoto *et al.*[76] in respect of non-optically active carbazole polymers.

C. Polymers as Acceptor Molecules

In contrast to the large number of examples of polymeric donors and small molecule acceptors, there are very few reported examples of the inverse combination, e.g. polymeric acceptors and small molecule donors. In fact there have been very few acceptor polymers reported in the literature, and in several of the reported cases apparently no studies of their CT properties were made. Before dealing with specific examples of acceptor polymers, it is worth discussing briefly why there are so few of them.

For vinyl type polymers, where the acceptor function is pendant to the backbone, classical addition type polymerization of monomers is not favoured. Most acceptors, for example, are free-radical inhibitors. Therefore, free-radical techniques are unfeasible in most polymerizations involving acceptor monomers. Anionic polymerization of monomers containing strong acceptor groups generally would fail because of electron transfer reactions. On the other hand, the acceptor function would most likely not interfere with cationic propagation. However, there are few, if any, acceptor monomers known that contain a vinyl group amenable to cationic polymerization. Consequently the best examples of acceptor polymers have been

prepared by condensation or ring-opening techniques. Post-modification of polymers to acceptor polymers has also been employed.

Polymers containing pendant nitrated phenyl groups account for most acceptor polymers. Although there are earlier examples of acceptor polymers, e.g. nitrophenyl acrylates and methacrylates,[89,90] the first example in which the CT characteristics were studied was reported by Smets *et al.*[91] and concerned poly-(2,4-dinitrostyrene) (**36**) as the acceptor. The CT spectrum of this polymer and α-naphthylamine was compared with that of the model

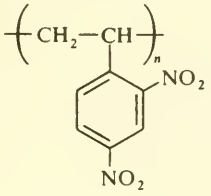

(**36**)

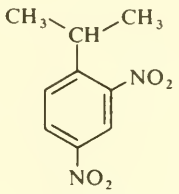

(**37**)

system 2,4-dinitrocumene (**37**) and α-naphthylamine. The absorption maximum in the polymer system was 430 nm compared with 410 nm for the model system. However, the study was complicated because of shifts in the absorption with concentration and time. It was suggested that the initial complex was reacting with another molecule of the primary amine. Consistent with this idea was the observation that the band became more asymmetric with increasing concentration of donor and acceptor. This suggests that more than one equilibrium was involved.

Because of the polymerization problems discussed earlier, the best examples of acceptor polymers, and consequently of their complexes, involve polymers prepared by condensation techniques. Schulz and Tanaka[92] have prepared and studied polyesters based on spiro cyclopropane–tetranitrofluorene units (**38**). (Copolymers of this structure, which result in intramolecular complexes, were also prepared and are discussed in another section.) Complexing studies of this strong acceptor polymer were carried out with both the donor fluorene and the polyester based on fluorene without the nitro groups. The results with the polymer were compared with the model compound (**39**). For this system a CT band in the 400 nm region was observed. From the $K\epsilon$ and K values the polymer appears to complex more efficiently than the model compounds. For example at 410 nm the value of $K\epsilon$ for fluorene as the small molecule donor and (**38**) the acceptor polymer was $603\ \text{mol}^{-2}\,\text{l}^2\,\text{cm}^{-1}$ whereas for the model compound it was $462\ \text{mol}^{-2}\,\text{l}^2\,\text{cm}^{-1}$.

Complexation of a mixture of the acceptor polymer (**38**) with the corresponding polyester without the nitro substituents also, surprisingly, yielded

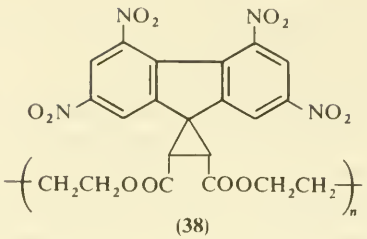

(38)

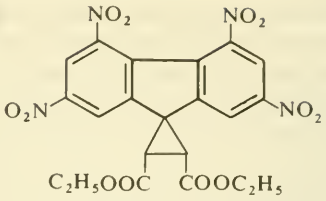

(39)

considerably higher values of $K\epsilon$ than the model compounds or the acceptor-polymer–small-molecule. At 410 nm for the mixture of polymers $K\epsilon$ was 2270 $mol^{-2}l^2\,cm^{-1}$, a value about four times that for either the model compounds or the acceptor-polymer–small-molecule complex. Since these two polymers would be expected to inhibit sterically the overlap of the aromatic chromophores, this result is very surprising. No explanation has been put forward to explain this dramatic effect.

Sulzberg and Cotter described unique acceptor polymers based on nitrated phthalic acid isomers and fluorenone-2,7-dicarboxylic acid derivatives as the acceptor units.[93, 94] These acceptor polymers were described as having excellent mechanical properties. Their CT complex characteristics were evaluated by forming EDA blends with donor polymers. For example the colourless acceptor polymer poly-(hexane-1,6-diol 5-nitroisophthalate) (**40**) turned yellow when combined in a 1:1 mixture with the donor polymer poly(phenyliminodiethanol isophthalate) (**41**). An absorption maximum

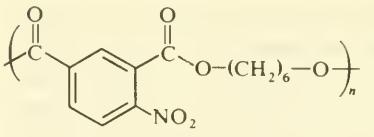

(40)

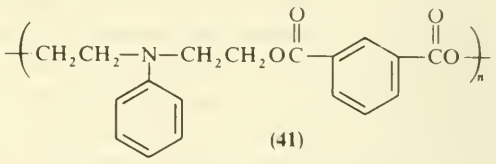

(41)

was noted at 391 nm. In addition the tensile modulus was 260000 for this blend compared with 90000 for the donor polymer and a very low value for the acceptor polymer. Similar results were obtained with other donor–acceptor polymer blends. Solution viscosities of the polymer blends were lower than would have been predicted by averaging the two components. This result was attributed to a decrease in polymer volume due to the inter-chain CT interactions. No studies were reported on the interactions of small molecule donors with these acceptor polymers.

A patent[94] by these authors also described acceptor polymers based on the fluorenone ring system. An example is the polyester based on dinitro-fluorenonedicarboxylic acid and hexanediol (**42**). These polymers would be

expected to be better acceptors than those based on the nitrated phthalic acid derivatives, but no complexing studies with these polymers have been reported other than the EDA blends described in the patent.

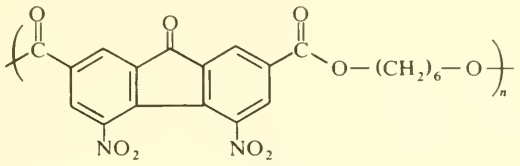

(42)

A new acrylic acceptor polymer, poly-(2,4,7-trinitro-9-fluorenyl methacrylate) (**43**) has recently been prepared and some properties have been studied.[95] With anthracene as donor, a CT band with λ_{max} 495 nm was found. In comparison, the CT complex of the model compound 2,4,7-trinitro-9-fluorenyl acetate (**44**) with anthracene exhibited λ_{max} 475 nm. From a Benesi–Hildebrand determination, $K\epsilon$ at 495 nm for the polymer system was 2000 $mol^{-2}\,l^2\,cm^{-1}$ compared with $K\epsilon$ at 475 nm of 1100 $mol^{-2}\,l^2\,cm^{-1}$ for the model system.

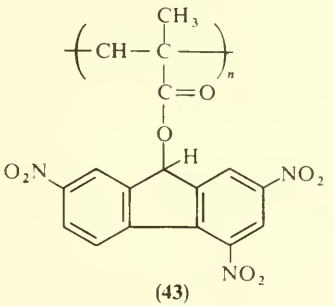

(43)

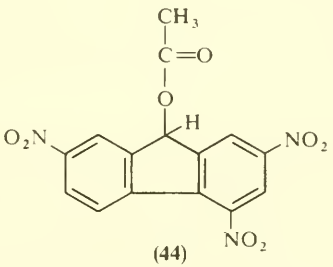

(44)

In a somewhat different vein, insoluble macromolecular acceptors have been prepared and studied by post-modification of insoluble polymeric materials. A divinylbenzene–polystyrene resin was benzylated via Friedel–Crafts techniques and then nitrated to a structure represented by (**45**).[96] This resin used as a column support was useful for separating mixtures of small molecule donors such as naphthalene, anthracene, pyrene, carbazole and other arylamines. CT bands in the 350–500 nm region were observed for these compounds.

Another insoluble macromolecular acceptor recently described is 3,5-dinitrobenzoyl cotton cellulose which was prepared by the reaction of 3,5-dinitrobenzoyl chloride and cellulose yarn in dimethylformamide.[97] Complexing with a series of small molecule donors was studied by measuring

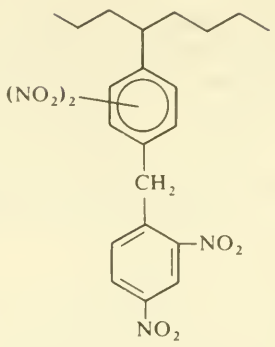

(45)

the weight increase of this material when treated with solutions of the respective donors. Presumably such a material could serve as a column support, although no studies were reported.

D. Polymeric Intramolecular Charge-transfer Complexes

Few examples of intrachain or polymeric intramolecular EDA complexes have been reported. Such copolymers are represented by the general structure (**46**). The donor and acceptor units can either be in the backbone or

—A—D—A—A—D—A—D—D—A—

(46)

pendant to it. The paucity of examples of this type of structure is most likely due to the small number of acceptor monomers available for incorporation into such a copolymer. This type of structure is unique because the influence of the polymer can result in constrained intramolecular interactions. The possible concentration of the complex, in such examples, depends on composition and also on the sequence distribution of the monomer units. When compared with model systems, in the few examples that have been reported, the CT absorption, as a function of concentration of monomer units, has generally been enhanced. Also, in such polymers the absorption decreases linearly with concentration (obeys the Lambert–Beer law) because of the intramolecular nature of the complexes. This is in contrast to the behaviour of intermolecular examples where the concentration of complex and hence the absorption is dependent on the equilibrium constant.

Such an intrachain complex was first reported by Yang and Gaoni.[98] These authors reported 2,4,6-trinitrostyrene to undergo spontaneous copolymerization with 4-vinylpyridine, 2-vinylpyridine or 4-dimethylaminostyrene to give copolymers assumed to have structures (**47**).

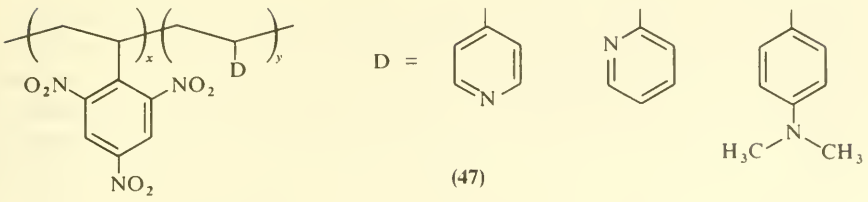

(47)

Schulz and Tanaka[92] recently reported the synthesis of polyesters based on the spiro cyclopropane–2,4,5,7-tetranitrofluorene monomer. The homopolymer based on this spirocyclic tetranitrofluorene group is reported in the section concerning acceptor polymers. Copolymers were prepared with the corresponding non-nitrated fluorene monomer and are represented in (**48**).

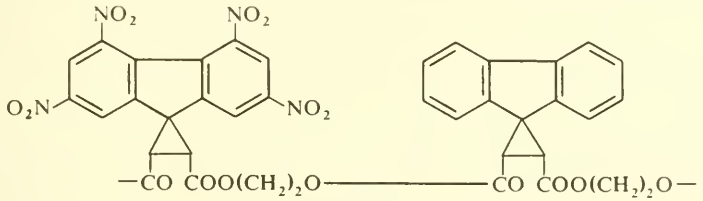

(48)

Polyesters were prepared containing donor to acceptor ratios of 4:1 and 1·4:1. In solution a greenish-brown colour was present and a strong absorption band was observed from 600 to 650 nm. The absorbance was proportional to the concentration of acceptor groups in the copolymer, and thus the authors concluded that the complexation was intramolecular. From model compound studies it was estimated that only about 10 per cent of the available acceptor groups were complexed. The very rigid nature of this copolymer was thought to play a role in its behaviour.

Seanor and Limburg[99] have studied copolymers of *N*-vinylcarbazole and *N*-vinylphthalimide (**49**) prepared by conventional free-radical techniques. A wide range of compositions was prepared and a broad CT band was observed from 350 to 470 nm. This band did not appear for a mixture of the two homopolymers poly-(*N*-vinylcarbazole) and poly-(*N*-vinylphthalimide), and also was absent for the poly-(*N*-vinylcarbazole)–*N*-ethylphthalimide model system. The intramolecular character of the CT interaction was established by observing that the intensity of the band followed the Lambert–Beer law. The composition versus the intensity of the CT complex was proportional to the phthalimide content up to about 50 per cent. At 50 per cent the intensity was less, presumably owing to the random nature of the copolymer and hence fewer adjacent donor–acceptor diads. The intramolecular nature of the CT band was manifested also in a broad, structureless

emission band from 400 to 600 nm. This band was not characteristic of either the carbazole or phthalimide groups. Other donor–acceptor systems were prepared from the *N*-vinylphthalimide–*N*-vinylcarbazole copolymers by first converting the phthalimide group in the copolymer into the primary amine by treating with hydrazine. This was followed by treatment with a halogenated phthalic anhydride. The chlorinated, brominated and iodinated phthalimide structures were prepared. No spectroscopic study of the CT characteristics of these modified copolymers has been made.

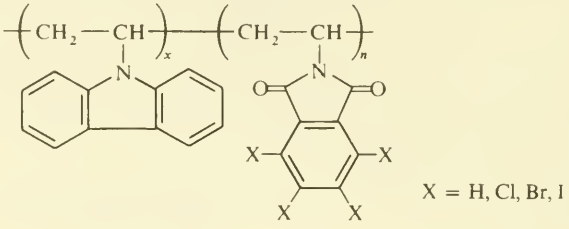

(49)

Tomono, Hasegawa and Tsuchida[100] have recently reported an unusual copolymer that exhibits intramolecular CT complexing. The polymer (**50**), prepared from the Mannich reaction of 2,4-dinitrotoluene, 1,3-di-(4-piperidyl)-propane and formaldehyde, is unique in that the π-type acceptor group is pendant to the backbone while the *n*-type donor is in the backbone. The

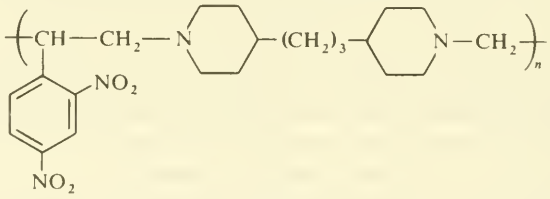

(50)

polymer gave an absorption in the 450–550 nm region similar to the small molecule model system 2,4-dinitrotoluene–*N*-methylpiperidine which gave a band from 490 to 510 nm. Neither chromophore absorbed in this region. The polymer solution obeyed the Lambert–Beer law over a wide range of concentrations. The CT band was destroyed by addition of hydrogen chloride because of the conversion of the piperidine units into their hydrochlorides which are not donors.

Inami, Morimoto and Hayashi[101] nitrated poly(acenaphthylene) (**51**) to various degrees to yield intramolecular donor–acceptor copolymers resulting from complexing of the nitrated and non-nitrated acenaphthylene units along the backbone. The degree of nitration was varied from 7·9 to

40·6 per cent. The copolymers were yellow but no spectral characterizations were made to ascertain if this originated from a CT complex. The greatly enhanced photoconductivity of the nitrated polymers over the non-nitrated poly(acenaphthylene) was attributed to the CT character of the copolymer.

In patents issued to two of these authors, Inami and Morimoto,[102] the

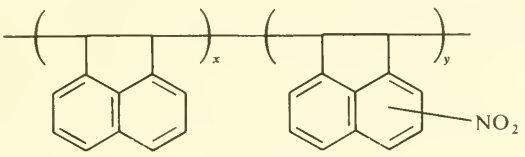

(51)

preparation of this copolymer by copolymerization of acenaphthylene and 5-nitroacenaphthylene is described. No data in support of the claimed structure are presented. In these patents several other examples of donor–acceptor type structures are given and photoconductive properties are claimed.

An equimolar copolymer of 2,4,7-trinitro-9-fluorenyl methacrylate and 1-(2-anthryl)ethyl methacrylate (**52**) has been prepared by conventional free-radical solution polymerization.[103] The copolymer exhibited a strong intramolecular CT band in the 450–550 nm region with λ_{max} at about 490 nm. This absorption was approximately an order of magnitude greater in intensity than that for the model systems anthracene–2,4,7-trinitro-9-fluorenyl acetate and anthracene–poly-(2,4,7-trinitro-9-fluorenyl methacrylate). As in the previously described cases, the intramolecular nature of the interaction was verified by the linear change in the CT absorption with concentration.

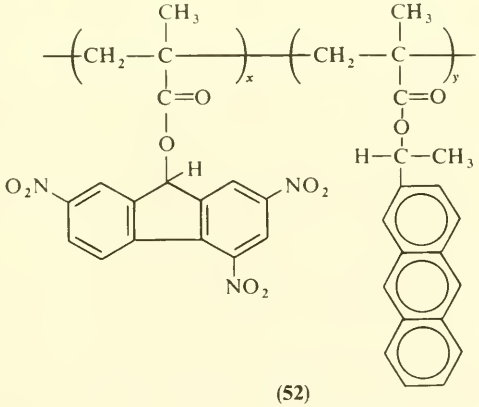

(52)

Other examples of intramolecular polymeric CT complexes are given in the section on electrical properties.

VI. ELECTRICAL PROPERTIES

Organic CT complex solids exhibit electrical properties ranging from those of typical insulators ($\sigma < 10^{-10}\,\Omega^{-1}\,cm^{-1}$) to semiconductors ($10^{-10}\,\Omega^{-1}\,cm^{-1} < \sigma < 10^{1}\,\Omega^{-1}\,cm^{-1}$) and more recently metals ($\sigma > 10^{1}\,\Omega^{-1}\,cm^{-1}$) and possibly superconductors. For complexes in which one or both of the components are polymeric, a similar range of properties, from insulating to semiconducting and metallic, has been achieved, but few commercial applications of polymeric CT complexes exist today, e.g. in electrophotography[104] [poly-(*N*-vinylcarbazole)–2,4,7-trinitrofluorenone (PVK–TNF)] and as a cell electrode [poly-(2-vinylpyridine)–iodine (P2VP–I_2)] in implantable cardiac pacemakers.[105]

The conductivity (σ) of a material is governed by the concentration (density) of charge carriers (n), their electronic charge which may be positive or negative (e), and the velocity of the carrier motion under unit electric field, i.e. a potential gradient of 1 V cm^{-1} (μ):

$$\sigma = ne\mu. \tag{1}$$

The conductivity, σ ($ohm^{-1}\,cm^{-1}$), is the reciprocal of the resistivity, ρ (ohm cm). The velocity of carrier motion is defined as the mobility, μ ($cm^2\,V^{-1}\,s^{-1}$). The carriers can be positively (holes) or negatively (electrons) charged, and can contribute independently to the current flow, i.e.

$$\sigma = n_+e_+\mu_+ + n_-e_-\mu_-$$

In order to understand and to control the conduction process it is necessary to know both the number and type of the charge carriers and their mobility, as well as the dependence of these parameters on variables such as temperature, applied field, etc. There are very few polymer based systems where these parameters have been clearly separated, one notable exception being poly-(*N*-vinylcarbazole) (PVK)[106] and a number of PVK–acceptor combinations.[107, 108] In general, it has been found that in polymeric CT complexes it is possible to achieve high values of n but not of μ. The development of a material exhibiting a high mobility, particularly at low applied fields, remains perhaps one of the greatest challenges in polymer science.

Charge transport in organic molecular solids results from transfer reactions of electrons (viewed in this molecular picture as radical anions) or holes (radical cations) through the appropriate weakly interacting (van der Waals forces) molecular states. In highly ordered ultra-pure systems such as single crystals, the electron transfer processes will occur with essentially equivalent rates, and the mobilities are clearly defined and generally high, e.g. anthracene[109] $\mu_+ \approx \mu_- \approx 1\ cm^2\,V^{-1}\,s^{-1}$, *N*-isopropylcarbazole[110] $\mu_+ \approx$

$\mu_- \approx 10^0$–10^{-1} $cm^2 V^{-1} s^{-1}$, pyrene–TCNE (1:1)[111] $\mu_+ \approx \mu_- \approx 10^0$–$10^{-2}$ $cm^2 V^{-1} s^{-1}$. The polymeric environment, however, imparts a high degree of both chemical and physical disorder, and therefore the electron transfer processes do not take place at the same rate and may actually involve different molecular species. This variation in electron transfer rates results from fluctuations in the interchromophore orientation and overlap and from inherent and adventitious chemical impurities (end groups, catalyst fragments, etc.). In such systems the charge transport process can be highly dispersive. Mobilities measured in polymers are very low, in the range 10^{-5} $cm^2 V^{-1} s^{-1}$, and they exhibit[112] strong electric field and temperature dependence.

Recent studies of transport in disordered amorphous molecular glasses, e.g. 2,4,7-trinitrofluorenone[113,114] (electron transport) and 1,3-diphenyl-5-(*p*-chlorophenyl)pyrazoline[115] (hole transport), indicate mobilities somewhat higher than those reported for amorphous polymeric materials. In amorphous TNF[113,114] electron mobilities in the range 10^{-4}–10^{-5} $cm^2 V^{-1} s^{-1}$ (at field of $\sim 5 \times 10^5$ $V cm^{-1}$) were reported, and the field dependence was similar to that measured for PVK and for the PVK–TNF combination.

The charge carrier can become localized or trapped during its transit across the sample. In this state it no longer contributes to the current flow. Once a carrier becomes trapped it can function as a recombination centre for carriers of opposite sign, it can acquire sufficient energy to escape from the trapping site or it can remain effectively trapped. The overall effect of trapping is to reduce the effective mobility of the carriers in the sample. Traps are usually defined in terms of their depth, i.e. shallow and deep, which is a crude measure of the ease with which the trapped carriers can escape. Our knowledge of the nature and the level of traps in organic molecules is weak, but it is clear that two kinds of trap exist. These are *chemical* (impurity molecules with lower ionization potential than the host transport molecules which constitute hole traps, and impurity molecules with higher electron affinities which constitute electron traps) and *physical* (structural defects such as chain folds, crystallite boundaries and chain ends which can cause discontinuities in the transport pathways). Even the most highly purified, single-crystal organic materials do not approach the state of purity of electronic grade silicon or germanium. The attainment of polymer based materials with high degrees of system purity and structural perfection is even more unlikely, particularly if processability is also a requirement.

Electronic transport in organic polymeric materials can be visualized as a series of electron-transfer reactions between the active molecular species. A detailed analysis is beyond the scope of this review, but a qualitative picture of the process can be obtained by considering a polymer possessing pendant

functional groups (B):

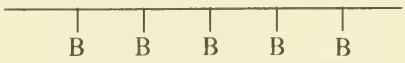

When a free carrier is introduced into such a molecular array (the carrier source can be ignored for the purpose of this argument) the transport will be governed by such factors as the molecular energy levels of B, the nature and distribution of the electronic overlap between the B sites, the molecular polarizability of the dielectric medium surrounding the carrier, the vibrational relaxation associated with removing ($B \rightarrow B^{+} + e$) or adding ($B + e \rightarrow B^{-}$) an excess electron to the molecular state, and the spin distribution of the unpaired electron in the ionized species (B^{+} or B^{-}). Chemical and physical disorder, as well as variables such as applied field, temperature etc., will also play a role. The transport process can be idealized as a series of electron exchanges between favourable adjacent B molecules, e.g.

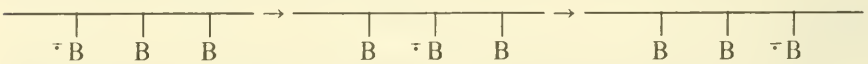

For hole transport the corresponding $B–B^{+}$ couple is invoked.

The neighbouring B sites can be on the same or different polymer chains. At our present level of understanding of the amorphous polymeric state, any attempt to differentiate between *intra-* and *inter-*molecular exchange is totally meaningless. It is perhaps more appropriate to consider any molecular solid, polymeric or not, as simply an array of transport sites. The function of the polymeric chain then is to control the microstructure and hence the nature and degree of interaction of the molecular species involved in charge transport. Exchange involves a hopping or tunnelling type process between ionized and non-ionized states. From a molecular orbital point of view the states involved are the highest occupied (HOMO) and the lowest unoccupied (LUMO) for holes and electrons respectively. In principle, provided that charge carriers can be introduced into the system, all polymers are intrinsically capable of transporting both holes and electrons. In practice, however, polymers generally exhibit unipolar transport characteristics, i.e. hole or electron transport is favoured. The vinylcarbazole polymers and model compounds illustrate this point. Both hole and electron transport were measured[110] in single crystals of the model compound *N*-isopropylcarbazole (NIPC), $\mu_{+} \approx 0{\cdot}33$ and $\mu_{-} \approx 1{\cdot}0\,cm^{2}\,V^{-1}\,s^{-1}$. In the vinylcarbazole polymers[116] and in molecular dispersions of NIPC in polycarbonate,[117] however, only hole transport has been observed and this has been attributed[118] to the strong electron trapping effects resulting from

oxygen and/or oxidative impurities having higher electron affinities than the carbazole chromophore. The equivalent but inverse situation can be envisaged in materials where electron transport predominates. In the case of CT complex systems the situation is somewhat different. The transport states need not be determined by the electronic structure of one molecular species, but can be assigned to the two components, i.e. the HOMO of the donor function to hole transport and the LUMO of the acceptor to electron transport. The electrical properties of this class of material will then be governed primarily by the concentration and distribution of the free and complexed components and by the nature of the ground state of the complex. Compared with single component systems, CT complexes exhibit enhanced long wavelength light absorption characteristics, and the efficiency of photo-induced formation of charge carriers may be enhanced by the ability of the donor and acceptor units to stabilize positive and negative carriers respectively. These factors are of obvious importance in practical applications of CT complexes, e.g. photoconductivity.

In CT complexes, monomeric or polymeric in nature, there exists a gradation in the degree of electron transfer in the ground state. It has been commonly assumed that weak complexes, where charge transfer plays a minor role in the formation of the ground-state complex, possess high resistivities. At the other extreme, strong complexes, which exist as salts in their ground states as a result of complete electron transfer, tend to be associated with low resistivities. There are many intermediate cases. Perhaps the best known examples of the ion-radical or charge-transfer salts are those involving tetracyanoquinodimethane (TCNQ) where conduction characteristic of an insulator, a semiconductor and a metal have been reported.[119] The formation and existence of ionic ground-states is therefore no guarantee of high conductivity in organic materials.

The theoretical problem of describing the transport of charge in disordered polymeric systems requires a detailed microscopic understanding of the relationship between structure and local electron transfer processes. The lack of reliable electrical conductivity measurements, plus our inadequate knowledge of polymer microstructure/morphology, have severely hindered progress in this area. It has been generally accepted that the transport of charge in organic materials occurs via a hopping process between localized molecular states, and a number of empirical hopping and tunnelling models have been suggested. Seki[120] and Scher and Montroll[121] have provided theories of transport processes in disordered systems which are claimed to account for the observed transport characteristics of PVK, PVK–TNF and other materials. With the emergence of more reliable experimental data on different systems there will probably be considerable progress in this area.

A. Experimental Techniques

The standard techniques used to study the electrical properties of organic materials have been detailed by Gutmann and Lyons[122] and Meier.[123] The usual measurement involves a determination of the current flowing through a sample under some given set of conditions. Surface or sandwich type cells are commonly employed. With high resistivity materials extreme caution must be exercised, particularly with respect to sample preparation, electrode formation and electronic circuitry.

Film-forming organic polymeric materials are considerably easier to evaluate than those requiring compaction into a suitable structure. With these polycrystalline or intractable samples the problems of ensuring particle–particle contact and reliable electrode formation are severe. Materials that form uniform, coherent films (by solvent coating, vacuum evaporation, etc.) are more amenable to investigation and generally provide more reliable data. As an example, the agreement in the electrical parameters of PVK and some PVK–acceptor combinations (which have been coated from a variety of solvents) measured by several independent investigators has been remarkable (see e.g. refs. 108 and 113).

Equation (1) shows that the conductivity of a sample is the product of two terms, n and μ, which are independent variables. Any interpretation of the conduction process that does not clearly separate n and μ, and their dependence on the experimental parameters, is dangerous. Comparison of the σ or ρ values within a series of related materials is certainly useful in establishing some level of activity. Its usefulness in providing mechanistic and structural correlations is, however, extremely limited. Unfortunately, much of the published work is of this nature, and this paucity of reliable experimental data is reflected in our current understanding of electronic conduction in organic materials. A limited number of experimental techniques have been developed to probe the number and the mobility of charge carriers in organic solids.

1. Dember Technique

In the Dember technique, the voltage across an organic material sandwiched between two transparent (or semitransparent), insulated capacitor plates is measured when one of the electrodes is illuminated. A modulated light source is employed and the wavelength is chosen to be strongly absorbed and to produce charge carriers at the interface. It is necessary in this technique to establish a carrier concentration gradient away from the illuminated electrode. Carriers with the highest mobility diffuse into the bulk of the material to create a potential difference between the sample bulk and the illuminated electrode. Application of a further constant voltage facilitates the

measurement of the small Dember voltage. The sign of the photovoltage gives the nature of the majority carrier, i.e. holes or electrons. In systems where the two carriers exhibit equivalent mobilities ($\mu_+ \approx \mu_-$) the photovoltage is too low to be detected. In low mobility organic materials, perturbations can arise from surface states (electrode effects), and there are many reported examples of inconsistencies with other experimental measurements (Seebeck coefficient, Hall effects, etc.).

2. Hall Technique

When any sample carrying a current is placed in a magnetic field, an electric field builds up perpendicular to both the current flow and the magnetic field. This is the Hall effect and it can be used to diagnose both the nature of the majority carrier and its mobility in organic solids. With high resistivity and low mobility materials the measurement of the Hall effect is extremely difficult. When both holes and electrons are active in carrying the current, the analysis of the data is even more complex.

The mobility determined from the Hall measurement is defined as the Hall mobility, μ_H, which is related to the drift mobility, μ, in the absence of any charge-trapping phenomena, but the two need not be equivalent.

3. Thermoelectric Effect; Seebeck Technique

The value of the thermoelectric potential in an organic material can provide information on both the nature and the mobility of the majority carriers. In the Seebeck technique a voltage difference is produced in an electroded sample in which a temperature gradient is maintained. The voltage difference divided by the temperature difference ($\Delta V/\Delta T$) is the Seebeck coefficient, Q. The voltage is produced as a result of the more mobile carriers diffusing from the hot to the cold regions of the sample. In organic materials the potential differences are generally very low (mV–μV range) and difficult to measure accurately. The Seebeck coefficient can give the sign of the majority carrier and some measure (order of magnitude) of the mobility. When both carriers contribute to the current the thermoelectric potential is zero.

All these techniques have been applied, with varying degrees of success, to the measurement of n and μ in organic materials. The techniques are difficult and the data often ambiguous. Two methods that have proved particularly successful and reproducible in probing the conduction process in high resistivity organic polymeric films are xerographic discharge measurements and transient-photocurrent or time-of-flight measurements. These are discussed in the following section.

4. Xerographic Technique

There are two variations of the xerographic discharge technique commonly

used. The first [see Fig. 5(a)] involves corona charging of the surface of a thin polymer film, which is generally solvent cast on a suitable conductive substrate, e.g. aluminium, and monitoring the decay in surface potential following exposure with a pulse of light of appropriate energy. The change in voltage during some time increment is measured, and from this the drift

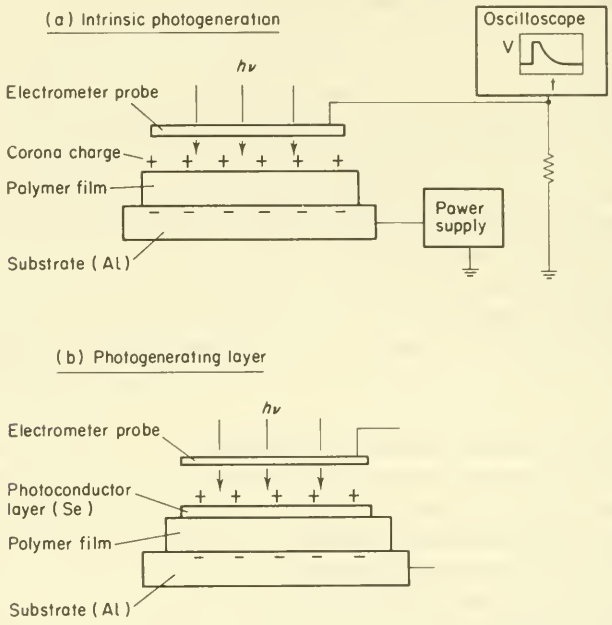

FIG. 5. Schematic diagram of the xerographic discharge apparatus for measuring the electrical properties of polymeric films, (a) utilizing intrinsic photogeneration, and (b) utilizing a thin overlayer of an efficient photogenerating material.

mobility can be calculated. This method requires that the absorbed photons generate charge carriers within the sample, and information on photogeneration processes as well as charge transport processes can be obtained. It has been applied both to PVK films[106] and to films of PVK doped with TNF[104] up to 1:1·1 mole ratios of PVK to TNF. The experimental details and the analysis of the data can be found in these publications.

In the second type of xerographic measurement [Fig. 5(b)] a thin layer of a highly efficient photogenerating material, e.g. selenium, is coated on the surface of the sample. This structure is corona charged and exposed with appropriate illumination. The rate of decay in the surface potential provides information both on the injection of charge carriers from the sensitizing

layer into the sample and on their transport through the material. This technique has been applied to many polymeric materials.[113, 116, 124] Provided that the transport levels in the sensitizer are known, information on the transport levels in the sample can also be obtained, e.g. PVK and TNF.

Some typical photoinduced discharge curves (PIDC) are reproduced in Fig. 6. Numerical differentiation of these voltage–time curves can then be

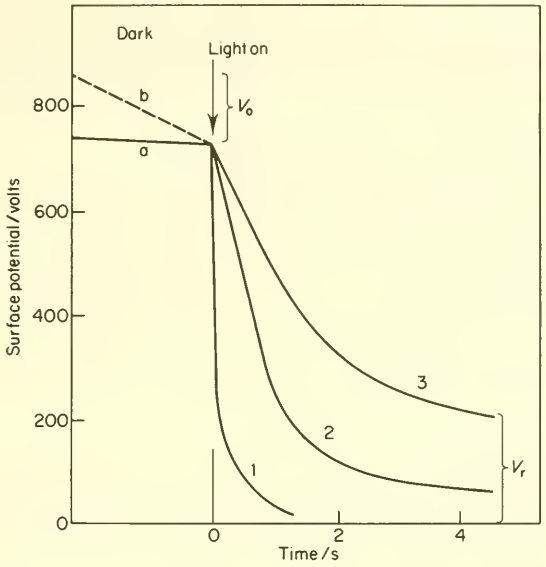

FIG. 6. Some typical photoinduced discharge curves (PIDC) from xerographic discharge technique measurements showing low (a) and high (b) dark decay, and high (1), intermediate (2), and low (3) light decay with increasing residual voltages (V_r) (V_0 = initial charging potential).

used to generate plots of $|dV/dt|$ versus E (electric field). Alternatively the film can be charged to a series of V_0 values and the initial slope of the discharge curve measured to generate $|dV/dt|_{t=0}$ versus E plots. The combined data from both analyses provide fundamental information about charge-carrier mobilities and their field and temperature dependence as well as charge-carrier trapping phenomena.

The current density (J) in the sample under the open circuit conditions of this experiment is related to the discharge rate, $|dV/dt|$, by the expression:

$$J = -C|dV/dt|$$

where C is the capacitance of the sample. There are two important limiting cases which should be considered. Depending on the initial electric field and

the light intensity, the discharge rate may be controlled by the rate of photoproduction of carriers, or the charge-carrier mobility in the sample. Since the photogeneration of charge carriers in a sensitizing layer such as selenium has been measured under a wide range of experimental conditions (electric field, temperature, sample thickness, etc.) this approach tends to be somewhat more convenient and is applicable to materials in which the photogeneration of carriers is very inefficient or has not been investigated in any detail.

In the case where the discharge rate is determined by the rate of production of charge carriers, the current is termed "emission limited" (J_e) and is given by:

$$J_e(\mathrm{E}) = \eta(\mathrm{E})eI$$

where η is the quantum efficiency of supply of carriers and is equal to the quantum efficiency of photogeneration in the absence of free carrier recombination or other loss processes, e is the electronic charge and I is the light intensity (photons $\mathrm{cm}^{-2}\,\mathrm{s}^{-1}$). In the case where the discharge rate is governed by the carrier mobility in the sample, the current becomes "space charge limited" (J_s). When there is no appreciable trapping in the sample, the current is given by the Childs law expression for a trap-free situation:

$$J_s = \mu(9/8)\epsilon'(V^2/l^3)$$

where ϵ' is the sample dielectric constant and l is the film thickness. Trapping effects during the discharge process can have a significant effect on the current flow, and a more complex analysis is required to evaluate carrier mobility and extract information on the nature and level of the trapping states. A recent review[125] describes in detail the application of space charge limited current (SCLC) theory to the study of electronic conduction in polymers.

5. Transient Photocurrent Technique[111]

In the time-of-flight or transient-current apparatus (Fig. 7) a high intensity, short duration light pulse of appropriate energy is applied through the semitransparent electrode to generate free carriers in the surface layer of the sample. A voltage step is applied across the sample just prior to the light pulse, and the transient current in the system is conveniently displayed on an oscilloscope. The transit times (τ) of the carriers are located and the carrier drift mobilities calculated using the expression:

$$\mu = l^2/V\tau$$

where l is the sample thickness and V is the applied voltage. These measurements can be made under both emission and space charge limited conditions.

Hole and electron drift mobilities in PVK[126] and the PVK–TNF complex[108] as a function of acceptor loading have been measured in several laboratories by both the transient current and xerographic techniques. The excellent agreement[108, 113] between the two sets of data attests to the reliability of the two techniques for evaluating charge carrier transport and trapping phenomena in organic materials.

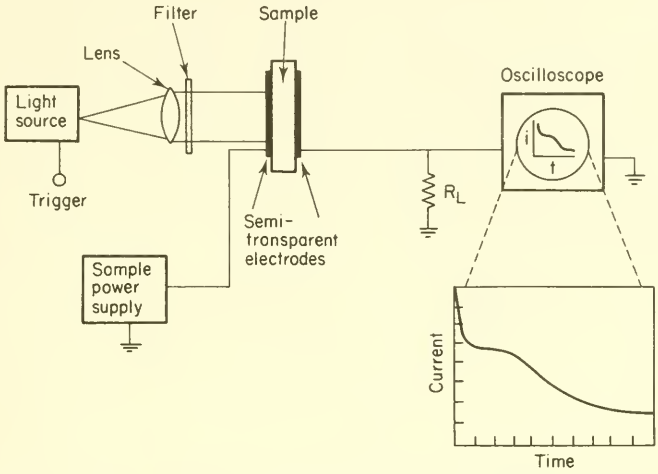

FIG. 7. Schematic diagram of the transient-photocurrent–drift mobility apparatus showing a typical current transient signal with the cusp defining the arrival of the fastest charge carriers at the collecting electrode.

B. Donor Polymers with Small Molecule Acceptors

1. Poly-(N-vinylcarbazole) (PVK) Systems

The combination of a polymeric donor and a small molecule acceptor has been the most widely studied of all the polymeric CT complexes, and poly-(*N*-vinylcarbazole) has been one of the most popular polymers. The electrical and photoelectrical properties of poly-(*N*-vinylcarbazole) (PVK) have been studied intensively since Hoegl[127, 128] first reported its unusual activity. The early work[129, 130] was mostly directed towards increasing the visible light photosensitivity of the polymer by doping with low levels (up to 10 mole per cent) of acceptor molecules. In this acceptor concentration range the hole transport characteristics of the donor polymer were not appreciably changed by the acceptor additive. The studies of Regensburger,[106] Pai[126] and Mort[131, 132] have considerably clarified electronic transport in PVK, and this is probably the only polymeric material for which the energy levels of the conducting states are known with any certainty.

Recently these investigations have been extended to the related vinylcarbazole polymers, poly-(3-vinyl-*N*-alkylcarbazole) (P3VK) and poly-(2-vinyl-*N*-alkylcarbazole) (P2VK) in an attempt to probe the role of polymer structure on the hole transport characteristics of these carbazole polymers.[116]

One of the first comprehensive studies of the electric and photoelectric properties of a polymeric CT complex solid was by Rembaum and Hermann[107] who investigated the PVK–I_2 system and also the PVK–TCNE system. From a comparison of the solution spectroscopic characteristics of PVK–I_2 and the model system *N*-ethylcarbazole–I_2 it was concluded that 1:1 complexes are formed. However, it was clearly recognized that, in the solid state, complex formation was incomplete, and free carbazole groups and free iodine molecules were present as well as possible multiple complexes. In compressed powders of the polymeric complex materials, conductivities were as high as $10^{-5}\,\Omega^{-1}\,cm^{-1}$. Hall mobility measurements[107d] indicated electron transport with mobilities in the range $0{\cdot}5\,cm^2\,V^{-1}\,s^{-1}$. Subsequent transit time measurements[107e] indicated $\mu_- \approx \mu_+ \approx 2 \times 10^{-2}\,cm^2\,V^{-1}\,s^{-1}$ for the PVK–I_2 complexes, and $\mu_- \approx \mu_+ \approx 1 \times 10^{-1}\,cm^2\,V^{-1}\,s^{-1}$ for the PVK–TCNE complexes. Dember voltage measurements suggested electrons as the majority carrier, while Seebeck coefficients were consistent with hole transport. These discrepancies are probably due to *n*-type surface phenomena to which the Hall and Dember measurements are particularly sensitive. All these mobility values are anomalously higher than reported values for μ_+ and μ_- in PVK and PVK–TNF (2,4,7-trinitrofluorenone) films. The high conductivities in these polymeric aromatic amine–iodine complexes are more consistent with charge migration along I_3^- like chains with little contribution from the organic radical cations (carbazole).

Esr measurements[107a] of this polymeric complex also revealed an increase in the free spin concentration as the concentration of I_2 increased. This paralleled the increase in conductivity. However, the free spin concentration is considerably higher (by $\sim 10^4$) than any realistic charge-carrier concentration, and the two phenomena appear not to be correlated. It is likely that the esr signals arise from paramagnetic centres produced in some manner in these samples and are not associated with charge-transport states.

Block *et al.*[133] have reported that the conductivity of PVK can be substantially increased by incorporating carbazole cation radical centres into the polymer. This was achieved by an oxidative procedure, using tri-(*p*-bromophenyl)aminium cation-radical salts as the oxidizing agent, to produce 3,3′-dicarbazolyl type radical cation crosslinks. In this case the conductivity was controlled by the radical cation content, and values as high as $\sim 10^{-5}\,\Omega^{-1}\,cm^{-1}$ were achieved at ~ 10 mole per cent level. Problems

with insolubility and material stability hindered investigations at higher radical cation concentrations.

The PVK–TNF (2,4,7-trinitrofluorenone) combination is the most thoroughly investigated polymer complex system.[104, 108] It is almost unique in that very high loadings (up to 1·2 moles of TNF per mole of vinylcarbazole repeat unit) of TNF can be accommodated in the amorphous polymeric solid without phase separation or crystallization of the small molecule. Many other acceptor molecules will form complexes with PVK, but these generally phase separate from the polymer at loadings higher than 10–20 mole per cent. Because the PVK–TNF complex can also be readily solvent cast into thin homogeneous films it is an ideal system for determining the electrical and spectroscopic properties over a wide range of composition.

Weiser[134, 135] carried out a detailed spectroscopic and mass density analysis of the PVK–TNF amorphous films in order to establish the composition (complexed and non-complexed components) of the solid. Absorption and electroabsorption measurements in the region of the CT absorption band were carried out on amorphous films (solvent cast) with increasing TNF/carbazole ratio. The absorption spectra of thin films are shown in Fig. 8 over the TNF–PVK composition range (molar) 0·1:1 to 1:1. It is

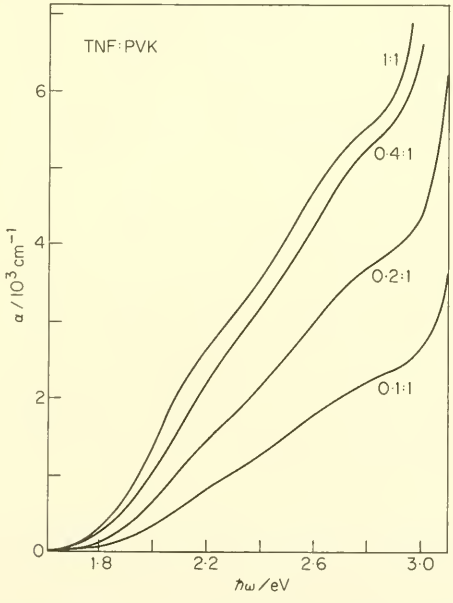

FIG. 8. Charge-transfer absorption spectra of TNF–PVK films with different molar ratios of TNF to PVK. [Reproduced with permission from G. Weiser, *J. Applied Physics*, **43**, 5018 (1972).]

evident that the absorption of the CT band increases appreciably with increasing TNF concentration. Above a ratio of 0·4:1, however, the absorption saturates and increases only slightly with increasing TNF. The electroabsorption spectra of the same amorphous films (Fig. 9) exhibit essentially the same saturation behaviour around a 0·4:1 molar ratio.

FIG. 9. Electroabsorption spectra (field induced change of the absorption constant, α) of TNF–PVK films with different molar ratios of TNF to PVK. [Reproduced with permission from G. Weiser, *J. Applied Physics*, **43**, 5028)1972).]

Both spectra are consistent with those measured in solution, exhibiting two CT absorption bands (at 2·17 and 2·83 eV in the solid state) originating from transitions between localized molecular states. The change in the absorption with increasing TNF concentration was used to estimate the degree of complex formation in the solid film. The procedure is similar to

that commonly used in solution studies. Table III shows the densities of the CT complexes, the free carbazole and free TNF molecules in films of different TNF/PVK ratios.

These values were derived from analysis of the spectra, assuming only

TABLE III. Densities of uncomplexed carbazole groups and TNF molecules and of charge-transfer complexes in TNF–PVK films of different TNF loadings

Molar ratio TNF:PVK	$N/10^{20}$ cm^{-3} Free TNF	Free PVK	Complexes	% TNF complexed
0:1	36·2			
0·1:1	30·6	0·93	2·37	71·8
0·2:1	25·9	1·96	4·00	67·3
0·4:1	19·0	3·93	6·10	60·7
0·6:1	14·9	6·30	6·60	51·2
0·8:1	12·0	8·20	6·45	45·9
0·9:1	10·8	9·05	7·01	43·7
1:1	9·9	9·9	7·00	41·5
1·1:1	9·1	10·7	6·40	39·2

localized excitation of the complex, and from the mass density measurements. The only other assumption was that formation of the complex maintains the chemical equilibrium:

$$\text{PVK} + \text{TNF} \rightleftharpoons [\text{PVK–TNF}]\ \text{complex}$$

with the slow solvent evaporation during formation of the film. This latter assumption may not be totally valid, particularly at higher concentrations of TNF in the films.

Figure 10 shows the ratios of the three components (CT complex and uncomplexed carbazole and TNF molecules) in films of different TNF/PVK ratios. It is interesting that, whereas some 72 per cent of the TNF molecules are complexed in 0·1 : 1 TNF–PVK films, only some 40 per cent are complexed in the 1:1 films. With the uncertainties in the changes occurring during formation of the films from solution, these are likely to be upper limits, but this does represent the first detailed compositional analysis of a solid polymeric CT complex.

The electroabsorption spectra (Fig. 9) show a field induced increase in the absorption constant α in the region associated with the CT complex. This increase is too great to be accounted for by an increase in the polarizability of the excited state of the CT complex. A more realistic explanation would be the formation of a significant molecular dipole in the complex resulting from appreciable electron exchange on excitation, with obvious implications for the photogeneration of charge carriers in this system.

Rochlitz[136] carried out an independent esr investigation of the PVK–TNF system. Irradiation (in the CT band) of thin films at low temperatures (below −40°C) results in formation of paramagnetic species. The esr spectra were structureless, but were assigned to the TNF radical anion ($TNF^{\cdot-}$). The signal intensity decreased with increasing temperature and increased with

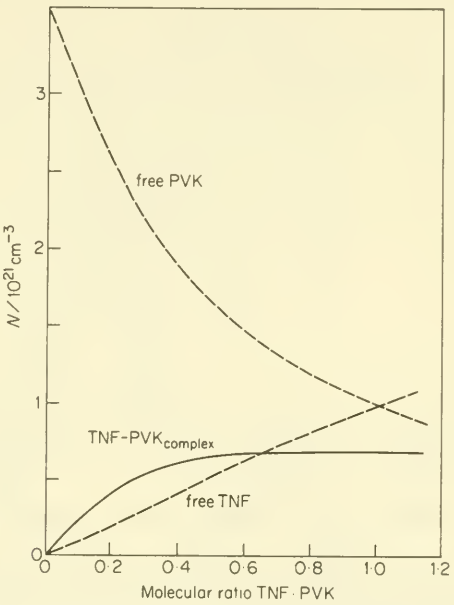

FIG. 10. Densities (N) of complexed molecules, of free TNF molecules and of free PVK units in amorphous TNF–PVK films. [Reproduced with permission from G. Weiser, *J. Applied Physics*, **43**, 5028 (1972).]

increasing TNF loading up to PVK to TNF ratios of 1:1. Parallel photoconductivity studies on films of equivalent composition revealed a correlation between the esr signal intensity and the photocurrent. These results were rationalized using a model in which excitation of the complex results in an electron-transfer reaction to produce the corresponding ion radical pair.

The TNF radical anion is stabilized at higher TNF loadings by electron exchange with neighbouring neutral TNF molecules. If one assumes that this state is the precursor to formation of free charge carriers (facilitated by the presence of an electric field), then the correlation between esr signal intensity and photocurrent can be explained. No explanation for the fate of the corresponding carbazole radical cation species was presented.

Detailed studies of the electrical properties of a series of PVK–TNF films were carried out by Gill.[108] Over the range of film compositions from 0·1:1 to 1:1, both hole (Fig. 11) and electron (Fig. 12) mobilities exhibit an identical field dependence even though within each series the drift mobilities vary by several orders of magnitude. The temperature dependence was also

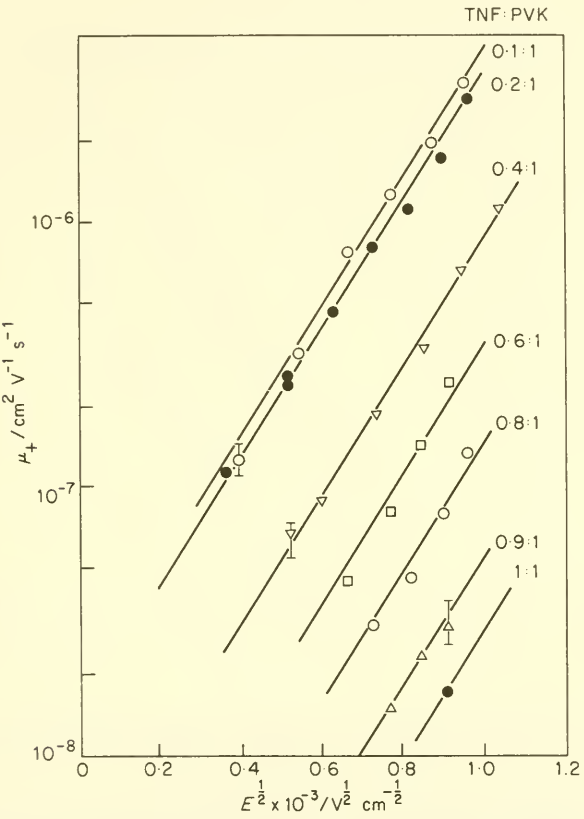

FIG. 11. Field (E) dependence of hole drift mobilities (μ_+) for TNF–PVK films of a series of compositions. [Reproduced with permission from W. D. Gill, *J. Applied Physics*, **43**, 5033 (1972).]

similar and showed that both the electron and hole mobilities are activated processes with significant activation energies. Zero field activation energies, E_0, for both hole and electron mobilities were estimated to be in the range 0·65–0·70 eV for films varying from pure PVK to 1:1 PVK–TNF.

Although both the field and temperature dependence of the mobilities were essentially independent of film composition, the drift mobilities were very sensitive to the PVK/TNF ratio. Figure 13 shows the variation in the

hole and electron drift mobilities in PVK–TNF films of different composition. The results of several independent investigators, using xerographic and time-of-flight techniques, clearly show (Fig. 13) that the hole mobility in PVK decreases as the TNF content increases: $\mu_+(\text{PVK}) \approx 10^{-6}\,\text{cm}^2\,\text{V}^{-1}\,\text{s}^{-1}$ ($E = 5 \times 10^5\,\text{V cm}$), $\mu_+(\text{PVK–TNF } 1{:}1) \approx 10^{-9}\,\text{cm}^2\,\text{V}^{-1}\,\text{s}^{-1}$. As the

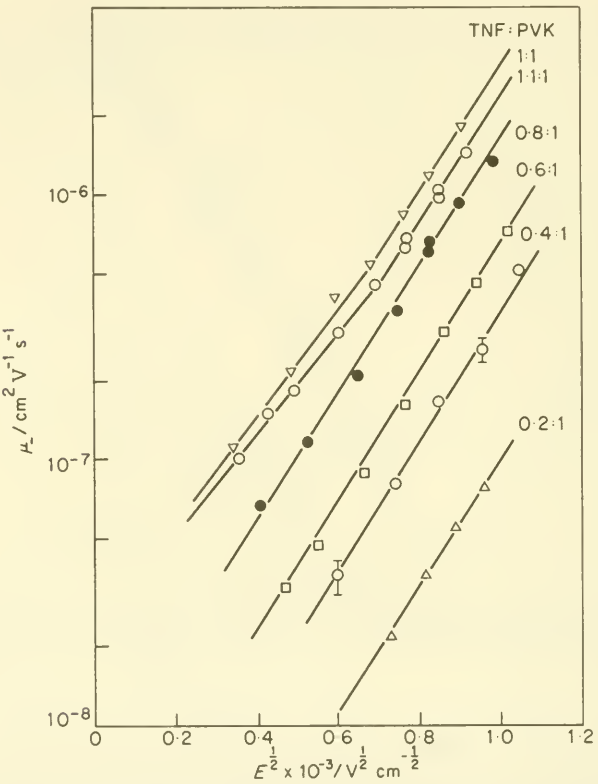

FIG. 12. Field (E) dependence of electron drift mobilities (μ_-) for TNF–PVK films of a series of compositions. [Reproduced with permission from W. D. Gill, *J. Applied Physics*, **43**, 5033 (1972).]

TNF content increases, the electron mobility becomes measurable and increases: $\mu_-(\text{PVK–TNF } 1{:}0{\cdot}1) \approx 10^{-9}\,\text{cm}^2\,\text{V}^{-1}\,\text{s}^{-1}$, $\mu_-(\text{PVK–TNF } 1{:}1) \approx 10^{-6}\,\text{cm}^2\,\text{V}^{-1}\,\text{s}^{-1}$. Measurement of electron transport[114] in pure amorphous films of TNF (prepared by a rapid quenching technique) gave drift mobilities in the range $4 \times 10^{-5}\,\text{cm}^2\,\text{V}^{-1}\,\text{s}^{-1}$ at fields of $5 \times 10^5\,\text{V cm}^{-1}$, with the same field dependence as in the PVK and PVK–TNF films. No hole transport was detected in the TNF films.

The hole/electron mobility results, in conjunction with the film composition data of Weiser,[134] provide key insights into the transport mechanism in these polymeric complex systems. The immediate conclusion is that hole transport is associated with the PVK (or the carbazole) component and electron transport with the TNF component. The electronic properties are

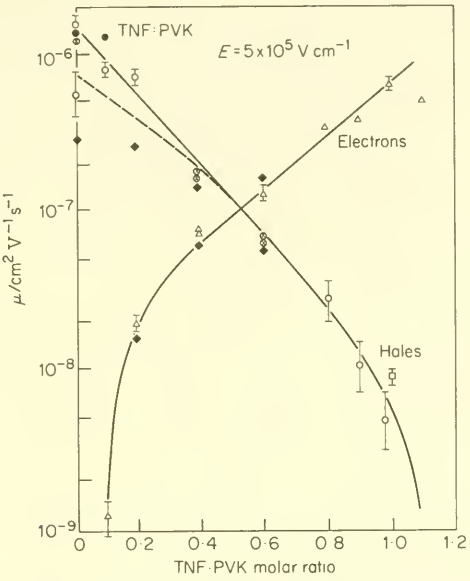

FIG. 13. Variation of hole (μ_+) and electron (μ_-) drift mobilities with TNF to PVK molar ratio in films of TNF–PVK; from ● Pai,[126] ⊗ Regensburger,[106] ◆ Mort and Emerald,[113] □, △, ○ Gill.[108]

very dependent on film composition: (a) below TNF/PVK ratios of 0·3, hole transport dominates; (b) for TNF/PVK ratios of 0·3–0·7, both hole and electron transport, with comparable mobilities, are observed; (c) above TNF/PVK ratios of 0·7 (up to the 1:1 limit where TNF phase separation occurs) electron transport is more efficient.

Figure 14 shows the effect of TNF content on the electron mobilities in PVK films and also in a non-complexing polyester matrix. Clearly, the electron mobility is a direct function of TNF content, irrespective of whether the TNF molecule is complexed or not. The molecular orbitals associated with electron transport in TNF (lowest unoccupied, LUMO) are antibonding and are spatially delocalized over the molecule. One might conjecture that these orbitals can tolerate the separations/perturbations associated with complex formation with carbazole groups, without impacting the electron exchange processes and the electron mobility. At low TNF

concentrations the exponential dependence of μ_-/r^2 versus r gives a measure of the wavefunction overlap of the transport states (α). A value of $\alpha = 1{\cdot}8 \times 10^{-8}$ cm is obtained from the linear portion of Fig. 14 for this overlap parameter. It is interesting that the electron mobility in amorphous films of pure TNF is also accommodated on the curve in Fig. 14, although the functional dependence at the very high TNF content is different from that at lower loadings.

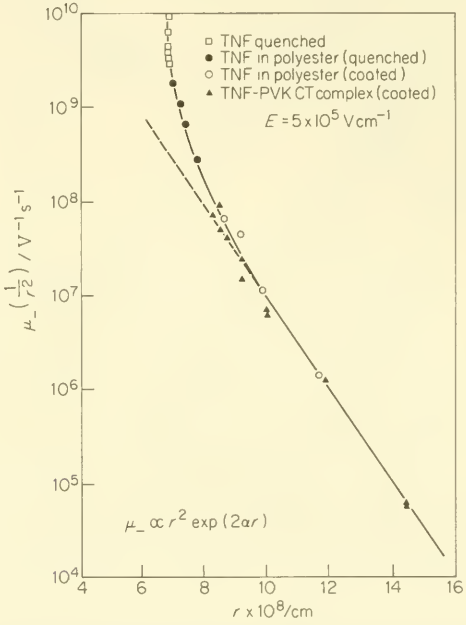

FIG. 14. Electron mobility as a function of TNF concentration, r being a measure of the average separation of TNF molecules in the system. [Reproduced with permission from W. D. Gill, in "Proceedings of the International Conference on Amorphous and Crystalline Semiconductors", Taylor and Francis, London (1973).]

It is more difficult to assess whether complex formation with TNF interferes with hole transport through the carbazole groups. Here the carbazole functions are covalently attached to the polymer backbone. If all the carbazole groups are involved in hole transport, then the presence of TNF molecules should not greatly impact the hole mobility. The results, however, are more consistent with a scheme in which the carbazole–TNF complexes effectively dilute the carbazole concentration, resulting in lower hole mobilities with increasing TNF content. Apparently, the exchange of holes between adjacent carbazole groups is very sensitive to the overlap of the appropriate

molecular orbitals (highest occupied, HOMO) and is perturbed by the presence of TNF molecules. Figure 13 shows that the hole mobility in PVK is significantly reduced even at low loadings of TNF molecules. It would be of interest to measure hole mobilities in amorphous films of a model carbazole compound, e.g. *N*-isopropylcarbazole, and in films of *N*-isopropylcarbazole dissolved in a non-complexing polymer binder in order to establish a compositional plot equivalent to Fig. 14. These results would aid in clarifying the concentration of carbazole groups involved in hole transport in PVK. Mort *et al.*[117] have reported electrical studies on dispersions of *N*-isopropylcarbazole in polycarbonates which support a mechanism involving hopping between carbazole molecules.

Similar conclusions were reached by Mort and Emerald[113] from their investigations of PVK, PVK–TNF and TNF systems. A thin amorphous selenium layer was used (Fig. 15) to photogenerate and inject carriers into

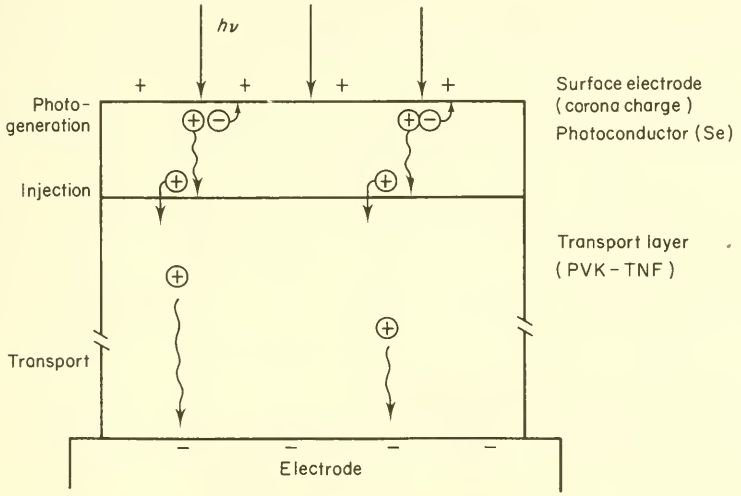

FIG. 15. Schematic diagram of the xerographic charge injection configuration used to measure drift mobilities and transport energy levels in TNF–PVK films. [Reproduced with permission from J. Mort and R. L. Emerald, *J. Applied Physics*, **45**, 175 (1974).]

the transport layer; the drift mobilities were measured and a reasonably detailed energy level diagram of the transport states in these materials could be constructed.

The discharge characteristics of this structure will be determined by the relative levels of the transport states for holes and electrons in the materials and by their relative mobilities in the transport layer. The results indicate a

large asymmetry in the discharge rates for holes compared to electrons in PVK films doped with 10 wt per cent TNF. At a given field, the discharge for holes is three orders of magnitude greater than for electrons, but at TNF loadings of 50 wt per cent no asymmetry exists. Two interpretations are possible: (a) a barrier to injection of electrons exists due to a misalignment of transport states in the Se and the polymer complex; (b) no injection barrier exists and the discharge rate is limited by the respective mobilities. It was clearly shown that the second interpretation is the valid one. Under the space charge limited conditions of the experiments, the asymmetry in the PVK–TNF (10 wt per cent) films is due to the electron mobility being three orders of magnitude lower than the hole mobility. At 50 wt per cent TNF loading the two mobilities are equivalent. The ability to inject electrons from Se into pure amorphous films of TNF supports the model in which the electron transport states in the two materials are favourably aligned.

These results suggest that negligible barriers exist between the transport states in amorphous Se and PVK–TNF films of any loading. Since the transport levels in Se have been well documented,[137] an energy level structure for the PVK–TNF system can be constructed (Fig. 16) which represents the

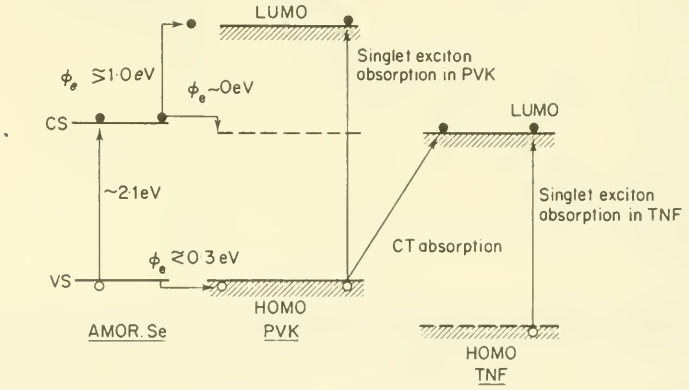

FIG. 16. Schematic diagram of the relative transport energy-level structure of amorphous Se and the TNF–PVK system. [Reproduced with permission from J. Mort and R. L. Emerald, *J. Applied Physics*, **45**, 175 (1974).]

most definitive analysis of transport states in any polymeric material at present.

Hermann and Nagao[138] have reported that orientation of PVK CT complexes (with TNF, TCNQ, I_2) by film formation in the presence of strong electric and magnetic fields can lead to materials with interesting birefringence properties. Since oriented liquid crystalline materials exhibit unusual dielectric and conductivity properties, enhanced charge transport might be

expected in these novel materials, but no electrical measurements have been reported on these interesting polymeric complex films.

Copolymerization of *N*-vinylcarbazole with a variety of co-monomers affects both the complexing characteristics and the electrical and photoelectric properties of the polymer. Copolymer structures ranging from random to alternating have been investigated.[139] In all cases the photocurrents were decreased. The effect was attributed primarily to a decrease in charge-carrier mobility resulting from perturbations in the carbazole group interactions. The role of the co-monomer structure in the trapping of charge was also recognized.

Pittman[140] investigated the electrical and photoelectric properties of copolymers of *N*-vinylcarbazole (NVK) with vinylferrocene (VF). Doping of the copolymers with TNF produced yellow to brown films with similar resistivities to the non-complexed materials. Copolymers containing 50–90 mole per cent NVK and 0·05–1·0 molar ratios of TNF to carbazole were examined. Oxidation of the TNF complexed copolymers with 2,3-dicyano-5,6-dichloroquinone, DDQ, caused a decrease in the resistivities of the products from 10^{14} to 10^{9} Ωcm. Control experiments demonstrated that TNF does not complex with, or oxidize, PVF and that DDQ does not complex with, or oxidize, PVK under the experimental conditions. Since these values are essentially identical to the resistivities obtained by direct DDQ oxidation of the copolymers, the effect is primarily due to the presence of the mixed valence ferrocene states (Fe^{II}/Fe^{III}) in the copolymer. It was concluded from this study that introduction of VF into the NVK polymer reduces the photoelectric activity, even in the presence of TNF. Oxidation of the ferrocene units (Fe^{II}/Fe^{III}) makes the copolymers (**53**) weakly semi-

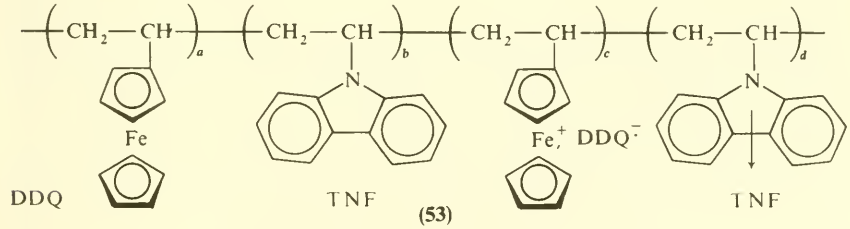

(**53**)

conducting, and the free TNF molecules and PVK–TNF complexes apparently play little role in the electrical properties. All the systems exhibited considerably lower levels of photoconductivity than PVK and PVK–TNF systems.

2. Other Donor Polymers

Litt and Summers carried out a detailed investigation of the synthesis,[83a]

characterization[83b,c] and electrical properties[83d] of one novel class of semiconducting polymeric CT complex based on *N*-acyl-polyethylenimines. This class of polymer was chosen on the basis of its ordered structure which allows control over the donor repeat distance along the chain as well as the space required for accommodating the complexing acceptor molecules.

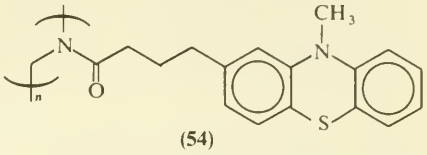

(54)

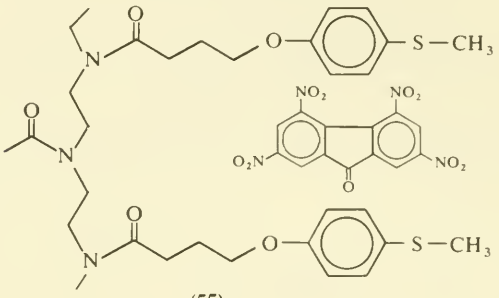

(55)

10-Methyl-3-phenothiazinyl (**54**) and 4-(methylthio)phenoxy (**55**) donor groups were used with the following acceptors: 2,3-dichloro-5,6-dicyanobenzoquinone (DDQ), tetracyanoquinodimethane (TCNQ), tetracyanoethylene (TCNE) and 2,4,5,7-tetranitrofluorenone (TENF). Solution spectroscopic studies of the (donor polymer)–(acceptor molecule) systems were claimed to support the existence of 2:1 complexes (one acceptor molecule sandwiched between two donors) with higher (by a factor of 3–50) equilibrium constants than were observed for the corresponding (donor molecule)–(acceptor molecule) case. The polymeric complexes also exhibited a red shift relative to their small molecule analogues. This was taken as evidence supporting the unique complexing geometry of the polymers (see discussion in Section V.B). Solid state infrared and X-ray analysis showed that the polymeric donors formed amorphous complexes with DDQ, TCNQ and TCNE, and crystalline complexes with TENF. The relative amounts of complexed and non-complexed components were not established. Compacted powders showed lower resistivities than the corresponding small molecule model complexes, one of the very few instances where this trend has been claimed. The best systems exhibited conductivities some 200 times higher than the non-polymeric donors. Esr data on the

polymeric complexes were inconclusive and indicative of impurity or trapped unpaired electrons. Seebeck and Dember coefficients were also determined in order to classify the majority carriers. Unfortunately, these experiments are extremely difficult with such high resistivity samples ($\rho > 10^{10}$–$10^{11}\,\Omega$cm) and no meaningful correlations with structure were obtained. The complexes were weakly photoconducting.

Some of the most conductive organic materials known are those based on 7,7,8,8-tetracyanoquinodimethane (TCNQ)[119] as the acceptor component. In the presence of a suitable donor molecule, electron transfer produces the ion radical pair. These ion radical salts provide a small but versatile class of π-molecular CT complex solids which exhibit conductivities spanning the range from insulators to semiconductors to "organic metals". In the simple molecule systems there are two distinct structural classes: 1:1 alternating mixed stack type, $\cdots D^{+}A^{-}D^{+}A^{-}\cdots$; and 1:1 segregated stack type, $\cdots D^{+}D^{+}D^{+}D^{+}\cdots\cdots A^{-}A^{-}A^{-}A^{-}\cdots$, which can be further subdivided to include the complex stoichiometry solids which contain an excess of neutral acceptor TCNQ molecules. Up to now all examples of conductive polymeric TCNQ salts are of the complex stoichiometry type. The extremely high conductivities in the TCNQ solids are a critical function of system purity and degree of structural order (high n and high μ), and it is unlikely that polymeric materials can meet these rigid criteria and retain any processing characteristics.

The first polymeric TCNQ complexes to be synthesized and investigated were those based on the poly(vinylpyridines).[141–143] Their mode of preparation was identical to that for their small molecule analogues. Following quaternization of the pyridine rings in the polymers, an exchange reaction was carried out with Li^{+} $TCNQ^{-}$. Addition of excess neutral TCNQ gave dark coloured products of different stoichiometries which are soluble in organic solvents and form generally brittle films with conductivities as high as 10^{-3}–$10^{-2}\,\Omega^{-1}\,cm^{-1}$. The presence of neutral TCNQ, e.g. (**56**), was

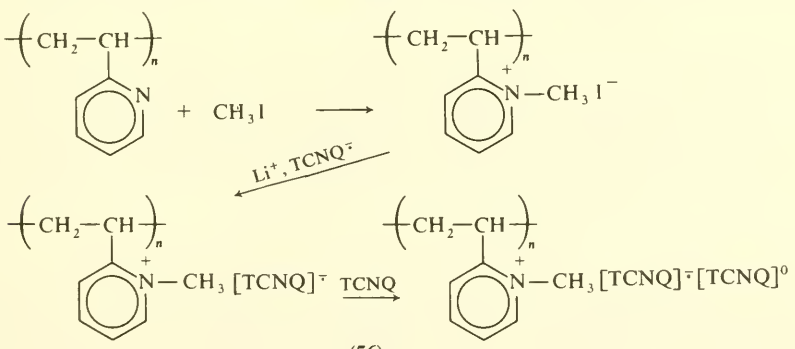

(**56**)

critical in achieving the high conductivity, and charge transport via electron exchange between the ionized and neutral TCNQ molecules was suggested.

3. Ionenes and Related Materials

Rembaum *et al.*[144–146] extended these studies to a new class of polymer, the ionenes (**57**), in which the N-containing function is incorporated into the polymer backbone, where R_1 is an akyl group, R_2 is $-(CH_2)_n-$ with $n \geqslant 3$,

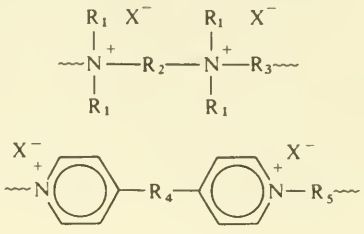

(57)

and R_3 can be the same as R_2 or have a different value of n. R_4 and R_5 can be the same as R_2 or can be aromatic or unsaturated groups. Examples covering a wide range of substituents have been synthesized and evaluated.

The electrical properties of the ionene–TCNQ complexes were primarily dependent on the $TCNQ^{\bullet-}/TCNQ$ ratio and to a lesser extent on the polymer structure. The aromatic ionenes were generally more conductive than the aliphatic series. Polymer structure was more important in determining the stability of the complex, and the aromatic ionene complexes were more stable.

Detailed electrical measurements[145] were carried out on ionene polymers based on the structures (**58**), (**59**) and their small molecule analogues. The

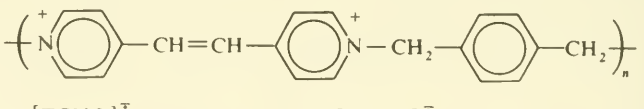

$[TCNQ]^{\bullet-}$ $[TCNQ]^{\bullet-}$

(58)

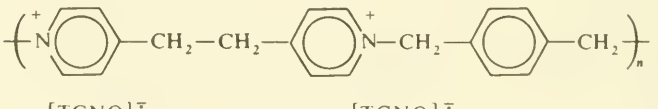

$[TCNQ]^{\bullet-}$ $[TCNQ]^{\bullet-}$

(59)

Hall mobilities (μ_H) were estimated to be $< 0{\cdot}1\ cm^2\ V^{-1}s^{-1}$ at 25°C with holes being the majority carrier. Seebeck coefficients were also consistent with a hole transport mechanism. These findings are inconsistent with

electron transport via the $TCNQ^{\cdot-}$–TCNQ couple. The mobility measurements were generally unsuccessful, and one example of a change in the sign of the Hall coefficient with time (from positive to negative carriers) was reported. An attempt was also made[147] to determine the drift mobility by investigating the change from ohmic to space charge limited currents in compacted and electroded structures. Mobilities in the range of 10^4 cm^2 V^{-1} s^{-1} were required to account for the observed results, and such a high value is clearly unrealistic.

Ashwell, Eley and Willis, in a short communication,[148] have reported a highly conducting TCNQ system (**60**) which exhibits a monotonic decrease in conductivity on cooling from ambient to 30 K. This is in contrast to other highly conducting TCNQ complexes[149,150] which undergo a metal–semiconductor transition in the region of 60 K. The 1,2-di-(*N*-ethyl-4-pyridinium)-ethylene complex (**60**) was grown as single crystals, and both metallic and

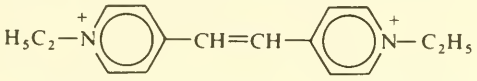

$[TCNQ]^{\cdot-}$ $[TCNQ]^0$ $[TCNQ]^{\cdot-}$ $[TCNQ]^0$

(60)

semiconducting behaviour was found for samples with identical stoichiometries. Preparative conditions have clearly yet to be optimized. Conductivities at 300 K of ~ 150–$2200\ \Omega^{-1}\ cm^{-1}$ were measured. This should be compared with $\sim 0{\cdot}26\ \Omega^{-1}\ cm^{-1}$ reported[145] for polycrystalline samples of the closely related 1,2-di-(*N*-methyl-4-pyridinium)ethylene complex (**61**).

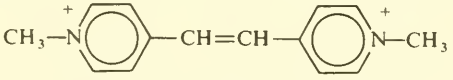

$[TCNQ]^{\cdot-}$ $[TCNQ]^0$ $[TCNQ]^{\cdot-}$

(61)

Clearly, subtle molecular structural changes (*N*-methyl to *N*-ethyl functions) and stoichiometries play a major role in determining the conductance behaviour of these systems. The electronic transport properties of aliphatic ionene type polymers (**62**) containing the dipyridylethylene function were reported in a preliminary communication by Rembaum and coworkers.[151]

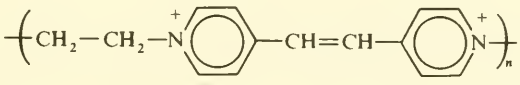

$[TCNQ]^{\cdot-}$ $[TCNQ]^0$ $[TCNQ]^{\cdot-}$

(62)

The most conductive polymer (**62**) had a room temperature conductivity (polycrystalline samples) of $\sim 6 \times 10^{-2}\,\Omega^{-1}\,cm^{-1}$, which is very similar to that of the closely related aromatic systems[145] and many other aromatic and aliphatic ionene polymers.

In further studies by Rembaum *et al.*[152] on some ionene polymers and model compounds, the separation of the positively charged nitrogen functions was systematically varied by modifying the number of CH_2 groups between them. Those model compounds and polymers that had high resistivities exhibited hole-type conduction as determined by Seebeck measurements. On the other hand, the low resistivity samples ($\rho \approx 10^2$–$10^3\,\Omega cm$) were characteristic of electron transport, as would be expected if the $TCNQ^{\cdot-}$–TCNQ couples were involved. Materials having their N^+ sites separated by sixteen CH_2 units gave indications of a mixed type of conductivity involving both holes and electrons. The wide variations in electrical properties could not be readily correlated with chemical structure, and it was shown that the nature of the solid state structure controls the conductivity. Only those systems where the TCNQ transport molecules adopt some chain-like paths through the materials display high levels of electron conduction. Clearly, the more order in the solid, the higher the conductivity, and single-crystal measurements support this model.

An interesting series of elastomeric ionenes was also studied.[153,154] They were synthesized from poly(propylene glycols) of varying molecular weights which were end-capped with dimethylamino groups. Coupling with appropriate halogen compounds gave the quaternary polymers which were reacted with Li^+ $TCNQ^{\cdot-}$ and excess TCNQ to give conductive elastomers. These polymers contain relatively low concentrations of quaternary nitrogens. Typical materials had resistivities of 10^7–$10^8\,\Omega cm$ at ambient temperatures, and the resistivity was a function of the concentration of positively charged nitrogen centres in the polymer. Conductivities increased as the distance between the $TCNQ^{\cdot-}$ molecules (associated with the positively charged nitrogen atoms) decreased. Temperature studies revealed breaks in the ρ versus T curves, associated with T_g of the system (Fig. 17). Conductivities were lower in the rubbery state than in the glassy state, and the authors attributed this to a decrease in the charge-carrier mobility resulting from motions of the ionized TCNQ molecules in the matrix. Another interesting observation[154] was that some of the elastomer–TCNQ samples showed no change in resistivity (some systems actually exhibited a slight decrease) at elongations up to 80 per cent. This is very unusual and in direct contrast to observations with, for example, known carbon black filled conductive elastomeric materials. The effect may be due both to the molecular nature of the TCNQ dispersion and to a stress induced orientation resulting in an increase in electron mobility.

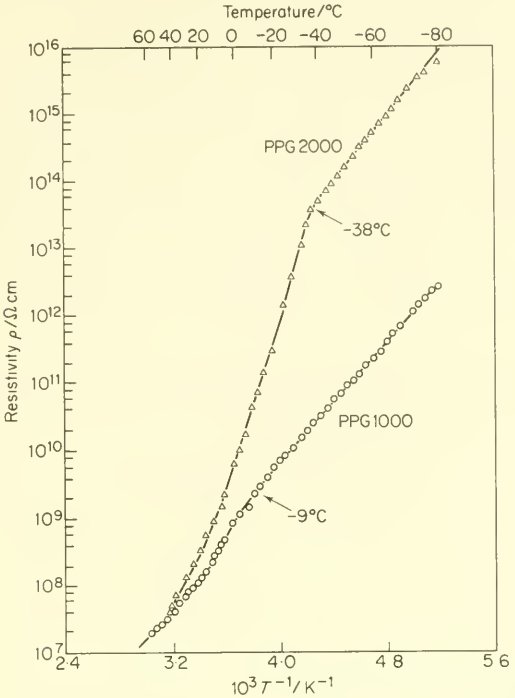

FIG. 17. Resistivity versus reciprocal temperature plots for two elastomeric ionene–TCNQ complex materials. [Reproduced with permission from R. Somoano, S. P. S. Yen and A. Rembaum, *J. Polymer Sci., Polymer Letters*, **8**, 467 (1970).]

Ionene polymers containing viologen (4,4′-bipyridylium) have been reported,[155,156] e.g. (**63**) and (**64**). TCNQ salts of the poly(xylyl-viologen)s (**63**) exhibited[156] conductivities in the range 10^{-3}–$10^{-5}\ \Omega^{-1}\ cm^{-1}$ which increased by approximately two orders of magnitude on doping with an excess of neutral TCNQ.

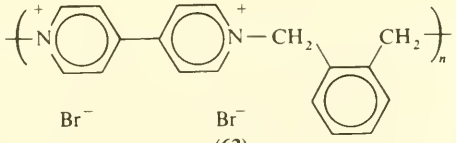

(**63**)

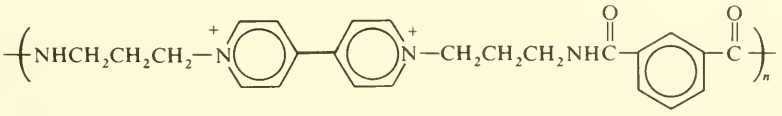

(**64**)

There have been only a small number of studies[142,143,157,158] on the effect of polymer tacticity and crystallinity on the electrical properties of CT complexes. Slough[157] and Lupinski[142] found equivalent conductivities in complexes of atactic and isotactic polymers of 1-vinylnaphthalene with chloranil and TCNE and of 2-vinylpyridine with TCNQ. Eley[158] also studied the electrical properties of some atactic and isotactic poly(vinylpyridinium)–TCNQ complexes. Using compressed pellet samples, these authors measured resistivities, Seebeck coefficients and microwave Hall mobilities in a series of poly-(2-vinylpyridine) complexes, P2VP–$[TCNQ]_2^-$. They found that the isotactic complexes were significantly better conductors than the corresponding atactic polymer complexes, but neither system approached the conduction levels achieved in the monomer model complex.

Seebeck and Hall mobility studies were indicative of electron transport with mobilities in the range 0·3–2·5 $cm^2 V^{-1} s^{-1}$ at ambient temperatures for both the atactic and isotactic complexes. It was suggested that the isotactic polymers behave as polycrystalline complex salts where the TCNQ molecules assume somewhat ordered structures in the matrix which increase electron mobility. The ordered polymer structure also tends to minimize polarization effects from the positively charged N atoms in the pyridine rings. In the atactic polymers the TCNQ molecules assume a more random distribution with a correspondingly lower mobility.

Analysis of all the investigations of the vinylpyridine and ionene polymer complexes with TCNQ would tend to favour a model in which the $TCNQ^{\cdot-}$–TCNQ arrays are responsible for charge-carrier (electron) transport. The more order the matrix polymer provides for these molecular arrays (channels) the higher the conductivity. Differences in conduction are then primarily due to matrix effects which can cause subtle or significant changes in the $TCNQ^{\cdot-}$–TCNQ chaining and in polarization influences which come from the cations present. It is probable that both molecular dispersions of the $TCNQ^{\cdot-}$–TCNQ molecules and also microcrystallites are present in some of the materials evaluated. Further work is needed on material characterization before these issues can be resolved.

4. Ferrocene-containing Polymers

Reports[119] of the extremely high conductivity, $\sim 10^0$–$10^3\ \Omega^{-1} cm^{-1}$, achieved in the CT complex salts of tetracyanoquinodimethane with phenazines, fulvalenes, ferrocenes and biferrocenes have stimulated renewed interest in organic polymeric semiconductors and conductors. Pittman *et al.*[159] described the synthesis of mixed valence (Fe^{II}/Fe^{III}) ferrocene polymers which had greater conductivities, $\sigma \approx 10^{-6}$–$10^{-7}\ \Omega^{-1} cm^{-1}$, than their Fe^{II} analogues, $\sigma \approx 10^{-13}$–$10^{-15}\ \Omega^{-1} cm^{-1}$. Picric acid, benzoquinone, TCNQ and chloranil were effective oxidizing agents, and the

polymer complex salts were generally intensely coloured and insoluble. Structure (**65**) has been suggested for these complex salts, e.g. for poly(vinylferrocene)–chloranil.

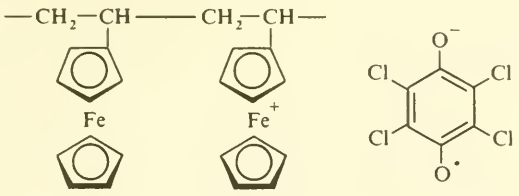

(**65**)

The polymeric complexes are amorphous and the conductivity appears to be insensitive to the nature of the anion species. Conductivity is a direct function of the Fe^{II}/Fe^{III} ratio with a maximum in the region of 70 per cent oxidation. Pittman also investigated the effect of introducing both extended conjugation and mixed valence states into the ferrocene polymer. Ethynylferrocene was synthesized and polymerized by free-radical techniques to give low yields of oligomeric products ($\overline{DP} \sim 10$–15). The intensely coloured poly(ethynylferrocene)s (**66**) were soluble, but somewhat unstable in solution, although they appeared to be stable in the solid state. Mixed valence salts

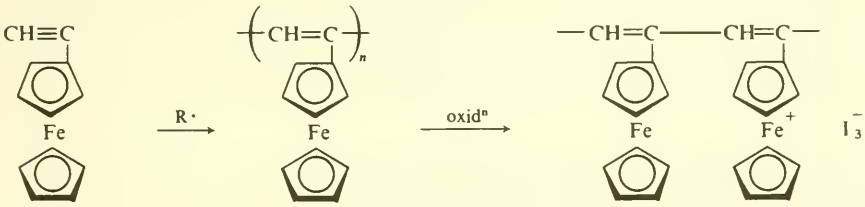

(**66**)

exhibited conductivities as high as $10^{-6}\,\Omega^{-1}\,cm^{-1}$ compared with the polymer, $10^{-4}\,\Omega^{-1}\,cm^{-1}$. This is comparable to the conductivity levels in the non-conjugated ferrocene polymers at equivalent degrees of oxidation. An electron hopping mechanism between neighbouring Fe^{II} and Fe^{III} sites, with little or no participation from the polymer backbone, the cyclopentadiene groups or the anions, has been suggested to account for these observations. Mueller-Westerhoff[160] and Cowan[161] showed that higher conductivities could be attained by using the symmetrical biferrocenylene (**68**) metallocenophane moiety rather than the ferrocene or biferrocene (**67**) structure in these complexes, $\sigma \approx 10\,\Omega^{-1}\,cm^{-1}$ at room temperature. The rigid geometry of (**68**) permits a much greater degree of interaction between the ferrocene units, and thus must be considered a completely delocalized

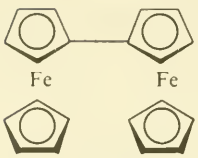

(67)

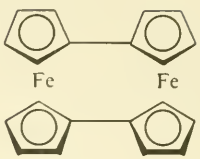

(68)

system in which the iron atoms are equivalent. The synthesis of 3-vinyl-bis-(fulvalene)di-iron (**69**) has been achieved.[162] The synthesis is difficult and the yields are extremely low but this unusual monomer can be polymerized by free radical initiation to low molecular weight homopolymer ($\overline{DP} \sim 12$) and copolymers.

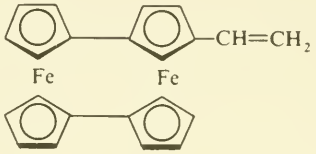

(69)

Complex salts of the $[TCNQ]_2^-$ type with degrees of oxidation of the biferrocenylene unit up to 70 per cent exhibit conductivities as high as 10^{-2}–$10^{-3}\ \Omega^{-1}\,cm^{-1}$. From an analysis of the dependence of the conductance on the degree of oxidation it has been postulated that a completely oxidized polymer should exhibit a conductivity of $1\ \Omega^{-1}\,cm^{-1}$.

5. Tetrathiafulvalene (TTF) and Related Materials

Compounds of the tetrathiafulvalene (TTF) and of the tetraselenafulvalene (TSeF) class form 1:1 complexes with TCNQ which are among the most highly conducting organic materials known. Very pure single-crystal

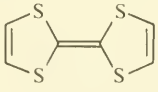

TTF

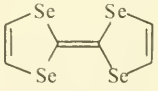

TSeF

samples exhibit conductivities up to 10^2–$10^3\ \Omega^{-1}\,cm^{-1}$. Melby *et al.*[163] reported the synthesis of a disubstituted TTF derivative (**70**) (a mixture of *cis* and *trans* isomers which were not separated), which possibly could be incorporated into a novel condensation polymer with TTF functions in the chain. Ueno *et al.*[164] subsequently described an alternative approach to a TTF containing polymer (**71**). The synthetic route involves a base coupling

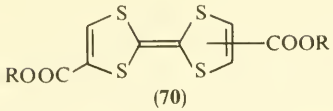

(70)

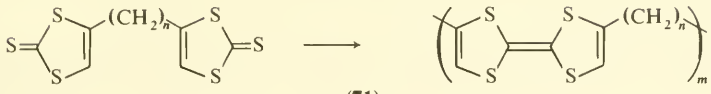

(71)

of 1,3-dithiol-2-thione rings to construct the TTF unit. The polymer with $n = 2$ and 3 was isolated as a green-brown solid, insoluble in common organic solvents. Molecular weights in the range 3000–4000, corresponding to $\overline{DP}$ of 15–25, were claimed, and these polymers were reacted with TCNQ

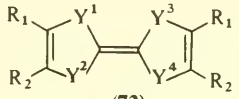

(72)

R_1	R_2	Y^1	Y^2	Y^3	Y^4
H	COOH	S	S	S	S
H	$COOCH_3$	S	S	S	S
H	CH_2OH	S	S	S	S
H	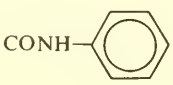	S	S	S	S
H	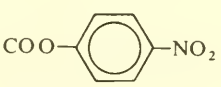	S	S	S	S
$COOCH_3$	$COOCH_3$	S	S	S	S
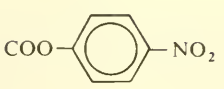	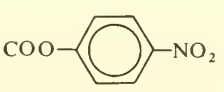	S	S	S	S
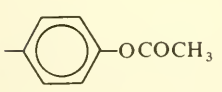	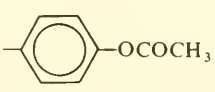	S	S	S	S
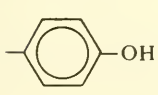	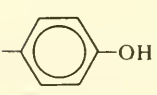	S	S	S	S
COOH	COOH	S	Se	S	S
$COOCH_3$	$COOCH_3$	S	Se	S	Se

and DDQ in refluxing acetonitrile to give CT complex products which were insoluble and intractable. Analytical data were consistent with a TTF to TCNQ 6:1 ratio which was clearly controlled by the heterogeneous nature of the (donor polymer)–(acceptor molecule) reaction. Attempts to achieve 1:1 complexes have so far been unsuccessful. The structural and electrical characterization of these materials has not yet been published.

Pittman *et al.*[165] described the synthesis of a number of functionalized tetrafulvalenes capable of being incorporated into a polymer via the traditional polycondensation reactions, e.g. (**72**). The complexing characteristics of these "TTF monomers" with TCNQ and DDQ were also investigated and found to be very dependent on the nature of the substituents.

These same authors have published[166] a preliminary report on the synthesis of a series of tetrathiafulvalene-containing polyamides, (**73**) and (**74**), using the diacid derivative described above with *N*-phosphonium salts of pyridine as the dehydrating agent. The major difficulties in this poly-

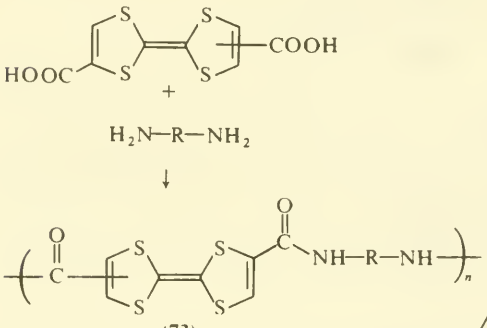

(73)

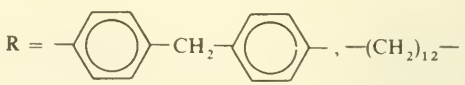

and

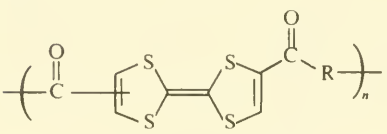

(74)

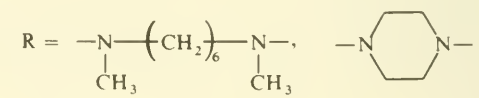

condensation were the thermal instability of the TTF nucleus at elevated temperatures and the insolubility of the product polymers. Attempted polytransesterification of the diester with diols such as bisphenol-A and ethylene glycol generally resulted in formation of low molecular weight polymeric products and recovery of the diacid of the starting material. Hertler[167] described a TTF-containing polyurethane formed by coupling 4,4′-bis(hydroxymethyl)-TTF with 4,4′-diisocyanato-TTF (**75**), but no CT complex formation studies or electrical measurements were conducted. The

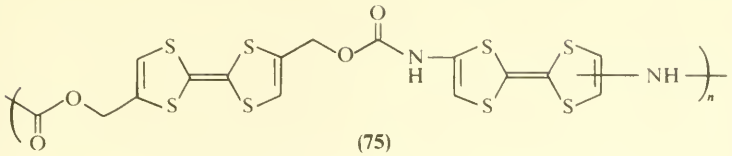

(75)

attainment of high molecular weight products in these polycondensations will be difficult. The polyamides did not form complexes with TCNQ or DDQ, and this was attributed to the effect of the amide functions in the polymer.

Pittman[168] has also succeeded in synthesizing a TTF-containing vinyl monomer (**76**). Green[169] has developed a novel and simple general procedure for the synthesis of monosubstituted TTF derivatives, which has been used to prepare vinyl-TTF (**77**). The monomer (**77**) polymerizes slowly even

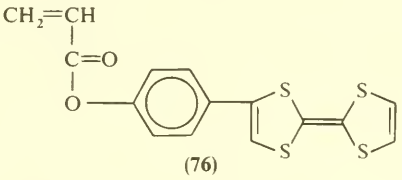

(76)

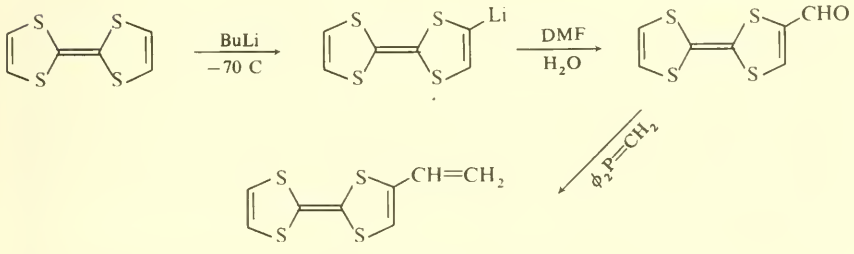

(77)

under inert atmosphere dry-box conditions. Controlled polymerization studies of both vinyl monomers are now in progress and the complexing characteristics and electrical properties of these polymeric salts are awaited with interest.

The conduction mechanism in these TCNQ systems is still not resolved. In the 1:1 polymeric salts the conduction appears to be dominated by hole transport, and conductivities in the 10^{-5}–$10^{-8}\ \Omega^{-1}\ cm^{-1}$ range are certainly consistent with a hopping process between, for example, the localized Fe^{II}/Fe^{III} states in the ferrocenes or the N/N^{+} states in the ionenes. The 1:2 D^{+}–[$TCNQ_2^{-}$ and higher] stoichiometry complexes are orders of magnitude more conductive than their 1:1 counterparts. Here, the transport mechanism

involves electron migration between the neutral and reduced TCNQ molecules in the system.

In the highly ordered, single-crystal model systems, e.g. TTF–TCNQ, the structural perfection and purity levels are critical in achieving high conductivity. The molecules must pack in segregated donor and acceptor stacks where the overlaps of the appropriate molecular orbital states are favourable for efficient hole and electron transfer interactions along the stacking axis (pseudo 1-D metals). Any structural perturbations lead to appreciable decreases in conductivity. In these systems the concept of complete radical ion formation by a formal one-electron transfer has been questioned.[170] In the solid, complete transfer will result in considerable instability as a result of the strong electrostatic repulsions within the molecular stacks. Partial electron transfer, on the other hand, will produce a more stable system by minimizing these intra-stack repulsive interactions. Recent X-ray,[171] neutron scattering[172] and other studies all indicate transfer of at least 0·5 of one electron, and definitely less than one electron, per TTF–TCNQ pair. This will be equivalent to molecular chains where the molecules exist in mixed valence states, i.e. TTF^{+}–TTF and $TCNQ^{-}$–TCNQ. Electron/hole migration along the chains is now less likely to produce undesirable doubly charged species, TTF^{2+} and $TCNQ^{2-}$, resulting in more efficient charge transfer. One of the issues that remains to be resolved in these systems is the nature and contribution of charge transport perpendicular to the chains. It seems reasonable to speculate that as electrons migrate along the acceptor chains and holes along the donor chains there will exist neutral donor and acceptor molecules adjacent to each other where interchain transfer can occur. In these highly ordered, defect free, single-crystal materials this lateral type conduction may be unimportant, whereas in the disordered TCNQ systems, e.g. polymeric materials, it may contribute significantly to the macroscopic conductivity.

The current conflicts that exist in this field may be largely due to the variable structures and stoichiometries resulting from slight differences in preparative procedures. In the polymeric complexes, the matrix materials and the fabrication procedures obviously play a major role in determining the morphology and the microstructure which control the conductive pathways. The presence of mixed valence states, i.e. TCNQ and $TCNQ^{-}$, is critical and is guaranteed by ensuring the presence of excess neutral TCNQ molecules. Conductivity is by electron transport. It remains to be seen whether both donor and acceptor morphological control can be achieved in a polymeric solid which would permit both holes and electrons to contribute to the conduction process.

The efforts of Pittman,[162,165,168] Ueno[164] and Hertler[167] to incorporate chromophores such as biferrocenylene (**68**) and tetrathiafulvalene

(TTF) into polymers (both directly in, and pendant to, the backbone) clearly illustrate the complex chemistry associated with this approach.

One of the major problems associated with conductive materials based on TCNQ and TTF is their oxidative instability which, as well as creating problems in the synthesis and evaluation of the materials, essentially precludes commercial exploitation. Nakatani[173] studied the effect of oxidation on the properties of the poly-(4-vinylpyridine)–TCNQ complex. The oxidation is accompanied by changes in the colour of the complex (dark green to light brown) and a decrease in conductivity. Chemical analysis of the oxidized films showed that α,α-dicyano-*p*-toluoyl cyanide is the major oxidation product. Tetrathiafulvalene (TTF) and many of its derivatives are also sensitive to oxidative and photo-oxidative degradation in air, producing violet, water-soluble products presumed to be the highly stable radical-cation (**78**) or dication salts (**79**).

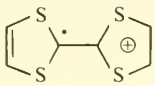

(78)

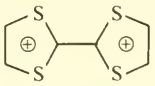

(79)

C. Acceptor Polymers with Small Molecule Donors

There are few known examples of materials of the opposite class to these (donor polymer)–TCNQ systems, i.e. (acceptor polymer)–(donor molecule). It is reasonable to expect that, based on the analysis presented in the preceding section, (acceptor polymer)–(donor molecule) conducting combinations should be feasible. In these systems hole transport should occur along (radical cation)–(neutral molecule donor) arrays. High conductivity has been reported[174] in the mixed valence halides of TTF; e.g. $(TTF)Br_{0.71}$, $(TTF)I_{0.71}$, $\sim 10^{11}\ \Omega^{-1}\,cm^{-1}$. Conductivity takes place through the TTF–$TTF^{\ddagger}$ networks with no contribution from the widely separated halide components. Barlow *et al.*[175] have also demonstrated high conductivities in neutral materials doped with controlled amounts of their radical-cation species, e.g. (**80**)–(**82**) BF_4^- or Br^- salts.

These examples show that hole transport via exchange between radical cation and neutral donor molecules, directly equivalent to the acceptor molecule systems, e.g. TCNQ, is known. The absence of examples of polymer based complex radical-cation salts in the literature is therefore a reflection of the lack of suitable acceptor-type polymers rather than stable radical-cation species.

As was stated in Section V.C, there are only a few examples of polymers containing typical acceptor groups, e.g. nitrofluorenones and substituted

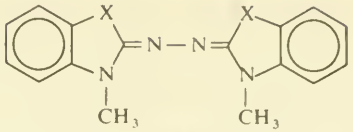

(80)

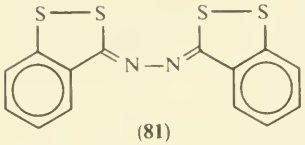

(81)

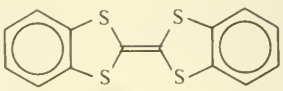

(82)

benzoquinones. Besides the acceptor polymers described earlier, other acceptor polymers have been synthesized and evaluated from an electrical properties standpoint. Poly-(2-vinylfluorenone) (**83**) has recently been prepared.[176] The fluorenone group is a relatively weak acceptor and, although this polymer formed complexes in solution with a variety of donors, in the solid state only very low complexing levels were observed.[177] The polymers exhibited poor electron transport capabilities, and electron drift mobilities were at the lower level of detection by xerographic or time-of-flight techniques, $< 10^{-8}$ cm^2 V^{-1} s^{-1}. Copolymers of 2-vinylfluorenone, e.g. with styrene, showed similar behaviour. Attempts to nitrate the fluorenone groups in the homopolymer and in a series of copolymers were unsuccessful. The nitration reactions invariably led to insolubilization and poorly defined products. Reaction of 2-vinylfluorenone or the fluorenone-containing polymers with malononitrile gave the corresponding 9-(dicyanomethylene)-fluorene derivatives (**84**).[178] Solubility problems with both the monomer and polymers precluded investigation of the complexing behaviour or electrical properties.

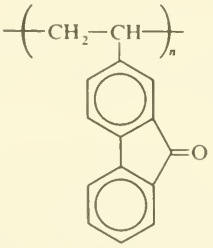

(83)

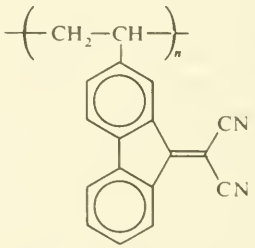

(84)

Two trinitrofluorenone-containing monomers, glycidyl 4,5,7-trinitrofluorenone-2-carboxylate and 2′-ethylmethacryl 4,5,7-trinitrofluorenone-2-carboxylate have been prepared and polymerized to low molecular weight

homopolymers (**85**) and (**86**) which complexed readily with a variety of donor molecules.[179] Electron mobilities estimated from xerographic data were about 10^{-8} cm^2 V^{-1} s^{-1} at a field of 50 V μ^{-1} (5×10^5 V cm^{-1}).

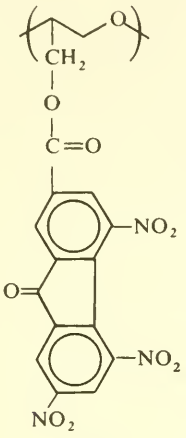

(**85**)

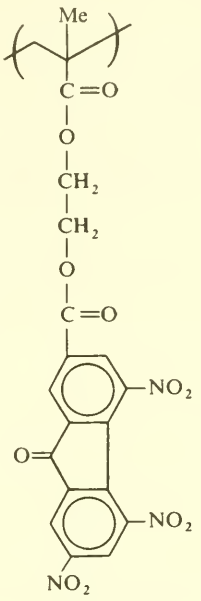

(**86**)

Both Cassidy[180] and Manecke[181] have investigated the polymerization and properties of some quinone-containing polymers which exhibit interesting redox behaviour, but there are no data on their complexing or electrical characteristics, e.g. (**87**)–(**89**).

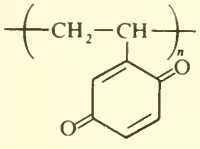

(**87**)

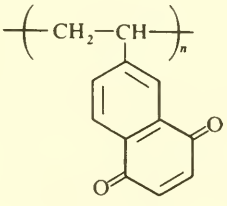

(**88**)

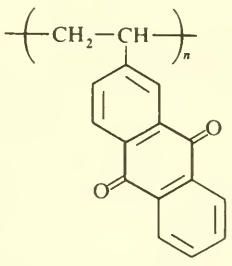

(**89**)

Copolyesters containing nitrofluorenone and dicyanomethylene-nitrofluorenone groups have been described by Sulzberg and Cotter.[93,94] These polymers, e.g. (**42**), form complexes with donor molecules and give soluble

products which can be cast into homogeneous films with good mechanical properties. The complexes exhibit semiconducting properties. Some of the other polyesters described in these reports include those based on fluorenone-2,7-dicarboxylic acid and the 9-dicyanomethylene analogue, 5-nitroisophthalic acid, 4,6-dinitroisophthalic acid and nitroterephthalic acid. Both the dinitrofluorenone and dicyanomethylene-dinitrofluorene polyesters have been investigated in regard to the xerographic properties of their 1:1 complexes with *N*-ethylcarbazole.[179] The dinitrofluorenone–*N*-ethylcarbazole systems gave a steeply field-dependent photodischarge at a field of 50 V μ^{-1}. The quantum efficiency of generation was estimated to be 3×10^{-3} at this field, compared with 5×10^{-2} for PVK–TNF (1:1). The dicyanomethylene-dinitrofluorene polyester behaved similarly but a higher dark decay was observed. The lower sensitivity of these systems than PVK–TNF is thought to be due partly to the steric consequences of putting the acceptor group in the polymer backbone. Detailed spectroscopic analysis has not been reported.

Schulz[92] described the synthesis of an interesting tetranitrofluorene-containing spiro-type polyester (**38**) but no electrical data for its complexes were reported. A copolyester based on the tetranitrofluorenone–fluorene couple was also prepared. Recent measurements have shown this material to be neither a bulk charge-carrier generating photoconducting system nor a measurable hole or electron transporter when used in conjunction with an amorphous selenium charge-carrier generating layer.[182]

Hertler[90] described a diol derivative of TCNQ which could be incorporated into a polymer, but only copolycondensations with donor functional monomers, e.g. ferrocene and TTF, were attempted.

There are only a few published[93,94] electrical investigations of (polymeric donor)–(polymeric acceptor) complexes. As a result of the phase separation problems commonly encountered on mixing polymers, it is highly unusual to find polymer combinations that will produce homogeneous solid structures. A typical (donor polymer)–(acceptor polymer) composition was prepared by solution casting or melt mixing the components, e.g. poly-(*p*-anisyliminodiethanol-bisphenol A carbonate) (**90**) with poly-[bis-(2-hydroxyethyl)-5-nitroisophthalate bisphenol A carbonate] (**91**) in a 1:1 ratio (by weight). The resulting films from this combination and others appeared to be homogeneous and yellow to orange in colour. They exhibited volume resistivities a factor of 10^3 lower than the individual component polymers.

This investigation was extended[93] to polyesters based on (**42**), and mixtures of these acceptor polyesters with polyester or polycarbonate donors gave highly coloured blends with volume resistivities as low as 10^5–10^6 Ω cm. These unique CT complex polyblends possess well-defined structures and useful mechanical properties, in contrast to many of the polymer–(small

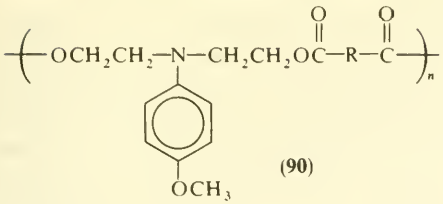

(90)

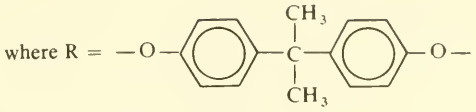

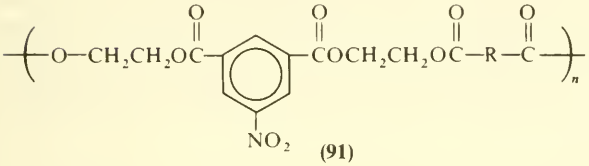

(91)

molecule) complexes which are generally of poorly defined structure, intractable and poorly processable.

Attempts[183] to use complex formation between donor and acceptor groups on different addition type homopolymers and copolymers to aid in rendering compatible otherwise incompatible systems have not been successful. It is unlikely that the complexes studied (involving carbazole, fluorenone and phthalimide groups) are strong enough to overcome the energetics of the phase separation process, and this may result partly from the severe steric constraints arising from the polymeric nature of the components.

D. Intramolecular Polymeric Complexes

Intramolecular CT transitions have been observed in molecules that possess both donor and acceptor functions. The transitions can arise from a direct conjugative interaction within the molecule, e.g.

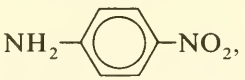

or from an across-space interaction where favourable conformations can be achieved.

In a polymeric system an intramolecular complex can, in principle, be formed between components on the same polymer molecule. The interacting groups need not be on adjacent positions in the chain. Conformational and

steric factors become extremely important and, although there are several examples of copolymers containing both donor and acceptor type groups, the evidence for intramolecular complex formation is generally confined to dilute solutions. In the solid state these copolymers can exhibit both inter- and intra-molecular complexation, the relative amounts depending on the structure, composition and the nature of chain conformations. There are no experimental techniques that can unequivocally distinguish between the two in a polymeric solid.

The product of spontaneous copolymerization of 2,4,6-trinitrostyrene with 2-vinyl- or 4-vinyl-pyridine or *p*-dimethylaminostyrene is commonly cited[98] as an example of a copolymer exhibiting intramolecular complexation. The reaction gives low molecular weight products having absorption bands in the 450–550 nm region and resistivities in the range of $10^{10}\,\Omega$cm. A recent report[184] indicates that the reported structures of these materials are probably in error. The mechanism and the products of this reaction have never been fully elucidated.

Donor–acceptor copolymers were the reported products from nitration reactions of poly(acenaphthalene),[185] poly-(*N*-vinylcarbazole)[186] and poly(vinylnaphthalene)[187] homopolymers. Enhancement in the photoconductive response of the nitrated polymers was attributed to formation of intramolecular complexes between the aromatic and nitro-aromatic groups resulting in an increased photogeneration of charge carriers. No detailed spectroscopic or electrical analyses were made on these materials.

Studies of the photoconductivity of a series of *N*-vinylcarbazole–*N*-vinylphthalimide random copolymers were carried out by Limburg and Seanor.[188] As has been described in Section V.D, detailed spectroscopic analysis confirmed the existence of intramolecular CT complexes in the copolymers (**49**) in solution. Variations in the structure of the phthalimide group were achieved by an exchange reaction, (**49**), X = H, Br, I. In this series the steric factors become appreciable and formation of complexes becomes more difficult as the size of the acceptor group increases. The photoconductivity of the copolymers also decreased along this series. There was very little difference in the photoelectric behaviour of the copolymers and of poly-(*N*-vinylcarbazole) doped with an equivalent concentration of the *N*-ethylphthalimide. The effective hole mobility in these copolymers decreased with increasing acceptor content similar to the observations in the PVK–TNF system. This has also been reported[139] for a number of *N*-vinylcarbazole copolymers with random and alternating structures.

Hertler[167] disclosed the synthesis of two TCNQ-containing polymers from the intermediate 2,5-bis-(2-hydroxyethoxy)-7,7,8,8-tetracyanoquinodimethane (**92**). Condensation with 1,1′-diisocyanatoferrocene and with 4,4′-diisocyanatotetrathiafulvalene gave the corresponding polyurethanes (**93**)

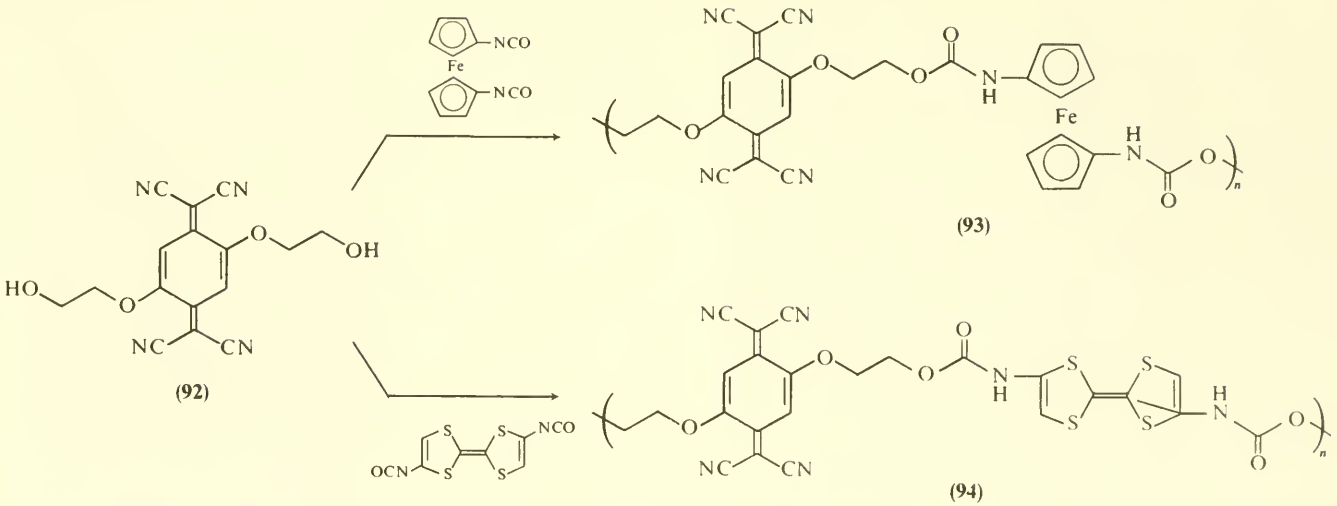
NCO
Fe
NCO
NC
CN
O
OH
HO
NC
CN
(92)
NC
CN
O
O
N
H
Fe
H
N
O
O
n
NC
CN
(93)
OCN
S
S
S
S
NCO
NC
CN
O
O
N
H
S
S
S
S
H
N
O
O
n
NC
CN
(94)

and (**94**). These polymers, which contain alternate donor and acceptor groups, were insoluble in organic solvents, and black. Molecular weights and structural confirmation were not provided. The ferrocene-containing polyurethane had a conductivity of $3{\cdot}3 \times 10^{-4}\,\Omega^{-1}\,cm^{-1}$ (compacted powder), which was two orders of magnitude lower than that of the complex formed between the corresponding TCNQ and ferrocene model compounds. This polymer contained both amorphous and crystalline components. The completely amorphous tetrathiafulvalene polyurethane had a conductivity of $1{\cdot}66 \times 10^{-11}\,\Omega^{-1}\,cm^{-1}$ (compacted powder). Disorder introduced into the polymer by the possible involvement of *cis* and *trans* (4,4′ and 4,5′) isomers of the substituted tetrathiafulvalene was the explanation offered for the substantially lower conductivity compared with the ferrocene polymer. It is likely that the polycondensation reaction is dominated by CT complexes formed between the reactants, and the ferrocene and TTF polymers could differ in structure, molecular weight, end group, etc. These effects will impact the resistivity and may account for the difference.

These donor–acceptor copolyurethanes possess rigid chain structures, and intrachain complex formation will not be favoured. In any case, in the solid state, intermolecular and intramolecular complex formation are indistinguishable and it seems probable that interchain complexes will dominate the properties.

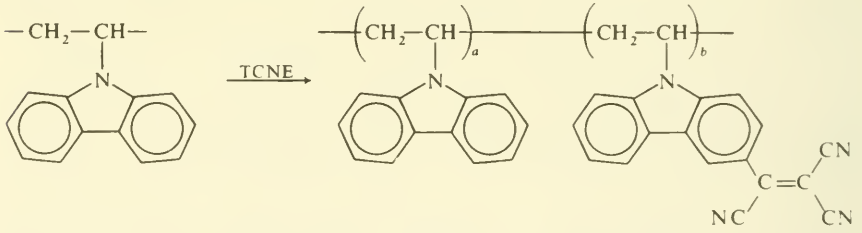

(**95**)

Polymeric systems can also be designed in which an intramolecular CT complex comprises the pendant group. An example of such a system is the copolymer of *N*-vinylcarbazole with *N*-vinyl-3-tricyanovinylcarbazole.[189] This unique polymer was synthesized by reaction of poly-(*N*-vinylcarbazole) with TCNE under controlled conditions (**95**). For degrees of tricyanovinylation below 10–15 mole per cent the copolymers are soluble and of comparable molecular weight to the starting polymers. Higher degrees of substitution can be achieved but at the expense of molecular weight control and solubility. The products become intensely coloured, increasingly intractable and more highly conducting. The increase in conductivity can possibly be attributed to contributions from intramolecular interactions, e.g. (**96**). Copolymers

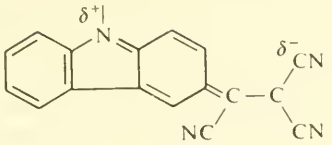

(96)

containing low levels of tricyanovinylcarbazole groups are considerably better photoconductors than poly-(*N*-vinylcarbazole) owing to the high extinction coefficient and visible light absorption characteristics ($\lambda_{max} \sim$ 500 nm) of the intramolecular complex. Hole mobilities decrease with increasing concentration of tricyanovinylcarbazole groups.

E. Charge-transfer Complexes in Polymeric Binders

Recently a number of publications have appeared on the optical and electrical properties of solutions of molecular CT complexes dissolved in polymeric matrices. Kryszewski has investigated the spectroscopic[190] and photoconductive[191] properties of the CT complexes of anthracene with chloranil and 1,3,5-trinitrobenzene in poly(methyl methacrylate) and polystyrene and of naphthalene, biphenyl, pyrene, durene, stilbene, carbazole and *N*-ethylcarbazole with TCNQ in a variety of polymer matrices.[192] The absorption, emission and photoconductive characteristics of the solid solutions were dependent on the concentration of the complex. Quenching of the donor emission was rationalized in terms of an energy-transfer process through free donor molecules to donor molecules in the complex. The excited complex centres can undergo a variety of deactivation processes, some of which can result in formation of charged species, i.e. photogeneration of charge carriers and observations of a photocurrent. The efficiency of photocurrent production correlates with the donor quenching, as observed experimentally. This mechanism is analogous to the electron transfer quenching suggested for complexes in liquid solutions, and is also consistent with the photogeneration mechanism suggested for the PVK–TNF system.[134] In optical and electrical properties these solid solutions are qualitatively similar to the solids in which one of the components (donor or acceptor) is chemically attached to a polymer backbone. The approach, however, does provide a

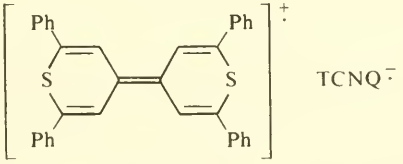

(97)

greater degree of freedom in evaluating CT complexes for which no polymeric component is known.

Perlstein, Van Allen, Isett and Reynolds reported[193] some very unusual and interesting results on films of the 2,2',6,6'-tetraphenyldithiapyranylidene–TCNQ complex dispersed in an inert polymer matrix (**97**). Compressed powder electrical measurements of the 1:1 complex showed conductivities comparable to the TTF–TCNQ system, i.e. ~ 10–$30\ \Omega^{-1}\ cm^{-1}$. The complex salt could be grown as fine filamentary structures in an insulating ($\sigma \approx 10^{-14}\ \Omega^{-1}\ cm^{-1}$) polyester matrix, and thin films ($\sim 1\ \mu m$) containing as little as 5 wt per cent complex had conductivities as high as $1\ \Omega^{-1}\ cm^{-1}$. This type of materials engineering approach will probably be pursued in the future to provide systems exhibiting unique processing, mechanical and electrical properties.

F. Polyacetylene Complexes

Doped polyacetylenes are new polymeric systems that are receiving much attention because of their broad range of electrical properties.[202] This new class of materials has exhibited conductivities that range over eleven orders of magnitude depending on the characteristics and concentration of the dopant. Conductivities at room temperature of about $10^3\ \Omega^{-1}\ cm^{-1}$ have been obtained. The electrical properties of these materials are thought to be a result of charge-transfer interaction between the dopant and polyacetylene. Dopants like iodine and bromine are postulated to behave as acceptors with the polyacetylene functioning as the donor, whereas doping with sodium, potassium and lithium results in the polyacetylene behaving as an acceptor polymer. Although a wide range of electrical properties has already been demonstrated, the exact chemical nature of these materials as well as the specific dopant interactions are as yet unclear. Because of their intriguing nature and their potential for practical applications, much activity in this field should be forthcoming.[203]

G. Present and Future Applications

In spite of the extensive world-wide studies on the electric and photoelectric properties of organic and polymeric charge-transfer complex materials, they have not yet found wide commercial exploitation. The success of the PVK–TNF complex in the electrophotographic industry[104,194] shows that organic systems can compete favourably with inorganic materials (selenium, zinc oxide, cadmium sulphide, etc.). Provided that the appropriate combination of conductive (or photoconductive) and mechanical and processing properties can be achieved, there will probably be further applications of polymeric CT complexes.

1. Electrophotography

A photoconductive material for use in the electrophotographic process is one that is insulating in the dark and becomes highly conducting when exposed to an appropriate light source. Charge carriers are generated by photons absorbed in the material. The mechanistic issues of the photogeneration process in organic systems have been reviewed recently.[195,196] Once

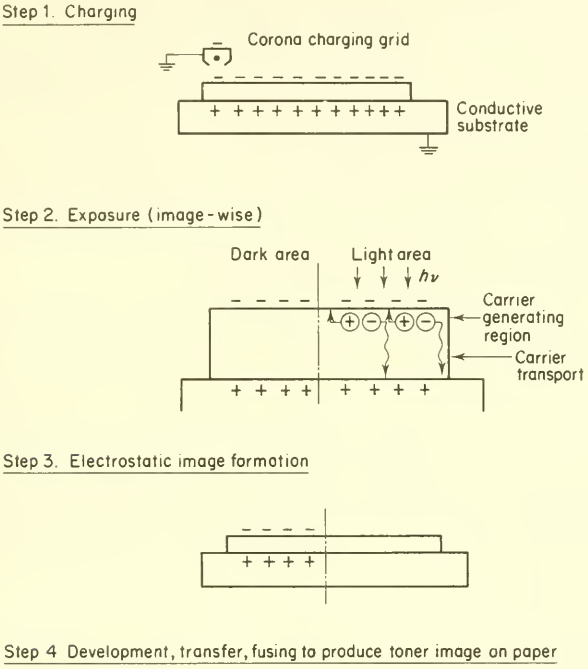

FIG. 18. Schematic diagram of the xerographic process.

produced, the charge carriers are transported through the material to the respective electrodes. A schematic diagram of the process is in Fig. 18.

The surface of the insulating photoconductive member is uniformly charged with a corona device consisting of a fine wire maintained at a high potential. Ionization of the air produces ionic species which are driven to the adjacent photoconductor surface by a bias potential on the grid. The surface charge polarity is determined by the photogeneration and transport characteristics of the system, e.g. Se, positive charging, majority carrier holes; PVK–TNF (1:1), negative charging, majority carrier electrons. This particular point is illustrated in more detail in step 2 for PVK–TNF (1:1). The absorption characteristics of this material at the wavelength and intensity of the light

used dictates that most of the charge carriers are produced within a relatively thin surface layer. Since electrons are the majority carrier in this material they are required to traverse the system to neutralize the positive charges on the back electrode. The positive holes are required to migrate only a relatively short distance to neutralize the surface negative charges. In the case of selenium, the opposite situation holds.

Following the charging step, the photoconductor is exposed to a light and dark image formed by reflecting light from the document to be copied. In the light-struck areas the charge carriers produced cause a reduction in the surface potential to form a latent electrostatic image on the surface of the member. This image is rendered visible by a developer consisting of a polymeric powder (toner) which is then transferred to a paper receiver sheet; the toned image is fused into the paper to become a permanent copy of the original document. To complete the xerographic process, the photoconductor surface is cleaned of any residual toner, any remaining electrostatic image is erased and the system is ready to repeat the cycle.

These basic steps in the xerographic process impose very rigid criteria on the photoconductive material. Among others, these include the ability to produce large area, defect free films of reproducible quality, long term stability and mechanical properties plus a set of demanding electrical capabilities. Many of these criteria can be met using organic polymeric materials and it is likely that other commercially viable systems will emerge in the future. It is perhaps unfortunate, in terms of our detailed understanding of photoelectric properties and particularly in establishing correlations with molecular structure, that most of these publications are in the patent and industrial literature.

2. Photoelectric Devices

Other potential photoelectric applications for polymer based CT complex materials include photocells, photomemory devices and radiation detectors. To our knowledge, organic systems are not at present used in any of these areas.

The development of a cheap, functional photovoltaic cell for efficient conversion of solar energy into a more usable energy form is of critical importance. Can organic-based systems compete in this area? Present solar cell technology uses silicon solid state *n–p* junction rectifiers which are both expensive and difficult to fabricate and which do not possess any storage capability. Conversion efficiencies of 10–15 per cent define the present state of the art. Devices based on organic polymeric materials certainly offer potential low cost, and easy fabrication advantages, but their photoelectric properties are at present far behind those of their inorganic competitors.

Reucroft *et al.*[197, 198] carried out both a theoretical and an experimental

analysis of photovoltaic conversion in their electroded structures using the PVK–TNF CT complex as the photoactive component. Using a hetero-junction model in which charge separation (free electron/free hole) occurs at the polymer–electrode interface, they showed that, for films of thickness $< 1\ \mu m$ in which the current flow through the cell becomes space charge limited, a modified model predicts even lower efficiencies, e.g. $1\ \mu m$, 10^{-3}–10^{-6} per cent and $10\ \mu m$, 10^{-7}–10^{-10} per cent. These extremely low efficiencies were verified experimentally. Clearly this particular system is impractical; whether other polymer based systems can be developed remains an open question.

Merritt and Hovel[199] have reported power conversion efficiencies of the order of 0·1–0·2 per cent for thin film (100–1000 Å) solar cells made from squaric acid based dyes (**98**), which possess broad absorption bands across

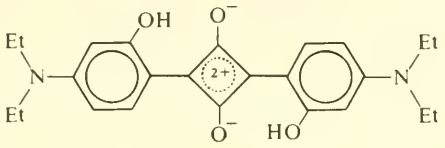

(**98**)

the visible region of the spectrum. Doping with bromine resulted in a 5-fold increase in efficiency, but this improvement degraded with time. Although these devices exhibited the characteristic (of organic systems) decrease in efficiency with increasing input light intensity, the effect was less pronounced than for other known systems. Interest in organic devices is obviously intensifying and a strong materials thrust can be expected in the next decade.

In view of the low charge-carrier photogeneration efficiencies and the low, and field dependent, mobilities exhibited by organic materials, the goal of an organic device must be regarded as a long range one.[111] It may well be that hybrid systems (organic–inorganic) can combine the best of both components (mechanical and photoelectrical).

3. Power Sources

Rembaum and coworkers[200] developed the first organic primary electrochemical solid-state cells containing metal anodes and charge-transfer complexes as cathodes. Some of the complexes used were iodine with perylene, phenothiazine, PVK, poly-(2-vinylquinoline) and poly(vinylpyridine). The poly-(2-vinylpyridine)–I_2 complex has since been developed as the cathode in the miniature Li–I_2 primary cell for implantable cardiac pacemakers.[105] This device (Fig. 19) weighs only 80 g, has dimensions of 5·2 × 4·4 × 1·2 cm, a voltage of 2·8 V (open circuit) and a capacity of 4 A h with an

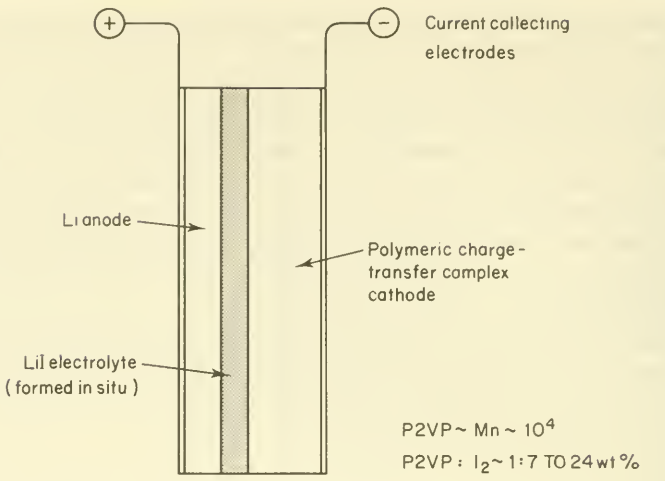

FIG. 19. Schematic diagram of the electrochemical cell based on the poly-(2-vinylpyridine) (P2VP)–I_2 charge-transfer complex.

energy density of 120 W h kg^{-1}. The reaction responsible for the electrochemical current generation is the formation of LiI. The polymeric complex serves a dual function, as a source of iodine for the cell reaction ($Li + \frac{1}{2}I_2 \rightarrow LiI$) and as an electronic conductor to carry the current to the collecting electrode. The conductivity of the complex remains constant around 10^{-3} $\Omega^{-1}\,cm^{-1}$ as the I_2 concentration falls from 90 to 75 per cent as the cell is discharged. These properties compare extremely favourably with those of the best lead–acid batteries, and the long service life (~ 10 years) has made the cell a competitive electromedical device. Vincent *et al.*[201] have shown that electrodes based on phenothiazine– and *N*-alkylphenothiazine–iodine complexes exhibit excellent properties (discharge and recharge characteristics) for solid-state cell applications. The polymeric analogues may also be competitive with the vinylpyridine systems.

VII. CONCLUSIONS

Charge-transfer complexes formed from polymeric donor or acceptor components are considerably more complex than their low molecular weight model analogues. The macromolecular environment imposes certain unique constraints on the nature and the formation of the complexes. Polymeric donors and acceptors are subject to conformational perturbations arising from the individual polymer backbone which introduce orientation and concentration effects absent in the simple molecular systems. Such

effects may result in an increased population of sites comprising more than one donor or acceptor unit and formation of higher order complexes. In studies of complex formation in solution these phenomena will be largely controlled by the actual donor–acceptor pair and by the polymer–solvent interactions which influence chain conformation. In the amorphous solid they will become especially important. Unfortunately our understanding of the molecular aspects of the polymeric solid state precludes any rigorous interpretation of the nature and structural issues involved in complex formation.

The pronounced effects observed for rigid small molecules such as paracyclophanes have very obvious relevance to the understanding and interpretation of the behaviour of polymeric donors and acceptors. Furthermore, comparison of polymers with carefully chosen low molecular weight models is extremely important in elucidating the polymer chain conformation effect. For this purpose it is desirable to have more reliable estimates of the values of association constants than are at present available. The rather limited amount of quantitative data can be taken to imply that there is a small but significant long wavelength shift in the λ_{max} value of CT transitions of polymeric donors in comparison with their small molecule models when complexed with some common acceptor.

Polymer based CT complexes are important from a practical point of view. Their physical, mechanical and processing properties make them attractive for many applications. These properties, coupled with their light absorption characteristics, have obvious potential in photoactivated systems. In addition to the properties associated with polymeric donor or acceptor materials, there are equally important advantages to be obtained in utilizing appropriate inert polymeric binders for small molecule complexes.

At the present the number of commercial applications of polymeric CT complexes is small. These novel materials have, however, made inroads into the electrophotographic and medical scene. Further applications in the electronics and energy industries seem possible. Other polymer based systems with tailored electrical, photoelectrical and mechanical properties for specialized applications can be developed. As we learn more about the electronic properties of organic materials, the evolution of new and improved functional systems appears to be both feasible and realistic.

REFERENCES

1. R. S. Mulliken, *J. Chem. Phys.*, **19**, 514 (1951); *J. Amer. Chem. Soc.*, **74**, 811 (1952); *J. Phys. Chem.*, **56**, 801 (1952).
2. R. Foster, "Organic Charge-Transfer Complexes", Academic Press, London and New York (1969).

3. R. Foster (ed.), "Molecular Complexes", Vol. 1, Elek Science, London: Crane Russak, New York (1973).
4. R. Foster (ed.), "Molecular Complexes", Vol. 2, Elek Science, London; Crane Russak, New York (1974).
5. R. Foster (ed.), "Molecular Association", Vol. 1, Academic Press, London and New York (1975).
6. M. Ottolenghi, *Accounts Chem. Res.*, **6**, 153 (1973).
7. P. Hyde and A. Ledwith, ref. 4, p. 173.
8. A. Weller, *Pure and Applied Chem.*, **16**, 115 (1968).
9. M. Gordon and W. R. Ware (eds.), "The Exciplex", Academic Press, New York (1975).
10. J. B. Birks (ed.), "Organic Molecular Photophysics", Vol. 1, Wiley, London (1973).
11. J. B. Birks (ed.), "Organic Molecular Photophysics", Vol. 2, Wiley. London (1975).
12. A. C. Somersall and J. E. Guillet, *J. Macromol. Sci., Revs. Macromol Chem.*, **C13**, 135 (1975).
13. J. M. Pearson, *Pure and Applied Chem.*, **49**, 463 (1977); J. Mort and D. M. Pai (eds.), "Photoconductivity and Related Phenomena", Elsevier, Amsterdam (1976); A. V. Patsis and D. A. Seanor (eds.), "Photoconductivity in Polymers", Technomic, Westport, Conn. (1976).
14. E. P. Goodings, *Endeavour*, **34**, 123 (1975); *Quart. Revs. Chem. Soc.*, **5**, 95 (1976).
15. E. M. Engler, *Chem. Tech.*, **6**, 274 (1976).
16. S. I. Peredereeva, I. G. Orlov and M. I. Cherkashin, *Russian Chem. Revs.*, **44**, 295 (1975).
17. T. Tomono and E. Tschida, *Kagaku No Ryoiki*, 903 (1975).
18. K. Komatsu and R. West, *Chem. Comm.*, 570 (1976).
19. L. B. Coleman, M. J. Cohen, D. J. Sandman, F. G. Yamagishi, A. F. Garito and A. J. Heeger, *Solid State Comm.*, **12**, 1125 (1973); J. P. Ferraris, D. O. Cowan, V. Walatka and J. Perlstein, *J. Amer. Chem. Soc.*, **95**, 948 (1973).
20. D. C. Green, *Chem. Comm.*, 161 (1977); R. C. Wheland and J. L. Gillson, *J. Amer. Chem. Soc.*, **98**, 3916 (1976).
21. E. M. Engler, F. B. Kaufman, D. C. Green, C. E. Kots and R. N. Compton, *J. Amer. Chem. Soc.*, **97**, 2921 (1975).
22. M. L. Kaplan, R. C. Hadden and F. Wudl, *Chem. Comm.*, 388 (1977).
23. D. J. Sandman, A. J. Epstein, T. J. Holmes and A. P. Fisher, *Chem. Comm.*, 177 (1977).
24. F. Wudl, M. L. Kaplan, B. K. Teo and J. Marshall, *J. Org. Chem.*, **42**, 1666 (1977).
25. N. F. Haley, *Chem. Comm.*, 207 (1977).
26. K. D. Truong and A. D. Bandrauk, *Chem. Phys. Letters*, **44**, 232 (1976).
27. B. Dodson, R. Foster, A. A. S. Bright, M. I. Foreman and J. Gorton, *J. Chem. Soc. (B)*, 1283 (1971); R. Foster and N. Kulevsky, *J. Chem. Soc. Faraday I*, **69**, 1427 (1973); R. J. Bailey, J. A. Chudek and R. Foster, *J. Chem. Soc. Perkin II*, 1590 (1976).
28. J. A. Chudek, R. Foster and E. Vogel, *J. Chem. Soc. Perkin II*, 994 (1977).
29. M. Yoshida, H. Tatemitsu, Y. Sakata, S. Misumi, H. Masuhara and N. Mataga, *Chem. Commun.* 587 (1976).
30. H. Masuhara, N. Mataga, M. Yoshida, H. Takemitsu, Y. Sakata and S. Misumi, *J. Phys. Chem.* **81**, 879 (1977).
31. H. Horita, T. Otsubo, Y. Sakata and S. Misumi, *Tetrahedron Lett.*, 3899 (1976); J. G. O'Connor and P. M. Keehn, *J. Amer. Chem. Soc.*, **98**, 8446 (1976); *Tetrahedron Lett.*, 3714 (1977).

32. R. Luhowy and P. M. Keehn, *J. Amer. Chem. Soc.*, **99**, 3797 (1977).
33. H. Beens and A. Weller, *Chem. Phys. Letters*, **2**, 140 (1968).
34. H. Masuhara and N. Mataga, *Chem. Phys. Letters*, **22**, 305 (1973).
35. T. Mimura and M. Itoh, *Bull. Chem. Soc. Japan*, **50**, 1739 (1977).
36. T. Mimura and M. Itoh, *J. Amer. Chem. Soc.*, **98**, 1095 (1976).
37. T. Mimura, M. Itoh, T. Ohta and T. Okamoto, *Bull. Chem. Soc. Japan*, **50**, 1665 (1977).
38. R. H. Boyd and W. D. Phillips, *J. Chem. Phys.*, **43**, 2927 (1965).
39. B. Badger and B. Brocklehurst, *Trans. Farad. Soc.*, **65**, 2159 (1969).
40. E. A. Chandross and C. J. Dempster, *J. Amer. Chem. Soc.*, **92**, 3586 (1970); T. Okada, T. Saito, N. Mataga, Y. Sakata and S. Misumi, *Bull. Chem. Soc. Japan*, **50**, 331 (1977).
41. R. S. Davidson and K. R. Trethewey, *Chem. Comm.*, 827 (1976).
42. R. A. Caldwell, D. Creed and H. Ohta, *J. Amer. Chem. Soc.*, **97**, 3246 (1975); G. N. Taylor, E. A. Chandross and A. H. Schiebel, *ibid.*, **96**, 2693 (1974).
43. N. C. Yang, M. H. Hui, D. M. Shold, N. J. Turro, R. R. Hautala, K. Dawes and C. J. Dalton, *J. Amer. Chem. Soc.*, **99**, 3023 (1977).
44. M. W. Wolf, R. E. Brown and L. A. Singer, *J. Amer. Chem. Soc.*, **99**, 526 (1977).
45. H. D. Becker and K. Sandros, *Chem. Phys. Lett.*, **53**, 228 (1978).
46. T. Okada, T. Fujita and N. Mataga, *Z. Phys. Chem.* (N.F.), **101**, 57 (1976); J. Prochorow and E. Bernard, *J. Luminescence*, **8**, 471 (1974).
47. C. K. Prout, ref. 3, p. 151.
48. M. Tanaka, *Bull. Chem. Soc. Japan*, **50**, 525 (1977).
49. R. S. Davidson and A. Lewis, *Tetrahedron Lett.*, 611 (1974).
50. J. H. Borkent, J. W. Verhoeven and Th. J. De Boer, *Tetrahedron Lett.*, 3363 (1972).
51. J. W. Verhoeven, I. P. Dirkx and Th. J. De Boer, *Tetrahedron*, **25**, 4037 (1969).
52. R. Carruthers, F. M. Dean, L. E. Houghton and A. Ledwith, *Chem. Comm.*, 1206, (1967).
53. H. A. H. Craenen, J. W. Verhoeven and Th. J. De Boer, *Rec. Trav. Chim. Pays-Bas*, **91**, 405 (1972).
54. K. Mutai, *Bull. Chem. Soc. Japan*, **45**, 2635 (1972).
55. M. Sisido, H. Takagi, Y. Imanishi and T. Higashimura, *Macromolecules*, **10**, 125 (1977).
56. H. A. Staab and H. Haffner, *Tetrahedron Lett.*, 4393, 4397 (1974).
57. M. W. Haenel, A. Flatow, V. Taglieber and H. A. Staab, *Tetrahedron Lett.*, 1733 (1977); H. A. Staab, C. P. Herz and Henke, *Chem. Ber.*, **110**, 3351 (1977).
58. T. Nakazawa and I. Murata, *J. Amer. Chem. Soc.*, **99**, 1996 (1977).
59. J. Prochorow, *J. Luminescence*, **9**, 131 (1974).
60. J. Prochorow and E. Bernard, *J. Luminescence*, **8**, 471 (1974).
61. J. H. Borkent, J. W. Verhoeven and Th. J. De Boer, *Chem. Phys. Letters*, **42**, 50 (1976).
62. H. A. Staab and C. P. Herz, *Angew. Chem. Int. Ed. Engl.*, **16**, 799 (1977).
63. L. E. Orgel, *J. Chem. Phys.*, **23**, 1352 (1955).
64. M. J. Mobley, K. E. Rieckhoft and E. M. Voigt, *J. Phys. Chem.*, **81**, 809 (1977); K. H. Michaelian, K. E. Rieckhoft and E. M. Voigt, *Proc. Nat. Acad. Sci. U.S.A.*, **72**, 4196 (1975).
65. J. Bendig, B. Dobslaw and D. Kreysig, *Z. Phys. Chem.* (Leipzig), **258**, 699 (1977); J. Bendig, B. Dobslaw, B. Ehmke, I. Juchert and D. Kreysig, *ibid.*, **258**, 705 (1977).
66. M. Rossi, U. Buser and E. Haselbach, *Helv. Chim. Acta*, **59**, 1039 (1976).
67. J. L. Lippert, M. W. Hanna and P. J. Trotter, *J. Amer. Chem. Soc.*, **91**, 4035 (1969).
68. W. C. Herndon and J. Feuer, *J. Amer. Chem. Soc.*, **90**, 5914 (1968).

69. D. D. Holder and C. C. Thompson, *Chem. Comm.*, 277 (1972).
70. H. Sakurai and M. Kira, *J. Amer. Chem. Soc.*, **97**, 4879 (1975).
71. W. Klöpffer, *Z. Naturforsch.*, **24a**, 1923 (1969).
72. U. Landman, A. Ledwith, D. G. Marsh and D. J. Williams, *Macromolecules*, **9**, 833 (1976).
73. H. J. Haink, J. E. Adams and R. J. Huber, *Ber. Bunsenges. Phys. Chem.*, **78**, 436 (1974); J. Behan, University of Liverpool, unpublished results.
74. E. Chiellini, R. Solaro and A. Ledwith, in the press.
75. H. Vogler, G. Ege and H. A. Staab, *Tetrahedron*, **31**, 2441 (1975).
76. K. Okamoto, M. Ozeki, A. Itaya, S. Kusabayashi and H. Mikawa, *Bull. Chem. Soc. Japan*, **48**, 1362 (1975).
77. H. Boudevska, G. Velinov and I. Ichobanova, *Makromol. Chem.*, **172**, 107 (1973).
78. S. Iwatsuki and K. Arai, *Makromol. Chem.*, **178**, 2307 (1977).
79. K. H. Brown and J. P. Montillier, *Photog. Sci. Eng.*, **22**, 22 (1978).
80. Y. Matsuyama and S. Tazuke, *Makromol. Chem.*, **176**, 1657 (1975); H. Ito, S. Tazuke and M. Okawara, *ibid.*, **177**, 621 (1976).
81. A. Ledwith and M. Keyanpoor-Rad, unpublished results.
82. R. C. Schulz and U. Geissler, *Makromol. Chem.* **179**, 1355 (1978), and personal communication.
83. M. H. Litt and J. W. Summers, *J. Polymer Sci., Polymer Chem. Ed.*, **11**. (*a*) 1339, (b) 1353, (c) 1359 (d) 1379 (1973).
84. A. Ledwith and K. C. Smith, unpublished results.
85. S. Tazuke, K. Sato, F. Banba and Y. Matsuyama, *J. Polymer Sci., Polym. Letters Ed.*, **14**, 653 (1976).
86. B. Gebus and R. Knoesel, *Makromol. Chem.*, **175**, 1439 (1974).
87. S. Iwatsuki and K. Inukai, *Makromol. Chem.*, **179**, 189 (1978).
88. S. Iwatsuki and K. Arai, *J. Polymer Sci., Polymer Chem. Ed.*, **10**, 3329 (1972); S. Iwatsuki and K. Inukai, *ibid.*, **12**, 1437 (1974).
89. H. A. Bruson and G. B. Butler, *U.S. Patent* 2,407,131 (September 3, 1946).
90. N. N. Tebedev and L. V. Andrianova, *J. Gen. Chem. USSR*, **25**, 193 (1955).
91. G. Smets, V. Balogh and Y. Castille, *J. Polymer Sci., Part C*, **4**, 1467 (1963).
92. R. C. Schulz and H. Tanaka, *Pure and Appl. Chem.*, **38**, 227 (1974).
93. T. Sulzberg and R. J. Cotter, *Macromolecules*, **1**, 554 (1968); T. Sulzberg and R. J. Cotter, *J. Polymer Sci., Part A-1*, **8**, 2747 (1970); R. J. Cotter and T. Sulzberg, *U.S. Patent* 3,536,781 (October 27, 1970).
94. H. Naarmann, *Angew. Chem.*, **81**, 871 (1969); *German Patent* 1,953,898.
95. S. R. Turner and C. AuClair, *Macromolecules*, **9**, 868 (1976).
96. J. T. Ayres and C. K. Marin, *Analytical Chem.*, **36**, 2185 (1964).
97. S. T. Snyder and C. M. Welch, *J. Polymer Sci., Polymer Letters Ed.*, **11**, 695 (1973).
98. N. C. Yang and Y. Gaoni, *J. Amer. Chem. Soc.*, **86**, 5022 (1964).
99. D. A. Seanor and W. W. Limburg, *U.S. Patent* 3,877,936 (to Xerox Corporation); W. W. Limburg, unpublished results.
100. T. Tomono, E. Hasegawa and E. Tsuchida, *J. Polymer Sci., Polymer Letters Ed.*, **12**, 139 (1974).
101. A. Inami, K. Morimoto and Y. Hayashi, *Bull. Chem. Soc. Japan*, **37**, 842 (1964).
102. A. Inami and K. Morimoto, *German Patent* 1,264,954 (to Matsushita) (March 28, 1968); *U.S. Patent* 3,418,116 (to Matsushita) (December 24, 1968).
103. S. R. Turner and M. Stolka, *Macromolecules*, **11**, 835 (1978).
104. R. M. Shaffert, *IBM Journal of Research and Development*, **15**, 75 (1971), and references therein.

105. A. A. Schneider, W. Greatbatch and R. Mead, *9th International Power Sources Symposium Paper No. 3*, Brighton, U.K. (1974).
106. P. J. Regensburger, *Photochemistry and Photobiology*, **8**, 429 (1968).
107. (a) A. M. Hermann and A. Rembaum, *J. Polymer Sci., Part C.* **17**, 107 (1967). (b) *ibid., Polymer Letters*, **5**, 445 (1967). (c) A. Rembaum, A. M. Hermann and R. Haack, *J. Polymer Sci.*, **6**, 1955 (1968). (d) A. Rembaum and A. M. Hermann, *J. Applied Phys.*, **37**, 3642 (1966). (e) A. M. Hermann, in "Electrical Properties of Polymers" (ed. K. C. Frisch and A. Patsis), Technomic Publ. Co., Conn. (1972).
108. W. D. Gill, *J. Applied Physics*, **43**, 5033 (1972).
109. O. H. Le Blanc, *J. Chem. Phys.*, **33**, 626 (1960).
110. J. H. Sharp, *J. Phys. Chem.*, **71**, 2587 (1967).
111. M. M. Labes, *J. Polymer Sci., Part C.*, **17**, 95 (1967).
112. D. A. Seanor, in "Polymer Science" (ed. A. D. Jenkins), Amer. Elsevier Publ. Co. N.Y. (1972), Ch. 17, pp. 1188–1280.
113. J. Mort and R. L. Emerald, *J. Applied Physics*, **45**, 175 (1974).
114. W. D. Gill, in "Proceedings of the Int. Conf. on Amorphous and Crystalline Semiconductors", Taylor and Francis, London (1973).
115. H. Mikawa, personal communication.
116. D. J. Williams, W. W. Limburg, J. M. Pearson, A. O. Goedde and J. F. Yanus, *J. Chem. Phys.*, **62**, 1501 (1975).
117. J. Mort, G. Pfister and S. Grammatica, *Solid State Comm.*, **18**, 693 (1976).
118. M. Froix, D. J. Williams and A. O. Goedde, *Bull. Amer. Phys. Soc.*, **20**, 473 (1975).
119. A. F. Garito and A. J. Heeger, *Accounts of Chemical Research*, **7**, 232 (1974); J. H. Perlstein, *Angew. Chem. Int. Ed. (Eng.)*, **16**, 519 (1977).
120. H. Seki, in "Amorphous and Liquid Semiconductors" (ed. J. Stuke and W. Brenig), Taylor and Francis, London (1975), p. 135.
121. H. Scher and E. Montroll, *Phys. Rev. B.*, **12**, 2455 (1975).
122. F. Gutmann and L. E. Lyons, "Organic Semiconductors", J. Wiley and Sons, New York (1967).
123. H. Meier, in "Organic Semiconductors", Monographs in Modern Chemistry, Vol. 2, Verlag Chemie, Weinheim (1974).
124. I. Chen and J. Mort, *J. Applied Phys.*, **43**, 1164 (1972).
125. M. Kryszewski and A. Szymanski, *J. Polymer Sci., Macromol. Revs.*, **D4**, 245 (1970).
126. D. M. Pai, *J. Chem. Phys.*, **52**, 2285 (1970).
127. H. Hoegl, O. Sus and W. Neugebauer, *German Patent* 1,068,115 (to Kalle A/G) (1957).
128. H. Hoegl, *J. Phys. Chem.*, **69**, 755 (1965).
129. M. Lardon, E. Lell-Doller and J. W. Weigl, *Molecular Crystals*, **2**, 241 (1967).
130. H. Hoegl and W. Neugebauer, *U.S. Patent* 3,162,532 (to Kalle A/G).
131. A. I. Lakatos and J. Mort, *Phys. Rev. Letters*, **21**, 1444 (1968).
132. A. I. Lakatos and J. Mort, *J. Non-Crystalline Solids*, **4**, 117 (1970).
133. H. Block, M. A. Cowd and S. M. Walker, *Polymer*, **18**, 781 (1977).
134. G. Weiser, *J. Applied Physics*, **43**, 5028 (1972).
135. G. Weiser, *Phys. Stat. Solid*, **18**, 347 (1973).
136. J. Rochlitz, in "Current Problems in Electrophotography" (ed. W. F. Berg and K. Hauffe), W. de Gruyter, Berlin (1972), p. 244.
137. J. Mort and H. Scher, *Phys. Rev. B.*, **3**, 334 (1971).
138. A. M. Hermann and M. Nagao, *J. Polymer Sci. Poly Letters Edition*, **12**, 69 (1974).

139. K. Okamoto, K. Kato, K. Murao, S. Kusabayashi and H. Mikawa, *Bull. Chem. Soc. Japan*, **46**, 2883 (1973).
140. C. U. Pittman and P. L. Grube, *J. Applied Polymer Sci.*, **18**, 2269 (1974).
141. J. H. Lupinski and K. D. Kopple, *Science*, **146**, 1038 (1964).
142. J. H. Lupinski, K. D. Kopple and J. J. Hertz, *J. Polymer Sci. C*, **16**, 1561 (1967).
143. H. Nomori, M. Hatano and S. Kambara, *J. Chem. Soc. Japan*, (*Ind. Chem. Section*), **67**, 1608 (1964).
144. A. Rembaum, A. M. Hermann and R. Haack, *J. Polymer Sci.*, **6**, 1955 (1968).
145. A. Rembaum, A. M. Hermann, F. E. Stewart and F. Gutmann, *J. Phys. Chem.*, **73**, 513 (1969).
146. V. Hadek, N. Noguchi and A. Rembaum, *Macromolecules*, **4**, 494 (1971).
147. A. Rembaum, A. M. Hermann and F. Gutmann, *Nature*, **221**, 1237 (1969).
148. G. J. Ashwell, D. D. Eley and M. R. Willis, *Nature*, **259**, 201 (1976).
149. J. Ferraris, D. O. Cowan, V. Walatka and J. H. Perlstein, *J. Amer. Chem. Soc.*, **95**, 948 (1973).
150. E. M. Engler and V. V. Patel, *J. Amer. Chem. Soc.*, **96**, 7376 (1974).
151. S. P. S. Yen, R. Somoano, V. Hadek, E. Cuellar, E. Washington and A. Rembaum, *Polymer Preprints*, **17**, 321 (1976).
152. V. Hadek, H. Noguchi and A. Rembaum, *Macromolecules*, **4**, 494 (1971).
153. R. Somoano, S. P. S. Yen and A. Rembaum, *J. Polymer Sci., Polymer Letters*, **8**, 467 (1970).
154. A. M. Hermann, S. P. S. Yen, A. Rembaum and R. F. Landel, *J. Polymer Sci., Polymer Letters*, **9**, 627 (1971).
155. M. S. Simon and P. T. Moore, *J. Polymer Sci., Polymer Chem. Ed.*, **13**, 1 (1975).
156. A. Factor and G. E. Heinsohn, *J. Polymer Sci., Polymer Letters, Ed.* **9**, 289 (1971).
157. W. Slough, *Trans. Faraday Soc.*, **58**, 2360 (1962).
158. O. W. Bonniface, M. J. Braithwaite, D. D. Eley, R. G. Evans, R. Pithig and M. R. Willis, *Disc. Faraday Soc.*, **51**, 131 (1971); but see also E. P. Goodings, *ibid.*, **51**, 157 (1971).
159. (a) D. O. Cowan, J. Park, C. U. Pittman, Y. Sasaki, T. K. Mukherjee and N. A. Diamond, *J. Amer. Chem. Soc.*, **94**, 5110 (1972). (b) Y. Sasaki, L. L. Walker, E. L. Hurst and C. U. Pittman, *J. Polymer Sci., Polymer Chem. Ed.*, **11**, 1213 (1973). (c) C. U. Pittman, Y. Sasaki and P. L. Grube, *J. Macromolecular Sci., A*, **8**, 923 (1974).
160. U. T. Mueller-Westerhoff and P. Eilbracht, *J. Amer. Chem. Soc.*, **94**, 9274 (1972).
161. D. O. Cowan and C. Le Vanda, *J. Amer. Chem. Soc.*, **94**, 9271 (1972).
162. C. U. Pittman and B. Surynarayanan, *J. Amer. Chem. Soc.*, **96**, 7916 (1974).
163. L. R. Melby, H. D. Hartzler and W. A. Sheppard, *J. Org. Chem.*, **39**, 2456 (1974).
164. Y. Ueno, Y. Masuyama and M. Okawara, *Chemistry Letters*, 603 (1975).
165. C. U. Pittman, M. Narita and Y. F. Liang, *Synthesis*, 489 (1976).
166. C. U. Pittman, M. Narita and Y. F. Liang, *Macromolecules*, **9**, 360 (1976).
167. W. R. Hertler, *J. Org. Chem.*, **41**, 1412 (1976).
168. C. U. Pittman, personal communication.
169. D. C. Green, *Chem. Comm.*, 161 (1977), and personal communication.
170. J. B. Torrance and B. D. Silverman, *Physical Review B.*, **15**, 788 (1977).
171. F. Denoyer, R. Comes, A. F. Garito and A. J. Heeger, *Phys. Rev. Letters*, **35**, 445 (1975).
172. R. Comes, S. M. Shapiro, G. Shirane, A. F. Garito and A. J. Heeger, *Phys. Rev. Letters*, **35**, 1518 (1975).
173. K. Nakatani, T. Sakata and H. Tsubomura, *Bull. Chem. Soc. Japan*, **48**, 2205 (1975).

174. J. Q. Chambers, D. C. Green, F. Kaufman, E. M. Engler, B. A. Scott and R. R. Schumaker, *Anal. Chem.*, **49**, 802 (1977).
175. W. A. Barlow, G. R. Davies, E. P. Goodings, R. L. Hand, G. Owen and M. Rhodes, *Molecular Crystals, Liquid Crystals*, **33**, 123 (1976).
176. J. F. Yanus and J. M. Pearson, *Macromolecules*, **7**, 716 (1974).
177. J. F. Yanus and J. M. Pearson, unpublished results.
178. J. F. Yanus and J. M. Pearson, *Macromolecules*, **7**, 951 (1974).
179. D. M. Pai and S. R. Turner, unpublished results.
180. H. G. Cassidy, *J. Polymer Sci., D*, **6**, 1 (1972).
181. G. Manecke, *Pure and Applied Chem.*, **38**, 181 (1974).
182. R. C. Schulz, H. Tanaka, D. M. Pai and S. R. Turner, unpublished results.
183. J. M. Pearson, unpublished results.
184. G. B. Butler and K. Sivaramakrishnan, *Polym. Prep.*, **17**, 608 (1976).
185. A. Inami, K. Morimoto and Y. Hayashi, *Bull. Chem. Soc. Japan*, **37**, 842 (1964).
186. K. Morimoto and A. Inami, *J. Chem. Soc. Japan (Ind. Chem. Sect.)*, **67**, 1938 (1964).
187. H. Kusagawa and S. Nishizaki, *Bull. Chem. Soc. Japan*, **38**, 2201 (1965).
188. (a) W. W. Limburg and D. A. Seanor, *Belgian Patent* 812,434 (1973) (to Xerox Corp). (b) personal communication of unpublished results.
189. (a) W. W. Limburg, *Belgian Patent* 816,552 (1974) (to Xerox Corp.). (b) Personal communication of unpublished results.
190. A. Degorski and M. Kryszewski, *J. Chem. Soc. Faraday II*, **71**, 1503 (1975).
191. A. Degorski and M. Kryszewski, *J. Chem. Soc. Faraday II*, **71**, 1513 (1975).
192. M. Kryszewski and P. Wojciechowski, *Molecular Crystals, Liquid Crystals*, **32**, 183 (1976).
193. New York Academy of Sciences Conference on Synthesis and Properties of Low Dimensional Materials, New York (June 1977), proceedings to be published.
194. M. D. Shattuck and U. Vahtra, *U.S. Patent* 3,484,237 (1969) (to I.B.M.).
195. D. J. Williams, *J. Chem. Phys.*, **61**, 2416 (1974).
196. J. H. Sharp and M. Smith, in "Physical Chemistry" (series ed. E. M. Loebl), Vol. 10 (ed. P. J. Holmes), Ch. 8, p. 435, Academic Press, New York (1969).
197. P. J. Reucroft, K. Takahashi and H. Ullal, *Applied Physics Letters*, **25**, 664 (1974).
198. P. J. Reucroft, K. Takahashi and H. Ullal, *J. Applied Physics*, **46**, 5218 (1975).
199. V. Y. Merritt and H. J. Hovel, *Applied Physics Letters*, **29**, 414 (1976).
200. F. Gutmann, A. M. Hermann and A. Rembaum, *J. Electrochem. Soc.*, **114**, 323 (1967).
201. M. Pampallona, A. Ricci, B. Scrosati and C. A. Vincent, *J. Applied Electrochem.*, **6**, 269 (1976).
202. A. G. Macdiarmid and A. J. Heeger, *Amer. Chem. Soc., Coatings and Plast. Prepr.*, **38**, 625, 631 (1978).
203. K. C. Yee and R. R. Chance, *J. Polymer Sci., Polymer Phys. Ed.*, **16**, 431 (1978).

3 Study of Complexation Phenomena by Gas–Liquid Chromatography

R. J. LAUB* and C. A. WELLINGTON

Department of Chemistry, University College of Swansea, Swansea SA2 8PP, U.K.

I. Introduction: Physicochemical Applications of Gas–Liquid Chromatography 172
A. The chromatographic method: advantages and limitations . . 173
B. Retention equations 173
C. Instrumentation 175
1. Column thermostats 176
2. Pressure controllers 177
3. Flow meters 177
4. Injectors 178
5. Detectors 178
6. Data acquisition systems 178
D. Sources of error 179
1. Systematic errors 179
2. Random errors 183
E. Accuracy of gas–liquid chromatographic data 184
II. Gas–Liquid Chromatographic Studies of Complexation Phenomena . 184
A. Evidence of complexation 186
B. Quantitative assessment of complexation phenomena . . . 187
1. General remarks 187
2. Approach of Gil-Av and Herling 188
3. Approach of Eon, Pommier and Guiochon 191
4. Approach of Martire and Riedl 194
5. Approach of deLigny 198
6. Approach of Langer, Johnson and Conder 200
7. Approach of Cadogan and Sawyer 200
C. Comparison of glc data with those of other techniques . . . 202
III. Recent Developments 206
A. Concentration effects in non-ionic solvent–additive systems . . 207

*Department of Chemistry, Ohio State University, Columbus, Ohio 43210, U.S.A.

B. Solvent effects 208
C. Diachoric solutions hypothesis 209
1. Evaluation by nmr spectroscopy 216
2. Evaluation by gas–liquid chromatography 217
D. Microscope partition (MP) theory of solutions 230
1. Extension to ultraviolet-visible spectroscopy 233
2. Extension to nmr spectroscopy 234
3. Disparity between chromatographic and spectroscopic data . 234
4. Interpretation of solvent effects 236
IV. Practical Consequences of MP Theory 237
A. The Laub–Purnell window diagram procedure 239
B. Extension to multi-component stationary phases 249
C. Extensions to solute mixtures of initially unknown content . . 250
D. Use with relative retention data 251
E. Application to gas–solid and gas–liquid–solid chromatography . 253
F. Applicants to liquid chromatography 253
G. Application to other system variables 254
1. The column temperature 254
2. The column pressure 255
References 256

I. INTRODUCTION: PHYSICOCHEMICAL APPLICATIONS OF GAS–LIQUID CHROMATOGRAPHY

The remarkable variety of separations to which gas chromatography has been applied is such that virtually every branch of science has at some time or other found it to be a useful (if not indispensable) analytical technique. An indication of the utility of the method is given by the temperature range over which it has been employed. For example, the nuclear and spin isotopes of hydrogen have been resolved at 32 K by Purer and Kaplan,[1] and Barrett[2] has patented a gas chromatograph capable of operation at 3000°C which was designed for the separation of cadmium from cadmium–mercury amalgams.

However, relatively few are aware of the potential of gas chromatography for physicochemical studies. Still others have noted that much of the early analytical work is irreproducible and have assumed that gas chromatography can accordingly have little relevance to physical measurements where accurate data are sought. In contrast, several workers[3–13] recognized in the period 1952–1956 that retention behaviour in gas–liquid chromatography (glc) is firmly linked to that of solutions in general, and that the glc method thus provides a dynamic approach analogous in all other ways to classical static procedures. Many glc studies relating in particular to complexation phenomena have since been reported and a review of these forms the substance of this chapter. In addition, a brief discussion of relations and procedures peculiar to glc is provided.[14–28] This is intended in part to intro-

duce what to many may be new or hitherto unrecognized areas of research and, further, to dispel the commonly held but specious notion that such studies, if chromatographic, are of little value.

A. The Chromatographic Method: Advantages and Limitations

The glc method has a number of inherent advantages when applied to acquisition of physicochemical data pertaining *inter alia* to complexation phenomena. The most significant of these are: (a) work at infinite dilution of the solute is "normal" in the elution mode of operation considered here; (b) high purity of solutes is not essential since separation can be achieved during the measurement process; (c) the technique demands neither sophisticated technical skill in the operator nor exceptionally sophisticated or expensive equipment; (d) studies may be carried out over wide temperature ranges. Yet glc is not limited solely to infinite-dilution studies. Thermodynamic data pertaining to solutions can in fact be obtained over widely extended mole-fraction ranges[21] and finite-dilution gas chromatography is today commonplace.[29–32] As a result of these advantages, both finite- and infinite-dilution investigations may be carried out rather more quickly than with other techniques, and little time need be spent on instrumentation or purity of materials.

The major limitation in the infinite-dilution mode of glc is volatility. Solutes must be able to withstand vaporization and elution, while liquid (stationary) phases must have vapour pressure at the column temperature sufficiently low that their mass in a column remains constant over a reasonable period. The employment of volatile stationary phases is not entirely precluded,[33–38] but difficulties associated with their use largely cancel advantages (c) and (d) mentioned above.

There are, of course, other advantages as well as a few disadvantages to be recognized. These are all well documented and understood (e.g. ref. 14), and few problems arise on their account.

B. Retention Equations

Partitioning of solutes between flowing mobile (gas) and stationary (liquid) phases requires for equilibrium that the solute free energy be minimized. This condition provides, upon replacement of activities by concentrations:

$$K_R = C_L/C_M \tag{1}$$

where K_R is the solute liquid–gas partition coefficient and C_L and C_M are the respective concentrations of solute in the stationary and mobile phases.

When a solute is dissolved in the stationary phase it is assumed to be immobile; movement down the column occurs only when it vaporizes and enters the mobile (carrier) stream. The linear rate of solute movement is therefore equal to the product of the average carrier velocity $\bar{u}$ and the fraction of time spent in the mobile phase:

$$\begin{aligned}\text{Rate of travel} &= \bar{u}[C_M V_M/(C_M V_M + C_L V_L)] \\ &= \bar{u}[1 + K_R(V_L/V_M)]^{-1} \end{aligned} \tag{2}$$

where V_M and V_L are the mobile- and stationary-phase volumes, respectively. Alternatively:

$$\text{Rate of travel} = \text{Column length, } L/\text{Elution times, } t_R. \tag{3}$$

Combination and rearrangement of equations (2) and (3) produces:

$$t_R = (L/\bar{u})[1 + K_R(V_L/V_M)] \tag{4}$$

$L/\bar{u}$ is just the "dead" time t_A in which a non-sorbed ($K_R = 0$) solute is eluted. The partition coefficient is therefore related to the retention and dead times and the column parameters by:

$$K_R = V_M(t_R - t_A)/V_L t_A. \tag{5}$$

The quotient V_M/t_A is just the corrected carrier flow rate F_c (which is commonly measured at the column outlet, with a soap-bubble flow-meter), multiplied by a gas compressibility correction factor j:

$$\frac{V_M}{t_A} = \underbrace{\frac{3}{2}\left[\frac{(p_i/p_o)^2 - 1}{(p_i/p_o)^3 - 1}\right]}_{j}\underbrace{\left[F\left(\frac{T}{T_{fm}}\right)\left(\frac{p_{fm} - p_w}{p_w}\right)\right]}_{F_c} \tag{6}$$

where p_i and p_o are the column inlet and outlet pressures; T, T_{fm}, and p_{fm} are the column and flow-meter temperatures and pressures; and p_w is the vapour pressure of the soap solution (generally taken to be that of water) at T_{fm}. Equation (5) now becomes:

$$K_R = (t_R - t_A) j F_c / V_L \tag{7}$$

which is one form of the fundamental retention relation which can be used to determine partition coefficients from purely chromatographic data.

It is a simple matter to show, further, that:

$$K_R = RT/\gamma_p^\infty p_1^0 \bar{V}_L = \rho_L RT/\gamma_p^\infty p_1^0 M_L \tag{8}$$

where R is the gas constant, γ_p^∞ and p_1^0 are the solute Henry's law activity coefficient and bulk vapour pressure, and $\bar{V}_L$, ρ_L, and M_L are the liquid-phase bulk molar volume, density, and molecular weight. Equation (8)

thus relates partition coefficients to parameters that are generally argued to be of fundamental significance, namely, the solute activity coefficient and its vapour pressure. However:

$$\ln K_R = \ln(RT/\bar{V}_L) - \Delta\bar{H}_s/RT + C \tag{9}$$

where $\Delta\bar{H}_s$ is the solute molar heat of solution. Since the logarithmic term on the right-hand side is temperature-dependent, plots of $\ln K_R$ versus $1/T$ are expected to be curved. To circumvent this difficulty a quantity called the solute specific retention volume, corrected to 0°C, is defined:

$$V_g^0 = K_R(273/T\rho_L) = 273R/\gamma_p^\infty p_1^0 M_L \tag{10}$$

such that:

$$\ln V_g^0 = \ln(273R/M_L) - \Delta\bar{H}_s/RT + C. \tag{11}$$

Plots of $\ln V_g^0$ versus $1/T$ are linear over moderate ranges of temperature and are therefore most often employed for measurement of heats of solution.

Activity coefficients which have been corrected for fugacity and virial effects γ_1^∞ (see below) may be calculated from equations (8) or (10), and excess thermodynamic properties of mixing may then be determined via plots of $\ln \gamma_1^\infty$ versus $1/T$:

$$\ln \gamma_1^\infty = \Delta\bar{H}^e/RT + C \tag{12}$$

where $\Delta\bar{H}^e$ is the solute excess enthalpy of solution. Finally, activity coefficients may be used to calculate Flory-type interaction parameters χ from the expression:

$$\ln \gamma_1^\infty = \ln(1/r) + (1 - 1/r) + \chi \tag{13}$$

where r is the ratio of solvent and solute ($\bar{V}_1$) molar volumes $\bar{V}_L/\bar{V}_1$. The gas–liquid chromatographic technique thus provides thermodynamic data which are commonly supposed to be pertinent to studies of solution phenomena, thence to formulation and identification of physically meaningful models of solution interactions.

C. Instrumentation

Chromatographic acquisition of data of accuracy sufficient for physicochemical studies generally precludes the use of commercial analytical instruments since, broadly speaking, these are not designed or fabricated for high-precision measurements. For example, partition data vary by about 1 per cent per 0·1°C and so gradients and fluctuations in the column temperature must be maintained at less than ±0·03°C. Similarly, the flow rate and inlet and outlet pressures must be held constant. Each of these parameters

must, in addition to $(t_R - t_A)$ and V_L, be measured such that the resultant partition coefficients are of a level of accuracy which in the present context of the study of complexation should not exceed ± 2 per cent.

In a gas chromatograph (Fig. 1) carrier gas from a cylinder is passed through a drying train and pressure and/or flow controllers, to thermostatted reference and sample columns. The effluents are then directed to a detector system and from there to a flow-meter. Solutes are generally introduced into the sample column via a heated injection system.

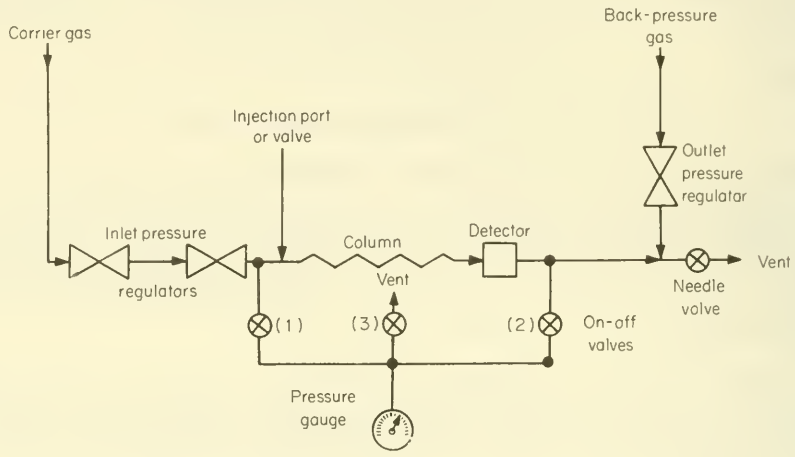

FIG. 1. Schematic diagram of the pneumatic circuit of a gas chromatograph

1. Column Thermostats

Of the numerous methods[39–44] used to thermostat sample and reference columns, the two most commonly used now consist of air ovens[45–49] and liquid baths.[50–53] Since most studies of complexation phenomena rarely involve temperatures above 75°C, the latter technique is the more useful.

Many examples of the construction and use of liquid column thermostats have been reported and require little comment other than to note specific cases which relate to gas chromatography. Thus, for example, Wicarova *et al.*[50] and Goedert and Guiochon[51] employed glycerol (30–150°C) and ethylene glycol (30–130°C) liquid baths, respectively. Temperature in the latter varied less than 0·01°C over 15 hours with gradients everywhere within the bath less than 0·05°C. Rijks and Cramers[52] reduced gradients in their system to less than 0·01°C. Laub *et al.*[53] reported that their commercial

unit was stable over the range 0–70°C to ±0·03°C, while in another of their studies[54] a laboratory-constructed model was reported to maintain 30·00 ± 0·01°C.

2. Pressure Controllers

It has been recognized for a number of years[55, 56] that flow controllers are generally less satisfactory than pressure regulators for high-precision measurements by gas chromatography. This is due mainly to sensitivity of the former to temperature and input-pressure fluctuations, while the latter appear to be relatively insensitive to such variations. Also, fluctuations in the post-column pressure seem to have little effect on inlet pressure regulation.

A variety[57–61] of manostat devices have been employed in gas chromatography; however, by far the most common in high-precision studies consists of one or two (tandem) lagged Negretti-Zàmbra R182 regulators. Goedert and Guiochon[51] showed, for example, that these units are capable of maintaining an inlet pressure of 2500 mbar with a stability of ±0·3 mbar. Wicarova *et al.*[50] found a standard deviation of approximately 0·01 per cent on p_i with their system, which consisted of two precision needle valves used in series with a Cartesian manostat. Rijks and Cramers[52] employed two Becker–Delft pressure controllers in series to obtain a column pressure drop which was said to be constant to about 0·002 atm. Laub and coworkers[53, 54] have consistently used R182 regulators with equally satisfactory results.

Many high-precision gas chromatographic systems do not incorporate controlled column outlet pressure but rely on constant ambient pressure, since small barometric variations cause only negligible fluctuations in the flow rate and j-correction which are approximately self-cancelling. For example, if the column inlet pressure is 1100 torr and during elution the column outlet (ambient) pressure changes from 760 to 770 torr, j will increase by less than 0·75 per cent which will be partially offset by a concomitant decrease in the flow rate. Overall, the product jF_c will be altered by less than 0·3 per cent. Controlled pressure at the column outlet is therefore unnecessary for the studies described here, especially in view of the magnitude (~1 per cent) of errors associated with determination of V_L (see below).

3. Flow Meters

Control of the inlet and outlet (ambient) pressures will, with constant column temperature, fix the flow rate. Measurement of the flow rate at the detector outlet is most convenient and is particularly simple; the effluent is passed through a 50–100 ml soap-bubble flow-meter of uniform diameter which can be constructed from a glass tee and a burette. Enclosure of the unit in a

water jacket will ensure constant temperature as well as facilitate observation of the soap film. Flow rates determined in this manner are generally accurate[62] to $\pm 0{\cdot}2$ per cent. Other techniques have been described[63–68] but soap-bubble flow-meters will suffice for low to moderate (< 150 ml min^{-1}) carrier velocities which are commonly employed in the studies under consideration here.

4. Injectors

A remarkable variety of sample introduction devices have been reported[69–85] but by far the most common variants consist of a heated chamber into which solutes are injected as vapours with a microlitre syringe. Alternatively, the column may be placed such that solutes are injected directly on to the inlet-end packing. (The authors have found no measurable difference in partition coefficients obtained with both techniques.) Heated injection ports require only that the vaporization space be small ($< 0{\cdot}5$ ml) so that solutes are swept downstream as a "plug"; its temperature must therefore be sufficient to prevent sample condensation.

Automated injection systems contribute unnecessarily complicated difficulties and are not recommended, especially since retention times can be made of duration sufficient to ensure that manual (syringe) techniques introduce less than 0·1 per cent error on t_R.

5. Detectors

Numerous reviews (e.g. refs. 86–88) describe over thirty types of detector that have been used in gas chromatography. The most widely employed, and the simplest and most versatile for physicochemical studies, is a hot-wire katharometer (helium or hydrogen are prescribed as carriers). Many units are available commercially at low cost, and almost all are suitable for gas chromatographic studies of complexation phenomena. Apparatuses have been described[89,90] which reduce peak asymmetry due to excess detector cell volume and slow response time. The filaments of modern units of some models are contained in volumes of less than 25 μl and have response times less than 0·5 s.

6. Data Acquisition Systems

Computerized[91,92] acquisition of retention data is of little advantage in measurement of partition coefficients, the parameter of primary interest here; a strip-chart recorder will suffice. The quantity that must be determined is the chart *difference* ($l_R - l_A$) between the solute peak and the "air" or "dead" peak which when divided by the chart speed gives the quantity $t_R - t_A$ ($= t'_R$). The *absolute* measurement of these data is therefore not required, which obviates the need for high-speed digital systems. For

example, Wicarova *et al.*[50] found that their recorder and manual data acquisition procedures contributed a relative standard deviation of only 0·06 per cent to specific retention volumes; the authors have encountered similar trivial errors with several types of recorder.

D. Sources of Error

Acquisition of precision data by gas chromatography requires that several sources of error, both systematic and random, be recognized and taken into account. The former arise from mass transfer non-equilibrium effects, fugacity and virial phenomena, solute adsorption at the gas–liquid interface, non-inert support materials, retention of supposedly non-sorbed solutes, and determination of V_L, the last in fact being the most troublesome in glc. Random errors can be identified and hence reduced via statistical assessment of each of the parameters of equation (7).

1. Systematic Errors

(a) *Peak asymmetry.* The symmetry of chromatographic peaks is an important criterion for judgement of the presence/absence of several sources of systematic error. Band-spreading in gas chromatography produces solute peak shapes at the detector that should be nearly symmetric and should closely approximate a Gaussian error curve. There are several tests for symmetry of the bands. For example,[93–95] the ratio η of the slopes of front and rear tangents to the sides of a peak should be unity. Values of η of $1 \pm 0{\cdot}2$ are generally accepted as indicative of symmetry. In another method[96] the asymmetry A_S is defined as:

$$A_S = (B - F)/(B + F) \tag{14}$$

where B and F are the respective baseline distances as measured from the peak rear and front tangents to a vertical line drawn through the peak maximum. η and A_S are related through:

$$\eta = F/B = (1 - A_S)/(1 + A_S). \tag{15}$$

Ettre[97] has also pointed out that for Gaussian peaks the ratio of the tangents baseline distance to that at half the peak height should be 1·698.

Peaks for which none of the above criteria is met must be regarded with considerable suspicion since there is every likelihood that phenomena other than those corresponding to solution are operative. Further, absence of peak asymmetry does not preclude the presence of these extraneous phenomena.

(b) *Mass transfer non-equilibrium effects.* Since chromatography is by definition a dynamic technique it may be supposed that partition coefficients so obtained could not correspond to those found with static methods. Sorption–desorption processes are, however, of such a rate that these effects are not seen even at high flow rates.[98] Further, static measurement of isotherms has confirmed that spreading of a liquid phase as a thin film on diatomaceous earth support serves only to increase the rate at which equilibration is achieved.[99, 100] Indeed, gas chromatographic measurement of K_R data at several flow rates with helium or hydrogen carriers provides means of testing the chromatographic system for leaks etc., since the partition coefficients thereby obtained should be identical.

(c) *Fugacity and virial effects.* Bulk fugacity and vapour pressure are related through:

$$f_1^0 = p_1^0 \exp(B_{11} p_1^0 / RT) \tag{16}$$

where B_{11} is the solute fugacity coefficient. In the absence of solute–carrier second-interaction virial effects (B_{12}), γ_p^∞ and γ_1^∞ are therefore related by:

$$\ln \gamma_1^\infty = \ln \gamma_p^\infty - B_{11} p_1^0 / RT. \tag{17}$$

Strictly,[93] the term on the right-hand side of equation (17) should take into account the change of the solute chemical potential upon being taken to infinite dilution; the correction is, however, trivial.

Fugacity corrections are of the order of 1 per cent for common hydrocarbon solutes and should be applied when high accuracy is, as here, required. B_{11} data are commonly calculated from the McGlashan–Potter[101] modification of the Beattie–Bridgeman[102] equation or measured directly.[103, 104]

When carriers other than helium or hydrogen are employed, K_R data must be corrected for second-interaction virial effects. The correction at low ($< 1{\cdot}5$ atm) column inlet pressure, and in the absence of carrier solubility in the stationary phase, is:[98, 105, 106]

$$\ln K_R = \ln K_R^0 + \beta p_0 J_3^4 \tag{18}$$

where K_R and K_R^0 are the solute partition coefficients at finite and zero column pressure drop, and β and J_3^4 are defined by:

$$\beta = (2B_{12} - v_1^\infty)/RT \tag{19a}$$

$$J_3^4 = (3/4)[(p_i/p_o)^4 - 1]/[(p_i/p_o)^3 - 1] \tag{19b}$$

where v_1^∞ is the solute molar volume at infinite dilution which can be measured directly[107] or replaced by $\bar{V}_1$ without introduction of noticeable error.[108] Since, with helium or hydrogen carriers, β is negligible below 1·5 atm, K_R at

finite pressure will correspond with these mobile phases to K_R^0. K_R must with other carriers be determined at several pressures, and plots of ln K_R versus $p_0 J_3^+$ then extrapolated to ln K_R.

(d) *Gas–liquid interfacial adsorption.* One of the most misleading and unfortunate errors made consistently in early glc studies resulted from lack of recognition of effects pertaining to solute adsorption at the mobile-phase–stationary-phase interface.[109–112] Peak asymmetry is usually marked in such cases because the surface area of liquid phase on a support is small; injection of even trivial amounts of solute will therefore "overload" the surface, causing asymmetric band-broadening. Introduction of different amounts of solute thus produces variation of retention times measured from the peak maximum.

Correction for adsorption effects requires, first, that sample size be such that retentions with any one column are invariant, and that, secondly, peaks be symmetric. When these conditions (at times difficult to achieve) are met, plots of V_N/V_L versus $1/V_L$ in accordance with the relation:[111, 112]

$$V_N/V_L = K_R + K_S A_L/V_L \tag{20}$$

are used to determine bulk-solution partition coefficients from columns containing various liquid loadings. V_N is the solute net retention volume ($= t'_R j F_c$), and K_S and A_L are the surface adsorption coefficient and liquid surface area, respectively. Since $K_S A_L/V_L$ is not linear in $1/V_L$, the plots will be convex to the abscissa if gas–liquid interfacial adsorption is present. In the absence of these effects the plots will be horizontal lines.

(e) *Support and column materials.* Modern gas chromatography support materials which have been acid-washed and deactivated with dimethyldichlorosilane offer few problems in physicochemical studies, and retention behaviour with stationary-phase loadings of 5–30 per cent (w/w) appears to be independent of the choice of support material. Particle sizes of 60–80 or 80–100 mesh are most convenient from the standpoints of reasonable efficiency and low-pressure drop. Quarter-inch copper, stainless steel, nickel, or dimethyldichlorosilane-treated glass tubes 2–6 ft long are suitable for most studies of complexation.

Stationary phases tend to "pool" in the pores of diatomaceous earths,[98] and it might be suspected that the decrease of solute vapour pressure due to capillary phenomena (which is called the "Kelvin contribution" to retention) would adversely affect accuracy of K_R data. These effects are, however, apparent only at very low liquid loadings, and even at that level are at best trivial.

(f) *Retention of non-sorbed solutes.* Syringe injection of solute vapours introduces some air which gives a peak with katharometer detectors from which solute retentions can be measured. Since air will not be sorbed except at cryogenic column temperatures it is an adequate measure of the dead time. Use of the other detectors such as flame ionization types may require rather more protracted methods[113–121] of determination of t_A.

(g) *Determination of* V_L. Measurement of the column liquid volume introduces the largest systematic error in physicochemical data obtained by gas–liquid chromatography. The procedure generally followed is, first, drawing the used column packing by aspiration into a tared flask which gives the weight of the support plus liquid phase. The weight per cent of liquid loading must next be determined and this is where the difficulties are encountered (it is usually not sufficient to assume that amounts originally weighed out in fabrication of the packing correspond to those of the used material). Several methods such as Soxhlet extraction and low to moderate temperature evaporation have been studied.[50, 122–125] The most accurate and reproducible for organic stationary phases seems, however, to be ashing of the packing at high (900–1100°C) temperature in a muffle furnace.[53, 54] This requires that a correction be made for bare-support weight loss which can be as much as 0·25 per cent. Table I presents data derived from typical ashing experiments by Laub *et al.*[53]

Once the total column packing weight and weight per cent stationary-phase loading have been determined, V_L is found from their product and the liquid-phase density at the column temperature; several variants of dilatometry[105, 126–128] or other techniques[129] are suitable for measurement of the latter. The data of Orwoll and Flory[126] for n-hexane (−15 to 89°C) and for n-hexadecane (18 to 207°C) are particularly useful for calibration of density apparatus.

TABLE I. Determination of weight per cent of n-octadecane liquid phase on Chromosorb G (60–80 mesh, AW-DMCS treated) by ashing[53] [Reproduced with permission from R. J. Laub and R. L. Pecsok, "Physico-Chemical Applications of Gas Chromatography", Wiley-Interscience, New York (1978)]

Run	Wt. packing/g	Wt. loss/g	Corrected[a] wt. %	$\Delta X\ (=X_i - \bar{X})$	$\Delta X/X_i$/%
1	0·9973	0·0746	7·33	−0·03	−0·41
2	0·9365	0·0706	7·38	0·02	0·27
3	0·8489	0·0641	7·40	0·04	0·54
4	1·0181	0·0763	7·34	−0·02	−0·27
5	1·0308	0·0773	7·34	−0·02	−0·27
			Average 7·36		

[a]For bare-support weight loss; ~0·0017 g/g ashed support.

2. Random Errors

The fractional standard deviation σ_{K_R}/K_R in terms of each of the parameters of equation (7) is given by:[54, 130]

$$\frac{\sigma_{K_R}}{K_R} = \left[\left(\frac{\sigma_{t'_R}}{t'_R}\right)^2 + \left(\frac{\sigma_j}{j}\right)^2 + \left(\frac{\sigma_{F_c}}{F_c}\right)^2 + \left(\frac{\sigma_{V_L}}{V_L}\right)^2\right]^{1/2} \tag{21}$$

σ_{K_R} may therefore be calculated from standard deviations of the means of t'_R, j, F_c, and V_L. This procedure simplifies considerably that reported by Wicarova *et al.*[50] and Goedert and Guiochon[51] in that random errors are taken in equation (21) to be reflected by the parameters indicated rather than terms comprising them. For example, calculation of j requires measurement of p_i and p_o for which an expression of the form of equation (21) could be written. The relative standard deviation thereby obtained, σ_j/j, must however correspond to that calculated from the mean of measurements of j. Equation (21) therefore provides a reasonable estimate of contributions from each of the parameters comprising equation (8) to the overall random error on K_R.

Table II lists calculated and experimental relative standard deviations

TABLE II. Comparison of predicted with experimental σ_{K_R}/K_R data for indicated solutes with squalane and dinonyl phthalate stationary phases at 30°C[54] [Reproduced with permission from R. J. Laub, J. H. Purnell, P. S. Williams, M. W. P. Harbison and D. E. Martire, *J. Chromatogr.*, **155**, 233 (1978)]

		$(\sigma_{K_R}/K_R) \times 100$			
		Squalane		Dinonyl phthalate	
	Solute	Predicted	Experimental	Predicted	Experimental
Series A					
	n-Pentane	0·45	0·04	1·86	0·53
	n-Hexane	0·41	0·19	1·13	0·11
	Cyclohexane	0·41	0·12	1·21	0·29
	n-Heptane	0·43	0·05	1·08	0·02
	Methylcyclohexane	0·47	0·18	1·05	0·21
	n-Octane	0·47	0·10	1·02	0·34
	Benzene	0·48	0·55	1·02	0·18
	Toluene	0·43	1·04	1·02	0·38
	Average:	0·44	0·28	1·17	0·26
Series B					
	n-Pentane	0·76	0·62	0·91	0·58
	n-Hexane	0·65	0·00	0·70	0·75
	n-Heptane	0·65	0·02	0·71	0·81
	Benzene	0·65	0·08	0·73	0·64
	Toluene	0·65	0·49	0·71	0·07
	Average:	0·67	0·24	0·75	0·57

for K_R data which were determined by Laub and coworkers[54] in two sets of experiments (Series A and B) each of which made use of slightly different apparatus and ashing techniques. The average of all data shows that the experimental relative standard deviations are well within those predicted from equation (21); the largest contribution to σ_{K_R}/K_R was that from measurement of V_L as might have been inferred from Table I. Further, since the squares of relative standard deviations are additive, sources of error other than that of V_L become important in complexation studies only when their magnitudes approach approximately half that for this parameter. For example, suppose that all terms except V_L are precise to $\pm 0{\cdot}1$ per cent while σ_{V_L}/V_L is 1 per cent; σ_{K_R}/K_R is calculated to be 1·1 per cent. Increase of $\sigma_{t'_R}/t'_r$ and σ_j/j to 0·5 per cent produces an increase of only 0·3 per cent in σ_{K_R}/K_R. Clearly, therefore, there is little point in controlling the column outlet pressure or flow rate, or indeed employing computerized digital data acquisition systems, as long as V_L cannot be determined with precision better than about 1 per cent.

E. Accuracy of Gas–Liquid Chromatographic Data

Early work[10, 131] in gas–liquid chromatography showed that static (non-chromatographic) and glc partition and activity coefficient data agreed only to within about ± 5 per cent. A recent survey[27] of glc-determined γ_1^∞ data seems to have affirmed that this level is approximately that to be expected generally. However, much of the cited irreproducibility of glc data can be traced to impure or contaminated solvents, to the use of "initial" retention times, failure to recognize and to correct for fugacity and virial effects, incorrect measurement of V_L, and so forth. When all these factors are taken into account a more favourable picture of glc data emerges. For example, Table III gives partition coefficients of n-alkane solutes with n-alkane stationary phases; inter-laboratory agreement is excellent. The glc partition coefficients determined by Laub *et al.*[54] are compared, further, with static data of Ashworth[134] for squalane and dinonyl phthalate phases in Table IV. Gas–liquid chromatography therefore appears capable of providing partition data of sufficient accuracy ($< \pm 1$ per cent) for all but the most demanding solution studies.

II. GAS–LIQUID CHROMATOGRAPHIC STUDIES OF COMPLEXATION PHENOMENA

Gas–liquid chromatography has proved to be a powerful tool for the study of complexation phenomena and, following initial[135] recognition of the exist-

TABLE III. Comparison of partition coefficients of n-alkane solutes with n-alkane solvents obtained at 80°C by gas–liquid chromatography [Reproduced with permission from R. J. Laub and R. L. Pecsok, "Physico-Chemical Applications of Gas Chromatography", Wiley-Interscience, New York (1978)]

Solute	n-$C_{24}H_{50}$		n-$C_{30}H_{62}$		n-$C_{36}H_{74}$			
	Ref. (49)	(132)	(49)	(132)	(49)	(53)	(132)	(133)
n-Hexane	61·97	61·84	57·16	57·01	52·91	53·56	52·83	53·40
n-Heptane	145·7	146·5	134·1	134·7	123·4	123·5	125·3	125·2
n-Octane	340·8	339·0	311·8	317·5	285·6	291·6	289·5	291·2

TABLE IV. Comparison of chromatographic[54] with static[134] partition coefficients of indicated solutes with squalane at 30°C as the stationary phase

Solute	Series A			Series B			Static
	Col. 1	Col. 2	Av.	Col. 1	Col. 2	Av.	
n-Pentane	98·73	98·78	98·76	98·66	97·80	98·23	98·08
n-Hexane	305·3	304·5	304·9	307·1	307·1	307·1	305·5
Cyclohexane	578·5	579·5	579·0	—	—	—	584·4
n-Heptane	926·4	927·0	926·7	934·0	933·8	933·9	927·0
Methylcyclohexane	1163	1166	1164	—	—	—	—
n-Octane	2795	2791	2793	—	—	—	2790
Benzene	431·7	435·1	433·4	437·1	436·6	436·9	434·8
Toluene	1414	1435	1425	1439	1429	1434	—

ence of such interactions in glc, was applied to measurement of activity coefficients, association (stability) constants K_1 and, from temperature-dependence of the latter, other thermodynamic information. A review of the techniques used in glc studies of complexation has recently been provided by Laub and Pecsok (ref. 14, Ch. 6) and a review of the literature, including a tabulation of the majority of association constants reported to 1973, has been given by Wellington.[136] deLigny[137] has also presented a useful critique of techniques with selected comparisons of data. It is intended in this section to bring these reviews up to date and to offer a prelude to presentation of more recent (and controversial) developments. The approach taken here is therefore sequential; ultimately, the field of complexation is considered in the light of current theories, in view of which it seems that no definitive position can yet be taken as to the proper description of behaviour of third-component solutes in mixed solvents, and in particular as to whether complexation phenomena *as currently measured* are in fact real (as indicated by the wealth of studies detailed below) or whether the entire basis of solution theory (including complexation) requires re-evaluation.

A. Evidence of Complexation

There are a number of reports of complex formation in glc studies in which, for one reason or another the results were not quantified in terms of association constants or other thermodynamic parameters (these add weight to the assertion that complexation appears on occasion to occur, but must be regarded only as inferential). For example, Langer *et al.*[138] found that tetrahalophthalate esters were selective stationary phases for the separation of aromatic hydrocarbons. Purnell *et al.*[139] used retention volumes to show that liquid surface excess concentrations could be determined by gas chromatography. They also inferred that complex formation occurred with their mixed phases—magnesium sterate and n-octadecan-1-ol. Bighi *et al.*[140] found that alkali-metal chlorides and KOH, when added to polyethylene glycol 400, affected the retention volumes of aliphatic, aromatic and alcohol solutes. Wasik and Tsang[36] showed that mercury(II), when mixed with Ag^+ in aqueous stationary phases, complexed strongly with olefin solutes but not with alkane or aromatic hydrocarbons. The latter, however, complexed weakly with silver.

As regards more quantitative studies, there is a review[141] of complexation involving metal ions in chromatographic separations with references to early 1971. Work reported since then has involved studies of complexation of lanthanum(facam)$_3$ compounds with tetrahydrofuran, ketones, acetates, and alcohols,[142] europium(fod)$_3$ with ketones and alcohols,[143] $PdCl_2$ and $AgNO_3$ in *N*-methylacetamide with butenes,[144] and rhodium(II)

compounds[145] such as the benzoate with ethers, ketones, and esters,[146] and the acetate with butenes.[147] Comparisons have also been made of other species with silver ion as, for example, that of $TlNO_3$ with $AgNO_3$ (water solvent) with olefin and toluene solutes.[148] Complexation with silver nitrate–ethylene glycol phases has also been studied by deLigny *et al.*[149] who employed an extended version of the theory of Gil-Av and Herling,[150] the techniques and procedures relating to which are discussed below.

B. Quantitative Assessment of Complexation Phenomena

1. General Remarks

As summarized in the reviews by Laub and Pecsok,[14] Wellington[136] and Foster,[207] there is no thermodynamic standard state that gives association constants that are independent of the choice of supposed "inert" solvent. The commonly adopted experimental procedure in glc has been that in which the solvent is in excess over the additive (often necessitated anyway by the weak miscibility of most additives in stationary phases) which is usually presumed largely to negate activity effects. Under these conditions,[136] molar (or molal) or volume-fraction units should be employed to avoid effects generally attributed to disparity in solute/additive/solvent molecular dimensions. Wellington[136] has further pointed out that the allowance made by Homer *et al.*[152] for differences in molecular size between hydrocarbon solutes and benzene and chloroform interactive species in an nmr study amounts only to a transformation from graphical representation of the data in terms of mole fraction to that in volume fraction, and that the resultant "mole fraction" constants were in effect nothing more than volume-fraction based stability constants.

Alternatively, it may be supposed that when the additive mole-fraction is high (0·9–1·0) the effects of solvents will be diminished. There exists the danger in this mode of measurement of K_1 that higher-order (A_nD; $n > 1$) complexes will be produced. Usually, therefore, the first procedure (excess solvent) is used and hence association constants will be given here in units of molar concentration and written as K_1, or volume fraction K_1^{ϕ}, whenever possible.

The above remarks apply equally to all methods (e.g. ref. 153) in which equilibrium constants are measured in liquid media (it appears that only gas-phase measurements would obviate problems associated with solvent and size effects.[151,154,155] Furthermore, physicochemical techniques used for determination of the extent of complexation generally exhibit disadvantages that are inherent in and peculiar to each. In gas–liquid chromatography, as pointed out by Wellington[136] and in Section I.D.1(d), a potentially important source of systematic error is that attributable to interfacial

adsorption. Studies of concurrent solution, adsorption, and complexation phenomena have been reported by Liao and Martire,[156] Cadogan and Purnell,[157] Pecsok and Gump,[158] Meen, Morris and Purnell,[159] Crowne, Harper and Farrell,[160] Martire, Pecsok and Purnell[111] and Pecsok, deYllana and Abdul-Karim.[110] Crowne *et al.* found, for example, that surface adsorption of aniline and *N*,*N*-dimethylaniline solutes with columns of 0·2M 2,4,7-trinitrofluorenone in tritolyl phosphate was severe, but could be minimized with stationary-phase loadings in excess of 10 per cent w/w (silanized Celite support). Langer and Purnell[161] showed that interactions involving other than those of bulk solution may result in complexation phenomena (as measured by glc) being at considerable variance with those determined by other techniques. Generally speaking, however, these effects are easily discerned since peak asymmetry is often severe and anyway the techniques described earlier for measurement of bulk solution properties may be applied in such cases for quantitative evaluation of K_R, hence K_1.

2. Approach of Gil-Av and Herling

In practice, two approaches have been used in glc for measurement of stability constants. In the first (I), the concentration of additive C_A in a mixed-liquid stationary phase is varied and the corresponding (interactive) solute partition coefficients are plotted as a function of C_A. K_1 is then taken as the slope/intercept quotient. This method pertains to a reference of pure solvent. The other approach (II) refers to use of columns of pure additive and of pure solvent in which solute retentions are measured on a relative basis from which, as detailed below, association constants can be deduced.

Gil-Av and Herling[150] first described the theory underlying method (I). They showed that solute partition coefficients with mixed phases should vary as C_A according to the relation:[14, 136]

$$K_R = K^0_{R(S)} + K^0_{R(S)} K_1 C_A \tag{22}$$

where $K^0_{R(S)}$ is the solute partition coefficient with pure solvent S, and K_1 is the association constant in terms of concentrations:

$$K_1 = C^{A,S}_{DA} / C^{A,S}_{D} C^{A,S}_{A}. \tag{23}$$

Data derived via equation (22) by, amongst others, Muhs and Weiss,[162] Cvetanovic *et al.*,[163] Schnekcko,[164] Queignec and Wojtkowiak[165] and Wasik and Tsang[36] have been abstracted and compared previously.[136] Examples of more recent studies of 2,4,7-trinitrofluorenone by Crowne *et al.*[160] are in Table V. Meen *et al.*[159] published stability constants for aromatic hydrocarbons with TNF in dialkyl phthalate and thiodipropionitrile solvents as given in Table VI. Purnell and Sriastava[166] extended their study of 2,4,7-trinitrofluorenone to di-n-butyl succinate, di-n-butyl adipate

TABLE V. Association constants K_1, enthalpies ΔH^c, free energies ΔG^c, and entropies ΔS^c of complexation for the substituted aniline–2,4,7-trinitrofluorenone complexes in tritolyl phosphate[160]

Donor	K_1/l mol^{-1} 130°	140°	150°	$-\Delta H^c$/ kcal mol^{-1}	140° ΔG^c/ kcal mol^{-1}	$-\Delta S^c$/ cal mol^{-1} K^{-1}
N,*N*-Dimethylaniline	0·44	0·39	0·34	4·37	0·79	12·5
N,*N*-Diethylaniline	0·24	0·21	0·17	5·84	1·28	17·2
N-Ethyl-*N*-methylaniline	0·33	0·27	0·24	5·39	1·07	15·6
N,*N*-Dimethyl-*p*-toluidine	0·54	0·48	0·43	3·86	0·60	10·8
N,*N*-Dimethyl-*o*-toluidine	0·19	0·16	0·14	5·18	1·50	16·2
N,*N*-Dimethyl-2,4-xylidine	0·13	0·11	0·09	6·23	1·81	19·5
N,*N*-Dimethyl-2,6-xylidine	0·10	0·07	0·04	11·74	2·93	35·5
Aniline	0·39	0·34	0·30	4·45	0·89	12·9
o-Toluidine	0·40	0·36	0·33	3·26	0·86	9·9
m-Toluidine	0·45	0·41	0·38	2·98	0·73	9·0
p-Toluidine	0·49	0·44	0·40	3·44	0·67	9·9
2,4-Xylidine	0·45	0·39	0·35	4·25	0·77	12·2
p-Ethylaniline	0·49	0·44	0·41	3·02	0·67	8·9
N-Methylaniline	0·35	0·31	0·27	4·40	0·96	12·9
N-Ethylaniline	0·26	0·24	0·22	2·83	1·17	9·7
N-n-Propylaniline	0·24	0·21	0·19	3·95	1·28	12·7
N-n-butylaniline	0·21	0·19	0·17	3·58	1·36	12·0

TABLE VI. Stability constants, $K^0_{R(S)}$ values, and γ_1^∞ data for 2,4,7-trinitrofluorenone with named solutes and solvents at 60°C[159]

Solvent	Toluene			Ethylbenzene			*o*-Xylene			*m*-Xylene			*p*-Xylene		
	K_1 M	$K^0_{R(S)}$	γ_1^∞	K_1/M	$K^0_{R(S)}$	γ_1^∞	K_1/M	$K^0_{R(S)}$	γ_1^∞	K_1/M	$K^0_{R(S)}$	γ_1^∞	K_1/M	$K^0_{R(S)}$	γ_1^∞
Di-n-propyl phthalate	0·237	532·5	1·182	0·161	1158·5	1·352	0·319	1603·6	1·326	0·331	1210·2	1·397	0·281	1252·8	1·404
Diisopropyl phthalate	0·193	520·6	1·192	0·128	1141·5	1·353	0·308	1558·8	1·345	0·291	1177·4	1·415	0·262	1217·7	1·429
Di-n-pentyl phthalate	0·430	518·7	0·944	0·348	1144·1	1·066	0·493	1616·0	1·024	0·476	1243·1	1·060	0·466	1277·3	1·072
Diisooctyl phthalate	0·240	473·9	0·779	0·184	1051·4	0·874	0·331	1492·1	0·836	0·318	1161·4	0·854	0·293	1188·7	0·868
Di-(3,5,5-trimethyl hexyl) phthalate	0·289	439·1	0·773	0·226	976·8	0·865	0·421	1393·1	0·824	0·416	1080·2	0·844	0·378	1119·0	0·848
Di-n-butyl maleate	0·339	559·2	1·067	0·295	1288·7	1·227	0·458	1795·5	1·195	0·453	1392·6	1·225	0·415	1430·6	1·241
β,β'-Thiodipropionitrile	0·509	187·7	6·247	0·376	304·2	9·518	—	—	—	0·670	341·2	9·473	0·675	343·4	9·164

TABLE VII. Stability constants and γ_1^∞ data for 2,4,7-trinitrofluorenone with named solutes and solvents at three temperatures[166]

Solute	Di-n-butyl succinate						Di-n-butyl adipate						Di-n-butyl sebacate					
	40°		50°		60°		40°		50°		60°		40°		50°		60°	
	K_1/1 mol^{-1}	γ_1^∞	K_1/1 mol^{-1}	γ_1^∞	K_1/1 mol^{-1}	γ_1^∞	K_1/1 mol^{-1}	γ_1^∞	K_1/1 mol^{-1}	γ_1^∞	K_1/1 mol^{-1}	γ_1^∞	K_1/1 mol^{-1}	γ_1^∞	K_1/1 mol^{-1}	γ_1^∞	K_1/1 mol^{-1}	γ_1^∞
Benzene	0·590	0·709	0·464	0·739	0·423	0·731	0·481	0·641	0·416	0·656	0·374	0·612	0·353	0·537	0·309	0·517	0·262	0·516
Toluene	0·702	0·808	0·521	0·836	0·449	0·816	0·491	0·700	0·451	0·727	0·417	0·678	0·332	0·569	0·281	0·568	0·240	0·559
Ethylbenzene	0·615	0·915	0·444	0·944	0·317	0·919	0·448	0·800	0·388	0·824	0·288	0·766	0·355	0·644	0·251	0·639	0·208	0·633
p-Xylene	0·764	0·917	0·649	0·939	0·613	0·924	0·624	0·780	0·550	0·807	0·498	0·791	0·425	0·620	0·381	0·619	0·322	0·619
m-Xylene	0·825	0·871	0·638	0·937	0·628	0·919	0·615	0·747	0·561	0·810	0·470	0·796	0·401	0·589	0·343	0·626	0·329	0·617
o-Xylene	0·871	0·914	0·671	0·926	0·603	0·906	0·606	0·776	0·581	0·797	0·506	0·780	0·393	0·613	0·371	0·614	0·327	0·610

and di-n-butyl sebacate solvents; their glc K_1 data are in Table VII where solvent effects are clearly evident.

3. Approach of Eon, Pommier and Guiochon

Eon, Pommier and Guiochon[167] and Eon and Karger[168] reported what was claimed to be a more exacting thermodynamic treatment of method (I) in terms of mole-fraction units (curiously, they did not then re-formulate the partition coefficient in the appropriate units which would have simplified considerably their derivation). They used an expression for K_R of a donor solute D which forms a 1:1 complex DA with the stationary phase additive A which, consistent with method (I), was of the form:

$$K_R = (C_D^{A,S} + C_{DA}^{A,S})/C_D^M \tag{24}$$

where the superscript M indicates the mobile phase. From Raoult's law:

$$f_D^{A,S} = f_D^0 x_{D(A,S)} \gamma_{D(A,S)} \tag{25}$$

where $f_D^{A,S}$ and f_D^0 are the fugacity of D above solutions of (A + S) which contain $x_{D(A,S)}$ amounts of D, and above bulk D, and where $\gamma_{D(A,S)}$ is the activity coefficient of D in (A + S). Since:

$$C_D^M = f_D/RT = f_D^0 x_{D(A,S)} \gamma_{D(A,S)}/RT \tag{26}$$

it follows that, since D is at infinite dilution:

$$\begin{aligned} K_R &= (RT/f_D^0 x_{D(A,S)} \gamma_{D(A,S)}^\infty)(C_D^{A,S} + C_{DA}^{A,S}) \\ &= (RT/f_D^0 x_{D(A,S)} \gamma_{D(A,S)}^\infty)(x_{D(A,S)}/\overline{V}_{A,S} + x_{DA(A,S)}/\overline{V}_{A,S}) \end{aligned} \tag{27}$$

where $\overline{V}_{A,S}$ is the molar volume of the solution of (A + S), where the volume of D has been ignored (see, however, ref. 136). Defining the thermodynamic equilibrium constant K_1^{th} in terms of mole-fraction units K_1^x:

$$K_1^{th} = (x_{DA}/x_D x_A)(\gamma_{DA}^\infty/\gamma_D^\infty \gamma_A)_{A,S} = K_1^x(\gamma_{DA}^\infty/\gamma_D^\infty \gamma_A)_{A,S} \tag{28}$$

followed by substitution into equation (27) yields:

$$K_R = (RT/f_D^0 \overline{V}_{A,S} \gamma_{D(A,S)}^\infty)[1 + x_A K_1^{th}(\gamma_D^\infty \gamma_A/\gamma_{DA}^\infty)_{A,S}]. \tag{29}$$

Noting that in the absence of excess mixing volumes:

$$\overline{V}_{A,S} = x_A \overline{V}_A + x_S \overline{V}_S = \overline{V}_S + x_A(\overline{V}_A - \overline{V}_S) \tag{30}$$

and further, that:

$$RT/f_D^0 = \gamma_{D(S)}^\infty \overline{V}_S K_{R(S)}^0 \tag{31}$$

gives, upon substitution into equation (29):

$$\overline{V}_{A,S} K_R = \overline{V}_S K_{R(S)}^0 \gamma_{D(S)}^\infty [1/\gamma_{D(A,S)}^\infty + x_A K_1^{th}(\gamma_A/\gamma_{DA}^\infty)_{A,S}]. \tag{32}$$

Eon and coworkers then argued that if the thermal contribution to the activity coefficient of D in (A + S) can be approximated by:

$$t_{\gamma^{\infty}_{D(A,S)}} = t_{\gamma^{\infty}_{D(S)}} \tag{33}$$

then, according to their interpretation of Flory–Huggins theory:

$$1/\gamma^{\infty}_{D(A,S)} \approx 1/\gamma^{\infty}_{D(S)} + x_A(1/\gamma^{\infty}_{D(A)} - 1/\gamma^{\infty}_{D(S)}). \tag{34}$$

Equation (32) therefore becomes:

$$\overline{V}_{A,S}K_R = \overline{V}_S K^0_{R(S)}[1 + x_A(\gamma^{\infty}_{D(S)}/\gamma^{\infty}_{D(A)} - 1 + K_1^{th}\gamma_{A(A,S)}\gamma^{\infty}_{D(A,S)}/\gamma^{\infty}_{DA(A,S)})] \tag{35}$$

which, if a quantity ψ is defined such that:

$$\psi = \gamma^{\infty}_{D(S)}/\gamma^{\infty}_{D(A)} - 1 \tag{36}$$

is the relation originally derived in ref. 167. It predicts that plots of $\overline{V}_{A,S}K_R$ versus x_A will be linear if the ratio $\gamma_{A(A,S)}/\gamma^{\infty}_{DA(A,S)}$ remains constant in x_A. Since all plots were indeed linear and since, further:

$$x_A/\overline{V}_{A,S} \equiv C_A^{A,S} \tag{37}$$

equation (36) must reduce to the Gil-Av–Herling relation equation (22), which is the case if the identification:

$$K_1 = [(\overline{V}_S - \overline{V}_A) + (\gamma^{\infty}_{D(S)}/\gamma^{\infty}_{D(A)} - 1 + K_1^{th}\gamma_{A(A,S)}\gamma^{\infty}_{D(S)}/\gamma^{\infty}_{DA(A,S)})] \tag{38}$$

is made.

However, surely such a treatment requires that the partition coefficient *also* be defined in terms of activities a_D^i:

$$K_R = (a_D^{A,S} + a_{DA}^{A,S})/a_D^M \tag{39}$$

which, since the solute is at infinite dilution, is approximately equivalent in any event to equation (24). Proceeding as before:

$$a_D^M = f_D^0(x_D\gamma^{\infty}_D)_{A,S}/RT \tag{40}$$

$$K_R = [RT/f_D^0(x_D\gamma^{\infty}_D)_{A,S}\overline{V}_{A,S}](x_D\gamma^{\infty}_D + x_{DA}\gamma^{\infty}_{DA})_{A,S}. \tag{41}$$

Upon substitution of equation (31):

$$\overline{V}_{A,S}K_R = \overline{V}_S K^0_{R(S)}\gamma^{\infty}_{D(S)}(1 + x_A K_1^{th}\gamma_{A(A,S)}). \tag{42}$$

Thus, a plot of the left-hand side against x_A gives $K_1^{th}\gamma_{A(A,S)}$ (without ψ) when partition coefficients are defined, consistent with a rigorous thermodynamic treatment, in terms of activities.

Eon and Karger[168] used equation (35) with ψ defined as:

$$\psi = (\overline{V}_A/\overline{V}_S)[\exp(\overline{V}_D/\overline{V}_A)/\exp(\overline{V}_D/\overline{V}_S) - 1] \tag{43}$$

TABLE VIII. Mole-fraction stability constants[168] (K^x) and corrected stability constants (in $1\,mol^{-1}$) (K_1) of complexes of alkylbenzene solutes with 2,4,7-trinitrofluorenone in named solvents at 60°C

Solvent	Toluene		Ethylbenzene		*o*-Xylene		*p*-Xylene		*m*-Xylene	
	K_1^x	K_1	K_1^x	K_1	K_1^x	K_1	K_1^x	K_1	K_1^x	K_1
Di-n-propyl phthalate	0·98	0·82	0·67	0·48	1·32	1·13	1·37	1·18	1·16	0·98
Diisopropyl phthalate	0·78	0·61	0·52	0·32	1·24	1·05	1·18	0·98	1·06	0·86
Di-n-pentyl phthalate	1·38	1·19	1·12	0·89	1·58	1·35	1·53	1·30	1·49	1·27
Diisooctyl phthalate	0·58	0·39	0·45	0·22	0·81	0·57	0·77	0·55	0·71	0·49
Di-(3,5,5-trimethylhexyl) phthalate	0·67	0·45	0·51	0·29	0·94	0·72	0·93	0·71	0·85	0·62
Di-n-butyl maleate	1·42	1·32	1·28	1·10	1·92	1·81	1·90	1·79	1·74	1·62

for a study of alkylbenzenes with 2,4,7-trinitrofluorenone; their results are in Table VIII. Castells[169] studied the complexation of aromatic hydrocarbons with 1,3,5-trinitrobenzene in dinonyl phthalate solvent, for which a careful appraisal of activity coefficients was offered. Mathiasson and Jonsson[170] found excellent straight lines for plots of $\overline{V}_{A,S}K_R$ versus x_A for alkanes, olefins, and aromatic hydrocarbons with dodecyl laurate–squalane. The slopes gave what were taken to be values of $(\psi + K_1^{th})$.

4. Approach of Martire and Riedl

This approach (method II) and its later developments have proved to be popular because they allow measurement of association constants with only two columns. Following the approach taken by Langer and coworkers.[138] Martire and Riedl[122] derived an expression for the specific retention volume of solute D (which forms 1:1 complexes) with pure stationary phase A which was of the form:

$$V_{g(A)}^{0(D)} = 273R/\gamma_{D(A)}^{\infty'} p_D^0 M_A = 273R/\gamma_{D(A)}^{\infty}(1 - c)p_D^0 M_A \tag{44}$$

where $\gamma_{D(A)}^{\infty'}$ is the apparent (experimentally measured) solute activity coefficient, $\gamma_{D(A)}^{\infty}$ is the activity coefficient of uncomplexed solute, and c is the fraction of solute which is complexed. Thus, the complex is assumed to be involatile, and only $(1 - c)$ amount of free solute moves down the column [$\gamma_{D(A)}^{\infty'} = \gamma_{D(A)}^{\infty}(1 - c)$, c being determined by the association constant].

As the concentration of solute approaches infinite dilution, $\gamma_{DA(A)}^{\infty} \to 1$, $\gamma_{D(A)}^{\infty} \to 1$, and $C_{DA}^{A} \to 0$ as $C_D^A \to 0$ and so:

$$K_1^{th} \approx C_{DA}^{A}/C_D^A a_A = K_1. \tag{45}$$

Now, for a column of pure A:

$$c = C_{DA}^{A}/(C_D^A + C_{DA}^{A}) \tag{46}$$

or

$$1/(1 - c) = 1 + K_1 a_A \tag{47}$$

so that

$$V_{g(A)}^{0(D)} = (273R/\gamma_{D(A)}^{\infty} p_D^0 M_A)(1 + K_1 a_A). \tag{48}$$

The appropriate expression for the complexing solute with a non-complexing phase S is:

$$V_{g(S)}^{0(D)} = 273R/\gamma_{D(S)}^{\infty} p_D^0 M_S. \tag{49}$$

The analogous expressions for a non-complexing solute N with S and with A are:

$$V_{g(S)}^{0(N)} = 273R/\gamma_{N(S)}^{\infty} p_N^0 M_S \tag{50}$$

$$V_{g(A)}^{0(N)} = 273R/\gamma_{N(A)}^{\infty} p_N^0 M_A. \tag{51}$$

Taking ratios of equations (48)–(51):

$$1 + K_1 a_A = V^{0(N)}_{g(S)} V^{0(D)}_{g(A)} / V^{0(N)}_{g(A)} V^{0(D)}_{g(S)} \tag{52}$$

where Martire and Riedl assumed that, for stationary phases of the same size, shape and polarizability, the activity coefficient ratio of complexing and inert (reference) solutes will give a measure of the potential energy difference between A and S, and should be independent of the choice of solute:

$$\gamma^{\infty}_{N(S)} / \gamma^{\infty}_{N(A)} = \gamma^{\infty}_{D(S)} / \gamma^{\infty}_{D(A)}. \tag{53}$$

Recognizing next that $a_A = \gamma_A C_A$ and that $C_A = \bar{V}_A^{-1}$ for pure A, it appeared that γ_A would, for closely related phases, be given by:

$$\gamma_A \approx \gamma^{\infty}_{N(S)} / \gamma^{\infty}_{N(A)} = V^{0(N)}_{g(A)} M_A / V^{0(N)}_{g(S)} M_S \tag{54}$$

which when combined with equation (52) produced:

$$K_1 = (V^{0(N)}_{g(S)} V^{0(D)}_{g(A)} / V^{0(N)}_{g(A)} V^{0(D)}_{g(S)} - 1)(V^{0(N)}_{g(S)} M_S \bar{V}_A / V^{0(N)}_{g(A)} M_A) \tag{55}$$

K_1 is therefore said to be calculable from retention data obtained from two columns, each containing a pure stationary phase.

Some of the results of Martire and Riedl[122] for hydrogen-bonding complexation between alcohol and amine solutes with di-n-octyl ether and di-n-octyl ketone stationary phases (n-heptadecane reference solute) are given in Table IX. Martire and his coworkers have also applied their method to hydrogen-bonding studies with the stationary-phase additives: di-n-octyl thioether,[171] di-n-octylmethylamine[172,173] and tri-n-hexylamine.[173]

Liao, Martire and Sheridan[172] made an important comparison of the Martire–Riedl and Gil-Av–Herling techniques in 1973. They used di-n-octylamine additive with n-octadecane reference solvent since the two

TABLE IX. Stability constants at 50°C and enthalpies of hydrogen-bond formation for di-n-octyl ether and di-n-octyl ketone with various solutes in n-heptadecane[122]

Solute	Di-n-octyl ether		Di-n-octyl ketone	
	K_1/l mol^{-1}	$-\Delta H^c$/kcal mol^{-1}	K_1/l mol^{-1}	$-\Delta H^c$/kcal mol^{-1}
Methanol	0·938	5·12 ± 0·48	2·84	—
Ethanol	0·688	4·22 ± 0·14	2·16	—
Propan-1-ol	0·672	3·97 ± 0·06	1·98	3·79 ± 0·19
Propan-2-ol	0·520	4·21 ± 0·09	1·70	3·73 + 0·29
Butan-1-ol	0·612	4·66 ± 0·30	1·91	4·20 ± 0·14
Butan-2-ol	0·637	4·51 ± 0·23	1·91	4·27 ± 0·14
s-Butanol	0·444	4·40 ± 0·28	1·42	3·67 ± 0·13
t-Butanol	0·349	4·40 ± 0·28	1·31	3·65 ± 0·13

TABLE X. Stability constants with di-n-octylmethylamine at 40°C[172] [Reproduced with permission from H.-L. Liao, D. E. Martire and J. P. S. Sheridan, *Anal. Chem.*, **45**, 2087 (1973)]

Solute	K_1/l mol^{-1}	
	G-A-H method (I)	M-R method (II)
Chloroform	0·405 ± 0·019	0·403
Dichloromethane	0·179 ± 0·014	0·187
Dibromomethane	0·222 ± 0·004	0·219

liquids have the same molecular size, shape and polarizability (M_A = 255·5, M_S = 254·5 g mol^{-1}; $\overline{V}_A$ = 325·4, $\overline{V}_S$ = 331·2 ml mol^{-1}). The "inert" solutes N were n-alkanes, specific retentions for which were identical with A and with $S(V_{g(S)}^{0(N)}/V_{g(A)}^{0(N)}$ = 1·012 ± 0·002; γ_A = 0·993 ± 0·002). K_1 data obtained for haloform solutes with these phases by methods (I) and (II) are given in Table X, which indicates that the two glc techniques give what appear to be internally consistent results.

Chamberlain and Drago[174] used the Martire–Riedl method to measure hydrogen-bonding interactions between di-n-octyl ether and several Lewis acid solutes, including alcohols, by glc. They also compared heats of complexation determined from these data with those obtained from calorimetry and from infrared spectroscopic measurements. The results are in Table XI and show good agreement.

Techniques similar to those of Liao, Martire and Sheridan have been used by Zlatkis and coworkers[175] to study the molecular association of a range of solutes, including alcohols, esters, ethers and sulphides, with dimeric

TABLE XI. Enthalpies for acid–di-n-octyl ether complexation[174]

Acid	$-\Delta H^c$(static)/ kcal mol^{-1}	$-\Delta H$(glc)/ kcal mol^{-1}
Tetrafluoroethylene	5·8, 5·9	6·0
Pyrrole	3·7	—
t-Butanol	3·0	3·1
Propan-2-ol	3·2	3·2
Propan-1-ol	3·5	3·8
Butan-1-ol	3·5	3·8
Isobutanol	3·4	3·9
s-Butanol	3·2	3·4

TABLE XII. Stability constants of named solutes with $[M(tfacCam)_2]_2$ in squalane at 75°C[175] [Reproduced with permission from V. Schurig, R. C. Chang, A. Zlatkis and B. Feibush, *J. Chromatogr.*, **99**, 147 (1974)]

Solute	K_1/l mol^{-1} Mn(II)	Co(II)	Ni(II)
Methyl formate	2·64	2·35	19·64
Ethyl formate	4·08	5·40	21·60
Methyl acetate	8·27	9·62	32·92
Ethyl acetate	12·14	13·52	41·14
Vinyl acetate	2·58	3·64	9·10
Methyl propionate	7·00	6·74	18·99
Ethyl propionate	10·05	9·10	23·90
Methyl butyrate	7·55	7·06	19·46
Ethyl butyrate	10·78	9·82	27·96
Propanone	11·94	18·55	60·16
Butan-2-one	10·60	14·47	54·0
Pentan-2-one	11·68	17·42	56·2
Acetaldehyde	3·13	5·30	31·76
Acrolein	4·86	7·96	25·84
Propanal	3·10	7·08	31·12
Butanal	3·72	7·57	30·03
2-Methylpropanal	3·00	6·98	29·33
Diethyl ether	2·92	6·40	21·03
Di-n-propyl ether	1·32	2·20	8·01
Diisopropyl ether	0	0	0·35
Propylene oxide	7·36	16·15	53·23
Tetrahydrofuran	33·85	131·52	594·1
p-Dioxan	18·81	93·0	782·9
Furan	0·16	0	0·87
Pyrrole	1·50	3·23	6·43
Thiophen	0·2	0·8	0·4
Benzene	0·15	0·6	0·5
Nitromethane	0·83	2·92	9·43
1-Nitropropane	1·58	1·81	3·85
Dimethyl sulphide	1·58	19·30	178·0
Diethyl sulphide	1·50	16·72	126·6
Propylene sulphide	1·03	6·66	51·16
Ethanol	159·2	165·1	>200·00
Propan-1-ol	175·9	185·5	>200·00
Propan-2-ol	99·5	102·8	189·4
Butan-1-ol	187·3	212·9	>200·00
Butan-2-ol	83·7	86·1	151·95
Pentan-2-ol	89·4	94·6	156·6

3-trifluoroacetylcamphorates (tfacCam) of Mn(II), Co(II) and Ni(II). No activity coefficients were reported, but plots of $[(V^{0(D)}_{g(A)} V^{0(N)}_{g(S)}/V^{0(D)}_{g(S)} V^{0(N)}_{g(A)}) - 1]$ versus C_A or versus the molality m_A were excellent straight lines. Table XII gives K_1 values evaluated from their data.

5. Approach of deLigny

deLigny[137] has deduced relations which are essentially identical to those of Martire and his coworkers: from equations (1), (5) and (10), and letting n^S_D be the total number of moles of donor in the stationary phase:

$$V^{0(D)}_{g(S)} = 273 n^S_D x_{D(S)} w_S / C^M_D T \tag{56}$$

$$V^{0(D)}_{g(A,S)} = 273 n^{A,S}_D (x_D + x_{DA})_{A,S} w_{A,S} / C^M_D T \tag{57}$$

where w_i is the weight of liquid phase in each column. Taking the ratio of equations (56) and (57), and recognizing that from Raoult's law, $x_{D(S)}\gamma^\infty_{D(S)} = x_{D(A,S)}\gamma^\infty_{D(A,S)}$:

$$V^{0(D)}_{g(A,S)}/V^{0(D)}_{g(S)} = (n^{A,S}_D \gamma^\infty_{D(S)}/n^S_D \gamma^\infty_{D(A,S)})(1 + x_{DA(A,S)}/x_{D(A,S)}). \tag{58}$$

Since, from equation (28):

$$(x_{DA}/x_D)_{A,S} = x_{A(A,S)} K^{th}_1 (\gamma_A \gamma^\infty_D / \gamma^\infty_{DA})_{A,S} \tag{59}$$

equation (58) becomes:

$$V^{0(D)}_{g(A,S)}/V^{0(D)}_{g(S)} = (n^{A,S}_D \gamma^\infty_{D(S)}/n^S_D \gamma^\infty_{D(A,S)})[1 + x_{A(A,S)} K^{th}_1 (\gamma_A \gamma^\infty_D / \gamma^\infty_{DA})_{A,S}]. \tag{60}$$

To avoid calculation of the activity coefficient ratio $\gamma^\infty_{D(S)}/\gamma^\infty_{D(A,S)}$ deLigny used a reference (non-interactive) solute N which closely resembled D but which did not complex with A:

$$V^{0(N)}_{g(A,S)}/V^{0(N)}_{g(S)} = n^{A,S}_N \gamma^\infty_{N(S)}/n^S_N \gamma^\infty_{N(A,S)}. \tag{61}$$

Equation (60) may thus be cast in the form:

$$V^{0(D)}_{g(A,S)} V^{0(N)}_{g(S)} / V^{0(D)}_{g(S)} V^{0(N)}_{g(A,S)} = 1 + x_{A(A,S)} K^{th}_1 (\gamma_A \gamma^\infty_D / \gamma^\infty_{DA})_{A,S} \tag{62}$$

which is identical to the relation (52) derived by Martire and Riedl except that it pertains to a mixed phase (A + S) as shown previously by Martire and coworkers.[172]

Equation (62) or its equivalent in terms of molar concentration ($C^{A,S}_A K_1$) has been used to study a number of systems. For example, deLigny *et al.*[149] used silver nitrate–ethylene glycol and lithium nitrate–ethylene glycol (reference) phases, and found that the ratio $V^{0(N)}_{g(S)}/V^{0(N)}_{g(A,S)}$ was close to unity for n-alkane solutes. It was, however, 1·07–1·19 for n-propyl acetate and considerably less than 1 for n-propyl halides, falling from 0·95 to 0·20 as the molality of the metal nitrate phases was increased from 0·25 to 3·0 due,

TABLE XIII. Stability constants of β-substituted ethanol solutes at 62·6°C[176] [Reproduced with permission from C. L. deLigny, N. J. Koole, H. D. Nelson and G. H. E. Nieudorp, *J. Chromatogr.*, **114**, 63 (1975)]

Additive	K_1^{th} —H	$-CH_3$	$-C_2H_5$	—F	—Cl	—Br	$-OCH_3$	$=CH_2$	$-C_2H_3$	$\equiv N$	—CN	$-SCH_3$
Hexadecyl fluoride	0·47	0·42	0·44	0·35	0·55	0·60	0·24	—	0·44	0·95	0·39	0·36
Hexadecyl chloride	0·38	0·34	0·36	0·28	0·43	0·45	0·22	—	0·38	0·44	0·22	0·30
Hexadecyl bromide	0·55	0·51	0·52	0·43	0·59	0·62	0·37	—	0·54	1·51	0·61	0·45
Hexadecyl iodide	0·41	0·37	0·38	0·32	0·44	0·45	0·26	—	0·42	0·69	0·42	0·36
Hexadecyl cyanide[a]	2·82	2·71	2·72	2·55	3·48	3·88	1·33	2·92	2·67	12·2	4·0	2·27
Hexadecyl cyanide[b]	2·42	2·27	2·36	2·72	3·98	4·36	1·29	3·40	2·33	—	6·3	2·06
Pentadecan-2-one	2·54	2·44	2·50	2·46	3·50	3·99	1·14	—	2·46	—	4·20	1·98
Dioctyl ether	1·35	1·31	1·36	1·50	1·78	1·88	0·63	—	1·23	7·68	2·72	1·00
Dioctyl ketone	2·12	2·00	2·11	1·95	2·93	3·35	0·89	—	2·04	10·0	3·31	1·65
Dioctyl sulphide	0·77	0·77	0·78	0·88	1·10	1·19	0·54	—	0·79	5·77	1·96	0·65
Dioctyl disulphide	0·52	0·49	0·50	0·39	0·61	0·66	0·28	—	0·51	1·17	0·50	0·43
Dioctylmethylamine	2·59	2·51	2·51	3·50	4·84	5·46	1·54	—	2·54	—	13·9	3·87

[a]Average of results with n-hexadecane and n-octadecane solvents. [b]n-Hexadecane solvent only.

presumably, to halide complexation with silver but not with lithium. The association constants of a variety of solutes were presented. deLigny *et al.*[176] have also used equation (62) to study the association of substituted alcohols with monofunctional hexadecyl derivatives and in particular 1-cyanohexadecane. The results are in Table XIII.

As mentioned earlier, complexes of $Eu(fod)_3 \cdot H_2O$ with butenes and alcohols have been studied by these methods.[143] Complexation of a series of lanthanide compounds $Ln(faCam)_3$ with various donors has also been investigated,[142] and interactions of Tl(I) tetraphenylborate with various unsaturated compounds have been reported.[177]

6. Approach of Langer, Johnson and Conder

Langer, Johnson and Conder[178] used a variation of method (I) in which a series of tetrahalophthalate esters with alkyl groups of varying chain length were employed. Solute partition coefficients with each of the pure phases were then plotted versus the inverse molar volumes of the phases from which values of K_1 were calculated. Several of the plots were curved which, it was postulated, may have resulted from formation of higher-order complexes.

7. Approach of Cadogan and Sawyer

Cadogan and Sawyer[179] applied the Gil-Av–Herling technique to gas–solid chromatography, where mixtures of $LaCl_3$ were used with NaCl. They plotted solute retention versus the surface concentration of the former and found straight lines for the solutes examined. The results of this interesting treatment of gas–solid phenomena are in Table XIV.

Eutectic melts of fused salts have also been used as liquid phases by a number of workers.[180] Juvet and coworkers,[181] for example, have employed several such mixtures for the study of volatile chloride solutes such as $SbCl_3$, $NbCl_5$ and $TaCl_5$.

TABLE XIV. Stability constants and heats of formation of aromatic–$LaCl_3$ complexes at 200°C[179]

Solute	$10^{-5} K_1/m^2$ mol^{-1}	$-\Delta H^c$/kcal mol^{-1}
Benzene	2·09	3·6
Toluene	4·37	4·8
Ethylbenzene	5·06	4·8
Isopropylbenzene	4·43	4·5
Fluorobenzene	3·00	4·6
Chlorobenzene	2·17	2·8
Bromobenzene	2·84	3·1
Iodobenzene	2·75	6·6
Hex-1-ene	1·62	—

TABLE XV. Values of K_1^C, K_1^x, and K_1^ϕ derived via ultraviolet and nmr techniques for 2,4,7-trinitrofluorenone at 40°C[166] [Reproduced with permission from J. H. Purnell and O. P. Srivastava, *Anal. Chem.*, **45**, 1111 (1973)]

Solvent	Toluene			*m*-Xylene			*p*-Xylene		
	K_1^C	K_1^x	K_1^ϕ	K_1^C	K_1^x	K_1^ϕ	K_1^C	K_1^x	K_1^ϕ
A. Ultraviolet technique (Benesi–Hildebrand method)									
Di-n-butyl succinate	0·116	−0·045	1·087	0·210	0·210	1·670	0·167	0·241	1·357
Di-n-butyl adipate	−0·030	−0·710	−0·272	0·082	−0·246	0·654	—	—	—
Di-n-butyl sebacate	−0·008	−0·730	−0·075	0·065	−0·448	0·522	0·145	−0·180	1·177
B. Nmr technique (Foster method)									
Di-n-butyl succinate	−0·019	−0·624	−0·168	0·072	−0·173	0·565	0·105	−0·033	0·850
Di-n-butyl adipate	−0·010	−0·571	−0·087	0·096	−0·198	0·769	—	—	—
Di-n-butyl sebacate	0·053	−0·519	0·491	0·041	−0·448	0·333	0·098	−0·356	0·800

Units of K_1^ζ are $1\,mol^{-1}$.

C. Comparison of Glc Data with Those of Other Techniques

Studies described in the above section would seem to have established conclusively that complexation phenomena occurred in the systems examined and that the glc methods enabled quantification of the extent of the interactions. Indeed, some authors[142] have quoted X-ray studies which support the view that complexes were formed in their systems. However, when comparisons are made between glc and other methods, doubts arise as to the exact physicochemical significance of the data from either. For example, Purnell and Srivastava[166] found that glc association constants were invariably higher than those measured by nmr or ultraviolet spectrophotometry, as shown by a comparison of their chromatographic data (Table VII) with those of Table XV. Although there is other evidence[171,173,182] apart from that of Purnell and Srivastava for glc stability constants being higher than those from ultraviolet and nmr measurements, nevertheless there is also evidence of glc results being in good agreement with those of other methods. The glc data of Chamberlain and Drago[174] quoted earlier gave enthalpies of complexation which were in good agreement with those obtained from calorimetry and infrared frequency measurements for di-n-octyl ether with tetrafluoroethylene, pyrrole and a series of alcohols, as shown in Table XI. Queignec and Wojtkowiak[165] have studied the hydrogen bonding between a series of alkynes and *N,N*-diethylacetamide by measurement of the absorbance of the C—H stretching band of the alkyne at 3300 cm^{-1} at different concentrations of alkyne. Benesi–Hildebrand type plots were excellent straight lines with CCl_4 as the solvent, and the values of complexation constants in $l\,mol^{-1}$ units are in Table XVI. Also included are the

TABLE XVI. Comparison of stability constants for *N,N*-diethylamine with named solutes from infrared and glc measurements[165]

Solute	glc K_1/l mol^{-1} 0°C	glc K_1/l mol^{-1} 25°C	ir 28°C	$-\Delta H^c$/ kcal mol^{-1}
$n\text{-}C_5H_{12}$	0·0	0·0	—	—
$(CH_3)_3CC{\equiv}CH$	0·96 ± 0·04	0·58 ± 0·03	0·60	3·3 ± 0·6
$(CH_3)_3SiC{\equiv}CH$	1·12 ± 0·04	0·66 ± 0·03	0·65	3·4 ± 0·6
$(CH_3)_2ClCC{\equiv}CH$	1·48 ± 0·06	0·90 ± 0·04	0·87	3·2 + 0·5
$CH_2ClC{\equiv}CH$	2·78 ± 0·10	1·73 ± 0·07	1·54	3·0 ± 0·5
$CH_2BrC{\equiv}CH$	2·74 ± 0·10	1·67 ± 0·07	1·50	3·0 ± 0·5
$CH_3(CH_2)_5C{\equiv}CH$	—	0·60 ± 0·03	0·60	—
$CH_3CH_2C{\equiv}CCH_2CH_3$	0·0	0·0	—	—

method (I) glc K_1 values, where squalane was used as the solvent. Thus, the position is far from clear as to agreement of glc with spectroscopic data, and appears to depend upon the system being studied.

Eon and Guiochon[183] concluded that results from various techniques would be in much closer agreement if the reactants had low "polarities", and if the solvent had the same refractive index as the additive. They would then have the same dispersion solubility parameters, and the thermal part of the activity coefficient of the additive in the solvent would be constant as the volume fraction of the additive was varied. It would also be advantageous to use solutes, additives and solvents of similar molar volumes. Further, it was said to be particularly important in nmr to use solvents and additives of nearly equal molar volumes. All these criteria are designed to minimize effects of the activity coefficient of the additive.

Martire[184] considered various types of interaction which can occur between two species A and D. He defined a 1:1 complex as that formed when the number of DA pairs is in excess of that expected on the basis of random encounters such that their lifetime is long when compared with the duration of a molecular collision. Any "loose" contacts between A and D were then termed "contact pairs", as suggested originally by Orgel and Mulliken[185] (see Chapter 5). Martire next asserted that the partition coefficient is affected both by complexation and by contact pairing, and hence one obtains the sum of the complexation constant and the contact-pair contribution α from glc experiments. For nmr, on the other hand, he states that K_1 can be measured uniquely even in the presence of appreciable contact pairing. The equation that Martire developed depends on a built-in difference between contact pairing and true (albeit weak) complex formation which is expressed in the interaction parameter of uncomplexed A with D in glc through the activity coefficient of the D-term. However, contact pairing does not, in Martire's theory, enter the nmr equation in the same manner. If it did so, then the measured complexing constants would obviously be $(K_1 + \alpha)$ for both methods. Further, while Martire suggests that there is a finite concentration C_{A-D} of contact pairs, he treats this concentration as though it somehow is different. Clearly, both types of complex are in dynamic equilibrium with free reactants, and since the point is such a crucial one it could well have received more extensive justification. If, on the other hand, it is accepted that Martire's approach can be justified, then the equation that he deduced is useful; from the Martire–Riedl theory, Martire showed that the correction factor for first-order contact pairing of C_A is:

$$\alpha = \overline{V}_D[\overline{V}_S - \overline{V}_A)/\overline{V}_S] + \overline{V}_A[\chi_{D(S)} - \chi_{D(A)} + (\overline{V}_D/\overline{V}_S)\chi_{A(S)}] \qquad (63)$$

where χ is the interaction parameter[186] of the indicated species (the sum of

the structural and energetic contributions to the logarithm of the corresponding reactant). Thus, Martire derived:

$$\alpha C_A = \ln(\gamma^{\infty}_{D(S)}\overline{V}_S/\gamma^{\infty}_{D(A)}\overline{V}_A) \tag{64}$$

and then showed that:

$$V^{0(D)}_{g(A)}V^{0(N)}_{g(S)}/V^{0(D)}_{g(S)}V^{0(N)}_{g(A)} = 1 + (K_1 + \alpha)C_A. \tag{65}$$

Turning next to nmr, Martire suggested that in principle four distinct proton frequencies could be identified, namely, that for free D, that perturbed by A–D contact pairing, and that for each of two types of DA complex formation. Letting $C_{A-D} = \alpha C_A C_D$. Martire obtained for the time-averaged proton frequency:

$$\nu = \frac{(C_D - \alpha C_A C_D)\nu_D + \alpha C_A C_D \nu_{A-D} + C^a_{DA}\nu^a_{DA} + C^b_{DA}\nu^b_{DA}}{C_D + C^a_{DA} + C^b_{DA}} \tag{66}$$

where the superscripts a and b indicate two types of complex. Thus, instead of introducing only the simple term $C_{A-D}\nu_{A-D}$ for contact pairing, Martire effectively introduced the term $C_{A-D}(\nu_{A-D} - \nu_D)$. This crucial difference means that a plot of Δ/C_A against Δ yields a slope of $-(K^a_1 + K^b_1)$, i.e. α is excluded. It may well be that, because of extremely rapid exchange of D between the free state and that of contact pairing, the average proton shift is indeed distorted, but surely not to the extent that it can be taken to be the effective difference between that of A–D and free D; the latter must in fact be extremely small when compared with the values of ν_D and ν_{DA}. Omission of the term C_{A-D} from the denominator of equation (66) is also of not inconsiderable importance but is justified presumably on the basis that A perturbs only D and that C_{A-D} does not represent a true concentration.

An alternative approach which yields the same result as that of Martire is that in which use is made of ν as the random averaged frequency of A–D, which is then treated in the same way as DA^a and DA^b (algebraically but not necessarily chemically); this would seem to be a more justifiable formulation.

If one *were* to accept the view that glc-measured stability constants amount to $(K_1 + \alpha)$ while nmr and ultraviolet-visible measurements give true K_1, then it may be explained why in some systems K^{glc}_1 is larger than that given by spectroscopy. For example, for $C(Hal)_4$ with aromatics, Martire[187] found no nmr shift differences and so ascribed association constants as measured by glc (0·34–0·65 l mol^{-1}; enthalpies of ~4·5 kcal mol^{-1}) for these systems to α. He also calculated α values for the systems studied by Purnell and Srivastava[166] from their spectroscopic data, and concluded that the glc stability constants were due essentially to contact pairing. Martire and

his coworkers[171,173,182] studied in addition the interactions between $CHCl_3$ and $CHBr_3$ with di-n-octyl ether, di-n-octyl thioether and di-n-octylmethylamine by glc and by nmr. In the nmr study the solvent was cyclohexane while in that by glc it was n-octadecane since the latter solvent was apparently viscous at the temperatures employed and so gave broad nmr bands. The system chloroform–di-n-octyl ether–n-octadecane was, however, examined by nmr and gave a value of K_1 of $0{\cdot}27 \pm 0{\cdot}02$ l mol^{-1} which was in agreement with that obtained with cyclohexane solvent ($0{\cdot}285 \pm 0{\cdot}003$ l mol^{-1} at 28°C). The values of α and of ΔH_α were, however, surprisingly large in these studies, so much so that one is led to doubt whether they can be realistic.

Martire and his coworkers[188] extended their analysis of these equations by comparison of polarization, nmr, ultraviolet and glc measurements.[189–192] These indicated that the concentration of complexes of CBr_4 with aromatic hydrocarbons in squalane was negligibly small and that the evidence therefore pointed to the predominance of electrostatic or van der Waals interactions. Hence, the glc K_1 data were said to yield α directly. The data were then analysed in terms of the configurational energy parameters of the systems, and it was shown that A–D interactions were self-consistent for like species. A subsequent study[193] of aromatic solutes with n-octadecane solvent and n-hexadecyl chloride, bromide, and iodide additives yielded interaction parameter differences which were again related to molecular energetic terms.

Similarities between the α of Martire and the ψ of Eon and coworkers have been pointed out[194] in a study of interactions of chloroform and methanol with tetradecylamine in n-octadecane. Here, α was calculated from the relationship:[172] $\overline{V}_D(1 - \overline{V}_A/\overline{V}_S)$. For chloroform, $\alpha = 0{\cdot}02$ and K_1 was found to be $1{\cdot}46$ l mol^{-1}. For methanol, plots of $K_R/K^0_{R(S)}$ against C_A were curved and both 1:1 and 1:2 complexes were thought to be present. The following values were obtained for this system: $\alpha = 0{\cdot}01$, $K_1 = 0{\cdot}45$ l mol^{-1}, and $K_2 = 1{\cdot}64$ l mol^{-1}.

The properties of complexing mixtures have also been examined by glc by Janik[195] and, more recently, a study of activity coefficients of alkanes, alicyclics and benzene with cycloalkanols in heptanol and benzyl alcohols has been reported.[196] Reznikov and coworkers[197–199] used relative retention times to measure equilibrium constants for several systems, and correlated the results with exchange parameters derived from the Barber molecular theory of solutions.

Thus, in-depth studies of solution properties have been made by glc and in conjunction with other, usually spectroscopic, methods. Differences between sets of data have been rationalized on the basis of one or other type of complexation. The subject is, however, open to considerable debate.

III. RECENT DEVELOPMENTS

There are implied limitations as well as practical difficulties associated with application of the Gil-Av–Herling method [equation (22)] as was pointed out in 1966 by Purnell.[200] For example, equation (22) in a rearranged form is:

$$K_R - K^0_{R(S)} = K^0_{R(S)} K_1 C_A. \tag{67}$$

If K_1 is of the order of 0·1 l mol^{-1} for a solute of $K^0_{R(S)}$ 100, the difference $(K_R - K^0_{R(S)})$ will be only 2 at $C_A = 0{\cdot}2$ M. The chromatographic data must in this case therefore be of accuracy sufficient to reflect a 2 per cent change in solute partition coefficients. Since, because of difficulties surrounding measurement of V_L, a figure of ± 1 per cent is at present the limit of precision of K_R data, K_1 will be accurate only to ± 50 per cent.

Laub and Pecsok[201, 202] and others have attempted to overcome the requirement of data of high precision by relating partition coefficients to "standard" solutes which are not expected to exhibit complexation, much in the manner of Martire and Riedl. The approach rests on the assumption implicit in the Gil-Av–Herling relation that the solubility of non-interactive solutes remains unchanged by addition of small amounts of additive to supposed "inert" solvents. However, numerous examples have recently been cited[203] which show that this behaviour is fortuitous and that both positive and negative stability constants may in fact be observed for "non-interactive" solutes with various solvent–additive systems.

The difficulty of small K_1 for solutes of low $(K_R - K^0_{R(S)})$ is exacerbated by the finding that, with few exceptions, most additives that are commonly recognized as "strong" complexing agents exhibit only weak miscibility with solvents of vapour pressure sufficiently low to be useful as gas–liquid chromatographic stationary phases. 2,4,7-Trinitrofluorenone, for example, is soluble only to the extent of ~0·2 M in dialkyl phthalate solvents at room temperature. This has promoted development of the Martire–Riedl method discussed earlier in which fully miscible solvent–additive pairs were employed. Eon, Pommier and Guiochon[167, 168, 204] also found that di-n-butyl tetrachlorophthalate was miscible in all proportions with squalane. Surprisingly, plots of K_R versus C_A were in these cases found to be linear over the entire range $C_A = 0$ to $\bar{V}_A^{-1}$.

The alternative approach to use of additives such as di-n-butyl tetrachlorophthalate which are fully miscible with common glc stationary phases is employment of various and less-common solvents with additives such as 1,3,5-trinitrobenzene, 2,4,7-trinitrofluorenone and tetracyanoethylene. 1,3,5-Trinitrobenzene, for example, is soluble[169] to ~0·8 M in dinonyl phthalate

and tetracyanoethylene to[205] 0·5 M in di-n-butyl adipate. However, stability constants with these additives are found by glc to vary somewhat with the solvent,[166] although to a degree which is considerably less than that noted in spectroscopic studies.[206]

Thus, it has been found in glc that those (few) non-ionic systems for which miscibility of solvent–additive pairs extends over considerable ranges of concentration exhibit plots of K_R versus C_A which are linear. Yet, concentration-based stability constants are solvent-dependent and, further, supposed non-interactive solutes often exhibit negative values of K_1.

The fact that glc and spectroscopic results, even when obtained by the same workers in the same laboratory,[166] are at times not self-consistent prompts only further doubt concerning the validity of experimental K_1 data. These anomalies are, of course, not uncommon in spectroscopic studies, and hence thorough formulation and evaluation of the glc method must apparently also find importance in and be related directly to optical and nmr techniques.

A. Concentration Effects in Non-Ionic Solvent–Additive Systems

Linearity of plots of K_R over extended ranges of C_A is not expected on the grounds that, if nothing else, the activity of the additive would not be supposed to vary linearly with concentration. Nevertheless, with very few exceptions, K_R is found in glc to be related directly to C_A for non-ionic stationary-phase mixtures, including those cases where solvent–additive miscibility is complete. Foster[207] has reviewed and commented upon similar linearity of ultraviolet-visible and nmr data; in one case[208] cited, solvent–additive Raoult's law data were shown unambiguously to deviate appreciably from ideal solution behaviour, yet association constants were consistent only with concentration (not activity) units. One of the explanations that purported to rationalize this phenomenon (e.g. ref 207, p. 98) is that *measured* association constants in, for example, concentration units are related to thermodynamic equilibrium quotients via:

$$K_1^{th} = K_1^C(\gamma_{DA}^{\infty,C}/\gamma_D^{\infty,C}\gamma_A^C) \tag{68}$$

where the superscript C refers to units appropriate to molar concentration and the subscripts to the relevant species (DA and solute D are at infinite dilution in glc and so are appropriately superscripted with ∞). Plots of K_R may therefore be linear in C_A because the term on the right-hand side of equation (68) is linear in C_A. Alternatively, it may be supposed that the ratio $\gamma_{DA}^{\infty,C}/\gamma_D^{\infty,C}$ is invariant and that γ_A^C varies as C_A. In either case, a function such as:

$$\gamma_{DA}^{\infty,C}/\gamma_D^{\infty,C}\gamma_A^C = a + bC_A \tag{69}$$

may accordingly be written, where a and b are constants. Substitution of equations (68) and (69) into the Gil-Av–Herling relation equation (67) produces:

$$K_R - K^0_{R(S)} = K^0_{R(S)} K^{th}_1 C_A/(a + bC_A) \tag{70}$$

which, however, can correspond to experiment, i.e. be linear in C_A, only if b is negligibly small, which implies that the activity coefficient ratio must remain constant. In contrast, the inverse of equation (70) is:

$$1/(K_R - K^0_{R(S)}) = a/K^0_{R(S)} K^{th}_1 C_A + b/K^0_{R(S)} K^{th}_1 \tag{71}$$

where $(K_R - K^0_{R_{(S)}})^{-1}$ will be linear in C_A^{-1} which is generally not observed.

Further expansion of equation (69) into a power series of the form:

$$\gamma^{\infty,C}_{DA}/\gamma^{\infty,C}_{D}\gamma^{C}_{A} = a + bC_A + cC_A^2 + \ldots \tag{72}$$

if realistic, would result in pronounced curvature of plots of K_R versus C_A, so this possibility must too be discarded as not conforming to experiment.

B. Solvent Effects

Perhaps the most disturbing aspect of complexation studies regardless of the experimental approach taken is the dependence of K_1 on the choice of "inert" solvent.[166, 206] Several explanations of the phenomena have been suggested[207] but none seems to be all-encompassing. Nor can any correspondence be claimed between K_1 data obtained in the vapour state and

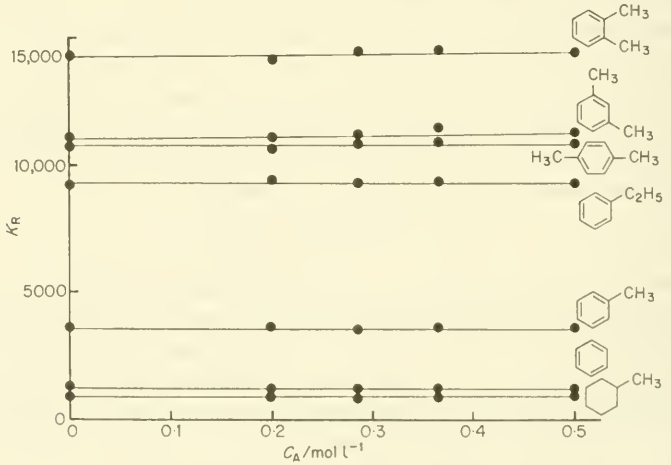

FIG. 2. Plots of K_R versus C_A for indicated solutes with tetracyanoethylene–di-n-butyl adipate stationary-phase mixtures at 25 °C. Data of Laub, Meen and Purnell[205]

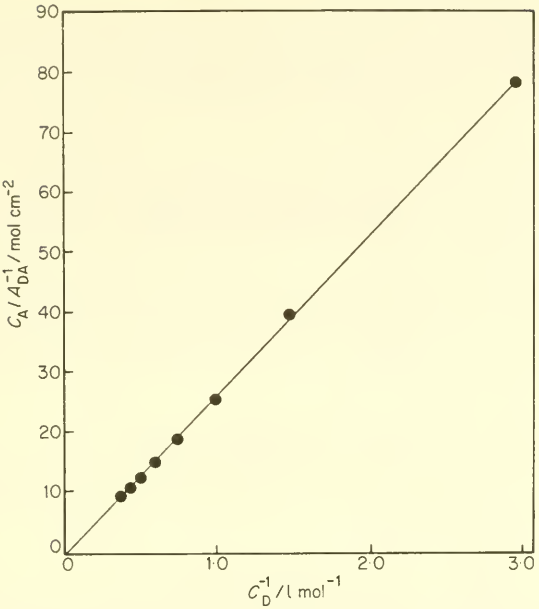

FIG. 3. Benesi–Hildebrand plot of $C_A l/A_{DA}$ versus $1/C_D$ for *o*-xylene with tetracyanoethylene–di-n-butyl adipate mixtures at 25°C. Data of Laub, Meen and Purnell[205]

those found with condensed (liquid) media[154] irrespective of the manner in which these are rationalized.[206] For example, there is strong (albeit largely inferential) evidence for π–π complexation of tetracyanoethylene with aromatic hydrocarbons. Figure 2, however, shows plots of K_R obtained via glc for such solutes with tetracyanoethylene additive in the solvent di-n-butyl adipate at 25°C;[205] similar results are obtained in di-n-butyl sebacate at 60°C.[205] The horizontal lines result in evaluation of K_1 according to the Gil-Av–Herling relation as approximately zero. A Benesi–Hildebrand type plot[205] is shown in Fig. 3 for *o*-xylene solute with the former system where again $K_1 = 0$ since the plot passes through the origin. Yet, these systems involve supposed "strong" complexation wherein solvent effects are generally considered to be minimal.

C. Diachoric Solutions Hypothesis

Prospective models of solution equilibria which purport to encompass complexation phenomena must, if to conform to experiment, predict and simultaneously rationalize the two well established findings noted above,

TABLE XVII. Test of equation (75)[209] [Reproduced with permission from J. H. Purnell and J. M. Vargas de Andrade, *J. Amer. Chem. Soc.*, **97**, 3585 (1975)]

Solute	Di-n-octyl ether–n-Heptadecane				Di-n-butyl tetrachlorophthalate–squalane			
	$K^0_{R(A)}$	$K^0_{R(S)}$	K_1/l mol^{-1}	$\bar{V}_A\Delta K^0_R/K^0_{R(S)}$	$K^0_{R(A)}$	$K^{0\,S}_{R(S)}$	K_1/l mol^{-1}	$\bar{V}_A\Delta K^0_R/K^0_{R(S)}$
Chloroform	579	250	0·407	0·398	718	232	0·640	0·664
1,2-Dichloroethane	535	317	0·215	0·208	984	294	0·745	0·744
Benzene	663	509	0·093	0·092	1218	442	0·548	0·557
Toluene	2189	1718	0·083	0·083	4141	1446	0·572	0·591
Ethylbenzene	5787	4619	0·077	0·077	8805	3688	0·410	0·440
o-Xylene	8508	6816	0·075	0·075	18034	5405	0·698	0·741
m-Xylene	6930	5804	0·059	0·059	12118	4408	0·521	0·555
p-Xylene	6735	5595	0·062	0·062	12896	4379	0·580	0·609

Data at 30°C: $\bar{V}$(di-n-octyl ether) = 0·30251 mol^{-1}; $\bar{V}$(di-n-butyl tetrachlorophthalate) = 0·31711 mol^{-1}.

namely, that K_R varies linearly with C_A over extended ranges of concentration, and that concentration-based stoichiometric equilibrium quotients are solvent-dependent to such an extent that zero or even negative values of K_1 may be obtained.

Purnell and Vargas de Andrade[209] approached the first of these problems by re-examination of two of those systems that had previously been reported to exhibit complexing and for which additive–solvent miscibility was extant in all proportions. The solutes and stationary phases, and their associated partition coefficients at 30°C are listed in Table XVII. Plots of K_R versus ϕ_A, as exemplified by those in n-heptadecane, are given in Fig. 4. Clearly, linearity obtains over the entire range $\phi_A = 0$–1, and since, in the absence of mixing volumes:

$$\bar{V}_i C_i = \phi_i \tag{73}$$

the plots must also be linear in C_A. The data were then treated as follows: according to the Gil-Av–Herling relation equation (22):

$$K_1 = (K_R - K^0_{R(S)})/K^0_{R(S)} C_A. \tag{74}$$

At the extremity of K_R/C_A plots (which are linear over the entire range of C_A) K_R becomes $K^0_{R(A)}$ (the partition coefficient with pure A) and C_A^{-1} is equal to $\bar{V}_A$ (the molar volume of bulk additive). It follows *necessarily* that equation (74) may be written as:

$$K_1 = \bar{V}_A(K^0_{R(A)} - K^0_{R(S)})/K^0_{R(S)} = \bar{V}_A \Delta K^0_R / K^0_{R(S)} \tag{75}$$

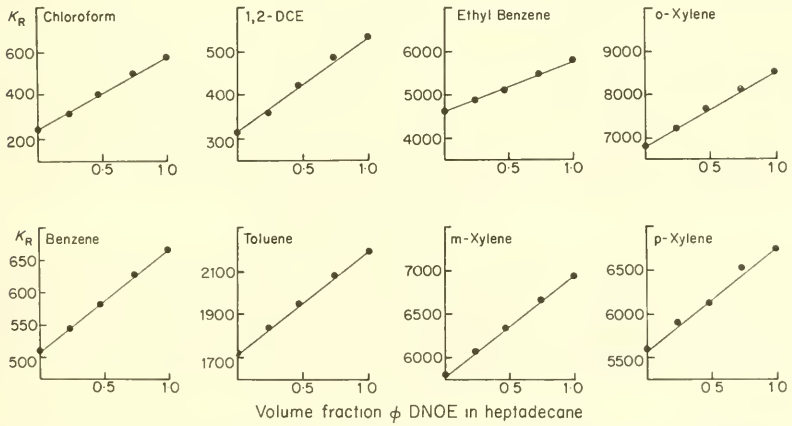

FIG. 4. Plots of K_R for named solutes versus volume fraction of di-n-octyl ether in n-heptadecane at 30°C. [Reproduced with permission from J. H. Purnell and J. M. Vargas de Andrade, *J. Amer. Chem. Soc.*, **97**, 3585 (1975)]

where the symbol ΔK_R^0 has been used to represent the numerical difference between the ordinate end-point values of the plots. Note that equation (75) has at this stage been formulated *only* as a consequence of the linearity of K_R in C_A, that is, the experimentally established validity of the Gil-Av–Herling relation for these systems.

Equations (74) and (75) must be formally identical since the slope of a straight line is constant whether taken at either end-point or at intermediate regions; equating the two relations, solving for K_R, and recalling equation (73) produces:

$$K_R = \phi_A \Delta K_R^0 + K_{R(S)}^0 = \phi_A K_{R(A)}^0 + \phi_S K_{R(S)}^0 \tag{76}$$

which is what would have been derived anyway from the plots shown in Fig. 4.

Equation (76) is currently the focal point of considerable controversy, and discussion and application of the relation form the basis of the remainder of this chapter.

The first and most obvious feature of the relation is that K_1 data are said, surprisingly, to be predictable solely from solute partition coefficients pertaining to the two pure solvents A and S, and $\bar{V}_A$. That is, values of K_1 derived from the conventional experimental procedure indicated by equation (22) should be identical to $\bar{V}_A \Delta K_R^0 / K_{R_{(S)}}$. Purnell and Vargas de Andrade[209] showed that this was indeed the case to well within any reasonable assessment of experimental error as shown for the systems listed in Table XVII. They noted further that values of K_1 which Martire and coworkers had obtained via the technique of Martire and Riedl conformed moderately well to equation (75), and hence retentions with these systems would be described by equation (76). This would, of course, be expected to be the case since the Gil-Av–Herling relation, as shown above, is merely one form of the more general expression (76), and since, as Martire and coworkers[172] themselves showed, the Martire–Riedl and Gil-Av–Herling methods yield values of K_1 that agree to within ~3 per cent. The proof of this proposition is as follows: the term γ_A in the Martire–Riedl formulation is given by:

$$\gamma_A = V_{g(A)}^{0(N)} M_A / V_{g(S)}^{0(N)} M_S. \tag{77}$$

Since γ_A is said to be a measure of the activity of the pure complexing phase with respect to that of the inert solvent, it should be independent of the choice of alkane solute used in its assessment. Suppose that this is in fact observed and, further, that the ratio $V_{g(A)}^{0(N)} / V_{g(S)}^{0(N)}$ is unity; equation (55) reduces in such a case to:

$$K_1 = \bar{V}_A (M_S / M_A)(V_{g(A)}^{0(D)} / V_{g(S)}^{0(D)} - 1). \tag{78}$$

Now, in order that, in application, the Martire–Riedl method conform to

assumptions and constraints specified originally in its derivation, the molecular weights, densities, polarizabilities, etc. of the two phases must be nearly identical. Thus, $M_S/M_A = 1$ and, recalling equation (10), since $K^0_{R(i)} = (V^0_{g(i)}\rho^0_i)(T/273)$:

$$K_1 = \bar{V}_A(K^0_{R(A)}/K^0_{R(S)} - 1) = \bar{V}_A\Delta K^0_R/K^0_{R(S)} \tag{79}$$

which is identical to that derived above by Purnell and Vargas de Andrade from plots of K_R which were linear in ϕ_A. Thus: K_1(Martire–Riedl) $\equiv$ K_1(Gil-Av–Herling) $\equiv$ K_1(Purnell–Vargas de Andrade) when γ_A is unity.

Suppose that $\gamma_A \neq 1$ but that $M_A = M_S$ and that $\rho^0_A = \rho^0_S$ is still true; equation (55) then becomes:

$$K_1 = (V^{0(N)}_{g(S)}/V^{0(N)}_{g(A)}(\bar{V}_A\Delta K^0_R/K^0_{R(S)}. \tag{80}$$

In the event that $M_A \neq M_S$ and $\rho^0_A \neq \rho^0_S$, then the full correction in terms of γ_A must be employed:

$$K_1 = (1/\gamma_A)(\bar{V}_A\Delta K^0_R/K^0_{R(S)})/\rho^0_S/\rho^0_A). \tag{81}$$

Table XVIII lists average values of the ratio $V^{0(N)}_{g(S)}/V^{0(N)}_{g(A)}$ and γ_A and $\bar{V}_A$ which were reported for the complexing phases di-n-octyl ether, di-n-octyl thioether and di-n-octylmethylamine with n-octadecane reference phase at 30–50°C. These data show that $\gamma_A \rightarrow$ unity only in the case of di-n-octylmethylamine at 30°C and at 40°C which accounts for the moderate discrepancies between K_1 and $\bar{V}_A\Delta K^0_R/K^0_{R(S)}$ found by Purnell and Vargas de

TABLE XVIII. Values of $V^{0(N)}_{g(S)}/V^{0(N)}_{g(A)}$, $\bar{V}_A^{-1}$, and γ_A for di-n-octyl ether, di-n-octyl thioether, and di-n-octylmethylamine[156] [Reproduced with permission from H.-L. Liao and D. E. Martire, *J. Amer. Chem. Soc.*, **96**, 2058 (1974)]

	30°C	40°C	50°C	60°C
A. Di-n-octyl ether				
$V^{0(N)}_{g(S)}/V^{0(N)}_{g(A)}$	0·987	1·005	1·022	1·039
$\bar{V}_A^{-}$/mol l^{-1}	3·299	3·270	3·241	3·212
γ_A	0·966	0·948	0·932	0·917
B. Di-n-octyl thioether				
$V^{0(N)}_{g(S)}/V^{0(N)}_{g(A)}$	1·089	1·087	1·085	1·083
$\bar{V}_A^{-1}$/mol l^{-1}	3·238	3·211	3·184	3·157
γ_A	0·932	0·934	0·936	0·938
C. Di-n-octylmethylamine				
$V^{0(N)}_{g(S)}/V^{0(N)}_{g(A)}$	1·004	1·012	1·018	1·024
$\bar{V}_A^{-1}$/mol l^{-1}	3·096	3·072	3·045	3·018
γ_A	1·000	0·993	0·986	0·981

TABLE XIX. Comparison of experimental[a] stability constants (K_1) with values calculated via equation (81) for solute interactions with (A) di-n-octyl ether, (B) di-n-octyl thioether, (C) di-n-octylmethylamine, all in n-octadecane at 30°C.

	K_1/l mol^{-1}					
	A		B[b]		C	
Solute	Exptl.	Calcd.	Exptl.	Calcd.	Exptl.	Calcd.
n-Propanol	1·20	1·22	0·72	0·66	2·47	2·46
Isopropanol	0·90	0·93	0·60	0·55	1·53	1·52
n-Butanol	1·15	1·17	0·72	0·66	2·41	2·40
Isobutanol	1·15	1·17	0·74	0·68	2·53	2·52
s-Butanol	0·77	0·79	0·54	0·50	1·34	1·34
t-Butanol	0·62	0·64	0·48	0·44	0·89	0·89
Dichloromethane	0·28	0·30	0·36	0·33	0·21	0·21
Bromochloromethane	0·29	0·31	0·41	0·37	0·22	0·23
Dibromomethane	0·30	0·31	0·45	0·42	0·25	0·26
Chloroform	0·39	0·41	0·42	0·38	0·47	0·47
Bromodichloromethane	0·41	0·42	0·50	0·46	0·51	0·52
Chlorodibromomethane	0·42	0·43	0·61	0·56	0·58	0·59
Bromoform	0·41	0·43	0·73	0·67	0·64	0·65
Carbon tetrachloride	0·07	0·08	0·14	0·12	0·06	0·07
Bromotrichloromethane	0·11	0·12	0·29	0·27	0·21	0·22
Carbon tetrabromide	0·12	0·14	0·93	0·85	—	—
1,1,1-Trichloroethane	0·10	0·12	0·16	0·15	0·07	0·08

[a]Refs. 122, 156, 171, 173. [b]Corrected for gas–liquid interfacial adsorption; these data suggest systematic experimental error of ~5 per cent.

Andrade (cf. Tables II–IV of ref. 209) referred to earlier. Near-perfect agreement is found if the fully corrected relation equation (81) is employed in making the comparison, as shown in Table XIX. The Martire–Riedl relation equation (55) is therefore only another (and specialized) form of equation (76).

Purnell and Vargas de Andrade[209] at this stage offered preliminary assessment of models of solutions from which equation (76) might be derived. They found that it could be obtained only by assuming that there were no interactions, specific or otherwise, between A and S. This implied either that A and S form solutions which in the nomenclature of conventional theories would be termed "perfect", or that pure A and pure S are separately aggregated on the microscopic level (see, however, the recent work of Nagy and coworkers[210]). Since the solute activity coefficients ranged within an order of magnitude about unity, the former possibility was considered unlikely, and Purnell and Vargas de Andrade were left with the task of deriving relations consistent with equation (76) on the assumption of the latter postulate. This proved to be straightforward; since the activity coefficient of solute D in (A + S) is said to be a linear function of that of D in A

and that of D in S then, from Raoult's law:

$$p_D/p_D^0 = \gamma_{D(A)}x_{D(A)} = \gamma_{D(S)}x_{D(S)} = \gamma_{D(A,S)}x_{D(A,S)} \quad (82)$$

where p_D and p_D^0 are the donor solute vapour pressure and saturation vapour pressure respectively, and $x_{D(i)}$ represents the solute mole-fraction in the ith medium. But in the elution mode of glc the solute is at infinite dilution, so:

$$1/\gamma^{\infty}_{D(A,S)} = x_A/\gamma^{\infty}_{D(A)} + x_S/\gamma^{\infty}_{D(S)}. \quad (83)$$

When this expression is combined with that commonly associated with the solute partition coefficient [equation (8)], and provided that there are no excess volumes of mixing, equation (76) is formed directly.

Purnell and Vargas de Andrade remarked that, consistent with the findings of Young,[211] they were unable to derive equation (76) on the basis of any theories of solutions currently accepted as "conventional". It could accordingly be evaluated only in terms of, and with reference to, published studies of systems wherein data pertaining to partitioning of a third component between (binary) mixed solvents and the vapour state had been reported. Laub and Purnell[203] subsequently located and tabulated a variety of such systems, all of which were derived from glc studies and which appeared without exception to exhibit plots of solute partition coefficients that were linear to, at worst, ± 10 per cent (and at this level only rarely) in ϕ_A. They noted, further, that many other workers had reported data for solute retentions with mixed-column compositions which conformed to one or another variant (cf. Section IV) of equation (76). These included, for example, steroid solutes with mixed silicone polymer stationary phases.[212–215]

Additional studies in which plots of K_R have been assessed as a function of some or other (A + S) compositional variable for fully miscible systems include those by Eon, Pommier and Guichon[167] and Mathiasson and Jonsson[170] ($\overline{V}_{A,S}K_R$ versus x_A). In the former, the pronounced curvature in the plots originally reported (K_R versus x_A) appears only to be a consequence of the fact that, in the absence of mixing volumes, ϕ_A is not related linearly to x_A:

$$\phi_A = x_A\overline{V}_A/[x_A(\overline{V}_A - \overline{V}_S) + \overline{V}_S]. \quad (84)$$

In contrast, since $x_A/\overline{V}_{A,S} = C_A$, plots of $\overline{V}_{A,S}K_R$ versus x_A would, on the basis of equation (76), be expected to be linear. Table XX gives the linear regression correlation coefficients of the data of Mathiasson and Jonsson obtained after conversion to K_R as a function of ϕ_A. Clearly, these systems obey equation (76) to, at worst, ± 3 per cent.

Equation (76) had to this point been shown to apply to several hundred (A + S) systems, each containing an infinite-dilution third component D. Since each comprised an average of six data points, well over a thousand

TABLE XX. Partition coefficient data[170] and linear regression correlation coefficients[14] for listed solutes with squalane–dodecyl laurate at 60°C [Reproduced with permission from R. J. Laub and R. L. Pecsok, "Physico-Chemical Applications of Gas Chromatography", Wiley-Interscience, New York (1978)]

Solute	$K^0_{R(S)}$	$K^0_{R(A)}$	r
p-Xylene	1119	1559	0·9996
Toluene	424·4	592·8	0·9997
Benzene	153·7	216·8	0·9994
Fluorobenzene	150·4	236·0	0·9995
Chlorobenzene	789·1	1271	0·9998
Benzotrifluoride	174·1	300·3	0·9999
Octafluorotoluene	96·93	166·8	0·9948
Methoxybenzene	1325	2329	0·9992
Di-n-butyl ether	1202	1308	0·9688
Cyclohexane	194·7	184·3	0·9796
Methylcyclohexane	353·5	338·5	0·9652
Ethylcyclohexane	981·5	937·4	0·9634
n-Heptane	273·7	261·4	0·9649
cis-Hept-2-ene	282·2	293·3	0·9698
trans-Hept-2-ene	269·4	280·1	0·9702
Trichloroethylene	222·5	328·3	0·9997
Tetrachloroethylene	695·6	818·2	0·9978

solutions of varying composition were found to conform. Moreover, these consisted of a range of compound types of considerable diversity, including many for which charge-transfer or hydrogen-bonding interactions ($K_1 > 3\,l\,mol^{-1}$) are traditionally considered to obtain; for others for which zero or even negative putative equilibrium quotients are evident; and for systems for which no conceivable form of complexation can be envisaged yet for which positive or negative K_1 could, variously, be evaluated depending upon the choice of identity of A and of S.

In view of the remarkable catholicity of equation (76), Laub and Purnell[203] suggested that solutions conforming to it be called *diachoric* (διαχωρισμως, partitioned-volume) and that the relation be termed the *diachoric solutions hypothesis*.

1. Evaluation by Nmr Spectroscopy

Purnell and Vargas de Andrade[216] attempted in view of the foregoing to evaluate equation (76) by nmr spectroscopy. The systems studied were those shown previously[209] to conform to the diachoric solutions hypothesis, which consisted of several solutes with di-n-octyl ether–n-heptadecane and di-n-butyl tetrachlorophthalate–squalane. They then related the nmr data

to the chromatographic partition coefficients through an expression consistent with equation (9) and with that derived by Foster, and found:

$$\Delta/\Delta_0 = \phi_A K^0_{R(A)}/K_R \tag{85}$$

where Δ_0 is the nmr shift difference between pure acceptor and pure complex and Δ is the observed nmr shift difference at intermediate composition of A with S. Plots of Δ versus ϕ_A/K_R (cf. Figs. 2–4 in ref. 216) were in most cases found to be linear; two systems gave what appeared to be pronounced curvature.

Martire[184] subsequently argued that these data, when plotted as the inverse of equation (85), were *all* curved and that it was therefore an ill-chosen method of relating nmr with glc data. He offered in its stead the hypothesis discussed earlier, that contact pairwise interactions were responsible for much of the discrepant chromatographic/spectroscopic data.

At this point, therefore, nmr and glc stability constant data appeared to be in serious disagreement, and the veracity of the diachoric solutions hypothesis appeared to be questionable insofar as it pertained to data measured by other techniques. The matter is deferred to Section III.D.3 since, first, equation (76) must be evaluated with respect to those remaining glc studies described in the literature or in contemporary work which may give further evidence for or against linearity of K_R as a function of ϕ_A.

2. Evaluation by Gas–Liquid Chromatography

(a) *Polymer solvent systems.* Thus far, Niederstrass[217] (cited by Braun and Guillet[218]) and Klein and Widdecke[219] are the only workers to have used polymer stationary phases with the expressed intent of evaluation of equation (76). They pointed out that the diachoric solutions relation could be cast in the form:

$$V^0_g = w_A V^0_{g(A)} + w_S V^0_{g(S)} \tag{86}$$

where w_A and w_S are the weight fractions of the respective components of the (A + S) mixed phase, and $V^0_{g(i)}$ the relevant solute specific retention volumes. Klein and Widdecke then obtained retention data for benzene and alkanes with columns containing polystyrene, polybutadiene, and mixtures comprising statistical, graft + homopolymer, graft, and block copolymer ("intimate") blends of these materials. It was assumed that V^0_g was linear in w_A and that compositions of the mixed polymer phases could therefore be obtained from V^0_g/w_A plots constructed from retention data for the two pure materials and from elution behaviour observed with the mixed phases. Table XXI presents the results of this work, where glc-determined polymer compositions are compared with those specified by the manufacturers which were measured by static techniques. Clearly, the integrity of equation (76)

TABLE XXI. Validity of equation (86) for copolymers of different sequence structure[219] [Reproduced with permission from J. Klein and H. Widdecke, *J. Chromatogr.*, **74**, 2210 (1978)]

Copolymer	Producer	Sequence structure	Composition, % Exptl. (glc)	Theoret.
Duranit 15S	Hüls	statistical	15	15
C118	Höchst	graft + homopolymer	25	22
C26II	Höchst	graft	52	51
Solprene 303	Phillips	11 block	53	52
Solprene 410	Phillips	32 block	55	52
Solprene 1205	Phillips	18 block	78	75
Solprene 1204	Phillips	statistical	80	75

with regard to these systems has been verified, even though, as emphasized by Klein and Widdecke, very different sequence length distributions obtained.

(b) *Partially-miscible solvent systems.* The most intriguing and simultaneously demanding test of equation (76) is the suggestion of linear K_R/ϕ_A plots for solutes with mixtures of stationary phases that exhibit only partial macroscopic miscibility over some or other portion of the volume fraction range 0–1 since, for such systems, there is no question of "perfect" solution behaviour. Further, aggregation within mixtures of these kinds is given credence not only on the basis of phase separation but also by opalescence phenomena observed at phase boundaries and, in particular, around the consolute temperature.

Equation (76) must apply within the two-phase region of systems of these kinds since here the composition of each phase remains invariant. Designating the volume fraction of each phase as ϕ_1 and ϕ_2:

$$K_R = \phi_1 K_{R(1)} + \phi_2 K_{R(2)} \tag{87}$$

where $K_{R(i)}$ is the solute partition coefficient with the ith phase which can in addition be defined in the manner of equation (76):

$$K_{R(1)} = K^0_{R(S)} + {}^1\phi_A \Delta K^0_R \tag{88}$$

$$K_{R(2)} = K^0_{R(S)} + {}^2\phi_A \Delta K^0_R \tag{89}$$

and which, upon combination and substitution into equation (87), provides:

$$K_R = K^0_{R(S)} + (K^0_{R(A)} - K^0_{R(S)})({}^1\phi_A\phi_1 + {}^2\phi_A\phi_2) \tag{90}$$

where ${}^1\phi_A$ and ${}^2\phi_A$ are the left- and right-side extremum points along the

volume fraction abscissa which define the two-phase region (i.e. $\phi_A = {}^1\phi_A$ to ${}^2\phi_A$). However:

$$ {}^1\phi_A = {}^1V_A/V_1 \tag{91} $$

$$ {}^2\phi_A = {}^2V_A/V_2 \tag{92} $$

where V_1 and V_2 are the total volumes of the conjugate phases 1 and 2, and ${}^1V_A$ and ${}^2V_A$ are the respective volumes of component A in each. Thus, the term $({}^1\phi_A\phi_1 + {}^2\phi_A\phi_2)$ corresponds to the overall volume fraction of A in the mixture, namely, bulk ϕ_A; equation (90) therefore reduces immediately to equation (76), and hence plots of K_R versus ϕ_A should exhibit uniform and contiguous linearity across the *entire* range $\phi_A = 0$–1 irrespective of phase separation at intermediate regions of composition.

Pakhomova and Vigdergauz[220] showed that equation (76) was not obeyed by several solutes with phases comprising the partially miscible pair squalane–tritolyl phosphate. Marked gas–liquid interfacial adsorption effects obtained in this study, so Laub, Purnell and Summers[221] carried out an investigation with the solvent system ethylene glycol–tributyl phosphate, the consolute temperature curve for which is shown in Fig. 5. The consolute

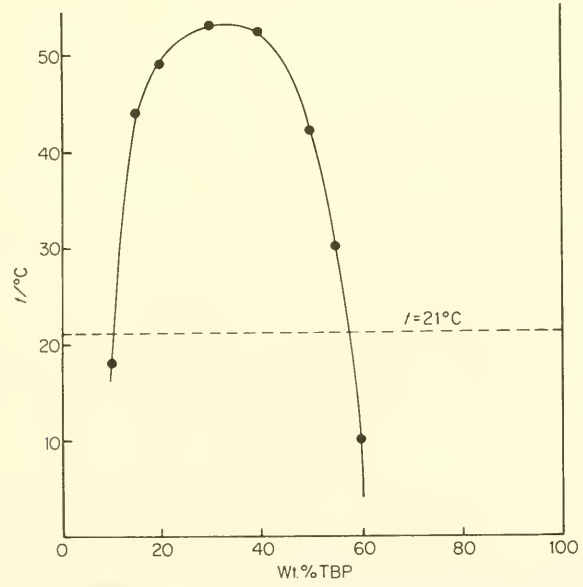

FIG. 5. Consolute temperature curve for tributyl phosphate–ethylene glycol. [Reproduced with permission from R. J. Laub, J. H. Purnell and D. M. Summers, *J. Chem. Soc. Faraday Trans. II*, submitted]

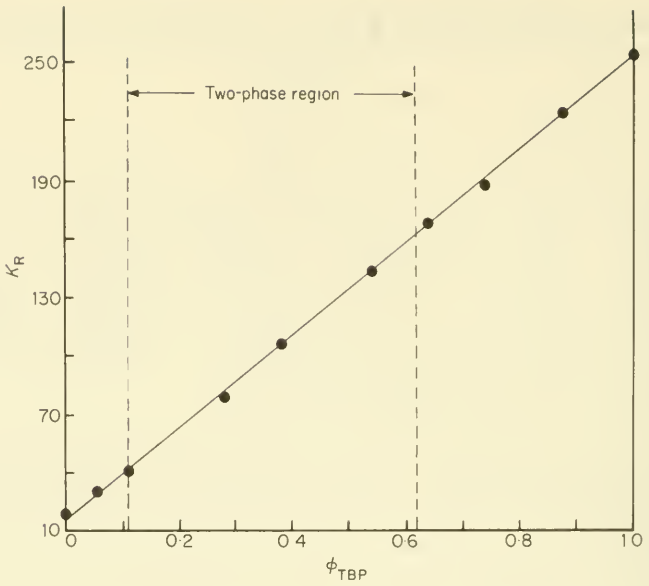

FIG. 6. Plots of K_R versus ϕ_{TBP} for furan solute with tributyl phosphate–ethylene glycol stationary-phase mixtures at 21°C. [Reproduced with permission from R. L. Laub, J. H. Purnell and D. M. Summers, *J. Chem. Soc. Faraday Trans. II*, submitted]

temperature is approximately 53°C over a plateau of ϕ, and there are broad ranges of one- and two-phase miscibility at lower temperatures. Further, preliminary experiments indicated that solute retentions were independent of liquid loadings with either of the pure phases. The system was therefore ideally suited for test of the above hypothesis.

Figure 6 shows a plot of K_R as a function of ϕ_A for the solute furan at 21°C. Similar plots were obtained for the solvents diethyl ether and methyl formate. To within ± 3 per cent or better all three are linear.

The diachoric solutions hypothesis was therefore demonstrated to apply to at least one solvent system with three solutes which involved non-ideality in the extreme, i.e. phase separation, and in which "small" molecules of additive and solvent were used which corresponded roughly to the size and shape of the solutes.

Martynyuk and Vigdergauz[222] have reported an evaluation of the use of colloidal mixtures of stationary phases. These comprised polyvinyl alcohol, polystyrene, or polyethylene dispersed in squalane, dinonyl phthalate, or polyethylene glycol 400. Plots of V_g^0 versus composition were linear over the ranges examined for ethanol, methyl ethyl ketone, benzene, nitromethane, pyridine, n-nonane, n-decane, toluene, and ethylbenzene solutes at 80 and

100°C. It was also demonstrated that retention characteristics of other pure phases could be duplicated by appropriate choice of composition of mixed-solvent systems.

(c) *Mechanically blended solvent systems.* Equation (76) must, as shown above, apply to mixed stationary phases constructed from pure-phase packings, that is, mechanical mixtures of (support + S) plus (support + A) whereby total "immiscibility" is guaranteed. Further, it must be presumed that intimately and mechanically mixed packings yield identical retentions.

The first to test these suggestions was McFadden[223] in 1958, who showed that retentions of alkyl halides with mixtures of methylsilicone and Tween 60 were identical whether the stationary phases were mixed intimately or mechanically, or constructed from tandem pure-phase columns. Series columns and those containing mechanically blended phases were, however, shown by Barnard and Hughes[224] to give slightly different results for ethane, propane, ethylene, and propylene with silver nitrate–ethylene glycol in admixture with triisobutylene. Variation in retention for segment-packed and series-connected columns was also noted by Haahti, Vandenheuvel and Horning[225] for steroids with methylsilicone–polyethylene glycol isophthalate solvents.

Matsuda and Yatsugi[226] compared intimate and mechanical blends of a variety of phases in 1962 and found no difference in retentions obtained from each. Maier and Karpathy[227] found similar results with di-2-methoxyethyl adipate–di-2-ethylhexyl sebacate. Darbre and coworkers[228, 229] indicated that segment-packed columns yielded retentions for derivatized amino-acids which corresponded closely to those measured with columns containing mechanically mixed phases; intimately blended solvents were said to be somewhat at variance with either, which may have been due to surface adsorption with their nitrile phases. Keller and Stewart,[230] Hildebrand and Reilley[231] and Pilgrim and Keller[232] subsequently reviewed the use of mixed phases in analytical glc, and showed that, because of carrier compressibility effects, tandem column systems are expected to yield retentions that are, depending on the pressure drop across each, at variance with single-column mixed-bed packings. Hildebrand and Reilley demonstrated, however, that solute capacity factors obtained from the latter were identical to those found with intimately blended phases.

Most recently, Lynch and coworkers[233] have demonstrated that mechanical mixtures of dimethylsilicone with methylphenylsilicone give retentions that are identical ($\pm 0{\cdot}5$ per cent) to those with other copolymer phases of intermediate phenyl content. Niederstrass[217] and Klein and Widdecke[219] showed in similar work that mechanical mixtures of packings of polystyrene with polybutadiene gave retentions that were the same as those with

("intimate") statistical, graft, block, or graft + homopolymer copolymer solvents [cf. Section III.C.2(a)].

(d) *n-Alkane solvent systems.* Laub, Martire and Purnell[53, 234] have recently reported studies of mixtures of n-alkanes which were designed to provide additional evaluation of the diachoric solutions hypothesis and, in particular, to allow comparison of partition data predicted from equation (76) with those from solution theories that are generally considered to be more "conventional" and, in this sense, well-founded. They first[234] extended the Janini–Martire[235] modification of Prigogine's treatment to binary (solute + solvent) hydrocarbon mixtures and showed that activity coefficients of n-alkane solutes could be predicted *a priori* from molecular properties to within ±1 per cent. Based upon the high degree of success of this study, they then[53] derived relations which permitted prediction of partition coefficients of n-alkane solutes with intimately blended binary n-alkane stationary phases which was of the form:

$$\ln K_R = \phi_S \ln K^0_{R(S)} + \phi_A \ln K^0_{R(A)} + (\bar{V}_1/\bar{V}_A)\chi_{A(S)}\phi_A\phi_S \qquad (93)$$

where $\bar{V}_1$ is the molar volume of the solute and where the "additive" was taken to be the solvent component of lower molecular weight. $\chi_{A(S)}$ is the additive–solvent Flory type interaction parameter. Equation (93) clearly predicts that plots of K_R will be curved in ϕ_A although the degree of curvature, depending upon the two n-alkane solvents and respective $\chi_{A(S)}$, may be slight.

Laub, Martire and Purnell chose to examine mixtures of n-octadecane with n-hexatriacontane since these solvents were available in pure form, were of sufficiently low vapour pressure for use as glc stationary phases at moderate temperatures, and differed by a factor of 2 in molecular weight. Furthermore, reliable data which could be related to partition coefficients had previously been reported by reputable laboratories for several n-alkane solutes with these pure solvents (cf. ref. 234). Plots of K_R versus ϕ_A were predicted, however, to exhibit only slight (< 1 per cent) curvature at $\phi \sim 0{\cdot}5$, which required development of techniques and procedures capable of yielding K_R data of precision at a level of ±1 per cent. This done (cf. ref. 54) they proceeded to determine the partition coefficients of n-pentane through n-octane with n-octadecane, n-hexatriacontane, and seven intimate mixtures of intermediate composition of the two phases at 80°C. Figure 7 shows the plots of $K_R/K^0_{R(S)}$ versus ϕ_A which they obtained for the mixed stationary phases, where the circles with error bars are the experimental data, the open circles are those calculated via equation (93), and the half-filled circles are those calculated from Orwoll–Flory theory.

The experimental data are seen to be indistinguishable from those calculated on the basis either of equation (76) or of equation (93), as emphasized

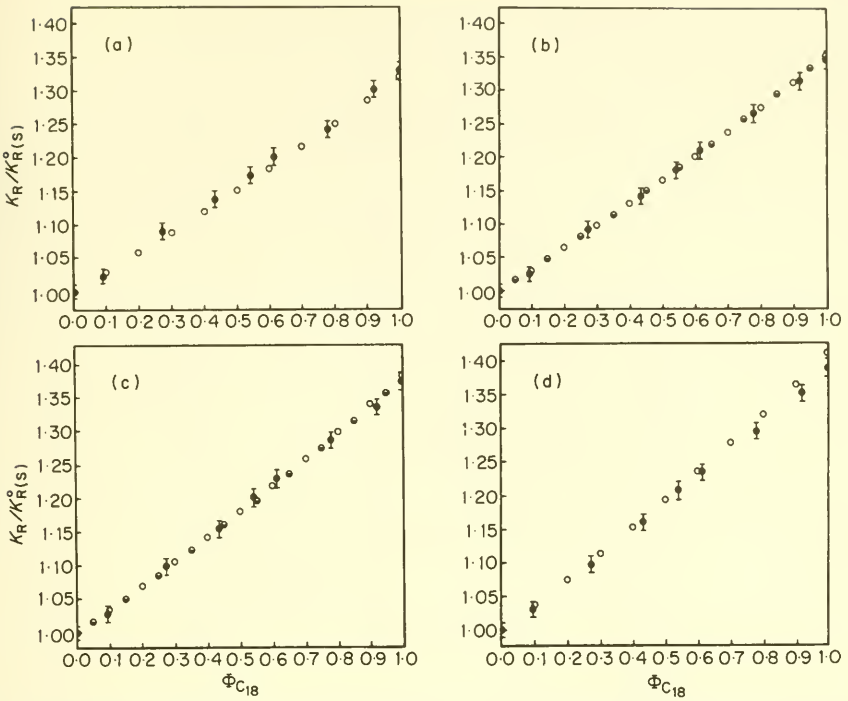

FIG. 7. Plots of $K_R/K^0_{R(S)}$ versus ϕ_A for (a) n-pentane, (b) n-hexane, (c) n-heptane, and (d) n-octane solutes with n-octadecane–n-hexatriacontane stationary-phase mixtures at 80°C. Filled circles, experimental data; open circles, Janini–Martire[235] theory; half-filled circles, Orwoll–Flory (cf. ref. 53) theory. [Reproduced with permission from R. J. Laub, D. E. Martire and J. H. Purnell, *J. Chem. Soc. Faraday Trans. II*, **74**, 213 (1978)]

by the linear regression correlation coefficients which were >0·9995 for all solutes. Nevertheless, all experimental points fall marginally below lines connecting $K^0_{R(S)}$ with $K^0_{R(A)}$ which could on statistical grounds be argued to imply real, albeit shallow, negative curvature.

It appears that the only other comprehensive study of n-alkane solutes with mixed n-alkane solvents is that reported by Hayduk and Cheng[236] for ethane with n-hexane–n-hexadecane solutions at 25°C. The K_R/ϕ_A plot for this system (cf. Fig. 6.17 of ref. 14) shows deviation from linearity which reaches about −17 per cent at $\phi_{C6} = 0{\cdot}6$.

(e) *Unsaturated hydrocarbon solutes with silver nitrate.* Equation (75) in the form:

$$K_1 = \bar{V}_A K^0_{R(A)}/K^0_{R(S)} - \bar{V}_A \tag{94}$$

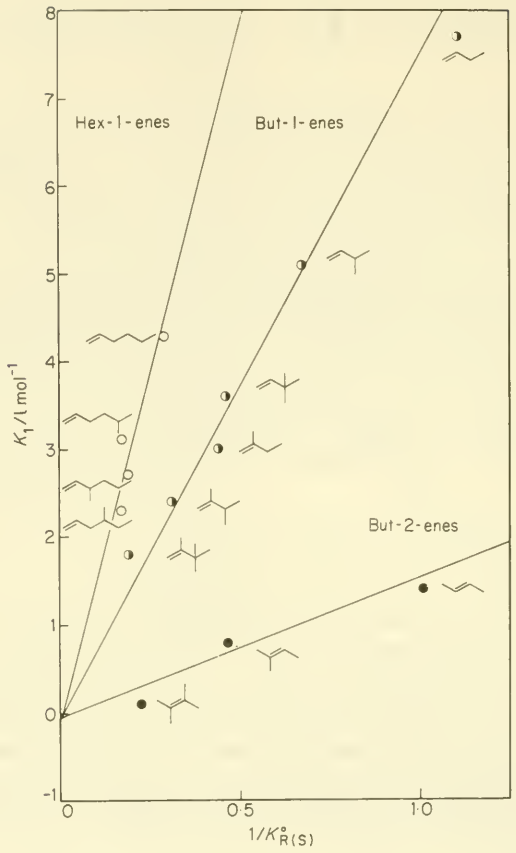

FIG. 8. Plots of K_1 versus $1/K^0_{R(S)}$ for indicated solutes with silver nitrate–ethylene glycol stationary-phase mixtures. [Reproduced with permission from R. J. Laub and J. H. Purnell, *J. Chem. Soc. Perkin Trans.* II, 895 (1978)]

indicates that plots of K_1 versus $1/K^0_{R(S)}$ will, for solutes with a common stationary-phase additive, be linear of slope $K^0_{R(A)}$ and intercept $-\bar{V}_A$ for data obtained with a series of related solvents. Laub and Purnell[237] pointed out that this approach might prove useful in quantitative assessment of solvent effects. Unfortunately, data of suitable form and of sufficient accuracy are not currently available for evaluation of the diachoric solutions hypothesis in this manner. However, several groups (cf. ref. 162) have reported K_1 data for a wide range of unsaturated hydrocarbon solutes with Ag^+ which were obtained by glc from silver nitrate–ethylene glycol stationary phases in the manner of Gil-Av and Herling, i.e. equation (22). There is some disagreement

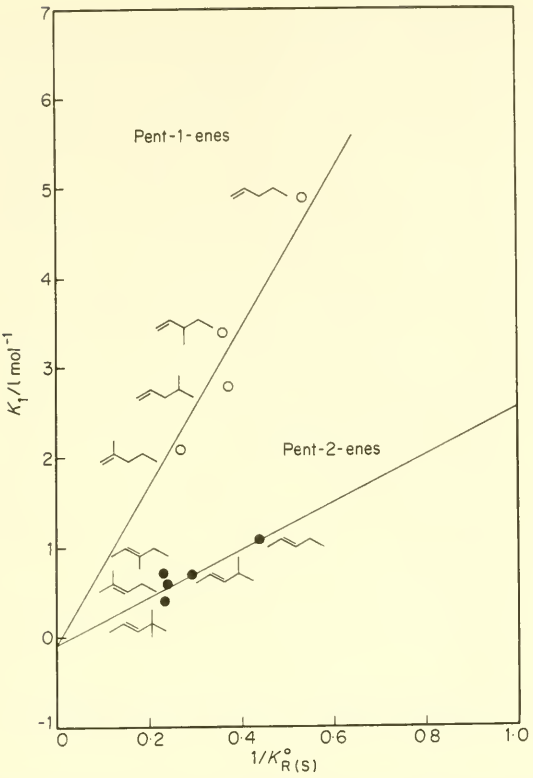

FIG. 9. Plots of K_1 versus $1/K^0_{R(S)}$ for indicated solutes with silver nitrate–ethylene glycol stationary-phase mixtures. [Reproduced with permission from R. J. Laub and J. H. Purnell, *J. Chem. Soc. Perkin Trans*, II, 895 (1978)]

as to the magnitude and importance of "salt" effects with systems of these types; nevertheless, the plotting procedure suggested by equation (94) seemed likely to bring out whatever consistencies there were in the data.

Figures 8–10 show plots of K_1 versus $1/K^0_{R(S)}$ for the indicated solutes at 40°C. These were drawn to intercept the ordinate at a value of $-\overline{V}_A$ for hypothetical "liquid" silver nitrate which Laub and Purnell estimated from density measurements of $AgNO_3$–ethylene glycol solutions.

There can be little doubt that these figures give strong indication of "family" behaviour which, however, is of a totally unexpected nature. Thus, for example, for olefins, methyl substitution seems relatively unimportant in comparison with the position of the double bond and with the carbon number of the solute backbone. Similarly, the position of the triple bond in acetylenes defines members of a family of common length of carbon skeleton.

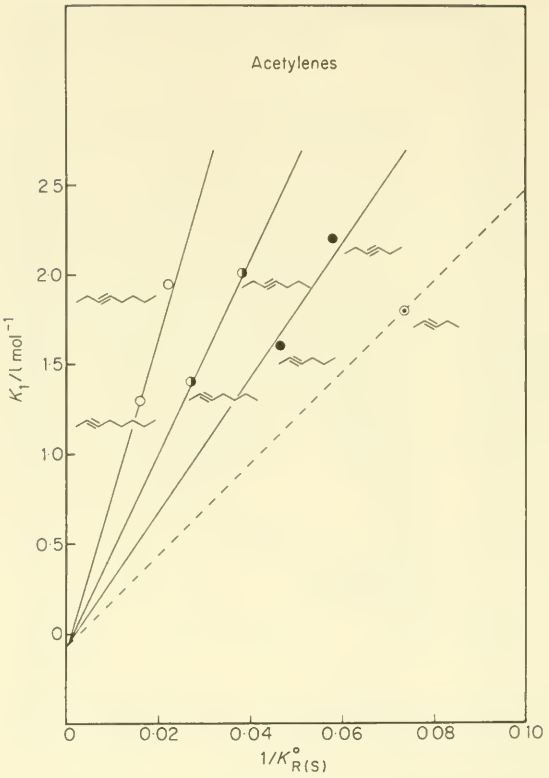

FIG. 10. Plots of K_1 versus $1/K^0_{R(S)}$ for indicated solutes with silver nitrate–ethylene glycol stationary-phase mixtures. [Reproduced with permission from R. J. Laub and J. H. Purnell, *J. Chem. Soc. Perkin Trans.* II, 895 (1978)]

These findings represent, insofar as the data are accurate, the first demonstrated coherence of complexation of unsaturated compounds with Ag^+, for which systems charge transfer is universally accepted to occur. The family behaviour found by Laub and Purnell is, to say the very least, novel, and clearly warrants further and comprehensive investigation. Use of equation (94) appears to offer significant advantages relating to studies of these systems.

(f) *Contemporary studies.* Laub, Martire, Purnell and their coworkers Harbison and Williams[238, 239] have recently determined partition data for several solutes with squalane/dinonyl phthalate mixtures by glc over the temperature range 0–70°C. This work was prompted by the study reported by Ashworth and Hooker[240] which showed that activity coefficients for these systems, as measured with a static technique and extrapolated to

infinite dilution, did not conform to equation (83) and hence could not be said to obey equation (76). Laub and coworkers confirmed that K_R was not a linear function of ϕ_A for the solutes examined (10 per cent positive deviations). Furthermore, plots of K_R versus ϕ_A for alkane and alicyclic hydrocarbons were asymmetric toward the squalane ordinate, while those for the two aromatic hydrocarbons (benzene and toluene) were asymmetric toward the dinonyl phthalate ordinate. In addition, asymmetry was not a linear function of temperature, this behaviour being in accordance with that predicted by Rowlinson[241] and confirmed by Patterson.[242, 243] (*Relative* partition coefficient data conformed remarkably well to the diachoric solutions hypothesis and are considered in detail in Section IV.A.)

Parcher and Westlake[244] reported finite-concentration gas chromatographic studies of eleven solutes of varied chemical type with mixtures of the solvents benzene–squalene, benzene–dinonyl phthalate, n-heptane–squalane, and n-heptane–dinonyl phthalate, all at 45°C. Several sets of partition data appeared to be curved slightly over the volume-fraction range permitted by the technique (ϕ_A = 0–0·5) while others appeared to be linear. These data may, however, be somewhat equivocal (see, for example, ref. 245) since, apparently, no allowance was made for the likely possibility of gas–liquid interfacial adsorption for several of the solutes, no account was taken of carrier virial or viscosity effects, nor could the concentration of the volatile component of the binary solvent mixture be determined accurately.

Kopecni and coworkers[246, 247] showed recently that plots of $\overline{V}_{A,S}K_R$ versus x_A and of K_R versus C_A were curved positively for alkanes, cyclohexane, benzene, and chlorinated hydrocarbon solutes with n-tetradecane–tri-n-butyl phosphate at 25 and 50°C. They attributed the non-linear behaviour to supposed[248, 249] dimerization of tri-n-butyl phosphate and, based upon the assumption that this phase exists solely as dimer in the bulk state, showed that the self-association constant K_d must lie between 1 and 10. Bogoslovsky *et al.*[250] have also presented examples which show extrema in plots of K_R versus ϕ_A for a variety of solutes with several interactive pairs of stationary phases.

Association of the components of an (A + S) stationary phase must yield curved plots of K_R versus *bulk* ϕ_A since, at every composition, the solvent would comprise three species: A, S, and an adduct. Assume that the additive dimerizes:

$$2A(1) \overset{K_d}{\rightleftharpoons} A(2) \tag{95}$$

where the 1 and 2 indicate monomer and dimer, respectively. The total concentration of additive C_A^t is related to K_d via:

$$C_A^t = C_{A(1)} + 2C_{A(2)} \tag{96}$$

$$K_d = C_{A(2)}/(C_{A(1)})^2 = (C_A^t - C_{A(1)})/2(C_{A(1)})^2. \tag{97}$$

Solving for $C_{A(1)}$:

$$C_{A(1)} = [-1 \pm (1 + 8K_d C_A^t)^{1/2}]/4K_d. \tag{98}$$

The net retention volume of a solute with the three-component solvent is given, according to the diachoric solutions hypothesis, by:

$$K_R(V_S + V_{A(1)} + V_{A(2)}) = V_N = V_S K^0_{R(S)} + V_{A(1)} K^0_{R(A)1} + V_{A(2)} K^0_{R(A)2}. \tag{99}$$

Recognizing that the total volume of A, V_A^t, is $(V_{A(1)} + V_{A(2)})$ or $V_{A(2)} = V_A^t - V_{A(1)}$, recalling that $\phi_i = C_i \bar{V}_i$ and substitution of equation (98) for $C_{A(1)}$ in equation (99) produces, since the root term must be positive:

$$K_R = \left[K^0_{R(S)} - \frac{\bar{V}_{A(1)}(K^0_{R(A)1} - K^0_{R(A)2})}{4K_d} \right] + \phi_A^t (K^0_{R(A)2} - K^0_{R(S)}) + \frac{\bar{V}_{A(1)}(K^0_{R(A)1} - K^0_{R(A)2}) \left(\frac{\bar{V}_A^t + 8K_d \phi_A^t}{\bar{V}_A} \right)^{1/2}}{4K_d} \tag{100}$$

which is of the form

$$K_R = (a - c) + b\phi_A^t + c(1 + d\phi_A^t)^{1/2} \tag{101}$$

where

$$a = K^0_{R(S)} \tag{102}$$

$$b = K^0_{R(A)2} - K^0_{R(S)} \tag{103}$$

$$c = \bar{V}_{A(1)}(K^0_{R(A)1} - K_{R(A)2})/4K_d \tag{104}$$

$$d = 8K_d/\bar{V}_A^t. \tag{105}$$

Equation (100) permits calculation of K_R as a function of ϕ_A^t provided that $\phi_{A(1)}$, $K_{R(A)1}$, and $K_{R(A)2}$ are known or can be measured or estimated.

In the event that solutes also complex with, say, monomer A, then the c-term must according to equation (22) be modified to:

$$K_{R(A)1} = K^{0,A(1)}_{R(A)}(1 + K_1^{A(1)} C_{A(1)}). \tag{106}$$

Table XXII gives the data required by equation (100) for calculation of K_R as a function of ϕ_A^t which were measured or estimated from those obtained by Laub and coworkers for benzene with squalane–dinonyl phthalate mixtures at 30°C. Figure 11 shows the experimental points plotted versus ϕ_A^t, and those calculated for $K_d = 0{\cdot}05$ ($K_1^{A(1)} = 0$) and for $K_d = 0{\cdot}05$ with $K_1^{A(1)} = 0{\cdot}2\ \mathrm{l\,mol^{-1}}$.

As seen in Fig. 11, both positive and negative curvature can be introduced into K_R/ϕ_A^t plots which is of the order of that observed for at least one

TABLE XXII. Values of parameters required by equation (100)

Term	Value	Method of determination
$K^0_{R(S)}$	433	exptl.
$K^0_{R(A)}$	667	exptl.
$K^0_{R(A)1}$	771	extrap.
$K^0_{R(A)2}$	127	calcd.
$\phi_{A(1)}$	0·838	calcd.
$\phi_{A(2)}$	0·162	calcd.
$\bar{V}_{A(1)}$	0·4341 mol^{-1}	exptl.
K_d	0·051 mol^{-1}	estim.
$K_1^{A(1)}$	0·201 mol^{-1}	estim.

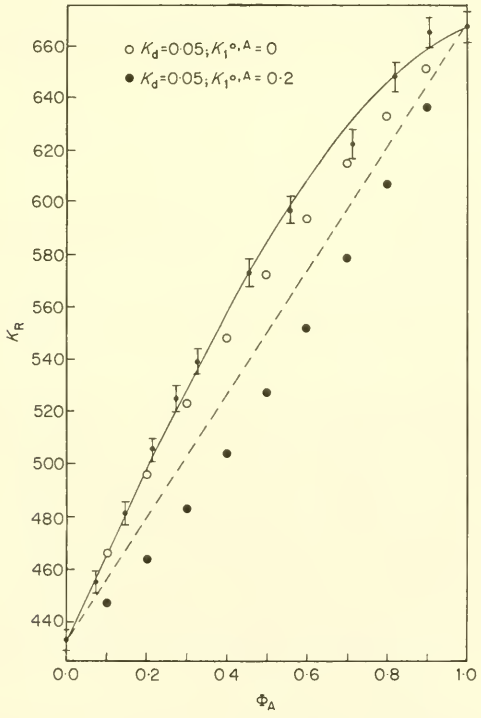

FIG. 11. Plot of K_R versus volume fraction of dinonyl phthalate for benzene solute with dinonyl phthalate–squalane stationary-phase mixture at 30°C. Experimental points indicated by error bars; open circles, calculated from equation (100) with data of Table XXII with $K_1^{A(1)} = 0$; filled circles, $K_1^{A(1)} = 0{\cdot}21\,\text{mol}^{-1}$.

system[238–240] which was found not to be described by the diachoric solutions relation. In the case cited the value of $K_{R(A)2}$ is unrealistically low, but nevertheless the point is made that a variety of heretofore unrecognized phenomena such as self-association may well cause equation (76) to fail. This view is lent further weight by the fact that a value of K_d of as little as 0·05 l mol^{-1} was enough to produce 10 per cent positive deviation from linearity in Fig. 11, and that subsequent addition of $K_1^{A(1)}$ of only 0·21 mol^{-1} produced ~10 per cent negative curvature. Alternatively, of course, the possibility must be recognized that equation (76) is altogether inappropriate for all binary systems, each containing a third infinite-dilution ("probe" solute) component, thus far noted in this section. Alternative relations, if to be given serious consideration, must presumably be at least as effective as equation (76) for prediction of partition coefficients with binary stationary phases for those systems that have been found to conform. Thus, in future such relations and their associated theories must predict linear or near-linear K_R/ϕ_A behaviour for wide ranges of solutes with equally diverse pairs of stationary phases which include mixtures of n-alkanes, silicone polymers, polyfunctional aromatic systems, and hydrogen-bonding and charge-transfer Lewis acids and bases.

D. Microscopic Partition (MP) Theory of Solutions

In view of the large number of systems that appeared to conform to the diachoric solutions hypothesis, Laub and Purnell[251] examined in detail the model from which it could be derived, namely, that of localized aggregation of A and of S. Parenthetically, this postulate is not novel or without precedent as some have mistakenly (and at times emotively) argued. For example, Table XXIII lists references to a portion of work in this field of some fifty years ago which precluded clarification of the basic concepts of micelle formation.[282] (Stewart referred originally to close-range molecular ordering as *cybotactic* behaviour, *cybotaxis* being synonymous in the present context with *diachoresis*.) In more recent years micelle phenomena have been said to be demonstrable in mixtures of liquid crystals (e.g. refs. 283–285), in soap solutions (e.g. refs. 282, 286, 287), and in biologically related systems (e.g. ref. 288). Franks[289,290] has shown that clustering or "swarming" occurs in water–alcohol solutions, which he termed the *hydrophobicity effect*. Toukubo and Nakamishi[291] argued, further, that molecular dynamics calculations offered evidence of long-time solvent clustering in solutions of Lennard-Jones particles. Compelling evidence for aggregation phenomena in mixtures of n-alkyl halides has also been reported by Brady,[292] and micelle formation in non-aqueous non-polar media was in part the subject of a recent symposium.[293]

TABLE XXIII. Systems said to exhibit cybotaxis[a]

Compound type	Ref.
Alcohols (methyl to lauryl)	252
Alcohols	253
Isomeric alcohols (butyl through heptyl)	254
Normal, branched alcohols	255
Octyl alcohols	256
Acetone	257
Normal alcohols; α- and β-naphthols; camphor	258
Fatty acids	259
Normal alkanes	260
Diethyl ether; chlorobenzene; quinoline	261
Alkanes; alcohols; acids; ethers; pyridine; piperidine; quinoline	262
Normal and branched alkanes	263
Aromatics; alicyclics; phenol; ketones; ethers	264
Water	265
Alcohols	266
Diethyl ether; nitrobenzene	267
Liquid crystals	268
Normal alkanes	269
Diethyl ether	270
Saturated solutions of LiCl in alcohols	271
Isopentane	272
Isopentane	273
Electrolytes in water and ethanol	274
Cyclohexane, benzene, and their mixtures	275
Reviews	276–280

[a]Alternative interpretations of these data are presented in ref. 281.

Thus, beginning with the *assumption* of aggregation of A and of S in (A + S) mixtures, Laub and Purnell[251] derived relations which arose strictly as a consequence of the diachoric solutions hypothesis and which pertained in particular to complexation phenomena.

The model on which their microscopic partition (MP) theory is based is shown in Fig. 12. Since A and S are presumed to be immiscible on the microscopic level, a hypothetical phase boundary is shown which separates additive from solvent in addition to that for each component with the gas phase. As indicated, several equilibria are possible:

(a) $$K^{0}_{R(A)} = (nC^{A}_{DA} + C^{A}_{D})/C^{M}_{D} \tag{107a}$$

where the apparent partition coefficient of D with pure A is the ratio of complexed plus free D in A to that in the mobile phase (M).

(b) $$K^{0,t}_{R(A)} = C^{A}_{D}/C^{M}_{D}. \tag{107b}$$

The true partition coefficient of D with A is given by the ratio of free D to that in the mobile phase. Similarly for S:

(c) $$K^{0}_{R(S)} = (qC^{S}_{DS} + C^{S}_{D})/C^{M}_{D} \tag{108a}$$

(d) $$K^{0,t}_{R(S)} = C^{S}_{D}/C^{M}_{D} \tag{108b}$$

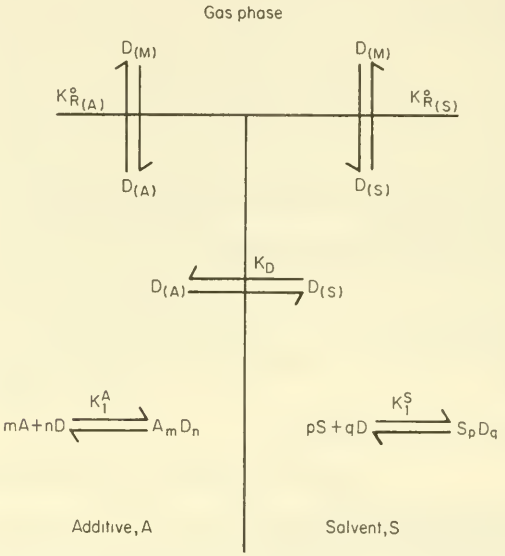

FIG. 12. Schematic diagram of microscopic partition (MP) model of solutions. [Reproduced with permission from R. L. Laub and J. H. Purnell, *J. Amer. Chem. Soc.*, **98**, 35 (1976)]

Partitioning of D between A and S is represented by:

(e) $$K_{d} = (nC^{A}_{DA} + C^{A}_{D})/(qC^{S}_{DS} + C^{S}_{D}) \tag{109a}$$

(f) $$K^{t}_{d} = C^{A}_{D}/C^{S}_{D}. \tag{109b}$$

Assuming that only 1:1 complexing occurs in either phase:

$$K^{A,t}_{1} = C^{A}_{DA}/C^{A}_{D}C^{A}_{A} \tag{110a}$$

$$K^{S,t}_{1} = C^{S}_{DS}/C^{S}_{D}C^{S}_{S}. \tag{110b}$$

Solving for C^{i}_{Di}, recognizing that $C^{i}_{i} \approx \bar{V}_{i}^{-1}$ since the solute is at infinite dilution, and relating each species to the total solution volume by dividing both sides by $(V_A + V_S)$ produces:

$$C^{A,S}_{DA} = K^{A,t}_{1}C^{A}_{D}\phi_{A}/\bar{V}_{A} \tag{111}$$

$$C^{A,S}_{DS} = K^{S,t}_{1}C^{S}_{D}\phi_{S}/\bar{V}_{S}. \tag{112}$$

Mole balance in the system requires that:

$$n_D^{A,S} = n_D^A + n_D^S + n_{DA}^A + n_{DS}^S \tag{113}$$

which, when divided by $(V_A + V_S)$, followed by substitution from equations (111) and (112), gives:

$$C_D^{A,S} = C_D^A\phi_A + C_D^S\phi_S + K_1^{A,t}C_D^A\phi_A/\bar{V}_A + K_1^{S,t}C_D^S\phi_S/\bar{V}_S. \tag{114}$$

Since the overall partition coefficient of D with (A + S) and the gas phase is $C_D^{A,S}/C_D^M$:

$$K_R = \phi_A[K_{R(A)}^{0,t}(1 + K_1^{A,t}/\bar{V}_A)] + \phi_S[K_{R(S)}^{0,t}(1 + K_1^{S,t}/\bar{V}_S)]. \tag{115}$$

Equation (115) can be arrived at more directly by supposing that the Gil-Av–Herling relation may be applied to solute interactions with pure A and with pure S in accordance with:

$$K_{R(i)}^0 = K_{R(i)}^{0,t}(1 + K_1^{i,t}/\bar{V}_i). \tag{116}$$

Substitution of this relation for $K_{R(A)}^0$ and for $K_{R(S)}^0$ in equation (22) produces equation (115), and hence the latter must contain and account for any equilibria, stoichiometric or otherwise, which occur between D and A and between D and S. Further, when $K_1^{A,t} = K_1^{S,t} = 0$, equation (115) reduces directly to the diachoric solutions hypothesis since, in such a case, $K_{R(A)}^{0,t} = K_{R(A)}^0$ and $K_{R(S)}^{0,t} = K_{R(S)}^0$. Experiment may still yield a value for K_1^{glc}, of course, which may be positive, zero, or negative depending on the solubility of D in A and in S.

When $K_1^{A,t} \neq K_1^{S,t} \neq 0$, equating equation (22) with equation (115) and solving for K_1^{glc} gives:

$$K_1^{glc} = \frac{(\bar{V}_A\bar{V}_S\Delta_R^{0,t}) + (\bar{V}_SK_{R(A)}^{0,t}K_1^{A,t}) - (\bar{V}_AK_{R(S)}^{0,t}K_1^{S,t})}{\bar{V}_SK_{R(S)}^{0,t} + K_{R(S)}^{0,t}K_1^{S,t}} \tag{117}$$

which when $K_1^{S,t} = 0$ reduces to:

$$K_1^{glc} = (\bar{V}_A\Delta K_R^{0,t} + K_{R(A)}^{0,t}K_1^{A,t})/K_{R(S)}^0 \tag{118}$$

and when $K_1^{A,t} = 0$, to equation (75).

Unfortunately, the product terms $K_{R(i)}^{0,t}$ and $K_1^{i,t}$ cannot be evaluated unless one or the other can be determined separately, for which gas-phase ultraviolet techniques appear to hold some promise.

1. Extension to Ultraviolet–Visible Spectroscopy

Laub and Purnell[251] next extended MP theory to ultraviolet–visible studies

and showed that for the case in which $K_1^{S,t} = 0$:

$$\frac{C_D^{A,S} l}{A_{DA}} = \frac{1}{K_1^{A,t} K_d^t C_A^{A,S} \epsilon_{DA}} + \left(1 + \frac{\overline{V}_A}{K_1^{A,t}} - \frac{\overline{V}_A}{K_1^{A,t} K_d}\right) \frac{1}{\epsilon_{DA}} \tag{119}$$

Dividing the intercept which would be found from a plot of $C_D^{A,S}/A_{DA}$ versus $1/C_A^{A,S}$ by the slope produces:

$$K_1^{uv} = (\overline{V}_A \Delta K_R^{0,t} + K_{R(A)}^{0,t} K_1^{A,t})/K_{R(S)}^0 = K_1^{glc} \tag{120}$$

which predicts that stability constants as measured by ultraviolet spectroscopy and by glc should be identical.

2. Extension to Nmr Spectroscopy

The form of equation (115) pertinent to nmr spectroscopy was shown by Laub and Purnell[251] in the case where $K_1^{S,t} = 0$ to be:

$$\frac{1}{\Delta} = \frac{K_{R(S)}^0}{K_{R(A)}^{0,t} \overline{V}_A C_A^{A,S} \Delta_0^t} + \left(\frac{\Delta K_R^{0,t}}{K_{R(A)}^{0,t}} + \frac{K_1^{A,t}}{\overline{V}_A}\right) \frac{1}{\Delta_0^t}. \tag{121}$$

Again dividing the intercept to be expected from this relation from a plot of $1/\Delta$ versus $1/C_A^{A,S}$ by the slope:

$$K_1^{nmr} = (\overline{V}_A \Delta K_R^{0,t} + K_{R(A)}^0 K_1^{A,t})/K_{R(S)}^0 = K_1^{uv} = K_1^{glc}. \tag{122}$$

3. Disparity Between Chromatographic and Spectroscopic Data

In practice, chromatographic and spectroscopic K_1 data have been found to agree in only one case, namely, that carried out by infrared spectroscopy[165] as noted in Section II. Further, heats of complexation obtained via calorimetric methods were shown to be in moderate agreement[174] with those found from the Martire–Riedl glc technique. In all other studies reported, $K_1^{nmr} \neq K_1^{glc} \neq K_1^{uv}$.

In spectroscopic studies, D is usually maintained in large excess over A in a third solvent S; in glc, of course, the (donor) solute is always at infinite dilution. Thus, comparisons heretofore made of chromatographic with spectroscopic data do not correspond to the same systems. Furthermore, Dodson, Foster and coworkers,[294] in commenting upon the disagreement between the values of stability constants derived from ultraviolet-visible measurements and those from nmr measurements, showed that termolecular complexation was undoubtedly responsible, at least in part, for the disparities. Thus, Δ_0 and ϵ_{DA} appeared to be concentration-dependent in several cases. If, as Foster has found, even moderate concentrations of D with A yield higher (than 1:1) complexes, spectroscopic and chromatographic data must *of necessity* be in disagreement.

According to MP theory, however, nmr and ultraviolet K_1 data may still

be correlated.[251] The relevant expressions for each technique are:

$$1/\Delta = 1/\Delta_0 K_1^{nmr} C_A^{A,S} + 1/\Delta_0 \tag{123}$$

$$C_D^{A,S} l/A_{DA} = 1/\epsilon_{DA} K_1^{uv} C_A^{A,S} + 1/\epsilon_{DA}. \tag{124}$$

Therefore, at equal values of $C_A^{A,S}$ for those cases for which $K_1^{nmr} = K_1^{uv}$:

$$C_D^{A,S} l/A_{DA} = \Delta_0/\epsilon_{DA}\Delta. \tag{125}$$

Plots of $C_D^{A,S} l/A_{DA}$ versus $1/\Delta$ are thus predicted to be linear of slope Δ_0/ϵ_{DA} and zero intercept. Figure 13 shows such plots for toluene with 2,4,7-trinitro-

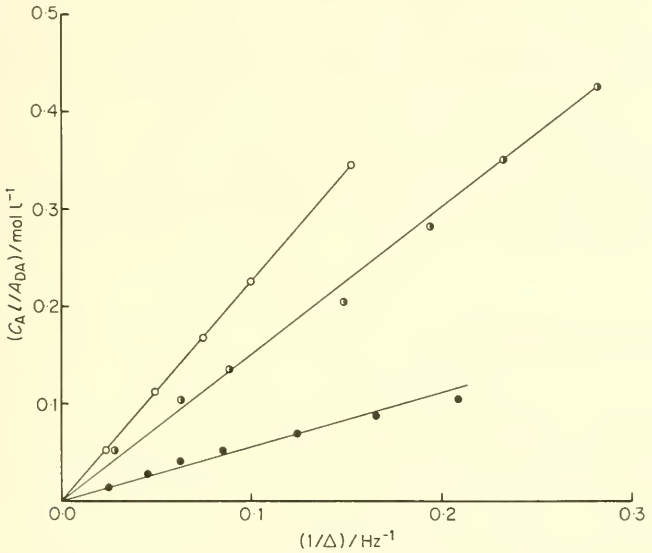

FIG. 13. Plots of $C_A l/A_{DA}$ versus $1/\Delta$ for toluene with 2,4,7-trinitrofluorenone and the solvents: di-n-butyl adipate (empty circles), di-n-butyl succinate (half-filled circles), and di-n-butyl sebacate (filled circles) at 40°C. [Reproduced with permission from R. J. Laub and J. H. Purnell, *J. Amer. Chem. Soc.*, **98**, 35 (1976)]

fluorenone in the solvents di-n-butyl phthalate, di-n-butyl succinate and di-n-butyl sebacate reported by Laub and Purnell[251] which appear to conform precisely to the behaviour predicted by equation (125). They also noted that ratios of Δ_0/ϵ_{DA} calculated from data determined in separate ultraviolet and nmr experiments differed by up to a factor of 3 from the slopes of the lines of this figure which they took to be a consequence of difficulties associated with evaluation of ϵ_{DA} from Benesi–Hildebrand type plots.

4. Interpretation of Solvent Effects

The MP model provides[251] means, at least in principle, of evaluation of solvent effects. Several possibilities may be considered in turn in terms of K_1:

(a) $$K_1^{S,t} = 0;\ K_{R(A)}^{0,t} = K_{R(S)}^{0}.$$

According to equation (117), K_1^{exptl} will, in this case only, be equal to $K_1^{A,t}$. The situation is, however, highly unlikely since it requires that complexing solutes be as soluble in "inert" solvents as in additives.

(b) $$K_1^{S,t} = 0;\ K_{R(A)}^{0,t} > K_{R(S)}^{0}.$$

Here $K_1^{A,t} < K_1^{exptl}$ must be true since K_R and $K_1^{A,t}$ must be zero or positive.

(c) $$K_1^{S,t} = 0;\ K_{R(A)}^{0,t} < K_{R(S)}^{0}$$

$K_1^{A,t}$ will be greater than K_1^{exptl} but the situation is even more unlikely than that of (a) in that solute solubility in S is said to be greater than that in A.

(d) $$K_1^{S,t} = K_1^{exptl} = 0$$

Equation (117) becomes in this instance:

$$K_1^{A,t} = -(K_{R(A)}^{0,t} - K_{R(S)}^{0})\bar{V}_A/K_{R(A)}^{0,t}.$$

But, since $K_1^{A,t} \geqslant 0$ must be true, it follows that $K_{R(S)}^{0} \geqslant K_{R(A)}^{0,t}$ must also obtain.

(e) $$K_1^{S,t} = 0;\ K_1^{A,:} < (K_{R(S)}^{0}/K_{R(A)}^{0,t} - 1)\bar{V}_A$$

K_1^{exptl} will for these cases be negative of limiting value $-\bar{V}_A$ (cf. Figs. 8–10).

(f) $$K_1^{S,t} \neq K_1^{A,t} \neq 0.$$

Assuming the not unreasonable values $\bar{V}_A = \bar{V}_S = 0{\cdot}51\,\mathrm{mol}^{-1}$, $K_{R(S)}^{0,t} = \Delta K_R^{0,t} = 500$, $K_{R(A)}^{0,t} = 1000$, $K_1^{A,t} = 0{\cdot}51\,\mathrm{mol}^{-1}$, and $K_1^{S,t} = 0{\cdot}11\,\mathrm{mol}^{-1}$, K_1^{exptl} would, according to equation (117), be evaluated as $1{\cdot}1671\,\mathrm{mol}^{-1}$, more than double the actual value of $K_1^{A,t}$. The situation is made even more discrepant if $K_1^{S,t}$ is assumed to be very small, say, $0{\cdot}01\,\mathrm{l\,mol}^{-1}$, since K_1^{exptl} is then $1{\cdot}461\,\mathrm{l\,mol}^{-1}$, almost treble $K_1^{A,t}$.

Thus, it seems feasible to rationalize solvent effects in terms of the MP model although, as noted above, $K_{R(i)}^{0,t}$ and $K_1^{i,t}$ have yet to be determined separately. Evaluation of this feature of the Laub–Purnell microscopic partition solutions theory must therefore await further experiment.

IV. PRACTICAL CONSEQUENCES OF MP THEORY

The choice of stationary phase, column length, temperature, and other operating conditions for a given separation has heretofore been made in analytical gas–liquid chromatography largely on the basis of what can most charitably be described as "hit or miss". The usual procedure (e.g. ref. 295) amounts to initial use of a solvent which is thought to be selective for the type of sample at hand (*similis similibus solvantur*) if guidelines for the separation cannot be found in the literature. A column of length often dictated by "standard" sizes available to the analyst is then packed with this stationary phase/support material and used at some operating temperature. If the resultant analysis is not considered satisfactory the column temperature is lowered and the run repeated. If it is still less than adequate from whatever point of view the procedure may be repeated several times with different stationary phases. Finally, the analyst may resort to capillary columns which offer the advantage of separation efficiency (however this is defined) which is greater than that possible with packed columns.

This scenario represents with few exceptions the current state-of-the-art procedure in choosing the pure-phase column and conditions that are thought to be appropriate for the separation of a given mixture. It is hardly surprising therefore that multi-component sorbents have been little used in analytical glc since prediction of retention behaviour with pure stationary phases, let alone their mixtures, would seem to be intractable. Nevertheless, there have been several noteworthy efforts in this direction. The strategies developed have without exception been founded upon some or other function that relates solute retention with pure solvents to that obtained with their admixtures.

The first reports of the use of mixed phases in glc were those by Martin and James[3] and James, Martin and Smith[296] in 1952. Phases were used in these instances to modify sorption properties of supports. Early studies which employed mixed phases in the form of tandem columns were those reported by Keulemans, Kwantes and Zaal[297] in 1955 and by Fredericks and Brooks[298] in 1956. Other work in this field includes that by Purnell and Spencer,[299] Zlatkis,[300] Bayer and coworkers,[301] Raupp[302] and others. McFadden[223] in 1958 was the first to show that mechanically mixed packings could be used in place of tandem columns, slightly at variance with the findings of Barnard and Hughes[224] in 1959.

Compositions of mixed phases in these early studies were formulated on a purely empirical basis and it was not until later in 1959 that the first *quantitative* study of the prediction of solute elution as a function of column composition was reported by Primavesi.[303] Series columns of triisobutylene

and silver nitrate–ethylene glycol were used in that investigation to measure the specific retention volumes of ethane, ethylene, propane and propylene at 12°C. The series columns corresponding to each composition were then unpacked, their contents were mixed mechanically, and were then repacked in a single column. Plots of V_g^0 versus w_A showed that, within an experimental error of ± 5 per cent, series columns provided retentions for these systems which were identical to those found with mixed packings and, further, that V_g^0 was linear in w_A. Thus, retentions with composite packings appeared to be predictable from data pertaining to the pure phases in accordance with equation (86).

Singliar and coworkers[304] found that series columns containing diglycerine and polyethylene glycol did not give the same number of theoretical plates N (column efficiency) as a single column containing mixed phases for isobutyraldehyde, n-butyraldehyde, toluol, isobutanol, and n-butanol solutes; however, surface adsorption effects are evident in this work. Haahti, Vandenheuvel and Horning[225] used mixed-packing columns in 1962, but found that the retention of steroid solutes was not a linear function of the phase composition. Waksmundzki and coworkers,[305, 306] following Kemula and Buchowski,[307] used an equation of the form:

$$\log k' = \phi_A \log k'_{(A)} + \phi_S \log k'_{(S)} \tag{126}$$

which they found to be obeyed by a variety of solutes with diethylene glycol–benzyl alcohol and diethylene glycol–decalin solvents. They also pointed out that only a few points were required to establish linearity of the plots and that inspection of such figures could provide a basis upon which to choose the optimum stationary-phase mixture for a given separation.

Zhukhovitskii and coworkers[308] were the first in 1962 to resolve the question of disparities between retentions obtained with series columns and with mixed-bed single columns. They showed that gas compressibility effects result in dependence of retention on the order of connection of tandem columns, especially if adsorbent phases are employed. This work was extended by Maier and Karpathy,[227] Jordan,[309] Keller and Stewart[230] and in particular by Hildebrand and Reilley in 1964 who showed that an expression of the form:

$$k' = w_A k'_{(A)} + w_S k'_{(S)} \tag{127}$$

was adequate for formulation of mixed phases in analytical glc and was independent of their construction as intimate or mechanical blends (cf. Fig. 1 of ref. 231). Rohrschneider,[310] Mitooka and coworkers,[311, 312] Pauschmann,[313] Littlewood and Willmott,[314] Waksmundzki and coworkers,[306] Touchstone and coworkers,[212–213] Darbre and coworkers,[228, 229] Windham,[315] Pakhomova and Vigdergauz,[220] Pilgrim

and Keller,[232] Melnikov and Aivazov,[316] Suzuki and coworkers[317] and Lynch and coworkers[233] have all used similar expressions for predictive purposes or for indentification of combinations of phases which duplicate (hence can replace) other pure solvents. Porter and coworkers,[318] Molera, Dominguez and Biarge[319] and Melnikov and Aivazov[320] have provided algorithm strategies for computerized selection of optimum stationary-phase mixtures.

Zielinski and Martire,[321] Risby and coworkers[322,323] and others (e.g. ref. 324) have evaluated and tabulated functional-group contributions to retentions with various pure phases in efforts to predict separations: often the data have been related through the solute retention index.[325] However, while these efforts have met with some success, their predictive capabilities insofar as practical selection of solvents is concerned, leave much to be desired. Part of the difficulty stems from the use of equivocal data of dubious accuracy. For example, McReynolds[326] determined specific retention volumes of solutes with columns of several types containing phases to which had been added small amounts of various surfactants. This is sufficient to alter retention times and even retention order, as was pointed out in 1955 by Purnell and Spencer.[299] Thus, McReynolds found that chloroform eluted after n-hexane with his mixed-phase solvent system whereas chloroform elutes before n-hexane with pure squalane. Risby and coworkers[322,323] unfortunately failed to take this into account when they calculated functional-group contributions to retention from McReynolds' data. Their method of predicting specific retention volumes at temperatures other than those which McReynolds used also fails badly. For example, the specific retention volume of n-hexane with squalane is forecast according to their relations[323] to be 186·5 ml g^{-1} at 30°C whereas the average of a number of independent glc and static measurements of high accuracy[238–240] gave 343·3 ml g^{-1}.

Thus, it seems that the use of mixed liquids offers a fruitful approach to separations since retentions can be forecast accurately from those obtained with pure solvents, rather than requiring *a priori* calculation of elution with individual phases (success of the latter approach rests ultimately upon development of adequate theories of solutions pertaining to mixtures of other than n-alkanes).

A. The Laub–Purnell Window Diagram Procedure

Development of techniques capable of prediction of solute retentions with mixed phases (or serial columns) as described above from data relating to pure solvents is an important advance in analytical gas chromatography. Consider, for example, the separation of a three-component solute mixture

in which two of the components overlap with one phase and where another pair overlaps with a second phase. Even though neither of the two pure solvents will provide resolution there is every likelihood that some mixture of the two phases will effect the desired separation.

Figure 14 illustrates the situation for the solutes labelled 1, 2, and 3 with the phases A and S, where straight lines have been drawn between the two

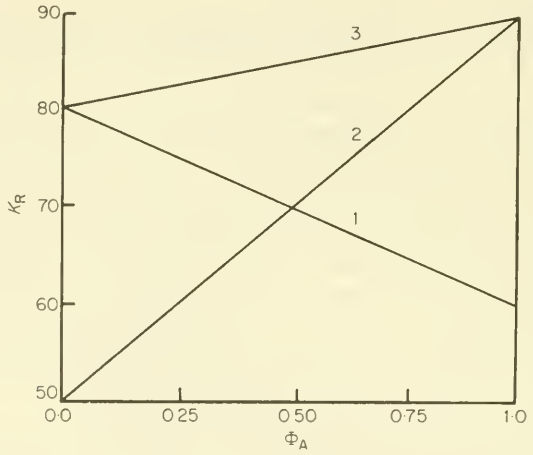

FIG. 14. Plots of K_R versus ϕ_A for three hypothetical solutes.

end-points $K^0_{R(S)}$ and $K^0_{R(A)}$ for each solute in accordance with equation (76). Inspection of the plots shows that overlap will occur at $\phi_A = 0{\cdot}5$ in addition to those at $\phi_A = 0$ and at $\phi_A = 1$, but that separation will be achieved at roughly $\phi_A = 0{\cdot}25$ and $0{\cdot}75$. More precise values of optimum column compositions ϕ_A^{opt} could be determined by calculation and tabulation of all K_R data at intervals of ϕ_A, the volume fraction which gives the largest difference (separation) between partition coefficients being that which offers the highest resolution. Manual data reduction with such a procedure becomes somewhat tedious for more than a few solutes but it can be computerized for up to fifty solutes with mixtures of three or more stationary phases (e.g. ref. 319).

The innovation offered by Laub and Purnell[329] was a development of a method of graphical representation of retention data which simplifies considerably the prediction of optimal mixtures of stationary phases. However, their techniques are based upon MP theory and in particular the diachoric solutions hypothesis. Thus, close inspection of the apparent success of their work will produce further and important insight of relevance to the veracity of the microscopic partition model of solutions.

First, these workers noted[327] that the parameter of fundamental and predominant interest in analytical glc, namely, the relative retention $\alpha_{i/j}$ of two solutes i and j, could according to equation (76) be cast in the form:

$$\alpha_{i/j} = \frac{K_{Ri}}{K_{Rj}} = \frac{\phi_A K_{R(A)i} + \phi_S K_{R(S)i}}{\phi_A K_{R(A)j} + \phi_S K_{R(S)j}}. \tag{128}$$

Separation of solutes therefore appears to be calculable as a function of ϕ_A from data pertaining only to the pure phases provided that, for each solute, K_R is linear in ϕ_A.

Laub and Purnell next constructed plots of α versus column composition such that α is maintained $\geqslant 1$ by inversion, where necessary, of the i/j assignment of identity of the solutes. Such a plot is illustrated in Fig. 15 where the

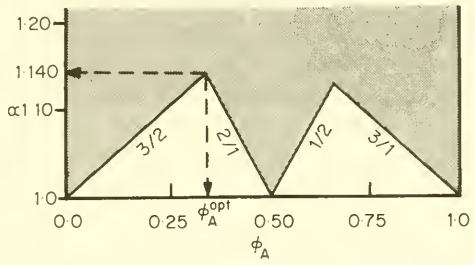

FIG. 15. Window diagram for three solutes of Fig. 14.

end-point of data of Fig. 14 have been used. Calculation is facilitated by recognizing that in practice only two values of α, 1·00 (impossible separation) and 1·10 (easy separation), need be considered. Equation (128) is therefore rearranged to:

$$\phi_A = \frac{K^0_{R(S)i} - \alpha_{i/j} K^0_{R(S)j}}{\alpha_{i/j} \Delta K^0_{Rj} - \Delta K^0_{Ri}} \tag{129}$$

where values of ϕ_A corresponding to the α-limits are calculated directly. Straight lines are then drawn between the points 1·10, 1·00 and 1·10 for each solute pair which, as shown in Fig. 15, produces a set of what appear to be inverted and partially overlapped triangles. Regions in which no overlaps occur amount to "windows" of separation which provide upon inspection additional quantitative information concerning the separation at hand. First, the optimum (A + S) stationary-phase blend is found from location of the highest window. In the present instance, the highest is marginally that at $\phi_A = 0{\cdot}348 = \phi_A^{opt}$. Secondly, the α-lines which form the sides of the window identify the two pairs of solutes which are the most difficult to

resolve at that column composition. Here the pairs 3/2 and 2/1 offer the greatest difficulty (lowest α) at ϕ_A^{opt}. Next, the height of the window yields the value of α of the most difficult pairs which in the present case is 1·140. Since the number of plates required to effect resolution of a given solute pair may be calculated from the relation:[328]

$$N_{req} = 36[\alpha/(\alpha - 1)]^2[(k' + 1)/k']^2 \qquad (130)$$

where the capacity factor, k', is defined as $(t_R - t_A)/t_A$, this value of α gives for $k' > 10$ (usually the case in packed-column glc) immediate assessment of the column efficiency necessary to perform the separation. Since, further, the analyst will have determined from earlier measurement of K_R^0 and in the course of practical experience the number of plates obtained per foot of column, the column length L_{req} which will baseline-resolve the most difficult solute pairs, hence the rest of the mixture as well, is specified. Finally, reference back to the "straight-line" diagram Fig. 14 allows deduction of the order of elution at the optimum (A + S) composition (here 2, 1, and 3 at $\phi_A^{opt} = 0{\cdot}348$). Thus, the window diagram procedure provides upon inspection: (a) the optimum stationary-phase composition for the separation at hand; (b) the pairs of solutes which offer the greatest difficulty at the chosen stationary-phase blend; (c) the value of α of the most difficult solute pairs; (d) the number of plates required to effect the separation; (e) the column length required to baseline-resolve the solute mixture; (f) the elution order.

Figure 16 shows the straight-line diagram[329] of a 30-component mixture with squalane and dinonyl phthalate at 100°C where it was *assumed* that K_R is a linear function of ϕ_A. This example is of complexity such that mere inspection of the plots yields little information concerning the separation. The window diagram in Fig. 17 shows immediately, however, that the optimum column composition occurs at $\phi_A = 0{\cdot}081$, at which point $\alpha = 1{\cdot}06$. Figure 18 presents the relevant chromatograms with columns of pure squalane (a), pure dinonyl phthalate (b), an intimate mixture of the phases such that $\phi_A = 0{\cdot}0807$ (c), and (d) a mechanical mixture of packings corresponding to ϕ_A of that in (c). Two full overlaps are seen in (a) while the pure dinonyl phthalate column (b) shows five pairs which are not resolved. Baseline resolution was found in the first run with each of the columns (c) and (d), and in accordance with MP theory these are identical.

Cursory assessment of the window diagram procedure, hence analytical aspects of the diachoric solutions hypothesis as embodied in equation (129), shows that the technique is highly successful when applied as in the cited examples[327,329] to *quantitative* prediction of optimum combinations of phases and other practical operating conditions which will effect a given separation; further, retention behaviour obtained with intimately mixed solvents appears to be identical to that observed with mechanically blended

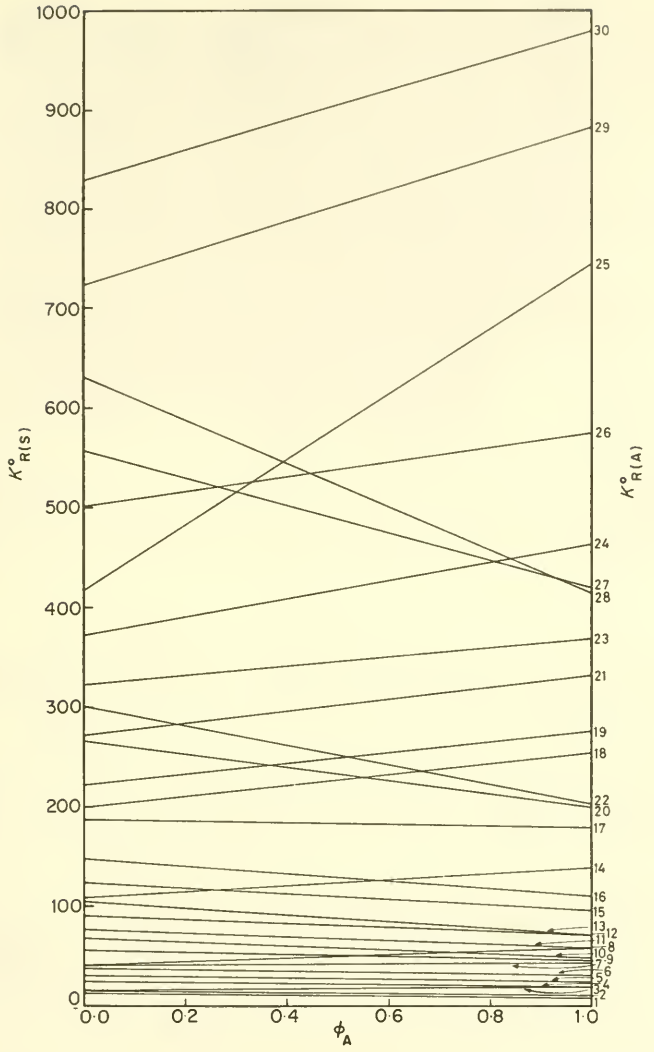

FIG. 16. Plots of K_R versus ϕ_A for hydrocarbon solutes with squalane and dinonyl phthalate at 100°C. [Reproduced with permission from R. J. Laub and J. H. Purnell, *Anal. Chem.*, 48, 799 (1976)]

packings. However, Ashworth and Hooker[240] showed via static measurement of activity coefficients that equation (83) was accurate to no better than ± 5 per cent. In addition, Laub, Martire, Purnell and their coworkers Harbison and Williams[238, 239] found that plots of K_R versus ϕ_A for aliphatic,

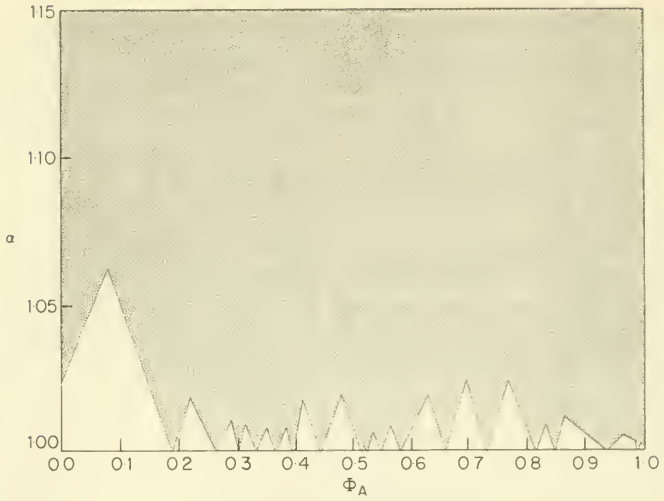

FIG. 17. Window diagram for solutes of Fig. 16. Best window is that at $\phi_A = 0{\cdot}0807$. [Reproduced with permission from R. J. Laub and J. H. Purnell, *Anal. Chem.*, **48**, 799 (1976)]

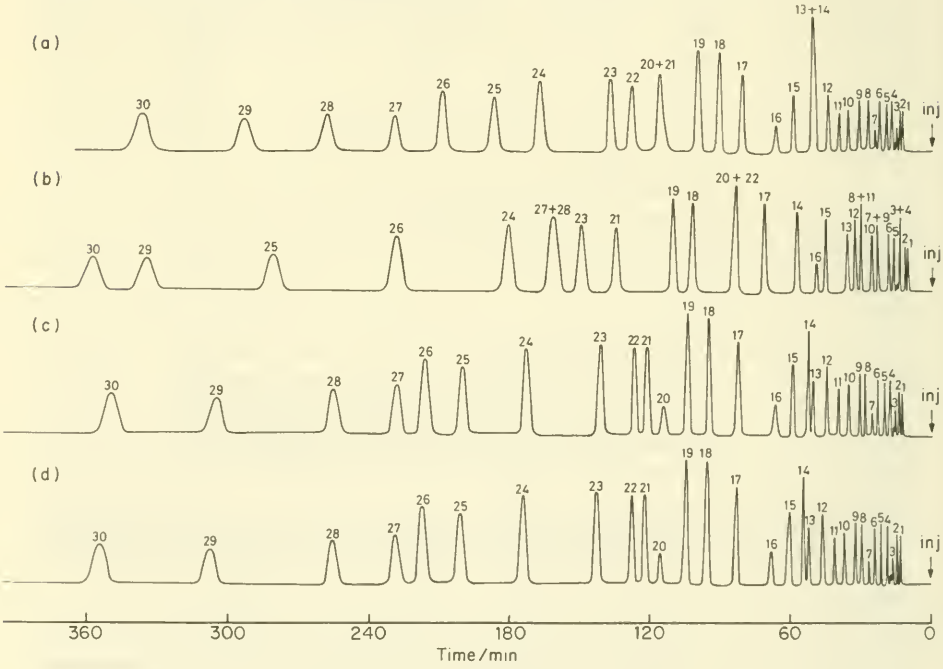

FIG. 18. Chromatograms of solutes of Fig. 16 with: (a) pure squalane, (b) pure dinonyl phthalate, (c) intimate mixture of phases such that $\phi_A = 0{\cdot}0807$, and (d) mechanical mixture of packings of (a) and (b) such that $\phi_A = 0{\cdot}0807$. [Reproduced with permission from R. J. Laub and J. H. Purnell, *Anal. Chem.*, **48**, 799 (1976)]

alicyclic, and aromatic hydrocarbons with squalane and dinonyl phthalate were curved over the temperature range 0–70°C as discussed in Section III. The apparent efficacy of the window diagram procedure of Laub and Purnell therefore seemed questionable, as also did the reported identity of retentions with mechanically and intimately mixed phases.

Laub and coworkers[238] carried out a comparative study by high-precision gas–liquid chromatography which was initiated in order to examine in detail these apparent anomalies; Table XXIV lists the solutes and respective K_R^0

TABLE XXIV. Partition coefficients[54, 238] of named solutes with squalane (S) and dinonyl phthalate (A) at 30°C employed for test of equation (128)

	$K^0_{R(S)}$	$K^0_{R(A)}$
1. n-Hexane	304·7	197·1
2. Benzene	433·2	666·9
3. Methylcyclohexane	1164	744·7
4. Toluene	1424	2069
5. n-Octane	2791	1685

data with squalane and with dinonyl phthalate at 30°C which were used in their work. The partition coefficients were taken from a previous investigation[54] in which agreement with static K_R data was found to within at worst ± 1 per cent. Using only these end-point K_R^0 values, linear (MP-predicted) plots of K_R versus ϕ_A were constructed as shown in Fig. 19. Also given are the actual glc and static K_R data obtained with intimate mixtures of squalane and dinonyl phthalate.

The window diagram constructed from equation (129) indicated that a composition of $\phi_A = 0{\cdot}270$ would resolve the mixture provided that the column yielded a number of plates sufficient to separate a pair of solutes with $\alpha = 1{\cdot}497$.

Figure 20 illustrates the chromatograms obtained with 3 ft $\times$ $\frac{1}{4}$ in columns where the flow rate ($\sim$400 ml min^{-1}) has been adjusted such that only 325 plates are obtained for each, that is, so that solutes of $\alpha = 1{\cdot}5$ would just be resolved. Chromatogram (a), that with pure squalane, shows two partial overlaps: solute 1 with 2 and solute 3 with 4. Chromatogram (b), pure dinonyl phthalate, also gives two overlaps and in addition solute 4 has eluted after solute 5, the reverse of that found in (a). Chromatogram (c) shows the results obtained with a mechanical mixture of pure-phase packings such that $\phi_A = 0{\cdot}270$ where all solutes have been baseline-resolved. The peak positions relative to toluene (no. 4) as predicted from the MP model are given as vertical lines. Chromatogram (d) was obtained with the packing of (c) after

it had been removed from the the column, slurried ("intimized") with dichloromethane, dried, and repacked. The predicted peak positions are again given as vertical lines. Table XXV gives the experimentally observed and MP-predicted K_R data for the solutes with the mechanically mixed packing (c). Also presented are the actual and predicted [equation (128)] α-values (toluene = 1·00). Table XXVI shows the data obtained for the solutes with the column containing the intimately mixed packing (d).

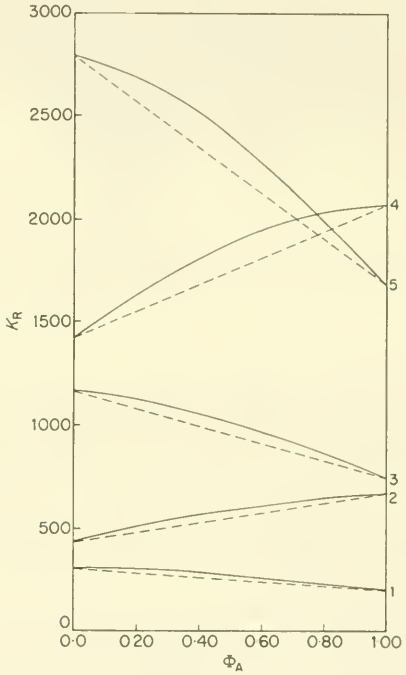

FIG. 19. Plots of K_R versus ϕ_A for solutes of Table XXIV with squalane and dinonyl phthalate stationary phases at 30°C. Dashed lines, MP-predicted; curves; experimental data with intimately mixed phases. After Laub and coworkers.[238]

There is no observable difference between chromatograms (c) and (d) irrespective of the fact that the former was obtained with a mechanical mixture of packings and the latter with intimately blended phases. This may at first be somewhat surprising in view of the curvature of the experimental K_R/ϕ_A data noted earlier for these systems. Close examination of Tables XXV and XXVI reveals, however, that equivalence of the chromatograms is expected *on the basis of relative retentions*. Consider first the partition coefficients of Table XXV. The actual and MP-predicted K_R values correspond to within ± 2 per cent and most likely to within a factor of 2 better

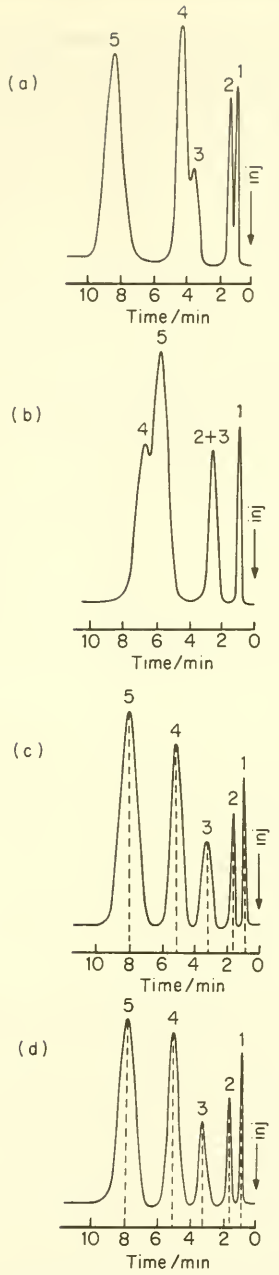

FIG. 20. Chromatograms of solutes of Table XXIV with (a) pure squalane, (b) pure dinonyl phthalate, (c) mechanical mixture of packings such that $\phi_A = 0{\cdot}270$, and (d) packing of (c) after treatment with dichloromethane, all at 30°C. After Laub and coworkers[238]

TABLE XXV. Experimental[238] and MP-predicted K_R and α values for solutes of Table XXIV with mechanically mixed packing of $\phi_A = 0.270$

Solute No.	K_R, act	K_R, MP-pred	α, act	α, MP-pred
1	270·4	275·7	0·17	0·17
2	490·1	496·3	0·30	0·31
3	1043	1051	0·65	0·66
4	1611	1598	(1·00)	(1·00)
5	2540	2493	1·58	1·56

TABLE XXVI. Experimental[238] and MP-predicted K_R and α values for solutes of Table XXIV with intimized packing of table XXV ($\phi_A = 0.270$)

Solute No.	K_R, act	K_R, MP-pred	α, act	α, MP-pred
1	287·0	275·7	0·17	0·17
2	515·5	496·3	0·30	0·31
3	1084	1051	0·64	0·66
4	1706	1598	(1·00)	(1·00)
5	2676	2493	1·57	1·56

than this since the high flow rate could not be measured with accuracy of better than about $\pm 1\frac{1}{2}$ per cent. In any event, the actual and MP-predicted values of α correspond precisely. The supposition that the diachoric solutions hypothesis strictly applies in the case of mechanically mixed packings therefore appears to be justified for these systems.

Turning now to the intimately mixed phase data of Table XXVI, a different picture emerges. Clearly, the experimental partition coefficients are larger than those expected on the basis of MP theory by on average 5 per cent. *However, the actual and MP-predicted α-values are nearly identical.* Thus, whatever curvature is extant in K_R/ϕ_A data with intimately blended phases appears in effect to have been divided out since the data were considered on a relative basis, as was also found by Melnikov and Aivazov for their results.[316,320] Furthermore, the experimental α-values obtained with the mixed-solvents packing correspond exactly to those found with the mixed-bed materials (Table XXV); chromatograms (c) and (d) of Fig. 20 are therefore identical as were those cited earlier for a wider range of solutes with squalane and dinonyl phthalate solvents at 100°C. Thus, the success of equation (129) with intimately mixed phases can be reconciled with the curvature observed in plots of K_R versus ϕ_A on the basis that relative retention data were used in analytical applications of the former.

Equation (129) must in any case be obeyed[221] by mechanically blended packings. Indeed, employment of such packings from a practical view facilitates considerably implementation of the window diagram procedure and hence quantitative prediction of parameters relating to a given separation.[329] Solute mixtures would first be run on each of several pure phases, well-characterized (as regards weight per cent liquid loadings) packings for which may be contained ready-made on a shelf. Measurement of partition coefficients of each of the solutes is facilitated if those of a standard solute have already been determined (alternatively, α-values and capacity factors may be used; cf. Section V.D). Next, straight-line plots of the K_R^0 data for all solutes with all possible pairs of stationary phases would be constructed [the number of combinations of pairs of solvents is $n!/2(n-2)!$]. Optimum column compositions for a given separation could then be predicted on a quantitative basis via the window diagram technique from data pertaining only to pure-solvent packings.

Since the calculations required are straightforward, the entire procedure may easily be computerized as shown by Laub, Purnell and Williams.[330] The logic is not as simple, however, as one might suppose since the algorithm must *inter alia* take into account the possibility of flat-topped windows. Nevertheless, application of their computer programs in analyses by glc showed that the limiting factor of the above optimization strategy amounted only to the turn-around time of their computer installation.

B. Extension to Multi-component Stationary Phases

According to MP theory, solute retention with multi-component stationary phases may be predicted from pure-component data via:

$$K_R = \sum_{i=1}^{n} \phi_i K_{R(i)}^0. \tag{131}$$

Laub and Purnell[329] found that this relation described the elution behaviour of several solutes with ternary stationary phases composed of squalane, dinonyl phthalate and dibutyl tetrachlorophthalate, irrespective of their constitution as intimately or mechanically mixed packings. It may be supposed that identity of the two column types can in this case be attributed, as above, to use of relative retention data. The *general* applicability of equation (131) is not of major consequence in analytical packed-column glc, however, and the relation must be obeyed by mechanically constituted multi-component stationary-phase mixtures which are in any case simpler to use than their intimately blended counterparts. As a result, Laub, Purnell and Williams[331] expanded their binary-solvent computer program to permit its

use with n-component stationary phases. They recognized, first, that volume compositions could for $n > 2$ be represented as lattice points on a multi-dimensional surface bounded by the condition $\Sigma\phi_i = 1$ such that location of the "highest" n-dimensional point of intersection of tie-lines (or surfaces) of α versus ϕ_i would pin-point the optimum column composition. For example, the ϕ-space for a three-component solvent system is an equilateral triangle above which tie-planes of α would produce pyramidal windows formed from intersection of three or more planes and/or the boundaries of the base. In practice this approach, while conceptually sound, was found to be difficult to apply even to three-component solvent mixtures owing primarily to problems associated with location of the highest point of intersection of planes. It was also found difficult to take into account the possibility that the optimum column composition might correspond to an n-dimensional plateau. As a result an alternative logic called DIACHOR was employed. K_R data and α-values were calculated from equation (131) at sequential intervals $\delta\phi_i$ of stationary phase compositions. The worst α-value, i.e. that corresponding to the most difficult solute pair, was located at each value of ϕ_i and compared with that obtained at the previous interval, the larger of the two values being retained. Upon completion of consideration of all possible compositions the final α retained is that of the most difficult solute pair at the optimum stationary-phase mixture. The choice of magnitude of the interval need be based only upon the computer time available to the user. In practice one of 0·02 or 0·03 was found to provide accuracy (2–3 per cent) sufficient for use with up to five solvents.

C. Extension to Solute Mixtures of Initially Unknown Content

Laub, Purnell and their coworkers had to this point shown that the diachoric solutions hypothesis [equation (76)] was obeyed for several intimately and mechanically mixed binary stationary phases, and that the generalized additivity principle of MP theory [equation (131] described retentions with at least one ternary mixed phase. Further, data manipulation was computerized such that optimum compositions of phases could be determined merely by programming pure-phase partition coefficients of each solute through the DIACHOR algorithm. Rarely, however, does an analyst have prior knowledge of the number of solutes in a given sample or in many cases its origin, let alone its history. The window diagram was therefore modified by Laub and Purnell[332] for use with samples of initially unknown content. As they emphasized, this application is of some importance in that it showed their technique to be capable of providing a quantitative basis for prediction of separations without requiring prior knowledge of the number or kind or, indeed, the identity of the sample constituents.

D. Use with Relative Retention Data

Measurement of partition coefficients is not often undertaken and, in fact, is usually considered to be an onerous task in analytical glc. This is due primarily to the supposition that considerable time and equipment are required for such measurements. In contrast to this somewhat specious view, Laub and coworkers[54] have shown that inexpensive and simple equipment and techniques can yield partition coefficients of accuracy better than ± 1 per cent (cf. Section I.E). Nevertheless, the vast majority of retention data have been reported as relative to some or other standard available to the analyst since α-values with a given stationary phase are calculable directly from raw retention and "dead" times, and to a first approximation are independent of flow rate, liquid loading and type of length of column. Laub, Purnell and coworkers[333] therefore recast their relations and procedures entirely in terms of α-values and capacity factors, and showed that the window diagram technique could be implemented solely with data of these kinds.

As Hildebrand and Reilley[231] pointed out, α-values alone are insufficient to construct straight-line type plots, since whatever (internal or external) standard to which solutes are related will in all probability not exhibit partition coefficients identical with dissimilar stationary phases. That is, in order to make use solely of relative retention data, the standard solute would have to be such that $K^0_{R(S)} = K^0_{R(A)}$, i.e. such that K_R versus ϕ_A is a horizontal line. While it is not inconceivable that solutes could be found which conform to this requirement, it nevertheless places an impractical constraint upon employment of the window diagram technique. An alternative and more general method was therefore required.

In terms of partition coefficients or specific retention volumes, the retentions of a solute with pure S and with pure A are related by:

$$K^0_{R(A)} = K^0_{R(S)}(k'_{(A)}/k'_{(S)})(V_S/V_A) \tag{132}$$

$$V^0_{g(A)} = V^0_{g(S)}(k'_{(A)}/k'_{(S)})(w_S/w_A) \tag{133}$$

where $k'_{(i)}$ is the solute capacity factor with a pure phase of volume V_i and weight w_i in the ith column, and where it has been assumed that each column has been constructed from the same size support and thus contains equivalent dead space per unit length. Equation (133) is the more practicable of these two relations since it requires information pertaining only to weight per cent liquid loadings and not [as equation (132)] densities. It will therefore be employed in what follows.

Consider now the use of equation (133) in calculation of the α-values of solute i relative to standard solute j with two pure phases A and S. That for

pure S is:

$$\alpha^0_{(S)i/j} = V^0_{g(S)i}/V^0_{g(S)j} = t'_{R(S)i}/t'_{R(S)j} \tag{134}$$

and that for pure A is:

$$\alpha^0_{(A)i/j} = V^0_{g(A)i}/V^0_{g(A)j} = t'_{R(A)i}/t'_{R(A)j}. \tag{135}$$

Equations (134) and (135) correctly order the retention of solute i with respect to solute j with the two pure phases. However, the *magnitude* of the $\alpha^0_{(A)}$ value will not be correct with respect to that for $\alpha^0_{(S)}$ unless, as noted above, $t'_{R(S)j}/t'_{R(A)j} = 1$. Straight-line plots in which $\alpha^0_{(S)}$ and $\alpha^0_{(A)}$ data are used as ordinate end-points hence will give an incorrect description of the variation of solute retention with column composition [here described in terms of the weight fraction of component A of the (A + S) binary phase]. This can be remedied by multiplying $\alpha^0_{(A)i/j}$ by the capacity factor ratio $k'_{(A)j}/k'_{(S)j}$ of the standard solute, which is given the symbol $\beta^0_{(A)}$:

$$\alpha^0_{(A)i/j} \cdot \beta^0_{(A)j} = \frac{t'_{R(A)i}}{t'_{R(A)j}} \cdot \frac{k'_{(A)j}}{k'_{(S)j}} = \frac{t'_{R(A)i}}{t'_{R(A)j}} \cdot \frac{t'_{R(A)j}}{t'_{R(S)j}}. \tag{136}$$

Equation (136) relates the retention of solute i with phase A to that obtained with phase S by what amounts in effect to definition of a hypothetical horizontal line extending across the straight-line diagram from $t'_{R(S)j}$, the standard. $\alpha^0_{(A)}\beta^0_{(A)}$ data are therefore correctly ordered with respect to $\alpha^0_{(S)}$ both in elution and in magnitude, and the diachoric solutions hypothesis may therefore be written as:

$$\alpha = w_S\alpha^0_{(S)} + w_A\alpha^0_{(A)}\beta^0_{(A)} \tag{137}$$

which is precisely equivalent to equation (133) and hence equation (76). Thus, straight-line plots and window diagrams may be constructed solely from α-values and capacity factors in terms of weight fractions from data pertaining only to pure stationary phases. Further, retentions with multicomponent packings must by analogy be described by the relation:

$$\alpha = w_S\alpha^0_{(S)} + \sum_{i=1}^{n} w_i\alpha^0_{(i)}\beta^0_{(i)} \tag{138}$$

and so the techniques and equations relating to ternary, quaternary.... mixed phases as described in Section IV.B. and in particular the DIACHOR algorithm, may also be used with data of these kinds.

One might suppose that analysis of mixtures of unknown content as mentioned in Section IV.C must also be amenable to the above relations. Laub and Purnell[334] showed that this was in fact the case and that the only additional refinement required was description of α-values at intermediate column compositions. These, they recognized, were ordered with respect

to elution and to magnitude by multiplication of intermediary α data by a factor β_{wA}, where:

$$\beta_{wA} = k'_{(wA)j}/k'_{(S)j} \tag{139}$$

that is, the ratio of the standard solute capacity factors with columns containing w_A amounts of A and S, and pure S.

The Laub–Purnell window diagram technique has been applied in the above form with complete success to analyses of what are generally considered to be "difficult" solutes with mixed packings comprising 2,4,7-trinitrofluorenone–SE-30 methylsilicone, with OV-17 methylphenylsilicone–polyethylene glycol 20M, and with methylsilicone–trifluoropropylsilicone stationary phases.[330, 333, 334] Use was made in these cases solely of α-values, capacity factors, and weight per cent packing compositions, and hence the techniques cited in this section find immediate and practicable utility at all levels of analytical gas–liquid chromatography.

E. Application to Gas–Solid and Gas–Liquid–Solid Chromatography

Since relative retentions appear to be additive in weight fraction of mechanically mixed phases, the relations discussed above must also apply to mixtures of gas–solid chromatographic (gsc) adsorbents. An example of the linearity present in such systems has been presented by Cadogan and Sawyer[179] as discussed earlier. Al-Thamir, Laub and Purnell[335] and others[336] have also shown that retention behaviour with mixtures of gas–liquid–solid (glsc) packings may be forecast in accordance with one or another form of equation (76).

F. Application to Liquid Chromatography

At this stage in the development of so-called "high-performance" liquid chromatography (HPLC), the general trend seems to be toward almost exclusive use of "reverse-phase" elution for non-ionic mixtures. This is due in part to the finding that, other than with regard to particle size, the type of solid support or adsorbent employed appears to be of little significance relative to multi-component mobile-phase compositional variations. Solutes are eluted therefore according to their solubility in the carrier fluid and are not retained selectively by the stationary phase.

Because in the case of HPLC carrier compressibility effects are negligible and in reverse-phase modes with deactivated supports C_L remains constant, equation (1) may be cast in the form:

$$C_M = \text{constant}/V_R. \tag{140}$$

The reciprocal of solute retention volumes will therefore vary with C_M, that is, with the mobile-phase concentration.

Scott and Kucera[337] were the first to show that equation (140) was obeyed over selected ranges of mobile-phase concentrations for a range of solutes and mixed carrier liquids. The Laub–Purnell window diagram technique is therefore applicable and has in fact been used recently by Deming and Turoff[338] for optimization of mobile-phase pH for the separation of several aromatic acids. It can be expected that the techniques and procedures of Sections IV.A–D will thus become of some importance in future analytical applications of liquid chromatography.

G. Application to Other System Variables

The foregoing examples have established that the procedures and relations developed in accordance with the diachoric solutions hypothesis find application in optimization of parameters relating to column composition. It is apparent at this point that in fact the method may be applied to quantitative preselection of other operational variables of chromatographic systems; indeed, the basic approach advocated by Laub and Purnell is such that it should find utility in *any* area of analytical chemistry wherein separations can be described as a function of one or more parameters of the technique under consideration.

1. The Column Temperature

Plots of log(retention) versus reciprocal absolute temperature are with few exceptions linear over extended ranges in chromatography. Occasionally, mixed sorption phenomena result in solute overlaps at one or more temperatures. Improved resolution may be obtained in such cases by decreasing *or increasing T*. For example, Laub and Purnell[339] considered plots[340] of $\log t'_R$ versus $1/T$ for n-alkane and benzene solutes with *N*,*N*-di-(2-cyanoethyl)formamide over the range 40–180°C. Benzene could not be separated from n-dodecane at the lower limit or from n-octadecane at the higher end of the temperature scale with this phase. At intermediate temperatures, further, it overlapped with n-tetradecane and with n-hexadecane. As was shown,[339] this was a situation in which quantitative selection of operating temperature could be made by reference to a window diagram.

Few studies have been reported of temperature effects in HPLC; a notable exception is that recently presented by Kraak, Jonker and Huber.[341] These workers eluted amino acids from a column of C_8-bonded silica with a buffered aqueous mobile phase over the temperature range 20–50°C. Their data are shown plotted[339] in Fig. 21 as $\log k'$ versus $1/T$ over a range which has been extended beyond the limits considered originally. The window

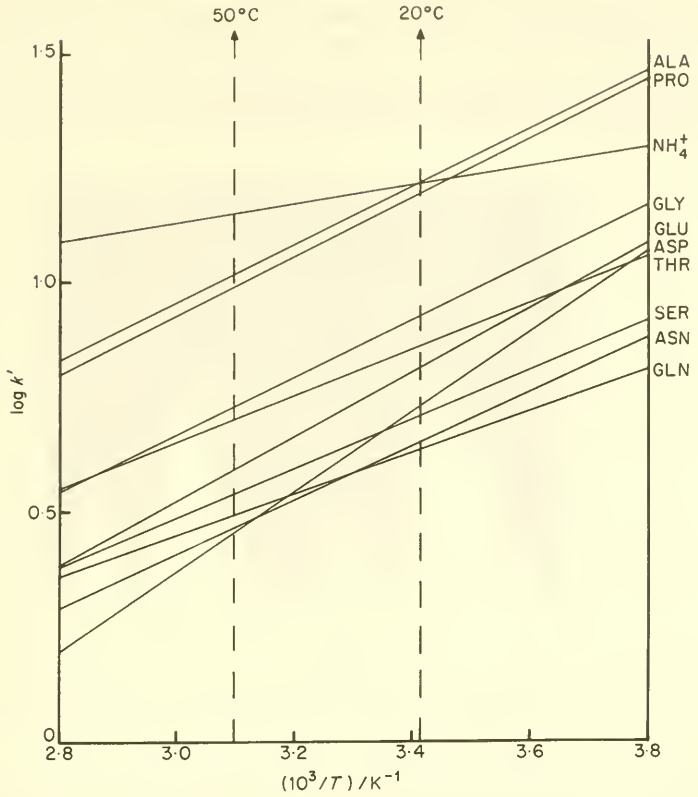

FIG. 21. Plots of $\log k'$ versus $10^3/T$ for the indicated amino-acids and NH_4^+ with a buffered mobile phase (nominal pH = 2·60) and C_8-bonded silica column packing. HPLC data of Huber and coworkers.[341] [Reproduced with permission from R. J. Laub and J. H. Purnell, *J. Chromatogr.*, **161**, 49 (1978)]

diagram is given in Fig. 22, where, in fact, two more or less equally good values of α (1·058 at 55°C and 1·054 at 15°C) are found outside the temperatures used in the original study. Since the α-values and analysis times are roughly comparable, choice of the appropriate window may be made on the basis of practical convenience which in this case specifies that at 15°C.

2. The Column Pressure

It was early established[342–344] in glc that the use of different carriers may alter elution times. In rare cases these (virial) effects can cause reversals in retention order.[345] Situations in which compositional optimization of binary carriers might play an important role in separations can therefore

be visualized. Consider the case in which a separation is so complex that even after column and stationary-phase optimization the most difficult solute pair still corresponds to $\alpha = 1{\cdot}01$. A mere 2 per cent increase to 1·03 will reduce the column length required for resolution by a factor of 10.

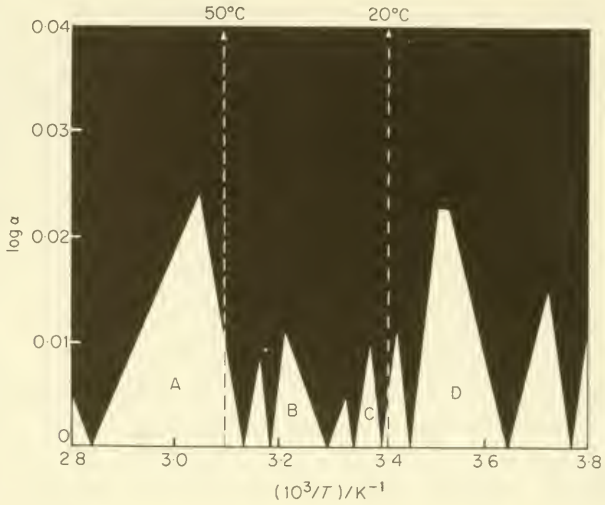

FIG. 22. Window diagram for data of Fig. 21. [Reproduced with permission from R. J. Laub and J. H. Purnell, *J. Chromatogr.*, **161**, 49 (1978)]

Studies of optimization of virial effects with regard to resolution have yet to be reported but are likely to be useful as a kind of "fine tuning". The Laub–Purnell window diagram technique is, of course, well suited to such studies, and as more data become available it should prove of considerable utility in quantitative development of this method of enhancement of separations.

REFERENCES

1. A. Purer and R. L. Kaplan, *J. Chromatogr. Sci.*, **9**, 59 (1971).
2. J. W. Barrett, *U.S. Patent* 3,237,380 (1966).
3. A. J. P. Martin and A. T. James, *Biochem. J.*, **50**, 679 (1952).
4. A. T. James, *Biochem. J.*, **52**, 242 (1952).
5. F. R. Cropper and A. Heywood, *Nature*, **172**, 1101 (1953); **174**, 1063 (1954).
6. D. H. James and C. S. G. Phillips, *J. Chem. Soc.*, 1600 (1953); 1066 (1954).
7. J. H. Griffiths and C. S. G. Phillips, *J. Chem. Soc.*, 3446 (1954).
8. N. H. Ray, *J. Appl. Chem.*, **4**, 21 (1954).
9. G. J. Pierotti, C. H. Deal, E. L. Derr and P. E. Porter, *J. Amer. Chem. Soc.*, **78**, 2989 (1956).

10. P. E. Porter, C. H. Deal and F. H. Stross, *J. Amer. Chem. Soc.*, **78**, 2999 (1956).
11. G. Dijkstra, J. G. Keppler and J. A. Schols, *Rec. Trav. Chim. Pays-Bas*, **74**, 805 (1955).
12. A. B. Littlewood, C. S. G. Phillips and D. T. Price, *J. Chem. Soc.*, 1480 (1955).
13. M. R. Hoare and J. H. Purnell, *Research*, **8**, S41 (1955); *Trans. Faraday Soc.*, **52**, 222 (1956).
14. R. L. Laub and R. L. Pecsok, "Physico-Chemical Applications of Gas Chromatography", Wiley-Interscience, New York (1978).
15. R. A. Keller, G. H. Stewart and J. C. Giddings, *Ann. Rev. Phys. Chem.*, **11**, 347 (1960).
16. J. H. Purnell, *Endeavour*, **23**, 142 (1964); *Ann. Rev. Phys. Chem.*, **18**, 81 (1967).
17. D. E. Martire and L. Z. Pollara, *Adv. Chromatogr.*, **1**, 335 (1965).
18. J. C. Giddings and K. L. Mallik, *Ind. Eng. Chem.*, **59**(4), 18 (1967).
19. R. Kobayashi and H. A. Deans, *Ind. Eng. Chem.*, **59**(5), 11 (1967).
20. R. Kobayashi, P. S. Chappelear and H. A. Deans, *Ind. Eng. Chem.*, **59**(10), 63 (1967).
21. J. R. Conder, *Adv. Anal. Chem. Instrum.*, **6**, 209 (1968); *Chromatographia*, **7**, 387 (1974).
22. S. Trestianu, *Rev. Chim.*, **19**, 709 (1968).
23. C. L. Young, *Chromatogr. Rev.*, **10**, 129 (1968).
24. M. S. Vigdergauz and R. I. Izmailov, "The Application of Gas Chromatography in the Physico-Chemical Characterization of Substances", Nauka, Moscow (1970).
25. A. N. Korol, *Usp. Khim.*, **41**, 321 (1972).
26. A. V. Kiselev, A. V. Iogansen, K. I. Sakodynskii, V. M. Sakharov, Y. I. Yashin, A. P. Karnaukhov, N. Y. Buyanova and G. A. Karkchi, "Physico-Chemical Applications of Gas Chromatography", Khimiya, Moscow (1973).
27. D. C. Locke, *Am. Lab.*, **7**(5), 17 (1975); *Adv. Chromatogr.*, **14**, 87 (1976).
28. K. L. Mallik, "An Introduction to Nonanalytical Applications of Gas Chromatography", Peacock Press, New Delhi (1976).
29. P. Valentin and G. Guiochon, *Sep. Sci.*, **10**, 245, 271, 289 (1975).
30. V. Rezl, B. Kaplanova and J. Janak, *Anal. Chem.*, **47**, 159 (1975).
31. J. R. Conder, *Anal. Chem.*, **48**, 917 (1976).
32. J. F. Parcher and T. N. Westlake, *J. Phys. Chem.*, **81**, 307 (1977).
33. A. Kwantes and G. W. A. Rijnders, in "Gas Chromatography 1958", ed. D. H. Desty, Butterworths, London (1958), p. 125.
34. J. Novak and J. Janak, *Anal. Chem.*, **38**, 265 (1966).
35. R. E. Pecsar and J. J. Martin, *Anal. Chem.*, **38**, 1661 (1966).
36. S. P. Wasik and W. Tsang, *J. Phys. Chem.*, **74**, 2970 (1970); *Anal. Chem.*, **42**, 1648 (1970).
37. A. Hartkopf and B. L. Karger, *Accounts Chem. Res.*, **6**, 209 (1973).
38. P. H. Weiner, H.-L. Liao and B. L. Karger, *Anal. Chem.*, **47**, 288 (1974).
39. S. A. Green, *J. Chem. Educ.*, **34**, 194 (1957).
40. G. K. Ashbury, A. J. Davies and J. W. Drinkwater, *Anal. Chem.*, **29**, 918 (1957).
41. J. N. Roper, Jr., *Anal. Chem.*, **32**, 447 (1960).
42. J. H. Purnell, "Gas Chromatography", Wiley, New York (1962), pp. 255–260.
43. F. Sicilio, H. Bull, R. C. Palmer and J. A. Knight, *J. Chem. Educ.*, **28**, 194 (1964).
44. J. M. Miller, *J. Chem. Educ.*, **47**, 306 (1970).
45. J. E. Oberholtzer and L. B. Rogers, *Anal. Chem.*, **41**, 1234 (1969).
46. R. S. Swingle and L. B. Rogers, *Anal. Chem.*, **43**, 810 (1971).

47. R. A. Culp, C. H. Lockmüller, A. K. Moreland, R. S. Swingle and L. B. Rogers, *J. Chromatogr. Sci.*, **9**, 6 (1971).
48. L. Premru and M. Kremser, *J. Chromatogr.*, **51**, 65 (1970).
49. J. F. Parcher, P. H. Weiner, C. L. Hussey and T. N. Westlake, *J. Chem. Eng. Data*, **20**, 145 (1975).
50. O. Wicarova, J. Novak and J. Janak, *J. Chromatogr.*, **51**, 3 (1970).
51. M. Goedert and G. Guiochon, *J. Chromatogr. Sci.*, **7**, 323 (1969); *Anal. Chem.*, **42**, 962 (1970); **45**, 1180, 1188 (1973).
52. J. A. Rijks and C. A. Cramers, *Chromatographia*, **7**, 99 (1974).
53. R. J. Laub, D. E. Martire and J. H. Purnell, *J. Chem. Soc. Faraday Trans. II*, **74**, 213 (1978).
54. R. J. Laub, J. H. Purnell, P. S. Williams, M. W. P. Harbison and D. E. Martire, *J. Chromatogr.*, **155**, 233 (1978).
55. L. Mikkelsen, *J. Gas Chromatogr.*, **5**, 601 (1967).
56. D. R. Deans, in "Gas Chromatography 1968", ed. C. L. A. Harbourn, Institute of Petroleum, London (1969). p. 447.
57. D. H. James and C. S. G. Phillips, *J. Sci. Instrum.*, **29**, 362 (1952).
58. J. H. Knox, *Chem. Ind.*, 1085 (1959).
59. H. W. Habgood and W. E. Harris, *Anal. Chem.*, **32**, 450 (1960).
60. O. Knapp and M. Lochner, *Chromatographia*, **3**, 378 (1970).
61. B. E. Bowen, S. P. Cram, J. E. Leitner and R. L. Wade, *Anal. Chem.*, **45**, 2185 (1973).
62. A. Levy, *J. Sci. Instrum.*, **41**, 449 (1964).
63. M. van Swaay, *J. Chromatogr.*, **12**, 99 (1963).
64. G. W. Munns, Jr and J. V. Frilette, *J. Gas Chromatogr.*, **3**, 145 (1965).
65. J. J. Czubryt and H. D. Gesser, *J. Gas Chromatogr.*, **6**, 528 (1968).
66. R. G. Thurman and M. F. Burke, *J. Chromatogr. Sci.*, **9**, 181 (1971).
67. Y. Hori and R. Kobayashi, *Bull. Chem. Soc. Japan*, **47**, 1791 (1974).
68. J. A. Jonsson, *J. Chromatogr.*, **111**, 271 (1975).
69. D. W. Carle, in "Gas Chromatography", eds. V. J. Coates, H. J. Noebels and I. S. Fagerson, Academic Press, New York (1958), p. 67.
70. B. O. Ayres, in "Gas Chromatography", eds. V. J. Coates, H. J. Noebels and I. S. Fagerson, Academic Press, New York (1958), p. 93.
71. D. A. Forss, M. L. Bazinet and S. M. Swift, *J. Gas Chromatogr.*, **2**, 134 (1964).
72. C. H. Hamilton, in "Instrumentation in Gas Chromatography", eds. J. Krugers, Centrex, Eindhoven (1968), p. 33.
73. R. D. Condon and L. S. Ettre, in "Instrumentation in Gas Chromatography", ed. J. Krugers, Centrex, Eindhoven (1968), p. 87.
74. H. Abegg, *J. Chromatogr.*, **9**, 519 (1962).
75. M. Ellison, *Analyst*, **93**, 264 (1968).
76. P. Pitt, *Chromatographia*, **1**, 252 (1968).
77. L. J. Lorenz, R. A. Culp and R. T. Dixon, *Anal. Chem.*, **42**, 1119 (1970).
78. T. H. Glenn and S. P. Cram, *J. Chromatogr. Sci.*, **8**, 46 (1970).
79. H. D. Axelrod, R. J. Teck, J. P. Lodge and R. H. Allen, *Anal. Chem.*, **43**, 496 (1971).
80. R. L. Wade and S. P. Cram, *Anal. Chem.*, **44**, 131 (1972).
81. F. Bruner, A. Liberti, M. Possanzini and I. Allegrini, *Anal. Chem.*, **44**, 2070 (1972).
82. F. Bruner, C. Canulli and M. Possanzini, *Anal. Chem.*, **45**, 1790 (1973).
83. B. E. Bowen and S. P. Cram, *J. Chromatogr. Sci.*, **12**, 579 (1974).

84. G. Schomburg, R. Dielman, H. Husmann and F. Weeke, *J. Chromatogr.*, **122**, 55 (1976).
85. G. Schomburg, H. Behlau, R. Dielmann, F. Weeke and H. Husmann, *J. Chromatogr.*, **142**, 87 (1977).
86. V. V. Brazhnikov, "Differential Detectors for Gas Chromatography", Nauka, Moscow (1974).
87. D. J. David, "Gas Chromatographic Detectors", Wiley-Interscience, New York (1974).
88. J. Sevcik, "Detectors in Gas Chromatography", Elsevier, Amsterdam (1976).
89. R. Kieselbach, *Anal. Chem.*, **35**, 1342 (1963).
90. I. G. McWilliam and H. C. Bolton, *Anal. Chem.*, **41**, 1755 (1969).
91. D. A. Leathard, *Adv. Anal. Chem. Instrum.*, **11**, 29 (1973).
92. S. P. Cram and J. E. Leitner, in "Computers in Chemical and Biochemical Research", eds. C. E. Klopfenstein and C. L. Wilkins, Academic Press, New York (1974) p. 235.
93. D. H. Everett and C. T. H. Stoddart, *Trans. Faraday Soc.*, **57**, 746 (1961).
94. A. J. B. Cruickshank and D. H. Everett, *J. Chromatogr.*, **11**, 289 (1963).
95. A. J. B. Cruickshank, D. H. Everett and M. T. Westaway, *Trans. Faraday Soc.*, **61**, 235 (1965).
96. S. Dal Nogare and R. S. Juvet, Jr., "Gas–Liquid Chromatography", Interscience, New York (1962), p. 168.
97. L. S. Ettre, *J. Chromatogr.*, **11**, 267 (1963).
98. A. J. B. Cruickshank, M. L. Windsor and C. L. Young, *Proc. Roy. Soc.* **A295**, 259, 271 (1966).
99. A. J. Ashworth and D. H. Everett, *Trans. Faraday Soc.*, **56**, 1609 (1960).
100. G. F. Freeguard and R. Stock, in "Gas Chromatography 1962", ed. M. van Swaay, Butterworths, London (1962), p. 102.
101. M. L. McGlashan and D. J. B. Potter, *Proc. Roy. Soc.*, **A267**, 478 (1962).
102. J. A. Beattie and O. C. Bridgeman, *J. Amer. Chem. Soc.*, **49**, 1665 (1927).
103. P. Y. Feng and M. Melzer, *J. Chem. Educ.*, **49**, 375 (1972).
104. R. B. Spertell and G. T. Chang, *J. Chromatogr. Sci.*, **10**, 60 (1972).
105. M. L. Windsor and C. L. Young, *J. Chromatogr.*, **27**, 355 (1967).
106. D. H. Everett, *Trans. Faraday Soc.*, **61**, 1637 (1965).
107. L. G. Hepler, J. M. Stokes and R. H. Stokes, *Trans. Faraday Soc.*, **61**, 20 (1965).
108. E. M. Dantzler, C. M. Knobler and M. L. Windsor, *J. Chromatogr.*, **32**, 433 (1968).
109. R. L. Martin, *Anal. Chem.*, **33**, 347 (1961); **35**, 116 (1963).
110. R. L. Pecsok, A. deYllana and A. Abdul-Karim, *Anal. Chem.*, **36**, 452 (1964).
111. D. E. Martire, R. L. Pecsok and J. H. Purnell, *Nature*, **203**, 1279 (1964); *Trans. Faraday Soc.*, **61**, 2496 (1965).
112. J. R. Conder, D. C. Locke and J. H. Purnell, *J. Phys. Chem.*, **73**, 700 (1969).
113. J. F. Smith, *Nature*, **193**, 679 (1962).
114. H. Gold, *Anal. Chem.*, **34**, 174 (1962).
115. S. Masukawa and R. Kobayashi, *J. Gas Chromatogr.*, **6**, 257 (1968).
116. R. E. Kaiser, *Chromatographia*, **2**, 215 (1969).
117. B. Versino, *Chromatographia*, **3**, 231 (1970).
118. C. A. Cramers, J. A. Luyton and J. A. Rijks, *Chromatographia*, **3**, 441 (1970).
119. M. Riedmann, *Chromatographia*, **7**, 59 (1974).
120. S. Ebel and R. E. Kaiser, *Chromatographia*, **7**, 696 (1974).
121. F. Riedo, D. Fritz, G. Tarjan and E. sz. Kovats, *J. Chromatogr.*, **126**, 63 (1976).

122. D. E. Martire and P. Riedl, *J. Phys. Chem.*, **72**, 3478 (1968).
123. N. D. Petsev, R. N. Nikolov and A. Kostova, *J. Chromatogr.*, **93**, 369 (1974).
124. N. D. Petsev, V. H. Petkov and Chr. Dimitrov, *J. Chromatogr.*, **114**, 204 (1975).
125. R. N. Nikolov, N. D. Petsev and A. D. Stefanova, *Chromatographia*, **9**, 81 (1976).
126. R. A. Orwoll and P. J. Flory, *J. Amer. Chem. Soc.*, **89**, 6814 (1967).
127. R. J. Laub and R. L. Pecsok, *Anal. Chem.*, **46**, 2251 (1974).
128. Y. A. Kanchencko, V. G. Berezkin, A. Y. Mysak and L. P. Paskal, *Zavod. Lab.*, **40**, 1450 (1974).
129. D. F. Folland, *Instrum. Control Syst.*, **41**, 97 (1968).
130. H. D. Young, "Statistical Treatment of Experimental Data", McGraw-Hill, New York (1962), Ch. IV.
131. J. R. Anderson and K. H. Napier, *Austl. J. Chem.*, **10**, 250 (1957).
132. Y. B. Tewari, D. E. Martire and J. P. Sheridan, *J. Phys. Chem.*, **74**, 2345 (1970).
133. E. C. Pease and S. Thorburn, *J. Chromatogr.*, **30**, 344 (1967).
134. A. J. Ashworth, *J. Chem. Soc. Faraday Trans. I*, **69**, 459 (1973).
135. B. W. Bradford, D. Harvey and D. E. Chalkley, *J. Inst. Petrol.*, **41**, 375 (1955).
136. C. A. Wellington, *Adv. Anal. Chem. Instrum.*, **11**, 237 (1973).
137. C. L. deLigny, *Adv. Chromatogr.*, **14**, 265 (1976).
138. S. H. Langer, C. Zahn and G. Pantazoplos, *J. Chromatogr.*, **3**, 154 (1960).
139. J. H. Purnell, S. P. Wasik and R. S. Juvet, Jr., *Acta Chim. Acad. Sci. Hung.*, **50**, 201 (1966).
140. C. Bighi, A. Betti and F. Dondi, *J. Chromatogr.*, **39**, 125 (1969).
141. O. K. Guha and J. Janak, *J. Chromatogr.*, **68**, 325 (1972).
142. B. Feibush, M. F. Richardson, R. E. Sievers and C. S. Springer, *J. Amer. Chem. Soc.*, **94**, 6717 (1972).
143 J. J. Brooks and R. E. Sievers, *J. Chromatogr. Sci.*, **11**, 303 (1973).
144. M. Kraitr, R. Komers and F. Cuta, *J. Chromatogr.*, **86**, 1 (1973); *Anal. Chem.*, **46**, 974 (1974).
145. E. Gil-Av and V. Schurig, *Anal. Chem.*, **43**, 2030 (1971).
146. V. Schurig, J. L. Bear and A. Zlatkis, *Chromatographia*, **5**, 301 (1972).
147. F. Mikes, V. Schurig and E. Gil-Av, *J. Chromatogr.*, **83**, 91 (1973).
148. A. G. Vitenberg, B. V. Ioffe, Z. St. Dimitrova and T. P. Strukova, *J. Chromatogr.*, **126**, 205 (1976).
149. C. L. deLigny, T. van't Verlaat and F. Karthaus, *J. Chromatogr.*, **76**, 115 (1973).
150. E. Gil-Av and J. Herling, *J. Phys. Chem.*, **66**, 1208 (1962).
151. M. Kroll, *J. Amer. Chem. Soc.*, **90**, 1101 (1968).
152. J. Homer, M. H. Everdell, C. J. Jackson and P. M. Whitney, *J. Chem. Soc. Faraday Trans. II*, **68**, 874 (1972).
153. T. F. Hunter, N. C. Cutvers, K. M. Mitchinson, G. N. Rowley and M. Stillman, *Spectrochim. Acta*, **27A**, 1207 (1971).
154. M. Tamres, in "Molecular Complexes", Vol. 1, ed. R. Foster, Elek Science, London (1974), Ch. 3.
155. R. S. Mulliken and W. B. Person, "Molecular Complexes", Wiley-Interscience, New York (1969), p. 92.
156. H.-L. Liao and D. E. Martire, *Anal. Chem.*, **44**, 498 (1972); *J. Amer. Chem. Soc.*, **96**, 2058 (1974).
157. D. F. Cadogan and J. H. Purnell, *J. Phys. Chem.*, **73**, 3489 (1969).
158. R. L. Pecsok and B. H. Gump, *J. Phys. Chem.*, **71**, 2202 (1967).
159. D. L. Meen, F. Morris and J. H. Purnell, *J. Chromatogr. Sci.*, **9**, 281 (1971).
160. C. W. P. Crowne, M. F. Harper and P. G. Farrell, *J. Chromatogr.*, **61**, 7 (1971).

161. S. H. Langer and J. H. Purnell, *J. Phys. Chem.*, **70**, 964 (1966).
162. M. A. Muhs and F. T. Weiss, *J. Amer. Chem. Soc.*, **84**, 4697 (1962).
163. R. J. Cvetanovic, F. T. Duncan, W. E. Falconer and R. S. Irwin, *J. Amer. Chem. Soc.*, **87**, 1827 (1965).
164. H. Schnecko, *Anal. Chem.*, **40**, 1391 (1968).
165. R. Queignec and B. Wojtkowiak, *Bull. Soc. Chim. France*, 3829 (1970).
166. J. H. Purnell and O. P. Srivastava, *Anal. Chem.*, **45**, 1111 (1973).
167. C. Eon, C. Pommier and G. Guiochon, *J. Phys. Chem.*, **75**, 2632 (1971).
168. C. Eon and B. L. Karger, *J. Chromatogr. Sci.*, **10**, 140 (1972).
169. R. C. Castells, *Chromatographia*, **6**, 57 (1973).
170. L. Mathiasson and R. Jonsson, *J. Chromatogr.*, **101**, 339 (1974).
171. J. P. Sheridan, D. E. Martire and Y. B. Tewari, *J. Amer. Chem. Soc.*, **94**, 3294 (1972).
172. H.-L. Liao, D. E. Martire and J. P. Sheridan, *Anal. Chem.*, **45**, 2087 (1973).
173. J. P. Sheridan, D. E. Martire and F. P. Banda, *J. Amer. Chem. Soc.*, **95**, 4788 (1973).
174. C. S. Chamberlain and R. S. Drago, *J. Amer. Chem. Soc.*, **98**, 6142 (1976).
175. V. Schurig, R. C. Chang, A. Zlatkis and B. Feibush, *J. Chromatogr.*, **99**, 147 (1974).
176. C. L. deLigny, N. J. Koole, H. D. Nelson and G. H. E. Nieudorp, *J. Chromatogr.*, **114**, 63 (1975).
177. G. E. Baiulescu and V. A. Ilie, *Anal. Chem.*, **46**, 1847 (1974).
178. S. H. Langer, B. M. Johnson and J. R. Conder, *J. Phys. Chem.*, **72**, 4020 (1968).
179. D. F. Cadogan and D. T. Sawyer, *Anal. Chem.*, **43**, 941 (1971).
180. R. S. Juvet, Jr. and F. M. Wachi, *Anal. Chem.*, **32**, 290 (1960).
181. R. S. Juvet, Jr., V. R. Shaw and M. A. Khan, *J. Amer. Chem. Soc.*, **91**, 3788 (1969).
182. D. E. Martire, J. P. Sheridan, J. W. King and S. E. O'Donnell, *J. Amer. Chem. Soc.*, **98**, 3101 (1976).
183. C. Eon and G. Guiochon, *Anal. Chem.*, **46**, 1393 (1974).
184. D. E. Martire, *Anal. Chem.*, **48**, 398 (1976).
185. L. E. Orgel and R. S. Mulliken, *J. Amer. Chem. Soc.*, **79**, 4839 (1957).
186. D. E. Martire, *Anal. Chem.*, **46**, 626 (1974).
187. D. E. Martire, *Anal. Chem.*, **46**, 1712 (1974).
188. G. M. Janini, J. M. King and D. E. Martire, *J. Amer. Chem. Soc.*, **96**, 5368 (1974).
189. C. J. Creswell and A. L. Allred, *J. Amer. Chem. Soc.*, **85**, 1723 (1963).
190. K. W. Jolley, L. M. Hughes and I. D. Watson, *Austl. J. Chem.*, **27**, 287 (1974).
191. C. J. Creswell and A. L. Allred, *J. Phys. Chem.*, **66**, 1469 (1962).
192. D. Patterson, Y. B. Tewari and H. P. Schreiber, *J. Chem. Soc. Faraday Trans. II*, **68**, 885 (1972).
193. G. M. Janini and D. E. Martire, *J. Phys. Chem.*, **78**, 1644 (1974).
194. T. Czajkowska and A. Waksmundzki, *J. Chromatogr.*, **119**, 91 (1976).
195. A. Janik, *Chromatographia*, **6**, 514 (1973).
196. R. K. Kurchal, K. L. Mallik and P. L. Gupta, *Can. J. Chem.*, **55**, 1273 (1977).
197. S. A. Reznikov, R. I. Sidorov and E. R. Veber, *Zh. Fiz. Khim.*, **49**, 356 (1975).
198. S. A. Reznikov and R. I. Sidorov, *Zh. Fiz. Khim.*, **49**, 376 (1975).
199. S. A. Reznikov, Yu. A. Batyrev and R. I. Sidorov, *Zh. Fiz. Khim.*, **49**, 440 (1975).
200. J. H. Purnell, in "Gas Chromatography 1966", ed. A. B. Littlewood, Institute of Petroleum, London (1967), p. 3.
201. R. J. Laub and R. L. Pecsok, *Anal. Chem.*, **46**, 1214 (1974).
202. R. J. Laub, V. Ramamurthy and R. L. Pecsok, *Anal. Chem.*, **46**, 1659 (1974).

203. R. J. Laub and J. H. Purnell, *J. Amer. Chem. Soc.*, **98**, 30 (1976).
204. C. Eon, C. Pommier and G. Guiochon, *C.R. Acad. Sci.*, **270**, 1436 (1970); **276**, 1337 (1973); *Chromatographia*, **4**, 235, 241 (1971).
205. R. J. Laub, D. L. Meen and J. H. Purnell, unpublished work.
206. R. J. Laub and R. L. Pecsok, *J. Chromatogr.*, **113**, 47 (1975).
207. R. Foster, in "Molecular Complexes", Vol. 2, ed. R. Foster, Elek Science, London (1974), Ch. 3.
208. R. S. Drago, R. L. Carlson, N. J. Rose and D. A. Wenz, *J. Amer. Chem. Soc.*, **83**, 3572 (1961).
209. J. H. Purnell and J. M. Vargas de Andrade, *J. Amer. Chem. Soc.*, **97**, 3585 (1975).
210. M. wa. Muanda, J. B. Nagy and O. B. Nagy, *Tetrahedron Lett.*, 3421 (1974); *J. Chem. Soc. Faraday Trans. 1*, **74**, 2210 (1978).
211. C. L. Young, *J. Chromatogr. Sci.*, **8**, 103 (1970).
212. J. C. Touchstone, A. Nikolski and T. Murawec, *Federation Proc.*, **24**(2), Pt. 1, 534 (1965).
213. J. C. Touchstone, C.-H. Wu, A. Nikolski and T. Murawec, *J. Chromatogr.*, **29**, 235 (1967).
214. J. C. Touchstone, T. Murawec and A. Nikolski, *J. Chromatogr. Sci.*, **8**, 221 (1970).
215. J. C. Touchstone and T. Murawec, *J. Chromatogr. Sci.*, **9**, 446 (1971).
216. J. H. Purnell and J. M. Vargas de Andrade, *J. Amer. Chem. Soc.*, **97**, 3590 (1975).
217. H. Niederstrass, Dr. Rer. Nat., Braunschweig (1975).
218. J.-M. Braun and J. E. Guillet, *Adv. Polymer Sci.*, **21**, 107 (1976).
219. J. Klein and H. Widdecke, *J. Chromatogr.*, in press.
220. V. I. Pakhomova and M. S. Vigdergauz, *Izv. Akad. Nauk SSSR, Ser. Khim.*, 2135 (1971).
221. R. J. Laub, J. H. Purnell and D. M. Summers, *J. Chem. Soc. Faraday Trans. II*, *submitted.*
222. R. N. Martynyuk and M. S. Vigdergauz, *Chromatographia*, **9**, 454 (1976).
223. W. H. McFadden, *Anal. Chem.*, **30**, 479 (1958).
224. J. A. Barnard and H. W. D. Hughes, *Nature*, **183**, 250 (1959).
225. E. O. A. Haahti, W. J. A. Vandenheuvel and E. C. Horning, *Anal. Biochem.*, **2**, 344 (1961).
226. T. Matsuda and H. Yatsugi, *Bunseki Kagaku* **11**, 1116 (1962).
227. H. J. Maier and O. C. Karpathy, *J. Chromatogr.*, **8**, 308 (1962).
228. A. Darbre and K. Blau, *J. Chromatogr.*, **29**, 49 (1967).
229. A. Islam and A. Darbre, *J. Chromatogr.*, **43**, 11 (1969).
230. R. A. Keller and G. H. Stewart, *Anal. Chem.*, **36**, 1186 (1964).
231. G. P. Hildebrand and C. N. Reilley, *Anal. Chem.*, **36**, 47 (1964).
232. G. W. Pilgrim and R. A. Keller, *J. Chromatogr. Sci.*, **11**, 206 (1973).
233. D. F. Lynch, F. A. Palocsay and J. J. Leary, *J. Chromatogr. Sci.*, **13**, 533 (1975).
234. R. J. Laub, D. E. Martire and J. H. Purnell, *J. Chem. Soc. Faraday Trans. 1*, **73**, 1686 (1977).
235. G. M. Janini and D. E. Martire, *J. Chem. Soc. Faraday Trans. II*, **70**, 837 (1974).
236. W. Hayduk and S. C. Cheng, *Can. J. Chem. Eng.*, **48**, 93 (1970).
237. R. J. Laub and J. H. Purnell, *J. Chem. Soc. Perkin Trans.*, II, 895 (1978).
238. M. W. P. Harbison, D. E. Martire, R. J. Laub, J. H. Purnell and P. S. Williams, *J. Amer. Chem. Soc.*, submitted.
239. R. J. Laub, J. H. Purnell, P. S. Williams, M. W. P. Harbison and D. E. Martire, *J. Chem. Soc. Faraday Trans. II*, in preparation.
240. A. J. Ashworth and D. M. Hooker, *J. Chromatogr.*, **131**, 399 (1977).

241. J. S. Rowlinson, "Liquids and Liquid Mixtures", Butterworths, London (1959), Chs. 4, 5.
242. D. Patterson, *Macromolecules*, **2**, 672 (1969).
243. D. Patterson, *Pure Appl. Chem.*, **31**, 133 (1972).
244. J. F. Parcher and T. N. Westlake, *J. Phys. Chem.*, **81**, 307 (1977).
245. J. R. Conder, *Chromatographia*, **7**, 387 (1974).
246. M. M. Kopecni, S. K. Milonjic and N. M. Djordjevic, *J. Chromatogr.*, **139**, 1 (1977).
247. M. M. Kopecni, Z. E. Ilic and S. K. Milonjic, *J. Chromatogr.*, **139**, 1 (1977).
248. Dj. M. Petkovic, *J. Inorg. Nucl. Chem.*, **30**, 603 (1968).
249. A. Poczynailo, P. R. Danesi and G. Scibona, *J. Inorg. Nucl. Chem.*, **35**, 3294 (1973).
250. Yu. N. Bogoslovsky, V. M. Sakharov and I. M. Shevchuk, *J. Chromatogr.*, **69**, 17 (1972).
251. R. J. Laub and J. H. Purnell, *J. Amer. Chem. Soc.*, **98**, 35 (1976).
252. G. W. Stewart and R. M. Morrow, *Proc. Nat. Acad. Sci.*, **13**, 222 (1927).
253. G. W. Stewart and R. M. Morrow, *Phys. Rev.*, **30**, 232 (1927).
254. G. W. Stewart and E. W. Skinner, *Phys. Rev.*, **31**, 1 (1928).
255. G. W. Stewart, *Phys. Rev.*, **35**, 296 (1930).
256. G. W. Stewart and R. L. Edwards, *Phys. Rev.*, **38**, 1575 (1931).
257. G. S. Parks and C. S. Chaffee, *J. Phys. Chem.*, **31**, 439 (1927).
258. G. W. Stewart, R. M. Morrow and E. W. Skinner, *Phys. Rev.*, **27**, 104 (1926).
259. R. M. Morrow, *Phys. Rev.*, **31**, 10 (1928).
260. G. W. Stewart, *Proc. Nat. Acad. Sci.*, **13**, 787 (1927).
261. J. Rolinski, *Phys. Zeit.*, **29**, 658 (1928).
262. C. M. Sogani, *Indian J. Physics*, **1**, 357 (1927); **2**, 97 (1927).
263. G. W. Stewart, *Phys. Rev.*, **32**, 153, 558 (1928).
264. G. W. Stewart, *Phys. Rev.*, **33**, 889 (1929).
265. G. W. Stewart, *Phys. Rev.*, **37**, 9 (1931).
266. G. W. Stewart and R. D. Spangler, *Phys. Rev.*, **36**, 472 (1930).
267. G. W. Stewart, *Phys. Rev.*, **39**, 176 (1932).
268. G. W. Stewart, *Trans. Faraday Soc.*, **29**, 982 (1933).
269. A. Müller, *Trans. Faraday Soc.*, **29**, 990 (1933).
270. R. D. Spangler, *Phys. Rev.*, **42**, 907 (1932); **46**, 698 (1934).
271. G. W. Stewart, *J. Chem. Phys.*, **2**, 147 (1934).
272. C. A. Benz and G. W. Stewart, *Phys. Rev.*, **46**, 703 (1934).
273. C. A. Benz, *Proc. Iowa Acad. Sci.*, **41**, 249 (1934).
274. G. W. Stewart, *Proc. Iowa Acad. Sci.*, **41**, 250 (1934).
275. H. K. Ward, *J. Chem. Phys.*, **2**, 153 (1934).
276. G. W. Stewart, *Rev. Modern Phys.*, **2**, 116 (1930); *Proc. Iowa Acad. Sci.*, **36**, 305 (1929).
277. G. W. Stewart, *Indian J. Physics*, **7**, 603 (1933).
278. F. I. G. Rawlins, *Trans. Faraday Soc.*, **29**, 993 (1933).
279. G. W. Stewart, *Kolloid-Zeit.*, **67**, 130 (1934).
280. C. Drucker, *Phys. Zeit.*, **29**, 273 (1928).
281. B. E. Warren, *Phys. Rev.*, **44**, 969 (1933).
282. F. Reiss-Husson and V. Luzzati, *J. Coll. Interface Sci.*, **21**, 534 (1966).
283. A. DeVries, *Mol. Cryst. Liq. Cryst.*, **10**, 219 (1970); **11**, 361 (1970).
284. G. W. Brady, C. Cohen-Addad and E. F. X. Lyden, *J. Chem. Phys.*, **51**, 4309 (1969).

285. G. W. Brady, *J. Chem. Phys.*, **57**, 91 (1972).
286. W. Phillipoff, *Discuss. Faraday Soc.*, **11**, 96 (1951).
287. W. D. Harkins, "The Physical Chemistry of Surface Films", Reinhold, New York (1966).
288. A. R. Oseroff, P. W. Robbin and M. M. Borger, *Ann. Rev. Biochem.*, **42**, 835 (1973).
289. F. Franks, ed., "Physico-Chemical Processes in Mixed Aqueous Solvents", Elsevier, New York (1967); "Water: A Comprehensive Treatise", Vol. 4, Plenum, New York (1975).
290. F. Franks and D. J. G. Ives, *Quart. Rev.*, **20**, 1 (1966).
291. K. Toukubo and K. Nakamishi, *J. Chem. Phys.*, **65**, 1937 (1976).
292. G. W. Brady, *Accounts Chem. Res.*, **7**, 174 (1974); *J. Chem. Phys.*, **60**, 3466 (1974); *Polymer Prepr.*, **14**, 181 (1973).
293. K. L. Mittal, ed., "International Symposium on Micellizations, Solubilization, and Microemulsions", Vols. 1 and 2, Plenum, New York (1978).
294. B. Dodson, R. Foster, A. A. S. Bright, M. E. Foreman and J. Gorton, *J. Chem. Soc. B*, 1283 (1971).
295. W. R. Supina, in "Modern Practice of Gas Chromatography", ed. R. L. Grob, Wiley-Interscience, New York (1977), p. 137.
296. A. T. James, A. J. P. Martin and G. H. Smith, *Biochem. J.*, **52**, 238 (1952).
297. A. I. M. Keulemans, A. Kwantes and P. Zaal, *Anal. Chim. Acta*, **13**, 357 (1955).
298. E. M. Fredericks and F. R. Brooks, *Anal. Chem.*, **28**, 297 (1956).
299. J. H. Purnell and M. S. Spencer, *Nature*, **175**, 988 (1955).
300. A. Zlatkis, *Anal. Chem.*, **30**, 332 (1958).
301. E. Bayer, K. H. Reuther and F. Born, *Angew. Chem.*, **69**, 640 (1957).
302. G. Raupp, *Angew. Chem.*, **71**, 284 (1959).
303. G. R. Primavesi, *Nature*, **184**, 2010 (1959).
304. M. Singliar, A. Bobak, J. Brida and L. Lukacovic, *Z. Anal. Chem.*, **177**, 11 (1960).
305. A. Waksmundzki, E. Soczewinski and Z. Suprynowicz, *Collect. Czech. Chem. Commun.*, **27**, 2001 (1962).
306. A. Waksmundzki and Z. Suprynowicz, *J. Chromatogr.*, **18**, 232 (1965).
307. W. Kemula and H. Buchowski, *Rev. Chim.*, **1**, 285 (1962).
308. A. A. Zhukhovitskii, M. S. Selenkina and N. M. Turkeltaub, *Russ. J. Phys. Chem.* (Engl. Transl.), **36**, 519 (1962).
309. J. H. Jordan, *J. Gas Chromatogr.*, **2**, 346 (1964).
310. L. Rohrschneider, *Z. Anal. Chem.*, **170**, 256 (1959).
311. M. Mitooka, *Bunseki Kagaku*, **20**, 1542 (1971); **21**, 189, 197, 354, 614, 717, 729, 867, 1043, 1242, 1437, 1447 (1972).
312. H. Miyake and M. Mitooka, *Bull. Japan Petrol. Inst.*, **5**, 58 (1963); *Nippon Kagaku Zasshi*, **84**, 593, 923 (1963); **85**, 326 (1964); *Bull. Chem. Soc. Japan*, **38**, 1062 (1965).
313. H. Pauschmann, *Z. Anal. Chem.*, **211**, 32 (1965).
314. A. B. Littlewood and F. W. Willmott, *J. Gas Chromatogr.*, **5**, 543 (1967).
315. E. S. Windham, *J. Assoc. Offic. Anal. Chem.*, **52**, 1237 (1969).
316. A. S. Melnikov and B. V. Aivazov, *Zh. Anal. Khim.*, **28**, 791 (1973).
317. M. Suzuki, Y. Yamato and T. Watanabe, *J. Assoc. Offic. Anal. Chem.*, **58**, 297 (1975).
318. R. S. Porter, R. L. Hinkins, L. Tornheim and J. F. Johnson, *Anal. Chem.*, **36**, 260 (1964).
319. M. J. Molera, J. A. G. Dominguez and J. F. Biarge, *J. Chromatogr. Sci.*, **7**, 305 (1969); **11**, 538 (1973).

320. A. S. Melnikov and B. V. Aivazov, *Zh. Anal. Khim.*, **29**, 365 (1974).
321. W. L. Zielinski, Jr. and D. E. Martire, *Anal. Chem.*, **48**, 1111 (1976).
322. T. H. Risby, P. C. Jurs and B. L. Reinbold, *J. Chromatogr.*, **99**, 173 (1974).
323. C. E. Figgins, T. H. Risby and P. C. Jurs, *J. Chromatogr. Sci.*, **14**, 453 (1976).
324. L. Sojak, J. Janak and J. A. Rijks, *J. Chromatogr.*, **142**, 177 (1977).
325. E. sz. Kovats, *Helv. Chim. Acta*, **41**, 1915 (1958).
326. W. O. McReynolds, "Gas Chromatographic Retention Data", Preston Technical Abstracts, Niles, Ill. (1966).
327. R. J. Laub and J. H. Purnell, *J. Chromatogr.*, **112**, 71 (1975).
328. J. H. Purnell, *J. Chem. Soc.*, 1268 (1960).
329. R. J. Laub and J. H. Purnell, *Anal. Chem.*, **48**, 799 (1976).
330. R. J. Laub, J. H. Purnell and P. S. Williams, *J. Chromatogr.*, **134**, 249 (1977).
331. R. J. Laub, J. H. Purnell and P. S. Williams, *Anal. Chim. Acta*, **95**, 135 (1977).
332. R. J. Laub and J. H. Purnell, *Anal. Chem.*, **48**, 1720 (1976).
333. R. J. Laub, J. H. Purnell, D. M. Summers and P. S. Williams, *J. Chromatogr.*, **155**, 1 (1978).
334. R. J. Laub and J. H. Purnell, *J. Chromatogr.*, **161**, 59 (1978).
335. W. K. Al-Thamir, R. J. Laub and J. H. Purnell, *J. Chromatogr.*, **142**, 3 (1977).
336. A. DiCorcia and R. Samperi, *J. Chromatogr.*, **107**, 99 (1975).
337. R. P. W. Scott and P. Kucera, *J. Chromatogr.*, **112**, 425 (1975).
338. S. N. Deming and M. L. H. Turoff, *Anal. Chem.*, **50**, 546 (1978).
339. R. J. Laub and J. H. Purnell, *J. Chromatogr.*, **161**, 49 (1978).
340. M. Rogozinski and I. Kaufman, *J. Gas Chromatogr.*, **4**, 413 (1966).
341. J. C. Kraak, K. M. Jonker and J. F. K. Huber, *J. Chromatogr.*, **142**, 671 (1977).
342. A. Kwantes and G. W. A. Rijnders, in "Gas Chromatography 1958", ed. D. H. Desty, Butterworths, London (1958), p. 125.
343. D. H. Desty and A. Goldup, in "Gas Chromatography 1960", ed. R. P. W. Scott, Butterworths, London (1960), p. 162.
344. D. H. Everett and C. T. H. Stoddart, *Trans. Faraday Soc.*, **57**, 746 (1961).
345. A. Goldup, G. R. Luckhurst and W. T. Swanton, *Nature*, **193**, 333 (1962).

4 The Study of Intermolecular Interactions in the Liquid Phase Using Infrared and Raman Band Shapes and Intensities

J. YARWOOD

Department of Chemistry, University of Durham, Durham City DH1 3LE, U.K.

R. ARNDT

Institut für Physikalische Chemie, Technische Universität, Hans Sommer Strasse 10, D3300 Braunschweig, West Germany

I. Introduction 267
II. Background Theory 272
A. Introduction 272
B. Reorientational motions 275
1. Introduction 275
2. Comparison of single-particle and pair correlation times . . 276
3. Band moments 278
4. Models for rotational motion 280
C. Vibrational relaxation 285
1. Transition-dipole–transition-dipole interactions . . . 289
2. Dipole–dipole interactions 290
3. Repulsive (short range) interactions 292
III. Examples of the Determination of Intermolecular Forces using Infrared and Raman Spectroscopy 296
A. Simple liquids (CH_3I, CHF_3, $CHCl_3$, CCl_4, CS_2, CH_2Cl_2, C_6H_6) . 296
B. Associated liquids (C_6H_5CHO, $C_4H_8O_2$, CH_3CN) . . . 312
References 325

I. INTRODUCTION

Important information about the nature and extent of intermolecular forces can be obtained from vibrational spectroscopic data in a number of ways—some obvious and some more subtle. We shall review these general methods and then assess critically the quality and quantity of information available.

(1) The formation of a molecular complex[1–4] or the onset of strong intermolecular interactions often leads to gross changes of band position, intensity and shape which are relatively easily interpreted in terms of a model for the interaction. Good examples of this situation are the formation of hydrogen-bonded[3] or other molecular complexes[1, 2] between a potential electron donor and a potential acceptor. Figures 1 and 2 illustrate the kind

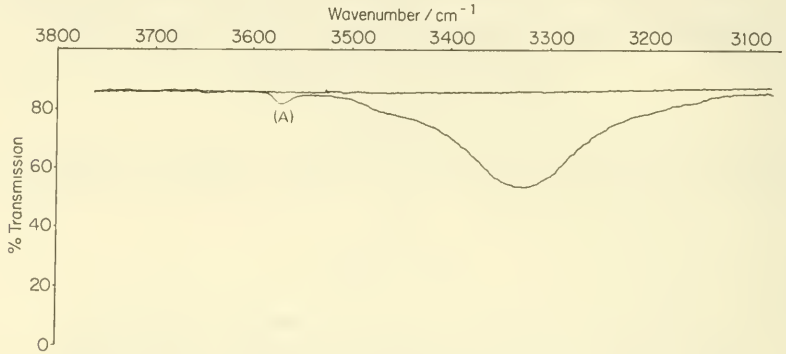

FIG. 1. The infrared spectrum of the C_6H_5OH–CH_3CN hydrogen-bonded complex in CCl_4 showing large shift and band-shape change of the ν(OH) vibration on complexation (A indicates "free" phenol in the equilibrium mixture).

of extensive spectral changes that may occur. The large observed frequency shifts and intensity changes can often be explained[1–4] in terms of the changes of force constants, normal coordinates and electron distribution due to the

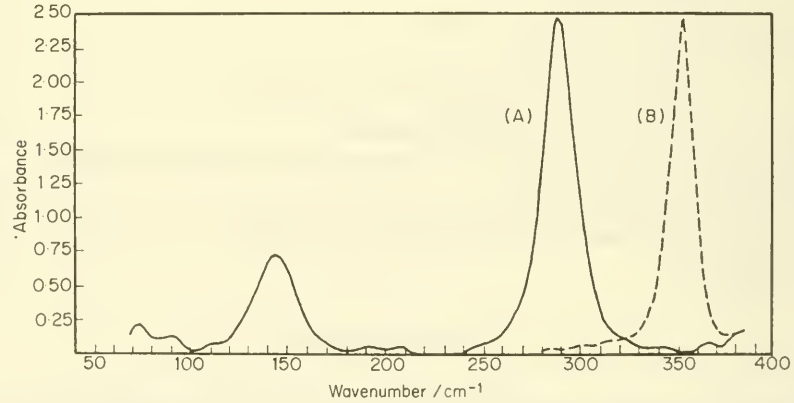

FIG. 2. Far-infrared spectrum of (A) pyridine–ICl in benzene, and (B) "free" ICl in benzene. An illustration of the effect of complexation on the ν(I—Cl) band. [Reproduced with permission from J. Yarwood (ed.), "Spectroscopy and Structure of Molecular Complexes", Plenum, London (1973)]

possible modes of interaction. Although the relative extents of coulombic, inductive, repulsive or donor–acceptor interaction for a given complex are usually not known, some deductions as to the *predominant* mode of interaction are possible if the data are analysed properly. It has been possible,[1] in favourable cases, to separate the effects of classical and quantum mechanical contributions to complex stability and spectral properties. The interpretation of band shapes[5–7] is still in its infancy, but a number of recent developments will undoubtedly help in future work not only on relatively stable complexes but also on the elucidation of intermolecular interactions in simple liquids and solutions, in which forces of interaction are less easily quantified (see below). These advances[8–11] centre on an awareness that important information can be obtained by studying the time development of the correlation functions associated with absorption or scattering of light from a molecular ensemble. By using the Heisenberg[12] approach to formulate the equations of motion for a given system, attention can be focused on the dynamic properties of the molecules in the system. By this method one can, for example, derive valuable information on the *lifetimes* of interactions and the *rates* at which the molecular motions (especially reorientational and translational motions) proceed. These dynamic properties may then be used as a probe to investigate the nature and extent of the intermolecular potential (see below and Section II for more details).

(2) When the extent of intermolecular forces is relatively weak, as is the case, for example, between molecules in a simple organic liquid or between the components of a "weak"† molecular complex, then the observed spectral changes become more subtle. Although these spectral changes are usually well defined and reproducible, their interpretation must rely on less quantitative models, and the difficulties and pitfalls are thereby multiplied. Nevertheless, there has been a concentration of effort during the past 10 years on the ways of obtaining information about the intermolecular potential from band shapes (or correlation functions) obtained for simple molecular liquids as a function of solvent concentration, density and temperature. When sufficiently accurate spectral data are available it is possible, for example, to derive intermolecular torques[13] directly from band moments. Also, information can often be obtained about the type of intermolecular potential that predominates, by studying the environmental dependence of the vibrational relaxation process or of the reorientational correlation function. The problems, both experimental and theoretical, with this approach will be illustrated in Sections II and III. The experimental separation of vibrational, reorientational and translational motions, although possible in principle using infrared,[5,6]

† The description "weak" here means that enthalpies of formation are less than about 25–30 kJ mol^{-1}.

Raman[7, 14] and neutron spectroscopy,[15–17] is often not straightforward.[18] Furthermore, available models for vibrational relaxation or reorientational motions in liquids are always much oversimplified and therefore sometimes inadequate to explain the observed data. Nevertheless, the use of techniques described in this chapter has proved extremely valuable and they will be used extensively in the future.

(3) There have been attempts[19–22] to interpret band splittings or band asymmetry in terms of intermolecular interactions or "ordering" of dipolar molecules in the liquid phase. If the lifetimes of the various possible species are long compared with the vibrational frequencies, there is no reason why splittings should not be observed (assuming that the instrument resolution is sufficiently high). Such information would undoubtedly be useful but extreme care should be exercised. The observed phenomena may sometimes be interpreted reasonably as being due to "hot" bands, i.e. combination bands of the type[23] $\nu_n + \nu_m - \nu_m$ (where ν_m is a low-lying vibrational level) whose frequency does not, because of anharmonicity, lie at ν_n. There may even be overtone or other combination bands in the vicinity of an observed fundamental band, although this ought to be readily identified for simple molecules. Finally, bands that arise in this way due to high "ordering" in the liquid phase should show the appropriate changes when the molecules are diluted in a non-polar solvent. Unless the solvent is such that further strong interactions are expected, the spectral "structure" ought to disappear gradually. There seem to be few, if any, proven cases of this phenomenon occurring in an organic liquid (see Section III). Detailed examples of the use of these techniques are given in Section III, but it is appropriate here to consider the general type of information that is obtained and the range of problems to which they are applicable.

In order to determine the reorientational and vibrational correlation functions separately and accurately, one must study the band shapes of well-isolated vibrational modes using *both* Raman and infrared spectroscopy. In general, this means that relatively simple or highly symmetrical molecules are needed to avoid extensive band overlap. (However, *too* high a symmetry can also be a disadvantage in that some modes may be infrared or Raman inactive.) It is also a considerable advantage if nuclei with high natural abundances of several isotopes are avoided. Figure 3 shows, for example, what can happen if the molecule considered contains chlorine nuclei (for those modes involving Cl atom displacements). Although this problem can be dealt with using the shift theorem,[24] it is clearly better to avoid such a situation if possible. If severe distortions due to finite instrument resolution are to be avoided it is essential to be able to study the band with good signal/noise ratio under high resolution conditions (slit width $< 0{\cdot}2$ apparent half band-width).[25] For dilute solutions, which are essential

for interpretative reasons, it is therefore necessary to have to make fairly large laser power (~3–6 watt) with Raman experiments and large path-lengths with infrared experiments. Both of these conditions have associated problems, mainly local sample heating and solvent absorption respectively. It is

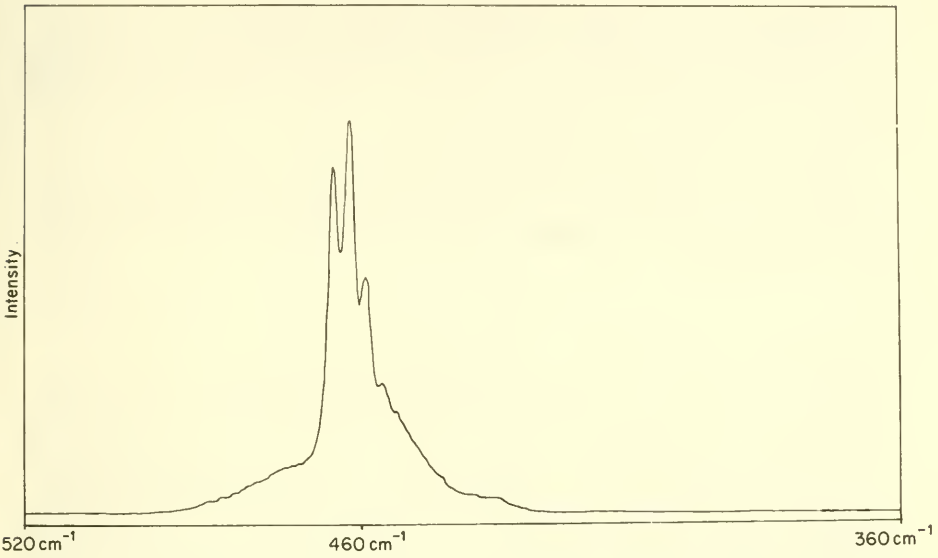

FIG. 3. Isotropic Raman spectrum of ν_1 band of liquid CCl_4 illustrating the "structure" produced by isotopically modified molecules.

preferable if the molecule is available (or can be made) in the fully deuterated form; in vibrational spectroscopy this permits selective removal of the effects of resonance vibrational energy transfer[26–30] between adjacent molecules using the deuterated molecule as a solvent. The deuterated material is also an important solvent in quasi-elastic incoherent neutron scattering[15] measurements for the determination of diffusive motions.

It should be emphasised that the transport and relaxation processes for a simple organic liquid or solution have correlation times [equation (7)] between about 0·1 and 10 ps. Thus vibrational spectroscopic techniques (with observation times $1/\omega_0$ of between 0·01 and 3·3 ps) are ideal for the study of the molecular correlation function over the time period between 0 and 10 ps.

II. BACKGROUND THEORY

A. Introduction

In this section we shall provide background for an understanding of how band-shape data can yield information about the nature and extent of intermolecular interactions. There are excellent reviews[12, 31–33] of molecular dynamic properties and relaxation processes in dense fluids, so we shall just emphasise the aspects considered in Section III in describing the experimental work on some typical systems.

Infrared and Raman rotational–vibrational band shapes may be conveniently considered to be the Fourier transforms of certain time autocorrelation functions $\Phi(t)$. For an infrared band with *normalised*[12] intensity $I_{IR}(\omega)$ we have[18]

$$\phi_v(t)\phi_{1R}(t) = \langle Q_i(0).\, Q_i(t)\rangle\langle P_1[\boldsymbol{\mu}_i(0).\, \boldsymbol{\mu}_i(t)]\rangle = \int_{band} I_{IR}(\omega)\exp(i\omega t)\,d\omega \quad (1)$$

where $\boldsymbol{\mu}$ is a unit vector along the direction of the transition moment corresponding to the normal coordinate Q_i of the ith molecule, and where $\langle P_1[\boldsymbol{\mu}_i(0).\, \boldsymbol{\mu}_i(t)]\rangle$ is the first-order tensor pure rotational (or orientational) correlation function [$P_1 = \cos\theta_i(t)$ where $\theta_i(t)$ is the angle between the transition dipoles of the ith molecule at time $t = 0$ and $t = t$]. For Raman spectra with a vertically polarised (laser) source the parallel (VV) and perpendicular (VH) components of the scattered light are related[14] to the isotropic and anisotropic parts of the scattering tensor by

$$I_{iso}(\omega) = I_{VV}(\omega) - (4/3)I_{VH}(\omega) \quad (2a)$$

$$I_{aniso}(\omega) = I_{VH}(\omega) \quad (2b)$$

where

$$\phi_v(t) = \langle Q_i(0).\, Q_i(t)\rangle = \int_{band} I_{iso}(\omega)\exp(i\omega t)\,d\omega \quad (3)$$

and

$$\phi_v(t)\phi_{2R}(t) = \langle Q_i(0).\, Q_i(t)\rangle\langle P_2[\boldsymbol{\mu}_i(0).\, \boldsymbol{\mu}_i(t)]\rangle = \int_{band} I_{aniso}(\omega)\exp(i\omega t)\,d\omega \quad (4)$$

where P_2 (the second-order Legendre polynomial) $= \frac{1}{2}[3\cos^2\theta_i(t) - 1]$.

In equations (1), (3) and (4) the autocorrelation function $\langle Q_i(0).\, Q_i(t)\rangle$ is usually known as the vibrational relaxation function but it must be remem-

bered that this function encompasses *all* non-reorientational contributions to the decay of the total $\Phi(t)$ function. These include the various possible modes[28,30] of vibrational relaxation (see Section II.C) and collision-induced[28,34] effects (Section II.B). Furthermore, there are several complicating factors that may lead to problems in separating $\phi_v(t)$ and the various reorientational correlation functions; these are as follows.

(i) The effects of finite slit. If the instrument resolution function is characterised by a function whose Fourier inversion leads, in the time domain, to $\phi_s(t)$, then one should write

$$\Phi_{IR}(t) = \phi_v^{IR}(t)\phi_{1R}(t)\phi_s(t) \tag{5a}$$

$$\Phi_{iso}(t) = \phi_v^{iso}(t)\phi_s(t) \tag{5b}$$

$$\Phi_{aniso}(t) = \phi_v^{aniso}(t)\phi_{2R}(t)\phi_s(t) \tag{5c}$$

so that

$$\phi_v^{iso}(t) = \Phi_{iso}(t)/\phi_s(t) \tag{6a}$$

$$\phi_{1R}(t) = \Phi_{IR}(t)/\Phi_{iso}(t) \tag{6b}$$

$$\phi_{2R}(t) = \Phi_{aniso}(t)/\Phi_{iso}(t). \tag{6c}$$

Thus the resolution function is most important for the determination of $\phi_v(t)$, which, unless the liquid is near its melting point, provides the *narrowest* contribution to the overall band contour. Notice that the use of equation (6b) is valid only if $\phi_s(t)$ is the same for infrared and Raman experiments. This will not generally be the case but it may, in principle, be made so by use of the same experimental slit conditions. Otherwise the contributions $\phi_v(t)\phi_{1R}(t)$ and $\phi_v(t)\phi_{2R}(t)$ must be separately corrected for the effects of finite slit.

(ii) If transition-dipole–transition-dipole interactions (Section II.C) are important, and if there is partial ordering of the molecules in the liquid phase (due to "clustering"), the infrared and Raman selection rules[22,114] are different for a given mode and there may be a considerable difference between $\phi_v^{IR}(t)$ or $\phi_v^{aniso}(t)$ and $\phi_v^{iso}(t)$. This would again invalidate the use of equations (6b) and (6c) to derive values for $\phi_{1R}(t)$ and $\phi_{2R}(t)$.

(iii) In equations (1)–(6) it is tacitly assumed that the various processes giving rise to decay of $\Phi_{IR}(t)$, $\Phi_{iso}(t)$ or $\Phi_{aniso}(t)$ are statistically uncorrelated. This has been assumed in almost all the published work on liquids but in practice it is unlikely to be strictly valid (the "best" situation arises in this respect when coupling of the various motions involved has very different rates or correlation times—see below). For example, it is evident that vibrational relaxation processes are often controlled largely by hard collisions[28,36] in the medium, so the rotational–translational motions of the molecules[37]

must be correlated with vibrational dephasing and vibrational energy level (population) relaxation (see Section II.C). Further, for degenerate vibrational modes it is obvious that coupling of vibrational and rotational angular momenta (e.g. Coriolis coupling)[38,39] will affect the decay of the $\Phi(t)$ functions.

(iv) For some molecules, especially those of low symmetry, it can be shown[18] that there are restrictions on the use of equations (6). For example, complete separation of the orientational and vibrational parts for a degenerate band (of E or T symmetry) is not possible.[14] Since such bands are depolarised, $I_{VH}/I_{VV} = \rho = 3/4$. The use of equation (2) to calculate I_{iso} is then not possible, and some alternative method[18,40] is needed to derive $\phi_v(t)$. On the other hand, totally symmetric bands (of A symmetry) have, in theory, totally polarised Raman bands ($\rho = 0$), and these contain no contribution from the anisotropic part of the scattering tensor.[41] Clearly, if $I_{VH} = 0$, no rotational correlation function can be derived. As seen in Section III, there are many totally symmetric bands for which $\rho > 0$, so a $\phi_{2R}(t)$ can be obtained, or resort can be made to the infrared spectrum to obtain $\phi_{1R}(t)$ if the mode is infrared active.

When separation of the various correlation functions is achieved (albeit making a number of assumptions) it is often convenient to characterise the function by the corresponding correlation time, τ_x, where

$$\tau_x = \int_0^{t_L} \phi_x(t)\, dt \tag{7}$$

and t_L is the expected time limit, controlled by the resolution.[42] If, as is often the case for models[31,62] describing rotational or vibrational relaxation functions [see e.g. equations (59) and (78)], the $\phi_x(t)$ function can be written as $\phi_x(t) = \exp(-t/\tau_x)$, the integrated value $\langle \tau_x \rangle$ in equation (7) is equivalent[43] to the "decay" time τ_x^e measured directly from the $\phi_x(t)$ versus t curve (see Fig. 4), i.e. the time required for $\phi_x(t)$ to fall from 1 to 1/e). For experimental reasons (usually poor signal/noise ratio or overlapping bands), it may not be possible to calculate $\phi_x(t)$ accurately; then, again assuming $\phi_x(t) = \exp(-t/\tau_x)$, one can calculate τ_x^h from $(\pi c \Delta\bar{\nu}_{\frac{1}{2}})^{-1}$ where $\Delta\bar{\nu}_{\frac{1}{2}}$ is the apparent full-width at half-maximum (FWHM). If $\phi_x(t)$ can be obtained but integration is not possible, it is often possible to calculate τ_x^s from the slope of the plot of $\ln \phi_x(t)$ against t at *long* times when $\phi_x(t)$ becomes exponential regardless of the details of the band-shape.

Having described the principles of the separation of reorientational and non-reorientational effects to the observed spectral band-shape, we shall now consider each of these contributions in turn and examine the value of each in the search for information on intermolecular forces.

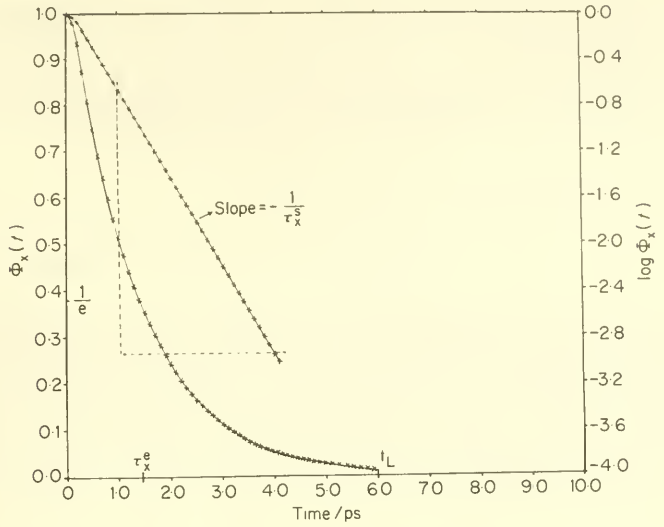

FIG. 4. Correlation function for a pure Lorentzian band of half-width (FWHM) = 7 cm^{-1}, showing the various correlation times that can be deduced.

B. Reorientational Motions

1. Introduction

Some authors (e.g. ref. 12, p. 230) have commented that observed rates of rotational diffusion very often appear not to reflect strongly the degree of intermolecular interaction expected. Nevertheless, some differences in such diffusion coefficients *have* been observed for molecules of differing polarities,[44] and it seems fairly clear that the nature and rate of collisions and reorientations which lead to decay of the correlation function $\langle P_l[\boldsymbol{\mu}(0).\boldsymbol{\mu}(t)]\rangle$ *must*,[45] to some extent, depend on the intermolecular potential if the interaction is such that "pairs" (or larger "clusters") of molecules are involved in cooperative motions, i.e. where the motion of one molecule is affected significantly by the motion of its interacting neighbour(s). This is why the investigation of intermolecular forces has mainly been carried out using depolarised Rayleigh[46] and far-infrared[33,47–49] spectra which depend on autocorrelation functions of the type

$$\sum_i \langle P_l[\boldsymbol{\mu}_i(0).\boldsymbol{\mu}_i(t)]\rangle + \sum_{j\neq 1} \langle P_l[\boldsymbol{\mu}_i(0).\boldsymbol{\mu}_j(t)]\rangle \qquad (8)$$

where $l = 1$ for far-infrared and $l = 2$ for depolarised Rayleigh spectra. The second term, involving cross correlations between molecules i and j has usually, but not always,[50] been considered unimportant for vibrational–

rotational (infrared and Raman) spectra. Infrared ($l = 1$) and Raman ($l = 2$) spectra usually give the first term in equation (8) but it should be noticed that the cross correlations may be observed in the anisotropic Raman spectrum if vibrational relaxation occurs via the exchange term in equation (49) since then resonant vibrational energy transfer will lead to

$$\Phi_{\text{aniso}}(t) \propto \sum_i \langle Q_{vi}(0) . Q_{vi}(t) \rangle \langle P_2[\boldsymbol{\mu}_i(0) . \boldsymbol{\mu}_i(t)] \rangle + \sum_{i \neq j} \langle Q_{vi}(0) . Q_{vj}(t) \rangle \langle P_2[\boldsymbol{\mu}_i(0) . \boldsymbol{\mu}_j(t)] \rangle . \quad (9)$$

A comparison of the single-particle and multi-particle reorientational correlation times (or functions if this is feasible) therefore gives important information about the degree to which motions of different molecules are coupled via intermolecular forces. Information about intermolecular torques is available, in principle, from rotational band moment measurements[1,12] on rotational–vibrational spectra, provided that the vibrational and rotational parts can be separated. Finally, the use of models that describe the reorientational motions of simple molecules may often contain, or be modified to contain, parameters such as collision times,[51] residence times, jump times or friction constants,[52] which imply a deviation from what is expected either in the gas phase or in the solid phase. Interactions such as arise from coulombic and polarisation forces (long range forces) usually affect only the time evolution of $\langle P_l[\boldsymbol{\mu}(0) . \boldsymbol{\mu}(t)] \rangle$ when $t \gg t'$ where t' is the time interval (usually between 0·1 and 0·5 ps) over which "pseudo-free" rotation is performed. The short time part of the reorientational correlation function ($t < t'$) is controlled by inertial effects but may also be affected by short range collision induced interactions (giving rise to "extra" intensity in the wings of the band).[107] Thus, a detailed study of the applicability or otherwise of a particular reorientational model may also provide evidence for or against the use of a particular model for interaction.

We shall now examine these three methods of investigating intermolecular interactions through reorientational band profiles in somewhat more detail. (Some examples of the use of these techniques are given in Section III.)

2. Comparison of Single-particle and Pair Correlation Times

As mentioned above, the first term in equation (8)—the single particle correlation function—is usually obtainable[31,53] from infrared ($l = 1$) (and in cases where the permanent dipole and transition dipole are in the same direction, from microwave[53]) or from Raman or nmr spectra ($l = 2$). Depolarised Rayleigh ($l = 2$) and far-infrared ($l = 1$) spectra reflect the inclusion of *both* terms in equation (8). Comparison of light scattering measurements and correlation times obtained from rotational Raman or spin–

lattice relaxation[54] measurements may be used to study intermolecular interactions in the following way. It may be shown[54, 55] that for cylindrically symmetric molecules (symmetric tops) and in the rotational diffusion approximation the two parts of (8) are given, respectively, by

$$G^s(t) = \tfrac{1}{15}N\beta^2 \exp(-6D_\perp t) \tag{10}$$

and

$$G^d(t) = \tfrac{1}{15}N\beta^2\left\{(1 + fN)\exp\left[-6D_\perp\left(\frac{1 + gN}{1 + fN}\right)t\right] - \exp(-6D_\perp t)\right\}. \tag{11}$$

N is the number density (number of molecules for a pure liquid), β is the molecular optical anisotropy and $D_\perp$ is the rotational diffusion coefficient of the symmetric-top axis (tumbling motion). The quantities f and g are the "static" and "dynamic" orientational correlation factors respectively. They are related,[54, 56, 57] for a symmetric-top molecule, to the Kirkwood[58] $g^{(1)}$ factor and $g^{(2)}$ factor[59] by

$$g^{(1)} \equiv 1 + gN \tag{12a}$$

and

$$g^{(2)} \equiv 1 + fN. \tag{12b}$$

In the absence of dipole–dipole, dipole–induced-dipole or other multipole interactions there is no reorientational order and then the g and f factors are zero and both $g^{(1)}$ and $g^{(2)}$ are 1. Antiparallel or perpendicular arrangement of pairs of molecular axes will[56] tend to reduce the value of the Kirkwood $g^{(2)}$ factor below 1 and thus fN is negative. For parallel arrangements of pairs of molecular axes the value of fN is positive and $g^{(2)} > 1$. The values of fN are obtained from the total integrated intensity since[54]

$$I_{VH}(\text{integrated}) = \tfrac{1}{15}AN[\tfrac{1}{3}(n^2 + 2)]^2\beta^2(1 + fN) \tag{13}$$

(n is the refractive index) and the relationship between the light scattering and single particle correlation times[54, 56] [equations (9) and (10)]

$$\tau_{LS} = \left[\frac{(1 + fN)}{(1 + gN)}\right]\tau_s \tag{14}$$

provides a method of obtaining gN when τ_s is known from Raman, nmr or from light scattering measurements extrapolated to infinite dilution.[54, 56, 60] At low concentrations the pair correlations are expected to be of little importance, the total correlation function for light scattering is given by equation (10) (for $|g|N$ and $|f|N \ll 1$), and the light scattering correlation time is

$$\tau_s = 1/6D_\perp \tag{15}$$

which acts as a check on the degree to which orientational correlation is important.

To conclude this section it is worth noting that much has been written about the linear viscosity dependence of the various reorientational[43] correlation times; that, for example,[54] the single particle correlation time appears to be dependent only on solution viscosity. It should be remembered, however, that the (microscopic) viscosity depends[61] not only on the molecular shape and size but also on the way in which the molecules interact with one another. This point is taken up again in Section III.

3. Band Moments

It is well known[9–12, 62] that the general correlation function may be expanded in terms of the frequency moments[63] of the experimental intensity distribution. Thus

$$\phi(t) = \sum_{n=0}^{\infty} \frac{M_n}{n!}(it)^n \tag{16}$$

where the normalised truncated moments are

$$M_n = \frac{\int_{\text{band}} (\omega - \omega_0)^n I(\omega - \omega_0)\, d\omega}{\int_{\text{band}} I(\omega - \omega_0)\, d\omega} \tag{17}$$

and ω_0 is a suitably chosen band origin. [Note that $M_0 = 1$ (or the total intensity if unnormalised moments are used) and M_1 is the average frequency shift $\langle \omega - \omega_0 \rangle$ which can be used to detect the true band centre.]

In this section we shall be concerned with the investigation of intermolecular forces using orientational moments (there being moments arising from the vibrational or non-reorientational intensity distribution[28] as well). For a classical system (relatively heavy molecules[12, 63]) only even values of n need be considered since odd moments are zero. Thus the value of the third moment provides a good measure of band asymmetry which may be caused by non-classical (quantum mechanical) effects.[63] Each coefficient M_n in the expansion of equation (16)

$$\phi(t) = 1 - M_2 t^2/2! + M_4 t^4/4! - M_6 t^6/6! + \ldots \tag{18}$$

is an equilibrium property of the system (which may be evaluated without solution of any equation of motion). Thus equation (18) holds for gas, liquid or solid provided that proper equilibrium averaging is carried out.

Gordon[63] and others[64, 65] have evaluated the coefficients M_n for simple molecules in both the classical limit, with quantum corrections, and with modification of vibration–rotation interaction. It is found that in the classical limit the second moment M_2 gives an upper limit to the rotational kinetic energy of the molecule but that M_4 contains terms that depend on the average intermolecular torque acting on the probe molecule due to its neighbours. Such intermolecular torques represent angular derivatives of the intermolecular potential[63] and are clearly of importance in studying molecular interactions in gases and liquids.

For the *parallel* band of a linear molecule the expansions[12] (18) are:

Infrared spectrum

$$\langle P_1[\boldsymbol{\mu}(0).\boldsymbol{\mu}(t)]\rangle = 1 - \left(\frac{kT}{I}\right)t^2 + \left[\tfrac{1}{3}\left(\frac{kT}{I}\right)^2 + \frac{1}{24I^2}\langle(OV)^2\rangle\right]t^4 + (t^6). \quad (19)$$

Raman spectrum

$$\langle P_2[\boldsymbol{\mu}(0).\boldsymbol{\mu}(t)]\rangle = 1 - \left(\frac{3kT}{I}\right)t^2 + \left[4\left(\frac{kT}{I}\right)^2 + \frac{I}{8I^2}\langle(OV)^2\rangle\right]t^4 + (t^6) \quad (20)$$

or in terms of the rotational constant[64] B (for the infrared case)

$$M_2 = 4(kT/hc)B \quad (21)$$

$$M_4 = 32(kT/hc)^2B^2 + 4B^2\langle(OV)^2\rangle \quad (22)$$

so that

$$\langle(OV)\rangle^2 = [M_4 - 2(M_2)^2]/4B^2 \quad (23)$$

where in each case $\langle(OV)^2\rangle$ is the mean square torque. For a parallel band of a symmetric top molecule, again for the infrared case, we have[64]

$$M_2 = 4(kT/hc)B + 4B^2 \quad (24)$$

$$M_4 = 32(kT/hc)^2B^2(1 + B/4A) + 4B^2\langle(OV)^2\rangle \quad (25)$$

so that

$$\langle(OV)^2\rangle = [M_4 - (2 + B/2A)(M_2)^2](1/4B^2) \quad (26)$$

(here A and B are the two rotational constants, and the mean square torque is for rotation of the symmetry axis (about I_B).

For a spherical top molecule[65] it has been shown that

$$\langle(OV)^2\rangle = [M_4 - (5/2)(M_2)^2][(3/2)B^2]. \quad (27)$$

Although the experimental determination of M_2 and M_4 is by no means straightforward[12, 53] there have been attempts to derive intermolecular

torques for some simple molecules, and some of these are mentioned in Section III.

4. Models for Rotational Motion

One of the most extensively used models of rotational motion in liquids is the "extended diffusion" model of Gordon[66] which is based on the original classical diffusion process of Debye[67] but which does not have the restriction of small angle diffusive steps inherent in the classical theory. The application of the Gordon M and J diffusion model to the study of rotational processes in liquids is mainly the work of Kivelson and McClung.[68–75] and numerous experimental tests of the theory have now been made (see Section III). The theory is characterised by an angular momentum correlation time, τ_J, which measures the rate at which the memory of angular momentum is lost by molecular collisions. The equation of motion for angular momentum is a Langevin equation[76] and it can be shown that in the Debye limit ($\tau_\theta \gg \tau_J$) the reorientational correlation times $\tau_\theta^{(1)}$ and $\tau_\theta^{(2)}$ [equivalent to τ_{1R} and τ_{2R} corresponding to the functions of equations (6b) and (6c)] are given by

$$\tau_\theta^{(2)}\tau_J = I/6kT = (1/3)\tau_\theta^{(1)}\tau_J \tag{28}$$

for a spherical top molecule. The M and J diffusion models[66,68–70] do, however, allow investigation of the relationship between τ_θ and τ_J over the whole range from the Debye limit to the perturbed free rotor ($\tau_\theta \gtrsim \tau_J$). In the Debye limit the reorientational correlation τ_θ is expected to be proportional to the macroscopic viscosity via Stokes–Einstein relationship

$$\tau_\theta = 4\pi a^3\eta/3kT \tag{29}$$

where a is the molecular radius and η is the viscosity coefficient. This has, however, been found to be inadequate[77] for studies on simple liquid systems (since Debye assumed that the rotating body was macroscopic) and a parameter κ has been introduced[68] on the right-hand side of equation (29) in order to account for intermolecular effects. κ is a solvent and pressure dependent parameter[77] which gives the ratio of correlation functions of the intermolecular torque and the intermolecular force in the liquid. Thus κ lies between 0 and 1 and has its maximum value for the extreme anisotropy of the intermolecular potential whereas κ is very small for weak intermolecular anisotropic potentials (and weak coupling of translational and rotational motions). Kivelson and McClung[68] show that, for a spherical top molecule,

$$\tau_J = I_\alpha/8\pi\kappa r_0^3\eta \tag{30}$$

(where r_0 is the mean molecular radius) while for non-spherical molecules

with anisotropic intermolecular potentials,[61]

$$\tau_\alpha^{-1} = (8\pi\eta r_\alpha^3 \kappa_\alpha / I_\alpha) + 4(\Delta_\alpha)^2[\tau_\beta^{-1} + \tau_\gamma^{-1}]^{-1}. \tag{31}$$

The three principal axes of inertia are labelled α, β and γ, and

$$\Delta_\alpha = (I_\beta - I_\gamma)(kT)^{\frac{1}{2}}/(I_\alpha I_\beta I_\gamma)^{\frac{1}{2}}.$$

A comparison of τ_θ and τ_J measured by two different techniques over a reasonable temperature range may therefore be used to get information on intermolecular forces in the following ways.

(1) An estimate of the value of κ and its dependence on temperature, solvent and pressure gives a good idea of the anisotropy of the intermolecular potential.

(2) The degree to which the liquid behaviour resembles that of an M or J diffusional rotator also gives information about the nature and anisotropy of the intermolecular forces. The M and J diffusion models focus attention on the short time part of the motion. In other words, the angular-momentum correlation function is controlled largely by the effects of short range forces which are collision controlled.[34] Any effects on $\phi_{lR}(t)$ by long range forces such as dipole–dipole interactions will be expected to lead to discrepancies[78–81] in the relationship between τ_θ and τ_J. However, it should be noted[43, 83] that apparent disagreement[82] with the diffusion theory must be examined properly in the light of the nature of the rotational correlation function actually calculated and its relationship[43] to the angular-momentum correlation function.

Models of a somewhat different (although related) nature have been constructed[84] for use with spectra arising in the far-infrared region. It is known that for a polar molecule this absorption process is a result of several different (and simultaneous) phenomena. Of these, the contributions from the short time part of the overall Debye relaxation process and from the collision induced enhancement of the transition dipole both provide information about the intermolecular potential. The far-infrared spectral density is related to the Rotational Velocity Correlation Function (RVCF), $\langle \dot{\boldsymbol{\mu}}_1(0) . \sum_i \dot{\boldsymbol{\mu}}_i(t) \rangle$, where

$$-\langle \dot{\boldsymbol{\mu}}(0) . \sum_i \dot{\boldsymbol{\mu}}_i(t) \rangle = \mathrm{d}^2(\langle \boldsymbol{\mu}(0) . \sum_i \boldsymbol{\mu}_i(t) \rangle)/\mathrm{d}t^2 \tag{32a}$$

or

$$-f_2(t) = +\mathrm{d}^2[f_0(t)]/\mathrm{d}t^2 \tag{32b}$$

by the expression

$$\alpha(\bar{\nu}) = \frac{2\pi N_i \mu^2}{3kTcn(\bar{\nu})} \int_{-\infty}^{+\infty} \exp(-2\pi i \bar{\nu} ct) f_2(t)\, \mathrm{d}t \tag{33}$$

($\boldsymbol{\mu}$ is a unit vector along the direction of the permanent dipole $\boldsymbol{\mu}_0$). The correlation function $f_2(t)$ may therefore be obtained by direct Fourier transform of the observed spectral distribution $\alpha(\bar{\nu})$. Including the correction for an Onsager or Lorentz[84, 85] internal field (for a collection of correlated molecules) we have[84]

$$f_2(t) = \frac{3kT}{\pi^2 N\mu^2}\left[\frac{9n_0}{(n_0^2+2)^2}\right]c^2\int_0^\infty \alpha(\bar{\nu})\cos(2\pi\bar{\nu}ct)\mathrm{d}\bar{\nu} \tag{34}$$

where N is the number density and n_0 the refractive index (in the visible region). The various models[84, 86] available for the prediction of molecular rotational velocities may then be compared with the result for $f_2(t)$ obtained from equation (34). By this method one can not only test and compare the various models but one may also investigate[84–91] the importance of the absorption due to fluctuating electrical fields caused by collision induced forces (see below).

The models used include that originally suggested by Lassier and Brot[92] and developed by Larkin[93–95] This is based on a classical vectorial correlation function for angular (librational) harmonic motion of dipolar molecules (subjected to instantaneous hard collisions as in the Gordon M and J diffusion model[66]) in a multi-well potential of neighbours. The characteristics of this potential in terms of molecular interactions are not included explicitly in this model (except insofar as the librational motion is restricted by thermal collisions) since it is assumed that the potential is of the form

$$U(\theta) = V\sin^2(\pi\theta/2\xi) \tag{35}$$

where V and ξ are the potential depth and angular aperture respectively. Further, this model does not (as mentioned above) allow for the creation of induced dipoles and absorption due to fluctuations of the induced dipoles on collision.

Another model that has been tried[84] is the Wyllie–Hill–Larkin itinerant oscillator.[31, 93, 96, 97] In this model the librator is assumed to be damped (restricted) by the surrounding "cage" rigidity rather than by collisional interaction, and reorientational diffusion is against a viscosity dependent drag. Both inertial and damping effects are considered[93] in solving the appropriate (Langevin) equations of motion. It has been shown[84, 86] for a range of polar liquids that neither of these models produces correlation functions that agree well with the form of the experimental RVCF, $f_2(t)$. In addition to the neglect of induced dipole absorption there are two main reasons for this. Firstly the two models represent unrealistic extremes in the way in which the molecules are envisaged to interact. In particular, the potential represented by equation (35) leads to a mean square torque $\langle(OV)^2\rangle$ that is too large. This torque is given at short times for a linear

molecule[63] by

$$f_2(t) = \frac{\langle \dot{\boldsymbol{\mu}}(0) \cdot \dot{\boldsymbol{\mu}}(t) \rangle}{\langle \dot{\boldsymbol{\mu}}(0) \cdot \dot{\boldsymbol{\mu}}(0) \rangle} = 1 - \frac{1}{I}\left(2kT + \frac{\langle (OV)^2 \rangle}{4kT}\right)t^2 + O(t^4) \tag{36}$$

(I is the moment of inertia). Since the torque is the angular derivative of $U(\theta)$ [equation (35)] this becomes

$$f_2(t) = 1 - \frac{1}{I}\left[2kT + \left\langle \frac{\pi^2 V^2}{16kT\xi^2} \sin 2\left(\frac{\pi\theta}{2\xi}\right)\right\rangle\right]t^2 + O(t^4) \tag{37}$$

in which the coefficient of t^2 gives a much faster decay of $f_2(t)$ than that actually observed (and an associated high-frequency tail which is not present in the experimental spectrum). This is because the empirical fitting of V to the observed librational frequency "maximum"

$$\bar{\omega}_{\max} = (\pi/\xi)(V/2I)^{\frac{1}{2}} \tag{38}$$

takes no account of the band shape. For the Wyllie–Larkin model this is a consequence of the lack of explicit definition of the form of $U(\theta)$. For the Brot–Larkin model, on the other hand, the intermolecular torque tends to infinity for $t \to 0$ and the zero slope of the RVCF is never reached. Secondly there is a problem with the exact form of the internal field correction since a non-dispersive correction [equation (34)] does not affect $f_2(t)/f_2(0)$ and there is an almost total lack of $n(\bar{\nu})$ data in this frequency range. Thus, in principle, from equations such as (36) one can obtain intermolecular torques from far-infrared spectra but this involves using more reliable techniques than those described above.

Recently a number of authors[32, 33, 87–90, 97] have shown how more reliable far-infrared spectra of both polar and non-polar molecules can be simulated using a correlation function written[87, 89, 90, 97] in terms of a series of memory functions using the Mori formalism.[98] For any time-dependent correlation function, $C(t)$, it can be shown[97, 98] that

$$\partial[C(t)]/\partial t = -\int_0^t K_0(t - \tau)C(\tau)\,\mathrm{d}\tau \tag{39a}$$

$$\partial K_0(t)/\partial t = -\int_0^t K_1(t - \tau)K_0(\tau)\,\mathrm{d}\tau, \text{ etc.} \tag{39b}$$

where the set of memory functions $K_0(t) \ldots K_n(t)$ obey the set of coupled Volterra equations

$$\partial[K_{n-1}(t)]/\partial t = -\int_0^t K_n(t - \tau)K_{n-1}(\tau)\,\mathrm{d}\tau \tag{40}$$

Taking the Laplace transform of equation (40) gives[89]

$$C(p) = \frac{C(0)}{p + K_0(p)} = \frac{C_0}{p + K_0(0)/[p + K_1(p)]} = \ldots \tag{41}$$

which may be truncated at a convenient point and used for comparison with either the observed correlation function, e.g. in equation (34), or with the observed spectral profile, i.e. the Fourier transform of $C(t)$. The memory functions $K_n(t)$ have equilibrium averages $K_n(0)$ which may be related to the time expansion[89] of the correlation time [c.f. equation (18)]

$$C(t) = 1 - a_1 t^2/2 + a_2 t^4/4! - a_3 t^6/6! + \ldots. \tag{42}$$

For example

$$K_0(0) = -a_1 \tag{43a}$$

and

$$K_1(0) = a_1 - a_2/a_1. \tag{43b}$$

The $K_n(0)$ coefficients can be shown[63] to be torque dependent, and therefore information about intermolecular forces can be obtained by fitting the observed $C(t)$ or $\alpha(\omega)$ to expressions containing these quantities. It is usual to truncate equation (40) to include only $K_0(t)$ and $K_1(t)$. For far-infrared correlation functions (corresponding to absorption via permanent[87, 99, 100] or induced dipole[89, 90, 101] absorption) one then has

$$K_1(t) = K_1(0) \exp(-\gamma t) \tag{44}$$

assuming that $K_1(t)$, the normalised autocorrelation function of the torque derivative, is exponential and statistically Markovian.[102]

This gives

$$K_1(p) = K_1(0)/(p + \gamma) \tag{45}$$

and the inverse Fourier–Laplace transform of $C(p)$, equation (41), leads to

$$\alpha(\omega) = \frac{AK_0(0)K_1(0)\omega^2\gamma}{\gamma^2[K_0(0) - \omega^2]^2 + \omega^2\{\omega^2 - [K_0(0) + K_1(0)]\}^2} \tag{46}$$

with $A = (\epsilon_0 - \epsilon_\infty)/n(\bar{\nu})c$.

For rotational motions of linear and symmetric top molecules[89] $K_0(0)$ is simply $2kT/I_B$. $K_1(0)$ and γ are stochastic parameters, $K_1(0)$ being given by its relation via equation (43b) to a_2 where

$$a_2 = \tfrac{1}{3}\left(\frac{kT}{I_B}\right)^2 + \frac{1}{24I_B^2}\langle (OV)^2 \rangle \tag{47}$$

γ^{-1} is a correlation time distinct from, but related[100] to, the Debye rotational relaxation time. In the case of induced dipole absorption both $K_0(0)$ and $K_1(0)$ are related[31] to intermolecular torques. The approach using equations (41)–(47) has been considerably more successful in explaining the far-infrared spectra of polar and non-polar molecules than the approaches that employ modified instantaneous collision models[85] (for example modified M and J diffusion models). Some examples of the usefulness of this approach are given in Section III.

C. Vibrational Relaxation

As indicated in Section II.A it is necessary to include in the $\phi_v(t)$ function all the *non-rotational* contributions to the decay of $\Phi_{IR}(t)$, $\Phi_{iso}(t)$ or $\Phi_{aniso}(t)$ [equations (5) and (6)]. For a given mode (v) of a given molecule, i, these processes may include[28,103] one or all of the following: (a) vibrational energy transfer[28] to the "lattice" via rotational–translational degrees of freedom; (b) vibrational energy relaxation,[30,37,104–107] or energy redistribution, between various internal modes of the molecule; (c) resonance vibrational energy transfer[28,30,37,103,107] involving coupling of adjacent molecules via a particular vibrational coordinate; (d) band broadening effects occurring because of loss of phase coherence of the excited vibrations in a particular mode.[6,7,26,29,30,107–115] This progressive loss of phase coherence occurs because there is a distribution of the interaction of given "probe" or "active" molecules with surrounding molecules and this leads to a "spread" of transition frequencies. Effects (a) and (b) are essentially vibrational depopulation effects and as such are usually known as "energy relaxation" processes. Effects (c) and (d) are phase relaxation processes and are sometimes given the collective title of "inhomogeneous broadening". It was, until recently, thought that energy relaxation processes were much slower[116] than phase relaxation processes but Lauberau and coworkers[105,106,108] have shown that if the molecular level considered (an excited vibrational state) has one or more other levels in the neighbourhood then the energy redistribution process *may* have a relaxation time of the order of 1–5 ps.[108] Assuming, however, statistical independence of these two types of process we can write

$$\phi_v(t) = \phi_E(t)\phi_{pp}(t). \tag{48}$$

Both "self" and "exchange" terms occur in the phase relaxation function which is written[30,114]

$$\phi_{pp}(t) = \sum_{i,j} \langle Q_{vi}(0) . Q_{vj}(t) \rangle = \sum_{i} \langle Q_{vi}(0) . Q_{vi}(t) \rangle + \sum_{i \neq j} \langle Q_{vi}(0) . Q_{vj}(t) \rangle \tag{49}$$

where i and j refer to different molecules [cf. equation (9)]. Since the broadening processes depend on the spread of different vibrational frequencies of the "active" molecule (see above) it follows that they depend on the nature and extent of the interactions between the active molecule and its neighbours. Hence the rate of vibrational relaxation via these processes is a result of the extent of frequency distribution caused by the surrounding intermolecular potential. Thus, in principle, vibrational relaxation functions provide an invaluable "probe" for the study of such potentials. The major difficulty is that phase coherence loss may occur through many *different* types of molecular interaction, and in theory we must include all possible modes of interaction in $\phi_{pp}(t)$ [equation (49)]. Again assuming statistical independence, we have

$$\phi_{pp}(t) = \Pi_k \phi_{pp}^{(k)}(t) \tag{50}$$

where individual $\phi_{pp}^{(k)}(t)$ functions may be due to attractive interactions of the of the dipole–dipole, transition-dipole–transition-dipole, dipole–quadrupole (etc.) types or due to repulsive potentials. Fortunately, however, these different types of interaction may sometimes be distinguished experimentally[27, 30, 37, 53, 107] and it can sometimes be shown[30] that any one particular type of interaction affects a particular vibrational mode (at least to an overwhelming extent). In these favourable cases the variation of temperature, concentration and density will enable the nature and behaviour of the interaction to be studied in detail. Some examples of how this may be achieved are given in Section III.

As in the case of rotational and translational motions, it is necessary, for a detailed description of the mechanism of vibrational relaxation, to resort to models. As far as vibrational dephasing is concerned the principal model to have been constructed is that first applied to liquid phase data by Döge[26, 27] and others.[6, 7, 29, 109] Essentially, inhomogeneous broadening is assumed to arise from vibrational energy level shifts due to a stochastic perturbation which couples the oscillator to the surrounding potential. This results in each active molecule having a slightly different vibrational frequency due to its different interaction energy in the surrounding medium. If the vibrational frequency shift is $\Delta\omega$, it can be shown[62, 124] that the relaxation function $\phi_{pp}(t)$ is given by

$$\phi_{pp}(t) = \langle \exp[i\Delta\omega(t)] \rangle \tag{51}$$

since $\Delta\omega$ is time dependent owing to the (time dependent) stochastic variation of the intermolecular potential. Thus $\Delta\omega(t)$ represents a random process in the liquid. Assuming that this process is stationary in time and has Gaussian marginal distribution, the average value of $\exp[i\Delta\omega(t)]$ is obtained[62, 124] by taking a cumulant expansion and truncating after the

second term.[6,7] (All cumulants vanish except the second for a process having zero mean and Gaussian distribution.) Thus we get

$$\phi_{pp}(t) = \exp\left\{-\tfrac{1}{2}\left\langle\left(\int_0^t \Delta\omega(t)\,dt\right)^2\right\rangle\right\}. \tag{52}$$

If the time-dependent perturbation has a correlation function $g_\omega(t)$ and the mean square shift $\langle\Delta\omega^2\rangle$ is the same as in the absence of motion, then we can write

$$G_\omega(t) = \langle\Delta\omega^2\rangle g_\omega(t) \tag{53}$$

and the average in equation (52) is given by

$$\left\langle\left(\int_0^t \Delta\omega(t)\,dt\right)^2\right\rangle = 2\int_0^t (t-\tau)G_\omega(\tau)d\tau. \tag{54}$$

Introducing $G_\omega(t)$ from equation (53) and using (54) and (52) we then have

$$\phi_{pp}(t) = \exp\left\{-\langle\Delta\omega^2\rangle\int_0^t (t-\tau)g_\omega(\tau)d\tau\right\}. \tag{55}$$

If the correlation function, $g_\omega(t)$, of the modulation is exponential, i.e.

$$g_\omega(t) = \exp(-t/\tau_c) \tag{56}$$

then it can easily be shown that equation (55) reduces to

$$\phi_{pp}(t) = \exp\{-\langle\omega^2\rangle[t\tau_c + \tau_c^2[\exp(-t/\tau_c) - 1]]\}. \tag{57}$$

Notice that Lynden-Bell[117] has obtained this expression using an equivalent approach involving the solution of a Langevin equation for the diffusion of *angular velocity*. This emphasises that the stochastic modulation via $g_\omega(t)$ results in a modulation time τ_c which depends on the rate of *relative reorientational* (and/or collisonal[28,37,50,103]) motions of the surrounding molecules. The dephasing process is thus orientation dependent unless the intermolecular potential is orientation independent (for example, if short range, repulsive forces are predominant). At long and short times equation (57) may be simplified as follows.

For $t \ll \tau_c$ the oscillators vibrate with random phases in a "quasi-static" environment which has not had time to change. In this case the decay of $\phi_{pp}(t)$ is expected[62] to follow the Gaussian distribution of the environmental interactions. From (57) we obtain

$$\phi_{pp}(t) \approx \exp(-\tfrac{1}{2}\langle\omega^2\rangle t^2). \tag{58}$$

(This is valid in the whole experimental time domain if the slow modulation limit is valid.)

For $t \gg \tau_c$, i.e. for times much longer than the correlation time of the perturbation, it is clear from equation (57) that the $\phi_{pp}(t)$ function will be represented by a single exponential

$$\phi_{pp}(t) \simeq \exp(-\langle\omega^2\rangle\tau_c t) = \exp(-t/\tau_p) \tag{59}$$

where

$$(\tau_p)^{-1} = \langle\omega^2\rangle\tau_c \tag{60}$$

These two situations are shown in Fig. 5.

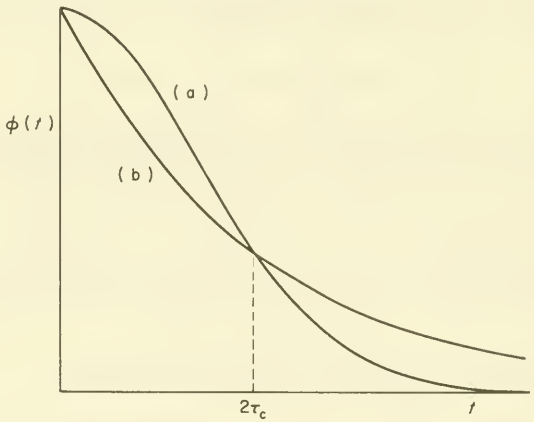

FIG. 5. Illustrating the behaviour of the correlation function $\phi(t)$ for $t \ll \tau_c$ (curve a) and for $\tau \gg \tau_c$ (curve b) for a Gaussian random modulation. [Reproduced with permission from R. Kubo, in "Fluctuation Relaxation and Resonance in Magnetic Systems" (ed. D. Ter Haar). Oliver and Boyd, London (1962), p. 26]

Depending on the rate of the modulation process due to fluctuations of the intermolecular potentials, prediction can be made about the band profile.

In the slow modulation limit ($\tau_c\langle\omega^2\rangle^{\frac{1}{2}} \gg 1$) the perturbation effectively lasts for a long time and the phase memory of the oscillators is rapidly lost.[28] The $\phi_{pp}(t)$ function therefore decays rapidly and has essentially Gaussian form [equation (55) and Fig. 6] with a small long time exponential tail. The band profile is obtained by Fourier transformation of equation (51).

$$I(\Delta\omega) = \exp[-\tfrac{1}{2}(\Delta\omega)^2/\langle(\Delta\omega)^2\rangle]. \tag{61}$$

For rapid modulation ($\tau_c\langle\omega^2\rangle^{\frac{1}{2}} \ll 1$) the perturbation due to fluctuations in the intermolecular potentials rapidly decays and the phase memory of the oscillators is retained for longer times.[28, 30] $\phi_{pp}(t)$ therefore decays more slowly and hence the band profile significantly narrows and for times $t > \tau_c$

an exponential decay is observed [equation (59) and Fig. 6]. Fourier transformation of equation (59) then yields the band profile as

$$I(\Delta\omega) = \frac{1}{\pi}\left\{\frac{\gamma}{\Delta\omega^2 + \gamma^2}\right\} \tag{62}$$

where

$$\gamma = \langle\omega^2\rangle\tau_c \tag{63}$$

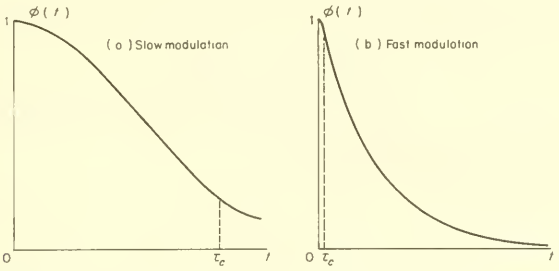

FIG. 6. Illustrating the behaviour of $\phi(t)$ in the slow modulation ($\tau_c\langle\omega^2\rangle^{1/2} \gg 1$) and rapid modulation ($\tau_c\langle\omega^2\rangle^{1/2} \ll 1$) limits. [Reproduced with permission from R. Kubo, in "Fluctuation Relaxation and Resonance in Magnetic Systems" (ed. D. Ter Haar), Oliver and Boyd, London (1962), p. 26]

(the band half-width). Since $\tau_c\langle\omega^2\rangle^{\frac{1}{2}} \ll 1$ it follows that $\gamma \ll \langle\omega^2\rangle^{\frac{1}{2}}$, and a "motional narrowing" situation[26, 30, 118–123] arises. It should be noticed, however, that at *short* times (high frequency displacements from the band centre) the $\phi(t)$ function will eventually reflect a Gaussian intensity distribution. This is essential to retain the correct behaviour of the band moments (since a Lorentzian profile has no finite second or higher moments).

If it is possible to obtain reliable second-moments from integration of the isotropic Raman band profile or by calculating $(\mathrm{d}\ln\phi_{pp}(t)/\mathrm{d}t)_{t=0}$ [see equation (58)] then both τ_c and $\langle\omega^2\rangle$ can be obtained experimentally and both contain valuable information about the nature of the intermolecular potential. Since τ_c represents a modulation time it is related to the time scale of the molecular fluctuations in the medium. The second moment measures the range of frequency distribution due to the various molecular interactions.[26–30] Three types of contributing molecular interaction have so far been considered in detail in the interpretation of experimental vibrational relaxation times and (vibrational) second-moments.

1. Transition-dipole–Transition-dipole Interactions[26–30]

These cause resonance energy transfer between oscillators on adjacent molecules.

The transition moment for transitions between states v and v' is[125]

$$\boldsymbol{\mu}'_{v'v} = \left(\frac{\partial \boldsymbol{\mu}}{\partial Q}\right)_{Q=0} \langle v' | Q | v \rangle \tag{64}$$

where $(\partial\boldsymbol{\mu}/\partial Q)_0$ is obtained via infrared intensity data. The interaction energy between two such dipoles is ϵ_{ij} where

$$\epsilon_{ij} = \int \phi_i V_{ij} \phi_j \mathrm{d}t \tag{65}$$

and the intermolecular potential V_{ij} is assumed to be given by

$$V_{ij} = (-\boldsymbol{\mu}'_{v'v}/R_{ij}^3)K_{ij} \tag{66}$$

where K_{ij} describes the relative orientations of the coupled oscillators and R_{ij} is the intermolecular distance.

It can then be shown[26,27] that

$$\epsilon_{ij} = \frac{-K_{ij}}{R_{ij}^3}\left(\frac{\partial \boldsymbol{\mu}}{\partial Q}\right)_{Q=0}^2 \frac{1}{2\gamma} \tag{67}$$

($\gamma = 2\pi\nu_0/\hbar$). Averaging the frequency distribution ($\epsilon_{ij}/\hbar$) over all K_{ij} and R_{ij}, one gets the second moment for the fundamental band ($v' = 1, v = 0$) as

$$\langle \omega^2 \rangle_{II} = \bar{Z}\left(\frac{AB\boldsymbol{\mu}_{10}^2}{R_{ij}^3\hbar}\right)^2 \tag{68}$$

where $\boldsymbol{\mu}_{10}^2 = (\partial\boldsymbol{\mu}/\partial Q)^2(1/2\gamma)$. The constants A and B are related to the radial distribution function and the transition-dipole length respectively. $\bar{Z}$ is the mean number of molecules in the first coordination shell.

A similar expression has been obtained[109a] independently by van Woerkom and his coworkers. The most important general conclusion reached by both groups was that the distribution of frequencies due to this type of interaction depends on the infrared fundamental intensity ($\propto \partial\boldsymbol{\mu}_0/\partial Q_i$, Q_i being the normal coordinate of the relevant mode). Except in the extreme slow modulation limit, the observed band shape also depends on a modulation time τ_c [see equation (57)]. For transition-dipole–transition-dipole (i.e. long range) interactions the τ_c parameter depends on the rate of reorientational and/or translational motions. In this case therefore $\tau_c \propto \tau_{1R'}$.

2. Dipole–Dipole Interactions[30,53,107]

Such interactions give rise to spectral broadening because, for an anharmonic oscillator, the time average of the dipole moment in the two states v and v' is different. This means that the interaction of the vibrating molecule with the surrounding permanent dipoles influences the energy of the transition

$v' \leftarrow v$. The dipole moment difference for the fundamental mode ($v = 1 \leftarrow 0$) is $\Delta_{01}\boldsymbol{\mu} \equiv \boldsymbol{\mu}_{11} - \boldsymbol{\mu}_{00}$ where

$$\Delta_{01}\boldsymbol{\mu} = \left(\frac{\partial \boldsymbol{\mu}}{\partial Q_{iv}}\right)_0 [\langle 1|Q|1\rangle - \langle 0|Q|0\rangle] + \tfrac{1}{2}\left(\frac{\partial^2 \boldsymbol{\mu}}{\partial Q_{iv}}\right)_0 [\langle 1|Q^2|1\rangle - \langle 0|Q^2|0\rangle]. \tag{69}$$

The interaction of $\Delta_{01}\boldsymbol{\mu}_i$ with the permanent (ground state) dipole $\boldsymbol{\mu}_{0j}$ is then

$$\Delta D_{ij} = (\Delta_{01}\mu)_i \mu_{0j} K_{ij}/R_{ij}^3. \tag{70}$$

The second moment of the distribution of $\Delta D_i = \Sigma \Delta D_{ij}$ (summed over all pairwise interactions) can be shown[30, 107] to be

$$\langle \omega^2 \rangle_{dd} = \bar{Z}\{(\Delta_{01}\mu)\mu_{0j} AB/R_{ij}^3 h\}^2. \tag{71}$$

From (69) it is clear that $\Delta_{01}\boldsymbol{\mu}$ depends on the extent of both mechanical and electrical anharmonicity, and so (70) can, in principle, be calculated if $\partial^2\boldsymbol{\mu}/\partial Q^2$ is obtainable from the intensity of the *infrared* first overtone band and the mechanical anharmonicity is ignored. Again, because these interactions are due to long range forces, the τ_c modulation time corresponds to a rotational or translational correlation time.

The principles outlined above demonstrate clearly the importance of *combined* Raman and infrared band shape and intensity studies in attempting to elucidate the type of intermolecular potential responsible for Raman (isotropic) band-broadening. Lynden-Bell[114] in a recent paper has emphasised the complementary nature of the techniques but has also shown that, when resonant vibrational energy transfer via dipolar interactions is important, i.e. when there is a non-zero exchange term in equation (49), then cross terms may occur between "self" (F_s) and "exchange" (F_e) contributions to the broadening

$$F_s \propto \mu_{0j} \cdot \partial^2 \mu_i / \partial Q_i^2 \tag{72a}$$

$$F_e \propto \frac{\partial \mu_i}{\partial Q_i} \cdot \frac{\partial \mu_j}{\partial Q_j} \tag{72b}$$

(i and j refer to different molecules). These cross terms enter only for dephasing processes affecting the isotropic Raman band profile, and therefore the vibrational part of the $l = 0$ spectrum is *different* from that of the $l = 1$ (infrared) and $l = 2$ (anisotropic Raman). There are also symmetry restrictions on the terms in the intermolecular potential which can lead to relaxation, and so not all possible long range interactions may affect all vibrational modes. The terms which contribute to the normal modes of molecules which belong to some commonly studied point groups are summarized in Table 1.

TABLE I. Contributions to vibrational relaxation for normal modes of various symmetries. Capital letters denote self terms; lower case, exchange terms; W = dispersion; D = dipolar; and Q = quadrupolar [Reproduced with permission from Ref. 114]

	Mode	VV Raman $l = 0$	VH Raman $l = 2$	Infrared $l = 1$
C_{3v}	A_1	$(W + w)^2 + (D + d)^2$	$W^2 + w^2 + D^2 + d^2$	$W^2 + w^2 + D^2 + d^2$
	E		$W^2 + D^2 + d^2$	$W^2 + D^2 + d^2$
D_{3h}	A_1	$(W + w)^2 + (Q + q)^2$	$W^2 + w^2 + Q^2 + q^2$	
	A_2			$w^2 + d^2 + Q^2$
	E		$W^2 + d^2 + Q^2 + q^2$	$w^2 + d^2 + Q^2 + q^2$
	E		$W^2 + Q^2 + q^2$	
$C_{\infty v}$	Σ	$(W + w)^2 + (D + d)^2$	$W^2 + w^2 + D^2 + d^2$	$W^2 + w^2 + D^2 + d^2$
	Π		$W^2 + D^2 + d^2$	$W^2 + D^2 + d^2$
$D_{\infty h}$	Σ_g^+	$(W^2 + w)^2 + (Q + q)^2$	$W^2 + w^2 + Q^2 + q^2$	
	Σ_u^+			$W^2 + d^2 + Q^2$
	Π_u			$W^2 + d^2 + Q^2$
	Π_g		$W^2 + Q^2 + q^2$	
T_d	A_1	$(W + w)^2$		
	E		$W^2 + q^2$	
	T_2		$W^2 + d^2(+q^2)$	$W^2 + d^2(+q^2)$
O_h	A_{1g}	$(W + w)^2$		
	E_g		$W^2 + q^2$	
	T_{2g}		$W^2 + q^2$	
	T_{1u}			$W^2 + d^2$

3. Repulsive (Short Range) Interactions

There have recently been a number of attempts to interpret measured vibrational relaxation times in terms of models that rely on an entirely repulsive intermolecular potential. For example, calculation[103] of vibrational band-widths due to resonant transfer of vibrational energy by repulsive interaction has been compared with broadening effects due to TD–TD interactions. Other authors[37] have used a repulsive model for comparison of the expected rates of energy relaxation and vibrational dephasing, in attempting to estimate the relative importance of these possible broadening processes.

Rothschild[103] has used the exponential repulsive potential

$$V = V_0 \exp(-\alpha r_{ij}) \tag{73}$$

(where r_{ij} is the radial distance between the interacting molecules) to obtain an expression for the value of matrix elements of the Hamiltonian $\hat{\mathscr{H}}'_{\text{rep}}$ for

the kth fundamental vibration as

$$\langle 1,0|\hat{\mathscr{H}}'_{\text{rep}}|0,1\rangle = -\alpha^2 V_0 \exp(-\alpha R_{ij})\left(\sum_n \frac{\partial s_n^i}{\partial Q_k}\right) \times \left(\sum_n \frac{\partial s_n^j}{\partial Q_k}\right)\frac{\hbar}{2\omega_k}\frac{(\boldsymbol{R}_{ij}.\boldsymbol{s}_k^i)(\boldsymbol{R}_{ij}.\boldsymbol{s}_k^j)}{\boldsymbol{R}_{ij}^2}. \tag{74}$$

Here s^i and s^j are the atomic displacement coordinates for the kth normal mode Q_k (frequency ω_k) and $\boldsymbol{R}_{ij}$ is the distance between the centres of the molecules i and j, i.e.

$$r_{ij} \simeq \boldsymbol{R}_{ij} - s^i + s^j. \tag{75}$$

(It should be noted, as pointed out by Fischer and Laubereau,[108] that the linear terms in s are eliminated in calculating $\hat{\mathscr{H}}'_{\text{rep}}$ since they contribute only to dissipative vibrational relaxation, i.e. population relaxation.) The rms frequency displacement (cm^{-1}) due to resonance energy transfer is then

$$\Delta\omega_{\text{rep}} \simeq \hbar^{-1}\{\langle|\hat{\mathscr{H}}'_{\text{rep}}|^2\rangle\}^{\frac{1}{2}} \simeq \frac{V_0}{12}(\rho/\pi^3)^{\frac{1}{2}}\exp(-\alpha d)\left(\frac{d^2\alpha^3}{2} - \frac{d\alpha^2}{2}\right)^{\frac{1}{2}}\left(\sum_n \frac{\partial s_n}{\partial Q_k}\right)^2 \frac{v_k^{-1}}{c} \tag{76}$$

where d is the distance of closest approach of the molecules (which can be estimated from Lennard-Jones diameters[103]) and ρ is the number density. The parameters α and V_0 of equation (76) can be estimated using known repulsive potentials of rare-gas atoms.[112]

It should be noted that the broadening $\Delta\omega_{\text{rep}}$ due to this mechanism is independent of temperature since the zero modulation limit is assumed to apply, i.e. that the rotational and translational motions of the molecule are ignored (see Section II.B) and the potential (73) has been averaged over all intermolecular orientations and distances. The broadening calculated from (76) is thus a Gaussian, full half-width *increment* which is caused by a static distribution of interactions. Any motional narrowing introduced for a repulsive potential would be mainly from translational motions since orientational diffusion would affect mainly long range forces. It should also be noted that the observed isotopic dilution sensitive part of ν_4 of $CHCl_3$ (see Section III) can be equally well predicted using a model based on a transition-dipole–transition-dipole mechanism[111] or using a Lennard-Jones 6-12 potential.[112]

The calculation of relative relaxation rates due to dephasing and level depopulation has also been achieved using the theory of collinear isolated binary collisions (i.e. using short range interactions). The work of Laubereau and Fischer[108] illustrates the general level of theoretical development

carried out so far. To a first approximation energy relaxation and dephasing processes are assumed to be independent of each other, and

$$1/\tau = 1/\tau_{ph} + 1/\tau' \tag{77}$$

where τ is the total relaxation time and τ_{ph} and τ' are relaxation times due to loss of phase correlation and depopulation respectively. As mentioned above, dephasing occurs via interaction terms which are quadratic in the oscillator amplitude. Thus it is necessary to calculate an expression for τ_{ph} where

$$\langle Q_k \rangle^2 \propto \exp(-t/\tau_{ph}) \propto \exp(-\delta\phi^2(t)/2) \tag{78}$$

Q_k represents *both* amplitude and phase of the normal coordinate and $\delta\phi$ is the time dependent phase distribution caused by a phase change of $\Delta\phi$ at each collision. So

$$\delta\phi = a\,\Delta\phi N^{\frac{1}{2}} = a\Delta\phi t/\tau_c \tag{79}$$

where a is a constant, N is the collision number and τ_c the time between collisions.

From equations (78) and (79) it is easily shown that

$$\tau_{ph} = 2\tau_c/(a^2\Delta\phi^2) \tag{80}$$

where τ_c and $\Delta\phi$ depend on the temperature, density and intermolecular potential.

More rigorously, an expression for τ^{-1} has been obtained in terms of the interaction part of the Hamiltonian $\hat{\mathscr{H}}'(t)$ which depends on the frequency shift $\Delta\omega_j(t)$ caused by time dependent intermolecular interactions. The dephasing rate is then

$$\tau_{ph}^{-1} = \frac{1}{\tau_c}\left|\int_{-\infty}^{+\infty} \Delta\omega_j(t)\mathrm{d}t\right|^2 \tag{81}$$

and

$$\begin{aligned}\tau^{-1} &= \frac{1}{\tau_v}\sum_{j(E_i = E_f)}\left|\int_{-\infty}^{+\infty}\langle i|\hat{\mathscr{H}}'(t)|f\rangle\,\mathrm{d}t\right|^2 \\ &\quad + \frac{1}{\tau_c}\sum_{j(E_i \neq E_f)}\left|\int_{-\infty}^{+\infty}\langle i|\hat{\mathscr{H}}'(t)|f\rangle\,\mathrm{d}t\right|^2 \\ &= \tau_{ph}^{-1} + (\tau')^{-1}\end{aligned} \tag{82}$$

where the potential is assumed to be modulated by isolated binary collisions (i.e. instantaneous collisions). Equation (82) emphasises that dephasing occurs via quasi-elastic collisions corresponding to adiabatic fluctuations of the initial and final energy states, E_i and E_f (i.e. there is *no energy change*

between states of the same jth molecule). The energy relaxation process on the other hand is due to inelastic collisions and therefore non-adiabatic transitions between different vibrational states.

The intermolecular potential is assumed by Fischer and Laubereau to be of the form

$$V(Q, R) = E \exp(\gamma Q/L - R/L) \tag{83}$$

where L measures the range of the interaction[127] and R is the distance between the centre of mass of the oscillator AB and the atom C with which it collides (E and γ are energy and mass factors respectively). It may then be shown that for a time-dependent R

$$\hat{\mathscr{H}}'(t) = \tfrac{1}{2}E(\gamma/L^2)Q^2 \operatorname{sech}^2\{(E/2\mu)^{\frac{1}{2}}t/L\} \tag{84}$$

where μ is a reduced mass for the system A—B ... C. It then follows from equations (80)–(82) that

$$(\tau_{ph})^{-1} = \frac{9}{2}\frac{\mu\gamma^4}{M^2}\frac{k_B T}{\omega^2 L^2}\frac{1}{\tau_c} \tag{85}$$

where M is the reduced mass of the oscillator with frequency ω and E has been given the value $k_B T$. Using (82) one can obtain τ' as

$$(\tau')^{-1} \simeq \{2\pi^2\omega L^2\mu^2\gamma/M\tau_c\hbar\} \exp\{-2\pi mL(\mu/\hbar\omega)^{\frac{1}{2}}\} \tag{86}$$

It should be noticed that the frequency dependencies of these expressions (85) and (86) are different. The energy relaxation rate $(\tau')^{-1}$ depends exponentially on ω while the dephasing rate $(\tau_{ph})^{-1}$ has quadratic dependence on ω. Thus, if $\hbar\omega \gg k_B T$ dephasing is likely to dominate, while at low frequencies of vibration the interconversion of vibrational and translation energies becomes more favourable. Both experimental data and calculations have shown that $\tau' \gg \tau_{ph}$ (sometimes by many orders of magnitude) and it has become customary to ignore, sometimes maybe erroneously, the effects of energy relaxation processes in interpreting the correlation functions obtained from spontaneous Raman spectra.

Oxtoby and Rice[110a] using a similar but somewhat more general technique (but also employing an isolated binary collision model with an effectively predominantly repulsive potential) have shown that equation (85) needs a small numerical correction (the factor 9/2 becomes 4). This correction has been employed by subsequent users.[37]

One interesting feature of the calculation of $(\tau_{ph})^{-1}$ and $(\tau')^{-1}$ from equations (85) and (86) is the interpretation and determination of τ_c which is described using these models as the "time between collisions". Litovitz and coworkers[14, 51, 127, 150] using a previous IBC model approximated this time to an Enskog time for the rate of binary collision of hard spheres (which may

be calculated from the time between collisions in the dilute gas and the compressibility factor) using a "cell" model[57, 150] (for which one has to make an assumption about the "packing" properties of the liquid molecules). More recently several authors[37, 122] have used a τ_J value, which may be in principle measured using the Gordon J diffusion[66, 68–74] (collision-interrupted free rotation) model. Using the IBC model the energy relaxation time is given by

$$(\tau')^{-1} = P_{1\leftarrow 0}(T)[1 - \exp(\hbar\omega/k_B T)](1/\tau_c) \tag{87}$$

where $P_{1\leftarrow 0}(T)$ is the temperature dependent transition probability for the fundamental vibrational band. However $P_{1\leftarrow 0}(T)$ is not easy to evaluate and it appears that equation (86) provides the best means of calculating τ' at present.

III. EXAMPLES OF THE DETERMINATION OF INTERMOLECULAR FORCES USING INFRARED AND RAMAN SPECTROSCOPY

In this section we attempt to show how the techniques described in Sections I and II have been used to elucidate the nature and extent of the intermolecular forces in some simple liquids. There is no intention that this should be an exhaustive account, even for the molecules considered. Rather, we have tried to present an illustrative and critical account for a few examples, pointing out the achievements so far and the difficulties that hinder or prevent further progress.

A. Simple Liquids

We have used the term "simple liquids" for liquids consisting of small molecules for which the orientation dependent interactions are smaller than the thermal energy kT. This condition is described quantitatively for dipolar intermolecular interactions by

$$\mu_0^2/R_{ij}^3 < kT \tag{88}$$

where μ_0 is the permanent dipole-moment and R_{ij} are intermolecular distances. As described above, one of the techniques available for the study of molecular interactions is via the determination of vibrational relaxation functions (VRF) calculated from the isotropic parts of band profiles measured in a spontaneous Raman scattering experiment. These functions consist generally of a product of an energy relaxation function $\phi_E(t)$[30, 37, 104–107] and a pure phase-relaxation function $\phi_{pp}(t)$[6, 7, 26, 29, 30, 107–115] [equation

(48)]. The phase-relaxation functions obtained using the Kubo model [see Section II.C; equations (51)–(57)] are described in the slow modulation limit by the vibrational second-moment $(M2)_v$ (or $\langle\omega^2\rangle$)[6, 7, 28, 103, 115] and in the rapid modulation limit the vibrational relaxation rate is directly proportional to the product of the parameters $(M2)_v$ and τ_c.[6, 26, 28, 109, 114] Thus the relaxation rate (for this model) is given by

$$\tau_v^{-1} = (M2)_v \tau_c. \tag{89}$$

For reorientational/translational motions (depending principally on long-range dipolar-interactions), τ_c is directly proportional to the dynamic viscosity[151] (and inversely proportional to the absolute temperature) so

$$\tau_v^{-1} \propto \rho\eta/T \tag{90}$$

since the second moment is directly proportional to the liquid density. Notice, however, that using *other* models, for example, dephasing or energy relaxation by hard collisions (Fischer and Laubereau[108]) or the IBC model of energy relaxation used by Litovitz and coworkers,[127, 150] the vibrational relaxation rate is directly proportional to $1/\tau_c$ [equations (86) and (87)]. Using these models τ_c is equivalent to a time between collisions (given by τ_J[68, 69] or calculated from a "cell" or "Enskog" model[37, 122]) and it is therefore proportional[76] to $1/\eta$. It is thus evident that the τ_v^{-1} values should have the *same* viscosity dependence regardless of the model used. Thus current theories on vibrational dephasing predict the following behaviour for these two parameters under different experimental conditions.[6, 26, 28, 115]

(1) Variation of $(M2)_v$ in the pure liquid: (a) decrease with increasing temperature at constant pressure; (b) no variation with increasing temperature at constant density; (c) increase with increasing density at constant temperature.

(2) Variation of τ_c in the pure liquid and in mixtures: (a) for long range dipolar $\tau_c \propto \tau_{1R} \propto \eta/T$ (IR reorientational correlation time, for example); (b) for short range repulsive forces $\tau_c \propto \tau_J \propto 1/\eta$ (collision time in the J-diffusion model, for example).

(3) Variation of $(M2)_v$ in mixtures: (a) for band broadened by resonant transfer of vibrational energy; decrease on isotopic dilutions; (b) for band broadened by dipolar interaction; decrease on dilution in a non-polar solvent and increase on dilution in a solvent with a higher dipole moment; (c) for band broadened by a "specific" interaction; decrease by dilution with a solvent in which interaction is smaller or is removed.

To interpret the experimental results of a study of the VRF of a particular band in the pure liquid it is therefore useful to perform dilution studies in various solvents with the aim of changing the types of interaction of the active molecules with their neighbours. In this way one can expect to get

information about the interactions that influence the band shape in the pure liquid. The isotopic dilution method is important for the determination of those interactions that lead to a resonant transfer of vibrational quanta.[26–30, 109, 118] The experiment can be performed in those cases where the band under investigation is considerably shifted on deuteration (or generally on isotopic substitution of an atom or a group of atoms). Dilution studies in polar and non-polar solvents can give information about dipolar interactions and other specific types of intermolecular potential.[26, 30, 118, 129–131]

One of the substances most extensively studied by spontaneous Raman scattering is methyl iodide, CH_3I, since it is a small molecule with well separated vibrational bands and the band profiles are not disturbed by isotope effects. The study of the isotropic part (I_z) of the ν_3(C—I) stretching band has been the aim of many investigations. It was found[26, 30, 119, 120, 122, 123, 132–134] that the vibrational relaxation rate τ_v^{-1} decreased with increasing temperature. In one study[122] the pressure was also varied and it was shown that (i) the rate τ_v^{-1} increases with increasing density at constant temperature, and (ii) τ_v^{-1} remains approximately constant with increasing temperature at constant density. The whole vibrational relaxation function was attributed to energy relaxation and the experimental facts were theoretically explained on the basis of the IBC (binary collision) model[122, 132] that contains as parameters the transition probability and the collision rate [see equation (87)]. In recent paper[30] the three totally symmetry A_1 vibrations of CH_3I, ν_1, the CH_3 stretching vibration, ν_2, the CH_3 bending mode and ν_3 were compared. It was discovered that all three bands have about the same vibrational correlation time τ_v at room temperature, but that the temperature and solvent dependences were different for the three vibrations. This indicates that they are broadened by different types of intermolecular interaction. For ν_2 and ν_3 the correlation time τ_v increased and for ν_1 it decreased on raising the temperature (at constant pressure). From the results of dilution studies it was concluded that the VRF of ν_2 and ν_3 are due to the loss of phase coherence of the active molecules. The decay of the VRF of ν_3 seems to be caused by the (long range) interactions of the permanent dipoles of the CH_3I molecules with the mechanical and electrical anharmonicity of the C—I vibration (see Section II.C.2). The qualitative interpretation of the relaxation rate of ν_3 using the collision models[122] of equations (85)[108] and (86) assuming short range repulsive potentials to be the effective intermolecular potential seems to be incorrect . Although the pressure and (or) temperature dependence of τ_v^{-1} is predicted correctly the solvent dependence of τ_v^{-1} in non-polar solvents[30, 152] cannot be explained by these models, while all the experimental facts *can* be interpreted assuming that long range dipole–dipole interactions are dominant in the effective

intermolecular potential for this mode.[30, 152] Since physically totally different models are able to explain the experimental data qualitatively (at least in the pure liquid) one sees the importance of performing dilution studies in order to determine the type of intermolecular potential causing the decay of the VRF. Only then can one decide what is the best model to apply for a particular band.

The extensive narrowing of ν_2 on isotopic dilution[26, 30, 132] (see Fig. 7)

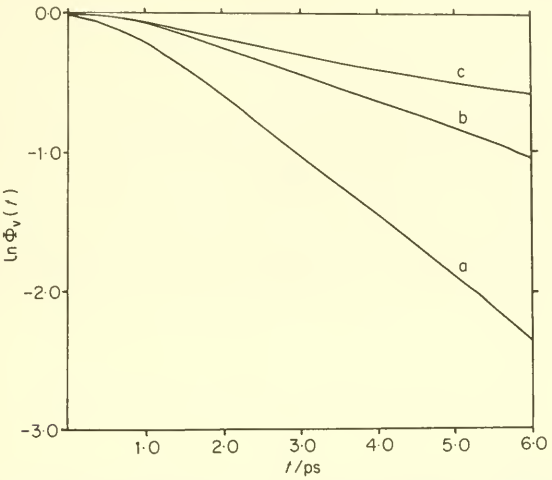

FIG. 7. Vibrational correlation functions for ν_2 of methyl iodide: a, pure liquid; b, solution in CD_3I, c, solution in CS_2. [Reproduced with permission from G. Döge, R. Arndt and A. Khuen, *Chem. Phys.*, **21**, 53 (1977)]

and the high infrared intensity indicate that ν_2 is mainly broadened by a resonant transfer of vibrational energy due to transition-dipole–transition-dipole interactions. In Table II one finds the results of a computer fit of the experimental VRF for ν_2 using equation (57). The vibrational second moment $(M2)_v$ decreases [see paragraph 1(a) above] and the τ_c modulation

TABLE II. Values for τ_c and $\langle\omega^2\rangle$ for ν_2 of methyl iodide (liquid) from a computer fit of the experimental vibrational relaxation functions

τ_c/ps	$10^{-24}(M2)_v$/rad^2 s^{-2}	Temperature/K
0·96	1·03	213
0·86	0·97	233
0·77	0·91	253
0·66	0·87	273
0·62	0·79	293

time (which is for this intermolecular potential proportional to τ_{1R}) shows the correct variation with increasing temperature. In a further investigation[135] the concentration dependence of $(M2)_v$ and τ_c of ν_2 on dilution with CD_3I and CS_2 was studied. In Fig. 8 it is shown that modulation time τ_c of the solvent dependent part of ν_2 does *not* vary on isotopic dilution as usually

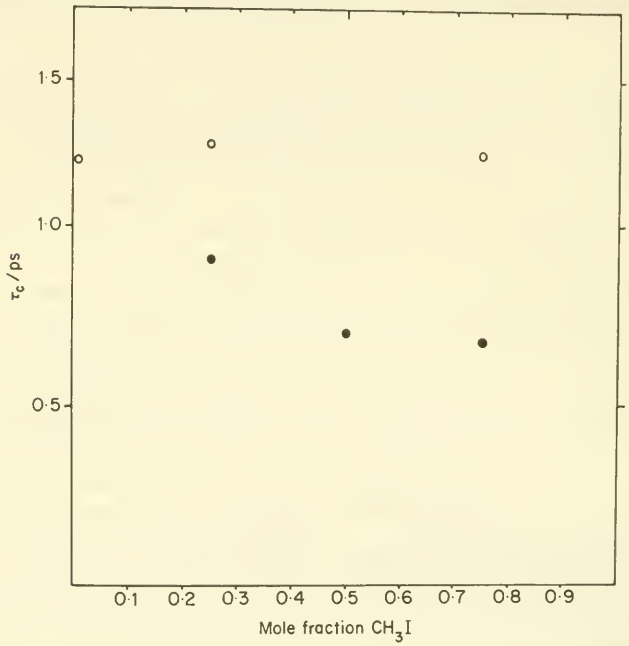

FIG. 8. Concentration dependence of the modulation time τ_c of the solvent dependent part of ν_2 of CH_3I; the solvents are CD_3I (○) and CS_2 (●).

assumed but decreases with increasing concentration of CS_2. This behaviour is similar to the results of variations[119] of τ_{2R} ($\approx \tau_{1R} \approx \tau_c$) of CH_3I in CS_2.

From a recent investigation[105] (probing the incoherent anti-Stokes scattering after an infrared excitation pulse) one can conclude that the main part of the VRF of ν_1 of CH_3I is due to energy relaxation and redistribution processes. This experimental result enables the direct study of energy relaxation using the method of spontaneous Raman scattering which is superior to the above method as far as time resolution and reproducibility are concerned. In Table III one finds the values of a computer fit of the VRF of ν_1 using equation (57). The variation of $(M2)_v$ contradicts the predictions of dephasing theories, 1(a), as it increases with increasing temperature at constant density. Dilution studies with CD_3I and CS_2 confirm the interpre-

TABLE III. Values for τ_c and $(M2)_v$ for ν_1 of methyl iodide (liquid) from a computer fit of the experimental vibrational relaxation functions

τ_c/ps	$10^{-24}(M2)$/rad^2 s^{-2}	Temperature/K
0·75	0·68	213
0·63	0·81	233
0·55	0·93	253
0·49	1·06	273
0·43	1·21	293

tation of the VRF as being due to intramolecular relaxation.[30,135] In mixtures of CH_3I with CCl_4 (Fig. 9) one observes a big frequency shift and a minimum in the τ_v value at intermediate concentrations.[135] These results can be interpreted in terms of an additional decay of the VRF due to the distribution of vibrational frequencies caused by concentration fluctuations in the neighbourhood of the active molecules. The variation of τ_v^{-1} as a function of frequency shift with concentration, $d\nu/dx$ is quantitatively

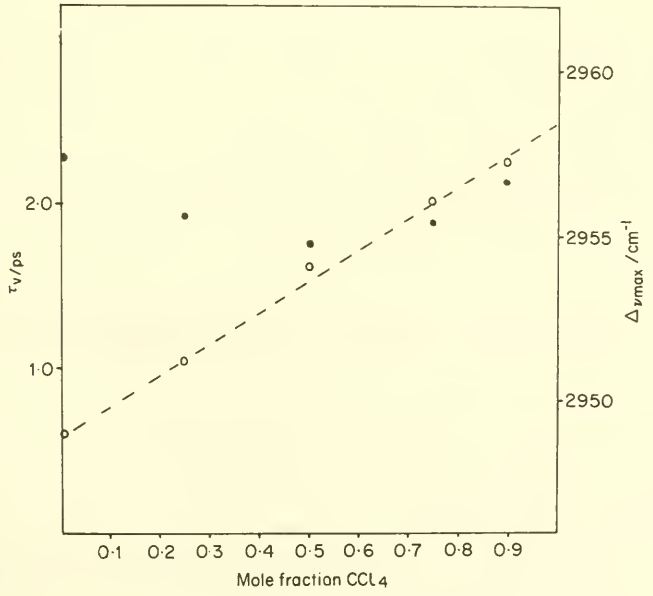

FIG. 9. Solvent dependence of τ_v and $\Delta\bar{\nu}_{max}$ for ν_1 of CH_3I mixtures with CCl_4 (filled circles refer to τ_v and open circles refer to $\Delta\bar{\nu}_{max}$).

described by the expression[136, 137]

$$\Delta\nu_{\frac{1}{2}} = 2(\ln 2)^{\frac{1}{2}} \frac{d\nu}{dx} \sqrt{\frac{C(1-C)}{n}} \frac{d\nu}{dx}$$

where $\Delta\nu_{\frac{1}{2}}$ is the full width at half-height (related to τ_v^{-1}), C the mole fraction of solute and n the number of molecules in the fluctuating volume. In infrared experiments the same effect was found for dilution of ν_1 of $CHCl_3$ in CS_2[136, 137] and for the isotropic part of ν_1 of $CDCl_3$ in CS_2 dilution.[129] The interpretation of an infrared dilution experiment in terms of vibrational relaxation is complicated, however, by the fact that both $\phi_v(t)$ and $\phi_{1R}(t)$ vary on dilution and this can lead to misinterpretation of the experimental results.

Another source of information about the ground state interactions in CH_3I is given by the analysis of the anisotropic part of the Raman bands $I(\omega)$. In addition to the determination of reorientational second moments and mean square torques $\langle(OV)_\perp^2\rangle$ (derived from fourth moments in the frequency domain[63]) one gets the reorientational correlation function in the time domain after deconvolution of the vibrational part and the apparatus profile [arising from the use of a finite slit; see equation (5)].

A comprehensive analysis of the reorientational part of all three A_1 vibrations seems to indicate that only the ν_1 vibration–rotation Raman band is affected by a Coriolis coupling of ν_1 with the neighbouring ν_4 mode and that this complicates the analysis of this band.[132] The results of studies[134] of the reorientational part of ν_3 and the depolarised Rayleigh wing show a significant difference in $D_\perp^{Ram}$ and $D_\perp^{Ray}$ indicating a collective contribution to the reorientational tumbling motion of the CH_3I molecules. The temperature dependence for both $D_\perp$ values is the same and is described by an activation energy $E_\perp^{Ram} = 8{\cdot}8\ \text{kJ mol}^{-1}$ and $E_\perp^{Ray} = 9{\cdot}2\ \text{kJ mol}^{-1}$. In some studies[119] the rotational second-moment of ν_3 was much smaller than the classical value[122, 123] while in another experiment[119] $(M2)^{exp}$ had the same size as $(M2)^{th}$.

The use of a pressure cell to perform temperature-dependent constant density experiments[122] provides valuable information about the separate effects of kinetic energy and density on the reorientational correlation functions of ν_3 of CH_3I, as can be seen in Figs. 10 and 11. It was shown that the variation of density is the dominant factor for changing the reorientational motion as a 10 per cent density increase gave more effect on $\phi_{2R}(t)$ than 33 per cent temperature change. The correlation functions showed a non-exponential part (Fig. 11) at short times which has a smaller slope at higher pressure. An analysis[122] of the intermolecular mean square torques $\langle(OV)_\perp^2\rangle$, acting on the rotating molecules, derived from the experimental fourth moments showed (despite a large uncertainty in the absolute value) the expected variations under different experimental conditions (see Table IV).

The values of $\langle (OV)_{\perp}^{2} \rangle$ increased at constant temperature with increasing pressure, decreased at constant pressure with increasing temperature and remained almost constant at constant density with increasing temperature. The activation volume was determined to be about 9 $cm^3\ mol^{-1}$ over the observed temperature range and had the same value as the activation volume for viscous flow.

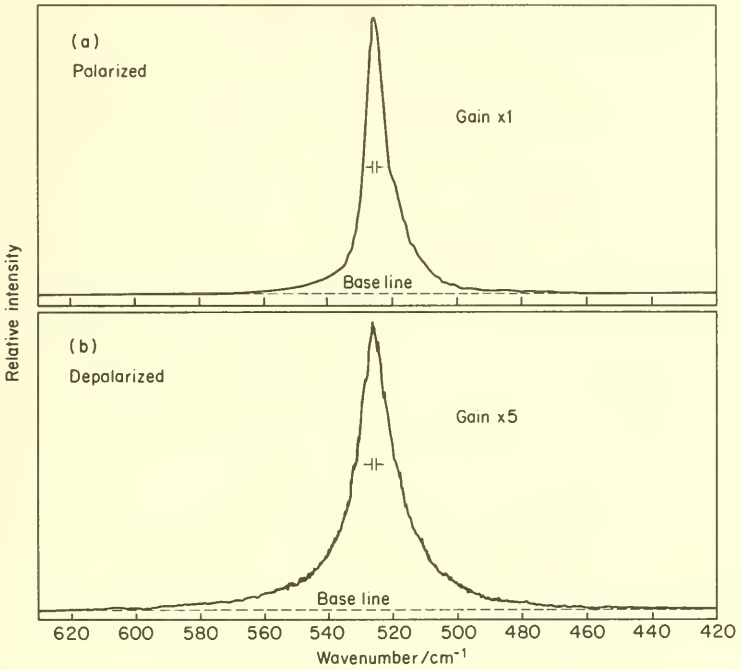

FIG. 10. Experimental polarised (a) and depolarised (b) spectra of the $\nu_3(a_1)$ Raman vibrational–rotational band of CH_3I at 526 cm^{-1} (P = 1000 bar and T = 333 K). Note the asymmetry due to the hot band on the low frequency side of the experimental spectra. [Reproduced with permission from H. J. Campbell, J.F. Fisher and J. Jonas, *J. Chem. Phys.*, **61**, 346 (1974)]

The activation energy for reorientational motion at constant pressure (E = 9·6 kJ mol^{-1}) was almost twice the size of the activation energy determined at constant density with E = 5·6 kJ mol^{-1}. This suggests that the physical significance of an activated process describing the molecular motion in liquid CH_3I is questionable.[122]

An investigation[119] of the temperature and solvent dependence of ν_2 and ν_3 of CH_3I indicated that the models of rotational diffusion and the J-diffusion are inadequate to describe the tumbling motion of the molecules.

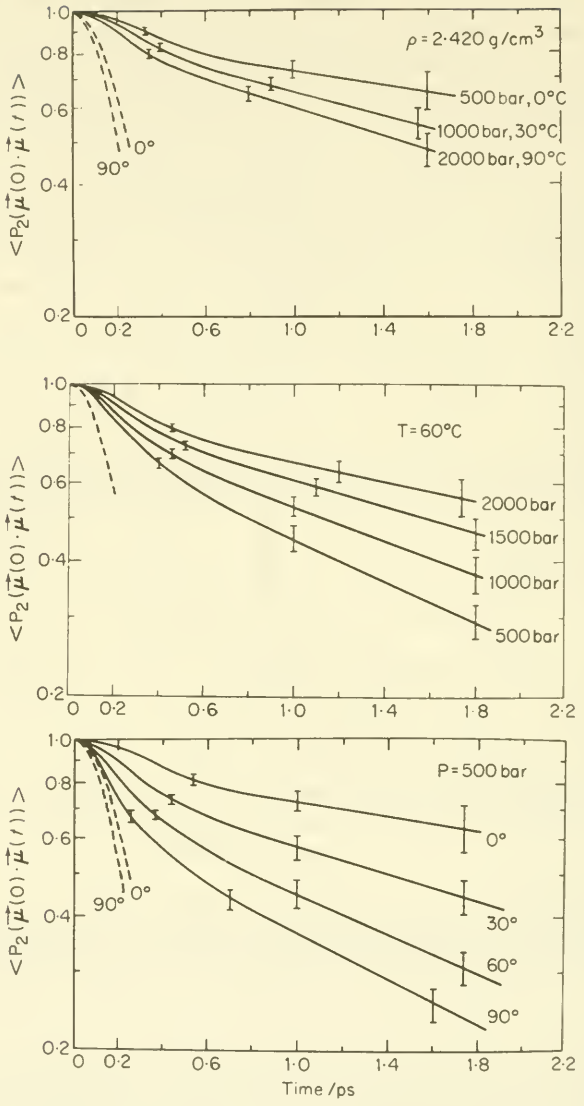

FIG. 11. The reorientational correlation function $\langle P_2[\mu(0)\ \mu(t)]\rangle$ for ν_3 of CH_3I calculated from the observed Raman spectra; top, constant density; middle, constant temperature; bottom, constant pressure. [Reproduced with permission from H. J. Campbell, J. F. Fisher and J. Jonas, *J. Chem. Phys.*, **61**, 346 (1974)]

TABLE IV. Intermolecular torques for CH_3I as a function of temperature and pressure

	Constant T (T = 333 K)		Constant pressure (P = 500 bar)			Constant density (ρ = 2·42 g cm^{-3})		
P/bar	$(M2)_{rot}$/cm^{-2}	$\langle(OV)^2\rangle^a$	T/K	$(M2)_{rot}$/cm^{-2}	$\langle(OV)^2\rangle^a$	T/K	$(M2)_{rot}$/cm^{-2}	$\langle(OV)^2\rangle^a$
500	174	20 ± 3	273	27	28 ± 3	273	27	28 ± 3
1000	128	24	303	91	25	303	48	28
1500	83	28	333	174	20	333	83	28
2000	51	30	363	271	14	363	97	30
2500	—	31						

[a] Unit is 10^{26} dyn^2 cm^2.

The solvent dependence of τ_{2R} was interpreted in relation to the viscosity of the solutions and it was found that viscous effects are not totally responsible for orientational relaxation in CH_3I.

The study[138] of vibrational and reorientational relaxation in liquid CHF_3 and CDF_3 showed that the isotropic line-width of ν_1 of CHF_3 was FWHM $> 20\,cm^{-1}$—(remarkably) broader than that of ν_3 of CHF_3 (FWHM $< 2\,cm^{-1}$). It could not be explained why the half-width of ν_1 of CHF_3 was constant with increasing temperature while that of ν_1 of CDF_3 decreased from $11{\cdot}3\,cm^{-1}$ to $8{\cdot}7\,cm^{-1}$ over the liquid range. An isotopic dilution experiment[138] excluded the effect of resonant transfer of vibrational energy on the band width of CHF_3. The rotational correlation functions for the ν_1 and ν_3 bands decay to 0·2 at 296 K before exponential decay. This indicated that the molecular reorientation proceeds through large angular steps. From the temperature dependence of τ_{2R}[138] an activation energy of $4{\cdot}0\,kJ\,mol^{-1}$ was derived—compared with a ^2H nmr value for CDF_3 of $4{\cdot}2\,kJ\,mol^{-1}$ and considerably smaller than the hydrodynamic value of $6{\cdot}7\,kJ\,mol^{-1}$. Although the process of determining an activation energy near kT seems to be questionable, this too means[138] that, especially at higher temperatures, the rotational motion is non-diffusive.

Detailed investigation[99] of the effects of intermolecular torques on liquid CHF_3 (and other symmetric top molecules) has been made using the far-infrared spectra and the Mori formalism for determination of the rotational velocity correlation function (see Section II.B.4) (the extent of induced dipole absorption for this molecule is shown to be small[99]). The observed band profile (Fig. 12) has been fitted to expression (46) (giving values of the stochastic parameters $K_1(0)$ and γ) and the observed rotational velocity correlation function [equations (32) and (34)] has been compared with that obtained from the Fourier transform of (46). The result of this comparison is shown in Fig. 12. The amplitudes of oscillations in the observed correlation function reflect the breadth of the spectrum in the frequency domain and hence the $K_1(0)$ value [see equation (44)]. Since $K_1(0)$ is related to the intermolecular torque [via equations (43b) and (47)] the band shape and correlation function give directly information about intermolecular forces. In the case of CHF_3, oscillations are observed at low temperatures[99b] but not at 296 K (Fig. 13), indicating that the torques are small at high temperatures but increase with decreasing temperature. This is interpreted as being due to an increase in "free volume" as the density decreases. The shapes of the RVCF have also been used to compare $\langle(OV)^2\rangle$ values for a number of simple molecules, and the importance of geometrical anisotropy (for example in propyne) in relation to the effective torques was noted. For symmetric top molecules of comparatively "spherical" shape the torques were generally low. It should be noticed that previous interpretation[84a] of the far-infrared

spectrum of CHF_3 using the Brot–Larkin model[92–95] was somewhat less successful (see Fig. 12) and this was attributed to a higher degree of freedom in the liquid than is allowed for by that model. However, even for the low density liquid (296 K) there is sufficient local ordering by transient cluster formation for there to be significant deviation from the J diffusion model (which embodies the collision interrupted "free rotation" concept).

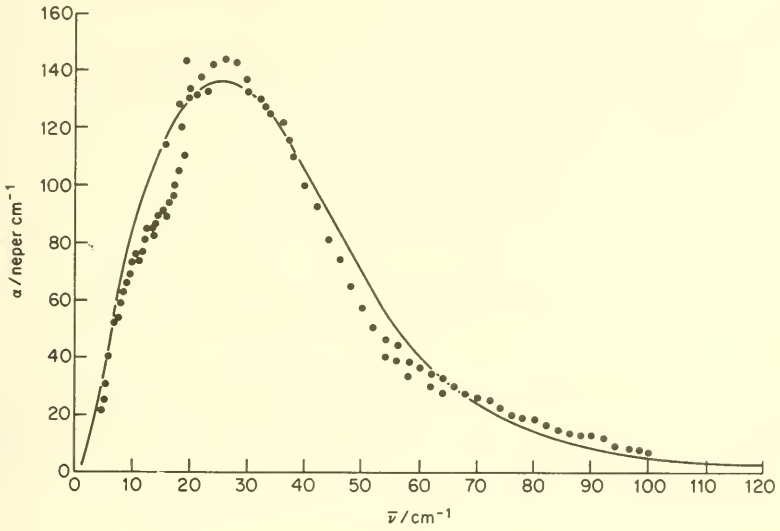

FIG. 12. Observed and calculated power spectrum for liquid CHF_3 at 296 K [·····, experiment; ——— equation (46)]. [Reproduced with permission from (a) G. J. Evans and M. W. Evans, *J. Chem. Soc., Faraday Trans. II*, 72, 1169 (1976); (b) A. Gerschel, Conf. on Molecular Motions in Liquids, Nancy (1974)]

The temperature and pressure dependence of the intermolecular torques of carbon tetrachloride and carbon disulphide[90] serves to emphasise the influence of molecular shape. Using the same far-infrared technique as that outlined above for CHF_3, data were obtained for these two molecules as a function of temperature (where now, of course, the observed spectra are due to the *induced* dipole fluctuations). Fitting of the data to equation (46) gave values of $K_1(0)$ which are in Table V. It can be seen that as the temperature increases the intermolecular torque increases for CS_2 but decreases for CCl_4. The behaviour of CCl_4 is exactly analogous to that of CHF_3, the degree of translation freedom (and free volume) increasing as the temperature increases. However, for CS_2 it is clear that the torques depend on the molecular thermal energy and appear to be controlled by hard core collisions since, for this type of potential, $\langle (OV)^2 \rangle \propto N'kT/\theta$ where N' is a force coefficient and θ a mean

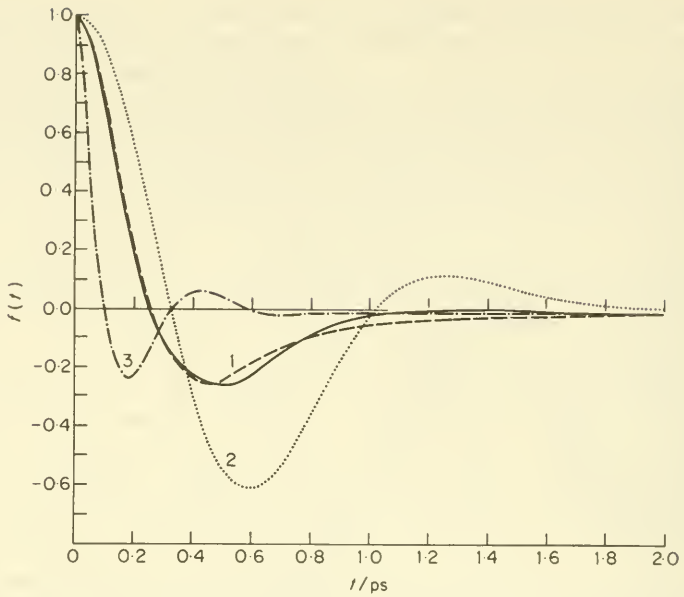

FIG. 13. Rotational velocity correlation functions for CHF_3 in the liquid phase at 296 K [– – –, observed data; ———, calculated using equation (34) with $\alpha(\bar{\nu})$ derived from (46); ·····, gas-phase free-rotor model at 296 K; – – –, Larkin–Brot model at 296 K]. [Reproduced with permission from (a) G. J. Evans and M. W. Evans, *J. Chem. Soc., Faraday Trans. II*, **72**, 1169 (1976); (b) A. Gerschel, Conf. on Molecular Motions in Liquids, Nancy (1974)]

free angle of rotation. Presumably as the pressure is increased at constant temperature θ decreases and N' increases for this "stick-like" molecule.

Another well studied liquid is $CHCl_3$ (or $CDCl_3$).[14, 28, 29, 103, 129, 53, 139, 140, 137, 141] It was found[29] that the ν_4, infrared band narrows on isotopic

TABLE V. Memory function parameters $K_1(0)$ for carbon disulphide and carbon tetrachloride from far-infrared spectra (Ref. 90).

	Temperature/K	Pressure/bar	$xK_1(0)^a$
CCl_4	296	1	80·6
	313	1	65·1
	328	1	51·2
	343	1	77·7
CS_2	232	1	114·3
	296	1	170·2
	293	11600	247·6
	315	1	212·0

[a] $x = I/2kT$.

dilution. This effect could be explained by the assumption that the band was partly broadened by transition-dipole–transition-dipole interaction. However, the results of an isotopic dilution study of the ν_4 Raman band of $CHCl_3$ were interpreted in terms of resonant transfer of vibrational energy due to repulsive potentials.[103] From theoretical calculations a distance of closest approach of the $CHCl_3$ molecules of 5·1 Å was derived. A calculation of the band-width due to resonant transfer of vibrational quanta caused by repulsive potentials showed[103] that ν_1 and ν_2 of $CHCl_3$ should not be affected in an isotopic dilution experiment. This was experimentally confirmed in another investigation[53] of reorientational and vibrational relaxation studies of the ν_1, ν_2, ν_3 and ν_4 bands of $CHCl_3/CDCl_3$. In a later paper[28] the whole VRF of ν_1 for $CDCl_3$ was attributed to dephasing effects and, by computer fitting of the VRF, the modulation time τ_c was determined to have the value of 0·13 ps. This time was compared to τ_M, the collision time derived from an M-diffusion model fit of the reorientational correlation function of ν_3 of $CDCl_3$. It was suggested[28] that the decay of the VRF is caused by the effect of repulsive potentials that are modulated by molecular collisions.

A recent study of the temperature dependence[129] of ν_1 of $CDCl_3$ showed that the vibrational second-moment $(M2)_v$ increases with increasing temperature. This behaviour is similar to that of ν_1 of CH_3I and contradicts the predictions of the dephasing models [see 1(a) above]. It seems reasonable to conclude that VRF of ν_1 of $CDCl_3$ is, to a certain extent, caused by energy relaxation and redistribution processes.[129] Whether or not this is the case could only be answered by a picosecond pulse experiment[106] which measures the correlation time of $\phi_E(t)$ directly.

The reorientational motion for $CHCl_3$ or $CDCl_3$ has also been studied by Raman spectroscopy,[53, 139, 140, 141] infrared spectroscopy,[53, 139, 142] depolarised Rayleigh scattering,[54, 134, 142] far-infrared spectroscopy[142] and nmr.[140–143]

A comprehensive investigation[53] of the ν_1, ν_2, ν_3 and ν_4 bands in a constant pressure Raman experiment showed that the correlation functions of ν_1 and ν_3 have a short Gaussian period of 0·15–0·2 ps, and from these data a jump angle θ of 1/3 radian was derived. The rotational correlation functions of ν_1 and ν_3 are almost identical and small differences may be due to the fact that for ν_1 the influence of vibrational relaxation is much larger. The ratio $\tau_1/\tau_2 = 2{\cdot}3$ indicates[53] too that the reorientational motion deviates from diffusive behaviour. The temperature dependence of τ_{2R}^{Ram} gives an activation enthalpy of $E^{Ram} = 6{\cdot}3\ kJ\,mol^{-1}$ for the tumbling motion of $CHCl_3$. The absolute values of τ_{2R}^{Ray} are bigger than τ_{2R}^{Ram}, indicating a collective contribution to the reorientational motion, and the activation energy[134] is also bigger since $E^{Ray} = 8{\cdot}4\ kJ\,mol^{-1}$.

Rotational correlation in chloroform has also been investigated by

Rosenthal and Strauss[142] using infrared, far-infrared, Raman and Rayleigh scattering techniques. Attempts have been made to determine the $g^{(1)}$ and $g^{(2)}$ factors [see equations (11) and (12)] and to extract the "distinct" correlation function $\phi_d^l(t)$ which is a measure of correlations involving many particles. For $l = 1$ a comparison of the far-infrared reorientational correlation function $\phi^1(t)$ [equation (8)] with that, $\phi_s^1(t)$, obtained from an infrared vibration–rotation band (using ν_3 of $CHCl_3$ with a correction for isotopic splitting and using the vibrational correlation function obtained from VV Raman scattering) gave a value of $g^{(1)}$ between 1·2 and 1·6 (using the analogous equation to (13) for the integrated intensity) depending on the nature of the dielectric internal field correction used. If one uses the data for $\tau_{1R}^s = 2{\cdot}8$ ps and $\tau_{1R}^{FIR} = 5{\cdot}0$ ps (estimated from Fig. 13 of Ref. 142) one is able to calculate a value of $(1 + gN) \approx 0{\cdot}7$ from equation (14). The static correlation parameter $(1 + fN) = 2{\cdot}0 \pm 0{\cdot}1$ obtained by Alms *et al.*[54] indicates, however, that in neat chloroform there is a tendency for the molecular axes (dipoles) to align themselves in a "parallel" configuration (see Section II.B.2). The distinct correlation function for $l = 1$ is shown in Fig. 14 and it is seen

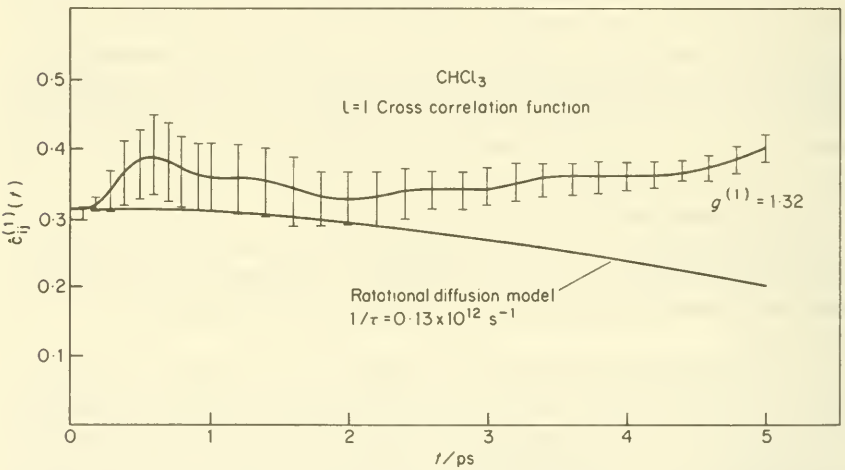

FIG. 14. The observed $l = 1$ "distinct" or cross-correlation function of liquid $CHCl_3$ compared with that calculated using the rotational diffusion model. [Reproduced with permission from L. C. Rosenthal and H. L. Strauss, *J. Chem. Phys.*, **64**, 282 (1976)]

that the correlation time $\tau_d^{(1)}$ is 7·7 ps. The distinct correlation decay rate is therefore slower than either the total (τ_{1R}^{FIR}) or single particle (τ_{1R}^s) correlation time. Comparison of $\phi^2(t)$ and $\phi_s^2(t)$ using Raman and depolarised Rayleigh scattering measurements was more difficult owing mainly to additional collision-induced effects[142] on the Rayleigh wing.

By comparison of τ_{2R} with the value calculated from the Debye expres-

sion[67] extended to include a microviscosity correction[68] a value of κ was determined [see equation (30)]. This κ may be interpreted as the ratio of the autocorrelation functions for the torque and the force on the molecules in the liquid,[68b] and its value is assumed to be constant for a given system. The value in chloroform at 303 K is 0·126 and one finds[143] that κ increases with temperature (at constant pressure) and decreases with increasing pressure (at constant temperature). Comparison of κ values for $CHCl_3$ (0·126) and SF_6 (0·1)[68b] indicates that the anisotropic part of the interaction potential is rather weak.

It is interesting that recent attempts[53] to establish a relation between vibrational relaxation rates in liquid chloroform and possible self-hydrogen-bonding interactions have proved negative. Rothschild and coworkers[53] deduced that hydrogen bonding was of little significance as a source of effective intermolecular potentials for the following reasons: (a) although the ν_1(CH) vibrational relaxation function has a shorter correlation time than the other A_1 vibrations, little evidence for resonance vibrational-energy transfer was found using isotopic dilution experiments (expected for a situation where close coupling of the hydrogen-bonded molecules is expected); (b) the behaviour of the C—H stretching vibrations, on both isotopic dilution and isotopic substitution, for $CHCl_3$ and CH_2Cl_2 was found to be identical. As Griffiths[133b] has pointed out, however, there is some evidence that pair correlations are more important for liquid chloroform than for other (surely) non-hydrogen bonded liquids (CH_3CN, C_6H_6 and CH_3I, for example). The differences between τ_{2R}^{Ray} and τ_{2R}^{Ram} and the different activation energies (indicated above) are both indications that a different type of intermolecular potential may have some importance.

Variable pressure measurements[141] of the ν_1 Raman band of $CHCl_3$ showed that the short time (inertial) part of $\phi_{2R}(t)$ remains mainly unaffected while the exponential part is strongly pressure dependent. The intermolecular mean square torques[141] vary from $8{\cdot}4 \times 10^{-26}$ (dyn cm)^2 at 1 atm to $11{\cdot}6 \times 10^{-26}$ (dyn cm)^2 at 2000 atm. The temperature dependent measurements of the spin–lattice relaxation time τ_1 of the D nucleus in $CDCl_3$ gave an activation energy of 8·6 kJ mol^{-1}. The variation of pressure allows one to calculate an activation volume of about 4·9 cm^3 mol^{-1} which was almost constant over the whole temperature range. The interpretation of the whole data in terms of activation and free volume models is not possible since each model describes only certain aspects of the results. The activation model fails to predict the correct behaviour at constant temperature, and free volume theories fail to predict the results at constant volume. Using the J-diffusion model, a collision time $\tau_c \equiv \tau_J$ was calculated but could not be fitted by cell models. This indicates that a more general model is needed to describe all the experimental data for this system.[143]

Isotopic dilution studies[29] of the ν_8 infrared band of CH_2Cl_2 resulted in a narrowing of the band. This was explained qualitatively with the model of resonant transfer of vibrational quanta due to transition-dipole–transition-dipole interactions. The corresponding calculation fitted the experimental results quite well.

The ν_2 vibrations of benzene and benzene-d_6 were studied[104] using spontaneous Raman scattering, and an isotopic dilution experiment showed a decrease of the band width of ν_2 for C_6H_6 in C_6D_6. A corresponding picosecond pulse experiment[104] measuring the vibrational lifetime of ν_2 was interpreted, together with the other data, on the basis of a model for collision induced intermolecular vibrational energy transfer. The activation energies for reorientational motion derived from vibration–rotation Raman bands and the depolarised Rayleigh wing show the same value of 10·9 kJ mol^{-1}. The absolute values of τ_{2R} and τ_{Ray} are almost the same, indicating that cross correlations between neighbouring molecules can be neglected for this system.[134]

In a recent paper[151] the temperature dependence of ν_2 at constant pressure and the solvent dependence of ν_2 in CCl_4 dilution was studied. Data analysis was attempted using an expression derived[26, 109] with the assumption of intermolecular dipole–dipole potentials. Since the solvent-dependent band broadening has been shown (see above) to be due to the effect of resonant energy transfer of vibrational quanta, the effective potential would then be a transition-dipole–transition-dipole interaction. However, since the ν_2 band of benzene is infrared forbidden (by symmetry), this intermolecular potential can have no effect on the band shape. The basis of the analysis is thus open to question and it is still unclear what kind of intermolecular potential causes the broadening of this band.

B. Associated Liquids

As mentioned previously the term "associated liquids" is here applied to liquids for which the orientation dependent intermolecular interactions are considerably greater than kT.

One molecule for which the condition for non-random distribution of the molecules due to the effect of dipolar forces is fulfilled (with $\mu_0^2/R_{ij}^3 > kT$) is benzaldehyde ($\mu_0 = 2{\cdot}77$ D). The influence of this effect on the isotropic part $I_\alpha(\omega)$ of a Raman band has been investigated[130, 131] by studying the temperature and solvent dependence of the line shape of the ν_4 [ν(C=O) symmetric stretching] vibration at 1697 cm^{-1}. As can be seen from Fig. 15, the isotropic part $I_\alpha(\omega)$ of the band in the pure liquid at 293 K shows an asymmetric shape with a steep wing at lower wavenumbers. The anisotropic part $I_\beta(\omega)$ is almost symmetric with its maximum ($\bar{\nu}_{max}$) shifted to higher

wavenumbers. On 98 mole per cent dilution of C_6H_5CHO in CS_2 the isotropic part narrows to a symmetric band with the same maximum frequency as I_β. An asymmetric band of this shape for I_α and the difference in $\bar{\nu}_{max}$ for $I_\alpha(\omega)$ and $I_\beta(\omega)$ are predicted[26] for a Raman band mainly broadened by the effect of transition-dipole–transition-dipole interaction if the reorientational distribution of the molecules in the liquid is non-random. With increasing temperature the band gets more symmetric since (with increasing kT) the distribution of the molecules becomes more randomised.[131]

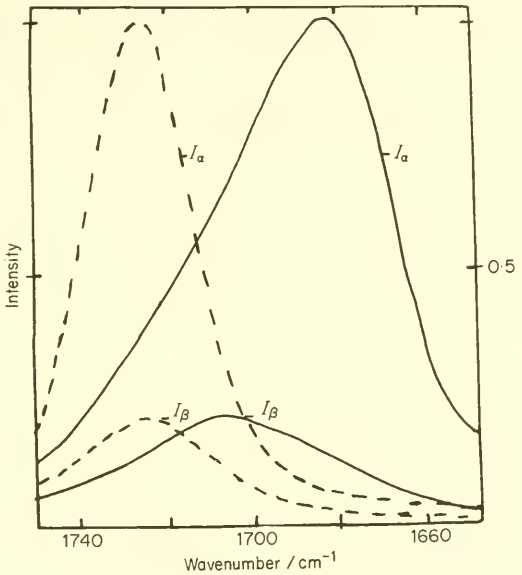

FIG. 15. Raman band shapes of the ν(C=O) vibration of benzaldehyde at 293 K. ———, pure liquid; – – – –, 2 mole per cent solution in CS_2. [Reproduced with permission from R. Arndt and D. Scheibe, Proc. 5th International Conference on Raman Spectroscopy, H. F. Schulz Verlag, Freiburg (1976), p. 52]

On dilution with CS_2 the effects of resonant transfer of vibrational energy due to transition-dipole–transition-dipole interaction on the band shape are removed as the benzaldehyde molecules become separated. [The CS_2 molecules have no spectral density in the frequency region of the ν(C=O) stretching vibration.] The same solvent dependence of the difference of $\bar{\nu}_{max}$ between $I_\alpha(\omega)$ and $I_\beta(\omega)$ has been observed for the ν(C=O) stretching vibrations of other molecules[22] and, in addition, it should be noted that the maximum of the corresponding infrared band coincides with that of $I_\beta(\omega)$. The difference in $\bar{\nu}_{max}$ was therefore interpreted[22] as the effect of transition-dipole–

transition-dipole interactions on the band shapes combined with the presence of partly ordered clusters of benzaldehyde molecules (resulting in differences[26, 114] between the infrared and Raman selection rules).

The interpretation of the frequency shift between $I_\alpha(\omega)$ and $I_\beta(\omega)$ and the concentration and temperature dependence of the solvent dependent part of $I_\alpha(\omega)$ as due to TD–TD interactions could be tested directly by an isotopic dilution experiment. A comparison of the isotropic band shape of the ν_4 bands of benzaldehyde and of benzaldehyde-d_6 showed that the deuterated compound behaved in the same way. Preliminary results[135] of an isotopic dilution study of C_6H_5CHO in C_6D_5CDO at concentrations of 75, 50 and 25 mole per cent benzaldehyde show that with increasing dilution the maximum shift between $I_\parallel(\omega)$ and $I_\perp(\omega)$ decreases from $\sim 4{\cdot}5\ cm^{-1}$ in the pure liquid to $\sim 1\ cm^{-1}$ in the most dilute solution. Using this result, together with the fact that the width of the ν_4 band decreases considerably, we can conclude that the ν(C=O) band is broadened by resonant energy transfer of vibrational quanta. This is most likely due to transition-dipole–transition-dipole interactions.[26, 109] Since at least one of the modes of behaviour typifying this band, i.e. the shift in frequency between $I_\parallel(\omega)$ and $I_\perp(\omega)$, is observed for many other compounds[22] it seems likely that such studies will in the future provide a valuable method of studying intermolecular potentials.

An endothermic excess enthalpy[128, 144] in mixtures of *p*-dioxan ($C_4H_8O_2$) with CS_2 and with cyclohexane indicates a self-association of the molecules in the pure liquid due to intermolecular interactions. The effect of dipole–dipole interaction is negligible owing to the permanent dipole moment of near zero (estimated to be $\sim 0{\cdot}1$ D.)[145] Infrared investigation[146] of the ν_{15}, ν_{33} and ν_{35} bands showed that vibrational relaxation in neat *p*-dioxan and solutions is relatively fast compared with reorientational relaxation.

The results of a systematic investigation[128] of the isotropic part of the C—H stretching vibration ν_1 at $2967\ cm^{-1}$ in the pure liquid and in various dilutions are in Table VI. The isotropic half-band width at half-height (HWHM) narrows by the same amount in a non-polar (CCl_4) and a polar ($CDCl_3$) solvent. An isotopic dilution experiment of dioxan diluted in dioxan-d_8 excluded the effect of resonant transfer of vibrational energy on the band shape. The assumption that the band broadening was caused by an interaction of oxygen "lone pair" electrons with the C—H bond of neighbouring molecules (formally written as C—H $\cdots$ O<) was confirmed by the results of dilutions of dioxan in acetone-d_6. In this solvent the band width remained approximately constant, indicating that the self interaction between dioxan molecules was replaced by a $C{-}H^{dioxan} \cdots O{=}C^{acetone}$ interaction causing approximately the same line broadening. In a further analysis the concentration dependence of the vibrational second-moment $(M2)_\nu$ for

TABLE VI. Solvent dependence of the half-width (FWHM) of the C—H stretching vibration ν_1 of *p*-dioxan at 303 K

Mole fraction CCl_4	$\Delta\nu_{1/2}/cm^{-1}$	Mole fraction $CDCl_3$	$\Delta\nu_{1/2}/cm^{-1}$	Mole fraction $C_4D_8O_2$	$\Delta\nu_{1/2}/cm^{-1}$	Mole fraction C_3D_6O	$\Delta\nu_{1/2}/cm^{-1}$
0·0	16·3	0·0	16·3	0·00	16·3	0·0	16·3
0·18	15·8	0·21	15·7	0·26	15·9		
0·37	15·1	0·41	14·6			0·34	16·2
0·57	13·3	0·61	12·5	0·58	16·3	0·66	15·9
0·73	11·9	0·76	11·6				
0·89	10·9	0·90	11·0	0·90	16·1		

CCl_4 and $CDCl_3$ solutions was calculated from the long time slope, $S(m)$, of the solvent-dependent part of the vibrational relaxation functions. This is shown in Fig. 16.

The apparent reduction of $(M2)_v$ on dilution of dioxan with CCl_4 or $CDCl_3$ can be explained by a replacement of the C—H $\cdots$ O< self interaction between adjacent dioxan molecules due to the stronger interaction

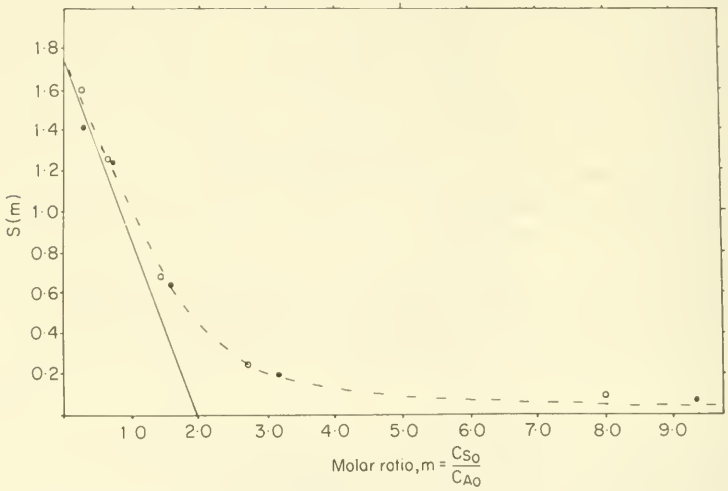

FIG. 16. Concentration dependence of the vibrational second moment of the solvent dependent part of v_1 of *p*-dioxane; the solvents are CCl_4 (●) and $CDCl_3$ (○).

of the solvent molecules (example CCl_4, $CHCl_3$) with dioxan[147–149] and can be described by the following scheme:

$$>O\cdots H—A + XB \overset{K}{\rightleftharpoons} >O\cdots X—B + HA$$

The concentration of oxygen functions blocked by solvent molecules C_{AS}, is given by

$$C_{AS} = \tfrac{1}{2}[(2 + m + 1/K) - \sqrt{(2 + m + 1/K)^2 - 8m}]$$

Here m is the molar ratio of solvent (C_{S_0}) to dioxan (C_{A_0}) initial concentrations and K is the equilibrium constant for the reaction as written above. Since the oxygen functions blocked by the solvent give no contribution to the vibrational second moment of v_1 [given by $S(m)$] it follows that

$$S(m) = S(0)(2 - C_{AS})$$

where $S(0)$ is the value of $S(A)$ at $m = 0$. The 2 must be introduced since the

concentration measure m refers to 1 mole dioxan which contains 2 mole oxygen atoms).

The solid curve in Fig. 16 is calculated for an infinite association constant of the dioxan–solvent complex (i.e. $K^{-1} = 0$) which describes the effect of totally blocked oxygen sites. The experimental values for CCl_4 and $CDCl_3$ solutions can be fitted very well by the dotted line which is given by a value of $K^{-1} = 0{\cdot}16$. Further evidence for the interaction of dioxan and $CDCl_3$ in mixtures with an excess of $CDCl_3$ has been obtained from an nmr study[148] of the spin–lattice relaxation time (T_1) of dioxan-d_8.

Correcting for viscosity effects, the reorientational correlation time for dioxan-d_8–$CDCl_3$ was 17 ps—considerably longer than in the pure liquid (7·5 kJmol^{-1}). This discrepancy was explained by the formation of a dioxan–10·9 kJ mol^{-1} and is larger than the activation energy of the viscosity (7·5 kJ mol^{-1}). This discrepancy was explained by the formation of dioxan–$CDCl_3$ complex that rotates as a single unit.

Apart from the methyl halides and the haloforms the most studied symmetric top molecule is probably acetonitrile (CH_3CN). The molecule is highly dipolar ($\mu_0 = 3{\cdot}9$ D), the dynamics are highly anisotropic[133b] and the vibrational relaxation process extremely complicated. Nevertheless, although much remains to be done to sort out the details of the intermolecular potential, some progress has been made in investigating possible models of orientation and relaxation. A number of Raman studies[14, 37, 50, 107, 119, 132, 152] have been made including studies in dilute solution[50, 107] and as a function of density.[37] As expected, the virtational parts of the four A_1 bands are different (Table VII) but measurements on the ν_2 and ν_4 bands are difficult

TABLE VII. Vibrational relaxation times (τ_v) for the ν_1, ν_2 and ν_3 vibrations of acetonitrile in the liquid phase

T/K	$\tau_v(\nu_1)$	$\tau_v(\nu_2)^a$	$\tau_v(\nu_3)$
252	1·50 ± 0·10	3·2 ± 0·1	1·2 ± 0·1
288	1·55 ± 0·10	3·3 ± 0·1	1·3 ± 0·1
318	1·50 ± 0·10	3·3 ± 0·1	1·4 ± 0·1
343	1·48 ± 0·10	3·3 ± 0·1	1·2 ± 0·1

[a] Values from ν_2 for high-frequency side of band.

because of interference[154] by hot bands (Fig. 17) of the type $\nu_2 + \nu_8 - \nu_8$ or $\nu_4 + \nu_8 - \nu_8$. The behaviour of the ν_1 and ν_3 bands on dilution and temperature variation is also different. For the ν_1 band the vibrational relaxation rate (τ_v^{-1}) is insensitive either to isotopic dilution or to temperature changes (at constant pressure) (Table VIII) but increases with density at constant

temperature and also increases with temperature at constant density. These facts would indicate that long-range interactions (dipolar interactions) are not of great significance for the broadening of the ν_1 band since resonance vibrational energy transfer via transition-dipole–transition-dipole interactions is obviously small [the intrared intensity is also small[155]—see equation (67)] and motional narrowing (which would be caused by strong dipolar interactions—see Section II.C) is *not* operative (this would lead to a *decrease*

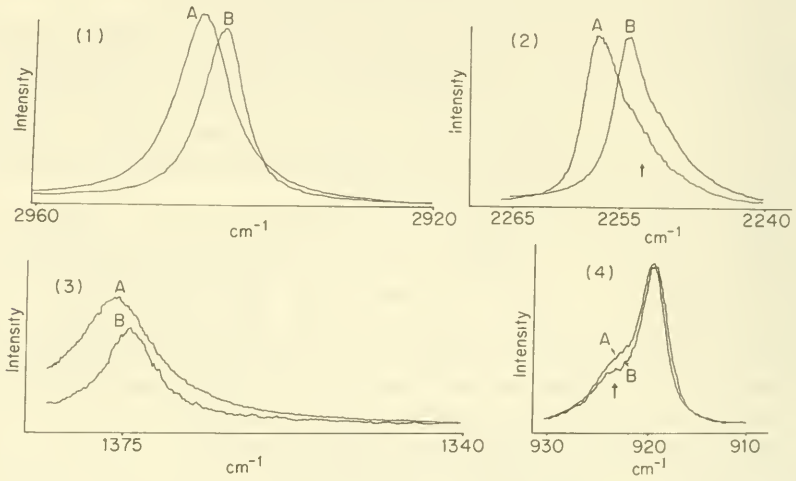

FIG. 17. Observed isotropic Raman spectra of acetonitrile in the liquid (A) and in a 0·16 mole-fraction solution in CCl_4 (B). (1) ν_1 at $\sim 2943\ cm^{-1}$; (2) ν_2 at $\sim 2256\ cm^{-1}$; (3) ν_3 at $\sim 1376\ cm^{-1}$; and (4) ν_4 at $\sim 918\ cm^{-1}$. In the cases of ν_2 and ν_4 the hot bands $\nu_n + \nu_8 - \nu_8$ are indicated by an arrow.

in τ_v^{-1} on increasing the temperature at constant density). That short-range repulsive interactions are predominant for this mode is indicated by the following observations: (a) dilution in carbon tetrachloride leads to only a small decrease in band width (or in τ_v^{-1}), showing that dipole–dipole interactions are of relatively minor importance; (b) the dephasing times calculated[37] (Table IX) using the model of Fischer and Laubereau[108] based on repulsive potentials and employing a modulation rate τ_c^{-1} proportional to the Enskog hard sphere[127] collision rate τ_E^{-1} [equation (87)] are in good agreement with the observed data; (c) on diluting further with carbon tetrachloride the vibrational second-moments increase, producing an increase in τ_c^{-1} and this increase is *non-linear* (Fig. 18), reflecting of course a non-linear variation in the overall τ_v when the Kubo model, equation (5b), is applied[107] to calculate τ_c values. This non-linearity and the increase in the second moments on

Table VIII. Isotropic and anisotropic line-widths for ν_1, ν_3 and $2\nu_3$ of acetonitrile for the liquid and for carbon tetrachloride solutions (all values in cm^{-1}) (Ref. 107).

Mode	Liquid				CCl_4 solution[a,b]						CD_3CN[a,b] solution
	252 K	288 K	318 K	343 K[c]	0·64	0·37	0·16	0·06	0·03	0·01	0·06
ν_1											
$\Delta\bar{\nu}^d_{1/2}$ (iso)	6·8	6·5	6·5	6·5	5·9	5·5	5·0	5·7	4·5	4·4	6·0
ν_3											
$\Delta\bar{\nu}_{1/2}$ (iso)	8·3	8·0	7·4	(8·8)	—	5·8	5·0	5·2	4·8	—	9·8[e]
$\Delta\bar{\nu}_{1/2}$ (aniso)	13·7	17·0	18·2	21·9	—	11·4	10·4	10·7	8·8	8·6	
$2\nu_3$											
$\Delta\nu_{1/2}{}^d$ (iso)	17·2	16·0	—	15·0	12·0	10·0	7·7	—	—	—	—

[a] Concentration is mole fraction of CH_3CN. [b] Temperature is 288 K. [c] Data are at 338 K for ν_3. [d] Assumed the same as $I_{\|}$ for these highly polarised bands. [e] Data for ν_3 in CD_3CN are for $I_{\|}$. The $I_{\|}$ half-width in the liquid is 11·0 cm^{-1} at 288 K.

TABLE IX. Calculated[a] and measured dephasing rates (ps^{-1}) for liquid acetonitrile (Ref. 37)

T/K	P/kbar	ρ/g cm^{-3}	τ_v^{-1} (obs)	τ_{ph}^{-1} (calc)
303	0·36	0·8000	0·64	0·61
333	0·74	0·8000	0·67	0·67
363	1·08	0·8000	0·70	0·72
393	1·44	0·8000	0·75	0·77
303	1·25	0·8500	0·70	0·74
333	1·72	0·8500	0·75	0·80
363	2·12	0·8500	0·79	0·86
393	2·54	0·8500	0·84	0·91
303	2·60	0·9000	0·82	0·88
333	3·12	0·9000	0·88	0·95
363	3·57	0·9000	0·94	1·02
393	4·07	0·9000	1·00	1·08

[a] Calculated using equation (85).

dilution raises the possibility of the importance of: (i) clustering of the acetonitrile molecules in such a way that the non-random molecular distribution becomes more important at low concentrations; (ii) repulsive (and therefore collisional) interaction between acetonitrile and the carbon tetrachloride molecules. More experimental work as a function of temperature at high dilution and as a function of solvent is needed before these ideas can be further tested. However, it is clear that the modulation rate τ_c^{-1} gets *faster* on *increasing* the amount of CCl_4 in the mixture. If this modulation rate is interpreted as a collision rate then the result fits in nicely with the observed decrease in translational and rotational[50, 107] diffusion rates of CH_3CN on dilution in CCl_4.

The behaviour of the ν_3 band is somewhat different in that τ_v^{-1} decreases a little on isotopic dilution (Table VIII) (however, transition-dipole–transition-dipole interaction is still probably small) and also decreases significantly on dilution in CCl_4. Signal/noise ratios[107] are too low to permit accurate determination of $\langle\omega^2\rangle$ $[\equiv (M2)_v]$ so τ_c cannot be determined quantitatively. However, a small amount of motional narrowing is observed (Fig. 19) at constant pressure, and the correlation functions in CCl_4 (Fig. 20) show qualitatively that the second moment, as measured from $\partial^2 \ln \phi(t)/\partial t^2$ at $t = 0$ [see equation (58)], decreases with decreasing concentration. Since τ_v^{-1} remains essentially constant (Fig. 19) it follows [equation (60)] that τ_c goes up on dilution. This is an indication that dipole–dipole interactions are important for the ν_3 band, τ_c^{-1} more accurately being described in this case as a reorientation rate. Additional evidence that this is

the case has been obtained from studies[107, 156] on the first overtone band, $2\nu_3$, both in the Raman (where narrowing on dilution in CCl_4 is drastic) and in the infrared[157] [extreme narrowing coupled with a high overall intensity; see equation (71)].

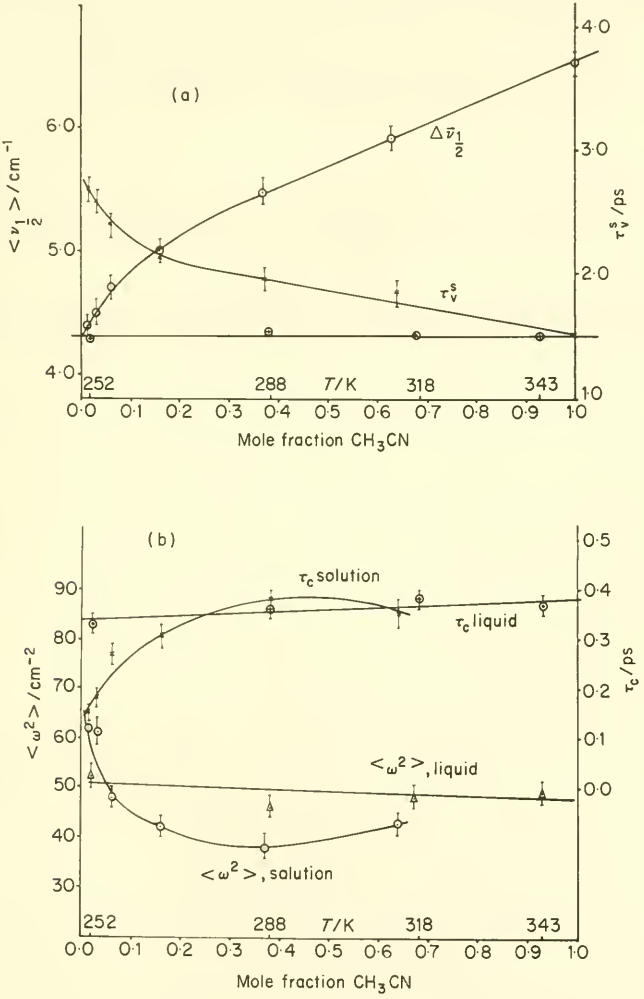

FIG. 18. (a) Changes in $\Delta\bar{\nu}_{1/2}$ and τ_v^s for ν_1 of acetonitrile as a function of temperature and concentration in carbon tetrachloride; solution data are at 288 K. (b) Changes of $\langle\omega^2\rangle$ and τ_c for ν_1 of acetonitrile (liquid and solution). [Reproduced with permission from J. Yarwood, R. Arndt and G. Döge, *Chem. Phys.*, ref. 107]

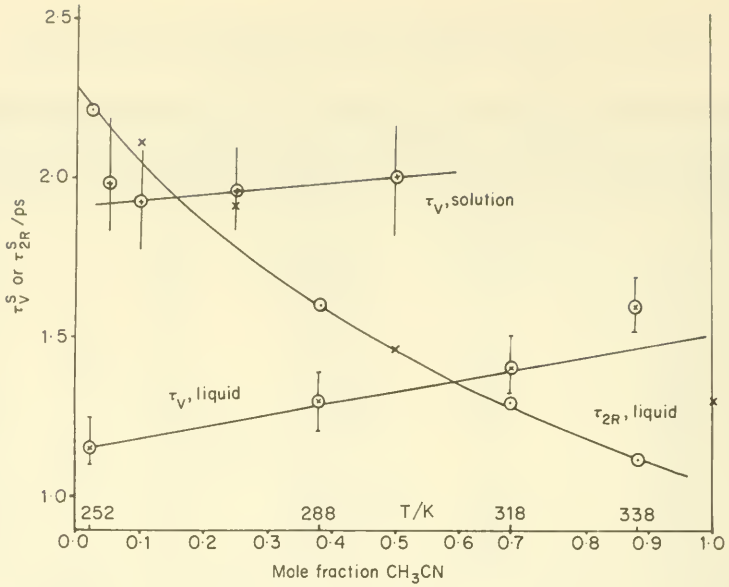

FIG. 19. Changes in τ_v^s and τ_{2R} for ν_3 of acetonitrile as a function of temperature and concentration in carbon tetrachloride. (Points marked × represent data for τ_{2R}^s in solutions.) [Reproduced with permission from J. Yarwood, R. Arndt and G. Döge, *Chem. Phys.*, ref. 107]

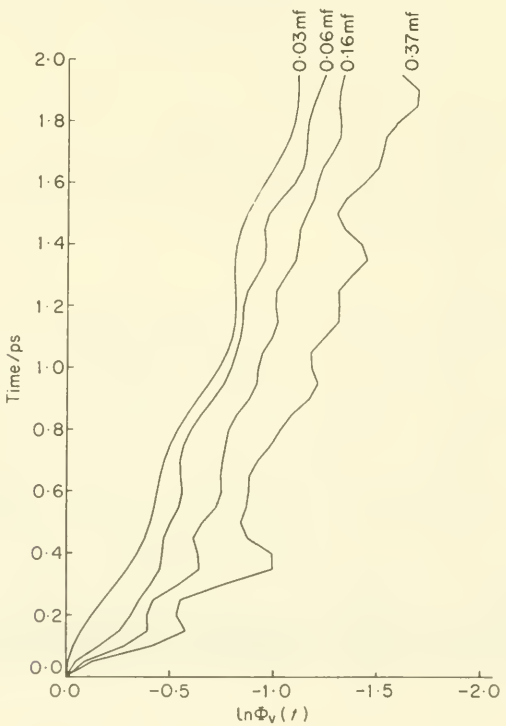

FIG. 20. Comparison of $\ln \Phi_v(t)$ for ν_3 of acetonitrile at different concentrations in carbon tetrachloride. [Reproduced with permission from J. Yarwood, R. Arndt and G. Döge, *Chem. Phys.*, ref. 107]

Study of the ν_2 and ν_4 bands is much complicated by the presence of hot bands (as mentioned above; see Fig. 17), and much of the work in the literature[14, 36, 50, 119, 158, 159] is in error because this has not been fully taken into account. At one time[21, 160] the "structure" of the ν_2 and ν_4 bands was throught to be due to liquid-phase ordering but it has since been shown[133b, 154] that this is not the case since the "structure" is retained even in dilute CCl_4 solutions and the temperature dependence of the ratio of the intensities of the ν_i and $\nu_i + \nu_8 - \nu_8$ components (separated[154] using realistic although probably not unique band profiles) is found to be in agreement with that expected on the basis of a Boltzmann population distribution.

The results of studies on the reorientation of CH_3CN in the liquid phase have been recently summarised in an excellent review by Griffiths.[133b] We are concerned here mainly with information obtained about intermolecular forces. Activation energies obtained for reorientation about the C_3 axis ($E_\parallel$ = 2·9–4·2 kJ mol^{-1}) and perpendicular to this axis ($E_\perp$ = 7·1–8·8 kJ mol^{-1}) have been obtained by a number of techniques (see Table 6 of Ref. 133b). Although these values demonstrate the anisotropic nature of the orientation they are clearly comparable to kT at 300 K (2·4 kJ mol^{-1}) and it is extremely doubtful whether rotation of such a molecule is an "activated" process. Certainly about the C_3 axis rotation is "pseudo-free" and a near-zero activation volume has been obtained.[78] A number of studies aimed at investigating the existence of pair correlations have been reported using Raman, nmr and depolarised Rayleigh scattering. According to equation (14) the difference between $\tau_{LS}(\tau_2^{Ray})$ and $\tau_S(\tau_2^{Ram}$ or $\tau_2^{nmr})$ gives a measure of the orientation correlation factor. Values obtained for τ_{LS} from depolarised Rayleigh scattering in liquid CH_3CN are mostly in the region 1·8–1·9 ps while τ_S values are about 1·1–1·3 ps from nmr[78, 161] data and 0·9–1·2 ps (ν_1)[36, 134, 152] or 1·4 ps (ν_3)[107] from Raman data. Despite claims[50] to the contrary (claims that arise from Rayleigh scattering measurements which are inexplicably[56] independent of concentration in CCl_4) the value of $(1 + fN)/(1 + gN)$ appears to be >1 and probably near 1·7. A recent analysis by Versmold[153] using more up-to-date Rayleigh measurements (including integrated intensities) [equation (13)] gives a value of $(1 + fN)/(1 + gN)$ between 1 and 1·4 depending on concentration in CCl_4. On the other hand Franck and coworkers[162] get values between 0·4 and 0·8 (indicating antiparallel alignment of dipole axes; Section II.B.2) for studies as a function of density. It is therefore extremely difficult at the moment to be certain whether or not the presence of pair correlations has been established. The high ground-state dipole moment would demand (intuitively) that such correlations might be expected. It should be noticed, however, that the effect of these dipoles on the vibrational relaxation functions is small, since

the intensity parameters in equations (68) and (71) for dipolar coupling are presumably *relatively* small. Furthermore, it appears that the rotational correlation times are well accounted for[78, 79] in terms of the J diffusion model, a model in which only hard collisions affect the rotational angular momentum.

Finally, it is interesting that CH_3CN is the only molecule for which it has so far been possible to test the recent predictions of Lynden-Bell (Table I) concerning the variation in vibrational relaxation function for a given mode on going from isotropic Raman to infrared band. We have recently pointed out[107] (Table X) that the reorientational half-widths of the ν_1 and ν_3 infrared

TABLE X. Measured half-widths (FWHM) for infrared and Raman ν_1 and ν_3 bands of liquid acetonitrile

	ν_1 (liquid)	ν_3 (liquid)
Infrared (total)	15 cm^{-1}	12 cm^{-1}
Raman, $I_{iso}(\omega)$	6·5 cm^{-1}	8 cm^{-1}
Infrared (rotational part)	8·5 cm^{-1}	4 cm^{-1}

bands (after subtracting the vibrational half-width obtained from isotropic Raman spectra) are very different, whereas for the same symmetry class they should be the same. This means that either or both $\phi_v(t)$ functions change on going to the infrared. This can be partly confirmed using the results of Breuillard-Alliot and Soussen-Jacob[159] who used the far-infrared data of

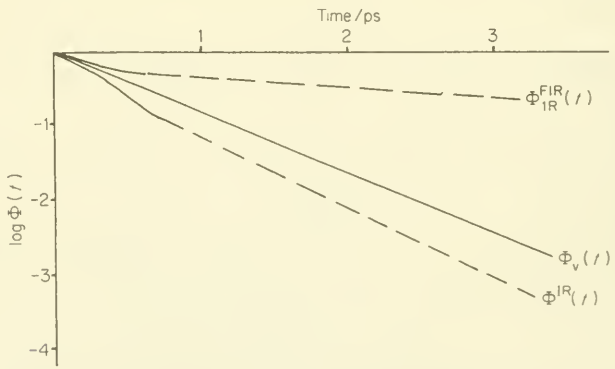

FIG. 21. Comparison of correlation functions for acetonitrile in carbon tetrachloride (1 mol dm^{-3}) from: far-intrared spectrum; the total infrared band profile of the ν_1 vibration; the derived vibrational correlation function for the ν_1 vibration. [Data taken from Refs. 159 and 163]

Fauquembergue *et al.*,[163] in CCl_4 solution in an effort to avoid the problem of measuring pair correlations [see equation (8)], to derive a $\phi_v^{IR}(t)$ function for ν_1. The correlation time is 1·2 ps as compared with a Raman correlation function $\phi_v^R(t)$, at about the same concentration, of about 2·3 ps (Fig. 21). The vibrational part of ν_1^{IR} is therefore very considerably broader than that of ν_1^{Ram}. We establish for the first time therefore that it is in general *wrong* to transfer[12, 36, 119] vibrational correlation functions from isotropic Raman spectra in order to compute $\phi_{1R}(t)$ functions from infrared spectra.

Acknowledgement

Valuable discussions with Prof. G. Döge and Prof. R. E. D. McClung are gratefully acknowledged. We should also like to thank NATO for a research grant and an exchange research fellowship (to R.A.).

REFERENCES

1. J. Yarwood (ed.), "Spectroscopy and Structure of Molecular Complexes", Plenum, London (1973).
2. R. Foster (ed.), "Molecular Complexes", Vols. 1 and 2, Elek Science, London; Crane Russak, New York, (1973, 1974).
3. "The Hydrogen Bond" (eds. P. Schuster, G. Zundel and C. Sandorfy), North Holland Publ. Co., New York (1976).
4. *Adv. Chem. Phys.* (ed. J. O. Hirschfelder), Wiley-Interscience, New York, (1967), Vol. 12, on Intermolecular Forces.
5. R. P. Young and R. N. Jones, *Chem. Rev.*, **71**, 219 (1971).
6. S. Bratos, J. Rios and Y. Giussani, *J. Chem. Phys.*, **52**, 439 (1970).
7. S. Bratos and E. Maréchal, *Phys. Rev.*, **4**, 1078 (1971).
8. R. G. Breene, "The Shift and Shape of Spectra lines", Pergamon, New York (1961).
9. B. J. Berne and G. D. Harp, *Adv. Chem. Phys.*, **17**, 63 (1970).
10. R. G. Gordon, *Adv. Magn. Resonance*, **3**, 1 (1968).
11. R. G. Gordon, *J. Chem. Phys.*, **43**, 1307 (1965).
12. R. T. Bailey, in "Molecular Spectroscopy", Vol. 2, (eds. R. F. Barrow, D. A. Long and D. J. Millen), The Chemical Society, London (1974).
13. A. Cabana, R. Bardoux and A. Chamberland, *Can. J. Chem.*, **47**, 2915 (1969).
14. F. J. Bartoli and T. A. Litovitz, *J. Chem. Phys.*, **56**, 404, 413 (1972).
15. J. G. Powles, in "Chemical Applications of Thermal Neutron Scattering" (ed. B. T. M. Willis), Oxford University Press, London (1973). Ch. 6.
16. T. Springer, "Quasi-elastic Neutron Scattering for the Investigation of Diffusive Motions in solids and liquids", Springer Tracts in Modern Physics, Vol. 64, Springer-Verlag, Berlin (1972).
17. F. Volino and A. J. Dianoux, Proceedings of Meeting on Structure and Dynamics of Organic Liquids, Mittenwald, 1976.
18. L. A. Nafie and W. L. Peticolas, *J. Chem. Phys.*, **57**, 3145 (1972).
19. J. A. Creighton and T. J. Sinclair, *Spectrochim. Acta*, **29A**, 817 (1973).
20. J. E. Griffiths, *Spectrochim. Acta*, **30A**, 169 (1974).

21. A. Loewenschuss and N. Yellin, *Spectrochim. Acta*, **31A**, 207 (1975).
22. G. Fini and P. Mirone, (a) *J. Chem. Soc., Faraday Trans. II*, **70**, 1776 (1974); (b) *Spectrochim. Acta*, **32A**, 625 (1976).
23. B. P. Stoicheff, *Can. J. Phys.*, **36**, 218 (1958).
24. P. van Konynenburg and W. A. Steele, *J. Chem. Phys.*, **56**, 4476 (1972).
25. D. A. Ramsay, *J. Amer. Chem. Soc.*, **74**, 72 (1952).
26. G. Döge, *Z. Naturforsch.*, **28A**, 919 (1973); G. Döge and A. Schäffer, *Ber. Bunsenges. Phys. Chem.*, **77**, 682 (1973).
27. G. Döge, in "Molecular Motions in Liquids" (ed. J. Lascombe), Reidel, Dordrecht (1974), p. 225.
28. W. G. Rothschild, *J. Chem. Phys.*, **65**, 455 (1976).
29. P. C. M. van Woerkam, J. de Bleyser, M. de Zwart, P. J. H. Burgers and J. C. Leyte, *Ber. Bunsenges. Phys. Chem.*, **78**, 1303 (1974).
30. G. Döge, R. Arndt and A. Khuen, *Chem. Phys.*, **21**, 53 (1977).
31. G. Wyllie, in "Dielectric and Related Molecular Processes" (ed. M. M. Davies), The Chemical Soicety, London (1972), Vol. 1, pp. 21–63.
32. D. Kivelson and P. A. Madden, *Mol. Phys.*, **30**, 1749 (1975).
33. J. S. Rowlinson and M. Evans, "Annual Reports, A, 1975", The Chemical Society, London (1975), p. 5.
34. P. van Konynenburg and W. A. Steele, *J. Chem. Phys.*, **62**, 2301 (1975).
35. R. M. Lynden-Bell, "Faraday Symposium No. 11", The Chemical Society, London (1977), p. 167.
36. A. M. Amorin da Costa, M. A. Norman and J. H. R. Clarke, *Mol. Phys.*, **29**, 191 (1975).
37. J. Schroeder, V. H. Schiemann, P. T. Sharko and J. Jonas, *J. Chem. Phys.*, **66**, 3215 (1977).
38. K. Müller, P. Etique and F. Kneubühl, "Molecular Motions in Liquids" (ed. J. Lascombe), Reidel, Dordrecht (1974), p. 265.
39. M. Gilbert and M. Drifford, Proceedings of the International Conference on Raman Spectroscopy, Freiburg, 1976; *J. Chem. Phys.*, **66**, 3205 (1977).
40. A. V. Rakov, *Opt. Spectrosc.* (U.S.S.R.), **13**, 203 (1962).
41. T. R. Gilson and P. J. Hendra, "Laser Raman Spectroscopy", Wiley-Interscience, London (1970).
42. K. Müller and F. Kneubühl, *Helv. Phys. Acta*, **46**, 38 (1973).
43. D. Kivelson, *J. Chem. Phys.*, **63**, 5034 (1975).
44. J. Yarwood, *Spectroscopy Lett.*, **5**, 193 (1972).
45. J. E. Anderson, *J. Chem. Phys.*, **50**, 3784 (1969).
46. B. J. Berne and R. Pecora, *Ann. Rev. Phys. Chem.*, **26**, 233 (1974).
47. A. Gerschel, I. Darmon and C. Brot, *Mol. Phys.*, **23**, 317 (1972).
48. A. Baise, *Chem. Phys. Lett.*, **9**, 627 (1971).
49. R. M. van Aalst, J. van der Elsken, D. Frenkel and G. H. Wegdam, "Faraday Symposium No. 6", The Chemical Society, London (1972), p. 94.
50. S. L. Whittenberg and C. H. Wang, *J. Chem. Phys.*, **66**, 4255 (1977).
51. H. Dardy, V. Volterra and T. A. Litovitz, "Faraday Symposium, No. 6", The Chemical Society, London (1972), p. 71.
52. T. B. MacRury, W. A. Steele and B. J. Berne, *J. Chem. Phys.*, **64**, 1288 (1976).
53. W. G. Rothschild, G. J. Rosasco and R. C. Livingston, *J. Chem. Phys.*, **62**, 1253 (1975).
54. G. R. Alms, D. R. Bauer, J. I. Brauman and R. Pecora, *J. Chem. Phys.*, **59**, 5310 (1973).

55. T. Keyes and D. Kivelson, *J. Chem. Phys.*, **56**, 1057 (1972).
56. C. W. Beer and R. Pecora, "Faraday Symposium No. 11", The Chemical Society, London (1977), paper 5.
57. T. Keyes, *Mol. Phys.*, **23**, 737 (1972).
58. J. G. Kirkwood, *J. Chem. Phys.*, **7**, 911 (1939).
59. A. Ben-Reuven and N. D. Gershon, *J. Chem. Phys.*, **51**, 893 (1969).
60. D. R. Bauer, G. R. Alms, J. I. Brauman and R. Pecora, *J. Chem. Phys.*, **61**, 2255 (1974).
61. D. Kivelson, M. Kivelson and I. Oppenheim, *J. Chem. Phys.*, **52**, 1810 (1970); discussion at the Faraday Symposium No. 11, Dec. 1976.
62. R. Kubo in "Fluctuations Relaxation and Resonance in Magnetic Systems" (ed. D. Ter Haar), Oliver and Boyd, London (1962), p. 26.
63. R. G. Gordon, *J. Chem. Phys.*, **38**, 1724 (1963); **39**, 2788 (1963); **40**, 1973 (1964); **41**, 1819 (1964).
64. I. Rossi-Sonnichsen, J. P. Bouanich and N-V-Thanh, *Compt. Rend.*, **273C**, 19 (1971).
65. R. L. Armstrong, S. M. Blumenfeld and C. G. Gray, *Can. J. Phys.*, **46**, 1331 (1968).
66. R. G. Gordon, *J. Chem. Phys.*, **44**, 1830 (1966).
67. P. Debye, "Polar Molecules", Reinhold, New York (1929).
68. (a) D. Kivelson and R. E. D. McClung, *J. Chem. Phys.*, **49**, 3380 (1968). (b) S. Sunder and R. E. D. McClung, *Can. J. Phys.*, **52**, 1209 (1974).
69. R. E. D. McClung, *J. Chem. Phys.*, **51**, 3842 (1969).
70. R. E. D. McClung, *J. Chem. Phys.*, **57**, 5478 (1972).
71. T. E. Eagles and R. E. D. McClung, *Chem. Phys. Lett.*, **22**, 414 (1973).
72. T. E. Eagles and R. E. D. McClung, *J. Chem. Phys.*, **59**, 435 (1973).
73. R. E. D. McClung and H. Versmold, *J. Chem. Phys.*, **57**, 2596 (1972).
74. R. E. D. McClung, *J. Chem. Phys.*, **55**,3459 (1971).
75. G. Levi, J. P. Marsault, F. Marsault-Herail and R. E. D. McClung, *J. Chem. Phys.*, **63**, 3543 (1975).
76. P. S. Hubbard, *Phys. Rev.*, **131**, 1155 (1963).
77. J. Jonas, *Ann. Rev. Phys. Chem.*, **26**, 167 (1975).
78. T. E. Bull and J. Jonas, *J. Chem. Phys.*, **53**, 3315 (1970).
79. T. E. Bull, *J. Chem. Phys.*, **62**, 222 (1975).
80. R. E. Assink, D. de Zwaan and J. Jonas, *J. Chem. Phys.*, **56**, 4975 (1972).
81. B. J. Berne, *J. Chem. Phys.*, **62**, 1154 (1975).
82. J. F. Dill, T. A. Litovitz and J. A. Bucaro, *J. Chem. Phys.*, **62**, 3839 (1975).
83. D. Kivelson, *Mol. Phys.*, **28**, 321 (1974).
84. M. Evans, *J. Chem. Soc., Faraday Trans. II*, **71**, (a) 843 (1975); (b) 2051 (1975).
85. C. Brot, "Dielectrics and Related Molecular Processes", Vol. 2 (Specialist Periodical Report), The Chemical Society, London (1975), Ch. 1.
86. M. Evans, *J. Chem. Soc., Faraday Trans. II*, **70**, 1620 (1974).
87. M. W. Evans, *Spectrochim. Acta*, (a) **32A**, 1253 (1976); (b) **32A**, 1259 (1976).
88. G. J. Davies and M. Evans, *J. Chem. Soc., Faraday Trans. II*, **71**, 1275 (1975); **72**, 40 (1976).
89. G. J. Davies and M. Evans, *J. Chem. Soc., Faraday Trans. II*, **72**, 1194 (1976).
90. G. J. Davies and M. Evans, *J. Chem. Soc., Faraday Trans. II*, **72**, 1206 (1976).
91. M. Evans, *J. Chem. Soc., Faraday Trans. II*, **71**, 71 (1975).
92. B. Lassier and C. Brot, *Chem. Phys. Lett.*, **1**, 581 (1968).
93. I. W. Larkin, *J. Chem. Soc., Faraday Trans. II*, **69**, 1278 (1973).
94. I. W. Larkin, *J. Chem. Soc., Faraday Trans. II*, **70**, 1457 (1974).

95. R. Haffmans and I. W. Larkin, *J. Chem. Soc., Faraday Trans. II*, **68**, 1729 (1972).
96. I. Larkin and M. Evans, *J. Chem. Soc., Faraday Trans. II*, **70**, 477 (1974).
97. B. Quentrec and P. Bezot, *Mol. Phys.*, **27**, 879 (1974).
98. H. Mori, *Prog. Theor. Phys.*, **33**, 423 (1965); B. S. Berne and J. D. Harp, *Adv. Chem. Phys.*, **17**, 63 (1970).
99. (a) G. J. Evans and M. W. Evans, *J. Chem. Soc., Faraday Trans. II*, **72**, 1169 (1976); (b) A. Gerschel, Conf. on Molecular Motions in Liquids, Nancy, 1974.
100. G. J. Evans, *J. Chem. Soc., Faraday Trans. II*, **73**, 729 (1977).
101. G. J. Davies and M. Evans, *J. Chem. Soc., Faraday Trans. II*, **72**, 2147 (1976).
102. B. J. Berne, "Physical Chemistry: An Advanced Treatise" (ed. H. Eyring, D. Henderson and W. Jost), Academic Press, New York (1971), Vol. 8B, Ch. 9.
103. T. Tokuhiro and W. G. Rothschild, *J. Chem. Phys.*, **62**, 2150 (1975).
104. J. E. Griffiths, M. Clerc and P. M. Rentzepis, *J. Chem. Phys.*, **60**, 3824, (1974).
105. K. Spanner, A. Laubereau and W. Kaiser, *Chem. Phys. Lett.*, **44**, 88 (1976).
106. A. Laubereau and W. Kaiser, *Ann. Rev. Phys. Chem.*, **26**, 83 (1975); A. Laubereau, *Chem. Phys. Lett.*, **27**, 600 (1974).
107. J. Yarwood, R. Arndt and G. Döge, *Chem. Phys.*, **25**, 387 (1977).
108. S. F. Fischer and A. Laubereau, *Chem. Phys. Lett.*, **35**, 6 (1975).
109. P. C. M. van Woerkom, J. de Bleyser, M. de Zwart and J. C. Leyte, (a) *Chem. Phys.*, **4**, 236 (1974); (b) *Chem. Phys. Lett.*, **20**, 592 (1973).
110. (a) D. W. Oxtoby and S. A. Rice, *Chem. Phys Lett.*, **42**, 1 (1976); (b) D. C. Krauss and R. S. Wilson, *Chem. Phys.*, to be published; (c) D. J. Diestler, *Chem. Phys. Lett.*, **39**, 39 (1976).
111. K. A. Valiev, *Opt. Spectroscopy*, **11**, 253 (1961).
112. M. Kakimoto and T. Fujiyama, *Bull. Chem. Soc. Japan*, **47**, 1883 (1974).
113. P. A. Madden and R. M. Lynden-Bell, *Chem. Phys. Lett.*, **38**, 163 (1976).
114. R. M. Lynden-Bell, *Mol. Phys.*, **33**, 907 (1977).
115. S. Bratos, *J. Chem. Phys.*, **63**, 3499 (1975).
116. A. Laubereau, D. von der Linde and W. Kaiser, *Phys. Rev. Lett.*, **28**, 1162 (1972).
117. R. M. Lynden-Bell, *Mol. Phys.*, **31**, 1653 (1976).
118. G. Döge, *Z. Naturforsch.*, **23A**, 1405 (1968); **24A**, 1130 (1968).
119. D. R. Jones, H. C. Anderson and P. Pecora, *Chem. Phys.*, **9**, 339 (1975).
120. M. Constant and R. Fauquembergue, *J. Chem. Phys.*, **58**, 4030 (1973); *Compt. Rend.*, **272B**, 1293 (1971).
121. M. Delhaye and R. Fauquembergue, *Compt. Rend.*, **271B**, 1177 (1971).
122. H. J. Campbell, J. F. Fisher and J. Jonas, *J. Chem. Phys.*, **61**, 346 (1974).
123. R. B. Wright, M. Schwartz and C. H. Wang, *J. Chem. Phys.*, **58**, 5125 (1973).
124. A. Abragam, "The Principles of Nuclear Magnetism", Clarendon Press, Oxford (1961), pp. 431–33.
125. A. S. Davydov, "Theory of Molecular Excitons", McGraw-Hill, New York (1962).
126. D. J. Diestler and R. S. Wilson, *J. Chem. Phys.*, **62**, 1572 (1975).
127. K. F. Herzfeld and T. A. Litovitz, "Absorption and Dispersion of Ultrasonic waves", Academic Press, New York (1959), p. 322.
128. R. Arndt, Dissertation, T.U. Braunschweig (1974).
129. R. Arndt and R. E. D. McClung, *J. Chem. Phys.*, **69**, 4280 (1978).
130. G. Döge, H. J. Geier and H. D. Günther, *Ber. Bunsenges. Phys. Chem.*, **72**, 1062 (1968).
131. R. Arndt and D. Scheibe, Proc. 5th International Conference on Raman Spectroscopy, H. F. Schulz Verlag, Freiburg (1976), p. 52.
132. H. S. Goldberg and P. S. Pershon, *J. Chem. Phys.*, **58**, 3816 (1973).

133. J. E. Griffiths, (a) *Chem. Phys. Lett.*, **21**, 354 (1973); (b) "Vibrational Spectra and Structure", (ed. J. R. Durig), Elsevier, Amsterdam (1977), Vol. 6.
134. G. D. Patterson and J. E. Griffiths, *J. Chem. Phys.*, **63**, 2406 (1975).
135. G. Döge and R. Arndt, unpublished results.
136. A. F. Bondarev and A. I. Mardaeva, *Opt. Spectrosc.*, **35**, 286 (1973).
137. T. Fujiyama, M. Kakimoto and T. Suzuki, *Bull. Chem. Soc. Japan*, **49**, 606 (1976).
138. J. de Zwaan, D. W. Hess and C. S. Johnson, *J. Chem. Phys.*, **63**, 422 (1975).
139. I. Rossi-Sonnichsen, C. Brodbeck, N. V. Thanh and A. Ruoff, *Compt. Rend.*, **279C**, 997 (1974).
140. D. A. Wright and M. T. Rogers, *J. Chem. Phys.*, **63**, 909 (1975).
141. (a) J. H. Campbell and J. Jonas, *Chem. Phys. Lett.*, **18**, 441 (1973). (b) J. Schroeder, V. H. Schieman and J. Jonas, *J. Chem. Phys.*, in press.
142. L. C. Rosenthal and H. L. Strauss,. *J. Chem. Phys.*, **64**, 282 (1976).
143. D. L. van der Hart, *J. Chem. Phys.*, **60**, 1858 (1974).
144. G. Fini, M. Giordini and P. Mirone, *Gazz. Chem. Ital.*, **102**, 288 (1972).
145. S. K. Garg, H. Kilp and C. P. Smyth, *J. Chem. Phys.*, **43**, 2341 (1965).
146. W. G. Rothschild, *J. Chem. Phys.*, **57**, 991 (1972).
147. M. L. McGlashan and P. R. Rastogi, *Trans. Faraday Soc.*, **54**, 496 (1958).
148. J. Czubryt, E. Tomchuk and E. Bock, *Ber. Bunsenges. Phys. Chem.*, **75**, 243 (1971).
149. D. D. Deshpande and S. L. Oswal, *J. Chem. Soc., Faraday Trans. I*, **68**, 1059 (1972).
150. (a) T. A. Litovitz, *J. Chem. Phys.*, **26**, 469 (1957). (b) W. M. Madigosky and T. A. Litovitz, *J. Chem. Phys.*, **34**, 489 (1961).
151. G. C. Tabisz and R. M. Lynden-Bell, *Chem. Phys. Lett.*, **46**, 175 (1977).
152. J. E. Griffiths, *J. Chem. Phys.*, **59**, 751 (1973).
153. H. Versmold, Proceedings of the meeting on Structure and Dynamics of Organic Liquids, Mittenwald, 1976; *Ber. Bunsenges. Phys. Chem.*, **82**, 451 (1978).
154. G. Fini and P. Mirone, *Spectrochim. Acta*, **32A** 439 (1976).
155. T. Fujiyama and M. Kakimoto, *Bull. Chem. Soc. Japan*, **45**, 3021 (1972).
156. J. Yarwood and R. Arndt, *Chem. Phys. Lett.*, **45**, 155 (1977).
157. J. Yarwood, unpublished data.
158. J. Yarwood, *Adv. Mol. Rel. Processes*, **5**, 375 (1973).
159. C. Breuillard-Alliot and J. Soussen-Jacob, *Mol. Phys.*, **28**, 905 (1974).
160. A. Loewenschuss and N. Yellin, *Spectrochim. Acta* **32A**, 1249 (1976).
161. T. T. Bopp, *J. Chem. Phys.*, **47**, 3621 (1967).
162. E. U. Franck, Proceedings of the meeting on Structure and Dynamics of Organic Liquids, Mittenwald, 1976.
163. R. Fauquembergue, Y. Leroy and P. Desplanques, *Compt. Rend.*, **269B**, 701 (1969).

5 Contact Charge-transfer Spectra

MILTON TAMRES

Department of Chemistry, University of Michigan, Ann Arbor, Michigan 48109, U.S.A.

ROBERT L. STRONG

Department of Chemistry, Rensselaer Polytechnic Institute, Troy, New York 12181, U.S.A.

I. Introduction 332
II. Theory of EDA Complexes 333
A. Ground-state stability 333
B. Absorption spectra 336
C. Solvent effects 338
III. Thermodynamic Properties from CT Spectra 339
A. Equilibrium constant 340
1. Benesi–Hildebrand (B–H) method 340
2. Constant activity method 342
3. Collision theory 343
4. Comments on K 344
B. Internal energy change 349
IV. Operational Criteria for Contacts 351
A. Internal energy change 352
B. Equilibrium constant 352
C. Wavefunction coefficient ratios 353
D. Viscosity and phase-change effects 354
V. Selection of Data for Contacts 357
VI. Molecular Halogen Acceptors 359
A. With alkanes 360
B. With cyclopropanes 365
C. With aromatic hydrocarbons 366
D. With alkenes 366
E. With alkyl halides 368
F. With halogen donors 378
G. With other donors 378
VII. Transient Halogen Atom Acceptors 379
A. Halogen atom recombination 380

1. Gas-phase recombination from flash photolysis studies . . 380
2. Liquid-phase photodissociation and recombination . . . 385
B. Charge-transfer spectra of halogen atoms 386
1. Spectral and thermodynamic measurements on transient halogen atom systems 386
2. Halogen atom charge-transfer spectra in the liquid phase . . 389
C. Vapour-phase halogen atom charge-transfer spectra . . . 393
D. Alkyl halide–halogen atom charge-transfer spectra . . . 393
VIII. Molecular Oxygen Acceptor 397
IX. Highest Valency Halides, Oxides and Oxyhalide Acceptors . . 416
X. Substituted Methane Acceptors 421
XI. π^*-Acceptors 432
XII. Miscellaneous 442
References 446

I. INTRODUCTION

When an electron donor, D, and an electron acceptor, A, interact, their physical properties are perturbed and new properties arise which are attributed to the formation of a complex, C. If a known relation exists between the new or perturbed properties and the concentration of complex, their investigation permits evaluation of the thermodynamic functions of the system. The kinds of physical (and chemical) measurements that have been made to study electron donor–acceptor (EDA) interactions are extremely varied. Many of these have been covered in several books under such titles as "electron donor–acceptor complexes[1] (or bonds[2])", "charge-transfer complexes",[3,4] and "molecular complexes[5–10] (or interactions[11] or association[12])", as well as numerous review articles.[3a,13–18]

Among the most widely used methods is that of spectroscopy, particularly involving the ultraviolet and visible regions. Impetus to these studies stems largely from the experimental paper of Benesi and Hildebrand[19] who drew attention to the appearance in solution of new ultraviolet spectral bands upon formation of 1:1 iodine complexes with aromatic hydrocarbons. These new bands were attributed by Mulliken[20] to an electronic excitation from an occupied level of the donor molecule to an empty level of the acceptor molecule, i.e. they are charge-transfer (CT) spectra.

The limiting case of weak EDA interactions which last sufficiently long for intermolecular CT absorption to occur can be called "contacts" or, simply "encounters" (such a term would signify that collisions need not be violent[21]). Because contacts are unstable, their concentrations are lower than the donor and acceptor concentrations, and sensitive methods often are required for their study. Charge-transfer bands usually are quite intense, with extinction coefficients of the order $10^4\,l\,mol^{-1}\,cm^{-1}$, and they provide

one of the commonly used means to study very weak complexes. The purpose of this chapter is to focus on the characterization of the most weakly interacting species, primarily of their contact charge-transfer (CCT) absorption spectra, i.e. the positions, shapes and intensities of the bands, and the thermodynamic properties derived from these spectra.

It is not easy to define the term "molecular complex".[9a, 13] One may agree that "a complex is a loose reversible association of two or more distinct chemical compounds",[22] but reaching agreement on what is meant by "loose" is more difficult. How strong should the association be before the system itself can be called a stable chemical compound, or how weak must it be to be called a contact?[9a] Stability is a function of temperature and will, of necessity, make the selection of systems dependent on temperature regardless of which criteria may be chosen. One suggestion in defining a complex is that the species stay together for more than one intermolecular vibration. This criterion is practically impossible to apply,[15] and the short lifetime would not make the definition suitable to most of the experimental methods used to study complexes. One approach is to consider "operational" definitions of contacts in searching for systems that are said to exhibit CCT spectra. Such definitions evidently contain an element of arbitrariness. In fact, distinction between very weak complexes and contacts may be a matter of semantics.[23, 24] Nevertheless, a distinction between these two terms is appropriate. For a very weak EDA pair there are likely to be several orientations, having slightly different strengths of interaction. The more favourable orientations may satisfy the arbitrary criteria selected for complex formation, while those less favourable would not. Therefore, we will maintain the distinction and we shall avoid using both terms in the same context, as in the phrase "contact charge-transfer complex."

There has been so much published on EDA theory, on the methods and reliability of determining thermodynamic and spectral properties of EDA complexes, and on the correlations involving the thermodynamic and spectral properties, that neither is it appropriate nor is it considered feasible to review them here. Brief mention will be made only of those aspects that bear on the problem of defining and characterizing contacts. References will be given to detailed accounts.

II. THEORY OF EDA COMPLEXES

The theory of EDA complexes has been amply covered in many books.[1–7, 11]

A. Ground-state Stability

Figure 1 is a potential energy diagram for the interaction of a neutral *isolated*

D molecule with a neutral *isolated* A molecule to form a 1:1 molecular EDA complex. It is simplified in that only one of the large manifold of excited states is shown. Following Mulliken's[7,20,25] notation, W_0 is the energy corresponding to the wavefunction for the "no-bond" structure, $\psi_{0(D,A)}$, and is the net energy from all the electrostatic attraction and repulsion between neutral D and A (coulomb, induction, dispersion and exchange repulsion;

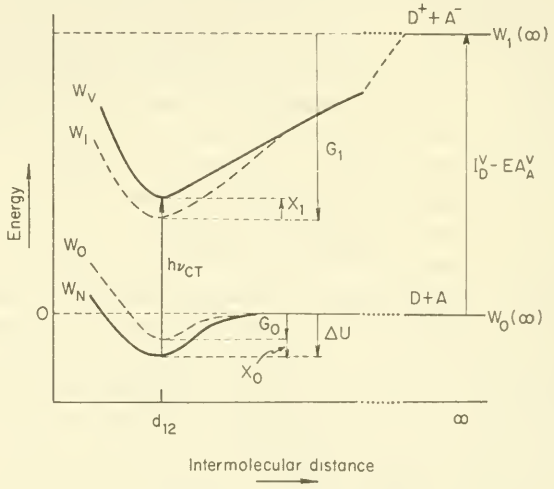

FIG. 1. Potential energy diagram for an electron donor–acceptor complex. [Adapted with permission from R. S. Mulliken and W. B. Person, "Molecular Complexes. A Lecture and Reprint Volume", Wiley, New York (1969)]

see Murrell[26]) including any reorganization energy in altering the structure of D and A to the geometry they have in the complex. The energy difference between D and A at infinite separation and at the intermolecular equilibrium distance (d_{12}) is G_0. The energy to transfer an electron from D to A at infinite separation is $I_D^V - EA_A^V$, where I_D^V is the vertical ionization energy of D and EA_D^V is the vertical electron affinity of A. W_1 is the energy corresponding to the wavefunction of the "dative" structure, $\psi_{1(D^+-A^-)}$, and represents the net energy from the interaction of two ions, D^+ and A^-, with pairing of their electrons. The energy to bring together D^+ and A^- from infinite separation is G_1 and is predominantly the coulombic energy, with some contribution from the other interactions (as for G_0). The wavefunctions of the singlet ground (N) state and singlet excited (V) state of the complex are taken to be a linear combination of ψ_0 and ψ_1:

$$\psi_N \approx a\psi_{0(D,A)} + b\psi_{1(D^+-A^-)} \tag{1}$$

and

$$\psi_V \approx a^*\psi_{1(D^+ A^-)} - b^*\psi_{0(D,A)} \quad (2)$$

where a and b are mixing coefficients, and $a \approx a^*$ and $b \approx b^*$. This mixing of states results in resonance stabilization to ψ_N at the distance d_{12} by X_0, and destabilization to ψ_V by X_1.

From Fig. 1, the ground-state stability, measured by the change in internal energy, ΔU, is:

$$\Delta U = G_0 + X_0. \quad (3)$$

Actually, a series of potential energy curves should be drawn for different orientations of the DA pair, each with its own d_{12} and ΔU.

For stable complexes, ΔU is large and negative, being much greater than RT. Here, X_0, which is always negative, is large, and G_0 may be either negative or positive (if large reorganization energy is involved as a result of formation of a D—A bond). For weak complexes, it has been shown (e.g., Hanna and coworkers,[27–29] Mantione,[30, 31] Dewar and Thompson,[32] Atack and Rice,[33] Cook and Schug,[34] LeFèvre and coworkers,[35] Morokuma and coworkers,[36] and references therein; see also Sambhi[37]) that the electrostatic energy is of prime importance in many of the cases examined theoretically, and it now seems accepted that the G_0 term is dominant.[7a, 15] Reorganization energy should be minimal here, so that G_0 is small and negative. In the absence of resonance stabilization, $W_N \equiv W_0$ and $W_V \equiv W_1$.

When ΔU approaches RT in magnitude there is, at best, a loose and rather brief association of D and A. Vibrational modes of very low frequency are present, and population of excited vibrational states at room temperature is expected to be high. The geometry no longer corresponds to a single DA orientation but, as suggested by Rice,[38] there may be almost free rotation of one molecule over the surface of the other. Here, at equilibrium, the system contains both complexes and contacts, in addition to free donor and acceptor, with the relative contributions being a function of temperature.

In the limiting case, i.e. $\Delta U = 0$, there is no longer a thermodynamically preferred orientation, although some orientations may be more favourable in regard to CCT absorption. Here, the interacting species can be thought of as consisting entirely of contacts. $W_N \equiv W_0$ is unchanged as D and A are brought together from infinity to the distance d_{12}, and then becomes increasingly positive at shorter intermolecular distances owing to repulsion of the nuclei and the interpenetration of electron clouds.

From a rigorous viewpoint, ΔU will not be exactly zero for the interaction between molecules of a real gas. Attraction between the same or different molecules is a prerequisite for condensation, with the formation of a bimolecular species being a first step in the condensation process.[24, 39] Therefore, ΔU

will be negative, *although small*, for molecules at van der Waals distance. If $\Delta U < 0$ were to be used as a rigid criterion for complexation then, in a strict sense, one might use the term "complex" for all interactions in the gas phase when the gas is below the Boyle temperature.[40] For D and A dissolved in a solvent, *S*, the London dispersion forces of D–S, A–S and S–S may cancel those of D–A.[7b] Thus, for interaction in solution, ΔU may be negative, zero, or even positive.

We shall adopt a more "liberal" approach in our definition of contacts, at least for the purposes of this chapter, by including systems that have a small, negative value for ΔU (Section IV).

B. Absorption Spectra

The position of the CT band maximum for EDA complexes (Fig. 1) is given by the equation:

$$h\nu_{CT} = W_V - W_N = I_D^V - EA_A^V + G_1 - G_0 + X_1 - X_0. \tag{4}$$

The last three terms in equation (4) are negligible for contacts, so the frequency of the CCT band maximum is approximated by:

$$h\nu_{CCT} \approx I_D^V - EA_A^V - e^2/d_{12}. \tag{5}$$

Here, $G_1 \approx e^2/d_{12}$, where e is the unit electron charge.

A more precise treatment of CT spectral properties requires consideration of other excited states in equations (1) and (2). These include states corresponding to structures for back charge-transfer (D^-–A^+), excited CT structures (D^+–A^-* and D^+*–A^-), and locally excited structures (D*, A and D, A*). The more general expressions for the wavefunctions then become

$$\psi_N = a\psi_{0(D,A)} + \sum_i b_i\psi_{i(D^+-A^-)} + \sum_j c_j\psi_{j(D^--A^+)} + \sum_k d_k\psi_{k(D^*,A)} + \sum_l e_l\psi_{l(D,A^*)} \tag{6}$$

and

$$\psi_V = \sum_i a_i^*\psi_{i(D^+-A^-)} - b^*\psi_{0(D,A)} + \sum_j c_j^*\psi_{j(D^--A^+)} + \sum_k d_k^*\psi_{k(D^*,A)} + \sum_l e_l^*\psi_{l(D,A^*)} \tag{7}$$

where the summation is over the appropriate manifold of CT and locally excited states.

Figure 2 is an energy level diagram, similar to that of Nagakura,[41] adapted for contacts and showing pertinent spectra among several singlet and

triplet states. It is assumed in this example that the local excitation of D lies highest in energy and that the triplet state $^3\psi_V$ is lower in energy than the singlet $^1\psi_V$.

Systems with no ground-state stability may form complexes with appreciable binding energy from the interaction of an excited state donor molecule with a ground state acceptor molecule, or vice versa (i.e. exciplexes[42]

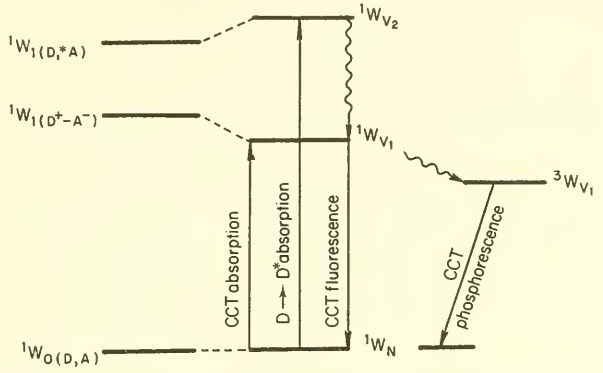

FIG. 2. Energy level diagram for contacts assuming that the triplet CT state is lower in energy than the singlet state. [Adapted with permission from S. Nagakura[41]]

and excimers[43,44].) For exciplexes, charge transfer results in a state such as $(D^+–A^-)^*$. Fluorescence from this state to the ground state is the reverse process of CCT absorption. Progress in nanosecond and picosecond time-resolved spectroscopy has resulted in increased attention in the study of excited state properties. The reader is referred to some recent reviews in this field[41,45–47] and to Chapter 1 of this volume. In keeping with the aim of this chapter, we will consider primarily the ground state characteristics.

As seen from Figs. 1 and 2, the presence of a CT band is no indication of stability *per se*. But there is a correlation between the CT band position with EDA stability which is most favourable for a homologous series of D–A pairs where there is systematic variation in I_D^V or EA_A^V [equation (4) or (5)].[1,2,7]

Similar comments apply to CT band intensities. The integrated intensity, or oscillator strength, of an electronic transition is related to the square of the electronic transition dipole, μ. For a CT transition from the N state to the V state, μ_{VN} is defined by:

$$\mu_{VN} = -e \int \psi_V \sum r_i \psi_N \, d\tau \tag{8}$$

where r_i is the vector distance of the ith electron from a convenient origin.

This can be shown to give approximately:[7c, 20]

$$\mu_{VN} \approx a^*b(\mu_{11} - \mu_{00}) + (aa^* - bb^*)(\mu_{01} - S_{01}\mu_{00}) + g\mu^*_{DD} + \ldots \quad (9)$$

S_{01} is the overlap integral $\int \psi_0\psi_1 \, d\tau$, and the μ terms are similar in definition to equation (8). The first two terms in equation (9) arise from using equations (1) and (2). The third (and other) terms arise when more excited states are included [equations (6) and (7)]. The first term, $(\mu_{11} - \mu_{00})$, corresponds essentially to the change in the dipole moment produced by transferring an electron from D to A keeping the nuclei fixed, and is large. For EDA complexes, where the coefficient b is appreciable, the first term may be the dominant contributor to the band intensity. For contacts, there may be an instantaneous small value for b; but even if $b = 0$ the other terms need not be zero. The second term can be related[7] to the overlap between the donor and acceptor orbitals. For an acceptor molecule such as iodine, its orbital (σ^*) is strongly antibonding and bloated in size,[48] so overlap occurs even in the absence of resonance stabilization between D and A, and this could result in appreciable intensity. For other D–A pairs, such as those of π–π^* type, this may be much less. A further important factor, as pointed out by Murrell,[49, 50] is that intensity can be borrowed through mixing of the CT state with the locally excited state of the donor (and/or acceptor) as given by the third term (see Fig. 2). These various contributions, which can make μ_{VN} rather large, may be quite different for unrelated type complexes, and it appears not to be possible in general to relate band intensity with stability. However, such correlation should be more favourable for a homologous series of complexes, and was so expected in the early theory.[7, 20] One problem in considering the question of band intensities is the reliability of the data. This is true particularly of the CCT bands where, in many instances, their reported characterization is in error (Section VI).

C. Solvent Effects

The theory of EDA interactions is a *gas-phase* theory,[7d] but most of the studies have been carried out in solution. Solvent effects on the spectral and thermodynamic properties of solutes, including CT complexes, have been studied extensively and have been the subject of many reviews.[24, 51–59]

Two recent reviews[24, 54] give data that compare the spectral and thermodynamic properties of iodine complexes in the gas phase and in n-heptane solution. Results reported for a range of complexes from strong to weak show trends that should extend to contacts. The solvent effects are rather large, and the following changes can be cited in going from the gas phase to solution for weak CT complexes: (1) a smaller equilibrium constant K;[3b, 60] (2) a larger molar absorption (extinction) coefficient (ϵ);[38, 61–63] (3) a

red shift of the CT band which becomes larger the weaker the complex; and (4) a smaller ΔU. (See the review by Tamres[24].)

Solvents are never completely "inert", although some such as the saturated hydrocarbons and carbon tetrachloride often are assumed to be nearly so. Yet it is known that these do behave as donors (toward halogens, Sections VI and VII), and the latter is an acceptor toward amines.[64,65] Fluorocarbons have a lower dielectric constant than the saturated hydrocarbons, and while this makes them more "inert" they are also poorer solvents.[66] For example, the spectrum of iodine in n-perfluoroheptane is similar to the spectrum of its vapour,[67] but the iodine solubility is low.

Interactions between solvent and solute molecules sometimes have been separated into two broad categories, namely, "specific" and "non-specific" effects. Specific interactions, of which hydrogen bonding is an example, generally would be expected to result in a preferred orientation of the species and would correspond to the formation of a complex. Non-specific interactions correspond to the classical electronic effects arising from random encounters and, as such, perhaps can be placed in the category of contacts. (It should be mentioned that to distinguish between specific and non-specific effects is likely to be just as difficult as it is to distinguish between contacts and complexes.) It is pertinent to note here a suggestion by Guggenheim[68] to use degree of "association" and degree of "sociation" to describe the fraction of interacting pairs of molecules, the former pertaining to all interactions and the latter to interactions in excess of that due to random encounters.

CT spectra involving solvents are well known. Some years ago, Blandamer and Fox[69] wrote an extensive review on charge-transfer-to-solvent (CTTS) spectra. These generally involve anions as the donor, and polar solvents as the acceptor. Various theoretical models have been suggested for the interaction[69] including that of CT complexation.[70] We shall not deal with systems involving ion–solvent interaction because the interactions are expected to be large. Even those cases where the overall energetics involving an anion donor are very small[71] are probably due to a cancellation from solvent effects.

III. THERMODYNAMIC PROPERTIES FROM CT SPECTRA

Since the CT spectral band characteristics do not serve as a criterion for defining contacts, it will be necessary to consider those properties that are determined from the spectra which are related to stability. These are primarily the thermodynamic properties, e.g. K and ΔU, or a combination of these with the spectral properties. If they are to be used as criteria, their reliability ought to be considered.

A. Equilibrium Constant

Much has been written about the problem of determining meaningful values of K (and ϵ) for weak complexes. There are too many papers to list individually, and attention is drawn to several excellent reviews.[2a, 3c, 72, 73]

1. Benesi–Hildebrand (B–H) Method

The classical procedure to determine K of EDA complexes from CT data is that of Benesi and Hildebrand,[19] or some modification of it[3, 73] (Scott,[74] Scatchard,[75] Foster and coworkers[76, 77]). The equilibrium constant for complex formation (neglecting activity coefficients) is:

$$K = C/D_0 - C)(A_0 - C) \tag{10}$$

where D_0 and A_0 are the initial concentrations of donor and acceptor, respectively. For contacts, where $C \ll D_0$ or A_0, the reciprocal of equation (10) becomes:

$$K^{-1} = D_0A_0/C - D_0 - A_0. \tag{11}$$

For the often used condition $D_0 \gg A_0$:

$$K^{-1} = D_0A_0/C - D_0. \tag{12}$$

This equation can be rearranged to give:

$$C = D_0A_0K/(1 + KD_0). \tag{13}$$

The spectrophotometric equivalent of equation (13) based on the Beer–Lambert law ($A = \epsilon bC$, where b is the cell path) is:

$$A = D_0A_0Kb\epsilon/(1 + KD_0). \tag{14}$$

This equation has the form of a typical adsorption isotherm, as shown in Fig. 3. Person[78] divided the figure into three regions. In region I, where $KD_0 \ll 1$:

$$A = D_0A_0Kb\epsilon. \tag{15}$$

Here, there is a linear dependence of A on D_0 for fixed A_0 (and also on A_0 for fixed D_0). The line goes through the origin with a slope of $A_0Kb\epsilon$. Such a dependence is what is expected from a "collision" model (Section III.A.3). Spectrophotometric studies can give only the product $K\epsilon$ in this case and not their separate values. It is apparent also in equation (14) that the donor concentration range where this dependence holds gets larger as the complex gets weaker, i.e. as $K \rightarrow 0$. Studies extending into region II permit the separate evaluation of K and ϵ by the typical B–H method. The initial section corresponds to weak complexation and the later one to strong complexation. [For the latter, the approximations leading to equation (11) from equation

(10) are no longer valid.[60]] In region III, the saturation region, $KD_0 \gg 1$, and $A = \epsilon bA_0$, i.e. the excess donor complexes all the acceptor, and only ϵ of the resulting compound is determined.

Equation (14) (or Fig. 3) represents a continuous function, and any division into regions I and II, or II and III, is arbitrary. Considering the errors associated with spectrophotometric measurements, Person suggested the reasonable limits for region II as $0{\cdot}1 \leqslant KD_0 \leqslant 9$ or, as shown in Fig. 3, $0{\cdot}1/K \leqslant D_0 \leqslant 9/K$.

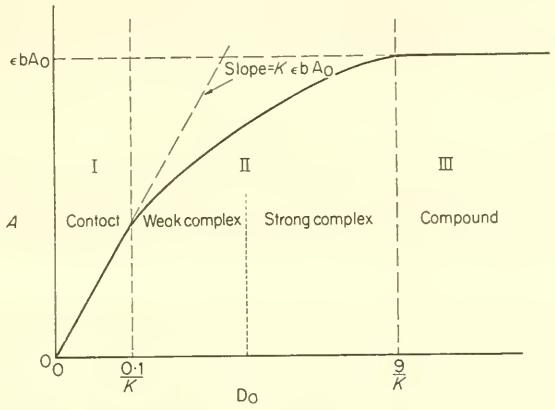

FIG. 3. Absorbance as a function of donor concentration at a fixed acceptor concentration (coordinates not drawn to scale). [Adapted with permission from W. B. Person, *J. Amer. Chem. Soc.*, **87**, 167 (1965)]

Similar conclusions are reached by looking at the well known spectrophotometric equivalent of equation (11):

$$D_0 bA_0/A = (1/\epsilon)[(D_0 + A_0) + 1/K] \tag{16}$$

which is the Scott modification[74] of the B–H equation. As $K \to 0$, $1/K$ becomes the dominant term in the brackets, i.e. the $(D_0 + A_0)$ contribution lies within the random error in measuring absorbance, and only the $K\epsilon$ product can be determined. Separation of K and ϵ is favoured when $(D_0 \ldots A_0)$ is comparable in magnitude to $1/K$, which occurs over the range suggested in the Person criteria. For strong complexes, where $D_0 \gg 1/K$ and $D_0 > A_0$, only ϵ of the complex can be determined.

The limit to which the concentration range of D_0 and A_0 can be extended experimentally depends on their solubilities in the chosen solvent and on the cell pressure in the gas phase. If, at the highest D_0 concentration used, the product KD_0 falls within Person's region I, analysis of the absorbance data

at a fixed temperature can lead only to results that are compatible with a contact model, even though the interaction may be quite strong.

A useful modification of equation (14) has been suggested by Cilento and Sanioto.[79] Letting m_D and m_A equal the number of moles of donor and acceptor present initially in volume V, then $D_0 = m_D/V$, $A_0 = m_A/V$, and equation (14) rearranges to:

$$1/V(A) = V/m_D m_A K b\epsilon + 1/m_A b\epsilon. \tag{17}$$

Thus, a plot of $1/V(A)$ versus V, obtained by dilution so that m_A and m_D are constant, should give a straight line with slope equal to $1/m_D m_A K b\epsilon$ and intercept (at $V = 0$) equal to $1/m_A b\epsilon$. Furthermore, as K approaches zero (contact, or Person's Region I):

$$A = m_D m_A K b\epsilon / V^2 \tag{18}$$

so the absorbance decreases as the square of the dilution. This treatment has been used extensively by Hammond and coworkers[80] to verify the contact character of many "ball plane" interactions as discussed later in Section IX.

2. Constant Activity Method

Overlap of component and complex bands requires determination of K to resolve the composite band. In the B–H procedure, if the complex is weak, K becomes less well determined and there may be considerable error in the characterization of the shape and position of the complexed band. An example of this, although involving a blue-shifted iodine visible band rather than a CT band, is the gas-phase study of the diethyl ether–iodine complex.[81]

The constant activity method circumvents this problem. The activity of a component can be controlled through a solid–vapour (or solid–solution) equilibrium. In the case of iodine complexes, it has been shown[82–86] that a useful system (one that provides a convenient concentration of iodine for spectrophotometric studies) is:

$$(CH_3)_4NI_5(s) \rightleftharpoons (CH_3)_4NI_3(s) + I_2(g)$$

or (19)

$$\tfrac{1}{2}(CH_3)_4NI_9(s) \rightleftharpoons \tfrac{1}{2}(CH_3)_4NI_5(s) + I_2(g).$$

Addition of a donor to form an iodine complex shifts the solid–vapour equilibrium to replace the complexed iodine. The difference spectrum of a donor + polyiodide mixture versus a polyiodide blank gives directly the CT band and the blue-shifted visible iodine band (assuming no absorbance by the donor). With this method it was possible to determine the band shape and position for the blue-shifted iodine visible band (and the CT band) in

the diethyl ether–iodine complex in the gas phase[85] *without* evaluation of K or ϵ.

Locally excited bands are perturbed on complexation. At the wavelength where the free and complexed bands cross (the isosbestic point), their molar absorption (extinction) coefficients are the same. By measuring the isosbestic point, in the absence of donor, the constant activity method can be used to obtain K directly, in a single measurement, from the increase in absorbance at the isosbestic point on adding donor.[82] This would apply, of course, to CT bands which overlap with one of the component bands. Again there is a practical limit to this procedure. As $K \rightarrow 0$, the enhancement in absorbance at the isosbestic point gets smaller. The uncertainty in determining quantitatively the increase in absorbance becomes sufficiently large that evaluation of K is no longer feasible.

3. Collision Theory

An equation similar to equation (15) is obtained from collision theory. The number of collisions per cubic centimetre per second between two gases D and A is:[87]

$$Z = \pi N_D N_A d_{12}^2 \bar{c} \tag{20}$$

where N_D and N_A are the concentrations of the species in molecules per cubic centimetre, d_{12} is the mean molecular diameter $[(d_1 + d_2)/2]$, and $\bar{c}$ is the average relative speed. The concentration of contacts in molecules per cubic centimetre is $Z \times t$, where t is the time of "sticking together"[87a] of the D–A pair. In the limiting case of "no sticking," i.e. a rebounding model, the time can be replaced by[88]

$$t = 2\Delta d/\bar{c} \tag{21}$$

where Δd is the distance between the pair within which electron transfer can occur.

The product $Z \times t$ $(= C)$ in units of mol l^{-1} is:[89]

$$C = 37{\cdot}84 \times 10^{-4} D_0 A_0 d_{12}^2 \Delta d \tag{22}$$

where d_{12} and Δd are in units of Å.

From the Beer–Lambert law

$$A = \epsilon b C = \epsilon b(37.84 \times 10^{-4} d_{12}^2 \Delta d) D_0 A_0. \tag{23}$$

Comparing equations (15) and (23):

$$K = 37{\cdot}84 \times 10^{-4} d_{12}^2 \Delta d. \tag{24}$$

If ν_{CCT}, I_D^V and EA_A^V are known, d_{12} can be calculated from equation (5).

According to Mulliken,[48] d_{12} may be larger than the intermolecular distance based on van der Waals radii, as in the case of complexes with molecular halogens where electron transfer is to the strongly antibonding σ^* orbital which is of large size.

From the data for D_0, A_0 and A it is possible to calculate C from equation (22), ϵ from equation (23), and K from equation (24) [or the more exact equation (10)] provided that an estimate is made of Δd. Prue[90] made the following estimate for contacts in solution. The "free volume" of liquids, i.e. the molar volume minus the volume of the molecules themselves, is approximately 0·5 ml mol^{-1} (or 8×10^{-25} ml $molecule^{-1}$), within a factor of 2 or 3. The cube root of this, assuming cubical packing, gives the average distance that a molecule can move with respect to a neighbour, Δd, and is $\sim$0·94 Å. Tamres and Grundnes[88] used a value of 1 Å in their gas-phase study of alkane–iodine CCT spectra. Morita and Tamres,[89] in a study of alkyl halide–iodine interactions, list several values of Δd from 1–4 Å and give the corresponding results for C, ϵ and K. (see Section VI.)

Both Z and t depend on the speed of the molecules, which is a function of temperature. Since Z changes directly with speed, whereas t changes inversely, the $Z \times t$ product is independent of temperature, assuming no change in d_{12} or Δd over a limited temperature range. Hence, the equilibrium constant remains independent of temperature, as indicated in equation (24). This means that $\Delta U \approx 0$, as would be expected for a purely collisional model.[88]

4. Comments on K

The fact that most of the data on equilibrium constants come from solution rather than gas-phase studies has complicated the interpretation of the results, particularly for weak complexes where the solvent effects are relatively large. The necessity to use high D_0 (or A_0) concentrations could well alter the dielectric properties of the medium which would affect the spectral band characteristics[7e, 51–59] (considered constant in the B–H treatment). Another problem is the neglect of activity.[7, 24, 54, 73, 91, 92] There has even been much discussion on the effect of the choice of concentration scale on K (see Foster[3c, 73] and references therein, and Lane and coworkers[92]). We shall discuss those interpretations of solution results that relate to the question of contacts.

The papers of Benesi and Hildebrand[19] and of Andrews and Keefer[93] on the homologous series of iodine complexes with methylbenzenes indicated that K increases with methyl substitution but ϵ decreases. The latter trend is opposite to what had been expected from simple orbital overlap considerations, and led Orgel and Mulliken[48, 94] to suggest the contribution from contacts as a possible explanation.

The B–H equation, derived from equation (12), is:

$$A_0 b/A = (1/K\epsilon)(1/D_0) + 1/\epsilon \tag{25}$$

ϵ and K are evaluated from the intercept and slope. A system containing several 1:1 complexes, each with a different K and ϵ, would behave in the B–H method as if there is present only a single complex (the CT band, locally excited bands, isosbestic points, etc.). The value of K obtained corresponds to the sum of the individual equilibrium constants, and the apparent ϵ to a weighted average absorption (extinction) coefficient:

$$K = \sum_i K_i \text{ and } \epsilon_{app} = (\sum_i K_i \epsilon_i)/K. \tag{26}$$

Orgel and Mulliken[94] noted there may be a continuous shading of species from complexes which are orientational isomers to contacts, but took as a simple model a division into two classes only, a 1:1 complex and 1:1 contacts. (Observation of a good isosbestic point suggests that there are no complications from complexes of stoichiometry other than 1:1.) The following relations then hold, where the subscript C is for complexes and CCT is for contacts. From equation (10):

$$C = K(D_0 - C)(A_0 - C) \tag{27}$$

and since the concentration of contacts is proportional to the free donor and acceptor concentrations:

$$(CCT) = \alpha(D_0 - C)(A_0 - C) \tag{28}$$

where, for $D_0 \gg A_0$, α is the number of sites of D around A multiplied by the molar volume of the solution (corresponds to a coordination number). Combining these equations with that for the total absorbance of complex and contacts, i.e. $b[\epsilon_C C + \epsilon_{CCT}(CCT)]$, gives:

$$\epsilon_{app} = \epsilon_C(1 + \rho/K) \tag{29}$$

where $\rho = \alpha\epsilon_{CCT}/\epsilon_C$. On rearrangement:

$$\epsilon_C = \epsilon_{app}K/(K + \rho). \tag{30}$$

Taking the Benesi–Hildebrand data for K and ϵ_{app} for the methylbenzene–iodine complexes, the trend in ϵ_C was found to increase with increasing stability of the complexes, as expected from theory,[7,20] when $\rho \approx 4$ or 5.

This analysis would imply that in the gas phase, where there would not be multiple sites of D around A, the experimental results should show a direct relation between K and ϵ. Gas-phase data for the iodine complexes with benzene,[33,95–97] *p*-xylene[97] (not at ν_{max} in this case) and mesitylene[97] have been reported, but only the $K\epsilon$ product is reliable and not the separated

values, for reasons discussed earlier for such weak complexes. It may be noted that the $K\epsilon$ product increases with increasing stability for both the gas phase and n-heptane solution.[24] A value of K for benzene–iodine in the gas phase has been reported from a PVT study[33] which, combined with the spectrophotometric data for $K\epsilon$, allows the determination of ϵ. Similar data for *p*-xylene–iodine or mesitylene–iodine are not yet available.

The reversal explained above in terms of contacts has been explained alternatively as arising from solvent effects. Carter, Murrell and Rosch[61] include the solvent (S) in the equilibrium expression:

$$AS_n + DS_m \rightleftharpoons DAS_p + qS \tag{31}$$

where n, m, p are the number of solvent molecules around the respective species, and q $(=n + m - p)$ is the number of solvent molecules squeezed out on complexation and returned to the bulk solvent. Then:

$$K = [DAS_p]X_S^q/[AS_n][DS_m] \tag{32}$$

where X_s is the free solvent concentration expressed in units of mole-fraction. For the initial conditions $D_0 \gg A_0$ and $S_0 \gg D_0$, the following approximate relation is obtained:[61]

$$\frac{A_0 b}{A} = \frac{1}{K\epsilon_C} \cdot \frac{1}{D_0} + \frac{1}{\epsilon_C}\left[1 - \frac{q(m+1)}{KS_0}\right]. \tag{33}$$

Comparing this to the usual B–H equation (25) for which the subscripts B–H are added:

$$K_{B\text{–}H} = K - q(m+1)/S_0 \quad \text{and} \quad \epsilon_{B\text{–}H} = \epsilon_C(K/K_{B\text{–}H}) \tag{34}$$

K and ϵ_C represent the true values. Thus, $K_{B\text{–}H} < K$ and $\epsilon_{B\text{–}H} > \epsilon_C$, but the respective products are equal, $K_{B\text{–}H}\epsilon_{B\text{–}H} = K\epsilon_C$.

Using a value of $q(m + 1) = 9$ as a correction to the data for the methylbenzene–iodine complexes, a plot of ϵ versus K gave a line of positive slope that passed through the origin, in accord with theory.[7, 20] The solvent and solute molecules are not very different in size, so $m \approx 4$ is reasonable for the number of solvent molecules around the donor, as is $q \approx 2$ for the number of solvent molecules squeezed out. Thus $q(m + 1) \approx 9$ seems reasonable. In this analysis, as the complex gets weaker and K approaches zero, it is possible for $K_{B\text{–}H}$ to become zero and even negative. The latter arises from a negative intercept in a B–H plot [or a negative slope in a Scott plot, equation (16)]. This was observed in a study by Davis and Farmer.[98]

For criticism and comments on this treatment the reader is referred to the literature.[24, 99–102] (See also the review by Davis.[54])

Prue[90] has argued that random pair-interactions between D and A in solution should lead to association constants appreciably greater than zero.

If two molecules of diameter d approach within a distance Δd to give a CCT band, the volume of the shell around one molecule available to the centre of its associated partner is $\pi d^2 \Delta d$. The fraction of molecules thus associated β is given by the ratio of the total volume of such shells to the volume of the solution:

$$\beta = [(\pi d^2 \Delta d) \times CV \times N]/V \tag{35}$$

where C is the stoichiometric molar concentration of D and A, V is the volume of solution, and N is the Avogadro number.

The association constant for these encounters:

$$\begin{array}{ccccc} D & + & A & \rightleftharpoons & DA \\ (1-\beta)C & & (1-\beta)C & & \beta C \end{array}$$

is

$$K = \beta C/(1-\beta)^2 C^2 \approx \beta/C \tag{36}$$

since β is quite small. Combining (35) and (36):

$$K = \pi d^2 \Delta d N. \tag{37}$$

In units of $1\,mol^{-1}$, with d and Δd in Å, this becomes:

$$K = 18{\cdot}92 \times 10^{-4} d^2 \Delta d. \tag{38}$$

The result for this collision model, again showing temperature independence, is quite the same as that from gas-phase theory [equation (24)]. The difference by a factor of 2 stems from expressing the lifetime of the contact as $2\Delta d/\bar{c}$ [equation (21)]. This applies to a head-on collision where the time of contact is a maximum. The minimum time, $t \approx 0$, is for D and A molecules passing each other in a grazing encounter at the separation Δd. Thus the average lifetime ought to be $\bar{t} = \Delta d/\bar{c}$, which brings the two results into agreement. Prue estimates $K \approx 0{\cdot}21\,mol^{-1}$, taking $\Delta d \approx 0{\cdot}94$ Å and $d \approx 10$ Å (which seems rather high). He points out that values reported to be smaller than this, assuming they are experimentally valid, provide no evidence for attraction between D and A in the ground state other than that due to normal dispersion forces.

Scott[103, 104] has re-emphasized the importance of the solvent model of Carter and coworkers.[61] In any random interaction, the solvent molecules must be considered because they occupy some of the coordination sites around the donor and acceptor. Scott determined the expression of K for weak complexes based on a quasi-chemical calculation for a lattice of D, A and S molecules, each with a lattice coordination number z in which the site fractions occupied by D, A and S are given by their mole-fractions X_D, X_A and X_S, respectively. All pair interactions are assumed to be the same except for a particular orientation of one of the z sites of D (labelled D′) with

a similar particular orientation of A (labelled A′) which differs from all the other pairs by an energy ω and has a molar absorption (extinction) coefficient ϵ.

In a lattice of N sites, the total number of random contacts DA is $NX_D X_A z$, but only $1/z^2$ of this will have the proper orientation to form the D′A′ "complex". Because of the energy difference the concentration of D′A′ will be higher than the completely random value. The solution to this model for the usual conditions of the B–H treatment, namely $X_D \gg X_A \approx 0$, gives the result:

$$\begin{aligned} K_{obsd} &= K - K_{random} \\ \epsilon_{obsd} &= K\epsilon/(K - K_{random}) \end{aligned} \tag{39}$$

Here, too, $K_{obsd}\epsilon_{obsd} = K\epsilon$.

Thus, the observed K (i.e. K_{B-H}) is just the excess over the random interactions. It is a "sociation" constant in Guggenheim's terminology.[68] Therefore, small values for K_{obsd} sometimes reported can be physically significant provided that they meet the experimental criteria[78, 105] for meaningful separation of K and ϵ.

This treatment can be generalized to include the case of several 1:1 complexes. The expressions in equation (26) then become

$$\begin{aligned} K &= \sum_i (K_i - K_{i\,random}) \\ \epsilon_{app} &= \sum_i K_i\epsilon_i / \sum_i (K_i - K_{i\,random}) \end{aligned} \tag{40}$$

In Scott's model, the stronger the D–A interaction, the greater will be the occupancy of the coordination sphere of D around A (or A around D) relative to that of the random distribution of solvent around D and A. This is rather analogous to a competition between solvent and donor molecules for A (or solvent and acceptor molecules for D) which has been treated in the literature.[3, 60, 99, 106, 106a] The weaker the D–A interaction, the larger is the underestimation of the equilibrium constant obtained by the B–H procedure. As pointed out by Merrifield and Phillips,[106] and later by Davis and Farmer,[98] for the competing equilibria:

$$D + A \overset{K_1}{\rightleftharpoons} DA$$

$$D + S \overset{K_S}{\rightleftharpoons} DS$$

a B–H treatment of the data (for the conditions $[D] \gg [DA]$, K is in mole-fraction units, and the mole-fraction of solvent is high) leads to K_{B-H} and

ϵ_{B-H} given by the equations:

$$K_{B-H} = \frac{K_1 - K_S}{1 + K_S} \qquad \epsilon_{B-H} = \frac{K_1}{K_1 - K_S}\epsilon. \tag{41}$$

Thus K_{B-H} and ϵ_{B-H} are functions of the solvent complexing ability and, as may be seen, the discrepancy between K_{B-H} and K_1 gets larger as K_1 decreases. If the complexing ability of the solvent is poor, such that $K_S \ll 1$, equations (41) and (39) become the same.

Another result for the competing equilibria for the conditions $S_0 \gg A_0$, where S_0 is the initial concentration of solvent, is:[60]

$$K_1 = K_{B-H}/(1 + K_S S_0) \tag{42}$$

Since S_0 will be of the order of 5–10 M for the more common organic solvents, neglect of solvent competition will lead to significant error if $K_S > 0{\cdot}1\,l\,mol^{-1}$.

Christian, Childs and Lane[82, 92, 107] have pointed out that K determined by the constant activity method includes both the specific and non-specific interactions between donor and acceptor. The non-specific effects of the donor are different from that of the solvent, and can change the activity and solubility of iodine in an equilibrium such as (19). These effects can be estimated from solubility theory.[108, 109]

The equilibrium constant they obtain has the form

$$K = K_{thermo} - \alpha_{I_2} \tag{43}$$

where α_{I_2} (a negative quantity) is the term due to non-specific interactions with the iodine acceptor. K is then the sum of the specific (K_{thermo} which should be compared to K_{B-H}) and non-specific interactions. Their experimental results for K for the methylbenzene–iodine complexes using the constant activity method give good agreement with the conventional K_{B-H} results after correction is made for α_{I_2}, which supports Scott's[104] interpretation of the latter method. It is of interest to note the magnitude of $-\alpha_{I_2}$, which is $\sim 0{\cdot}2$–$0{\cdot}3\,l\,mol^{-1}$ for this system. The $K\epsilon$ and $K_{B-H}\epsilon_{B-H}$ products are in good agreement. Although there still is a decrease in ϵ with increasing K for the homologous series, the inclusion of the non-specific effects makes it not nearly so drastic as in the B–H method.

B. Internal Energy Change

The internal energy change in the gas phase, ΔU^0, is determined from a van't Hoff plot of ln K_C versus $1/T$. Using pressure units for the equilibrium constant, i.e. K_P, such a plot gives the enthalpy change, ΔH^0.[110] For 1 : 1 complex

formation in the gas phase, $K_P = K_C(RT)^{-1}$ and $\Delta H^0 = \Delta U^0 - RT$. In solution, $\Delta H^0 \approx \Delta U^0$.

The classical (or conventional) B–H method to determine the $K\epsilon$ product at a single temperature requires absorbance measurements of several solutions in which the concentrations of donor, or acceptor, or both are varied. Separation of the terms in the $K\epsilon$ product, as discussed, often is not possible for very weak complexes, i.e. K and ϵ show large random variation with temperature and have large error limits. A feasible procedure to obtain ΔU^0 for contacts, then, is to assume that ϵ is temperature independent and to plot $\ln K\epsilon$ versus $1/T$. In actuality, there is a change in ϵ with temperature due to band broadening. If the absorbance data are taken at the band maximum, the ΔU^0 determined from the plot of $\ln K\epsilon_{max}$ versus $1/T$ is an upper limit value because ϵ_{max} decreases slightly with increasing temperature. This effect could amount to $\sim 1\,\mathrm{kJ\,mol^{-1}}$ (several tenths of a $\mathrm{kcal\,mol^{-1}}$) which can be a significant fraction of the total change in ΔU^0 for contacts. Grundnes and Christian[111] suggested that the relative increase in half-width of the CT band with increase in temperature be used as a correction for the relative decrease in ϵ_{max}. No information on the entropy change, ΔS^0, is obtained in this procedure because ϵ is unknown. If ϵ fluctuates within tolerable limits over the temperature range, an average value can be taken which then permits determination of ΔS^0.

Two other experimental procedures have been shown to be useful. Although they do not eliminate the problems cited above, at least they do eliminate the need to measure precise donor and acceptor concentrations and, further, allow the determination of ΔU^0 from the study of the temperature dependence of absorbance of only a *single* donor–acceptor mixture.[24, 112]

From equation (10) and the Beer–Lambert law:

$$K = (A/b\epsilon)/(\mathrm{D_0} - \mathrm{C})(\mathrm{A_0} - \mathrm{C}) \tag{44}$$

where A is the absorbance. Taking the logarithms, and assuming the condition $\mathrm{D_0} \gg \mathrm{A_0}$:

$$\ln K\epsilon + \ln b + \ln \mathrm{D_0} + \ln(\mathrm{A_0} - \mathrm{C}) = \ln A. \tag{45}$$

The temperature dependence of equation (45) is:

$$\frac{\mathrm{d}\ln K\epsilon}{\mathrm{d}(1/T)} + \frac{\mathrm{d}\ln b}{\mathrm{d}(1/T)} + \frac{\mathrm{d}\ln \mathrm{D_0}}{\mathrm{d}(1/T)} + \frac{\mathrm{d}\ln(\mathrm{A_0} - \mathrm{C})}{\mathrm{d}(1/T)} = \frac{\mathrm{d}\ln \mathrm{A}}{\mathrm{d}(1/T)}. \tag{46}$$

The coefficient of expansion of silica is small, so b is essentially temperature-independent. The temperature dependence of $\mathrm{D_0}$ is zero in the gas phase, but in solution a correction must be made for the change in density of the solution. If this correction were to be approximated by the temperature dependence of the density of the pure solvent, say n-heptane, this would be

~ 1 kJ mol^{-1} (0·2 kcal mol^{-1}).[86] The more closely the system approaches that for contacts, the better the approximation that $(A_0 - C)$ is nearly temperature-independent. Thus

$$\frac{d \ln K\epsilon}{d(1/T)} \approx \frac{d \ln A}{d(1/T)}$$

and plotting $\ln A$ versus $1/T$ for a single donor–acceptor mixture gives ΔU^0 directly. This result will be a *lower limit* because the term $d \ln (A_0 - C)/d(1/T)$ can only be positive.

Corresponding equations can be written for the constant-activity method. Here, equations (44), (45) and (46) become, respectively:

$$K = (A/b\epsilon)/(D_0 - C)(A_0)_t \tag{47}$$

$$\ln K\epsilon + \ln b + \ln D_0 + \ln (A_0)_t = \ln A \tag{48}$$

$$\frac{d \ln K\epsilon}{d(1/T)} + \frac{d \ln (A_0)_t}{d(1/T)} = \frac{d \ln A}{d(1/T)} \tag{49}$$

where $(A_0)_t$ is the saturation concentration of the acceptor at temperature t. The magnitude of $d \ln (A_0)_t/d(1/T)$ can be evaluated separately from data on the temperature dependence of the saturation concentration of the constant activity source. This correction is then used to obtain ΔU^0 from the plot of $\ln A$ versus $1/T$. Equation (49) is applicable to interactions over the full range from contacts to complexes.

ΔU^0 is itself temperature dependent, but is essentially constant over a short temperature range, i.e. the plot of $\ln K_C$ versus $1/T$ is linear. As pointed out by Orgel and Mulliken,[94] if several 1:1 contact and weak complex species are present, each with its individual ΔU^0, then the van't Hoff plot ought to be curved. ΔU^0 at a specified temperature is determined from the slope of the tangent at the appropriate point along the curve, and is a weighted average value. Experimentally, however, it would be almost impossible to detect the curvature because the differences in the ΔU^0 values of the species are so small to begin with.[113]

IV. OPERATIONAL CRITERIA FOR CONTACTS

Any measurement showing deviation from ideal behaviour could be used to indicate the strength of the perturbing interaction between D and A molecules (e.g. excess thermodynamic functions, solubility, relaxation times, shifts in infrared and nmr spectra, shifts in locally excited states, dipole moment[1–3]). In keeping with the stated aim of this chapter, we will select criteria that pertain to the spectral properties of CT bands and the thermodynamic properties derived therefrom. In later discussion, mention will be made of

other types of potential criteria which relate to the CT studies (e.g. blue shift of the iodine visible band; Section VI).

A. Internal Energy Change

As one operational definition of contacts in solution, we shall adopt as a criterion $-\Delta U^0 \leqslant 1{\cdot}0$ kcal mol^{-1} ($\leqslant \sim 4$ kJ mol^{-1}). This is only slightly greater than the RT value of 0·6 kcal mol^{-1} at room temperature. Considering also that the results for the spectrophotometric determination of ΔU^0 probably are no better than to $\sim \pm 0{\cdot}2$ kcal mol^{-1}, the above criterion seems of reasonable magnitude.[66] It is, however, an arbitrary choice, and any fraction or small multiple of RT could well have been taken. At such a low value of $-\Delta U^0$, it is hardly likely that a uniquely oriented D–A pair exists, i.e. the contribution from contacts to this system is expected to be significant.

The value of 1 kcal mol^{-1} is a little smaller than that for the benzene–iodine system in "relatively inert" solvents, e.g. n-heptane, cyclohexane and carbon tetrachloride, for which the range $\sim 1{\cdot}3$ to $\sim 1{\cdot}7$ kcal mol^{-1} has been reported[24] for $-\Delta U^0$. Benzene–iodine has been the classical example of a weak complex, and it will be assumed to be near the operational limit where such description might be preferable. (At low temperature, benzene–bromine forms a crystalline compound of 1:1 stoichiometry.[114] In the range 154–194°C, benzene–iodine interaction in the gas phase has been described as being of typical van der Waals type[33]).

Gas-phase data for weak complexes are relatively few. But, where available, it generally has been found that the $-\Delta U^0$ values in the gas phase are somewhat larger than those in solution[24] (Section II.C). The difference is even greater if ΔH^0 values are compared ($\Delta H^0 = \Delta U^0 - RT$). We shall retain the same operational definition of $-\Delta U^0 = 1$ kcal mol^{-1} for contacts in both phases. This means that some EDA interactions will be in the category of complexes in the gas phase and contacts in solution.

B. Equilibrium Constant

Reported CT studies more often provide data on K (and ϵ) than on ΔU^0. As discussed previously, such data for weak complexes have to be considered with caution because of the problem of separating K and ϵ from the $K\epsilon$ product. But even for cases that satisfy the Person[78] criterion for valid separation, there is the question of what value is appropriate for K as an operational definition for contacts.

Experimental values corresponding to the product function $K\epsilon$ are *finite* for complexes or contacts [equation (15)]. If K for contacts approaches zero, as sometimes is considered for the limiting case, then ϵ for contacts must

approach infinity. Equation (9) for the electronic transition dipole does not suggest such behaviour. A change of merely 1 (or a few) kcal mol^{-1} in ΔU^0, which can be achieved by substitution of groups in the donor and acceptor molecules, should not produce such drastic effects on the CT spectra (Fig. 2). Thus K for contacts must reach a limiting value appreciably greater than zero.[90] The estimates of Prue,[90] of Tamres and Grundnes,[88] and of Morita and Tamres,[89] based on equations (24) and (38), lead to a value $K \approx 0{\cdot}1$–$0{\cdot}2$ l mol^{-1} (depending on the estimate of Δd and d_{12}). We shall adopt a value of $\sim 0{\cdot}1$ l mol^{-1} *in solution* as a reasonable criterion. Literature reports of K_{B-H} smaller than this would be assumed to be at least equally well described in terms of contacts.

Most studies have been carried out at or near 25°C. However, the criteria are applicable at any temperature, which again emphasizes that a system considered to be composed primarily of contacts at a higher temperature would best be described in terms of a complex at a lower temperature.

Data for K in the gas phase for weak EDA interactions also are very few, and most come from non-spectrophotometric studies,[24] e.g. benzene–iodine (PVT),[33] and diethyl ether–iodine and n-hexane–iodine (isopiestic).[115] For these three cases, at least, the K values around 35°C are rather comparable, and all are appreciably larger than the corresponding solution values, by a factor of ~4–12. If correct, these data emphasize the difficulty in making any physical distinction between weak complexes and contacts.[115]

C. Wavefunction Coefficient Ratios

The coefficients of the "no-bond" and "dative bond" wavefunctions a and b in equation (1) give a measure of the ground-state stability of EDA interactions due to charge transfer, the magnitude of b relative to a becoming smaller as the charge-transfer contribution decreases. (Even in the limiting case for contacts b may not be exactly zero[7] and a may not be exactly 1, for normalized functions.)

In earlier work, the coefficients were estimated in several ways (see refs. 1a, 2c, 116, 117 for the simultaneous equations involved and the estimate of parameters). One of these was based on measuring the properties of the CT band, e.g. ϵ_{max} and band position (ν_{max}). Other measurements were based on the ground-state dipole moment and on the energy of interaction.

Expressions such as $b^2/(a^2 + b^2)$ and $(b^2 + abS_{01})$ represent the degree of charge transfer and were taken to be the measure of the ground-state polarity of the EDA pair. For quite weak interactions these expressions can be approximated by b^2/a^2. One of the equations used to calculate this ratio is:[1a, 2c, 116, 117]

$$b^2/a^2 \approx -\Delta U^0/h\nu_{CT}. \tag{50}$$

As stated in Section II.A, charge-transfer contribution may no longer be dominant in weak EDA interaction. Still, equation (50) may be used operationally to define contacts, much like ΔU^0 itself. For $-\Delta U^0 \approx 1{\cdot}0$ kcal mol^{-1} (~ 4 kJ mol^{-1}) and for CT bands in the range 200–300 nm, the ratio $b^2/a^2 \approx$ 0·007–0·010, and this value may serve as an operational upper limit for contacts.

Listed in Table I are the wavefunction coefficient ratios for some donor–iodine interactions. The variation in the data emphasizes the problems associated with obtaining reliable spectral and thermodynamic properties for these weakly interacting systems, a point that also will be evident in many of the data cited in subsequent tables. The values for $-\Delta U^0$ of Bhat, Bhaskar and Rao[23] for the interaction in n-heptane of iodine with cyclohexane and with methylcyclohexane may be high. Julien and Person[118] found for cyclohexane–I_2 in n-heptane that $-\Delta U^0 \approx 0$ within their experimental limits. The gas-phase results for n-butane–I_2[119] and methylcyclohexane–I_2[88] also are ~ 0. It would be expected that $-\Delta U^0$ for the gas phase should be larger than that in n-heptane solution.[24] Thus, the values reported by Bhat, Bhaskar and Rao for b^2/a^2 based on equation (50) are probably too high.

In Table I, comparison is made also for the wavefunction coefficient ratios of the weak benzene–iodine complex estimated by different methods. It is to be expected that the results would be nearly the same for all methods, but the solution data are rather dissimilar. Some of the difference may arise from the approximations made in the several approaches, but much of it must be attributed to a solvent effect. For weak complexes, the solvent increases ϵ_{CT} several-fold compared with the gas-phase value.[24] This gives a high result in solution for μ_{VN} and, hence, also for $b^2/(a^2 + b^2)$. The same may be true for the ground-state dipole moment μ_{DA} because of mutual polarization with the solvent. On the other hand, the solvent decreases the value for ΔU^0 by a factor that is bigger than the increase in ν_{CT}, thereby making the b^2/a^2 ratio too low. The overall agreement between methods is improved when gas-phase data are compared.

D. Viscosity and Phase-change Effects

It has been shown in Section III.A.3 that the concentration of contact pairs in the gas phase can be estimated from simple collision theory. Similarly, in fluid media the concentration of contacts will be determined by the bimolecular encounter rate in solution, which will be diffusion-controlled. For hard spheres diffusing in a continuum of viscosity η, combination of the Smoluchowski relation:

$$k = 4\pi d_{AB} D_{AB} N/1000 \text{ l mol}^{-1} \text{ s}^{-1} \qquad (51)$$

TABLE I. Wavefunction coefficient ratios for some EDA interactions[a] with iodine

System	Phase	λ_{max} /nm	$-\Delta U^0$ /eV	$h\nu_{CT}$ /eV	b^2/a^2	Ref.
n-Butane–I_2	gas	<210	~0	>5·90	<0·01	119
Methylcyclohexane–I_2	gas	<216	~0	>5·74	<0·01	88
	n-heptane	(~245)[b]	(0·061 ± 0·02)[c]		(0·013)[a,d]	17, 23
Cyclohexane–I_2	n-heptane	232	~0		<0·01	118
	n-heptane	(~245)[b]	(0·069 ± 0·02)[c]		(0·015)[c,d]	17, 23
n-Heptyl bromide–I_2	n-heptane	~245	0·069 ± 0·02		0·015[d]	17, 23
Benzene–I_2	gas	<282	0·0768 ± 0·007	>4·40	<0·017	24, 97
	gas	~268	0·087 ± 0·004	~4·63	~0·019	24, 96
	n-heptane	296	0·056	4·19	0·013	1a, 24, 116, 117
	n-heptane	288	0·0703	4·30	0·016	24, 100
	n-hexane	296	0·056	4·19	0·013	24, 116
	cyclohexane	289	0·0746	4·29	0·017	24, 100

System	Phase	μ_{DA} /debye	$b^2/(a^2+b^2)$	Ref.
Benzene–I_2	benzene	0·72	0·028	1a, 20, 120
	cyclohexane	1·80	0·082	1a, 121

System	Phase	ϵ_{max} /l mol^{-1} cm^{-1}	μ^2_{VN}	$b^2/(a^2+b^2)$	Ref.
Benzene–I_2	gas	(1650)[e]	7·90	0·018	24, 96
	n-heptane	17000[f]	81·4	——[g]	24

[a] Operational value for contacts is $b^2/a^2 < 0{\cdot}01$ (see text). [b] λ_{max} is undoubtedly at a shorter wavelength. [c] May be high (see text). [d] The reported value is ~0·001 unit high for the λ_{max} and ΔU^0 data given in ref. 23. [e] This value may not be precise because of the difficulty in separating K and ϵ for weak complexes, although it is probably of the correct order. [f] Several values reported of approximately this magnitude (see compilation in Ref. 24). [g] Following the literature procedure[1a] using $\epsilon = 17000$ l mol^{-1} cm^{-1} and $\mu_1 = 15{\cdot}6$ debye, no meaningful solution for the coefficients a, a^*, b, b^* were obtained for positive values of S_{01}.

where N is the Avogadro number, d_{AB} is the encounter diameter, and D_{AB} $(= D_A + D_B)$ is the diffusion coefficient for simultaneous motion of A and B, with the Stokes–Einstein equation:

$$D = RT/3\pi L\eta d_s \text{ cm}^2 \text{ s}^{-1} \tag{52}$$

gives the Debye equation for diffusion-controlled reaction rate constants, assuming $d_{s,A} = d_{s,B} = d_s$:

$$k = 8RTd_{AB}/3000\eta d_s. \tag{53}$$

It is generally assumed that the encounter diameter d_{AB} is equal to the diffusion diameter d_s, in which case the bimolecular rate constant (and hence

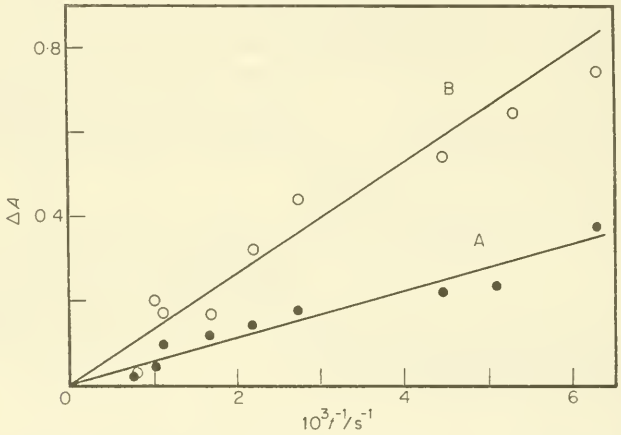

FIG. 4. The differences in absorbance, ΔA, between the nitrogen-purged and oxygenated solutions of benzene (A) at 235 nm (concentration 5×10^{-5} M) and *N*,*N*-dimethylaniline (B) at 268 nm (concentration 1×10^{-5} M), in ethanol–ethylene glycol mixtures plotted against t^{-1}, the reciprocal of the flow time in the Ostwald viscometer. [Reproduced with permission from C. J. Bolter, C. A. G. Brooks, K. M. C. Davis and M. E. Delf, *J. Chem. Soc., Perkin II*, 1350 (1973)]

the concentration of contacts from encounters) is inversely proportional to the viscosity, η, or directly proportional to the fluidity, ϕ. Thus, in contrast to complexes, the intensity of the CT absorption for contacts should vary linearly with solvent fluidity, with zero intercept in completely rigid media. Such an effect is shown in Fig. 4 for benzene–O_2 and *N*,*N*-dimethylaniline–O_2 contacts.[122] This is in contrast to the behaviour of complexes such as hexamethylbenzene–chloranil, in which the absorbance is essentially independent of viscosity.[122]

Similarly, the CT absorption spectrum for many contact pairs has been observed to disappear on freezing and to reappear on melting,[87a] exhibiting

thermochromic or "phase-change chromic"[123,124] behaviour. This behaviour serves as a useful operational criterion for establishing contact interaction in the absence of other thermodynamic justification. On the other hand, the absorption at 220 nm of an oxygen-saturated 1:1 mixture of methylcyclohexane in isopentane increases monotonically on cooling from room temperature to −160°C (rigid glass).[125] This indicates greater interaction on cooling (possibly because of closer contact due to contraction of the liquid), but does show that the CT absorption in this case cannot be due solely to contacts. Similar effects on cooling are shown in the absorption spectra of oxygen and organic molecules absorbed in porous glass or silica gel.[126]

V. SELECTION OF DATA FOR CONTACTS

The common thermodynamic properties for EDA interaction reported in the literature are ΔH^0 and K. These have been determined by many experimental techniques other than the investigation of their uv and visible spectra. Covering all these studies in a search for contacts would make the scope of this chapter too broad. Extensive compilations of such data from which examples of contacts can be selected are available in several instances, e.g. EDA pairs[17] including Lewis acid–base adducts[2] and hydrogen-bonding.[127] The present search was limited primarily to those studies involving CCT spectra, but comparison is made in some cases to results for the same systems studied by other techniques. A broad range of systems classified as contacts are discussed in Sections VI–XII, and the data are presented in Summary Tables at the end of each section. Gas-phase data are included where available.

Even with the "operational" definitions as a guide, there are many problems associated with searching the literature and selecting examples of contacts.

(a) Reliable thermodynamic data are difficult to obtain, particularly the equilibrium constants for weak complexes. Thus, for the same system studied in different laboratories, the results may be such that one set of data would fall in the contact category, as defined, whereas another set would not. This poses an additional arbitrariness whether to include all such data. We have made at least some selective comparisons.

(b) Most studies on EDA interactions have been made in solution. Solvent effects on the thermodynamic properties of EDA interactions need to be taken into account, especially if the solvents are themselves good electron donors or acceptors. Data obtained in relatively "inert" solvents such as n-heptane and carbon tetrachloride may place a system in the category of a complex, while in another solvent the choice would be different. Therefore,

data obtained in solvents, known to be involved in EDA interaction or hydrogen-bonding, e.g. benzene, ethers and dichloromethane, will be only selectively included, mostly when data in "inert" solvents are unavailable.

(c) If a system falls just barely within the category of contacts, by whatever definition is adopted, substitution of other groups at various positions in the molecular framework of the interacting species could cause a slight change in the strength of interaction sufficient to make the system fall into the other category. For example, dialkyl ethers form complexes with iodine, but there is no evidence for complexation between diperfluorohexyl ether and iodine.[67, 128] Thus, in large part, the data in the Summary Tables (Sections VI–XII) indicate the types of systems at or near the contact range *by the definition adopted.* Omission of data for quite similar systems is not intended to indicate an abrupt, complete absence of contacts.

(d) It is difficult to be consistent in the selection of systems as contacts because error limits on thermodynamic properties are not always reported. In some cases where they are reported these limits are sufficiently large to make ΔH^0 or K fall at or near the values suggested for the operational criteria. These data are included.

(e) Data for ΔH^0 and K may be such that one fits the operational definition but not the other. In some cases this may be due to experimental error in determining these quantities, but not necessarily so. Most solution data for K are near 25°C, which is an arbitrary choice. Often, ΔH^0 does not change much with temperature, but K does. In fact, relative stabilities based on comparison of K at room temperature can be reversed if the temperature is altered. Conversely, if the K values show a systematic trend at more than one temperature, the ΔH^0 values may show an opposite trend.[129] However, for the weakly interacting system of iodine with the methylbenzenes over the range studied, linear relations have been observed from plots of any two of the three thermodynamic functions (ΔG^0, ΔH^0, ΔS^0).[130, 131]

Considering these various possibilities, data where either $-\Delta U^0 (\approx -\Delta H^0$ for solution or $-\Delta H^0 + RT$ for vapour phase) $\leqslant 1$ kcal mol^{-1} or $K \leqslant 0{\cdot}1\,1\,\text{mol}^{-1}$ are included.

(f) In many of the systems no CCT absorption maximum is found owing to overlap with either the donor or acceptor bands. For those cases where enhanced absorption is reported, we have listed in the Summary Tables the wavelength for the approximate onset of the CCT band (λ_{onset}). Quantitative comparison of the absorbance at λ_{onset} is often not possible because the conditions (concentration, cell path, etc.) are not always specified. If criteria for λ_{onset} are established, e.g. as has been done for contacts with oxygen[132–134] (Section VIII), then it appears that $h\nu_{\text{onset}}$ of the CCT bands can be correlated with donor ionization potentials, as is the case for $h\nu_{\text{max}}$ [equation (5)]. This is also illustrated in the work of Hammond[135] on the interaction of

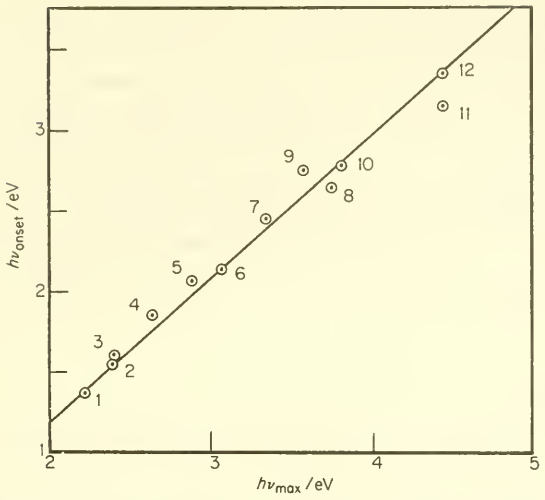

FIG. 5. Dependence of absorption onsets on absorption maxima for some intermolecular charge-transfer bands with the donor benzene. Acceptors are: 1, WCl_6; 2, MoF_6; 3, CrO_2Cl_2; 4, $WOCl_4$; 5, $VOCl_3$; 6, $NbCl_5$; 7, WF_6; 8, $TaCl_5$; 9, $TiCl_4$; 10, OsO_4; 11, TeF_6; and 12, PCl_5. Points 2, 9 and 10 are inferred from the positions with other donors, and 3, 5, 6, 8, 11 and 12 are partially screened by other bands. [Reproduced with permission from P. R. Hammond, *J. Chem. Soc.* (*A*), 3826 (1971)]

benzene with a series of highest valency halides, oxyhalides and oxides (Section IX), who observed a linear relation between $h\nu_{onset}$ and $h\nu_{max}$ (Fig. 5).

Data reported in the Summary Tables that are considered to be incorrect are enclosed in brackets.

VI. MOLECULAR HALOGEN ACCEPTORS

The molecular halogens, particularly iodine, have been among the classical acceptor molecules studied in weak molecular interaction. It has long been observed that solutions of molecular iodine show a range of colours, which led to the classification of solvents as being of "violet" or "brown" type (see the review by Kleinberg and Davidson[136]). Solvents in which iodine gives "violet" solutions with its visible band maximum at $\sim$520 nm are regarded as being relatively "inert".[137, 138] Solutions that are "brown" exhibit shifts in the visible iodine band to shorter wavelengths, and this is taken as evidence for complexation of iodine with the solvent. This *blue shift* is attributed to the perturbation by the donor of the molecular energy levels of the iodine (there

is a repulsive interaction between the electrons of the donor and the electron in the strongly antibonding orbital (σ_u^*) of the excited iodine molecule[7,48]. The magnitude of the blue shift has been correlated with the strength of interaction.[7,139–142] Hence, it can serve as a criterion for contacts, although again no sharp division can be drawn. Voigt[143] and also Hildebrand and coworkers[144] have published data on the visible iodine band maximum in solvents of different types and ionization potentials.

Often, observations on the visible iodine band are reported in the literature together with those on the CT band. In such cases the data are included in Summary Table A.

A. With Alkanes

The saturated hydrocarbons, being without functionally reactive groups, have commonly been included among the "inert" solvents. They are violet solvents for iodine and give "regular solutions",[109] although it has been noted in some cases that methyl substitution alters the iodine solubility somewhat from that expected from regular-solution theory.[145]

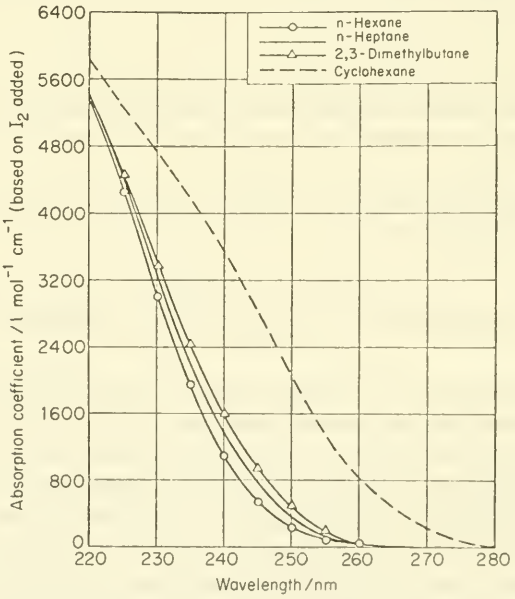

FIG. 6. Ultraviolet absorption of iodine in saturated hydrocarbons. [Reproduced with permission from S. H. Hastings, J. L. Franklin, J. C. Schiller and F. A. Matsen, *J. Amer. Chem. Soc.*, 75, 2900 (1953)]

An early attempt to establish the spectral characteristics of CCT bands of saturated hydrocarbon–iodine mixtures was that of Hastings and coworkers.[146] The spectra of the mixtures show a broad enhancement with a rising tail below ~250 nm and extending into the vacuum ultraviolet region, but no band maximum (Fig. 6). Since these are composite spectra, i.e. the absorbance is due to contacts plus the contributions of the free donor and free acceptor, corrections must be made for the latter. The problem here is one of selecting a *reference* solvent. Hastings and coworkers chose n-hexane because its iodine solution gave the smallest absorbance of the solvents studied. Subsequent work on n-hexane–iodine showed that there is an appreciable CCT contribution[67,119,128] at the shorter wavelengths which overlaps the CCT bands of the other systems. Consequently, the spectral bands they report have maxima that are at much too long wavelengths. Further, the data of Hastings and coworkers barely meet, at best, Person's criterion for reliable separation of K and ϵ from the $K\epsilon$ product. Therefore, the spectral and equilibrium constant data in Summary Table A are enclosed in brackets to indicate that they are not correct.[67,88,128]

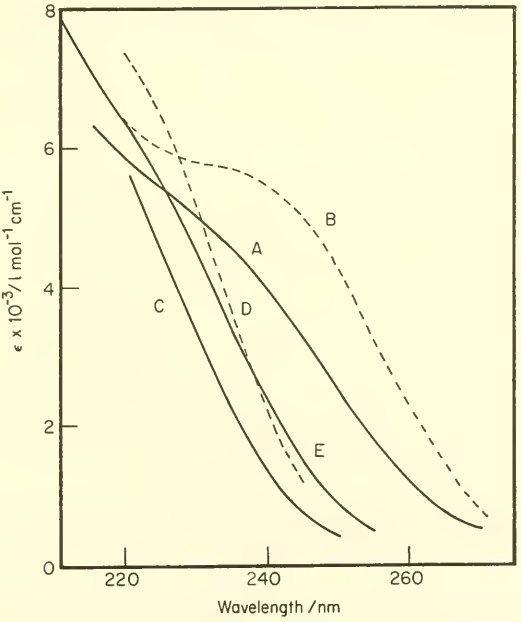

FIG. 7. Absorption spectra of iodine in hydrocarbon solution: A, methylcyclohexane at ~22°C; B, methylcyclohexane at −127°C; C, 2-methylpentane at ~22°C; D, 2-methylpentane at −127°C; E, methylcyclopentane at ~22°C. [Reproduced with permission from D. F. Evans, *J. Chem. Soc.*, 4229 (1957)]

Evans[67] has shown that the spectrum of iodine in n-perfluoroheptane and in diperfluorohexyl ether is almost like that of the gas phase (also for Br_2[147]). Adding n-heptane to a solution of n-perfluoroheptane of fixed iodine concentration gave an increase in absorbance near 220 nm in direct proportion to the concentration of n-heptane, as expected for a contact model (Person's region I).

A very large change with temperature of the CCT band intensity of iodine in saturated hydrocarbons has been observed for cyclohexane–iodine.[128,139] The spectrum reported by Evans[128] at $-127°C$ for methylcyclohexane–iodine (Fig. 7) shows a well defined shoulder at 240 nm, and presumably indicates that a CCT band maximum may be present in this region.

This is supported to some extent by the work of Julien and Person.[118] They determined the pressure-broadened gas-phase spectrum of iodine in 1 atm of nitrogen and used this to estimate the correction for the free iodine in n-heptane, cyclohexane and iso-octane in order to determine the CCT bands (Fig. 8). There is some arbitrariness in drawing the "tail" of the iodine reference band, which would affect both the CCT band maximum position and its intensity (perhaps by about 50 per cent).[118] Wobschall and Norton[148] studied the ultraviolet spectra of solutions of iodine and steroids containing various functional groups, and found that the spectral and thermodynamic properties compared well with those of simpler hydrocarbons with the same functional groups. This was also observed for contacts; the results in Freon solvent for 5α-cholestane–iodine were similar to those for cyclohexane–iodine.

More recently, attempts have been made to study CCT spectra of iodine with saturated hydrocarbons directly in the gas phase. Rao, Chaturvedi and Bhat[149] report for cyclohexane–iodine and methylcyclohexane–iodine a λ_{max} for the CCT bands of ~ 230 nm and ~ 235 nm, respectively. These maxima are not in accord with the expected blue-shift from the solution results of Julien and Person.[118] Subsequently, Tamres and Grundnes[88] reported a maximum for the cyclohexane–iodine CCT band in the gas phase at ~ 215 nm when n-pentane–iodine was used as the reference band for the "free" iodine. Using equations (5), (23) and (24), they estimated $K \approx 0{\cdot}13\,l\,mol^{-1}$ (based on $\Delta d = 1$ Å) and $\epsilon \approx 5{\cdot}9 \times 10^3\,l\,mol^{-1}\,cm^{-1}$. Later work[119] showed that n-pentane–iodine also has a CCT contribution, and therefore the above characterization is based on too low an absorbance. The gas-phase spectra of iodine in a series of hydrocarbons from methane through n-heptane, cyclohexane, methylcyclohexane and several gases (O_2, N_2, He)[119] are shown in Fig. 9. Taking as the reference system for "free" iodine its pressure broadened spectrum gives the CCT bands of Fig. 10. No maximum is observed, although an inflection point is indicated in one or two cases. These results are consistent with the expectation[24] that λ_{max}

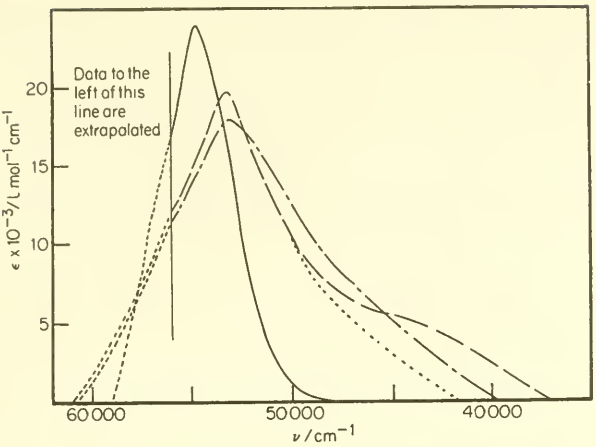

FIG. 8. The absorption spectrum near 200 nm of I_2 vapour (——), in n-heptane (—·—·), and in cyclohexane (– – – –). The dotted line (·····) gives the spectrum estimated for the I_2 "182 nm" band. Absorptivities are based on the total I_2 concentration in the solutions. [Reproduced with permission from L. M. Julien and W. B. Person, *J. Phys. Chem.*, **72**, 3059 (1968)]

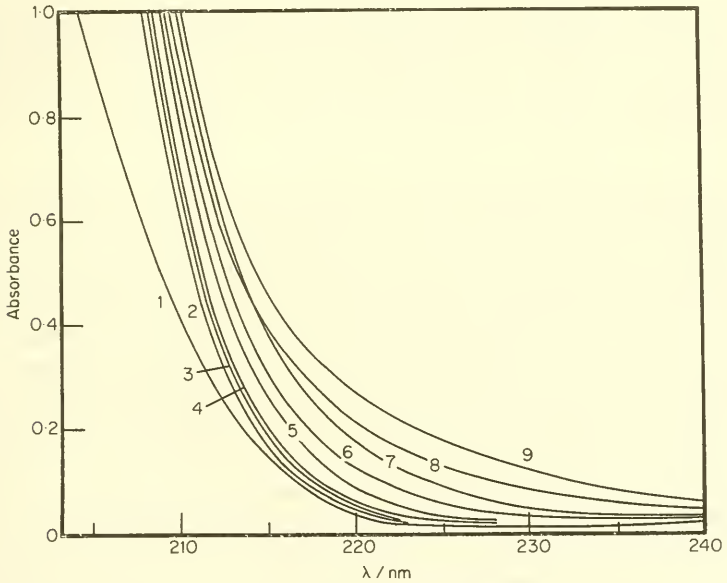

FIG. 9. Ultraviolet spectra of iodine at 110°C in the vapour phase: curves 1–5 for I_2 at 9·03 × 10^{-5} M in a 50·0-cm cell; curves 6–9 for I_2 at 6·50 × 10^{-5} M in a 75·0-cm cell; all gases and vapours are at 3·50 × 10^{-2} M; (1) no added gas, (2) N_2, O_2 or CH_4, (3) ethane, (4) n-butane, (5) n-pentane or neopentane, (6) n-hexane, (7) n-heptane, (8) cyclohexane, (9) methylcyclohexane. Curves 3–9 corrected for small alkane absorption. [Reproduced with permission from S. N. Bhat, M. Tamres and M. S. Rahaman, *J. Phys. Chem.*, **77**, 2756 (1973)]

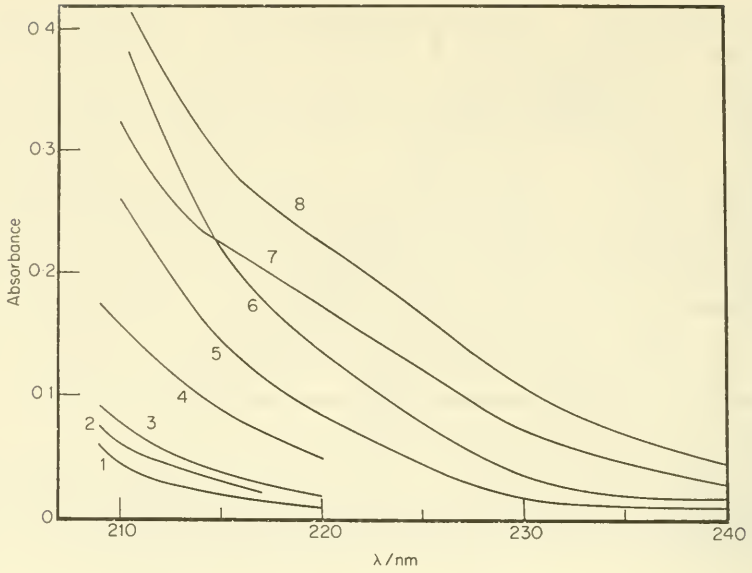

FIG. 10. CCT spectra of alkane–iodine systems at 110°C in the vapour phase: curves 1–4 for I_2 at $9{\cdot}03 \times 10^{-5}$ M in a 50·0-cm cell; curves 5–8 for I_2 at $6{\cdot}50 \times 10^{-5}$ M in a 75·0-cm cell; all alkanes at $3{\cdot}50 \times 10^{-2}$ M; (1) ethane-I_2, (2) propane-I_2, (3) n-butane-I_2, (4) n-pentane-I_2 or neopentane-I_2, (5) n-hexane-I_2, (6) cyclohexane-I_2, (7) n-heptane-I_2, (8) methylcyclohexane-I_2. [Reproduced with permission from S. N. Bhat, M. Tamres and M. S. Rahaman, *J. Phys. Chem.*, **77**, 2756 (1973)]

should be appreciably blue-shifted in the gas phase relative to that reported in solution.[118] There is also a direct dependence of absorbance on either the iodine or saturated hydrocarbon concentration.[88] Further, over a 20°C range, the absorbance of n-butane–iodine[119] and of methylcyclohexane–iodine[88] showed no change with temperature, within the limits of measurement; thus $\Delta U^0 \approx 0$. These findings are in accord with a contact model.

Although the alkane–iodine CCT bands in the gas phase are only partially characterized, the data in Fig. 10 indicate that the onset of the bands follows the order of decreasing I_D^V, as expected from equation (5). Further characterization will require extending these studies into the vacuum ultraviolet region and unravelling the overlap with the 182 nm band of iodine. Some work in this region has been done; for example, it is known that the presence of gases changes considerably the intense iodine spectrum at 182 nm and the Beer–Lambert law is not obeyed.[150,151] (It is obeyed for iodine in cyclohexane solution with ϵ_{max} 17 300 ± 300 l mol^{-1} cm^{-1} at λ_{max} 188 nm.[151] From the Julien and Person data[118] in Fig. 8, ϵ_{max} is estimated as ~19800 l mol^{-1} cm^{-1} at λ_{max} 188 nm).

Recently, Clark and Kolb[152] reported a large number of equilibrium constants for the weak interaction of iodine with aliphatic and aromatic donors in carbon tetrachloride solution, based on the competitive effect of the donor on the equilibrium of the cyclohexene–iodine addition reaction. The donors were substituted benzenes, polynuclear aromatics, haloalkanes and two alkanes (hexane and methylcyclohexane). With only a few exceptions, there is rather good agreement with the K values determined by the conventional Benesi–Hildebrand method, at least for those systems where the K values are larger than 0·1 l mol^{-1}. For hexane–I_2 and methylcyclohexane–I_2, the K values obtained at 25°C are 0·03 and 0·04 l mol^{-1}, respectively. These are rather close to the values at 25°C reported by Rao and coworkers[17,23] for cyclohexane–I_2 and methylcyclohexane–I_2 (data in Summary Table A). However, the agreement may be fortuitous considering the difficulty in separating K and ϵ from the $K\epsilon$ product for such weak interactions.

B. With Cyclopropanes

In an early study, Freed and Sancier[153] observed that iodine in cyclopropane at 230 K gives a violet solution, much like that of iodine in propane, but, unlike the latter, the cyclopropane solution exhibits an intense ultraviolet peak at 240 nm. Since iodine in propane does not absorb in this region, the CCT band position and shape seem established. However, the magnitude of ϵ for cyclopropane–I_2 at λ_{max} (240 nm), reported as 2900 l mol^{-1} cm^{-1} at 230 K and 5 100 l mol^{-1} cm^{-1} at 150 K, is only an apparent value. It is not known if further decrease in temperature would affect the ϵ_{app} beyond that of a density change. Hence, the latter value must be regarded as a lower limit. The integrated intensity of the band becomes considerably greater as the temperature is lowered from 25°C to −80°C, which would be expected for an increase in concentration of EDA pairs. Qualitative intensity measurements gave a value of ~2 kJ mol^{-1} (0·5 kcal mol^{-1}) for ΔH^0.

Aleksanyan and Gevorkyan[154] found a CCT band at 222 nm for cyclopropane–Cl_2. This value compares quite well with that calculated by them from the known difference in electron affinity between molecular iodine and molecular chlorine, and the observed CCT band for cyclopropane–I_2.[153] From a Raman study, they determined $-\Delta H^0$ as 0·5 ± 0·3 kcal mol^{-1} for cyclopropane–Cl_2.

Yoshida *et al.*[155] reported the spectral and thermodynamic properties of iodine interaction with several alkyl substituted cyclopropanes. The CCT bands were characterized by obtaining the spectrum of cyclopropane–I_2–n-hexane mixtures, and subtracting from it the spectra of solutions at the same concentration of cyclopropane–n-hexane and of I_2–n-hexane. This

procedure, while unsatisfactory for the alkane–I_2 system, may be applicable here because λ_{max} for the CCT band of the cyclopropanes–I_2 is above 250 nm at which wavelength the CCT band contribution of I_2–n-hexane is no longer a factor. It does become a factor below this wavelength and may account for the steep slope on the low wavelength side of the CCT band reported for n-pentylcyclopropane–I_2. A very large cyclopropane concentration range, from 0·1 to 6 M, was used in determining K by the Benesi–Hildebrand method.

C. With Aromatic Hydrocarbons

Benzene–iodine is the classical example of a weak EDA interaction exhibiting a CT band.[19, 20, 156] This system, by the definitions adopted in this chapter, is at about the boundary between being labelled a complex or a contact.[157] Regardless of the problems inherent in classification, discussed previously, it is clear that modifying the benzene ring or changing the halogen will alter the strength of interaction. The studies of Andrews and Keefer,[93, 158–160] Choi and coworkers,[161–165] as well as others[113, 166] show systematic effects on K in carbon tetrachloride for many of the substituted aromatic hydrocarbon–halogen systems with the range in K values overlapping those for complexes and contacts. The sequence of acceptor strengths of the halogens towards the aromatic hydrocarbons is chlorine < bromine < iodine < interhalogen. Monohalogen substitution in the benzene ring does not always lead to a decrease in stability, and it may be that in some cases the compound is an n-donor rather than a π-donor.[158] Karaianev, D'Alessio and Bonadeo[167] cite ultraviolet, infrared and nmr evidence that a contribution to the interaction in chlorobenzene–I_2 comes from the iodine behaving as the donor.

The aromatic hydrocarbon–halogen data obtained in "inert" solvents which meet the adopted criteria for contacts are given in Summary Table A.

Note should be taken that, to facilitate comparison of data in this and subsequent tables, literature values reported in mole-fraction units (K_x and ΔH_x^0) have been changed to units of molarity (K_c and ΔH_c^0). The conversions are based on the relation $K_c = K_x V_0$ (which holds for dilute solutions) where V_0 is the molar volume of the solvent. The difference in temperature dependence of K_c and K_x is due to the temperature dependence of V_0. For the temperature range usually studied, the following approximation will be used, $\Delta H_x^0 \approx \Delta H_c^0 - 0{\cdot}2$ kcal mol^{-1}.[168–170]

D. With Alkenes

Early CT studies on alkene–iodine systems[116, 139, 146, 153, 171–173] generally indicated that the interactions were comparable to those of iodine with

aromatic hydrocarbons. Traynham and Olechewski[174] made a systematic study of iodine interactions with cycloalkenes and with methylenecycloalkanes. When their spectral and thermodynamic data are compared with available ionization potentials of these cyclic alkanes,[175,176] an overall linear relation between I_D and $h\nu_{CT}$ is found, but the correlation is not as good as is usually obtained for a homologous series of donors. Also, in considering the strength of interaction, there is no apparent relation among the data for K_c, ΔH_c^0 and λ_{max}, which may be indicative of the difficulty in obtaining reliable results. There is some variation in the data from different laboratories, as in the case of cyclohexene–I_2.[139,146,171,174,175] Further, Andrews and Keefer[171] observed that λ_{CT} varied slightly with the solvent content of the solution. Photochemical reaction also occurs between I_2 and olefins.[176a]

Sergeev and coworkers[177–179] studied the interaction of the series I_2, Br_2, Cl_2 and ICl with hex-1-ene, cyclohexene, 4-methylpent-1-ene and hept-3-ene. (Ionization potential data[175,180,181] are available for some of the alkenes.[175,180,181]) Unlike the case of the aromatic hydrocarbon donors, there is no obvious correlation of the reported thermodynamic data, which are beyond the limit suggested for contacts, with the expected acceptor strength of the halogens. It should be noted, however, that Cl_2 and Br_2 react rapidly with olefins, making precise determination of K and ΔH^0 difficult. Sergeev and coworkers[177–179] observed appreciable reaction 15–30 s after mixing, and extrapolated the absorbance data to zero time for the Benesi–Hildebrand evaluation.

The reactivity of Cl_2 and Br_2 towards olefins has necessitated study of the intermediates by going to low temperature[182] or by using rapid measurement techniques. Dubois and Garnier[183,184] used fast mixing and scanning methods to determine λ_{max} of the CT bands for many olefins with Cl_2 and Br_2. Very good linear correlation of I_D with $h\nu_{CT}$ was obtained, with the lines for alkene–Cl_2 and alkene–Br_2 having different slopes and intercepts. Dubois and Garnier were unable to obtain K and ϵ from a B–H treatment of the data because, as they state, the interaction is too weak. Their data are included in Summary Table A.

Since the thermodynamic characteristics of the halogen interaction with alkenes are, on the whole, not so precisely established, as evidenced by the lack of correlation with expected donor and acceptor properties, it is difficult to apply in a meaningful way the criteria for contacts adopted for this chapter. Data have been compiled in Summary Table A in accordance with the criteria, but the selection of data (for inclusion or omission) quite likely will change as improved results are forthcoming.

E. With Alkyl Halides

Ultraviolet and visible spectroscopic studies of alkyl halides (RX) with molecular halogens are relatively few. Keefer and Andrews[185] observed for solutions of I_2 in RX a gradation in colour from pinkish violet to brown for the sequence RCl, RBr, RI, which is indicative of their relative strengths of interaction. The visible band maxima of iodine in n-butyl halides (Cl, Br and I) were reported by Voigt[143] to be 495, 491·5 and 479 nm, respectively, these bands being at least as much shifted as for iodine in toluene (λ_{max} 496 nm). Equilibrium constants determined by Keefer and Andrews[185] for iodine with methyl (Me), ethyl (Et), propyl (Pr) and butyl (Bu) halides also indicate an interaction as large as with toluene, e.g. in n-heptane solvent, with K (l mol^{-1}) at 25°C given in parentheses: MeI–I_2 (0·23), EtI–I_2 (0·36), i-PrI–I_2 (0·43), t-BuI–I_2 (1·33), n-BuBr–I_2 (0·18–0·25); and in carbon tetrachloride solvent: EtI–I_2 (0·29), toluene–I_2 (0.16). These determinations were based on absorbance data taken in the tail region of the CT band, 330–360 nm, rather than the band maximum because of the intense absorbance of RI at lower wavelengths. Keefer and Andrews[185] estimated a band plateau at ~280–300 nm with $\epsilon_{max} \sim 3 \times 10^4$ l mol^{-1} cm^{-1}. Similar study in carbon tetrachloride of MeI–Br_2 gave enhanced absorption at ~350 nm and K 0·07 l mol^{-1}; that of n-BuBr–Br_2 gave enhanced absorption at ~290 nm but K was too small to be evaluated.

Hastings and coworkers[146] reported single peaks for the CT bands of several RI–I_2 pairs. They also determined the spectral and thermodynamic properties of n-BuBr–I_2 from data at the CT band maximum: λ_{max} 244 nm, ϵ_{max} 23 400 l mol^{-1} cm^{-1}, and $K \approx$ 0·359 l mol^{-1} (presumably at room temperature) which is a little higher than that of Keefer and Andrews.[185]

Comparable extent of interaction of I_2 with RX in carbon tetrachloride was obtained in the competitive equilibria study of Clark and Kolb[152] who reported K (l mol^{-1}) at 25·0°C, given in parentheses, for the following donors: n-BuCl (0·11), chlorocyclohexane (0·15), n-PrBr (0·27), i-PrBr (0·33), MeI (0·67), EtI (0·82), n-PrI (0·79), i-PrI (0·77). Multihalogen substitution diminishes K; thus for tetrachloroethane–I_2 the value of K is zero.[152] Perfluoroalkyl solvents are essentially inert in their effect on the spectra of the halogens.[67, 143, 147]

There is one report of a gas-phase CT band maximum at 250 nm for n-heptyl bromide–I_2.[149] This is not likely to be correct because, in comparison with the result of Hastings and coworkers[146] for n-butyl bromide–I_2 in solution, there is an unexpected blue shift in going from solution to the gas phase.[24, 54]

In a detailed study, Morita and Tamres[89] found that the CT bands for RI–I_2 were complex and actually consisted of three bands, two being CT bands arising from the first and second ionization potentials of RI (which

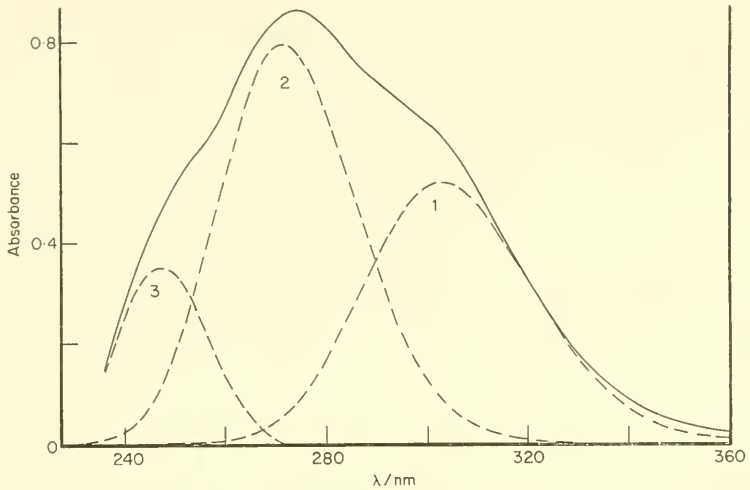

FIG. 11. Resolution of the ethyl iodide–I_2 spectrum: curves 1 and 2 are CT bands and curve 3 is a blue-shifted ethyl iodide band. [Reproduced with permission from H. Morita and M. Tamres, *J. Phys. Chem.*, **80**, 891 (1976)]

differ by $\sim 0{\cdot}6$ eV)[186–188] and the third being due to a blue-shifted and enhanced $n \rightarrow \sigma^*$ local excitation in the RI molecule (Fig. 11). The system n-propyl bromide–I_2 gave a single CT band, comparable to that reported by Hastings and coworkers[146] for n-butyl bromide–I_2, and n-propyl chloride–I_2 also gave a simple CT band. This is due to the fact that the $n \rightarrow \sigma^*$ transitions are much further in the ultraviolet region ($\sim$ 197 nm for n-PrBr and $<$ 190 nm for n-PrCl) and do not interfere with the CT bands. Also, the first and second ionization potentials are closer together in n-PrBr and especially in n-PrCl.[188]

Morita and Tamres[89] interpreted their data in terms of contacts. In order to study the CT band maxima, the concentrations of the highly absorbing RI and RBr were kept low, such that the experimental conditions fell in Person's region I (Section III.A.1). Plots of absorbance versus either the RX (at fixed I_2) or I_2 (at fixed RX) concentration gave straight lines which passed through the origin, in accord with a contact model [equation (15)]. But for n-PrCl–I_2, whereas a plot of absorbance against I_2 at constant n-PrCl concentration also gave a straight line through the origin, there was evident curvature in the plot of absorbance versus n-PrCl at constant I_2 concentration. The latter observation was attributed to a possible change in dielectric properties[3d, 7f] of the solution because of the large concentration range of n-PrCl used. An alternative interpretation is that the concentration of n-PrCl is sufficiently high for the KD_0 term in equation (14) to be significant, i.e. curvature arises because the data extend into Person's

TABLE II. Estimated values of contact pair size (d_{12}), equilibrium constant (K), maximum molar absorption (extinction) coefficient (ϵ_{max}), and oscillator strength (f) of alkyl halide–iodine contacts.

	MeI	EtI	n-PrI	i-PrI	n-PrBr	n-PrCl
$h\nu_{CCT}$[a]/eV	4·166	4·092	4·069	4·027	5·113[b]	5·617
I_D^V/eV	9·50	9·34	9·27	9·19	10·34[c]	10·88
d_{12}[d]/Å	6·39	6·64	6·79	6·91	6·71	6·60
D_0/mol l^{-1}	0·0848	0·0701	0·0645	0·0576	$0·167_0$	$1·86_0$
A_0/10^3 mol l^{-1}	7·82	7·82	7·81	7·83	3·91	1·96
Absorbance	0·461	0·518	0·549	0·512	0·536	0·942
Δd = 1·0 Å						
C[e]/mol l^{-1}	1·02 × 10^{-4}	$0·91_4$ × 10^{-4}	$0·87_8$ × 10^{-4}	$0·81_5$ × 10^{-4}	1·11 × 10^{-4}	6·00 × 10^{-4}
K/l mol^{-1}	$0·15_7$	$0·16_9$	$0·17_7$	$0·18_3$	$0·17_5$	$0·23_7$
ϵ_{max}[f,g]/l mol^{-1} cm^{-1}	4·33 × 10^4	5·44 × 10^4	6·01 × 10^4	6·04 × 10^4	4·64 × 10^4	1·51 × 10^4
f[g,h]	$0·83_0$	$0·99_4$	1·07	1·13	$0·88_8$	$0·26_2$
Δd = 2·0 Å						
C[e]/mol l^{-1}	2·04 × 10^{-4}	1·83 × 10^{-4}	1·76 × 10^{-4}	1·63 × 10^{-4}	2·22 × 10^{-4}	12·0 × 10^{-4}
K/l mol^{-1}	$0·31_8$	$0·34_3$	$0·35_8$	$0·37_0$	$0·36_1$	$0·85_0$
ϵ_{max}[f,g]/l mol^{-1} cm^{-1}	2·16 × 10^4	2·72 × 10^4	3·00 × 10^4	3·02 × 10^4	2·32 × 10^4	$0·75_4$ × 10^4
f[g,h]	$0·41_5$	$0·49_7$	$0·53_6$	$0·56_3$	$0·44_4$	$0·13_1$
Δd = 4·0 Å						
C[e]/mol l^{-1}	4·10 × 10^{-4}	3·66 × 10^{-4}	3·51 × 10^{-4}	3·26 × 10^{-4}	4·45 × 10^{-4}	($>n_A$)
K/l mol^{-1}	$0·65_4$	$0·70_4$	$0·73_4$	$0·75_9$	$0·76_9$	
ϵ_{max}[f,g]/l mol^{-1} cm^{-1}	1·08 × 10^4	1·36 × 10^4	1·50 × 10^4	1·51 × 10^4	1·16 × 10^4	
f[g,h]	$0·20_8$	$0·24_9$	$0·26_8$	$0·28_2$	$0·22_2$	

[a] n-Heptane solution result. [b] Composite band. [c] Average I_D. [d] Constant value of 0·5 eV added to $h\nu_{CCT}$ as the shift from solution to the vapour phase in calculating d_{12} from equation (5); EA_A^V of I_2 is 2·58 eV (ref. 189). [e] Based on the value calculated from equation (25) rather than half that value (see Section III.A.4). [f] Cell path length = 0·104 cm. [g] These values pertain to solution because the absorbances were measured in n-heptane solvent. [h] $f \simeq 4·32 \times 10^{-9}\, \epsilon_{max} \Delta\nu_{1/2}$ (ref. 7f).

SUMMARY · TABLE A. Molecular halogen acceptors.

Donor	Acceptor	Medium	T/°C	λ_{max}/nm	λ_{onset}/nm	ϵ_{max} /l mol^{-1} cm^{-1}	K_c[a] /l mol^{-1}	$-\Delta H^0$[b] /kcal mol^{-1}	Other data[c]	Ref.
Alkanes										
Ethane	I_2	gas	110	<210	~210[d]					119
Propane	I_2	gas	110	<210	~212[d]					119
	I_2	propane	−43	<210					λ_{bs} 520	153
n-Butane	I_2	gas	110	<210	~213[d]			~0[e]		119
n-Pentane	I_2	gas	110	<210	~220[d]					88, 119
Neopentane	I_2	gas	110	<210	~220[d]					119
n-Hexane	I_2	gas	110	<210	~224[d]					88, 119
	I_2	n-hexane	—[f]		~247[g]					146
2,3-Dimethylbutane	I_2	n-hexane	−[f]	{236}	251[g]	{19 200}[h]	{0·0034}[h]			146
2-Methylpentane	I_2	2-methylpentane	22	<220	~242[i]					128
	I_2	2-methylpentane	−127	<220	~245[i]					128
Cyclohexane	I_2	gas	110	<210	~228[d]					119
	I_2	gas		{~230}						149
	I_2	n-heptane	25	{~245}			0·043	{1·6 ± 0·5}		17, 23, 149
	I_2	cyclohexane	23	232		(> 2 × 10^4)[j]	<0·02[j]		$\Delta\nu_{1/2}$ 6 000 μ_{vn} 0·77 D f = 0·12	118
	I_2	n-heptane	—[f]	{242}	266[g]	{19 000}[h]	{0·0126}[h]		$\Delta\nu_{1/2}$ 5 000	146
	I_2	n-hexane	27 ± 1	238		19 400	0·021			155
	I_2	freon	20	243 ± 5		{19 100}	{0·013}			148
Methylcyclopentane	I_2	methylcyclo-pentane	22	<220	~248[i]					128
Methylcyclohexane	I_2	gas	110	<210	~238[d]			~0[e]		88, 119
	I_2	gas	−[k]	{~235}						149
	I_2	n-heptane	25	{~245}			0·054	{1·4 ± 0·5}		17, 23, 149
	I_2	methylcyclo-hexane	22	~235[l]	~261[i]					128
	I_2	methylcyclo-hexane	−27	240[m]	~268[i]	~5 800[n]				128

Summary Table A—*continued*

Donor	Acceptor	Medium	T/°C	λ_{max}/nm	λ_{onset}/nm	ϵ_{max} /l mol^{-1} cm^{-1}	K_c[a] /l mol^{-1}	$-\Delta H^{0}$[b] /kcal mol^{-1}	Other data[c]	Ref.
	I_2	methylcyclo-hexane + isopentane glass	< −126	~320						139
n-Heptane	I_2	gas	110	<210	~234[d]					88, 119
	I_2	n-heptane	—[f]		~250[g]					146
	I_2	n-heptane	23 ± 2	<220	245[e]					67
	I_2	n-heptane	—[f]	227					$\Delta\nu_{1/2}$ 6000 μ_{vn} 0·55 f 0·06	118
n-Octane	I_2	n-octane	−[f]	{234}						146
Isooctane	I_2	isooctane	—[f]	231					$\Delta\nu_{1/2}$ 6000 μ_{vn} 0·65 f 0·09	118
cis-Decalin	I_2	*cis*-decalin	—[k]	250[m]	~283[i]	~ 4000[n]				128
	I_2	n-hexane	27 ± 1	247		17400	0·023			155
trans-Decalin	I_2	*trans*-decalin	—[k]	—[p]	~278[i]					128
5α-Cholestane	I_2	freon	20	~240		{0·06}				148
Isopentane + 3-methylpentane	I_2	isopentane + 3-methyl-pentane glass	−196	—[q]						207
Cyclohexane	Br_2	cyclohexane	23 ± 2	<220	~263[r]					147
n-Heptane	Br_2	n-heptane	23 ± 2	<220	~245[r]					147
Cyclopropanes										
Cyclopropane	I_2	propane	−43	240		2900[s]		0·5	λ_{bs} 520	153
			−123	240		5100[s]			λ_{bs} 520	153
Isopropylcyclo-propane	I_2	n-hexane	27 ± 1	252		14600	0·050			155
n-Pentylcyclopropane	I_2	n-hexane	27 ± 1	253		15000	0·053			155
Bicyclo[4.1.0]heptane	I_2	n-hexane	27 ± 1	255		14700	0·064			155
Bicyclo[6.1.0]nonane	I_2	n-hexane	27 ± 1	256·5		15200	0·062			155
Cyclopropane	Cl_2	cyclopropane	{70}	222						154

Aromatic hydrocarbons								
Fluorobenzene	I_2	n-heptane	21	286	23 200	$0{\cdot}050 \pm 0{\cdot}006^a$	$1{\cdot}2^b \pm 0{\cdot}06$	113
	I_2	CCl_4	21	288	14 700	$0{\cdot}065 \pm 0{\cdot}012^a$	$1{\cdot}2^b \pm 0{\cdot}07$	113
	I_2	fluorobenzene	21–23	287				167
1,3-Difluorobenzene	I_2	n-heptane	21	278	37 900	$0{\cdot}015 \pm 0{\cdot}015^a$		113
	I_2	CCl_4	21	280	17 000	$0{\cdot}027 \pm 0{\cdot}003^a$		113
1,3,5-Trifluorobenzene	I_2	n-heptane	21	~264	—[t]	—[t]		113
	I_2	CCl_4	21	<274	>26 700	$0{\cdot}0097 \pm 0{\cdot}012^a$		113
o-Fluorotoluene	I_2	n-heptane	21	299	13 300	$0{\cdot}12 \pm 0{\cdot}018^a$		113
m-Fluorotoluene	I_2	n-heptane	21	300	15 300	$0{\cdot}096 \pm 0{\cdot}018^a$		113
p-Fluorotoluene	I_2	n-heptane	21	~284	(9 900)[u]	$0{\cdot}11 \pm 0{\cdot}043^a$		113
Chlorobenzene	I_2	cyclohexane	25	(300)[v]	(9 510)[v]	0·101		208
	I_2	n-hexane	25	290	12 600	$0{\cdot}087^a$	$0{\cdot}9^b$	116, 173
	I_2	CCl_4	25			0·106		163
	I_2	chlorobenzene	21–23	286				167
o-Dichlorobenzene	I_2	cyclohexane	25	(310)[v]	(15 370)[v]	0·0257		208
	I_2	n-hexane	25	294	8 400	$0{\cdot}086^a$	$0{\cdot}8^b$	116, 173
Bromobenzene	I_2	cyclohexane	25	(300)[v]	(10 240)[v]	0·127		208
	I_2	CCl_4	25	290	10 400	0·13		93
	I_2	bromobenzene	21–23	290				167
Benzene	Br_2	CCl_4	25	292	13 400	$0{\cdot}100^a$		158
	Br_2	CCl_4	25			0·137		161
Fluorobenzene	Br_2		rt[w]	~280		0·045		162
Chlorobenzene	Br_2	CCl_4	25	286	7 300	$0{\cdot}087^a$		158
Bromobenzene	Br_2	CCl_4	25	288	7 600	$0{\cdot}114^a$		158
Benzene	Cl_2	CCl_4	25	278	9 090	$0{\cdot}032^a$		159
	Cl_2	CCl_4	25			0·0643		161
m-Xylene	Cl_2	CCl_4	25	290	6 340	$0{\cdot}060^a$		159
Fluorobenzene	Cl_2	CCl_4	rt[w]	~280		0·035		162
Chlorobenzene	Cl_2	CCl_4	25			0·0400		163
Bromobenzene	Cl_2	CCl_4	—[k]			0·0485		164
Iodobenzene	Cl_2	CCl_4	21			0·070		165
Fluorobenzene	IBr	CCl_4	rt[w]	~280		0·072		162
Chlorobenzene	IBr	CCl_4	25			0·109		163

Summary Table A—*continued*

Donor	Acceptor	Medium	T/°C	λ_{max}/nm	λ_{onset}/nm	ϵ_{max} /l mol^{-1} cm^{-1}	K_c[a] /l mol^{-1}	$-\Delta H^{0}$[b] /kcal mol^{-1}	Other data[c]	Ref.
Alkenes										
Propene	I_2	propene	−43	270				0·5	λ_{bs} 480	153
			−196	280					λ_{bs} 435	153
cis-But-2-ene	I_2	*cis*-but-2-ene	−43	295				0·5	λ_{bs} 470	153
			−196	300					λ_{bs} 455	153
trans-But-2-ene	I_2	*trans*-but-2-ene	−43	297				0·2	λ_{bs} 475	153
			−196	298					λ_{bs} 465	153
Buta-1,3-diene	I_2	propane +	−80	—[x]						153
		propene	−121	278					λ_{bs} 440[y]	153
Isoprene	I_2	propane +	−43	—[x]						153
		propene	−196	315						153
Cyclopentene	I_2	2,2,4-trimethyl-pentane	25	298		14 200	0·462[a]	0·2[b]		174
2-Methylbut-1-ene	I_2	2-methylbut-1-ene	—[k]	292						146
2-Methylbut-2-ene	I_2	3-methylpentane	< −158	316						209
Methylene cyclobutane	I_2	2,2,4-trimethyl-pentane	25	283		15 300	0·459[a]	0·6[b]		174
Methylenecyclo-pentane	I_2	2,2,4-trimethyl-pentane	25	312		16 500	0·431[a]	0·8[b]		174
2,3-Dimethylbut-2-ene	I_2	2,3-dimethylbut-2-ene	—[k]	340					$\Delta\nu_{1/2}$ 5 800	146
Oct-1-ene	I_2	oct-1-ene	—[k]	275						146
cis-Cyclooctene	I_2	2,2,4-trimethyl-pentane	25	295		83 400	0·180[a]	0·3[b]		174
Ethylene	Br_2	freon	25	241						183
Propene	Br_2	freon	25	267						183
	Br_2	propene + propane[z]	−196	274						182
	Br_4	propene + propane[z]	−196	312·5						182
	Br_2 and Br_4	propene[aa]	−196	500–1000[bb]						182

But-1-ene	Br_2	freon	25	269				183
Pent-1-ene	Br_2	freon	25	269				183
Hex-1-ene	Br_2	freon	25	270				183
cis-But-2-ene	Br_2	freon	25	291				183
trans-But-2-ene	Br_2	freon	25	292				183
cis-Pent-2-ene	Br_2	freon	25	292				183
cis-Hex-2-ene	Br_2	freon	25	294				183
Cyclohexene	Br_2	freon	25	294				183
	Br_2	3-methyl-pentane	< -158	302				209
2-Methylbut-2-ene	Br_2	freon	25	312·5				183
	Br_2	3-methyl-pentane	< -158	314				209
2-Methylpent-2-ene	Br_2	freon	25	312·5				183
2,3-Dimethylbut-2-ene	Br_2	freon	25	343·5				183
	Br_2	3-methyl-pentane	< -158	322				209
Ethylene	Cl_2	freon	25	230				183
Propene	Cl_2	freon	25	246				183
But-1-ene	Cl_2	freon	25	246				183
Pent-1-ene	Cl_2	freon	25	248				183
Hex-1-ene	Cl_2	freon	25	248				183
cis-But-2-ene	Cl_2	freon	25	260				183
trans-But-2-ene	Cl_2	freon	25	261				183
cis-Pent-2-ene	Cl_2	freon	25	262				183
cis-Hex-2-ene	Cl_2	freon	25	264				183
cis-4-Methyl-pent-2-ene	Cl_2	freon	25	260				183
Cyclohexene	Cl_2	freon	25	263				183
2-Methylbut-2-ene	Cl_2	freon	25	278				183
1-Bromoprop-1-ene	I_2	n-hexane	25	278	18 500	0·069[a]		171
cis-Dichloroethylene	I_2	n-hexane	14	262	14 000	0·033[a]	< 1	172, 173
	I_2	n-hexane	25	262	12 000	0·042[a]		171
trans-Dichloro-ethylene	I_2	n-hexane	25	262	14 000	0·031[a]		171
Trichloroethylene	I_2	n-hexane	14·5	270	12 500	0·025[a]	< 1	172, 173
Tetrachloroethylene	I_2	n-hexane	14	277	16 600	0·014[a]	< 1	172, 173

Summary Table A—*continued*

Donor	Acceptor	Medium	T/°C	λ_{max}/nm λ_{onset}/nm	ϵ_{max} /l mol^{-1} cm^{-1}	K_c[a] /l mol^{-1}	$-\Delta H^{0}$[b] /kcal mol^{-1}	Other data[c]	Ref.
Alkyl halides									
1-Chloropropane	I_2	n-heptane	24	220·7				$\Delta\nu_{1/2}$ 4 010	89
	I_2	1-chloropropane	—[k]	224					1b, 146
2-Chloropropane	I_2	2-chloropropane	—[k]	224					1b, 146
2-Methyl-2-chloropropane	I_2	2-methyl-2-chloropropane	—[k]	224					1b, 146
1-Bromopropane	I_2	n-heptane	24	242·5				$\Delta\nu_{1/2}$ 4 430	89
	I_2	1-bromopropane	—[k]	244					1b, 146
2-Bromopropane	I_2	2-bromopropane	—[k]	244					1b, 146
1-Bromopentane	I_2	1-bromopentane	—[k]	244					1b, 146
1,1-Dimethyl-1-bromopropane	I_2	1,1-dimethyl-1-bromopropane	—[k]	244					1b, 146
1-Bromoheptane	I_2	gas	—[k]	{250}					149
Iodomethane	I_2	n-heptane	24	297·6[cc]				$\Delta\nu_{1/2}$ 4 440	89
				269·0[dd]				$\Delta\nu_{1/2}$ 4 000	
Iodoethane	I_2	n-heptane	24	303·0[cc]				$\Delta\nu_{1/2}$ 4 230	89
				271·5[dd]				$\Delta\nu_{1/2}$ 4 300	
	I_2	iodoethane	—[k]	{280}					1b, 146
1-Iodopropane	I_2	n-heptane	24	304·7[cc]				$\Delta\nu_{1/2}$ 4 130	89
				270·5[dd]				$\Delta\nu_{1/2}$ 4 800	
2-Iodopropane	I_2	n-heptane	24	307·9[cc]				$\Delta\nu_{1/2}$ 4 320	89
			24	275·0[dd]				$\Delta\nu_{1/2}$ 5 000	
	I_2	2-iodopropane	—[k]	{280}					1b, 146
Diiodomethane	I_2	3-methylpentane	< −158	245					209
Halogen donors									
Iodine	I_2	n-hexane	22·0 & 45·1	—[ee]			1·19 ± 0·20		192
	I_2	n-heptane	22·0 & 45·1	—[ee]			1·16 ± 0·30		192
	I_2	n-heptane	8 & 20	293·5					193

	I_2	n-heptane	23	(285)					67
	I_2	cyclohexane	22·0 & 45·1	—[ee]			1·03 ± 0·11		192
	I_2	CCl_4	22·0 & 45·1	~292			1·52 ± 0·29		192
	I_2	CCl_4	25	293·5	{780}[ff]	{2·05}[gg]	1·96 ± 0·15		193, 194
	I_2	CCl_4	25	280	{1 170}	{2·5}[gg]			195
	I_2	CCl_4	25·5	288	{16 000}[hh]	{0·13}[hh]	1·0 ± 0·2	$K\epsilon_{max}$ $2·04 \times 10^3$	169
	I_2	gas	332	230–255[ii]	~3 000	0·4 ± 0·1	2·9 ± 0·4[jj]		196, 197
	I_2	gas	110–140	~245			—[kk]		198
	I_2	gas		(267)[ll]					190
Bromine	Br_2	gas	25–225	(~205)[mm]	(1 000–1 400)[nn]		2·27 ± 0·25[oo]		196, 199
	Br_2	gas	25	(208)[pp]			{2·0}[qq]		200
	Br_2	gas	30	<220					201
	Br_2	gas	23	<215[rr]					147

[a] Literature data in mole-fraction units (K_x) have been changed to K_c based on $K_c = K_x V_0$ (Section VI.C). [b] Literature data reported as $\Delta H^0_x \approx \Delta H^0_c - 0·2$ kcal mol^{-1} (168–170) (Section VI.C). [c] Among the cited other data are: half-band width of the CCT band ($\Delta\nu_{1/2}$/cm^{-1}), oscillator strength of the CCT band (**f**), electronic transition dipole (μ_{VN}/debye), and blue-shifted iodine visible band (λ_{bs}/nm). [d] Estimated for an absorbance of 0·05 for comparable conditions of hydrocarbon concentration, iodine concentration and cell path (Fig. 3 of Ref. 119). [e] Value is for the internal energy change (ΔU^0_c). [f] Temperature not specified (probably ~25°C). [g] Based on $\epsilon_{app} \approx 400$ l mol^{-1} cm^{-1} (Fig. 1 of Ref. 146). [h] Does not meet Person's criteria[78] $KD_0 > 0·1$. [i] Based on $\epsilon_{app} \approx 1\,000$ l mol^{-1} cm^{-1} (Fig. in Ref. 128). [j] Estimated value. [k] Temperature not specified. [l] Inflection point. [m] Well defined shoulder. [n] ϵ_{app} at distinct shoulder. [o] Based on $\epsilon_{app} \approx 1\,000$ l mol^{-1} cm^{-1} (Fig. 1 of Ref. 67). [p] Broad band (probably composite) extending to below 210 nm. [q] Absorption could be changed by cooling the solution at different rates owing to precipitation of iodine, probably of different size and distribution. [r] Based on $\epsilon_{app} \approx 400$ l mol^{-1} cm^{-1} (Fig. 2 of Ref. 147). [s] Reported value is an apparent ϵ. [t] Attempted separation of K and ϵ at 270 nm gave negative values. From a correlation with Taft σ^* values, estimates of ϵ (~70 000 l mol^{-1} cm^{-1}) and K_c (~0·0041 mol^{-1}) were obtained. [u] At 290 nm. [v] Wavelength chosen to minimize absorbance corrections; not λ_{max}. [w] Room temperature. [x] Reaction occurs. [y] At 77 K. [z] Propene:propane:Br_2 ratio 1 500:33:1.

[aa] Propene:Br_2 ratio 1 500:1. [bb] For associated species Pr · A · Pr · A ... where Pr is propene and A is either Br_2 or Br_4. [cc] From first I_D of donor. [dd] From second I_D of donor. [ee] I_4 band centre not well defined. [ff] Literature value corrected by a factor of 2. [gg] Probably high. [hh] Estimated. [ii] Broad spectrum, overlapping unresolved bands. [jj] ΔH^0 over the range 150–420°C. [kk] ΔU^0 stated to be quite small. [ll] Composite spectrum of I_2 and I_4. [mm] Large uncertainty. [nn] Based on K values from *PVT* study (Ref. 203). [oo] ΔH^0 value of −2·6 kcal mol^{-1} obtained from *PVT* study (Ref. 203). [pp] Composite spectrum of Br_2 and Br_4. [qq] Value for $-\Delta U^0$. [rr] Spectrum in perfluoroheptane is similar to that in the gas phase.

region II (Section III.A.1). Treating the data (only 3 points) in the typical B–H fashion gives, at 24°C, K_c 0·191 l mol^{-1} and ϵ_{max} 17 600 l mol^{-1} cm^{-1}. These results are of comparable magnitude to those calculated by Morita and Tamres[89] based on contacts using equations (5), (22), (10) and (14) in sequence. The thermodynamic and spectral properties of several alkyl halide–I_2 pairs are given in Table II for different values of Δd (Section III.A.3). The solution value of $h\nu_{CCT}$ was adjusted to a gas-phase value by adding a correction estimated as 0·5 eV. (A smaller correction would decrease d_{12} and K, and increase ϵ.) Thus, the values for d_{12} and K should apply to the vapour phase, but those of ϵ_{max} and f (the oscillator strength) are for the solution phase because the absorbance was measured in n-heptane.

Studies that report spectral data for RX–I_2 systems but no thermodynamic values derived from these data are listed in Summary Table A. It is recognized, however, that many entries may be outside the limit set for contacts when comparison is made with some of the data cited above.

F. With Halogen Donors

Kortüm and Friedheim observed a band at ~267 nm in the spectrum of gaseous iodine for which the apparent ϵ was concentration dependent. The band was attributed to loosely bound molecules of I_4, and was interpreted by McConnell[191] as arising from an intermolecular CT transition. The iodine molecule functions both as the electron donor and as the acceptor, and is an example of a "two-way CT complex" in Mulliken's terminology.[7]

Thermodynamic data for the I_4 species have been reported in solution[169, 192–195] with somewhat scattered results, and in the gas phase[196–198] with the uncertainty reported to be rather large. Passchier and Gregory[197] point out that prediction of association from gas imperfection studies gives results similar to those based on a molecular association model,[33] so classification of I_4 as a molecule is regarded as being a matter of convenience and not of significance.

CT studies on Br_4 have been made mostly in the gas phase;[147, 196, 199–201] the band maximum is below 215 nm. (Study of a thin film of solid Br_2 at low temperature is reported to show distinct multiple CT bands at higher wavelengths.[202]) Separation of K and ϵ from the $K\epsilon$ product could not be achieved, although this could be done by relying on the K value obtained from a PVT study.[199, 203] (See ref. 24.)

G. With Other Donors

There is a large literature on CT spectra arising from halogen interaction with n-type donors, especially those containing O, S or N atoms. Generally,

the interactions are rather strong, and their consideration is beyond the scope set for this chapter. But altering the substituents in the donor molecule can greatly affect the extent of interaction. Cited earlier [Section V, paragraph (c)] is the inertness of diperfluorohexyl ether towards iodine. Examples can be found scattered in the literature of systems that meet the adopted criteria for contacts, e.g. trichloroacetonitrile–I_2 (from a study of the blue shift of the I_2 band)[17, 204, 205] and thiophen–I_2 (λ_{max} 285 nm and ΔH^0 $-0{\cdot}4$ kcal mol^{-1}; solvent not given);[206] and also ΔH^0 $-3{\cdot}7 \pm 0{\cdot}7$ kcal mol^{-1} and K_c $0{\cdot}12 \pm 0{\cdot}02$ l mol^{-1} in carbon tetrachloride).[206a]

VII. TRANSIENT HALOGEN ATOM ACCEPTORS

Conceptually, one of the simplest chemical reactions is the combination of atoms:

$$2X \rightarrow X_2. \tag{54}$$

In the homogeneous gas phase, simultaneous conservation of energy and momentum requires the presence of a third body, M:

$$2X + M \rightarrow X_2 + M. \tag{55}$$

Experimentally it is generally found that this reaction is kinetically third order:

$$d[X_2]/dt = k_{recomb}[X]^2[M]. \tag{56}$$

but that the rate has a negative temperature coefficient and is markedly dependent on the nature of M. In the liquid phase the omnipresence of solvent molecules eliminates the explicit need for M in the recombination mechanism expression, although of course energy and momentum are still conserved through solvent–molecule interaction.

A large number of studies has been made on halogen atom recombination, particularly since developments of the flash photolysis[210–212] and pulse radiolysis[213, 214] techniques which lead to production of relatively large atomic-halogen concentrations in the experimental systems. Generally in flash photolysis the halogen atoms result from the photodissociation of the parent halogen molecule, whereas in pulse radiolysis the atoms are often produced from fragmentation of molecular species such as bromobenzene or carbon tetrachloride. Kinetics of the recombination process are determined by following spectrophotometrically as a function of time the subsequent increase in absorbance in the visible region due to molecular halogen formation.

In many cases (both in liquid- and vapour-phase recombination studies) a transient absorbing species is produced, and this has been attributed to charge-transfer interaction between the acceptor halogen-atom X and donor third-body M or solvent species.[215] This spectral behaviour is discussed in Section VII.B. The strong dependence on the nature of M in gas-phase recombination suggests specific M—X interaction; whether or not this interaction is sufficiently weak in some cases to fall within the operational criteria established for contacts (Section IV) is developed in the following section.

A. Halogen Atom Recombination

1. Gas-phase Recombination from Flash Photolysis Studies

Gas-phase photoexcitation of halogen molecules leads to dissociation:

$$X_2 \xrightarrow{h\nu} 2X;\ d[X_2]/dt = -\phi I_a \tag{57}$$

with the primary quantum yield, ϕ, equal to 1 both below the convergence limit—due to direct dissociation—and above it even at moderately low pressures—resulting from several pressure-induced and direct predissociation processes.[216] Recombination is generally accepted to occur either via an energy-transfer (ET) mechanism involving an unbound quasidimer[217] X_2^*:

$$2X \rightleftharpoons X_2^* \tag{58}$$

$$X_2^* + M \rightarrow X_2 + M \tag{59}$$

or through an M—X intermediate (the radical-molecule, RMC, mechanism):

$$X + M \underset{r}{\overset{f}{\rightleftharpoons}} M—X \tag{60}$$

$$M—X + X \rightarrow X_2 + M \tag{61}$$

where the efficiency of the recombination is determined by the stability of M—X. If attraction in M—X is very strong, as for example with NO and I,[218] so that a significant fraction of X is in the form of M—X, then recombination may also occur by:

$$2M—X \rightarrow X_2 + 2M. \tag{62}$$

Extensive classical 3-D trajectory/Monte Carlo calculations have been made on gas-phase bromine or iodine recombination systems involving simple inert third-body gases.[219] In general it is found that neither the ET nor the RMC mechanism alone adequately describes atom recombination over wide temperature and pressure ranges, particularly for the lighter third

bodies. With M = He, the ET mechanism apparently dominates over the whole temperature range for bromine[220] and for iodine[221] recombination, but for M = Ar or Xe at low temperatures the RMC mechanism is more significant and leads to a large negative temperature-dependence.[220,221] The importance of the ET mechanism decreases as the mass of M increases, although at sufficiently high temperatures the ET mechanism contributes substantially even for the higher mass third bodies.[221] For the more complex molecular third bodies both mechanisms are involved, but the RMC mechanism appears to be the major contributor to halogen-atom recombination.[222,223]

Three-body recombination involving an orbiting pair quasidimer (M—X)*:

$$X + M \rightleftharpoons (M—X)^* \tag{63}$$

$$(M—X)^* + X \rightarrow X_2 + M \tag{64}$$

also occurs.[219] However, its contribution to the overall recombination is small, being less than 20 per cent for Br- or I-atom recombination in Xe at all temperatures but gaining in importance for recombination of light atoms.[224]

A critical parameter in the classical 3-D trajectory calculations and in the relative importance of the ET and RMC mechanisms is the extent of stabilization of M—X, i.e. the depth of the M—X potential energy well. Assuming classical Arrhenius behaviour with a temperature-independent pre-exponential factor:

$$k = Ae^{-E_a/RT} \tag{65}$$

from the RMC mechanism [equations (60) and (61)] it follows that:

$$(E_a)_{recomb} = (E_a)_{60,f} - (E_a)_{60,r} + (E_a)_{61}. \tag{66}$$

Thus, if the activation energies for formation and reaction of M—X [$(E_a)_{60,f}$ and $(E_a)_{61}$] are zero, then the observed negative temperature-coefficient, $(E_a)_{recomb}$, is the negative of the M—X dissociation energy.

Several representative values for k and E_a, obtained by flash photolysis from room temperature to ~ 500 K, are given in Table III for iodine-atom recombination in argon. The average of these five $(E_a)_{recomb}$ results, 1·5 kcal mol^{-1}, is about 4·6 times greater than the potential between an argon atom and a xenon atom (the closest inert gas atom to iodine), whereas the van der Waals potential between Ar and I is estimated to be only $\sim 1{\cdot}2$ times that between Ar and Xe.[230] This behaviour has been taken to indicate that more specific types of interaction, such as charge-transfer forces, are involved.[231,232] As pointed out above, however, this conclusion is based on the RMC mechanism being solely responsible for the recombination. On

TABLE III. Iodine-atom recombination in argon.

Source	$(k_{recomb})_{298} \times 10^{33}$ /cm^6 molecule^{-2} s^{-1}	$(E_a)_{recomb}$ /kcal mol^{-1}
Russell and Simons[225]	5·0	−2·1
Strong *et al.*[226]	8·6	−1·4
Bunker and Davidson[227]	8·0	−1·1
Porter and Smith[228]	8·2	−1·3
Blake and Burns[229]	6·6	−1·6[a]

[a] Obtained from k_{recomb} data at 298 K and 473 K.

the other hand, the more detailed classical 3-D trajectory calculations[221] give reasonably good agreement with the experimental recombination data covering a much wider temperature range[229] if a potential well of only 0·6 kcal mol^{-1} is used for I—Ar. This is less than half the experimental $(E_a)_{recomb}$ given above, and is only $\sim 1{\cdot}9$ times the interaction potential between Ar and Xe, in agreement with recent molecular beam results for I—Kr[233] and I—Ne[234] interactions. Similar interaction energetics result from 3-D trajectory calculations on bromine atom recombination in argon[220] and from classical similar trajectory (ST) calculations.[235] The fact that the magnitude of this interaction energy between a halogen atom and an argon atom is so close to the Xe—Ar potential energy and (within a factor of 2) is the same as that for thermal translational energy, clearly indicates a very unstable intermediate and that the interaction must be considered contact involving predominantly weak van der Waals forces.

The energetics of halogen-atom recombination in the presence of molecular third bodies are more difficult to interpret. The rate of recombination is strongly dependent on, but the Arrhenius activation energy is surprisingly insensitive to, the nature of the third body, as shown in Table IV for iodine-atom recombination. Similar activation energies are indicated for iodine-atom recombination in HCl (−2·1 kcal mol^{-1}), HBr (−2·2 kcal mol^{-1}) and SO_2 (−2·0 kcal mol^{-1}) (the values in parentheses calculated between 300 K and 500 K from data in ref. 222).

Russell and Simons[225] showed a correlation between log k_{recomb} and the boiling point or the critical constant of M, as well as a regular variation between k_{recomb} and the ionization potential of M, over quite a diverse range of third bodies. These correlations led to the conclusion that general van der Waals forces are involved rather than more specific types of interaction. Basila and Strong[236] point out, however, that for a given halogen-atom recombination the same general dependence on the ionization potential of

TABLE IV. Iodine-atom recombination rates and Arrhenius activation energies.

Third body	$k_{recomb} \times 10^{32}$ /cm^6 molecule^{-2} s^{-1}	$(E_a)_{recomb}$ /kcal mol^{-1}
Nitrogen[a]	1·3[a]	−2·0
Oxygen[b]	1·9[b]	−1·5
Carbon dioxide[b]	3·7	−1·75
Cyclohexane[a]	15[a]	−1·8
Benzene[b]	22[b]	−1·7
Toluene[b]	54	−2·7
Ethyl iodide[b]	72	−2·4
Mesitylene[b]	112	−4·1

[a] Ref. 225. [b] Ref. 228.

M would be expected for both charge-transfer and van der Waals interactions. On the other hand, for a given M and different halogen atoms recombining, opposite trends should be observed depending on the dominant nature of the intermolecular forces, based on relative electron affinities *EA* and polarizabilities α. Specifically, since $(EA)_{Br} > (EA)_I$, but $\alpha_{Br} < \alpha_I$, it follows that $(k_{recomb})_{Br} > (k_{recomb})_I$ for major charge-transfer interactions, while $(k_{recomb})_{Br} < (k_{recomb})_I$ if non-specific van der Waals forces are the key factors in recombination. As shown in Table V, it would appear that the relative contribution of charge-transfer interactions decreases with increasing third-body ionization potential.

Chang and Burns[223] have recently studied I-atom recombination in the presence of H_2, D_2 and HI, following flash photolysis of HI. The Arrhenius E_a is also low for HI as third body ($-1·7$ kcal mol^{-1}, between 206 K and 300 K) suggesting only weak interactions between I and HI. It was pointed out, however, that any activation energy associated with reaction (61) can lead to the observed small negative temperature coefficient even though M—X may be relatively stable, i.e. large dissociation energy [note equation (66)].

Extensive temperature-dependence data are not available for recombination of other halogen atoms as a function of third-body complexity. Some results for bromine and chlorine recombination are given in Table VI for a limited range of third bodies. Although there is some indication of a correlation between k_{recomb} and $(E_a)_{recomb}$ for bromine-atom recombination, such a correlation does not exist for the recombination of chlorine atoms. However, more wide-ranging temperature–third-body efficiency determinations are required for these halogens in order to establish reliable correlations.

In summary, it appears that, except for very efficient third bodies such as I_2,[238] NO[218, 239, 240] and NO_2[241] the classical Arrhenius *activation energy* $(E_a)_{recomb}$ for gas-phase halogen-atom recombination is small and

TABLE V. Gas-phase I- and Br-atom recombination rates at room temperature[236]

Third body	Ionization potential/eV	$k_{recomb} \times 10^{32}$/cm^6 molecule^{-2} s^{-1} Bromine	Iodine
Benzene	9·24	145	23
Ethyl bromide	10·29	69	22
Methyl bromide	10·53	33	15
Ethyl chloride	10·97	15	16
Methyl chloride	11·33	9·6	11

TABLE VI. Rates and Arrhenius activation energies for bromine and chlorine recombination[237]

Third body	Bromine $k_{recomb} \times 10^{32}$ /cm^6 molecule^{-2}s^{-1}	Bromine $(E_a)_{recomb}$ /kcal mol^{-1}	Chlorine $k_{recomb} \times 10^{32}$ /cm^6 molecule^{-2}s^{-1}	Chlorine $(E_a)_{recomb}$ /kcal mol^{-1}
Nitrogen	0·91	−1·5	2·2	−1·6
Sulphur hexafluoride	2·2	−1·8	3·3	−0·97
Carbon tetrafluoride	2·8	−2·3	3·4	−1·2
Carbon dioxide	2·2	—	5·2	−1·5

fairly insensitive to the nature of the molecular third body, although the recombination *rate* k_{recomb} varies greatly—particularly for recombination of iodine atoms. Furthermore, it is doubtful if $(E_a)_{recomb}$ is a valid measurement of the depth of the M—X potential well in most cases, particularly when both the ET and RMC recombination mechanisms are operative. In comparison with classical 3-D trajectory calculations on atomic inert-gas third-body systems it must be concluded that the transient intermediate binding energies may be appreciably less than the negative of the observed Arrhenius activation energies and within the operational criterion of 4 kJ mol^{-1} ($\sim$ 1 kcal mol^{-1}) for contacts.

If only the RMC mechanism is assumed to be operative and if equilibrium for reaction (60*j*) is maintained, then the formation constant for M—X can be calculated from experimental k_{recomb} values; such calculations have been carried out by Porter and Smith [228] for several inert third-bodies. However, Hippler, Luther and Troe[241–243] have shown that the ET mechanism cannot be neglected in the determination of the formation constant from data obtained at low (< 1 atm) pressure. In general, inclusion of the ET mechanism[242] leads to values for K at least a factor of 4 less than those based on the less refined analyses,[228] and of the order of magnitude to be associated with predominantly contact interactions in the gas phase.

2. Liquid-phase Photodissociation and Recombination

Halogen atom recombination in the liquid phase differs in several important aspects from that in the gas phase. As pointed out above, the intimate presence of solvent molecules during any encounter between halogen atoms in the liquid phase negates the explicit need for a third body in the recombination mechanism, and liquid-phase recombinations in inert solvents show kinetically a second-order dependence on halogen atom concentration:

$$d[X_2]/dt = k_{recomb}[X]^2. \tag{67}$$

On the other hand, the primary quantum yield of dissociation, ϕ [see equation (57)], is less than 1 in the liquid phase because of primary recombination[244] of atoms present before photodissociation in the same diatom ("geminate" recombination[245]) as a result of a cage[246] of solvent molecules. Non-geminant recombination between atoms that were not original partners is diffusion controlled[247, 248] in inert solvents and has a positive temperature coefficient which correlates reasonably well in most cases with the constant-pressure temperature dependence of the solution viscosity. Thus, although there undoubtedly is a small potential barrier associated with the solvent cage to be overcome in dissociation and in bringing the two atoms together,[249] the activation energy for actual atom–atom combination is essentially zero.

If 1:1 charge-transfer complexation occurs between solvent molecules and halogen atoms:

$$S + X \rightleftharpoons S{\cdot}X; \quad K_S = [S{\cdot}X]/[S][X] \tag{68}$$

and $[X]_{total} = [X] + [S{\cdot}X]$, the recombination mechanism becomes:

$$2X \rightarrow X_2 \tag{69}$$

$$X + S{\cdot}X \rightarrow X_2\ (+S) \tag{70}$$

$$2S{\cdot}X \rightarrow X_2\ (+2S) \tag{71}$$

where X_2 represents free plus complexed molecular halogen. It follows that:

$$d[X_2]/dt = k_{69}[X]^2 + 2k_{70}[X][S{\cdot}X] + k_{71}[S{\cdot}X]^2. \tag{72}$$

Assuming that the three rate constants are equal, $k_{69} = k_{70} = k_{71} = k_a$, then:

$$d[X_2]/dt = k_a\{[X]^2 + 2[X][S{\cdot}X] + [S{\cdot}X]^2\} = k_a[X]^2_{total} \tag{73}$$

in agreement with the observed second-order kinetics in these systems represented by (67).

B. Charge-transfer Spectra of Halogen Atoms

It is seen in the preceding section (VII.A) that no clear influence of charge-transfer complexation on halogen molecule photodissociation or on the atom recombination in the liquid phase has been detected, nor has the role of charge-transfer complexes in vapour-phase recombination been clearly separated from that of classical van der Waals interactions. On the other hand, transitory increases in absorption are detected in many photochemical or radiological systems containing halogen atoms. In general it is clear that these new absorption bands result from charge-transfer interactions, although in most cases it has not been possible to get accurate thermodynamic data on transient interactions in the same manner as with more stable systems. In this absence of reliable equilibrium data, we have included in Summary Table B the spectral results for halogen atom acceptors with all donors, recognizing that many of these species may fall outside the operational criteria for contacts specified in Section IV.

1. Spectral and Thermodynamic Measurements on Transient Halogen Atom Systems

Kinetic spectrophotometric and flash spectrographic analyses, both employing absorption spectroscopy, are the two methods most widely used in the physical detection of transients produced in flash photolysis and pulse

radiolysis studies. In the former, continuum light from a steady source is collimated through the absorption cell to a monochromator or filter system and the transmitted light is monitored at a single wavelength λ with a photomultiplier–oscilloscope system or other fast detector–recorder device, from which is obtained the transient change in absorbance, $\Delta A_\lambda = \log_{10}(I_0/I_\lambda)$, as a function of time. A complete kinetic run can be obtained from a single flash; absorption bands are obtained through point-by-point determination of ΔA_λ as a function of λ, each taken at the same specific time after discharge of the activating flash or radiation pulse. In flash spectrographic analysis, the continuum analysing light is replaced by a pulsed monitoring source, and detection is by a spectrograph; it has the advantage of providing a complete transient spectrum with a single flash, but kinetic data must be obtained from the analysis of a series of spectrographs taken at varying times after the flash. Spectral curves from the spectrophotometric technique, or kinetic data by spectrographic analysis, generally require photochemically stable systems and constant flash or pulse discharge energies. The absorption spectra obtained by either technique may be erroneous if several species are present with overlapping absorption bands, such as the halogen atom CT spectra in the near-ultraviolet and visible spectral regions where the parent halogen molecules also absorb. The error will be enhanced if two or more transient absorbing species have substantially different decay rates.

If the halogen-atom CT band and the molecular halogen band are separated, then the total atomic halogen concentration is obtained from ΔA_{X_2} in the molecular halogen band, since $[X] = -2\Delta[X_2] = -2\Delta A_{X_2}/\epsilon_{X_2} b$, where ϵ_{X_2} is the molar extinction coefficient for X_2 and b is the absorbing light path. If it is further assumed that all the halogen atoms are complexed with the donor solvent (S) in neat liquid systems, then the absorption (extinction) coefficient for S·X may be estimated from the concurrent change in absorbance measured in the halogen atom CT band since then $[X] = [S{\cdot}X]$ and $\Delta A_\lambda = \epsilon_{S\cdot X,\lambda}[S{\cdot}X]b$. In general, however, the assumption of complete complexation is too drastic for the vapour phase and for most liquid systems leading to values for $\epsilon_{S\cdot X,\lambda}$ that are too low, although the relative ΔA_λ values are adequate to show CT band shapes and maxima.

In most cases disappearance of the transient CT absorbance is kinetically second-order. Again assuming complete complexation between S and X:

$$2S{\cdot}X \rightarrow X_2(+2S); \quad -d[S{\cdot}X]/dt = 2k_{recomb}[S{\cdot}X]^2$$

which integrates to:

$$\left(\frac{b}{2}\right)\left(\frac{\epsilon_{S\cdot X,\lambda}}{k_{recomb}}\right)\left(\frac{1}{\Delta A_\lambda}\right) = t + C. \tag{74}$$

Slopes of $1/\Delta A_\lambda$ versus t second-order plots thus give "relative absorption (extinction) coefficients", $\epsilon_{S\cdot X}/k_{recomb}$. This quotient cannot be separated without additional assumptions or an independent measurement of one of the two quantities. For example, it is sometimes separated by assuming diffusion-controlled recombination and validity of the Debye equation given in Section IV.D.[250] However, if complexation is not complete—as for example in dilute solutions of a donor D, or in the vapour phase, or with contact charge-transfer systems—the two additional recombination steps given by equations (69) and (70), replacing S by D, must be included. If the three recombination rate-constants k_{69}, k_{70} and k_{71} are equal, recombination will remain kinetically second-order, but $\epsilon_{D\cdot X}/k_{recomb}$ calculated from the linear second-order plot of equation (74) will increase with increasing donor concentration.[251] Similar problems arise if competing complexation also occurs with the solvent,[252] so that in general data for $\epsilon_{D\cdot X}/k_{recomb}$ have not led to reliable estimates of the absorption (extinction) coefficients for the halogen atom complexes. Values of $\epsilon_{D\cdot X}/k_{recomb}$ at the wavelength of maximum absorption are given in Summary Table B for a few D·X species, but in virtually all cases reported in Table B λ_{max} has been obtained from measurements of ΔA_λ rather than from second-order kinetic measurements of $\epsilon_{D\cdot X}/k_{recomb}$.

In principle the classical Benesi–Hildebrand treatment or one of its modifications (see Section III.A.1) can be used to obtain the formation constant and molar absorption (extinction) coefficient for transient halogen atom complexes. An equation similar to (16) (Section III) was used by Gover and Porter to determine K for the C_2H_5Br–I and C_2H_5I–I complexes in cyclohexane.[250] It was assumed that at the wavelength, λ, where absorbance changes were measured, the only absorbing species was the CT complex:

$$b/\Delta A_\lambda = 1/\epsilon_{D\cdot I}[I_0] + 1/\epsilon_{D\cdot I}K[D_0][I_0] \qquad (75)$$

where $[I_0]$ is the total (complexed and free) iodine atom concentration at the time of the ΔA_λ measurement. Thus, the plot of $1/\Delta A_\lambda$ versus $1/[D_0]$ should be linear with the ratio intercept/slope equal to K. This treatment, however, neglects I-atom complexation with the solvent [equation (68)]. As discussed [see equation (42)], inclusion of this equilibrium results in the intercept/slope ratio from equation (75) being $K/(1 + K_S S_0)$ rather than K,[250] and may lead to significant error. (It should be pointed out that Halpern and Weiss estimate a lower limit for K_S of ~ 1 l mol^{-1} for methylcyclohexane solvent.[252]) $[I_0]$ was not known in the Gover and Porter work,[250] and therefore the molar extinction coefficient $\epsilon_{D\cdot I}$ could not be determined. However, since $[I_0] = -2\Delta[I_2]$, it can be obtained by independent measurements of ΔA_{I_2} in the I_2 absorption band taken at the same time after the flash as ΔA_λ, as was done for the I-atom–*o*-xylene complex.[253]

Realistic pressure limitations leading to very small percentage complexation, which results in large errors in absorbance change measurements, have so far precluded determination of formation constants in the vapour phase using the Benesi–Hildebrand treatment. A few vapour-phase formation constants, given in Summary Table B, have been estimated from recombination kinetic data (see Section VII.A.1), as have also several liquid-phase constants.[252]

2. Halogen Atom Charge-transfer Spectra in the Liquid Phase

Bühler[18] has reviewed the spectral, kinetic and thermodynamic properties of approximately sixty of the liquid-phase CT species involving chlorine, bromine or iodine atoms listed in Summary Table B which were studied prior to 1972. In addition, the spectral data (and hence the charge-transfer energies) have been correlated with the donor ionization potentials[254] using the parabolic relationship:[7g]

$$(h\nu_{CT})^2 = \left[\frac{I_D - C_1}{1 - S_{01}^2}\right]^2 \left[1 + \frac{4\beta_0\beta_1}{(I_D - C_1)^2}\right]. \tag{76}$$

In this equation, which is applicable to fairly strong complexes, S_{01} is the overlap integral, and β_0 and β_1 are the resonance integrals $(H_{01} - S_{01}W_0)$ and $(H_{01} - S_{01}W_1)$, respectively, related through:

$$\beta_1 = \beta_0 - S_{01}(I_D - C_1). \tag{77}$$

Equation (76) is used to explain the fact that, although in general $h\nu_{CT}$ increases approximately linearly for most homologous series of halogen atom complexes, the slopes of the $h\nu_{CT}$ versus I_D plots are less than 1 in all cases.

If β_0 is assumed to be constant for a given donor series, then equation (76) reduces to the quadratic relationship in I_D:[254]

$$(h\nu_{CT})^2 = \gamma_0 I_D^2 - \gamma_1 I_D + \gamma_2 \tag{78}$$

which in principle can be solved for C_1, S_{01}, and β_0 by the method of least squares. In practice it was necessary to estimate S_{01} independently; by analogy with weak molecular iodine complexes[7h] $S_{01} = 0{\cdot}1$ was chosen, after which the remaining two coefficients C_1 and β_0 were determined. The results are summarized in Table VII for π and ROH donors, and equation (76) is plotted in Figs. 12–14 for the halogen-atom complexes. In fact, β_0 and C_1 are quite insensitive to the choice of S_{01} for weak complexes. If, for example, $S_{01} = 0$ is chosen for the π and ROH donors with I, $\beta_0 = -1{\cdot}17$ eV, $C_1 = 8{\cdot}23$ eV, and virtually the same I_D versus $h\nu_{CT}$ correlation curve is obtained as that shown on Fig. 14 for $S_{01} = 0{\cdot}1$.

TABLE VII. Least-squares adjustment of equation (76) to the charge-transfer energy of halogen-atom complexes, assuming $S_{01} = 0{\cdot}1$

Donor type	Acceptor	β_0/eV	C_1/eV
π^a	I	−1·02	8·0
π and ROH^b	I	−1·17	8·5
π^a	Br	−0·94	7·8
π^a	Cl	−1·04	7·7

[a] Ref. 254. [b] Data from Summary Table B and Ref. 254.

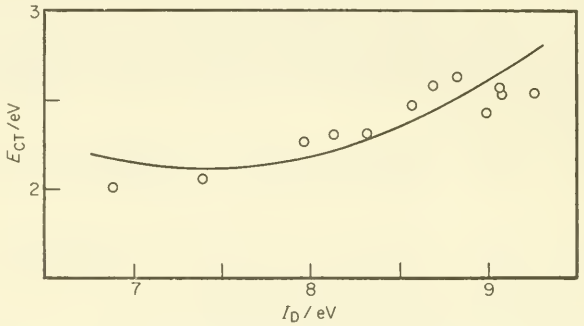

FIG. 12. Chlorine-atom CT complexes. [Reproduced with permission from R. E. Bühler, *J. Phys. Chem.*, **76**, 3220 (1972)]

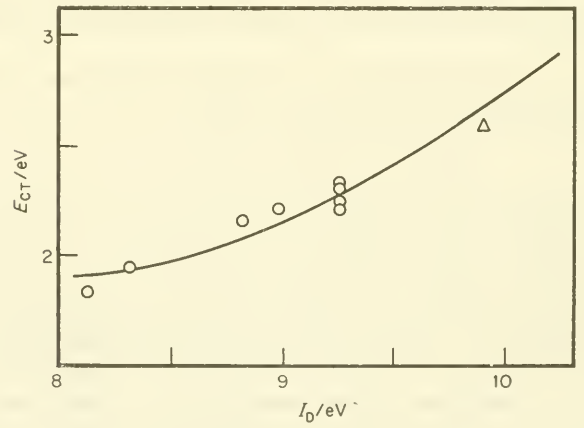

FIG. 13. Bromine-atom CT complexes. (The effect from the difference with and without bromocyclohexane, a non-π donor (Δ), is negligible on the curve fitting.) [Reproduced with permission from R. E. Bühler, *J. Phys. Chem.*, **76**, 3220 (1972)]

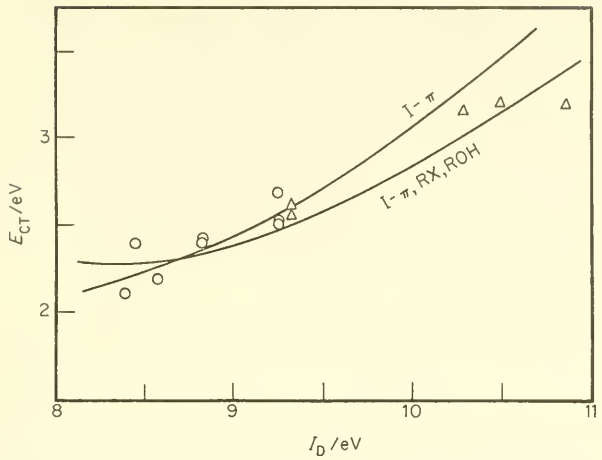

FIG. 14. Iodine-atom CT complexes. (O denotes the π donors.) [Reproduced with permission from R. E. Bühler, *J. Phys. Chem.*, **76**, 3220 (1972)]

It is worth pointing out that data-fitting to equation (76) leads naturally to a concave-curved plot of $h\nu_{CT}$ versus I_D, whereas it is seen in Figs. 12–14 that the data for Cl, Br, or I with π, RX, or ROH donors do not warrant such a curved dependence. Use of equation (76) is helpful in justifying a low dependence of $h\nu_{CT}$ on I_D. However, as pointed out by Mulliken and Person,[7i] change in donor size alone will also lead to a $h\nu_{CT}$ versus I_D slope less than 1, particularly for weak complexes involving high electron-affinity acceptors (such as the halogen atoms) where the Coulombic term involving charge separation becomes a major contributor to the charge-transfer energy. If it is assumed that the π and ROH interactions with I are essentially contact with zero ground-state binding and with only Coulombic attraction in the charge-transfer state (as is done for the RX—I species—see following section) then equation (5), Section II.B, applies. The charge separations given in Table VIII were obtained in this manner after applying a constant 0·30 eV solvent effect to $h\nu_{CT}$, based on the constant liquid–vapour blue shift in the RX—I systems. It is seen that, except for *p*-xylene (whose charge-transfer band is probably the resultant of two overlapping bands[255]), there is a gradual but general increase in charge separation with decreasing ionization potential and increasing size of the donor molecule, as expected for predominantly contact interactions. It thus seems that the observed $h\nu_{CT}$ versus I_D behaviour is satisfactorily explained solely on the basis of donor size alone, and estimates of resonance energies, ionic character, and complex strength based on curve-fitting to equation (76)[254] are not justified unless the predicted concave dependence of $h\nu_{CT}$ on I_D is clearly demonstrated.

TABLE VIII. Charge separations in I-atom–π or ROH donor contact-charge-transfer systems

Donor	I_D/eV	d_{12}/nm
Mesitylene	8·39	0·49
p-Xylene	8·44	0·54
o-Xylene	8·56	0·48
Toluene	8·82	0·47
Benzene	9·25	0·43
Propan-2-ol	10·16	0·41
Methanol	10·85	0·39
Water	12·59	0·32

Transient spectra in photolysed solutions of I_2 in saturated alkanes and cycloalkanes have recently been investigated by laser flash photolysis.[256] The transient absorbance changes with concentration of methylcyclohexane in methylcyclohexane–iodine–carbon tetrachloride solutions clearly showed contact charge-transfer behaviour. Unfortunately the spectral bands are so broad and apparently complex that band maxima are not clearly defined, although estimates for two alkanes are listed in Summary Table B. (The spectrum for methylcyclohexane actually appears to consist of at least two bands of about equal magnitude, although the resolution is very difficult from the limited data available.) Although absorbance does not vary linearly with donor concentration in n-hexane–iodine–perfluorohexane solutions, this effect is attributed to possible influences of relatively large changes in the dielectric constant of the medium at different hexane–perfluorohexane mixtures. Results suggest that the hexane–I spectrum may also be influenced by collisions of perfluorohexane molecules with the hexane–I pair.[256]

Flash photolysis of I_2 in hydroxylic solvents leads to several transient absorbing species. Conventional "microsecond" flash photolysis gives the predominant absorption band at 385 nm, and in the case of water solvent this at one time was attributed to CT absorption by the $H_2O \cdot I$ complex.[250, 257] However, more recent "nanosecond" flash studies on I_2[258] or I^-[259] in water,[258, 259] alcohols,[258] and nitriles[259] with single-pulse lasers show two types of transient absorption: a band between 250 and 450 nm produced during the lifetime of the laser pulse whose position depends on the ionization potential of the solvent, and a second band at ~ 385 nm which grows in as the earlier transient decays. The band produced initially is now attributed to solvent·I CT interaction (for $H_2O \cdot I$, λ_{max} 255 nm[258]) with the 385 nm peak reassigned[260] to the I_2^- radical anion.[261] Similarly, bands for $H_2O \cdot Br$ (λ_{max} 275 nm) and $H_2O \cdot Cl$ (λ_{max} 315 nm) have been determined,[262] with the λ_{max} dependence on halogen atom electron affinity being in qualitative agreement with equation (4) or (5) (Section II.B).

C. Vapour-phase Halogen Atom Charge-transfer Spectra

With the exception of the (alkyl halide)–(halogen atom) systems covered in the following section, there have been very few studies of vapour-phase transient halogen-atom spectra. This is unfortunate, since most theoretical treatments of charge-transfer interactions apply to isolated species present in the gaseous state at low pressures.[24] Charge separations for four weak (or contact) gas-phase halogen-atom interactions are given in Table IX.

TABLE IX. Some halogen-atom gas-phase CCT charge separations

Donor	I_D/eV	Acceptor	λ_{max}/nm	d_{12}/nm[b]
Dimethyl sulphide[263]	8·69	I	500	0·46
Benzene[264]	9·25	I	430	0·44
Cyclohexane[a]	9·88	I	339	0·46
Xenon[186]	12·13	Br	[257]	0·37

[a] R. L. Strong, unpublished data. [b] From equation (5), Section II.B.

D. Alkyl Halide–Halogen Atom Charge-transfer Spectra

On the basis of ionization potentials, vapour pressures, reactivities, and spectral absorption properties, the alkyl halides represent one of the most convenient homologous series for vapour and liquid phase studies of transient charge-transfer interactions with halogen atoms.

Charge-transfer spectra in various (alkyl halide)–(halogen atom) systems have been reported from several laboratories, both by flash photolysis and by pulse radiolysis, and these are given in Summary Table B. In spite of the apparent simplicity of these systems, results differ substantially from the different research groups.

Gover and Porter[250] flash photolysed iodine in pure ethyl iodide and in 3 per cent iodine–cyclohexane solution. Transient absorption maxima were observed at 490 and 475 nm, respectively, which were attributed to a charge-transfer spectrum from complexation between an iodine atom and ethyl iodide; in addition, there was increasing absorption below 440 nm with an apparent maximum at $\sim$390 nm, although not stated as such by the authors (see Fig. 4, ref. 250). Pulse radiolysis of liquid methyl, ethyl or isopropyl iodide produced a broad absorption band with maximum absorption near 400 nm in each case ($\sim$390 nm for ethyl iodide), but no absorption band at $\sim$490 nm.[264] In these cases the authors also attributed the 400 nm band to an (iodine atom)–(alkyl iodide) charge-transfer complex, stating that the 490 nm band observed by Gover and Porter in ethyl iodide could have

come from molecular iodine production following flash photodissociation of the ethyl iodide. On the other hand, more recent flash photolysis experiments of iodine in liquid methyl iodide give a transient absorption band centred at 480 nm [and also assigned as an (iodine atom)–(methyl iodide) charge-transfer spectrum] but no peak near 390 nm.[265] Bühler [18] attributes failure to observe the 480 nm peak in pulse radiolysis to overlapping of the long-wavelength tail of the 400 nm band; he assigns this 400 nm absorption to the complexed I_2^- transient formed by:[266]

$$I + RI \rightleftharpoons (RI \cdot I) \rightleftharpoons (R^+ \cdot I_2^-)_{solv} \tag{79}$$

where $RI \cdot I$ is an outer CT complex and $R^+ \cdot I_2^-$ is an inner complex found in high dielectric solvents.

Vapour-phase spectral studies of iodine-atom charge-transfer interactions have now been extended to a series of ethyl iodides and bromides.[267] In each case two bands are observed in the near ultraviolet and/or blue spectral regions. The separation between peaks is approximately constant for each RX series: 0·53 eV for RI, 0·28 eV for RBr. The fact that this separation is significantly different for the two structurally identical series clearly indicates that the multiple peaks come from charge-transfer donations from different energy levels in RX rather than from specific properties of the iodine atom or from different donor and acceptor orientations.

The ionization potential versus charge-transfer transition energy plot for the $RX \cdot I$ systems is shown on Fig. 15. Although a reasonable correlation exists for RI or RBr alone using only the lower or upper ionization potentials, it is clear that there is no correlation between the alkyl halide series or between the lower and upper ionization potentials for a given RX series. This lack of correlation may result from modification of the molecular spin–orbit decoupling in RX ionization as a result of rather strong charge-transfer interactions.[267] This may be unlikely, however, in view of the contact nature of the molecular-iodine–alkyl-halide interactions in the liquid phase.[89]

Perhaps a more rational interpretation for the behaviour shown in Fig. 15 is that the observed charge-transfer spectra are primarily contact, in which case equation (5), Section II.B, applies. Since spin–orbit splitting in RX does not produce orbits with different nodal planes, each $RX \cdot I$ species should have the same orientation and hence the same d_{12} for the two donor ionization potentials. This was shown to be the case, with d_{12} ranging from $\sim$0·40 nm for $CH_3Br \cdot I$ to 0·44 nm for 1-iodo-2-methylpropane·I.[267]

In view of the charge-transfer nature of the two transient bands in the vapour-phase alkyl halide systems the interpretation[266] of the 390–400 nm band in non-aqueous solvents as due to $(R^+ \cdot I_2^-)_{solv}$ is questionable. Strong

and Venditti[268] recently determined the transient spectra following flash photodissociation of I_2 in dilute (1 per cent) n-hexane solutions of the five alkyl iodides used in the vapour phase studies.[267] As in the vapour phase studies two bands were observed, red-shifted $\sim 0{\cdot}3$ eV from the vapour-phase spectra but with close to the same band separation (0·58 eV) and the

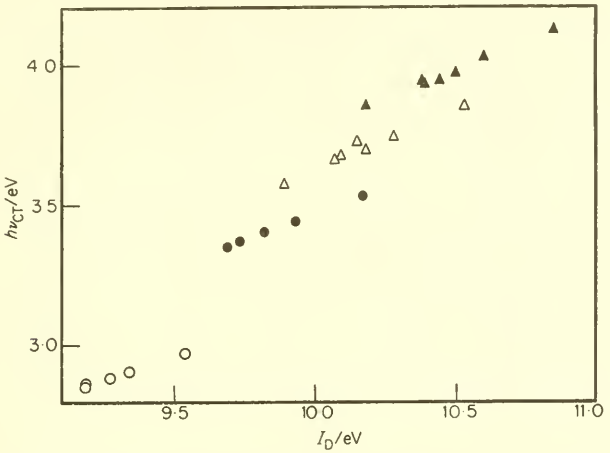

FIG. 15. Plot of charge-transfer transition energies, $h\nu_{CT}$, versus alkyl halide ionization potentials, I_D. Circles: alkyl iodides. Triangles: alkyl bromides. Open symbols: lower component of donor first ionization potential. Closed symbols: upper component of donor first ionization potential. [Reproduced with permission from R. L. Strong and J. A. Kaye, *J. Amer. Chem. Soc.*, **98**, 5460 (1976)]

same type of $h\nu_{CCT}$ versus I_D correlation as with the vapour phase results, as shown in Fig. 16. We therefore conclude that in flash photolysis of I_2–alkyl halide systems in low dielectric constant solvents the two transient absorption bands in the 390 and 480 nm regions are both attributable to RX·I charge-transfer absorption, although in flash photolysis studies in water or other solvents of high dielectric constant or in pulse radiolysis generation of iodine atoms the predominant absorbing species at 390 nm may well be the solvated dihalide ion.

Also plotted on Fig. 16 are the molecular-iodine–alkyl-iodide charge-transfer spectra from ref. 89. Since these $RI \cdot I_2$ absorbances were shown to be consistent with contact charge-transfer pairs within the concentration range studied,[89] the close correspondence among the three systems shown in Fig. 16 indicates similar contact interactions in RI·I. On the other hand, the magnitude of the CT transition energy red-shift in going from vapour to liquid suggests somewhat stronger interactions. The difference in charge-

transfer transition energies between the vapour and liquid phases is given by:[24]

$$\Delta h\nu_{CT} = h\nu_{CT}(\text{vapour}) - h\nu_{CT}(\text{liquid}) = \Delta X_N - \Delta X_V \qquad (80)$$

where ΔX_N and ΔX_V are the solvation stabilization energies of the complex in its ground (N) and excited (V) states, respectively. In general, the stronger

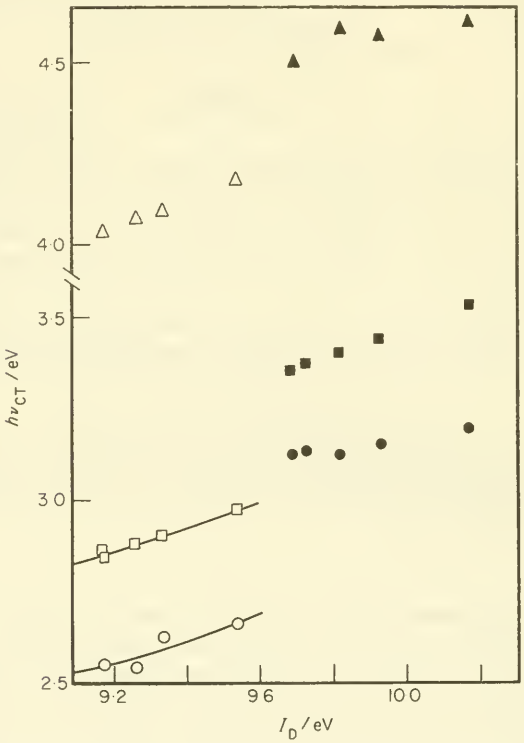

FIG. 16. Plot of charge-transfer transition energies, $h\nu_{CT}$, versus alkyl iodide ionization potentials, I_D. Open symbols: lower component of donor first ionization potential; closed symbols: upper component of donor first ionization potential. Circles: I acceptor in liquid phase; squares: I acceptor in vapour phase; triangles: I_2 acceptor in liquid phase. [Reproduced with permission from R. L. Strong and F. J. Venditti, Jr., *Chem. Phys. Lett.*, **46**, 546 (1977)]

the complex the smaller is the vapour–liquid red shift,[24] ranging from an estimated 0·5 eV for contacts[89] to 0 and even to a blue shift for the very strong trimethylamine–SO_2 complex.[111] The shift of $\sim$0·3 eV shown in Fig. 16 for the I-atom interactions suggests modest charge-transfer stabilization of

the ground state that may be beyond that expected solely from random encounters.

This suggestion may also be drawn from a comparison of the liquid-phase $RI \cdot I$ and $RI \cdot I_2$ spectra. It follows from equation (5), Section II.B, that:

$$h\nu_{RI \cdot I_2} - h\nu_{RI \cdot I} = (EA_A)_I - (EA_A)_{I_2} - e^2(1/d_{RI \cdot I_2} - 1/d_{RI \cdot I}). \quad (81)$$

From Fig. 16, $h\nu_{RI \cdot I_2} - h\nu_{RI \cdot I} \approx 1{\cdot}5$ eV; since $(EA_A)_I - (EA_A)_{I_2} \approx 0{\cdot}48$ eV, and assuming that the charge separations are the same in the liquid and vapour phases so that $d_{RI \cdot I} = 0{\cdot}43$ nm,[267] it follows that $d_{RI \cdot I_2} = 0{\cdot}62$ nm. The difference of 0·19 nm between $d_{RI \cdot I_2}$ and $d_{RI \cdot I}$ is beyond that to be expected solely from van der Waals radii (i.e. contact interactions), although it should be pointed out that this calculation assumes identical solvent effects for $RI \cdot I_2$ and $RI \cdot I$.

In contrast to the vapour studies[267] but in agreement with the comparable I_2 species,[89] only one transient band was observed when I_2 was flash photolysed in dilute (1 per cent) 1-bromopropane–hexane solution.[268] In view of the peak-broadening experienced with the RI–I systems in going from vapour to dilute solution, however, it is not surprising that two-peak resolution was not possible with the RBr–I system with its smaller (0·28 eV versus 0·53 eV) gas-phase separation. If it is assumed that the single peak consists of two bands of approximately equal intensities, then the vapour–liquid red shift of 0·28 eV is in excellent agreement with results for the comparable $RI \cdot I$ and $RI \cdot I_2$ systems.

Multiple absorption bands due to iodine atom CT interactions are also observed in glassy (77–82 K) γ irradiation or ultraviolet photolysis of alkyl iodides; these are summarized in Summary Table B. The γ-radiolysis of pure alkyl iodide glass at 77 K produces $RI \cdot I$[269] in which the two I atoms are inequivalent with the unpaired electron approximately equally distributed between the two I atoms. This behaviour may indicate rather strong CT complexation with equal dative and "no-bond" contributions under conditions of low temperature and rigid environment.

VIII. MOLECULAR OXYGEN ACCEPTOR

It has been known for some time that oxygen dissolved in a wide variety of solvents leads to absorption at longer wavelengths than for the solvent alone. In 1953 Evans reported[288] that freshly distilled *N,N*-dimethylaniline becomes yellow in air, the colour becoming much deeper when oxygen is bubbled through the solvent but disappearing completely on outgassing or flushing with nitrogen. New absorption bands for a variety of solvent–O_2 systems were presented, and although in most cases the ultraviolet *maxima*

SUMMARY TABLE B. Transient halogen atom acceptors

Donor	Medium[a]	T^b/°C	λ_{max}/nm	λ_{onset}/nm	$\epsilon_{max}/k^c_{recomb}$ /10^{-6} s cm^{-1}	ϵ_{max} /l mol^{-1} cm^{-1}	K_c /l mol^{-1}	$-\Delta H^0$ /kcal mol^{-1}	Ref.
			1. Iodine-atom Acceptor						
Pentane				350					250
Isopentane				350					250
Hexane			330						270
n-Hexane				350					250
			305		0·076				256
n-Octane				350					250
			290		0·10	1 700[d]			256
Isooctane				385[e]					256
Cyclohexane			—[h]						256
			339						271
			310[j]						272
		20–23	330[j]		0·3[k]	2 050[m]			273
Methylcyclopentane				—[i]					256
Methylcyclohexane			290, 335		0·13[f]				256
			330		0·1	1 600[m]	⩾1		252
Decane				350					256
Benzene			495		0·31	3 500[o]			255, 274
			500		0·33	1 600[p]			250
			465						275
Toluene			515		0·28	3 400[o]			255, 274
			520						250
o-Xylene			570		0·4	3 600[o]			255, 274
	CCl_4	25	570			3 400	0·9	4·4	253
p-Xylene			520		0·26	2 950[o]			255, 274
Mesitylene			590		0·56	5 800[o]			255, 274
Hexamethylbenzene	CCl_4						2·7		251
CCl_4			<280						270
				350[g]					256
			275						276
$CHCl_3$			~400						250

CH_3I	cyclohexane				0·7[q]			250
	water		310, 350			5 000[m]		277
			~400		1·2[r]	~9 000		264
	hexane		389, 467					268
C_2H_5I			390, 490		2·4[r]			250
	cyclohexane	27	475		1·0[q]		0·50	250
	hexane				0·5[q]			250
			390		2·9[r]	~9 000		264
	hexane		394, 473					268
1-Iodopropane	hexane		397, 488					268
2-Iodopropane			~400		1·8[r]	~9 000		264
	hexane		397, 487					268
1-Iodo-2-methyl-propane	hexane		396, 487					268
Iodocyclohexane		20–23	390[n]			~10^3–10^4[m]		273
C_2H_5Br			395		0·23	1 800[p]		250
	cyclohexane	27					0·33	250
H_2SO_4	H_2O			280				270
H_2O			395[s]		0·8	2 800[p]		250
			255			1 040[m]		258
CH_3OH			390[s]		3·0	1 7000[p]		250
			330			1 350[m]		258
C_2H_5OH			390[s]		0·71	1 900[p]		250
Propan-2-ol			380			1 550[m]		258
CH_3CN			274			2 300[m]		259
C_2H_5CN			280			1 800[m]		259
$CH_3(CH_2)_2CN$			300			8 500[m]		259
$CH_3O(CH_2)_2OCH_3$			420			4 000[m]		259
Diethyl ether			>430					250
CS_2			485					250
Ammonia	methylcyclohexane		350					252
Quinuclidine	methylcyclohexane		410					252
Pyridine			440					250
Benzene	vapour	92	430					186
Cyclohexane	vapour	87	310					186
Methyl iodide	vapour	100	420–430					250

Summary Table B—*continued*

Donor	Medium[a]	T^b/°C	λ_{max} /nm	λ_{onset} /nm	$\epsilon_{max}/k^c_{recomb}$ /10^{-6} s cm^{-1}	ϵ_{max} /l mol^{-1} cm^{-1}	K_c /l mol^{-1}	$-\Delta H^0$ /kcal mol^{-1}	Refs.
	vapour	88	351, 418						186, 267
Ethyl iodide	vapour	84	360, 428						186, 267
1-Iodopropane	vapour	125	365, 431						267
2-Iodopropane	vapour	91	370, 437						267
1-Iodo-2-methyl-propane	vapour	153	368, 434						267
Methyl bromide	vapour		313						186
	vapour	61	300, 322						267
Ethyl bromide	vapour		323						186
	vapour	55	308, 332						267
1-Bromopropane	vapour	78	312, 336						267
2-Bromopropane	vapour	63	316, 339						267
1-Bromo-2-methyl-propane	vapour	107	315, 338						267
2-Bromo-2-methyl-propane	vapour	73	322, 347						267
1-Bromobutane	vapour	110	315, 338						267
Methyl chloride	vapour		268						186
Ethyl chloride	vapour		279						186
Toluene	50:50 3MP–IP[w]	−196	490						278
Mesitylene	50:50 3MP–IP[w]	−196	570						278
Eight alkyl iodides	3MP[w]	−196	390, 480						278
Ethyl iodide	3:2 3MP–IP[w]	−196	472						207
HI	3:2 3MP–IP[w]	−196	392						207
Polyenes	film[x]		1205						279
3MP[w]		−196							280
Hexene	3MP[w]	−196	440						280
Ethylene	3MP[w]	−196	385						280
HI	3MP[w]	−187	390, 470						280
Methyl iodide	3MP[w]	−187	390, 470						280
Ethyl iodide	3MP[w]	−187	390, 470						280

2. Bromine-atom Acceptor

Benzene			560	0·6			274, 281
			555				275
Toluene			575				275
H_2SO_4	H_2O		330				270
CCl_4			305[y]				270
Hexane			290[y]				270
H_2O	aq. $HClO_4$		275		3 500[m]		262
Naphthalene	$CHBr_3$		680				282
Biphenyl	$CHBr_3$		640				282
Bromobenzene			560		2 800[m]		282
			560		26 000[m]		283
CBr_4	benzene		550				282
$CHBr_3$	benzene		540				282
CCl_3Br	benzene		535				282
Bromocyclohexane			480				282
Methyl bromide	vapour	25	335			2·9	236, 186
Ethyl bromide	vapour	25	345			6·5	236, 186
Methyl chloride	vapour	25	300			0·8	236, 186
Ethyl chloride	vapour	25	310			1·2	236, 186
Xenon	vapour		[257]				186
Toluene	3MP[w]	−196	500				284
2-Bromopropane	3MP[w]	—196	600				284
Polyenes	film[x]	−196	1430				279

3. Chlorine-atom Acceptor

H_2O	aq. $HClO_4$		~315		< 5 000[m]		262
Naphthacene	CCl_4		620				285, 286
Anthracene	CCl_4		605				285, 286
Naphthalene	CCl_4		540				285, 286
1-Methylnaphthalene	CCl_4		550				285, 286
Biphenyl	CCl_4		540				285, 286
o-Xylene	CCl_4		505				285, 286
Toluene	CCl_4		475				285, 286
Bromobenzene	CCl_4		510				285, 286

Summary Table B—*continued*

Donor	Medium[a]	T^b/°C	λ_{max} /nm	λ_{onset} /nm	$\epsilon_{max}/k^c_{recomb}$ /10^{-6} s cm^{-1}	ϵ_{max} /l mol^{-1} cm^{-1}	K_c /l mol^{-1}	$-\Delta H^0$ /kcal mol^{-1}	Refs.
Chlorobenzene	CCl_4		490						285, 286
Cumene	CCl_4		480						285, 286
t-Butylbenzene	CCl_4		480						285, 286
o-Dichlorobenzene	CCl_4		485						286
CCl_4	3MP	−196	470						287
Benzene	CCl_4	−196	~500						284
Toluene	CCl_4	−196	~500						284
Polyenes	film[x]		1540						279

[a] If medium is not specified, it is the liquid donor. [b] If temperature is not specified, it is assumed to be room temperature. [c] From kinetic second-order recombination plots. [d] Based on k_{recomb} (measured at 500 nm) = 1·7(±0·4) × 10^{10}/l mol^{-1} s^{-1}. [e] From Fig. 1, Ref. 256; ϵ/k_{recomb} = 0·02 × 10^{-6}/s cm^{-1}. [f] At 290 nm. [g] From Fig. 2, Ref. 256. [h] Closely resembles methylcyclohexane. [i] Absorption commences at only slightly higher wavelength than the alkanes. [j] From pulse radiolysis of iodine in cyclohexane. [k] At 340 nm. [m] Assumes complete complexation. [n] From pulse radiolysis of pure iodocyclohexane. [o] Assumes ($k_{recomb}\eta$) = constant (diffusion-controlled), and $(k_{recomb})_{CCl_4}$ = 7·5 × 10^9/l mol^{-1} s^{-1}. [p] Assumes diffusion-controlled recombination. [q] At 400 nm. [r] At 410 nm. [s] Probably the I_2^- radical-anion (see text). [t] At 430 nm and 29°C. [u] At 430 nm. [v] At 265 nm. [w] 3MP = 3-methylpentane glass; IP = isopentane glass. [x] 10 μm thick poly(vinyl chloride) film. [y] Estimated; actual maximum obscured by continuous absorption.

and apparent *band shifts* on dilution reported by Evans[288] were subsequently shown to be spurious instrumental effects,[289] the new "tailing" absorption in the presence of oxygen was clearly real. For aromatic solvents, Evans attributed this absorption to a CT interaction; however, for alkanes such as hexane or cyclohexane he first concluded that the enhanced absorption was due to oxygen itself, such as the forbidden $^3\Sigma_u^+ \leftarrow {}^3\Sigma_g^-$ transition, strengthened by intermolecular forces, but later[67] attributed it to weak, or collisional type, CT species.

Summary Table C gives spectral and thermodynamic data for many different solvent systems exhibiting this long wavelength structureless tailing absorption in the presence of oxygen. In general this O_2-enhanced absorbance is directly proportional to the partial pressure of oxygen above the solution.[133, 134, 290–292] Although Monck and Scott attributed this linear absorbance versus O_2 pressure to formation of a 1:1 molecular complex,[290] subsequent results on such systems as O_2–naphthalene (chloroform solvent)[291] show that behaviour of this type is in agreement with equation (15) (Section III.A.1) for solely contact or collisional interaction. Tsubomura and Mulliken[132] observed that, when *N*,*N*-dimethylaniline was diluted with n-heptane, the new ultraviolet absorption was approximately proportional to the volume fraction of the aniline. Molecular oxygen is more soluble in n-heptane than in *N*,*N*-dimethylaniline, so the linear dependence of absorbance on volume fraction of the aniline even when it is at a greater concentration than O_2 shows very little complex formation. This contact-behaviour agreement with equation (15) (Section III.A.1) with respect to changing donor concentration (constant O_2 pressure) has been confirmed for a wide variety of solvent systems.[134, 293] The absorption spectrum for O_2–*N*,*N*-dimethylaniline was also found to be independent of temperature,[132] showing essentially zero heat of formation and hence again no definite complex formation. Similar results were obtained with triethylamine.

Another indication of at best only very weak interactions between O_2 and many solvent systems is the fact that O_2 solubilities depend primarily on internal pressures rather than on solvent basicities.[132] Additional solubility data, for example that the heats of solution are the same order of magnitude for O_2, N_2 or Ar in water at 4°C or in benzene at 20°C, show no thermochemical evidence for any complex formation.[133]

The second cross virial coefficients for aromatic (benzene, naphthalene, anthracene)–oxygen and aromatic–argon are essentially the same;[294] since pure argon and pure oxygen have identical *PVT* behaviour, the similarities in the virial coefficients indicate zero ($\pm 0{\cdot}03$ l mol^{-1}) CT equilibrium constants. Similarly, second cross virial coefficients have been determined for O_2–C_2H_4, O_2–C_2F_6, and O_2–buta-1,3-diene mixtures that show essentially no specific interactions between molecular pairs.[295]

It was pointed out in Section IV.D that the intensity of absorption for contact interaction should be directly proportional to solvent fluidity, becoming zero in rigid media in the strict absence of any complex formation since the interacting species will be unable to diffuse together in this extreme case. This behaviour is clearly shown in Fig. 4 for benzene–O_2 and *N*,*N*-dimethylaniline–O_2 in various ethanol–ethylene glycol solutions.[122]

It is perhaps surprising that O_2 does not form definite complexes even with strong electron donors such as triethylamine, *N*,*N*-dimethylaniline, or the anion radicals of tetracyanoquinodimethane ($TCNQ^-$) and tetracyanoethylene ($TCNE^-$). However, the *vertical* electron affinity of O_2 is undoubtedly small and may even be negative.[132] Tsubomura and Mulliken have further pointed out that the increase in size in going from O_2 to O_2^- (the CT state) will be small because of the presence initially of two electrons in the acceptor π 2p orbitals, hence there will be very little overlap between the orbital of the transferred electron in O_2^- with those of donor molecules in contact with the O_2. The strong intensity of the CT band even in the absence of actual complexation comes for the most part through borrowing of intensity from one or more strongly allowed transitions in the donor molecule.[49]

The charge-transfer character of the spectral absorption is clearly shown by its dependence on the donor ionization potential. Since in general band maxima are not obtained owing to overlapping solvent absorption (see Figs. 17 and 18), it is necessary to plot transition energies, either at equal absorbance (e.g. 0·7)[132] on the long wavelength side corrected for oxygen solu-

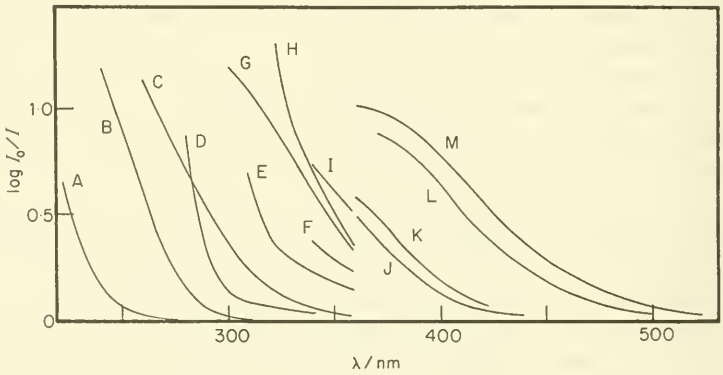

FIG. 17. Absorption bands induced by saturating organic liquids with oxygen: A, ethyl alcohol; B, dioxan; C, n-butylamine; D, benzene; E, mesitylene; F, 1 vol. aniline and 2 vol. ethyl alcohol; G, pyrrole; H, triethylamine; I, aniline; J, *N*,*N*-dimethyl-*o*-toluidine; K, *N*,*N*-dimethyl-2,6-xylidine (the spectrum for this case may be less accurate than the others); L, *N*,*N*-dimethylaniline; M, *N*,*N*-dimethyl-*p*-toluidine. [Reproduced with permission from H. Tsubomura and R. S. Mulliken, *J. Amer. Chem. Soc.*, **82**, 5966 (1960)]

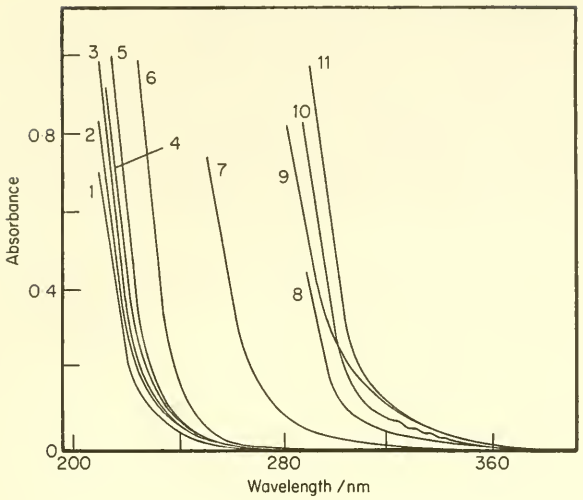

FIG. 18. Ultraviolet absorption spectra (1-cm path length, 1 atm of oxygen) of: (1) 2,2-dimethylbutane; (2) 2-methylpentane; (3) 2,3-dimethylbutane; (4) n-heptane, 2,2,4-trimethylpentane (isooctane) and 2,4-dimethylpentane; (5) 2.3-dimethylpentane; (6) cyclohexane and methylcyclohexane; (7) oct-1-ene; (8) chlorobenzene; (9) cyclohexene and cyclooctene; (10) benzene; (11) cumene and toluene. [Reproduced with permission from J. C. W. Chien, *J. Phys. Chem.*, **69**, 4317 (1965)]

bilities,[134] or at onset of absorption,[132, 296] versus I_D. Although such comparisons will be affected by band profiles and integrated absorption intensities, it is seen in Fig. 19 (equal absorbance = 0·7) and 20 (onset of CT absorption based on $\epsilon_{O_2,\,dissolved} = 10\,l\,mol^{-1}\,cm^{-1}$) that reasonably good linearity is obtained by either technique. It is thus concluded that the additional tailing in ultraviolet spectra observed in oxygen-containing solvents arises from weak, or contact, CT interactions.

In contrast to the tailing or unresolved spectra obtained in liquid solvents, the CT spectrum of an aromatic compound in an O_2 matrix at 10 K[297] or adsorbed with O_2 on to glass or silica gel[126, 297a] often has a clear maximum, as shown in Fig. 21 for O_2 and triethylenediamine adsorbed on to porous Vycor glass at 77 K.[297a] Sometimes two or more distinct maxima are observed. For example, the shoulder at 380 nm for *N*,*N*-dimethylaniline–O_2 in the liquid phase (2,2,4-trimethylpentane solvent)[298] is split into two bands at about 415 and 370 nm in the adsorbed configuration at room temperature.[126]† Cooling to 77 K leads to a slight blue shift and increases

†Somewhat different results from those cited in ref. 126 have been obtained in subsequent work by Professor Tsubomura (personal communication), which may be due to different porous glass substrates.

the intensity of the absorption bands. These results suggest strengthened interaction on cooling (an effect also shown for diethyl ether–O_2),[299] although they might also be due to closer contact between the adsorbed molecules at the lower temperature. Two CCT absorption bands (273 and < 260 nm) are also observed when polystyrene film is exposed to O_2 at high pressure,[300] presumably due to transitions from two molecular orbitals of the polystyrene aromatic groups. The polarized spectrum for

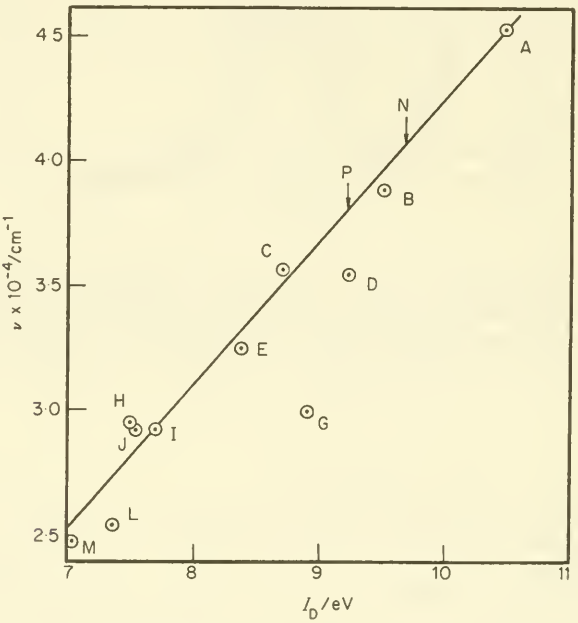

FIG. 19. Relationship between the wavenumbers of oxygen-induced absorption bands and the ionization potentials of organic molecules. The signs for the donors are the same as given in Fig. 17. The arrows in the figure marked with N and P show the ionization potentials of acetone and pyridine, respectively. [Reproduced with permission from H. Tsubomura and R. S. Mulliken *J. Amer. Chem. Soc.*, **82**, 5966 (1960)]

drawn polystyrene–adsorbed O_2 film is stronger for the parallel component than for the perpendicular component, suggesting that the CCT transition moment is perpendicular to the benzene ring.[300] On the other hand, the recent spectral measurements on styrene in an O_2 matrix at 10 K[297] suggest that the 273 nm band comes from residual unpolymerized styrene–O_2. The true polystyrene–O_2 band maximum should be near 230 nm.[301]

In addition to the contact CT absorption, molecular oxygen strongly induces the spin-forbidden singlet–triplet (S_0–T_1) bands of many types of

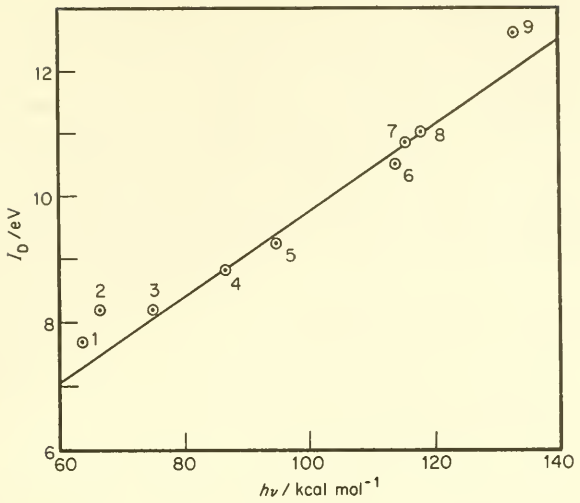

FIG. 20. The dependence of the equivalent energy of the charge-transfer band onset on the ionization energy of the solvent molecule; (1) aniline, (2) pyrrole, (3) anisole, (4) toluene, (5) benzene, (6) ethanol, (7) methanol, (8) cylcohexane, (9) water. [Reproduced with permission from J. Jortner and U. Sokolov, *J. Phys. Chem.*, **65**, 1633 (1961)]

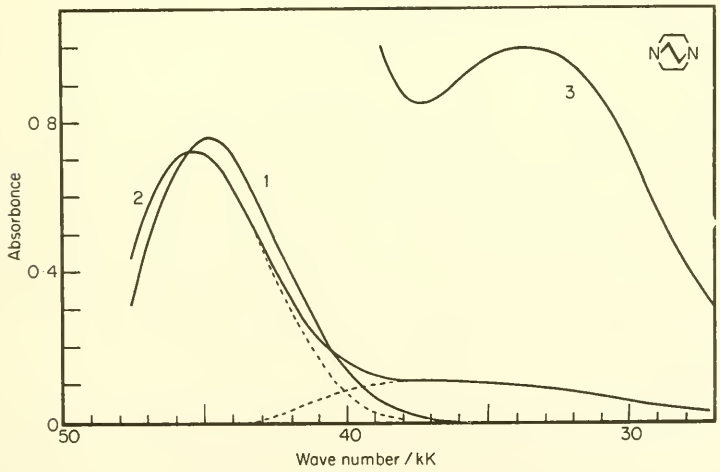

FIG. 21. Ultraviolet absorption spectra of O_2–triethylenediamine. Curve 1: absorption of diamine adsorbed on Vycor glass. Curve 2: same plus O_2 (spectrum can be divided into two bands, one for contact absorption and one for donor absorption). Curve 3: clear CCT band maximum obtained at much higher diamine concentrations. [Reproduced with permission from H. Tsubomura, "Prog. photobiol. Proc. Int. Congr., 6th, 1972", ed. G. O. Schenck, Bochum, Germany (1974)]

organic molecule, ranging from aromatic hydrocarbons to heterocyclics. This singlet–triplet enhancement has been attributed to the paramagnetic character of oxygen,[291] a position supported by the comparable effects in solvent complexes with various paramagnetic ions such as manganous, cobalt, nickel, or ferric, but not with gadolinium or dysprosium.[298] Tsubomura and Mulliken[132] suggested that the main reason for the enhancement of the singlet–triplet solvent bands is a multiplicity mixing and borrowing of intensity by the S_0–T_1 band from the CT band; this is in agreement with the theoretical treatment of these systems by Murrell.[302] In general the induced solvent singlet–triplet bands are well defined and appear at longer wavelengths than the contact CT bands.

It has been suggested that the oxygen–hydrocarbon CCT species is the precursor to thermal autoxidation of hydrocarbons,[303] and absorption in the CCT band leads to photooxidation in a variety of solvent systems. Chien measured the photooxidation rate dependence on O_2 pressure, substrate concentration, and light intensity for several aliphatic, olefinic, and aromatic hydrocarbons.[134] He concluded that a likely initiating step (particularly with methylcyclohexane) is:

$$RH + O_2 \overset{h\nu_{CCT}}{\rightleftharpoons} (RH^+ \cdots O_2^-) \tag{82}$$

by analogy with the primary process in CT excitation of aqueous halide ions.[304] Enhanced singlet–triplet absorption:

$$A + O_2 \xrightarrow{h\nu} {}^3A + {}^1O_2 \tag{83}$$

$$^3A + O_2 \rightarrow \text{peroxide} \tag{84}$$

was considered to be important in photooxidations of the olefins and aromatics. However, Wei and Adelman[305] found the same products and product ratios in the direct photoexcitation of toluene and in the photoexcitation only within the toluene–O_2 CCT band. They thus concluded that photooxidation of toluene proceeds via an excited state of the toluene–O_2 contact and not an excited state of toluene or oxygen, regardless of the mode of photoexcitation.

Kulevsky *et al.* have measured the O_2 CCT photooxidation of cyclohexane.[306] The only products found in greater than trace amounts were cyclohexanone and cyclohexanol, although iodometric titrations did indicate peroxide formation. In addition to reaction (82) they suggested a free-radical mechanism involving a second independent photochemical process:

$$(RH^+ \cdots O_2^-) \rightarrow R\cdot + HO_2\cdot \tag{85}$$

$$R\cdot + HO_2\cdot \rightarrow RO_2H \xrightarrow{h\nu} RO\cdot + HO\cdot \tag{86}$$

rather than a concerted insertion of O_2 into the CH bond:[307]

$$RH + O_2 \xrightarrow{h\nu_{CCT}} [R{-}H \cdots O_2]^* \rightarrow RO_2H. \quad (87)$$

Furthermore, by comparing relative rates of photooxidation of cyclohexane and cyclopentane (varying ring size) and relative reactivities of primary, secondary, and tertiary carbons in acyclic hydrocarbons, it was determined that C—H bonds, rather than C—C bonds, are the donor site in the CCT absorption.[308] These results indicate that some differential stability must exist in the charge-transfer precursors, although undoubtedly it is below the operational criterion for contacts.

Photolysis in the O_2–ethanol CCT band ($\lambda > 220$ nm) produces acetaldehyde, acetic acid, formaldehyde and hydrogen peroxide; the decomposition quantum yield at 254 nm is 0·43.[309] Similarly, absorption in the CCT band of O_2 in acyclic or cyclic ethers leads to photochemical oxidations, major products in all cases being the appropriate ester or lactone and peroxides.[310, 311] The initial step again is suggested to be photoexcitation in the CT band to form the intermediate 1-ethoxyethyl hydroperoxide:

$$CH_3CH_2OCH_2CH_3 + O_2 \rightleftharpoons CH_3CH_2\overset{\displaystyle O_2}{\overset{\vdots}{O}}CH_2CH_3 \xrightarrow{h\nu} CH_3CH_2\overset{\displaystyle O\ldots O^-}{\overset{\vdots}{\overset{+}{O}}}CH_2CH_3 \quad (88)$$

$$CH_3CH_2\overset{\displaystyle O{-}O^-}{\overset{\vdots}{\overset{+}{O}}}CH_2CH_3 \rightarrow CH_3CH_2\overset{\displaystyle O{-}OH}{\overset{|}{\overset{+}{O}}}CHCH_3 \rightarrow CH_3CH_2O\overset{\displaystyle O{-}OH}{\overset{|}{C}}HCH_3. \quad (89)$$

On the other hand, studies carried out at -30°C (which increases the O_2 concentration and reduces chain reactions) indicate radical cation formation as precursor to the photolysis products:[299]

$$CH_3CH_2\overset{\displaystyle O_2}{\overset{\vdots}{O}}CH_2CH_3 \xrightarrow{h\nu} CH_3CH_2\overset{+}{\overset{\cdot}{O}}CH_2CH_3 + O_2^-. \quad (90)$$

Irradiation in the CCT band of O_2–diethyl ether at 77 K leads to an esr signal for ethyl (or possibly methyl) radicals.[312] Upon warming, these radicals become mobile and either react with O_2 to produce the peroxy radical or abstract hydrogen atoms from ether. The major products are ethyl acetate ($\Phi = 0{\cdot}49$), ethanol and/or methanol ($\Phi = 0{\cdot}43$), ethyl formate ($\Phi = 0{\cdot}23$), and acetaldehyde ($\Phi = 0{\cdot}17$). The ethyl (methyl) radicals are produced by further photoexcitation of the excited CT state. Irradiation in the O_2–triethylamine CCT band at 77 K (n-heptane, acetonitrile, or 1:1 n-propyl–isopropyl alcohol solvent) also produced an esr signal attributable to the methyl radical, which disappeared on warming (i.e. matrix softening)

SUMMARY TABLE C. Molecular oxygen acceptor

Donor	Medium[x]	T^a/°C	λ_{max} /nm	λ_{onset} /nm	ϵ_{max} /l mol^{-1} cm^{-1}	K_c /l mol^{-1}	$-\Delta H^0$ /kcal mol^{-1}	Other data	Refs.
2,2-Dimethylbutane				214[b]					134
2-Methylpentane				211[c]					134
3-Methylpentane									308
2,3-Dimethylbutane				214[c]					134
n-Heptane				221[b]					134, 290
2,2,4-Trimethylpentane				220[b]					134
2,4-Dimethylpentane				223[b]					134
2,3-Dimethylpentane				220[c]					134
n-Hexane									290. 308
(+)-3-Methylhexane									306
Cyclohexane				233[b]					134, 306
		30		225[i]					290
Methylcyclohexane				230[c]					134
Cyclopentane									308
cis-Decalin									307
trans-Decalin									307
Ethylene	argon	−186		205[e]					319
Oct-1-ene				252[c]					134
Cyclohexene				285[c]					134
Cyclooctene				285[c]					134
Benzene				282[f]	>96[h]				132
				285[b]					122, 134, 288
		25		301[j]					133
	$CHCl_3$			358[k]					296
	CCl_4		⩽221·5						320
	vapour		219						321
	vapour								320
	matrix	−263	235						297
Toluene				300[b]					134, 288, 318

				350	305
	matrix	−263	246		297
Xylene				310[b]	134
Mesitylene				320[b]	134
				308[f]	132
Hexamethylbenzene	$CHCl_3$			420[k]	296
Ethylbenzene	$CHCl_3$				296
Cumene				293[b]	134
Styrene					288
	matrix	−263	268, 228		297
Indene			360		303
	matrix	−263	270, 230		297
Polystyrene	film		273, <260		300
Chlorobenzene				290[d]	134, 288
Bromobenzene					288
m-Cresol					288
Anisole					288
Biphenyl	$(CHCl_2)_2$				288
	$CHCl_3$				296
Naphthalene	$CHCl_3$			488[k]	296
	$CHCl_3$		345		322
	$(CHCl_2)_2$				288
	adsorbed[m]		370		126
2-Methylnaphthalene	$CHCl_3$				296
2,3-Dimethyl-naphthalene	$CHCl_3$			491[k]	296
Anthracene	$CHCl_3$			710[k]	296
	$CHCl_3$		440		323
Chrysene	$CHCl_3$			564[k]	296
Pyrene	$CHCl_3$			619[k]	296
Triphenylene	$CHCl_3$			508[k]	296
1,2:5,6-Dibenz-anthracene	$CHCl_3$			537[k]	296
3,4-Benzopyrene	$CHCl_3$			677[k]	296
1,2:7,8-Dibenz-anthracene	$CHCl_3$			574[k]	296

Summary Table C—*continued*

Donor	Medium[x]	T^a/°C	λ_{max} /nm	λ_{onset} /nm	ϵ_{max} /l mol^{-1} cm^{-1}	K_c /l mol^{-1}	$-\Delta H^\circ$ /kcal mol^{-1}	Other data	Refs.
1,2:3,4-Dibenz-anthracene	$CHCl_3$								296
1,2:4,5-Dibenzopyrene	$CHCl_3$			681[k]					296
Stilbene	$CHCl_3$								296
Fluorene	$CHCl_3$								296
Fluoranthene	$CHCl_3$								296
o-Terphenyl	$CHCl_3$								296
p-Terphenyl	$CHCl_3$								296
20-Methylcholanthrene	$CHCl_3$			580[k]					296
Methylamine	$CHCl_3$			375[k]					296
Trimethylamine	$CHCl_3$								296
Ethylamine	$CHCl_3$			405[k]					296
Diethylamine	$CHCl_3$			455[k]					296
Triethylamine	$CHCl_3$			488[k]					296
				340[f]					132
	n-heptane		290		1 550	0·05–0·08			313
n-Butylamine	$CHCl_3$			400[k]					296
				280[f]					132
t-Butylamine	$CHCl_3$			405[k]					296
N,*N*-dimethyl-p-phenylenediamine	adsorbed[m]		769, 625, 429						126
p-Phenylenediamine	cyclohexane		250, 310						312
Aniline				340[f]	>164[h]				132
									288
	$CHCl_3$								296
N-Methylaniline	adsorbed[m]		391, 350						126
N,*N*-Dimethylaniline	$CHCl_3$			500[k]					296
				393[f]					132, 288
	ethanol–ethylene glycol			340[p]					122

	2,2,4-trimethyl-pentane			380[q]		298
	adsorbed[m]		413, 369			126
N,*N*-Diethylaniline	adsorbed[m]		521[n], 452[n]			126
Pyrrole				333[f]		132, 288
Indole	$CHCl_3$					296
N,*N*-Dimethyl-*o*-toluidine				340[f]		132
N,*N*-Dimethyl-*m*-toluidine	adsorbed[m]		420, 375			126
N,*N*-Dimethyl-*p*-toluidine				404[f]		132
	adsorbed[m]		488, 424			126
N,*N*-Dimethyl-2,6-xylidine				367[q]		132
Formamide	$CHCl_3$			345[k]		296
Dimethylformamide	$CHCl_3$			380[k]		296
Dimethylacetamide	$CHCl_3$			393[k]		296
2-Fluorenylacetamide	$CHCl_3$					296
Quinoline	n-butanol					288
	$CHCl_3$			520[k]		296
Pyridine	$CHCl_3$			477[k]		296
Acridine	$CHCl_3$			663[k]		296
Methanol						290
		25		248[j]		133
Ethanol		−[a]		221[f]	>76[h]	132
				230[b]		134
		25		251[j]		133
Acetone	$CHCl_3$					296
o-Aminobenzoic acid	$CHCl_3$					296
Tetrahydropyran						311
Tetrahydrofuran				245[b]		134, 311
	$CHCl_3$					296
Diethyl ether			210			310
		28	215			299

Summary Table C—*continued*

Donor	Medium[x]	T^a /°C	λ_{max} /nm	λ_{onset} /nm	ϵ_{max} /l mol^{-1} cm^{-1}	K_c /l mol^{-1}	$-\Delta H^0$ /kcal mol^{-1}	Other data	Refs.
				265[b]					134, 290
Dioxan		–[a]		257[f]					132
Di-n-propyl ether									311
Diisopropyl ether									311
Di-n-butyl ether									311
Propylene oxide									311
Trimethylene oxide									311
Acetonitrile		25		<228[j]					133
Dialkyl sulphides				320[b]					134
Water		25		215[j]					133
		25		250[r]					324
Thiophen									325
Imipramine	$CHCl_3$								296
Reserpine	$CHCl_3$								296
Chloroquine	$CHCl_3$			545[k]					296
Phenothiazine	$CHCl_3$								296
Caffeine	$CHCl_3$								296
Tetramethyluric acid	$CHCl_3$								296
Alanine	water								296
Proline	water								296
Glycine	water								296
Tryptophan	water								296
$TCNE^{-v}$	adsorbed[s]	–196	~500						326
$TCNQ^{-w}$	adsorbed[s]	–196	~500						326
I^-	water	24	264			<0·3	1·2	$K\epsilon$ 871^2 mol^{-2} cm^{-1}	327
	ethanol	24	285[q]				0·0	$K\epsilon$ 391^2 mol^{-2} cm^{-1}	327
	ethylene glycol	24	286				–0·7	$K\epsilon$ 2071^2 mol^{-2} cm^{-1}	327

	chloroform	24	287			$K\epsilon$ $43\,l^2\,mol^{-2}\,cm^{-1}$	327
	acetonitrile	24	286			$K\epsilon$ $42\,l^2\,mol^{-2}\,cm^{-1}$	327
n-Decane		30		210[f]	−0·4		328
TMAE[y]	n-decane	30	450		−1·2		328
Dimethyl sulphoxide			273				329
Tetralin			310[u]				303
Cumene			~280				293
p-Cymene			~290				293
TMAE[y]	adsorbed[s]	−196	~460				297a
TMBI[z]	adsorbed[s]	−196	~460				297a
Triethylenediamine	adsorbed[s]	−196	297				297a
Benzene	adsorbed[s]	−196	227				297a
	adsorbed[aa]	−196		280			329a
Naphthalene	adsorbed[aa]	−196		350			329a
Anthracene	adsorbed[aa]	−196		445			329a

[a] If temperature not specified, it is assumed to be room temperature. [b] From Fig. 5 of Ref. 134. [c] From Fig. 2 of Ref. 134; P_{O_2} = 1 atm, 1 cm optical path-length, absorbance 0·7. [d] From Fig. 2 of Ref. 134; P_{O_2} = 1 atm, 1 cm optical path-length, absorbance 0·4. [e] From Fig. 1 of Ref. 319; $\epsilon = 1\,l\,mol^{-1}\,cm^{-1}$. [f] From Fig. 2 of Ref. 132; P_{O_2} = 1 atm, 1 cm optical path-length, absorbance 0·7. [g] From Fig. 1 of Ref. 132: P_{O_2} = 1 atm, 1 cm optical path-length, absorbance 0·5. [h] These values, based on the concentration of dissolved oxygen in solution and taken at absorbance ≈ 0·7 (1 cm cell), represent lower limits for ϵ_{max}. [i] From Fig. 1 of Ref. 290; P_{O_2} = 0·84 atm, 1 cm optical path-length, absorbance 0·7. [j] $\epsilon_{O_2,\,dissolved} = 10\,l\,mol^{-1}\,cm^{-1}$. [k] From Fig. 1, Ref. 296; P_{O_2} = 120 atm. [l] Film thickness 0·0023 mm, P_{O_2} = 59 atm. [m] Porous glass (surface area ≈ 271 $m^2\,g^{-1}$) or silica gel; P_{O_2} = 200 mm. [n] Slightly blue shifted on cooling to −196°C. [p] Estimated from Fig. 2. Ref. 122. [q] Shoulder. [r] Absorbance 0·01; P_{O_2} = 1 atm. [s] Porous Vycor glass. [t] From Fig. 2 of Ref. 328; P_{O_2} = 1 atm, absorbance 0·7. [u] Shoulder at ~315 nm. [v] Anion radical of tetracyanoethylene. [w] Anion radical of tetracyanoquinodimethane. [x] If medium is not specified, it is the liquid donor. [y] Tetrakis(dimethylamino)ethylene. [z] 1,1′,3,3′-Tetramethyl-$\Delta^{2,2'}$-bi(imidazolidine). [aa] Porous Vycor glass immersed in liquid O_2.

to the peroxy radical signal.[313] On the other hand, the peroxy radical esr signal appears on CCT irradiation of the O_2–triethylamine band in decalin or methylcyclohexane solution,[313] or the O_2–*p*-phenylenediamine band in cyclohexane,[312] at 77 K because the methyl radical is more mobile in these solvents than in the others given above and therefore unstable relative to interaction with O_2. In all cases, however, it is apparent that the initial act of absorption in the contact CT band is formation of the almost purely ionic pair corresponding to the CT excited state.

Molecular oxygen is an extremely efficient energy-transfer quencher of fluorescence (excited singlet state) and phosphorescence (triplet state), the former essentially diffusion-controlled and the latter at approximately one-ninth the diffusion-controlled rate for aromatic hydrocarbons, provided that the energy gap between the aromatic triplet and the low-lying oxygen singlet ($^1\Delta_g$) states is not large.[314] In either case an excited state association (i.e. a transient exciplex) is considered between the electronically excited aromatic molecule and oxygen:

$$^1M^* + {}^3O_2 \rightarrow {}^3(M \cdot O_2)^* \tag{91}$$

$$^3M^* + {}^3O_2 \rightarrow {}^1(M \cdot O_2)^*. \tag{92}$$

Brewer has shown[315] that O_2 fluorescence quenching rates for alkyl- and fluoro-benzenes are inversely dependent on the ionization potentials of the aromatic molecules, indicating a charge-transfer intermediate state at least for the singlet-state quenching. Lifetimes of the intermediate complexes involved in singlet or triplet quenching are apparently very short ($< 2 \times 10^{-10}$ s).[316]

An interesting type of static fluorescence quenching involving only very weak complexation or contact in the ground state is possible,[317] and this has been observed in the toluene–oxygen system.[318] This is due to excitation of the donor–acceptor pair in its CCT band and hence photoselection in competition with direct photoexcitation of the donor to its fluorescence state, and manifests itself in an unusual fluorescence-quenching wavelength dependence. For example, excitation of the toluene–O_2 system at 280 nm leads to substantially greater quenching than with excitation close to the toluene absorption maximum at 254 nm.[318]

IX. HIGHEST VALENCY HALIDES, OXIDES AND OXYHALIDE ACCEPTORS

Coloured solutions between organic molecules and highest valency group IV, V and VI metal halides, oxides and oxyhalides have been well known for

many years with a very extensive literature. For example, colourless tungsten hexafluoride gives deep red solutions in clear organic solvents such as benzene, toluene, acetone and cyclohexanone.[330] In general the oxygen- or nitrogen-containing *n*-donor organic compounds combine strongly with the evolution of heat to form 1:1, 1:2 and higher relatively stable complexes with these acceptors.[331] The strength of these complexes for the most part is well beyond the limits suggested in Section IV for contact charge-transfer interactions.

On the other hand, interactions with π-donor aromatic hydrocarbons or fluorocarbons appear to be very weak and to fall into the contact charge-transfer category. A concentration-spectral study of tungsten hexafluoride in benzene showed a 1:1 complex ratio.[330] In addition, it was shown that the mixture becomes colourless on freezing but regains its colour on warming ("phase-change chromism"), characteristic of contact charge-transfer behaviour in the liquid state.[124] Using essentially the Benesi–Hildebrand treatment, Tsubomura showed that the interaction between stannic chloride and naphthalene or benzene is very weak.[332] He also reported a direct relationship between absorbing wavelength and decrease in ionization energy for several aromatic and oxygen-containing donors and attributed the spectral absorption to weak charge-transfer.[332] Similar dependence on ionization potential was shown for the spectra of aromatic molecules with $TiCl_4$, $TiBr_4$ and $VOCl_3$,[333] again supporting the charge-transfer nature of the interaction. The Benesi–Hildebrand treatment of the spectral behaviour of $TiCl_4$ with several aromatic hydrocarbons also showed very weak interactions leading to essentially zero or small ($< 0{\cdot}1$ l mol^{-1}) formation constants.[334]

The continuous variation method[335] has frequently been used to establish the stoichiometry of the interaction, as for example stannic chloride and mesitylene in dichloromethane solvent shown in Fig. 22.[336] Neither stannic chloride nor mesitylene alone absorbs at the analysing wavelengths of 320 and 340 nm. At each wavelength the mixture absorbance passes through a maximum at 0·5 mole-fraction $SnCl_4$ (relative to mesitylene, neglecting the solvent), indicative of predominant 1:1 interaction. The absorbance decreases parabolically at lower and higher mole-fractions with the maximum being symmetric and well-rounded showing very little association. This behaviour appears to be generally followed by the systems covered in this section.

Hammond and coworkers have carried out the most detailed studies of charge-transfer interactions between aromatic hydrocarbons and fluorocarbons with highest oxidation state Group IV,[123] VA,[337] VB,[338] VIA[339] and VIB[340] metal halides, oxides and oxyhalides. Common to each system is the appearance of an intermolecular charge-transfer absorption band, although in most cases overlapping strong acceptor and/or donor bands

prevent determination of the new absorption band maximum. Formation constants and molar absorption (extinction) coefficients were determined by the dilution technique using modifications of the Benesi–Hildebrand equation[341] (see Section III.A.1), and the continuous variation technique established 1:1 interaction in all cases in which this procedure was followed. Spectral and thermodynamic results of these studies, with selected data from earlier investigations, are given in Summary Table D.

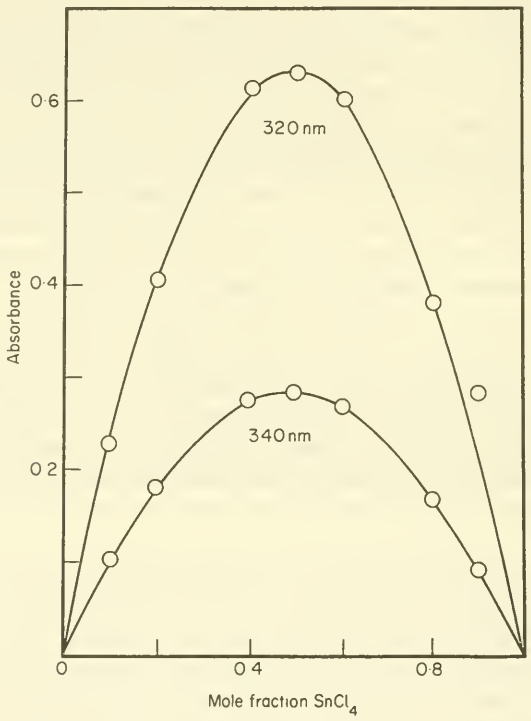

FIG. 22. Absorbance of solutions of stannic chloride and mesitylene in dichloromethane at 25°C. Mole-fraction of stannic chloride refers to the stannic chloride–mesitylene mixture, neglecting the solvent. [Reproduced with permission from J. J. Myher and K. E. Russell, *Can. J. Chem.*, **42**, 1555 (1964)]

Formation constants and heats of formation vary considerably among different sets of data. Thus, for the hexamethylbenzene–stannic chloride interaction (cyclohexane solvent), Burkardt *et al.*[123] report average values for K_c and ΔH^0 of 0·21 l mol^{-1} and $-0{\cdot}31$ kcal mol^{-1}, respectively, Hatano and Ito[342] found $K_c = 1{\cdot}68$ l mol^{-1} and $\Delta H^0 = -2{\cdot}8$ kcal mol^{-1} for the same solvent system, and Myher and Russell[336] estimated $\Delta H^0 = 0{\cdot}2$ kcal

mol^{-1} (dichloromethane solvent). Similar variations are reported for the CCl_4–hexamethylbenzene interactions.[123,342] Reasons for these discrepancies are not clear. However, the spectral measurements and use of the Benesi–Hildebrand equation are strongly sensitive to impurities, moisture, and stability of the mixtures. Furthermore, the formation constants appear to vary significantly with wavelength. This behaviour is observed in other cases as well;[3e] it has been attributed to the presence of ternary or higher complexes with different absorption bands,[17] although continuous-variation plots over wide concentration ranges fail to indicate other than 1:1 interactions for the systems included here. Although the two measurements of K_c for the $SnCl_4$–hexamethylbenzene interaction given above are reported for different wavelengths,[123,342] the measuring wavelengths are nevertheless quite close and it is doubtful if the wavelength difference in determination of K_c can account for the large discrepancy.

For most of the systems reported by Hammond and coworkers,[135] formation constants are generally very small—typically well below 0·5 $l\,mol^{-1}$ and often zero or even negative. Enthalpies of formation also are generally small and are found to be both negative and positive. Results for a typical aromatic donor–highest valency halide acceptor system, benzene–tungsten hexafluoride, are summarized in Table X. It is seen that not only is K_c (and hence ϵ) very sensitive to the wavelength of measurement, it is also very dependent on the solvent used in the dilutions. As Hammond has emphasized, a "conspiracy" of experimental errors obscures the individual K_c and ϵ values, and the negative values for these quantities are of course physically meaningless. In view of these factors plus uncertain solvent effects and component purities, it is obvious that the thermodynamic K and ΔH quantities given in Summary Table D are too small to imply any specific complex formation

The lack of complexation is perhaps surprising in view of the high electron affinities to be expected for the acceptor molecules, particularly where many electronegative atoms are attached to a central atom.[343] Hatano and Ito have carried out extended Hückel molecular-orbital calculations on Group IV tetrahalides.[342] These halides form stable 1:2 complexes with *n*-donors such as aromatic aldehydes. Although the free molecule is tetrahedrally shaped, the 1:2 complex has six-fold coordination leading to octahedral geometry with either *cis* or *trans* configuration.[344] Thus, charge transfer is directed to the electron core of the central metal atom leading to formation of sp^3d^2 (octahedral) hybrid orbitals and strong complexation. On the other hand, crystallographic data show that π-donating planar aromatic molecules transfer charge to the halogen atom and the tetrahedral shape of the metal tetrahalide is retained,[345] leading to "ball-plane" interaction. The lowest vacant d atomic orbital on the halogen atom is a logical acceptor orbital.[346]

TABLE X. Equilibria and spectral data for benzene–tungsten hexafluoride interactions at 26°C[339]

Solvent	λ/nm	$K_c \pm \sigma$/l mol^{-1}	ϵ^a/l mol^{-1} cm^{-1}	ϵ^b/l mol^{-1} cm^{-1}	f
Carbon tetrachloride	380	0·17 ± 0·03	330	640	0·029
	390	0·11 ± 0·03	480	620	(for $\lambda > 275$ nm)
	400	0·04 ± 0·03	1 300	580	
	410	0·07 ± 0·03	670	540	
$\lambda_{max} \approx 380$ nm; $\Delta H^0 = -0{\cdot}15$ kcal mol^{-1}					
Cyclohexane	410	−0·10 ± 0·03	−500		0·029
	420	−0·09 ± 0·04	−460		(for $\lambda > 275$ nm)
	430	−0·09 ± 0·05	−400		
Perfluoroalkane	400	0·00 ± 0·03	−3 700	580	0·07
	410	0·00 ± 0·03	−3 400	540	(for $\lambda > 275$ nm)
	420	−0·06 ± 0·04	−380	490	
$\lambda_{max} \approx 350$ nm; $\Delta H^0 = -0{\cdot}05$ kcal mol^{-1}					

[a] From dilution technique using modified Benesi–Hildebrand equation. [b] Assumes concentration of complex is the same as that of the minor component.

However, extended Hückel calculations of Hatano and Ito[342] suggest that higher vacant d-orbitals ($3d_{z^2}$ and $3d_{yz}$ for chlorides, $4d_{z^2}$ for bromides) are involved in charge transfer for the non-transition element tetrahalides, while the acceptor orbitals in the Group IV transition element halides are the lowest vacant molecular orbitals that do not necessarily involve empty atomic d-orbitals on the halogen atoms. Overlap between aromatic π-donor orbitals and these acceptor orbitals is geometrically highly unfavourable, hence the overlap integrals are very small for these ball-plane configurations leading to very weak or predominantly contact charge-transfer associations in spite of the very large acceptor electron affinities. Weak chemical bonding may result if the acceptor deviates from the ball-plane configuration; examples of this have been cited by Hammond.[135] Another contributing factor to the lack of complexation is the loss in symmetry and hence less loss in entropy when highly symmetric donors (e.g. benzene; symmetry number $\sigma = 12$) and acceptors ($\sigma = 12$ for $SnCl_4$) are complexed.[135, 347]

During the final stages of preparation of this chapter, a paper appeared reporting contact CT transitions for several Group VI metal fluorides with xenon.[348] Onset wavelengths are given at the end of Summary Table D; as with most of the extensive ball-plane interactions involving these metal fluorides, overlap of acceptor absorption prevented determination of λ_{max}. Stabilization energy for $IrF_6 \cdot Xe$ is very weak, 0·07 kcal mol^{-1}, even though the results confirmed the high electron affinities of the metal fluorides.[348] Although the intermolecular CT spectra are reported at 77 K in crystalline xenon, the purple colour of $IrF_6 \cdot Xe$ remains at the melting point of xenon (161 K) but is not present in the room-temperature vapour mixture of IrF_6 and Xe.[348]

X. SUBSTITUTED METHANE ACCEPTORS

The substituted methanes in Summary Table E contain halogen and nitro group substituents. Data on the aromatic hydrocarbon–CX_4 systems are included, although they also are examples of the ball-plane type interactions (Summary Table D).

Carbon tetrachloride, chloroform and dichloromethane are among the halocarbons commonly used as solvents. While chloroform and dichloromethane are known to interact through hydrogen bonding with σ- and π-donors,[127a] carbon tetrachloride often has been considered "inert". Yet, in some cases, the interaction of σ- and π-donors is found[98, 353] to be in the sequence $CCl_4 > CHCl_3 > CH_2Cl_2$.

Quite often, on mixing the donor and acceptor, an enhanced absorbance is observed in the ultraviolet region, but no band maximum. The effects

SUMMARY TABLE D. Highest valency halides, oxides and oxyhalide acceptors

Donor	Acceptor	Medium[f]	T^a /°C	λ_{max} /nm	λ_{onset} /nm	ϵ_{max} /l mol^{-1} cm^{-1}	K_c /l mol^{-1}	$-\Delta H^0$ /kcal mol^{-1}	Other data	Ref.
Benzene	$TiBr_4$	cyclohexane		370						333
Hexamethylbenzene	$TiBr_4$	cyclohexane		540						342
Naphthalene	$TiBr_4$	cyclohexane		469						333
Anthracene	$TiBr_4$	cyclohexane		437, 606						333
Phenanthrene	$TiBr_4$	cyclohexane		469						333
Chrysene	$TiBr_4$			541						333
Pyrene	$TiBr_4$	cyclohexane		595						333
Perylene	$TiBr_4$	cyclohexane		521, 704						333
Benzene	$TiCl_4$			360[b]		2 000[c]				123
	$TiCl_4$	cyclohexane		336						333
	$TiCl_4$	heptane	25	334		5 300[e]	0·04[d] ± 0·02			334
Toluene	$TiCl_4$	heptane	25	328						334
ααα-Trifluorotoluene	$TiCl_4$	heptane	25	313						334
p-Xylene	$TiCl_4$	heptane	25	335						334
m-Xylene	$TiCl_4$									123
Mesitylene	$TiCl_4$	heptane	25	330						334
	$TiCl_4$	cyclohexane		425[b]						123
Hexamethylbenzene	$TiCl_4$	cyclohexane	26	510[b]			0·41[d] ± 0·08			123
	$TiCl_4$	cyclohexane		510				1·8		342
Naphthalene	$TiCl_4$	cyclohexane	26	450		940[c]	0·15[d] ± 0·11			123
	$TiCl_4$	CCl_4	26				0·22[d] ± 0·08	0·18		123
	$TiCl_4$			388, 476						333
Phenenthrene	$TiCl_4$									123
	$TiCl_4$			455						333
Triphenylene	$TiCl_4$									123
Anthracene	$TiCl_4$			600		1 200				123
	$TiCl_4$	cyclohexane	26	576		1120[c]	0·05[d] ± 0·02			123
	$TiCl_4$	CCl_4	26	573		1120[c]	0·13[d] ± 0·05	0·28		123
Pyrene	$TiCl_4$									123
Anthracene	$TiCl_4$			400, 600						333
Chrysene	$TiCl_4$			370, 521						333

Pyrene	$TiCl_4$			426, 581						333
Perylene	$TiCl_4$			476, 690						333
Diethyl ether	$TiCl_4$	hexane	25	333			0·021[g]			334
Anisole	$TiCl_4$	hexane	25	330			0·007[g]			334
Diphenyl ether	$TiCl_4$	hexane	25	330						334
Hexamethylbenzene	$SnBr_4$	cyclohexane		370						342
Benzene	$SnCl_4$			275		3 500[c]				123
	$SnCl_4$				365[h]					332
	$SnCl_4$	dichloromethane	25					−1·2	—[i]	336
Toluene	$SnCl_4$	dichloromethane	25						—[i]	336
Mesitylene	$SnCl_4$	dichloromethane	25						—[i]	336
	$SnCl_4$	cyclohexane	24·5	300		1 000	0·43			342
Hexamethylbenzene	$SnCl_4$	dichloromethane	25					0·2	—[i]	336
	$SnCl_4$	cyclohexane		339			1·68	2·8		342
	$SnCl_4$	cyclohexane	26	340			0·21[d] ± 0·06	0·31		123
Naphthalene	$SnCl_4$	cyclohexane	18		405[j]		0·06			332
	$SnCl_4$	cyclohexane	26		400		0·15 ± 0·09	0		123
Anthracene	$SnCl_4$	cyclohexane	26		481		0·05 ± 0·08	0·26		123
Durene	$SnCl_4$	cyclohexane								123
Benzene	$PbCl_4$	CCl_4	26		485[j]		0·03[d] ± 0·04			123
Hexafluorobenzene	$PbCl_4$									123
Mesitylene	$PbCl_4$	CCl_4								123
Toluene	$PbCl_4$	CCl_4			510[j]					123
	$PbCl_4$									123
o-Xylene	$PbCl_4$	CCl_4								123
m-Xylene	$PbCl_4$	CCl_4		430						123
p-Xylene	$PbCl_4$	CCl_4								123
Naphthalene	$PbCl_4$	CCl_4								123
Octafluoro-naphthalene	$PbCl_4$									123
Anthracene	$PbCl_4$	CCl_4								123
Hexamethylbenzene	$GeBr_4$	cyclohexane		342						342
Naphthalene	$GeCl_4$									123
Hexamethylbenzene	$SiBr_4$	cyclohexane		250						342
	VCl_4	cyclohexane		550						342

Summary Table D—*continued*

Donor	Acceptor	Medium[f]	T^a /°C	λ_{max} /nm	λ_{onset} /nm	ϵ_{max} /l mol^{-1} cm^{-1}	K_c /l mol^{-1}	$-\Delta H^0$ /kcal mol^{-1}	Other data	Ref
Benzene	$VOCl_3$	cyclohexane	26		595		$-0{\cdot}01^d \pm 0{\cdot}08$	0·3		337
	$VOCl_3$	CCl_4	26		595		$-0{\cdot}06^d \pm 0{\cdot}08$	0·14		337
	$VOCl_3$			450						337
	$VOCl_3$	cyclohexane		420						333
	$VOCl_3$			430						349
Bromobenzene	$VOCl_3$			465						349
Chlorobenzene	$VOCl_3$			450						349
	$VOCl_3$									337
p-Dichlorobenzene	$VOCl_3$									337
Toluene	$VOCl_3$			470						349
p-Xylene	$VOCl_3$			490						349
Mesitylene	$VOCl_3$			515						349
Naphthalene	$VOCl_3$			570						349
	$VOCl_3$			625						333
	$VOCl_3$	cyclohexane	26	595			$0{\cdot}26^d \pm 0{\cdot}03$	1·7		337
Octafluoro-naphthalene	$VOCl_3$	CCl_4	26		650		$0 \pm 0{\cdot}08$			337
Anthracene	$VOCl_3$	cyclohexane		820						333
Phenanthrene	$VOCl_3$			617						333
	$VOCl_3$			570						349
Chrysene	$VOCl_3$			690						333
Pyrene	$VOCl_3$	cyclohexane		523, 800						333
Perylene	$VOCl_3$	cyclohexane		490, 658, 1 250						333
Camphor	$VOCl_3$			420						349
Acridine	$VOCl_3$			490						349
Octafluorotoluene	VF_5	C_7F_{13}	26							337
Me_4Si	NbF_5			230, 264[b]		—[k]				350
Me_4Ge	NbF_5			233		—[k]				350
Me_4Sn	NbF_5			275		—[k]				350
Benzene	$NbCl_5$			400		8 500[c]				337

	$NbCl_5$	cyclohexane	26		570[h]		$-0{\cdot}12^d \pm 0{\cdot}02$	2·4	337
	$NbCl_5$	CCl_4	26		590		$-0{\cdot}10^d \pm 0{\cdot}02$	2·1	337
Mesitylene	$NbCl_5$			490		4 140[c]			337
	$NbCl_5$	cyclohexane	26				$0{\cdot}12^d \pm 0$		337
	$NbCl_5$	CCl_4	26		682		$-0{\cdot}11^d \pm 0{\cdot}03$	1·2	337
Hexamethylbenzene	$NbCl_5$	CCl_4							337
Napthalene	$NbCl_5$	cyclohexane	26	530[b]			$0{\cdot}14^d \pm 0{\cdot}01$		337
Benzene	$TaCl_5$			340[b]					337
	$TaCl_5$	cyclohexane	26				$-0{\cdot}06 \pm 0{\cdot}06$	2·5	337
	$TaCl_5$	CCl_4	26		470[j]		$-0{\cdot}10^d \pm 0{\cdot}03$	1·1	337
Hexamethylbenzene	$TaCl_5$								337
Naphthalene	$TaCl_5$								337
Octafluoro-naphthalene	$TaCl_5$	CCl_4	26		500[j]		$0{\cdot}15^d \pm 0{\cdot}03$		337
Benzene	PCl_5			280		3 000[c]			338
Hexamethylbenzene	PCl_5	CCl_4							338
Naphthalene	PCl_5	CH_2Cl_2	26				$0{\cdot}10^d \pm 0{\cdot}09$	0·11	338
	PCl_5	CCl_4	26		455[h]		$0{\cdot}15^d \pm 0{\cdot}08$	0·07	338
Anthracene	PCl_5	CCl_4							338
Pyrene	PCl_5	CCl_4							338
Hexamethylbenzene	$POCl_3$	cyclohexane	26				$0{\cdot}03^d \pm 0{\cdot}05$	−0·59	338
Naphthalene	$POCl_3$				330				338
Pyrene	$POCl_3$				400				338
Anthracene	$POCl_3$				400				338
Hexamethylbenzene	$POCl_3$				330				338
Benzene	$SbCl_5$								338
	$SbCl_5$	cyclohexane	26				$0{\cdot}03^d \pm 0{\cdot}07$		338
	$SbCl_5$	CCl_4	26		500[h]		$-0{\cdot}08^d \pm 0{\cdot}02$		338
Hexafluorobenzene	$SbCl_5$								338
Mesitylene	$SbCl_5$								338
Octafluoro-naphthalene	$SbCl_5$			450		350[c]			338
	$SbCl_5$	CCl_4	26		550[h]		$0{\cdot}13^d \pm 0{\cdot}03$	−0·11	338
Benzene	CrO_2Cl_2	C_7F_{13}			830[j]				339
	CrO_2Cl_2	CCl_4							339
Octafluoro-naphthalene	CrO_2Cl_2	CCl_4							339

Summary Table D—*continued*

Donor	Acceptor	Medium[f]	T^a /°C	λ_{max} /nm	λ_{onset} /nm	ϵ_{max} /l mol^{-1} cm^{-1}	K_c /l mol^{-1}	$-\Delta H^0$ /kcal mol^{-1}	Other data	Ref
n-Hexane	WF_6	C_7F_{13}	26	240[b]			0·61[d] ± 0·06			351
	WF_6	CCl_4	26				0·18[d] ± 0·02			351
Cyclohexane	WF_6	C_7F_{13}	26	250			0·34[d] ± 0·03			351
	WF_6	CCl_4	26				0·41[d] ± 0·06			351
Benzene	WF_6	CCl_4	26	375			0·08[d] ± 0·06			341
	WF_6	CCl_4	26	380			0·10[d] ± 0·06	0·15		339
	WF_6			380		640[c]				339
	WF_6			< 295						350
	WF_6	cyclohexane	26		500[h]		−0·09[d] ± 0·01			339
	WF_6	perfluoroalkane	26	350			−0·02[d] ± 0·03	0·05		339
Hexafluorobenzene	WF_6				460[h]					339, 350
	WF_6	CCl_4	26				0·29[d] ± 0·06			339
	WF_6	CCl_4		330[b]						351
Toluene	WF_6			< 295						339, 350
Octafluorotoluene	WF_6									339
m-Xylene	WF_6									339
p-Xylene	WF_6									339
Perfluoro-*p*-xylene	WF_6									339
Naphthalene	WF_6	CCl_4		440			0·04[d] ± 0·03	0·17		339
	WF_6	cyclohexane		440			0·14[d] ± 0·02			339
Octafluoro-naphthalene	WF_6	CCl_4			400[l]		0·38[d] ± 0·02			339
Me_4Si	WF_6			248		−[k]				350
Me_4Ge	WF_6			287		−[k]				350
Me_4Sn	WF_6			336		−[k]				350
(n-Propyl)$_4$Sn	WF_6			290[b], 229		−[k]				350
(n-Butyl)$_4$Sn	WF_6			242, 315		−[k]				350
CCl_4	WF_6	C_7F_{13}	26			295[j]	0·18[d] ± 0·03			351
	WF_6			269						350
$SiCl_4$	WF_6			239						350
$SnCl_4$	WF_6			233						350

									350
Hexafluorobenzene	WF_5OMe			<295					350
CCl_4	WF_5OMe			269					350
Me_4Si	WF_5OMe			248		$-$[k]			339
Benzene	WCl_6			570		6 300[c]			339
	WCl_6	CCl_4	26				$-0{\cdot}12$[d] $\pm$ 0·03		339
	$WOCl_4$			480		2 000[c]			339
	$WOCl_4$	CCl_4	26				0·03[d] $\pm$ 0·02	$-0{\cdot}13$	339
	$WOCl_4$	cyclohexane	26				0·04[d] $\pm$ 0·01	$-0{\cdot}06$	351
n-Hexane	MoF_6	C_7F_{13}	26	360[b]			0·54[d] $\pm$ 0·04		339
Hexafluorobenzene	MoF_6			430		270[c]	$-$[d]		339, 351
	MoF_6	CCl_4	26	440			0·14[d] $\pm$ 0·02		339
	MoF_6	C_7F_{13}	26	420			$-0{\cdot}15$[d] $\pm$ 0·06		339
Octafluorotoluene	MoF_6								339
Perfluoro-*p*-xylene	MoF_6								350
Me_4Si	MoF_6			358					350
Me_4Ge	MoF_6			230					350
CCl_4	MoF_6	C_7F_{13}	26		350		0·21[d] $\pm$ 0·01		351
	MoF_6					$-$[k]			350
$SiCl_4$	MoF_6			372[b], 467					339
Naphthalene	MoO_2Cl_2	CH_2Cl_2							339
1-Chloronaphthalene	MoO_2Cl_2	CH_2Cl_2							339
1-Fluoronaphthalene	MoO_2Cl_2	CH_2Cl_2							339
Hexafluorobenzene	UF_6	CCl_4							339
Octafluorotoluene	UF_6	CCl_4							339
Perfluoro-*p*-xylene	UF_6	CCl_4							339
Cyclohexane	SeF_6								340
Benzene	SeF_6			400[j]					340
	SeF_6	CCl_4	26				0·13[m]		340
m-Xylene	SeF_6								340
p-Xylene	SeF_6								340
Mesitylene	SeF_6			310		160[c]			340
	SeF_6	CCl_4	26				$-0{\cdot}13$[d] $\pm$ 0·03		340
Naphthalene	SeF_6	CCl_4	26				0·25[d] $\pm$ 0·02		340
1,4-Dimethyl-naphthalene	SeF_6								340
Cyclohexane	TeF_6			205		760[c]			

Summary Table D—*continued*

Donor	Acceptor	Medium[f]	T^a /°C	λ_{max} /nm	λ_{onset} /nm	ϵ_{max} /l mol^{-1} cm^{-1}	K_c /l mol^{-1}	$-\Delta H^0$ /kcal mol^{-1}	Other data	Ref.
Benzene	TeF_6			280		585[c]				340
	TeF_6	CCl_4	26				0·32[d] ± 0·07			340
	TeF_6	cyclohexane	26				0·19[d] ± 0·03			340
m-Xylene	TeF_6									340
p-Xylene	TeF_6									340
Mesitylene	TeF_6			315		170[c]				340
	TeF_6	CCl_4	26				0·46[d] ± 0·07			340
Naphthalene	TeF_6	CCl_4	26				0·62[d] ± 0·09			340
	TeF_6	cyclohexane	26				0·42[d] ± 0·06			340
1,4-Dimethyl-naphthalene	TeF_6									340
Tetrakis(dimethyl-amino)ethylene	SF_6				525					352
Benzene	SO_2Cl_2			270		1 600[c]				340
Mesitylene	SO_2Cl_2									340
Hexamethylbenzene	SO_2Cl_2	CCl_4	26				−0·01[d] ± 0·04	−0·12		340
Naphthalene	SO_2Cl_2			280		730[c]				340
	SO_2Cl_2	CCl_4	26				0·19[d] ± 0·04	0·14		340
Phenanthrene	SO_2Cl_2									340
Triphenylene	SO_2Cl_2									340
Anthracene	SO_2Cl_2									340
Pyrene	SO_2Cl_2									340
Durene	SO_2Cl_2									340
Cyclohexane	ClO_2F				240[j]					340
Perfluoromethyl-cyclohexane	ClO_2F				220[j]					340
Benzene	ClO_2F				285[j]					340
Mesitylene	ClO_2F				325[j]					340
Naphthalene	ClO_2F									340
1,4-Dimethyl-naphthalene	ClO_2F									340

Hexafluorobenzene	IF_7							351
Octafluorotoluene	IF_7			360				340
Perfluoro-*p*-xylene	IF_7							340
Hexafluorobenzene	IOF_5	perfluoroalkane			475			340, 351
Benzene	RuO_4	CCl_4						340
Hexafluorobenzene	RuO_4	CCl_4						340
Toluene	RuO_4	CCl_4						340
m-Xylene	RuO_4	CCl_4						340
p-Xylene	RuO_4	CCl_4						340
Mesitylene	RuO_4	CCl_4						340
Octafluoro-naphthalene	RuO_4	CCl_4						340
Benzene	OsO_4					470[j]		340
	OsO_4	CCl_4	26			0·03[d] ± 0·02		340
	OsO_4	cyclohexane	26			−0·01[d] ± 0·06	0·525	340
m-Xylene	OsO_4							340
p-Xylene	OsO_4							340
Mesitylene	OsO_4			410		1 500[c]		340
	OsO_4	CCl_4	26			0·03[d] ± 0·01	0·77	340
Naphthalene	OsO_4							340
	OsO_4	CCl_4	26			0·05[d] ± 0·07	0·4	340
Octafluoro-naphthalene	OsO_4							340
1,4-Dimethyl-naphthalene	OsO_4							340
Xenon	IrF_6	crystal	−196		1 020		(0·07)	348
	ReF_6	crystal	−196		<455			348
	WF_6	crystal	−196		273			348
	MoF_6	crystal	−196		380			348
	UF_6	crystal	−196		<385			348

[a] If temperature not specified, it is assumed to be room temperature. [b] Shoulder. [c] Assuming 100 per cent complexation of the minor component. [d] Average value (±std. deviation) of at least three different wavelength modified Benesi–Hildebrand dilution plots. [e] Measured at 330 nm; at 340 nm, $\epsilon = 5700$; at 370 nm, $\epsilon = 6\,600\,l\,mol^{-1}\,cm^{-1}$. [f] If medium is not specified, it is the two-component mixture. [g] Measured at 420 nm. [h] Estimated from figure in reference: $\epsilon = 11\,l\,mol^{-1}\,cm^{-1}$, based on complete complexation of the minor component. [i] Significant absorption in the 320–360 nm range. [j] Estimated from figure in reference; $\epsilon = 51\,l\,mol^{-1}\,cm^{-1}$, based on complete complexation of the minor component. [k] $\epsilon = 5 \times 10^4$–$10^5\,l\,mol^{-1}\,cm^{-1}$. [l] Longest wavelength at which K_c was determined. [m] Measured at 350 nm only.

have been attributed as arising from perturbation of the local excitation of the acceptor, or the donor, or the appearance of a CT band, and the interpretations have not always been in accord. The interaction of benzene with CBr_4 produces no clear new band, rather there is an enhancement in the region of the CBr_4 absorption and a red shift on substituting methyl groups in the benzene. Tramer[354] considers a CT band to be present, whereas Bahnick, Bennett and Person[355] believe there is only enhancement of the local CBr_4 absorption in the region 230–265 nm. However, the latter authors do not rule out the possibility of a broad CT band which lies under the local CBr_4 band as suggested by Tramer.[354]

Davis and Farmer[353] found that addition of halomethanes to aromatic hydrocarbons, e.g. CCl_4 to tetracene in n-hexane solution, diminishes the peak height and simultaneously broadens the ^1B_a or ^1B_b band (Platt[356] notation) of the aromatic compound, with the total integrated intensity being the same. This evidence is taken by Davis and Farmer as pointing to the interaction being due mainly to contact effects in solution.

As with other studies on weak interactions, there is difficulty in obtaining precise thermodynamic values. Lautenberger, Jones and Miller[357] found a predominantly 1:1 interaction between n-butylamine and CCl_4 in cyclohexane, using the method of continuous variations on absorbance data from the side of the CT band. Separation of the $K_c\epsilon$ product was not achieved (the B–H plot gave an intercept of ~ 0), and the authors concluded that the observations could be due either to weak 1:1 complex formation or to 1:1 pairs giving rise to CCT spectra. Similar difficulties were encountered with other amine–halocarbon studies,[98,353,358] and in one case[358] an upper limit for K_c was estimated. In general, the thermodynamic data for the amine–halocarbon systems fall in the range considered as contacts by the definitions adopted for this chapter.

Results on the thermodynamic data on similar aromatic hydrocarbon–halomethane systems reported from different laboratories are more scattered. This may be seen from the data in Summary Table E for hexamethylbenzene–CCl_4[359–361] and benzene–CBr_4.[354,355] Rosseinsky and Kellawi[361] make a strong plea for inclusion in papers (or deposition in libraries) of sufficient details of original measurements to allow statistical evaluation. Data for many aromatic hydrocarbon–halomethane systems also are available from nmr studies, e.g.[362–365] with many examples where the interactions lie within the definition adopted for contacts,[362] and others better described as complexes.[363]

The K_c data of Tramer[354] for the aromatic hydrocarbon–CBr_4 interactions are quite low. The K_c of Bahnick and coworkers[355] for benzene–CBr_4 is probably better because they used short-path cells which enabled them to study the entire CBr_4 absorption band rather than just the tail. Their K_c

result suggests to them the formation of a true complex. However, the ΔH^0 value is almost zero. The authors point out that this value could be as high as -3 kcal mol^{-1} if the errors in K_c are of the order of ± 30 per cent. In an earlier study of Raman intensities of CCl_4 in various systems, Bahnick and Person[366] state that their interpretation of the intensification in terms of very weak complexes is consistent in explaining why the changes in bond polarizations seem concentrated in the properties of the C—Cl bond, but they also point out that this kind of intensity change may possibly result simply from "contact" interactions.

As is the case with molecular oxygen, fluorescence quenching and photochemical reaction with the halomethanes also occur. These have been viewed as proceeding via an intermediate contact or complex. For example, CCl_4 and $CHCl_3$ are quenchers of such molecules as aniline, 2-naphthylamine[367] and anthracene,[368] with the interaction between the donor in its excited state and the halomethane (Q) being represented by:

$$D^* + Q \rightarrow D^*Q \rightarrow \text{products} \quad \text{(contact or complex).} \tag{93}$$

Among the photochemical reactions studied which proceed via charge-transfer excitation are the amine–halomethanes[357, 358] with the order of reactivity[358] being $FCCl_3 < ClCCl_3 < BrCCl_3 < BrCBr_3$, and perhaps also anthracene–CCl_4.[358, 369]

It was pointed out by Evans[128] that CCT spectra involving saturated hydrocarbons should not be restricted to the molecular halogen and oxygen acceptors. However, most other electron acceptors absorb strongly below 270 nm which would obscure many CT bands. Evans chose to study the nitromethanes because they do not absorb strongly above 240 nm, with only a weak absorption maximum in the vapour phase at 275 nm. Also, tetranitromethane apparently is a good acceptor towards unsaturated hydrocarbons, giving rise to CT bands extending into the visible region. (Heilbronner[370] showed that the CT bands of olefin–$C(NO_2)_4$ interactions are in the visible region, and are shifted systematically to longer wavelengths by increased alkyl substitution at the site of the C=C bond.)

The nitromethane vapour spectrum is little affected by cyclohexane solvent.[128] "Active" solvents such as benzene, toluene and dioxan increase the intensity of the nitromethane absorption, but not by very much compared with the saturated hydrocarbons.[371] The spectral changes have been considered primarily as solvent-induced effects on the local excitation in nitromethane[128, 371] arising either from a weak 1:1 complex or a physical perturbation.[371] That the interaction is very weak also is shown in the work of Anderson, Cambio and Prausnitz[372] who report for K_c at 25°C (solvent

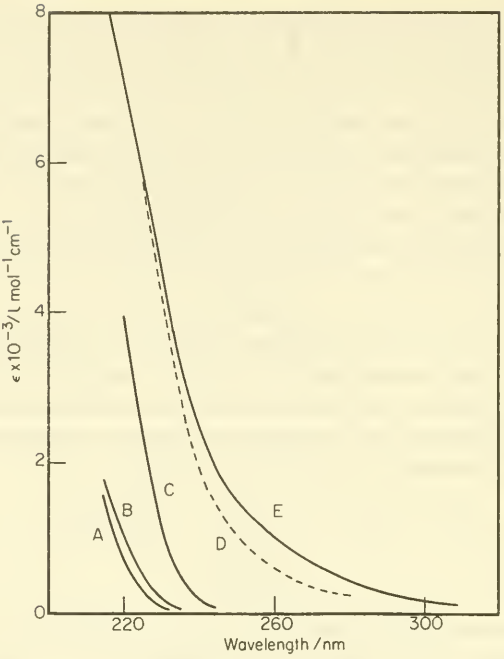

FIG. 23. Absorption spectra of electron acceptors: A, nitromethane vapour; B, nitromethane in cyclohexane; C, tetranitromethane vapour; D, tetranitromethane in 2,2,4-trimethylpentane; E, tetranitromethane in cyclohexane. [Reproduced with permission from D. F. Evans, *J. Chem. Soc.*, 4229 (1957)]

not given) for the interaction of nitromethane with benzene, toluene and mesitylene values of 0·029, 0·022 and 0·093 l mol^{-1}, respectively. On the other hand, the effects of saturated hydrocarbons on the vapour spectrum of tetranitromethane are quite large (Fig. 23), and Evans[128] suggested that this additional absorption is due primarily to CCT spectra.

XI. π^*-ACCEPTORS

There is a very extensive literature on EDA complexes where the electron acceptor is a π^*-acid.[1,2,17] Most commonly, the interaction involves a π-donor and is sufficiently strong to be a complex by the definitions adopted. However, there are examples of π, π^*-interactions that could be cited as contacts (see Section XII). There is also evidence for very weak interaction between π^*-acceptors (mostly TCNE) and a variety of σ-donors of relatively

SUMMARY TABLE E. Substituted methane acceptors

Donor	Acceptor	Medium	T /°C	λ_{max} /nm	λ_{onset} /nm	ϵ_{max} /l mol^{-1} cm^{-1}	K_c /l mol^{-1}	$-\Delta H^0$ /kcal mol^{-1}	Other data		Ref.
									λ	$K_c\epsilon$	
n-Butylamine	CCl_4	cyclohexane	25		~270		—[a]		265	1·35 ± 0·2	357
									270	0·95 ± 0·2	
									275	0·70 ± 0·2	
									λ	$K_c\epsilon$	
Triethylamine	$HCCl_3$	isooctane	—[b]	~230	~280[c]		{0·085}[d]		230	~160	358
	$FCCl_3$	isooctane	—[b]	(~245)[e]	~290[c]		{0·074}[d]		230	~450[e]	358
	$ClCCl_3$	isooctane	—[b]	~230	~320[c]		{0·096}[d]		230	~400	358
	$BrCCl_3$	isooctane	—[b]	~260	~360[c]				260	~1 600	358
N,*N*-Dimethyl-aniline	CCl_4	n-hexane	—[b]	—[f]			0·06	0·5			98
	$CHCl_3$	n-hexane	—[b]	—[f]			—[a]				98
	CH_2Cl_2	n-hexane	—[b]	—[f]			—[g]				98
N,*N*,*N*′,*N*′-Tetramethyl-*p*-phenylene-diamine	CCl_4	n-hexane	—[b]	—[f]	~400 to <310[h]		0·13	1·2			98
	$CHCl_3$	n-hexane	—[b]	—[f]	~390 to <310[h]		0·007	0			98
	CH_2Cl_2	n-hexane	—[b]	—[f]	~390 to <310[h]		—[a]				98
									λ	ϵ	
Benzene	CCl_4	n-hexane	25	233·5			{0·009 ± 0·004}		234·0	859	373
									234·5	795	
	CCl_4	n-hexane	25				{0·001 ± 0·02}[i]				361
	CCl_4	cyclohexane	25	~216[j]			0·076 ± 0·057		220	4 070 ± 2 840	361
p-Xylene	CCl_4	cyclohexane	25	~230[j]			0·136 ± 0·018		232	3 144[k]	361
									234	2 440[k]	
									236	1 871[k]	
									238	1 456[k]	
m-Xylene	CCl_4	cyclohexane	25	~230[j]			0·112 ± 0·028		232	3 850[k]	361
									234	2 989[k]	
									236	2 283[k]	
									238	1 698[k]	
Mesitylene	CCl_4	n-hexane	rt[l]		~286 to <238[h]						359
	CCl_4	n-hexane	25				0·113 ± 0·044		233·5	1 206	373
									234·5	1 174	

Summary Table E—*continued*

Donor	Acceptor	Medium	T /°C	λ_{max} /nm	λ_{onset} /nm	ϵ_{max} /l mol^{-1} cm^{-1}	K_c /l mol^{-1}	$-\Delta H^0$ /kcal mol^{-1}	Other data		Ref.
	CCl_4	n-hexane	25			7 125 ± 713[i]	0·144 ± 0·017[i]				361
	CCl_4	cyclohexane	25	~235[j]			0·252 ± 0·036		234	2 723[m]	361
									236	2 268[m]	
									238	1 820[m]	
Hexamethyl-benzene	CCl_4	n-hexane	rt[l]	242		(2·5 ± 2·5) × 10[4]	{0·02 ± 0·01}	0·54 ± 0·15			359
	CCl_4	cyclohexane	26		310[k]		0·04 ± 0·03[y]	0·2			123
									λ	ϵ	
	CCl_4	n-hexane	25	240·5			0·64 ± 0·12		243	923[n]	360
									245	962[n]	
									247	869[n]	
	CCl_4	n-hexane	25			902 ± 114[i]	0·648 ± 0·092[i]				361
	CCl_4	cyclohexane	25	~242[j]		1 150[o]	0·550 ± 0·160		244	1 109[o]	361
									246	1 062[o]	
Mesitylene	$CHCl_3$	n-hexane	rt[l]		~242 to ~222[h]						359
Hexamethyl-benzene	$CHCl_3$	n-hexane	rt[l]	234		(9 ± 1·5) × 10[3]	0·06 ± 0·015				359
Benzene	CBr_4	n-hexane	—[b]		295[p]	(~10[4])[q]	{0·01 ± 0·005}				354
	CBr_4	cyclohexane	25		—[r]		0·226 ± 0·06	~0			355
Toluene	CBr_4	n-hexane	—[b]		302[p]	(~10[4])[q]	{0·02 ± 0·005}				354
p-Xylene	CBr_4	n-hexane	—[b]		307[p]	(~10[4])[q]	{0·03 ± 0·005}				354
Mesitylene	CBr_4	n-hexane	—[b]		312[p]	(~10[4])[q]	{0·045 ± 0·005}				354
Hexamethyl-benzene	CBr_4	n-hexane	rt[l]	~303							359
2-Chloro-naphthalene	CBr_4	n-hexane	—[b]		~328[s]						354
Tetrahydrofuran	CBr_4	cyclohexane	25		—[r]		{0·08}[t]				355
Hexamethyl-benzene	$CHBr_3$	n-hexane	rt[l]	~263							359
2-Methylbut-2-ene	CBr_4	3-methyl-pentane	< −158	273							209
	CCl_2Br_2	3-methyl-pentane	< − 158	254							209
	CCl_3Br	3-methyl-pentane	< −158	242							209

2,3-Dimethyl-but-2-ene	CBr_4	3-methyl-pentane	< -158	285			209
	CCl_2Br_2	3-methyl-pentane	< -158	267			209
	CCl_3Br	3-methyl-pentane	< -158	257			209
Anthracene	CCl_4	n-hexane	—[b]	—[r]		—[a or g]	353
Tetracene	CCl_4	n-hexane	—[b]	—[r]		0·15	353
Perylene[u]	CCl_4	n-hexane					353
Naphthalene	CCl_4	n-hexane					353
Anthracene[v]	$CHCl_3$	n-hexane	—[b]	—[r]		—[a or g]	353
Tetracene							
Perylene							
Naphthalene							
Anthracene[v]	CH_2Cl_2	n-hexane	—[b]	—[r]		—[a or g]	353
Tetracene							
Perylene							
Naphthalene							
Cyclohexane	$C(NO_2)_4$	cyclohexane			{~300}[w]		128
2,2,4-Trimethyl-pentane (isooctane)	$C(NO_2)_4$	2,2,4-trimethyl-pentane			{~280}[w]		128

[a] Benesi–Hildebrand plot gave a nearly zero intercept. [b] Temperature not specified (probably room temperature). [c] Estimated from figure in Ref. 8 for the condition $K_c\epsilon \approx 21^2\,mol^{-2}\,cm^{-1}$. [d] Estimated upper limit. [e] Uncertain shoulder; broad (perhaps composite) band. [f] λ_{max} buried under the intense high-energy band of the amine. [g] Benesi–Hildebrand plot gave a negative intercept. [h] Region of enhanced absorbance. [i] Re-evaluation of literature data using a non-linear least-squares computation. [j] Value is approximate because of overlap with donor and acceptor bands. [k] Error to about 3 per cent. [l] Room temperature. [m] Error to about 4 per cent. [n] ϵ_c obtained by adding $\Delta\epsilon + \epsilon_A + \epsilon_D$ in Ref. 360. [o] Error to about 10 per cent. [p] Absorption edge given in Ref. 9. [q] Supposed value (Ref. 354). [r] See text for observations in ultraviolet region. [s] Obtained from data in Fig. 3 of Ref. 354. [t] Not significantly different from zero (Ref. 355). [u] Results similar to those for tetracene. [v] Data not given, but effects were similar, being in the order $CCl_4 > CHCl_3 > CH_2Cl_2$. [w] Estimated from Fig. 3 of Ref. 128 for an apparent $\epsilon \approx 200\,l\,mol^{-1}\,cm^{-1}$. [x] Longest wavelength at which K_c was determined. [y] Average value (±std. deviation) of three different wavelengths, modified Benesi–Hildebrand dilution plots.

low ionization potentials. These include organosilicon and organogermanium compounds,[374, 375] several peralkylmetals,[376–379] and even saturated hydrocarbons.[380–382] Hydrogen-bonding solvents have been used almost entirely in these studies. Data for these systems are given in Summary Table F.

Traven and West[374] and also Sakurai, Kira and Uchida[375] observed new absorption bands on mixing solutions of permethylpolysilanes with tetracyanoethylene (TCNE). These were attributed to charge transfer of σelectrons of low ionization energy, such as in donors with Si—Si and Ge—Ge bonds, to the π^*-acceptor. The high concentration of donor needed to observe the CT band is an indication that the interaction is quite weak (barring an unexpectedly small value for ϵ). This is substantiated by the fact that straight-line plots were obtained using the Benesi–Hildebrand method with intercepts that were near zero (or negative). While it appears that these systems fall in the category of contacts, such classification is forced in part by the experimental conditions employed. First, it should be noted that

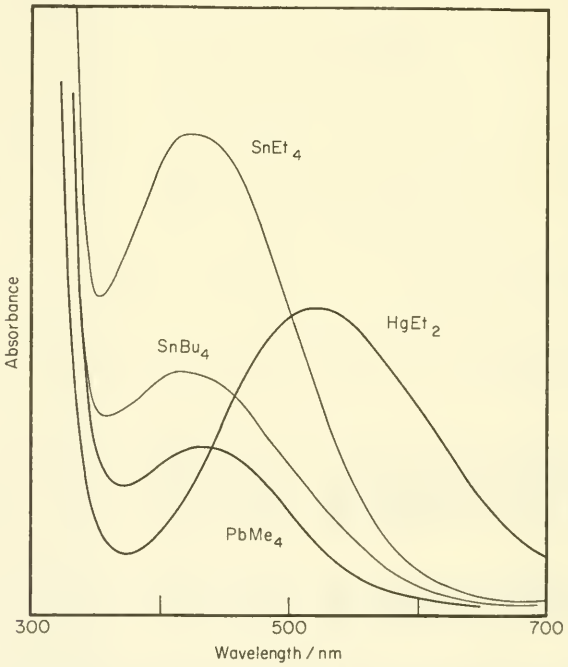

FIG. 24. Charge-transfer spectra of tetraethyltin (0·60 M), tetra-n-butyltin (0·46 M), and diethylmercury (0·41 M) with 0·015 M TCNE in chloroform solutions at room temperature. Spectrum of tetramethyllead (0·30 M) and 0·01 M TCNE in chloroform is at −10°C. [Reproduced with permission from H. C. Gardner and J. K. Kochi, *J. Amer. Chem. Soc.*, **98**, 2460 (1976)]

the highest donor concentration used was ~0·5 M in one study[374] and ~0·8 M in another,[377] and even benzene–iodine (with $K_c \approx 0{\cdot}13$ l mol^{-1} at 25°C) would be essentially in Person's Region I under these conditions. Second, the solvents used were chloroform, dichloromethane and 1,2-dichloropropane probably because the solubility of TCNE in "inert" solvents is low. These solvents, through hydrogen-bonding, can introduce competing equilibria and thereby decrease K for the permethylpolysilane–TCNE systems.

Distinct CT band maxima are observed and the bands are broad in some cases. For decamethyltetrasilane–TCNE there is a shoulder at 370 nm in addition to the band maximum at 520 nm. For dodecamethylcyclohexasilane–TCNE the broad band with maximum at 507 nm was separated into two bands with maxima at 555 and 477 nm. These bands are attributed to electron transfer from the two highest filled levels of $(SiMe_2)_6$ with ionization potentials of 7·79 and 8·16 eV. The energy difference of the CT transitions is about the same as the difference in the ionization potentials (0·37 eV).

Quite similar results have been reported by Traven and West[376] and by Gardner and Kochi[377–379] for the interaction of TCNE with peralkylmetal compounds of lead, tin and mercury. Typical spectra are shown in Fig. 24 and the spectral data are listed in Summary Table F. A plot of $h\nu_{CCT}$ against I_D^V (Fig. 25) shows good linearity, in accordance with equation (5).

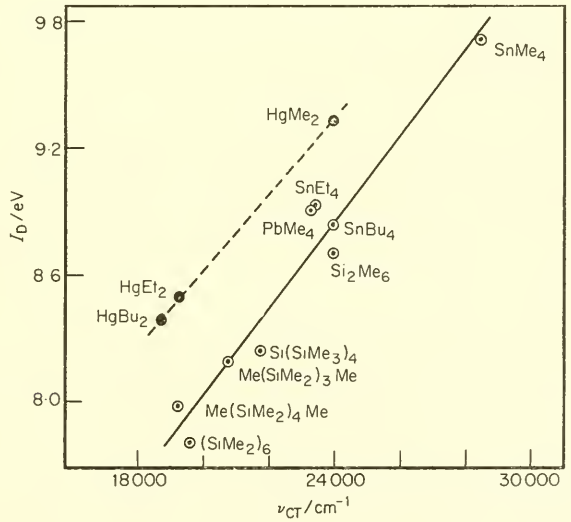

FIG. 25. Correlation of the maximum of the TCNE charge-transfer bands in chloroform with the vertical ionization potential of the alkylmetal. [Reproduced with permission from H. C. Gardner and J. K. Kochi, *J. Amer. Chem. Soc.*, **98**, 2460 (1976)]

The fact that the 2-coordinated organomercurials are not on the same line as the 4-coordinated (tetrahedral) organometallics has been attributed to less steric hindrance for the former.[377] This should increase the G_1 term which is inversely proportional to the encounter distance[377] since it involves primarily the Coulombic interaction of D^+ and A^-. However, solvent effects on systems of different coordination may also be a factor.

Many of the organometallics undergo rapid reaction with TCNE, and the CT band has had to be studied at low temperatures. The rate of reaction depends on both the metal and the alkyl group, as well as the solvent.[377] The reaction results in the insertion of the alkylmetal into TCNE:

$$\mathrm{RM + TCNE \rightarrow R{-}\overset{\mathrm{NC}}{\underset{\mathrm{NC}}{\overset{|}{\underset{|}{\mathrm{C}}}}}{-}\overset{\mathrm{CN}}{\underset{\mathrm{CN}}{\overset{|}{\underset{|}{\mathrm{C}}}}}{-}M} \qquad (94)$$

which goes quantitatively, with the initial step in the mechanism being an electron transfer:

$$\mathrm{RM + TCNE \rightleftharpoons [RM, TCNE] \rightarrow [RM^{\cdot +}, TCNE^{\cdot -}]}. \qquad (95)$$

A study of the kinetics of tetraalkyllead–TCNE showed a first-order dependence with respect to each reactant.

Tabushi and Yamamura[381] determined the spectral and thermodynamic properties of quadricyclane with a series of π^*-acids. They noted that the molar absorption (extinction) coefficient of the complex paralleled the electron affinity of the π^*-acid, but the equilibrium constant followed the opposite trend, in contrast to theory. The possible factors cited are similar to those suggested for the opposite trend in ϵ and K reported by Andrews and Keefer[383] for the alkylbenzene–iodine complexes. An additional possibility cited is a steric effect (due to the bulkiness of the acceptor).

Quadricyclane is a strained hydrocarbon whose highest occupied molecular orbitals (HOMO) have ethylene-like character which is attributed to the distortion of the valence angles of the carbon atoms in the ring.[382] Traven and coworkers[382] recently studied the CT spectra from the interaction of TCNE with saturated hydrocarbons that are free from geometric distortion. The spectrum of TCNE in chloroform shows a band at 276 nm ($\log \epsilon$ 4·17) with a shoulder at 300 nm ($\log \epsilon \approx 2$). In mixtures of TCNE with hexamethylethane, cyclohexane, bicyclohexyl, decalin, adamantane and 1,1′-biadamantyl, there is a distinct shift of the shoulder at 300 nm to longer wavelengths, and in the case of the two latter compounds it was possible to separate the bands.

SUMMARY TABLE F. π^*-Acceptors

Donor	Acceptor	Medium	T /°C	λ_{max} /nm	λ_{onset} /nm	ϵ_{max} /l mol^{-1} cm^{-1}	K_c /l mol^{-1}	$-\Delta H^0$ /kcal mol^{-1}	Other data	Ref.
Si_2Me_6	TCNE	chloroform	—[a]	417						374
		dichloro-methane	rt[b]	417						375
Si_3Me_8	TCNE	chloroform	—[a]	480						374
		dichloro-methane	rt[b]	474						375
$Si(SiMe_3)_4$	TCNE	chloroform	—[a]	458						374
Si_4Me_{10}	TCNE	chloroform	—[a]	520 (370)[c]						374
		dichloro-methane	rt[b]	510						375
Si_5Me_{12}	TCNE	dichloro-methane	rt[b]	543						375
$(SiMe_2)_6$	TCNE	chloroform	—[a]	555[d] (477)[d]						374
$PbMe_4$	TCNE	chloroform	−35 to −50	427						377
		1,2-dichloro-propane	−35 to −50	412						377, 378
$PbMe_3Et$	TCNE	1,2-dichloro-propane	−35 to −50	430						377, 378
$PbMe_2Et_2$	TCNE	1,2-dichloro-propane	−35 to −50	454						377, 378
$PbMeEt_3$	TCNE	1,2-dichloro-propane	−35 to −50	479 491						377, 378 378
$PbEt_4$	TCNE	1,2-dichloro-propane	−35 to −50	—[e]						377
		chloroform	—[a]	—[e, f]						376, 377
$PbBu_4$	TCNE	1,2-dichloro-propane	−35 to −50	—[e, f]						377

Summary Table F—*continued*

Donor	Acceptor	Medium	T /°C	λ_{max} /nm	λ_{onset} /nm	ϵ_{max} /l mol^{-1} cm^{-1}	K_c /l mol^{-1}	$-\Delta H^0$ /kcal mol^{-1}	Other data	Ref.
$SnMe_4$	TCNE	chloroform	—[a]	350						376, 377
		1,2-dichloro-propane		~330						377
$SnEt_4$	TCNE	chloroform	—[a]	427						376, 377
		1,2-dichloro-propane		409						377
$SnBu_4$	TCNE	chloroform		417						377
		chloroform	—[a]	{476}[g]						376
		1,2-dichloro-propane		393						377
Sn_2Me_6	TCNE	chloroform	—[a]	—[e,f]						376
Sn_2Pr_6	TCNE	chloroform	—[a]	—[e,f]						376
$GeBu_4$	TCNE	chloroform	—[a]	375						376, 377
Ge_2Me_6	TCNE	(dichloro-methane)		435						375
Ge_2Bu_6	TCNE	chloroform	—[a]	435						376
$(GeMe_2)_6$	TCNE	chloroform	—[a]	—[e,f]						376
$HgMe_2$	TCNE	chloroform	—[a]	415						376, 377
		1,2-dichloro-propane		395						377
$HgEt_2$	TCNE	chloroform		517						377
		1,2-dichloro-propane		500						377
$HgBu_2$	TCNE	chloroform		532						377
		1,2-dichloro-propane		508						377
$(SiMe_2)_6$	chloranil	chloroform	—[a]	430						374
Si_3Me_8	2,3,5,6-DDQ[j]	chloroform	—[a]	535						374
$SnEt_4$	2,5,3,6-DDQ[j]	chloroform	—[a]	431						376
$SnBu_4$	2,5,3,6-DDQ[j]	chloroform	—[a]	481						376

Quadricyclane[h]	maleic anhydride	cyclohexane		315	1 000		380
		dichloromethane	20	325	740	0·039[i]	381
	chloromaleic anhydride	dichloromethane	20	334	1 400	0·019[i]	381
	dichloromaleic anhydride	dichloromethane	20	346			381
	p-benzoquinone	dichloromethane	20	368	1 980 ± 110	0·013 ± 0·0006[i]	381
	2,5-dichloro-*p*-benzoquinone	dichloromethane	20	418			381
	chloranil	dichloromethane	20	474[k]	2 600 ± 600	0·015 ± 0·006[i]	381
	2,3,5,6-DDQ[j]	dichloromethane	20	536			381
Hexamethylethane	TCNE	$CHCl_3$	—[a]	310[l]			382
Cyclohexane	TCNE	$CHCl_3$	—[a]	320[l]			382
Bicyclohexyl	TCNE	$CHCl_3$	—[a]	330[l]			382
Decalin	TCNE	$CHCl_3$	—[a]	330[l]			382
Adamantane	TCNE	$CHCl_3$	—[a]	355			382
1,1′-Biadamantyl	TCNE	$CHCl_3$	—[a]	380			382

[a] Temperature not specified. [b] Room temperature. [c] Shoulder; presence of a second CT band. [d] See text. [e] Unstable. [f] $TCNE^-$ observed. [g] Probably incorrect; see Ref. 377. [h] Tetracyclo[3.2.0.$0^{2,7}$.$0^{4,6}$]heptane. [i] See footnote *a* of Summary Table A. [j] 2,3,5,6-DDQ = 2,3-dichloro-5,6-dicyano-*p*-benzoquinone; 2,5,3,6-DDQ = 2,5-dichloro-3,6-dicyano-*p*-benzoquinone. [k] Possibly a second CT band at a wavelength shorter than 330 nm. [l] Shoulder.

XII. MISCELLANEOUS

Data for miscellaneous systems studied in "inert" solvents are listed in Summary Table G. Initial entries are for π,π^* interactions, mostly from Hammond and coworkers[80, 343, 352, 384, 384a] (who also report data in dichloromethane solvent). Their study of the donor tetrakis(dimethylamino)-ethylene (TMAE) with a variety of π^*-acids gave values for K_c that did not differ significantly from zero. Castro, Andrews and Keefer[170] report an example of weak π,π^* interaction due to steric effects, e.g. hindered biphenyls and 1,3,5-trinitrobenzene.

Weimer and Prausnitz[385] reported enhanced absorbance of solutions of *p*-xylene dissolved in polar solvents commonly used in many typical chemical operations. These solvents act as electron acceptors (see data in Summary Table G), as indicated by the fact that K_c for the nitroethane interaction increases systematically with the donor series benzene ($0{\cdot}020 \pm 0{\cdot}010$ l mol^{-1}) < toluene ($0{\cdot}022 \pm 0{\cdot}010$ l mol^{-1}) < *p*-xylene ($0{\cdot}054 \pm 0{\cdot}012$ l mol^{-1}) < mesitylene ($0{\cdot}093 \pm 0{\cdot}020$ l mol^{-1}). Similar (although not always systematic) results are reported for solutions of aromatic hydrocarbon donors with nitromethane and with acetone as acceptors.[385]

Sulphur dioxide behaves much like the molecular halogens in its interaction with donors, its strength as an acceptor compared with the halogens being[386] $Cl_2 < SO_2 < Br_2 < I_2$. Like the halogens, the interactions cover the range from contacts to relatively strong complexes, the sequence being generally[386–388] saturated hydrocarbon donors < olefinic and aromatic donors < oxygen donors < nitrogen donors. This is indicated by the spectral shifts in the ultraviolet region of SO_2 solutions, e.g. there is very little effect on the ultraviolet spectrum of SO_2 dissolved in propane or cyclopropane[389] whereas there is a large effect with amines where complexation is quite strong.[111, 387]

The CT bands are in the region where SO_2 has a band maximum (~ 290 nm)[386] that is enhanced several-fold in intensity owing to interaction with the donor. The CT band maxima obtained by resolving the spectra show a fairly good linear relation between I_D and $h\nu_{max}$ with olefin and aromatic hydrocarbon donors. There is a generally consistent trend to longer wavelengths with increase in K_c. Further data on λ_{max} for SO_2 interactions, where K_c and ΔH^0 data are beyond the limits adopted for contacts, are 2-methylbut-2-ene (308 nm), 2,3-dimethylbut-2-ene (325 nm), xylenes (~ 296 nm) and mesitylene (~ 305 nm).[386, 389] No correlation is found between K_c and ϵ_{max}, a situation similar to that in studies with iodine.

An opposite trend is observed in the interaction of SO_2 with alcohols (λ_{max} and K_c given in parentheses): methanol (274·5 nm, $0{\cdot}229$ l mol^{-1}),

SUMMARY TABLE G. Miscellaneous

Donor	Acceptor	Medium	T^a /°C	λ_{max} /nm	λ_{onset} /nm	ϵ_{max} /l mol^{-1} cm^{-1}	K_c /l mol^{-1}	$-\Delta H^0$ /kcal mol^{-1}	Other data	Ref.
TMAE[b]	C_6F_6	cyclohexane	26		475[e]		−0·07 ± 0·05			384, 384a
	C_6ClF_5	cyclohexane	26		475[e]					384a
	$C_6Cl_3F_3$	cyclohexane	26		485[e]					384a
	C_6Cl_5F	cyclohexane	26		525[e]					384a
	C_6Cl_6	cyclohexane	26		540[e]		0·01 ± 0·04			384, 384a
	p-nitroanisole	n-hexane	24	474			−0·07 ± 0·04			80, 384
	p-methylnitro-benzene	n-hexane	24	482[c]						384
	nitrobenzene	cyclohexane		492						394
	nitrobenzene	n-hexane	24	493			0·01 ± 0·02	0·28		80, 384
	p-fluoronitro-benzene	n-hexane	24	511[c]						80
	p-chloronitro-benzene	n-hexane	24	533			0·08 ± 0·04	0·23		80, 384
	p-bromonitro-benzene	n-hexane	24	536						80
	acridine	n-hexane	24	462			−0·02 ± 0·04	0·18		80, 384
	pyrene	n-hexane	24		575[d]					80
	anthracene	n-hexane	24		600[d]					80
	perylene	n-hexane	24		500[d]					80
	phenazine	n-hexane	24	554			0·10			80
	pyridine	n-hexane	24		450[e]					80
	pyrazine	n-hexane	24		500[e]					80
	tetramethylurea	n-hexane	24		—[f]					80
	acrylonitrile	cyclohexane			—[g]					394
	perfluorobut-2-yne	—[h]			620					352
	perfluorobut-2-ene	—[h]			590					352
	hexafluorobenzene	—[h]			580					352
	naphthalene	—[h]			530					352
	perfluorocyclo-butane	—[h]			530					352
	perfluoromethyl-cyclohexane	—[h]			500					352
	CF_2Cl_2	—[h]			460					352

Summary Table G—*continued*

Donor	Acceptor	Medium	T^a /°C	λ_{max} /nm	λ_{onset} /nm	ϵ_{max} /l mol^{-1} cm^{-1}	K_c /l mol^{-1}	$-\Delta H^0$ /kcal mol^{-1}	Other data	Ref.
	perfluorocyclo-hexane	—[h]			460					352
	benzene	—[h]			450					352
Naphthalene	tetranitromethane	cyclohexane	26		525[r]		−0·07[j] ± 0·04			343
Tetramethyl-2-thiourea	1,3,5-trinitro-benzene	—[k]	27 ± 1		—[g]					384
Toluene	nitrobenzene	CCl_4	20	<310	315[t]	>1 580[m]	0·10 ± 0·08			395
	m-dinitrobenzene	CCl_4	20	<320	327[t]	>1 540[m]	0·32 ± 0·29			395
	p-dinitrobenzene	CCl_4	20	<335	350[t]	>1 840[m]	0·21 ± 0·15			395
m-Xylene	*m*-dinitrobenzene	CCl_4	20	<320	337[t]	>2 060[m]	0·09 ± 0·08			395
	p-dinitrobenzene	CCl_4	20	<340	358[t]	>1 850[m]	0·16 ± 0·02			395
Tetramethylethylene	1,3,5-trinitro-benzene	CCl_4	20	353		4 920	0·035	1·25		1, 396
Cyclohexene	1,3,5-trinitro-benzene	CCl_4	20	306		14 370	0·014	0·45		1, 396
m-Methylbiphenyl	1,3,5-trinitro-benzene	CCl_4	25	350[n]		1 300	1·2	1·1[o]		1, 170
o-Methylbiphenyl	1,3,5-trinitro-benzene	CCl_4	25	310		2 000	0·7	1·2[o]		170
2,2',6,6'-Tetramethyl-biphenyl	1,3,5-trinitro-benzene	CCl_4	25	320			<0·1	<0·2		1, 170
Bimesityl	1,3,5-trinitro-benzene	CCl_4	25	340			<0·1	0·4[p]		170
Benzene	oxalyl chloride[q]	n-heptane		<280		>3 333[m]	0·040			397
p-Xylene	cyclohexanone	n-hexane	25		286[r]		0·15 ± 0·05[s]		$(\epsilon'_c - \epsilon'_D)$ 20·9[t]	385
	triethyl phosphate	n-hexane	25		229[r]		0·14 ± 0·05[s]		111·1[t]	385
	methoxyacetone	n-hexane	25		286[r]		0·12 ± 0·06[s]		20·2[t]	385
	cyclopentanone	n-hexane	25		295[r]		0·12 ± 0·05[s]		22·9[t]	385
	γ-butyrolactone	n-hexane	25		285[r]		0·09 ± 0·05[s]		2·6[t]	385
	N-methyl-pyrrolidone	n-hexane	25		285[r]		0·09 ± 0·05[s]		44·0[t]	385
	propionitrile	n-hexane	25		229[r]		0·065 ± 0·002[s]		137·0[t]	385
	nitromethane	n-hexane	25		286[r]		0·055 ± 0·010[s]		62·4[t]	385
	nitroethane	n-hexane	25		286[r]		0·054 ± 0·012[s]		60·7[t]	385

	2-nitropropane	n-hexane	25		286[r]		0·048 ± 0·022[s]		51·5[t]	385
	citraconic anhydride	n-hexane	25		343[r]		0·040 ± 0·003[s,u]		173·4[t]	385
	2-nitro-2-methyl-propane	n-hexane	25		286[r]		0·027 ± 0·017[s]		73·5[t]	385
Oct-1-ene	SO_2	n-hexane	25	242		3 960	0·0438 ± 0·0011	1·04 ± 0·04		1, 389
Isobutene	SO_2	n-hexane	25	255		1 690	0·176 ± 0·012[v]	1·2 ± 0·04[v]		1, 389
cis-But-2-ene	SO_2	n-hexane	25	262		2 570	0·0755 ± 0·005	1·03 ± 0·04		1, 389
trans-But-2-ene	SO_2	n-hexane	25	262		2 290	0·082 ± 0·009	1·37 ± 0·12		1, 389
Cyclohexene	SO_2	n-hexane	25	272		3 430	0·0532 ± 0·0011	0·80 ± 0·05		1, 389
Cyclopentene	SO_2	n-hexane	25	271		4 170	0·0374 ± 0·0013	0·73 ± 0·06		1, 389
Chlorobenzene	SO_2	CCl_4	25	288		2 500–3 300	0·026–0·038			1, 386
Benzene	SO_2	CCl_4	25	280		3 850	0·046			1, 386
	SO_2	CCl_4	25·0	280		3 850	0·045	{7·6}[w]		388
	SO_2	n-hexane	25	<275		>5 000	0·0471 ± 0·0059	1·03 ± 0·15		1, 389
Toluene	SO_2	CCl_4	25	284		3 450	0·077			1, 386
Anthracene	SO_2	n-hexane	25	387						389
Stilbene	SO_2	n-hexane	25	342						389
Naphthalene	SO_2	n-hexane	25	496						389
Butan-1-ol	SO_2	CCl_4	24·0	279		920	0·077			1, 388
Anisole	NO	anisole			300–400[x]					326
N,*N*-Dimethylaniline	NO	*N*,*N*-dimethyl-aniline			300–400[x]					326
Methanol	NO	methanol			210–260[x]					133
n-Hexane	$CO(CN)_2$	n-hexane			<300[y]					62, 393

[a] If temperature is not specified, it is assumed to be room temperature. [b] Tetrakis(dimethylamino)ethylene. [c] Unstable. [d] From Fig. in Ref.; 5 cm optical path-length, absorbance 0·1. [e] From Fig. in Ref.; 1 cm optical path-length, absorbance 0·1. [f] Similar to, but much weaker than, the pyridine–TMAE spectrum. [g] Orange colour. [h] Possibly cyclohexane. [i] From Fig. in Ref.; 2 cm optical path-length, absorbance 0·1. [j] Average value (±std. deviation) of at least three different wavelengths; modified Benesi–Hildebrand dilution plots. [k] Medium not specified. [l] λ at which $\epsilon = 1\,000\,l\,mol^{-1}\,cm^{-1}$. [m] ϵ corresponds to the wavelength in the λ_{max} column. [n] An inflection point. [o] Average value. [p] To one significant figure. [q] $(COCl)_2$. [r] Region of enhanced absorbance; wavelength listed is the lowest of those cited in the reference. [s] Average of the values given at each wavelength in the reference. [t] ϵ_c and ϵ_D are the extinction coefficients of complex and donor at the wavelengths cited. [u] There is an apparent systematic change in K_c with wavelength. [v] Average of two results. [w] Seems high. [x] Reported absorption tail. [y] Observed in solution but not in the gas phase.

ethanol (277·5 nm, 0·218 l mol^{-1}), n-propanol (278·5 nm, 0·179 l mol^{-1}) and n-butanol (279 nm, 0·077 l mol^{-1}).[388] These data undoubtedly reflect the donor behaviour of alcohol aggregates rather than the monomeric species.[390]

Barb[391] observed the onset of a CT band for styrene–SO_2 in *o*-dichlorobenzene. Up to a concentration of styrene of 2·17 M, the optical density increased in direct proportion to the SO_2 concentration. A further indication that K is small is the fact that a freezing point measurement did not reveal the formation of a complex.[392] An enthalpy determination gave a value of ~ 12 kJ mol^{-1} ($\sim 3{\cdot}0$ kcal mol^{-1}).

Studies of molecular oxygen as an electron acceptor (Section VII) include its perturbing effect on the singlet–triplet transitions of aromatic molecules which is attributed to its paramagnetism. Nitric oxide, another simple paramagnetic molecule, shows similar behaviour.[326] When NO is dissolved in a donor such as *N*,*N*-dimethylaniline or anisole, there is an absorption tail in the 300–400 nm region which is attributed (as for O_2) to a CCT band because of its relatively high intensity and lack of fine structure. A similar observation has been made of NO dissolved in methanol.[133] Evidence for weak interaction also was found in the linear dependence of the optical density on NO concentration.[133]

Prochorow and Tramer[62,393] reported that n-hexane solutions of $CO(CN)_2$ show a continuous absorption in the region $\lambda < 300$ nm which they assigned to a CCT band. This band was not found in gaseous mixtures of $CO(CN)_2$ and n-hexane at the pressures used (27 and 120 mm Hg, respectively).

ACKNOWLEDGMENT

The authors express their appreciation to Professor R. S. Mulliken for helpful comments on the manuscript in its early stages. Partial support from the National Science Foundation is also gratefully acknowledged.

REFERENCES

1. G. Briegleb, "Elektronen-Donator-Acceptor Komplexe", Springer-Verlag, Berlin (1961), (a) pp. 21–25, (b) p. 34.
2. E. N. Gur'yanova, I. P. Gol'dshtein and I. P. Romm. "Donor-Acceptor Bond", Moscow (1973); English translation, Wiley, New York (1975), (a) chapter 2, (b) p. 289, (c) p. 10.
3. R. Foster, "Organic Charge-Transfer Complexes", Academic Press, New York (1969), (a) p. 17, (b) p. 127, (c) chapters 6 and 7, (d) p. 171, (e) 160.
4. S. Tazuke, H. Tsubomura, N. Tokura and H. Mikawa, eds., "Charge-Transfer Complexes I, II", Kagakudojin, Kyoto (1971) (in Japanese).

5. L. J. Andrews and R. M. Keefer, "Molecular Complexes in Organic Chemistry", Holden-Day, San Francisco (1964).
6. J. Rose, "Molecular Complexes", Pergamon Press, New York (1967).
7. R. S. Mulliken and W. B. Person, "Molecular Complexes: A Lecture and Reprint Volume", Wiley, New York (1969), (a) p. 302, (b) p. 95, (c) p. 219, (d) p. 2, (e) p. 97, (f) p. 26, (g) p. 12, (h) p. 150, (i) p. 146.
8. J. Yarwood, ed., "Spectroscopy and Structure of Molecular Complexes", Plenum Press, New York (1973).
9. R. Foster, ed., "Molecular Complexes", Vol. 1, Elek Science, London; Crane-Russak, New York (1973), (a) Introduction.
10. R. Foster, ed., "Molecular Complexes", Vol. 2, Elek Science, London; Crane-Russak, New York (1974).
11. N. Mataga and T. Kubota, "Molecular Interactions and Electronic Spectra", Dekker, New York (1970).
12. R. Foster, ed., "Molecular Association", Vol. 1, Academic Press, London and New York (1975).
13. S. P. McGlynn, *Radiat. Res. Suppl.*, **2**, 300 (1960).
14. E. Koros, *Kem. Kozlem.* **26**, 379 (1966) (in Hungarian).
15. R. S. Mulliken, Proceedings of the Robert A. Welch Foundation Conference on Chemical Research XI. Radiation and the Structure of Matter (1967), p. 109.
16. R. S. Mulliken and W. B. Person, "Physical Chemistry", Vol. 3 (eds. Eyring, Jost and Henderson), Academic Press, New York (1969), Chapter 10.
17. C. N. R. Rao, S. N. Bhat and P. C. Dwivedi, *Applied Spectrosc. Rev.*, **5**, 1 (1971).
18. R. E. Bühler, *Radiat. Res. Rev.*, **4**, 233 (1972).
19. H. A. Benesi and J. H. Hildebrand, *J. Amer. Chem. Soc.*, **71**, 2703 (1949).
20. R. S. Mulliken, *J. Amer. Chem. Soc.*, **74**, 811 (1952).
21. R. S. Mulliken, personal communication; see also refs. 49 and 90.
22. F. A. Matsen, in "Techniques of Organic Chemistry", ed. A. Weissberger, **9** (1956), p. 688.
23. S. N. Bhat, K. R. Bhaskar and C. N. R. Rao, *Proc. Indian Acad. Sci.*, **66A**, 97 (1967).
24. M. Tamres in ref. 9, chapter 2.
25. R. S. Mulliken, *J. Chem. Phys.*, **61**, 20 (1964).
26. J. N. Murrell, M. Randic and D. R. Williams, *Proc. Roy. Soc.* (London), **A284**, 566 (1965).
27. M. W. Hanna and J. L. Lippert in ref. 9, chapter 1.
28. M. W. Hanna, *J. Amer. Chem. Soc.*, **90**, 285 (1968).
29. J. L. Lippert, M. W. Hanna and P. J. Trotter, *J. Amer. Chem. Soc.*, **91**, 4035 (1969).
30. M. Mantione, in "Molecular Associations in Biology", ed. B. Pullman, Academic Press, New York (1968), p. 411.
31. M. Mantione, *Theoretica Chem. Acta*, **11**, 119 (1968).
32. M. J. S. Dewar and C. C. Thompson, Jr., *Tetrahedron Suppl.*, **7**, 97 (1966).
33. D. Atack and O. K. Rice, *J. Phys. Chem.*, **58**, 1017 (1954).
34. E. C. Cook and J. C. Schug, *J. Chem. Phys.*, **53**, 723 (1970).
35. R. J. W. LeFèvre, D. V. Radford and P. J. Stiles, *J. Chem. Soc., B*, 1297 (1968).
36. H. Umeyama, K. Morokuma and S. Yamabe, *J. Amer. Chem. Soc.*, **99**, 330 (1977).
37. M. S. Sambhi, *J. Phys. Chem.*, **77**, 2290 (1973).
38. O. K. Rice, *Int. J. Quantum Chem.*, Symp. No. **2**, 219 (1968).
39. E. J. Robbins and R. E. Leckenby, *Nature*, **206**, 1253 (1965).
40. G. W. Castellan, "Physical Chemistry", Addison-Wesley, Reading, Mass., 2nd ed. (1971), p. 37.

41. S. Nagakura in ref. 46, vol. **2**, p. 321.
42. J. B. Birks, *Nature*, **214**, 1187 (1967).
43. Th. Forster, *Pure and Applied Chem.*, **7**, 73 (1963).
44. Th. Forster, *Angew. Chem. Intern. Ed. Engl.*, **8**, 333 (1969).
45. M. Ottolenghi, *Accounts Chem. Res.*, **6**, 153 (1973).
46. E. C. Lim, ed., "Excited States", Vol. 1, Academic Press, New York (1974); Vol. 2 (1975).
47. M. Gordon, W. R. Ware, P. deMayo and D. R. Arnold, "The Exciplex", Academic Press, New York (1975).
48. R. S. Mulliken, *Rec. Trav. Chim. Pays-Bas.*, **75**, 845 (1956).
49. J. N. Murrell, *J. Amer. Chem. Soc.*, **81**, 5037 (1959).
50. J. N. Murrell, *Quart. Rev.* (London), **15**, 287 (1961).
51. W. Liptay, in "Modern Quantum Chemistry; Part II", ed. O. Sinanoglu, Academic Press, New York (1965), section II.B, part 5.
52. O. Sinanoglu, in "Molecular Associations in Biology", ed. B. Pullman, Academic Press, New York (1968), p. 427.
53. P. Suppan, *J. Chem. Soc.* (*A*), 3125 (1968).
54. K. M. C. Davis in ref. 12, chapter 3.
55. A. T. Amos and B. L. Burrows, *Advan. Quantum Chem.*, **7**, 289 (1973).
56. M. F. Nicol, *Applied Spectrosc. Rev.*, **8**, 183 (1974).
57. J. Homer, *Applied Spectrosc. Rev.*, **9**, 1 (1975).
58. S. D. Christian, Office of Saline Water Research and Development Progress Report No. 706, July (1971).
58a. M. Jauquet and P. Laszlo, in "Techniques of Chemistry, Vol. 8, part 1: Solutions and Solubilities", eds. A. Weissberger and M. R. J. Dack, Wiley-Interscience, New York (1975).
59. S. D. Christian, in "Techniques of Chemistry, Vol. 8, part 1: Solutions and Solubilities", eds. A. Weissberger and M. R. J. Dack, Wiley-Interscience, New York (1975).
60. M. Tamres, *J. Phys. Chem.*, **65**, 654 (1961).
61. S. Carter, J. N. Murrell and E. J. Rosch, *J. Chem. Soc.*, 2048 (1965).
62. J. Prochorow and A. Tramer, *J. Chem. Phys.*, **44**, 4545 (1966).
63. P. J. Trotter, *J. Amer. Chem. Soc.*, **88**, 5721 (1966).
64. C. J. Biaselle and J. G. Miller, *J. Amer. Chem. Soc.*, **96**, 3813 (1974).
65. D. V. Fenby, *Aust. J. Chem.*, **26**, 1143 (1973), and references therein.
66. E. M. Engler and P. Laszlo, *J. Amer. Chem. Soc.*, **93**, 1317 (1971).
67. D. F. Evans, *J. Chem. Phys.*, **23**, 1424 (1955).
68. E. Guggenheim, *Trans. Faraday Soc.*, **56**, 1159 (1960).
69. M. J. Blandamer and M. F. Fox, *Chem. Rev.*, **70**, 59 (1970).
70. M. F. Fox and T. F. Hunter, *Nature*, **223**, 177 (1969).
71. P. C. Dwivedi and C. N. R. Rao, *Spectrochim. Acta*, **26A**, 1535 (1970).
72. E. G. Polle, *Russian Chem. Rev.* (*Usp. Khim.*), **43**, 631 (1974).
73. R. Foster in ref. 10, chapter 3.
74. R. L. Scott, *Rec. Trav. Chim. Pays-Bas*, **75**, 787 (1956).
75. G. Scatchard, *Ann. New York Acad. Sci.*, **51**, 660 (1949).
76. R. Foster, D. L. Hammick and A. A. Wardley, *J. Chem. Soc.*, 3817 (1953).
77. R. Foster and C. A. Fyfe, *Trans. Faraday Soc.*, **61**, 1626 (1965).
78. W. B. Person, *J. Amer. Chem. Soc.*, **87**, 167 (1965).
79. G. Cilento and D. L. Sanioto, *Z. Phys. Chem.* (Leipzig), **223**, 333 (1963).
80. P. R. Hammond and R. H. Knipe, *J. Amer. Chem. Soc.*, **89**, 6063 (1967) and subsequent papers.

81. J. Grundnes, M. Tamres and S. N. Bhat, *J. Phys. Chem.*, **75**, 3682 (1971).
82. J. D. Childs, Ph.D. Dissertation, University of Oklahoma, Norman, Oklahoma (1971).
83. J. D. Childs, S. D. Christian, J. Grundnes and S. R. Roach, *Acta Chem. Scand.*, **25**, 1679 (1971).
84. J. D. Childs, S. D. Christian and J. Grundnes, *J. Amer. Chem. Soc.*, **94**, 5657 (1972).
85. M. Tamres and S. N. Bhat, *J. Amer. Chem. Soc.*, **95**, 2516 (1973).
86. H. C. Tse, Ph.D. Dissertation, University of Michigan, Ann Arbor, Michigan (1976).
87. W. J. Moore, "Physical Chemistry", Prentice-Hall, Englewood Cliffs, New Jersey, 4th ed. (1972), p. 149.
87a. R. E. Gibson and O. H. Loeffler, *J. Amer. Chem. Soc.*, **62**, 1324 (1940).
88. M. Tamres and J. Grundnes, *J. Amer. Chem. Soc.*, **93**, 801 (1971).
89. H. Morita and M. Tamres, *J. Phys. Chem.*, **80**, 891 (1976).
90. J. E. Prue, *J. Chem. Soc.*, 7534 (1965).
91. M. Kroll, *J. Amer. Chem. Soc.*, **90**, 1097 (1968).
92. E. H. Lane, S. D. Christian and J. D. Childs, *J. Amer. Chem. Soc.*, **96**, 38 (1974).
93. L. J. Andrews and R. M. Keefer, *J. Amer. Chem. Soc.*, **74**, 4500 (1952).
94. L. E. Orgel and R. S. Mulliken, *J. Amer. Chem. Soc.*, **79**, 4839 (1957).
95. F. T. Lang, Ph.D. Dissertation, Rensselaer Polytechnic Institute, Troy, New York (1964).
96. F. T. Lang and R. L. Strong, *J. Amer. Chem. Soc.*, **87**, 2345 (1965).
97. W. K. Duerksen and M. Tamres, *J. Amer. Chem. Soc.*, **90**, 1379 (1968).
98. K. M. C. Davis and M. F. Farmer, *J. Chem. Soc.* (*B*), 28 (1967).
99. T. F. Hunter and D. H. Norfolk, *Spectrochim. Acta*, **25A**, 193 (1969).
100. B. B. Bhowmik, *Spectrochim. Acta*, **27A**, 321 (1971).
101. P. H. Emslie, R. Foster, C. A. Fyfe and I. Horman, *Tetrahedron*, **21**, 2843 (1965).
102. S. Carter, *J. Chem. Soc.* (*A*), 404 (1968).
103. R. L. Scott and D. V. Fenby, *Ann. Rev. Phys. Chem.*, **20**, 111 (1969).
104. R. L. Scott, *J. Phys. Chem.*, **75**, 3843 (1971).
105. R. A. LaBudde and M. Tamres, *J. Phys. Chem.*, **74**, 4009 (1970).
106. R. E. Merrifield and W. D. Phillips, *J. Amer. Chem. Soc.*, **80**, 2778 (1958).
106a. I. Deperasińska, *Bull. Acad. Pol. Sci., Ser. Sci. Math Astron. Phys.*, **23**, 93 (1975).
107. S. D. Christian, J. D. Childs and E. H. Lane, *J. Amer. Chem. Soc.*, **94**, 6861 (1972).
108. J. H. Hildebrand and R. L. Scott, "The Solubility of Non-Electrolytes", Reinhold, New York (1950).
109. J. H. Hildebrand, J. M. Prausnitz and R. L. Scott, "Regular and Related Solutions", Van Nostrand, New York (1970).
110. D. M. Golden, *J. Chem. Ed.*, **48**, 235 (1971).
111. J. Grundnes and S. D. Christian, *J. Amer. Chem. Soc.*, **90**, 2239 (1968).
112. M. Tamres and J. Yarwood in ref. 8, chapter 3.
113. M. Tamres, *J. Phys. Chem.*, **68**, 2621 (1964).
114. O. Hassel and K. O. Stromme, *Acta Chem. Scand.*, **12**, 1146 (1958).
115. S. D. Christian and J. Grundnes, *J. Am. Chem. Soc.*, **93**, 6363 (1971).
116. J. A. A. Ketelaar, *J. Phys. Radium*, **15**, 197 (1954).
117. M. Tamres and Sr. M. Brandon, *J. Amer. Chem. Soc.*, **82**, 2134 (1960).
118. L. M. Julien and W. B. Person, *J. Phys. Chem.*, **72**, 3059 (1968).
119. S. N. Bhat, M. Tamres and M. S. Rahaman, *J. Phys. Chem.*, **77**, 2756 (1973).
120. (a) F. Fairbrother, *Nature*, **160**, 87 (1947). (b) *J. Chem. Soc.*, 1051 (1948).
121. G. Kortüm and H. Walz, *Z. Elektrochem.*, **57**, 73 (1953).

122. C. J. Bolter, C. A. G. Brooks, K. M. C. Davis and M. E. Delf, *J. Chem. Soc.* (*A*), 3789 (1971).
123. L. A. Burkardt, P. R. Hammond, R. H. Knipe and R. R. Lake, *J. Chem. Soc., Perkin II*, 1350 (1973).
124. P. R. Hammond and L. A. Burkhardt, *Chem. Commun.*, 986 (1968).
125. H. Tsubomura and R. P. Lang, *J. Chem. Phys.*, **36**, 2155 (1962).
126. H. Ishida, H. Takahashi, H. Sato and H. Tsubomura, *J. Amer. Chem. Soc.*, **92**, 275 (1970).
127. M. D. Joesten and L. J. Schaad, "Hydrogen Bonding", Marcel Dekker, New York (1974); (a) Appendix and references therein.
128. D. F. Evans, *J. Chem. Soc.*, 4229 (1957).
129. M. L. McGlashan, D. Stubley and H. Watts, *J. Chem. Soc.* (*A*), 673 (1969).
130. R. M. Keefer and L. J. Andrews, *J. Amer. Chem. Soc.*, **77**, 2164 (1955).
131. O. C. Kwun and H. Hartmann, *Z. Phys. Chem.* (N.F.), **100**, 139 (1976).
132. H. Tsubomura and R. S. Mulliken, *J. Amer. Chem. Soc.*, **82**, 5966 (1960).
133. J. Jortner and U. Sokolov, *J. Phys. Chem.* **65**, 1633 (1961).
134. J. C. W. Chien, *J. Phys. Chem.*, **69**, 4317 (1965).
135. P. R. Hammond, *J. Chem. Soc.* (*A*), 3826 (1971).
136. J. Kleinberg and A. W. Davidson, *Chem. Rev.*, **42**, 601 (1948).
137. G. Kortüm and W. M. Vogel, *Z. Electrochem.*, **59**, 16 (1955).
138. W. B. Jepson and J. S. Rowlinson, *J. Chem. Soc.*, 1278 (1956).
139. J. Ham, *J. Amer. Chem. Soc.*, **76**, 3875 (1954).
140. Sr. M. Brandon, M. Tamres and S. Searles, Jr., *J. Amer. Chem. Soc.*, **82**, 2129 (1960).
141. R. Lang, *J. Amer. Chem. Soc.*, **84**, 1185 (1962).
142. T. Kubota, *J. Amer. Chem. Soc.*, **87**, 458 (1965).
143. E. M. Voigt, *J. Phys. Chem.*, **72**, 3300 (1968).
144. J. Walkley, D. N. Glew and J. H. Hildebrand, *J. Chem. Phys.*, **33**, 621 (1960).
145. J. H. Hildebrand and J. Dymond, *Proc. Nat. Acad. Sci.*, **54**, 1001 (1965).
146. S. H. Hastings, J. L. Franklin, J. C. Schiller and F. A. Matson, *J. Amer. Chem. Soc.*, **75**, 2900 (1953).
147. D. F. Evans, *J. Chem. Phys.*, **23**, 1426 (1955).
148. D. C. Wobschall and D. A. Norton, *Arch. Biochem. Biophys.*, **122**, 85 (1967).
149. C. N. R. Rao, G. C. Chaturvedi and S. N. Bhat, *J. Mol. Spectrosc.*, **33**, 554 (1970).
150. L. C. Glasgow and J. E. Willard, *J. Phys. Chem.*, **77**, 1585 (1973).
151. K. Fuke, M. Tamres and S. Nagakura, unpublished results.
152. P. D. Clark and K. E. Kolb, *J. Org. Chem.*, **42**, 359 (1977).
153. S. Freed and K. M. Sancier, *J. Amer. Chem. Soc.*, **74**, 1273 (1952).
154. V. T. Aleksanyan and B. Z. Gevorkyan, *Zh. Strukt. Khim.*, **17**, 732 (1976).
155. Z. Yoshida, N. Ishibe and H. Kusumoto, *J. Amer. Chem. Soc.*, **91**, 2279 (1969).
156. H. A. Benesi and J. H. Hildebrand, *J. Amer. Chem. Soc.* **70**, 3978 (1948).
157. E. K. Plyler and R. S. Mulliken, *J. Amer. Chem. Soc.*, **81**, 823 (1959).
158. R. M. Keefer and L. J. Andrews, *J. Amer. Chem. Soc.*, **72**, 4677 (1950).
159. L. J. Andrews and R. M. Keefer, *J. Amer. Chem. Soc.*, **73**, 462 (1951).
160. R. M. Keefer and L. J. Andrews, *J. Amer. Chem. Soc.*, **72**, 5170 (1950).
161. S. U. Choi, S. J. Chang and S. J. Kwon, *Daehan Hwahak Hwoejee*, **9**, 153 (1965) (*C.A.*, **65**, 3078a).
162. S. U. Choi and B. J. Han, *Daehan Hwahak Hwoejee*, **11**, 89 (1967) (*C.A.*, **70**, 7056b).
163. S. U. Choi and S. J. Chang, *Daehan Hwahak Hwoejee*, **9**, 169 (1965) (*C.A.*, **65**, 3078d).

164. S. U. Choi and S. J. Chang, *Daehan Hwahak Hwoejee*, **10**, 46 (1966) (*C.A.*, **66**, 32412q).
165. S. U. Choi and E. R. Kim, *Daehan Hwahak Hwoejee*, **11**, 94 (1967) (*C.A.*, **70**, 7057c).
166. M. Tamres, D. R. Virzi and S. Searles, *J. Amer. Chem. Soc.*, **75**, 4358 (1953).
167. S. Karaianev, E. D'Alessio and H. Bonadeo, *J. Amer. Chem. Soc.*, **97**, 6474 (1975).
168. J. A. A. Ketelaar, C. van de Stolpe and H. R. Gersmann, *Rec. Trav. Chim. Pays-Bas*, **70**, 499 (1951).
169. R. M. Keefer and T. L. Allen, *J. Chem. Phys.*, **25**, 1059 (1956).
170. C. E. Castro, L. J. Andrews and R. M. Keefer, *J. Amer. Chem. Soc.*, **80**, 2322 (1958).
171. L. J. Andrews and R. M. Keefer, *J. Amer. Chem. Soc.*, **74**, 458 (1952).
172. J. A. A. Ketelaar and C. van de Stolpe, *Rec. Trav. Chim. Pays-Bas*, **71**, 805 (1952).
173. C. van de Stolpe, Thesis, Amsterdam (1953).
174. J. G. Traynham and J. R. Olechewski, *J. Amer. Chem. Soc.*, **81**, 571 (1959).
175. D. A. Demeo and M. A. El-Sayed, *J. Chem. Phys.*, **52**, 2622 (1970).
176. C. Batich, O. Ermer, E. Heilbronner and J. R. Wiseman, *Angew. Chem.*, **85**, 302 (1973).
176a. Y. Kubota, *Yukagaku*, **25**, 257 (1976).
177. G. B. Sergeev, V. V. Smirnov and G. A. Bakarinov, *Vestn. Mosk. Univ., Khim.*, **15**, 358 (1974).
178. G. B. Sergeev and Chen Ton-kha, *Theor. and Exptl. Chem.*, **3**, 240 (1967).
179. G. B. Sergeev and Yu. A. Serguchev, *Theor. and Exptl. Chem.*, **4**, 258 (1968).
180. K. Watanabe, T. Nakayama and J. Mottl, *J. Quant. Spectrosc. Radiat. Transfer*, **2**, 369 (1962).
181. P. Masclet, D. Grosjean, G. Mouvier and J. Dubois, *J. Electron Spectrosc. Relat. Phenomena*, **2**, 225 (1973).
182. V. A. Lichnevskii, *Kinet. Katal.*, **6**, 406 (1965).
183. J. E. Dubois and F. Garnier, *Spectrochim. Acta*, **23A**, 2279 (1967).
184. J. E. Dubois and F. Garnier, *J. Chim. Phys.*, **63**, 351 (1966).
185. R. M. Keefer and L. J. Andrews, *J. Amer. Chem. Soc.*, **74**, 1891 (1952).
186. V. A. Brosseau, J. R. Basila, J. F. Smalley and R. L. Strong, *J. Amer. Chem. Soc.*, **94**, 716 (1972).
187. F. Brogli and E. Heilbronner, *Helv. Chim. Acta*, **54**, 1423 (1971).
188. K. Kimura, S. Katsumata, Y. Achiba, H. Matsumoto and S. Nagakura, *Bull. Chem. Soc. Japan*, **46**, 373 (1973).
189. W. A. Chupka, J. Berkowitz and D. Gutman, *J. Chem. Phys.*, **55**, 2724 (1971).
190. G. Kortüm and G. Friedheim, *Z. Naturforsch.*, **2a**, 20 (1947).
191. H. McConnell, *J. Chem. Phys.*, **22**, 760 (1954).
192. M. M. deMaine, P. A. D. deMaine and G. E. McAlonie, *J. Mol. Spectrosc.*, **4**, 271 (1960).
193. P. A. D. deMaine, *J. Chem. Phys.*, **24**, 1091 (1956).
194. P. A. D. deMaine, *Can. J. Chem.*, **35**, 573 (1957).
195. D. D. Eley, F. L. Isack and C. H. Rochester, *J. Chem. Soc.* (*A*), 1651 (1968).
196. A. A. Passchier, Ph.D. Dissertation, University of Washington, Seattle, Washington (1968).
197. A. A. Passchier and N. W. Gregory, *J. Phys. Chem.*, **72**, 2697 (1968).
198. M. Tamres, W. K. Duerksen and J. M. Goodenow, *J. Phys. Chem.*, **72**, 966 (1968).
199. A. A. Passchier, S. D. Christian and N. W. Gregory, *J. Phys. Chem.*, **71**, 937 (1967).
200. E. A. Ogryzlo and B. C. Sanctuary, *J. Phys. Chem.*, **69**, 4422 (1965).
201. W. Y. Wen and R. M. Noyes, *J. Phys. Chem.*, **76**, 1017 (1972).

202. E. I. Yakovenko, G. B. Serteev and G. P. Kalinina, *Dokl. Akad. Nauk SSSR*, **173**, 240 (1967).
203. G. A. Kokovin, *Z. Neorgan. Khim.*, **10**, 287 (1965).
204. S. N. Bhat and C. N. R. Rao, *J. Amer. Chem. Soc.*, **88**, 3216 (1966).
205. W. B. Person, W. C. Golten and A. I. Popov, *J. Amer. Chem. Soc.*, **85**, 891 (1963).
206. I. G. Arzamanova and E. Gur'yanova, *Dokl. Akad. Nauk SSSR*, **157**, 683 (1964).
206a. J. R. Masaguer, A. Sousa-Alonso, R. Bastida, J. Romero and J. A. Garcia Vazquez, *An. Quim*, **73**, 647 (1977).
207. D. Timm, *Acta Chem. Scand.*, **20**, 2219 (1966).
208. W. K. Plucknett and H. L. Richards, *J. Chem. Eng. Data*, **8**, 239 (1963).
209. G. P. Brown and J. P. Simons, *Trans. Faraday Soc.*, **65**, 3245 (1969).
210. R. G. W. Norrish and G. Porter, *Nature*, **164**, 658 (1949); G. Porter, *Proc. Roy. Soc.* (London), **A200**, 284 (1950).
211. G. Herzberg and D. A. Ramsay, *Disc. Faraday Soc.*, **9**, 80 (1950).
212. N. Davidson, R. Marshall, A. E. Larsh and T. Carrington, *J. Chem. Phys.*, **19**, 1311 (1951).
213. R. L. McCarthy and A. MacLachlan, *Trans. Faraday Soc.*, **56**, 1187 (1960).
214. J. P. Keene, *Nature*, **188**, 843 (1960).
215. S. J. Rand and R. L. Strong, *J. Amer. Chem. Soc.*, **82**, 5 (1960).
216. E. Wassermann, W. E. Falconer and W. A. Yager, *Ber. Bunsenges. Phys. Chem.*, **72**, 248 (1968).
217. S. K. Kim and J. Ross, *J. Chem. Phys.*, **42**, 263 (1965).
218. G. Porter, Z. G. Szabo and M. G. Townsend, *Proc. Roy. Soc.* (London), **A270**, 493 (1962).
219. A. G. Clarke and G. Burns, *J. Chem. Phys.*, **55**, 4717 (1971) and subsequent papers by Burns.
220. W. H. Wong and G. Burns, *J. Chem. Phys.*, **59**, 2974 (1973).
221. W. H. Wong and G. Burns, *J. Chem. Phys.*, **58**, 4459 (1973).
222. H. W. Chang and G. Burns, *J. Chem. Phys.*, **62**, 2426 (1975).
223. H. W. Chang and G. Burns, *J. Chem. Phys.*, **64**, 349 (1976).
224. D. T. Chang and G. Burns, *Can. J. Chem.*, **54**, 1535 (1976).
225. K. E. Russell and J. Simons, *Proc. Roy. Soc.* (London), **A217**, 271 (1953).
226. R. L. Strong, J. C. W. Chien, P. E. Graf and J. W. Willard, *J. Chem. Phys.*, **26**, 1287 (1957).
227. D. L. Bunker and N. Davidson, *J. Amer. Chem. Soc.*, **80**, 5085 (1958).
228. G. Porter and J. A. Smith, *Proc. Roy. Soc.* (London), **A261**, 28 (1961).
229. J. A. Blake and G. Burns, *J. Chem. Phys.*, **54**, 1480 (1971).
230. T. Kihara and K. Yamazaki, *Chem. Phys. Lett.*, **16**, 32 (1972).
231. D. E. Hoare and A. D. Walsh, *Chem. Soc., Spec. Publ.*, No. 9, 17 (1957).
232. G. Porter and J. A. Smith, *Nature*, **184**, 446 (1959).
233. M. J. Cardillo, M. S. Chow and E. F. Greene, cited in Ref. 224.
234. Y. T. Lee, cited in Ref. 223.
235. W. K. Hackmann and A. Mann, *Chem. Phys. Lett.*, **28**, 72 (1974).
236. J. R. Basila and R. L. Strong, *J. Amer. Chem. Soc.*, **96**, 701 (1974).
237. R. P. Widman and B. A. DeGraff, *J. Phys. Chem.*, **77**, 1325 (1973).
238. M. I. Christie, A. J. Harrison, R. G. W. Norrish and G. Porter, *Proc. Roy. Soc.* (London), **A231**, 446 (1955).
239. H. Van den Bergh and J. Troe, *Chem. Phys. Lett.*, **31**, 351 (1975).
240. H. Van den Bergh and J. Troe, *J. Chem. Phys.*, **64**, 736 (1976).
241. H. Hippler, K. Luther and J. Troe, *Chem. Phys. Lett.*, **16**, 174 (1972).

242. H. Hippler, K. Luther and J. Troe, *Ber. Bunsenges. Phys. Chem.*, **77**, 1104 (1973).
243. H. Hippler, K. Luther and J. Troe, *Ber. Bunsenges. Phys. Chem.*, **78**, 178 (1974).
244. J. Franck and E. Rabinowitch, *Trans. Faraday Soc.*, **30**, 120 (1934).
245. R. M. Noyes, *J. Amer. Chem. Soc.*, **77**, 2042 (1955).
246. E. Rabinowitch and W. C. Wood, *Trans. Faraday Soc.*, **32**, 1381 (1936).
247. R. M. Noyes, *Progr. Reaction Kinetics*, **1**, 129 (1961).
248. G. T. Evans and M. Fixman, *J. Phys. Chem.*, **80**, 1544 (1976).
249. R. M. Noyes, *J. Amer. Chem. Soc.*, **86**, 4529 (1964).
250. T. A. Gover and G. Porter, *Proc. Roy. Soc.* (London), **A262**, 476 (1961).
251. R. L. Strong and J. Perano, *J. Amer. Chem. Soc.*, **83**, 2843 (1961).
252. A. M. Halpern and K. Weiss, *J. Phys. Chem.*, **72**, 3863 (1968).
253. R. L. Strong and J. Perano, *J. Amer. Chem. Soc.*, **89**, 2535 (1967).
254. R. E. Bühler, *J. Phys. Chem.*, **76**, 3220 (1972).
255. R. L. Strong, S. J. Rand and J. A. Britt, *J. Amer. Chem. Soc.*, **82**, 5053 (1960).
256. S. R. Logan, R. Bonneau, J. Joussot-Dubien and P. Fornier de Violet, *J. Chem. Soc. Faraday I*, **71**, 2148 (1975).
257. J. Faure, J. C. Soulignac and J. C. Dupuy, *Compt. Rend. Acad. Sci.* (Paris), **267C**, 673 (1968).
258. P. Fornier de Violet, R. Bonneau and J. Joussot-Dubien, *Chem. Phys. Lett.*, 19, 251 (1973); *J. Chim. Phys.*, **70**, 1404 (1973).
259. A. Treinin and E. Hayon, *Int. J. Radiat. Phys. Chem.*, **7**, 387 (1975).
260. P. Fornier de Violet, R. Bonneau and J. Joussot-Dubien, *Mol. Photochem.*, **5**, 61 (1973).
261. L. I. Grossweiner and M. S. Matheson, *J. Phys. Chem.*, **61**, 1089 (1957).
262. A. Treinin and E. Hayon, *J. Amer. Chem. Soc.*, **97**, 1716 (1975).
263. J. F. Smalley, Ph.D. Thesis, "A Flash Photolysis Study of Dimethyl Sulfide and Iodine in the Gas Phase", Rensselaer Polytechnic Institute, Troy, N.Y. (1975).
264. C. Capellos and A. J. Swallow, *J. Phys. Chem.*, **73**, 1077 (1969).
265. R. E. Bühler and F. Marchetti, unpublished results (1970) cited in Refs. 18 and 266.
266. U. Brühlmann, H. Büchler, F. Marchetti and R. E. Bühler, *Chem. Phys. Lett.*, **21**, 412 (1973).
267. R. L. Strong and J. A. Kaye, *J. Amer. Chem. Soc.*, **98**, 5460 (1976).
268. R. L. Strong and F. J. Venditti, Jr., *Chem. Phys. Lett.*, **46**, 546 (1977).
269. S. P. Mishra and M. C. R. Symons, *J. Chem. Soc., Perkin, II*, 1492 (1975).
270. N. K. Bridge, *J. Chem. Phys.*, **32**, 945 (1960).
271. R. L. Strong, unpublished data.
272. J. H. Baxendale, E. M. Fielden, C. Capellos, J. M. Francis, J. V. Davies, M. Ebert, C. W. Gilbert, J. P. Keene, E. J. Land, A. J. Swallow and J. M. Nosworthy, *Nature*, **201**, 468 (1964).
273. M. Ebert, J. P. Keene, E. J. Land and A. J. Swallow, *Proc. Roy. Soc.* (London), **A287**, 1 (1965).
274. R. L. Strong, *J. Phys. Chem.*, **66**, 2423 (1962).
275. N. Yamamoto, T. Kajikawa, H. Sato and H. Tsubomura, *J. Amer. Chem. Soc.*, **91**, 265 (1969).
276. V. A. Brosseau, Ph.D. Thesis, "Photokinetic, Spectral, and Thermodynamic Properties of the Iodine Atom–Toluene Charge Transfer Complex", Rensselaer Polytechnic Institute, Troy, New York (1970).
277. J. K. Thomas, *J. Phys. Chem.*, **71**, 1919 (1967).
278. J. P. Mittal and W. H. Hamill, *J. Amer. Chem. Soc.*, **89**, 5749 (1967).

279. V. V. Kolesnikova, O. V. Kolninov, V. K. Milinchuk and S. Ya. Pshezhetskii, *Polymer Sci. U.S.S.R.*, **16**, 2874 (1974).
280. T. E. Lantz, Ph.D. Thesis, "A Study of the Photolysis and Charge-Transfer Complexes of I_2, HI, and some Alkyl Iodides in Glassy Matrices at 77 K", University of Wisconsin, Madison (1968).
281. J. S. Bartlett, Ph.D. Thesis, "Flash Photolysis of Bromine in Benzene", Rensselaer Polytechnic Institute, Troy, N.Y. (1962).
282. J. M. Bossy, R. E. Bühler and M. Ebert, *J. Amer. Chem. Soc.*, **92**, 1099 (1970).
283. J. M. Bossy and R. E. Bühler, *Int. J. Radiat. Phys. Chem.*, **6**, 85 (1974).
284. P. W. F. Louwrier and W. H. Hamill, *J. Phys. Chem.*, **73**, 1707 (1969).
285. R. E. Bühler and M. Ebert, *Nature*, **214**, 1220 (1967).
286. R. E. Bühler, *Helv. Chim. Acta*, **51**, 1558 (1968).
287. P. W. F. Louwrier and W. H. Hamill, *J. Phys. Chem.*, **73**, 1702 (1969).
288. D. F. Evans, *J. Chem. Soc.*, 345 (1953).
289. D. F. Evans, *Chem. and Ind.*, 1061 (1953).
290. A. V. Monck and J. F. Scott, *Nature*, **177**, 587 (1956).
291. D. F. Evans, *J. Chem. Soc.*, 1351 (1957).
292. C. Dijkgraaf and G. J. Hoijtink, *Tetrahedron*, Suppl. 2, **19**, 179 (1963).
293. J. Betts and J. C. Robb, *Trans. Faraday Soc.*, **64**, 2402 (1968).
294. H. Bradley, Jr. and A. D. King, Jr., *J. Chem. Phys.*, **47**, 1189 (1967).
295. C. L. Manger, J. H. Moore, Jr and M. A. Alexander, *Physiol. Chem. Phys.*, **8**, 559 (1976).
296. M. A. Slifkin and A. C. Allison, *Nature*, **215**, 949 (1967).
297. A. J. Rest, K. Salisbury and J. R. Sodeau, *J. Chem. Soc. Faraday Trans. II*, **73**, 265 (1977).
297a. H. Tsubomura, in "Prog. Photobiol. Proc. Int. Congr., 6th, 1972", ed. G. O. Schenck, Bochum, Germany (1974).
298. D. F. Evans, *J. Chem. Soc.*, 1987 (1961).
299. C. von Sonntag, K. Neuwald, H.-P. Schuchmann, F. Welke and E. Janssen, *J. Chem. Soc. Perkin II*, 171 (1975).
300. N. Yamamoto, S. Akaishi and H. Tsubomura, *Chem. Phys. Lett.*, **15**, 458 (1972).
301. J. B. Birks, "Organic Molecular Photophysics", Vol. 2, John Wiley and Sons, New York, N.Y. (1975), p. 522.
302. J. N. Murrell, *Mol. Phys.*, **3**, 319 (1960).
303. D. J. Carlsson and J. C. Robb, *Trans. Faraday Soc.*, **62**, 3403 (1966).
304. J. Jortner, M. Ottolenghi and G. Stein, *J. Phys. Chem.*, **68**, 247 (1964).
305. K. S. Wei and A. H. Adelman, *Tetrahedron Letters*, 3297 (1969).
306. N. Kulevsky, P. V. Sneeringer, L. D. Grina and V. I. Stenberg, *Photochem. Photobiol.*, **12**, 395 (1970).
307. N. Kulevsky, P. V. Sneeringer and V. I. Stenberg, *J. Org. Chem.*, **37**, 438 (1972).
308. V. I. Stenberg, P. V. Sneeringer, C. Niu and N. Kulevsky, *Photochem. Photobiol.*, **16**, 81 (1972).
309. L. M. Gurdzhiyan, O. L. Kaliya and T. N. Fesenko, *Zh. Prikl. Spektrosk.*, **25**, 319 (1976).
310. V. I. Stenberg, R. D. Olson, C. T. Wang and N. Kulevsky, *J. Org. Chem.*, **32**, 3227 (1967).
311. N. Kulevsky, C. T. Wang and V. I. Stenberg, *J. Org. Chem.*, **34**, 1345 (1969).
312. K. Maeda, A. Nakane and H. Tsubomura, *Bull. Chem. Soc. Japan*, **48**, 2448 (1975).
313. H. Tsubomura, T. Yagishita and H. Toi, *Bull Chem. Soc. Japan.*, **46**, 3051 (1973).
314. O. L. J. Gijzeman, F. Kaufman and G. Porter, *J. Chem. Soc. Faraday II*, **69**, 708 (1973).

315. T. Brewer, *J. Amer. Chem. Soc.*, **93**, 775 (1971).
316. D. R. Kearns, *Chem. Revs.*, **71**, 395 (1971).
317. W. R. Ware and C. Lewis, *J. Chem. Phys.*, **57**, 3546 (1972).
318. C. Lewis and W. R. Ware, *J. Chem. Soc. Faraday II*, **72**, 1851 (1976).
319. H. W. Buschmann, *Ber. Bunsenges. Phys. Chem.*, **78**, 1344 (1974).
320. E. C. Lim and V. L. Kowalski, *J. Chem. Phys.*, **36**, 1729 (1962).
321. J. B. Birks, E. Pantos and T. D. S. Hamilton, *Chem. Phys. Lett.*, **20**, 544 (1973).
322. C. Dijkgraaf, R. Sitters and G. J. Hoijtink, *Mol. Phys.*, **5**, 643 (1962).
323. D. F. Evans, 2nd Internationales Farbensymposium, Optische Anregung Organischer Systeme (1964), p. 586; cited in G. J. Hoytink, *Acct. Chem. Res.*, **2**, 114 (1969).
324. L. J. Heidt and L. Ekstrom, *J. Amer. Chem. Soc.*, **79**, 1260 (1957).
325. D. F. Evans, *J. Chem. Soc.*, 3885 (1957).
326. T. Sakata, T. Okai and H. Tsubomura, *Bull. Chem. Soc. Japan*, **48**, 2207 (1975).
327. G. Navon, *J. Phys. Chem.*, **68**, 969 (1964); H. Levanon and G. Navon, *J. Phys. Chem.*, **73**, 1861 (1969).
328. C. A. Heller and A. N. Fletcher, *J. Phys. Chem.*, **69**, 3313 (1965).
329. W. M. Mazee and A. Van der Weil, *Rec. Trav. Chim. Pays-Bas*, **84**, 1044 (1965).
329a. H. Ishida and H. Tsubomura, *J. Photochem.*, **2**, 285 (1973).
330. H. F. Priest and W. C. Schumb, *J. Amer. Chem. Soc.*, **70**, 2291 (1948).
331. D. P. N. Satchell and R. S. Satchell, *Chem. Rev.*, **69**, 251 (1969).
332. H. Tsubomura, *Bull. Chem. Soc. Japan*, **27**, 1 (1954).
333. C. Dijkgraaf, *J. Phys. Chem.*, **69**, 660 (1965).
334. J. B. Ott, J. R. Goates, R. J. Jensen and N. F. Mangelson, *J. Inorg. Nucl. Chem.*, **27**, 2005 (1965).
335. P. Job, *C. R. Acad. Sci.* (Paris), **180**, 928 (1925).
336. J. J. Myher and K. E. Russell, *Can. J. Chem.*, **42**, 1555 (1964).
337. P. R. Hammond and R. R. Lake, *J. Chem. Soc.* (*A*), 3800 (1971).
338. P. R. Hammond and R. R. Lake, *J. Chem. Soc.* (*A*), 3806 (1971).
339. P. R. Hammond and W. S. McEwan, *J. Chem. Soc.* (*A*), 3812 (1971).
340. P. R. Hammond and R. R. Lake, *J. Chem. Soc.* (*A*), 3819 (1971).
341. P. R. Hammond, *J. Phys. Chem.*, **72**, 2272 (1968).
342. M. Hatano and O. Ito, *Bull. Chem. Soc. Japan*, **44**, 916 (1971).
343. P. R. Hammond and R. R. Lake, *Chem. Commun.*, 987 (1968).
344. S. Echiba, M. Mishima and H. Negita, *Bull. Chem. Soc. Japan*, **42**, 1486 (1969).
345. F. J. Streiter and D. H. Templeton, *J. Chem. Phys.*, **37**, 161 (1962).
346. J. R. Goates, R. J. Sullivan and J. B. Ott, *J. Phys. Chem.*, **63**, 589 (1954).
347. P. R. Hammond, *J. Chem. Soc.* (*A*), 145 (1968).
348. J. D. Webb and E. R. Bernstein, *J. Amer. Chem. Soc.*, **100**, 483 (1978).
349. H. L. Krauss and G. Gnatz, *Chem. Ber.*, **95**, 1023 (1962).
350. R. R. McLean, D. W. A. Sharp and J. M. Winfield, *J. Chem. Soc. Dalton Trans.*, 676 (1972).
351. P. R. Hammond, *J. Phys. Chem.*, **74**, 647 (1970).
352. P. R. Hammond, *J. Chem. Phys.*, **55**, 3468 (1971).
353. K. M. C. Davis and M. F. Farmer, *J. Chem. Soc.* (*B*), 859 (1968).
354. A. Tramer, *Bull. Acad. Pol. Sci., Ser. Sci. Math. Astron. Phys.*, **13**, 751 (1965).
355. D. A. Bahnick, W. E. Bennett and W. B. Person, *J. Phys. Chem.*, **73**, 2309 (1969).
356. J. R. Platt, *J. Chem. Phys.*, **17**, 484 (1949).
357. W. J. Lautenberger, E. N. Jones and J. G. Miller, *J. Amer. Chem. Soc.*, **90**, 1110 (1968).
358. D. P. Stevenson and G. M. Coppinger, *J. Amer. Chem. Soc.*, **84**, 149 (1962).

359. F. Dorr and G. Buttgereit, *Ber. Bunsenges. Phys. Chem.*, **67**, 867 (1963).
360. R. F. Weimer and J. M. Prausnitz, *J. Chem. Phys.*, **42**, 3643 (1965).
361. D. R. Rosseinsky and H. Kellawi, *J. Chem. Soc. (A)*, 1207 (1969).
362. J. Homer and M. C. Cooke, *J. Chem. Soc. (A)*, 777 (1969).
363. J. Homer and P. J. Huck, *J. Chem. Soc. (A)*, 277 (1968).
364. C. J. Creswell and A. L. Allred, *J. Phys. Chem.*, **66**, 1469 (1962).
365. H. Modaress and M. Edrissi, *Michrochem. J.*, **22**, 451 (1977).
366. D. A. Bahnick and W. B. Person, *J. Chem. Phys.*, **48**, 1251 (1968).
367. B. Stevens and M. Boudart, *Ann. New York Acad. Sci.*, **67**, 570 (1957).
368. W. H. Meluish and W. S. Metcalf, *J. Chem. Soc.*, 480 (1958).
369. E. J. Bower and K. K. Rohatgi, *Discuss. Faraday Soc.*, **14**, 147 (1953).
370. E. Heilbronner, *Helv. Chim. Acta*, **36**, 1121 (1953).
371. N. S. Bayliss and C. J. Brackenridge, *J. Amer. Chem. Soc.*, **77**, 3959 (1955).
372. R. Anderson, R. Cambio and J. M. Prausnitz, *Amer. Inst. Chem. Engineers J.*, **8**, 66 (1962).
373. R. Anderson and J. M. Prausnitz, *J. Chem. Phys.*, **39**, 1225 (1963).
374. V. F. Traven and R. West, *J. Amer. Chem. Soc.*, **95**, 6824 (1973).
375. H. Sakurai, M. Kira and T. Uchida, *J. Amer. Chem. Soc.*, **95**, 6826 (1973).
376. V. F. Traven and R. West, *J. Gen. Chem. U.S.S.R.*, **44**, 1803 (1974).
377. H. C. Gardner and J. K. Kochi, *J. Amer. Chem. Soc.*, **98**, 2460 (1976).
378. H. C. Gardner and J. K. Kochi, *J. Amer. Chem. Soc.*, **97**, 1855 (1975).
379. H. C. Gardner and J. K. Kochi, *J. Amer. Chem. Soc.*, **97**, 5026 (1975).
380. C. D. Smith, *J. Amer. Chem. Soc.*, **88**, 4273 (1966).
381. I. Tabushi and K. Yamamura, *Tetrahedron*, **31**, 1827 (1975).
382. V. F. Traven, V. F. Donyagina, N. S. Fedotov, G. V. Évert and B. I. Stepanov, *Zh. Obshch. Khim.*, **46**, 2761 (1976).
383. L. J. Andrews and R. M. Keefer, *J. Amer. Chem. Soc.*, **77**, 2164 (1955).
384. P. R. Hammond and L. A. Burkardt, *J. Phys. Chem.*, **74**, 639 (1970).
384a. P. R. Hammond, *J. Chem. Soc. (A)*, 145 (1968).
385. R. F. Weimer and J. M. Prausnitz, *Spectrochim. Acta*, **22**, 77 (1966).
386. L. J. Andrews and R. M. Keefer, *J. Amer. Chem. Soc.*, **73**, 4169 (1951).
387. J. A. Moede and C. Curran, *J. Amer. Chem. Soc.*, **71**, 852 (1949).
388. P. A. D. deMaine, *J. Chem. Phys.*, **26**, 1036 (1957).
389. D. Booth, F. S. Dainton and K. J. Ivin, *Trans. Faraday Soc.*, **55**, 1293 (1959).
390. H. C. Tse and M. Tamres, *J. Phys. Chem.*, **81**, 1367, 1376 (1977).
391. W. G. Barb, *Proc. Roy. Soc.* (London), **A212**, 66 (1952).
392. C. S. Marvel and F. J. Glavis, *J. Amer. Chem. Soc.*, **60**, 2622 (1938).
393. J. Prochorow, *J. Chem. Phys.*, **43**, 3394 (1965).
394. N. Wiberg and J. W. Buchler, *Chem. Ber.*, **97**, 618 (1964).
395. N. B. Jurinski and P. A. D. de Maine, *J. Amer. Chem. Soc.*, **86**, 3217 (1964).
396. G. Briegleb and J. Czekalla, *Z. Elektrochem.*, **59**, 184 (1955).
397. B. D. Saksena and R. E. Kagarise, *J. Chem. Phys.*, **19**, 994 (1951).

Author Index

Numbers in italics refer to pages where the reference is listed in full

A

Aalst, R. M., van, 275(49), *326*
Abdul-Karim, A., 181(110), 188(110), *259*
Abegg, H., 178(74), *258*
Abragam, A., 286(124), *328*
Achiba, Y., 60(148a, 148b, 148c, 152, 153), *76*, 369(188), *451*
Adams, J. E., 96(73), *166*
Adelman, A. H., 408(305), 411(305), *454*
Adrian, F. J., 70(185), *78*
Aivazov, B. V., 239(316, 320), 248 (316, 320), *264*, *265*
Akaishi, S., 406(300), 411(300), *454*
Akazawa, H., 63(162), *77*
Alchalal, A., 59(146), 60(146), *76*
Aleksanyan, V. T., 365(154), 372(154), *450*
Alexander, M. A., 403(295), *454*
Algar, B. E., 28(87), *74*
Allegrini, I., 178(81), *258*
Allen, R. H., 178(79), *258*
Allen, T. L., 366(169), 377(169), 378(169), *451*
Allison, A. C., 405(296), 410(296), 411 (296), 412(296), 413(296), 414(296), *454*
Allred, A. L., 205(189, 191), *261*, 430 (364), *456*
Alms, G. R., 277(54, 60), 278(54), 309 (54), *326*, *327*
Al-Thamir, W. K., 253(335), *265*
Amdur, I., 63(161), *77*
Amorin da Costa, A. M., 273(36), 323 (36), 325(36), *326*
Amos, A. T., 338(55), 344(55), *448*
Andersen, H. C., 289(119), 298(119), 300(119), 302(119), 303(119), 317(119), 323(119), 325(119), *328*
Anderson, J. E., 275(45), *326*
Anderson, J. R. A., 184(131), *260*
Anderson, R., 431(372), 433(373), *456*
Andrews, L. J., 332(5), 333(5), 344(93), 358(130), 366(93, 158, 159, 160, 170, 171), 367(171), 368(185), 373(93, 158, 159), 375(171), 430(93), 438(383), 442 (386), 444(170), 445(386), *447*, *449*, *450*, *451*, *456*
Andrianova, L. V., 107(90), 152(90), *166*
Arai, K., 100(78), 101(78), 105(78, 88), *166*
Arimitsu, S., 28(80a, 80b), 62(80a), *74*
Armstrong, A. T., 4(26b), *72*
Armstrong, R. L., 279(65), 296(65), *327*
Arndt, R., 271(30), 273(30), 276(107), 285(30, 107), 286(30, 107), 288(30), 289(30), 290(30, 107), 296(30, 107), 298(30, 129, 131), 299(30), 300(135), 301(30, 135), 302(129), 308(129), 309 (129), 312(131), 313(131), 314(128, 135), 317(107), 318(107), 319(107), 320 (107), 321(107, 156), 323(107), 324 (107), *326*, *328*, *329*
Arnold, D. R., 337(47), *448*
Arzamanova, I. G., 379(206), *452*
Ashbury, G. K., 176(40), *257*
Asher, M., 48(131), 54(131), 55(131), *76*
Ashwell, G. J., 139(148), *168*
Ashworth, A. J., 180(99), 184(134), 185 (134), 226(240), 230(240), 239(240), 243(240), *259*, *260*, *262*
Assink, R. E., 281(80), *327*
Atack, D., 335(33), 345(33), 346(33), 352 (33), 353(33), 378(33), *447*
Au Clair, C., 109(95), *166*
Axelrod, H. D., 178(79), *258*
Ayres, B. O., 178(70), *258*

Ayres, J. T., 109(96), *166*
Azumi, T., 4(26b), 28(90), 65(90, 168), *72*, *75*, *77*

B

Badger, B., 88(39), *165*
Bahnick, D. A., 430(355), 431(366), 434 (355), 435(355), *455*, *456*
Bailey, R. J., 85(27), 86(27), *164*
Bailey, R. T., 269(12), 272(12), 276(12), 278(12), 279(12), 325(12), *325*
Baise, A., 275(48), *326*
Baiulescu, G. E., 200(177), *261*
Bakarinov, G. A., 367(177), *451*
Bakshiev, N. G., 15(64a), *73*
Balogh, V., 107(91), *166*
Banba, F., 103(85), 104(85), *166*
Banda, F. P., 195(173), 202(173), 205 (173), *261*
Bandrauk, A. D., 85(26), *164*
Barb, W. G., 446(391), *456*
Bard, A. J., 8(43), 20(43, 44), 20(71), 21(43, 44), 22(43, 44, 71), *73*, *74*
Bardoux, R., 269(13), *325*
Barlow, W. A., 149(175), *169*
Barnard, J. A., 221(224), 237(224), *262*
Barrett, J. W., 172(2), *256*
Bartholomew, R. F., 61(156), *77*
Bartlett, J. S., 401(281), *454*
Bartoli, F. J., 270(14), 272(14), 274(14), 295(14), 308(14), 317(14), 323(14), *325*
Basila, J. R., 369(186), 382(236), 384 (236), 399(186), 400(186), 401(186, 236), *451*, *452*
Bastida, R., 379(206a), *452*
Batich, C., 367(176), *451*
Batyrev, Yu. A., 205(199), *261*
Bauer, D. R., 277(54, 60), 278(54), 309 (54), 310(54), *326*, *327*
Baxendale, J. H., 398(272), *453*
Bayer, E., 237(301), *264*
Bayliss, N. S., 431(371), *456*
Bazinet, M. L., 178(71), *258*
Bear, J. L., 187(146), *260*
Beattie, J. A., 180(102), *259*
Becker, H. D., 89(45), *165*
Bednar, T. W., 3(10), 52(10), *71*
Beens, H., 3(11, 13, 14), 4(13), 6(29b), 40(117), 41(117), 42(13, 117), 44(121), 58(117), *72*, *75*, 87(33), *165*
Beer, C. W., 277(56), 323(56), *327*
Behan, J., 96(73), *166*
Behlau, H., 178(85), *259*
Bendig, J., 93(65), *165*
Benesi, H. A., 332(19), 340(19), 344(19), 336(19, 156), *447*, *450*
Bennett, W. E., 430(355), 434(355), 435 (355), *455*
Ben-Reuven, A., 277(59), *327*
Benz, C. A., 231(272, 273), *263*
Berezkin, V. G., 182(128), *260*
Berkowitz, J., 370(189), *451*
Bernard, E., 89(46), 92(60), *165*
Berne, B. J., 269(9), 275(46), 276(52), 278(9), 281(81), 283(98), 284(102), *325*, *326*, *328*
Bernstein, E. R., 421(348), 429(348), *455*
Betti, A., 186(140), *260*
Betts, J., 403(293), 415(293), *454*
Bezot, P., 282(97), 283(97), *328*
Bhaskar, K. R., 333(23), 354(23), 355(23), 365(23), 371(23), *447*
Bhat, S. N., 332(17), 333(23), 342(81, 85), 343(85), 354(23, 119), 355(17, 23, 119), 357(17), 361(119), 362(119, 149), 364 (119), 365(17, 23), 368(149), 371(17), (23, 119, 149), 372(119), 376(149), 377(119), 379(17, 204), 419(17), 435 (17), *447*, *449*, *450*, *452*
Bhowmik, B. B., 346(100), 355(100), *449*
Biarge, J. F., 239(319), 240(319), *264*
Biaselle, C. J., 339(64), *448*
Bighi, C., 186(140), *260*
Birks, J. B., 2(4, 7), 9(4, 7, 47), 28(84, 85), *71*, *73*, *74*, 83(10, 11), 88(10), *164*, 337(42), 406(301), 410(321), *448*, *454*, *455*
Bixon, M., 18(66c), *74*
Blake, J. A., 382(229), *452*
Blandamer, M. J., 339(69), *448*
Blau, K., 221(228), 238(228), *262*
Bleyser, J., de, 271(29), 285(29, 109), 286(29, 109), 289(29), 290(109), 296 (29, 109), 297(109), 298(29, 109), 308 (29), 312(29, 109), 314(109), *326*, *328*
Block, H., 124(133), *167*
Blumenfeld, S. M., 279(65), 296(65), *327*
Bobak, A., 238(304), *264*
Bock, E., 316(148), 317(148), *329*
Bogoslovsky, Yu. N., 277(250), *263*

Bolter, C. J., 356(122), 404(122), 410 (122), 412(122), 415(122), *450*
Bolton, H. C., 178(90), *259*
Bonadeo, H., 366(167), 373(167), *451*
Bondarev, A. F., 302(136), *329*
Bonneau, R., 392(256, 258, 260), 398 (256), 399(258), 402(256), *453*
Bonniface, O. W., 142(158), *168*
Boos, H., 13(58b), 47(123), *73*, *75*
Booth, D., 442(389), 445(389), *456*
Bopp, T. T., 323(161), *329*
Borger, M. M., 230(288), *264*
Borkent, J. H., 89(50), 92(61), *165*
Born, F., 237(301), *264*
Bossy, J. M., 401(282, 283), *454*
Bouanich, J. P., 279(64), *327*
Boudart, M., 431(367), *456*
Boudevska, H., 100(77), *166*
Bowen, B. E., 177(61), 178(83), *258*
Bowen, E. J., 431(369), *456*
Boyd, R. H., 88(38), *165*
Brackenridge, C. J., 431(371), *456*
Bradford, B. W., 184(135), *260*
Bradley, H., Jr, 403(294), *454*
Brady, G. W., 230(284, 285, 292), *263*, *264*
Braithwaite, M. J., 142(158), *168*
Brandon, M., Sr, 353(117), 355(117), 360(140), *449*, *450*
Brant, G. J., 15(64b), *74*
Bratos, S., 269(6, 7), 270(7), 285(6, 7, 115), 286(6, 7), 287(6, 7), 296(6, 7, 115), 297(6, 7, 115), *325*, *328*
Brauman, J. I., 277(54, 60), 278(54), 309(54), 310(54), *326*,*327*
Braun, J-M., 217(218), *262*
Braunschweig, T. U., 298(129a), 301 (129a), 302(129a), 308(129a), 309 (129a), 314(129a), *328*
Brazhnikov, V. V., 178(86), *259*
Breene, R. G., 269(8), *325*
Breuillard-Alliot, C., 323(159), 324(159), *329*
Brewer, T., 28(89), *74*, 416(315), *455*
Brida, J., 238(304), *264*
Bridge, N. K., 398(270), 399(270), 401 (270), *453*
Bridgeman, O. C., 180(102), *259*
Briegleb, G., 34(101), *75*, 332(1), 333(1), 337(1), 351(1), 353(1), 355(1), 376(1), 432(1), 444(1, 396), 445(1), *446*, *456*
Bright, A. A. S., 85(27), 86(27), *164*, 234 (294), *264*
Britt, J. A., 391(255), 398(255), *453*
Brocklehurst, B., 70(182, 183, 187), *77*, *78*, 88(39), *165*
Brodbeck, C., 308(139), 309(139), *329*
Brogli, F., 369(187), *451*
Brooks, C. A. G., 356(122), 404(122), 410(122), 412(122), 415(122), *450*
Brooks, F. R., 237(298), *264*
Brooks, J. J., 186(143), 200(143), *260*
Brosseau, V. A., 369(186), 398(276), 399 (186), 400(186), 401(186), *451*, *453*
Brot, C., 275(47), 282(85, 92), 285(85), 307(92), *326*, *327*
Brown, G. P., 374(209), 375(209), 376 (209), 434(209), 435(209), *452*
Brown, K. H., 100(79), 101(79), *166*
Brown, R. E., 89(44), *165*
Brühlmann, U., 394(266), *453*
Bruner, F., 178(81, 82), *258*
Bruson, H. A., 107(89), *166*
Bube, W., 71(188), *78*
Bucaro, J. A., 281(82), *327*
Büchler, H., 394(266), *453*
Buchler, J. W., 443(394), *456*
Buchowski, H., 238(307), *264*
Bühler, R. E., 332(18), 389(18, 254), 390 (254), 391(254), 394(18, 265, 266), 399 (286), 401(282, 283, 285, 286), 402 (285, 286), *447*, *453*, *454*
Bull, H., 176(43), *257*
Bull, T. E., 281(78, 79), 323(78), 324(78, 79), *327*
Bunker, D. L., 382(227), *452*
Burgers, P. J. H., 271(29), 285(29), 286 (29), 289(29), 296(29), 298(29), 308(29), 312(29), *326*
Burkardt, L. A., 357(123, 124), 417(123, 124), 418(123), 419(123), 422(123), 423 (123), 434(123), 442(384), 443(384), 444(384), *450*, *456*
Burke, M. F., 178(66), *258*
Burns, G., 380(219), 381(219, 220, 221, 222, 223, 224), 382(220, 221, 222, 229), 383(223), *452*
Burrows, B. L., 338(55), 344(55), *448*
Buschmann, H. W., 410(319), 415(319), *455*
Buser, U., 93(66), *165*
Butler, G. B., 107(89), 154(184), *166*, *169*

Buttgereit, G., 430(359), 433(359), 434 (359), *456*
Buyanova, N. Y., 172(26), *257*

C

Cabana, A., 269(13), *325*
Cadogan, D. F., 188(157), 200(179), 253(179), *260*, *261*
Caldwell, R. A., 89(42), *165*
Cambio, R., 431(372), 456
Campbell, J. H., 289(122), 296(122), 297 (122), 298(122), 302(122), 303(122), 308(141a), 309(141a), 311(141a), *328*, *329*
Canulli, C., 178(82), *258*
Capellos, C., 393(264), 398(272), 399 (264), *453*
Cardillo, M. J., 382(233), *452*
Carle, D. W., 178(69), *258*
Carlson, R. L., 207(208), *262*
Carlsson, D. J., 408(303), 411(303), 415 (303), *454*
Carrington, T., 379(212), *452*
Carroll, F. A., 34(103), *75*
Carter, S., 338(61), 346(61, 102), 347(61), *448*, *449*
Carruthers, R., 89(52), *165*
Cassidy, H. G., 151(180), *169*
Casteilan, G. W., 336(40), *447*
Castells, R. C., 194(169), 206(169), *261*
Castille, Y., 107(91), *166*
Castro, C. E., 366(170), 444(170), *451*
Chaffee, C. S., 231(257), *263*
Chalkley, D. E., 184(135), *260*
Chamberlain, C. S., 196(174), 202(174), 234(174), *261*
Chamberland, A., 269(13), *325*
Chambers, J. Q., 149(174), *169*
Chance, R. R., 158(203), *169*
Chandross, E. A., 3(17), 5(27b), 7(17), 13(27b, 62), 21(70), 24(73), 35(27b), 37(17), 52(62, 138), *72*, *73*, *74*, *76*, 89 (40, 42), *165*
Chang, D. T., 381(224), *452*
Chang, G. T., 180(104), *259*
Chang, H. W., 381(222, 223), 382(222), 383(223), *452*
Chang, R. C., 196(175), 196(175), *261*
Chang, S. J., 366(161, 163, 164), 373(161, 163, 164), *450*, *451*
Chao, H. M., 61(155), *77*
Chappelear, P. S., 192(20), *257*
Chaturvedi, G. C., 362(149), 368(149), 371(149), 376(149), *450*
Chen, I., 121(124), *167*
Cheng, S. C., 223(236), *262*
Chen Ton-Kha, 367(178), *451*
Cherkashin, M. I., 84(16), 100(16), *164*
Chiellini, E., 97(74), 98(74), 106(74), *166*
Chien, J. C. W., 358(134), 382(226), 403(134), 405(134), 408(134), 410(134), 411(134), 413(134), 414(134), 415(134), *450*, *452*
Childs, J. D., 342(82, 83, 84), 343(82), 344(92), 349(82, 92, 107), *448*
Choi, S. U., 366(161, 162, 163, 164, 165), 373(161, 162, 163, 164, 165), *450*, *451*
Chow, M. S., 382(233), *452*
Chow, P. P., 15(64b), *73*, *74*
Chow, Y. L., 62(157), *77*
Chowdhury, M., 65(167), *77*
Christian, S. D., 338(58, 59), 342(83, 84), 344(58, 59, 92), 349(92, 107), 350(111), 353(115), 377(199), 378(199), 396(111), 442(111), *448*, *449*, *451*
Christie, M. I., 383(238), *452*
Christodonleas, N., 65(167), *77*
Chuang, T. J., 8(41), 11(56), 12(41), 14(56), 19(56), 26(56), *73*
Chudek, J. A., 85(27), 86(27, 28), *164*
Chupka, W. A., 370(189), *451*
Cilento, G., 342(79), *448*
Clark, P. D., 365(152), 368(152), *450*
Clarke, A. G., 380(219), 381(219), *452*
Clarke, J. H. R., 273(36), 323(36), 325(36), *326*
Clerc, M., 285(104), 296(104), 312(104), *328*
Cohen, J. I., 61(155), *77*
Cohen, M. J., 84(19), *164*
Cohen, S. G., 28(79), 29(79, 93), 61(79, 93, 155), 62(157), *74*, *75*, *77*
Cohen-Addad, C., 230(284), *263*
Coleman, L. B., 84(19), *164*
Comes, R., 148(171, 172), *168*
Compton, R. N., 84(21), *164*
Conder, J. R., 172(21), 173(21, 31), 181(112), 200(178), 227(245), *257*, *259*, *261*, *263*
Condon, R. D., 178(73), *258*

Constant, M., 289(120), 298(120), *328*
Cook, E. C., 335(34), *447*
Cooke, M. C., 430(362), *456*
Coppinger, G. M., 430(358), 431(358), 433(358), *455*
Cotter, R. J., 108(93), 151(93), 152(93), *166*
Cowan, D. O., 84(19), 139(149), 142 (159a), 143(161), *164*, *168*
Cowd, M. A., 124(133), *167*
Cox, R. J., 8(41), 12(41), *73*
Craenen, H. A. H., 89(53), *165*
Craig, B. B., 63(164), *77*
Cram, S. P., 177(61), 178(78, 80, 83, 92), *258*, *259*
Cramers, C. A., 176(52), 177(52), 182 (118), *258*, *259*
Creed, D., 89(42), *165*
Creighton, J. A., 270(19), *325*
Creswell, C. J., 205(189, 191), *261*, 430(364), *456*
Cropper, F. R., 172(5), *256*
Crowne, C. W. P., 188(160), 189(160), *260*
Cruickshank, A. J. B., 179(94, 95), 180(98), 181(98), *259*
Cuellar, E., 139(151), *168*
Culp, R. A. 176(47), 178(77), *258*
Curran, C., 442(387), *456*
Cuta, F., 186(144), *260*
Cutvers, N. C., 187(153), *260*
Cvetanovic, R. J., 188(163), *261*
Czajkowska, T., 205(194), *261*
Czekalla, J., 444(396), *456*
Czubryt, J. J., 178(65), *258*, 316(148), 317(148), *329*

D

Dainton, F. S., 442(389), 445(389), *456*
D'Alessio, E., 366(167), 373(167), *451*
Dal Nogare, S., 179(96), *259*
Dalton, C. J., 89(43), *165*
Danesi, P. R., 227(249), *263*
Dantzler, E. M., 180(108), *259*
Darbre, A., 221(228, 229), 238(228, 229), *262*
Dardy, H., 276(51), 295(51), *326*
Darmon, I., 275(47), *326*
David, D. J., 178(87), *259*
Davidson, A. W., 359(136), *450*
Davidson, N., 379(212), 382(227), *452*
Davidson, R. S., 4(24), 26(24), 61(156), *72*, *77*, 89(41, 49), *165*
Davis, A. J., 176(40), *257*
Davies, G. J., 282(88, 89, 90), 283(88, 89, 90), 284(89, 90, 101), 307(90), 308(90), *327*
Davies, G. R., 149(175), *169*
Davies, J. V., 398(272), *453*
Davies, K. M. C., 338(54), 344(54), 346 (54, 98), 345(98), 356(122), 368(54), 404(122), 410(122), 412(122), 415(122), 421(98, 353), 430(353), 433(98), 435 (353), *448*, *449*, *450*, *455*
Davydov, A. S., 290(125), *328*
Dawes, K., 89(43), *165*
Deal, C. H., 172(9, 10), 184(10), *256*, *257*
Dean, F. M., 89(52), *165*
Deans, D. R., 177(56), *258*
Deans, H. A., 172(19, 20), *257*
De Boer, Th. J., 89(50, 51, 53), 92(61), *165*
Debye, P., 280(67), 311(67), *327*
Degorski, A., 157(190, 191), *169*
De Graff, B. A., 384(237), *452*
Delf, M. E., 356(122), 404(122), 410(122), 412(122), 415(122), *450*
Delhaye, M., 289(121), 298(121), *328*
Demeo, D. A., 367(175), *451*
Deming, S. N., 254,(338), *265*
Dempster, C. J., 5(27b), 13(27b), 35(27b), *72*, 89(40), *165*
Denoyer, F., 148(171), *168*
Deperasinska, I., 348(106a), *449*
Derr, E. L., 172(9), *256*
Deshpande, D. D., 316(149), *329*
Desplanques, P., 324(163), 325(163), *329*
Desty, D. H., 255(343), *265*
DeVries, A., 230(283), *263*
Dewer, M. J. S., 335(32), *447*
Diamond, N. A., 142(159a), *168*
Dianoux, A. J., 270(17), *325*
Di Corcia, A., 253(336), *265*
Dielman, R., 178(84), *259*
Dielmann, R., 178(85), *259*
Diestler, D. J., 285(110c), *328*
Dijkgraaf, C., 403(292), 411(322), 417 (333), 422(333), 423(333), 424(333), *454*, *455*
Dijkstra, G., 172(11), *257*
Dill, J. F., 281(82), *327*

Dimitrov, Chr., 182(124), *260*
Dimitrova, Z. St., 187(148), *260*
Dirkx, I. P., 89(51), *165*
Dixon, R. S., 70(187), *78*
Dixon, R. T., 178(77), *258*
Djordjevic, N. M., 227(246), *263*
Dobslaw, B., 93(65), *165*
Dodiuk, H., 3(23a, 23b), 22(23a, 23b), 29(23a, 23b), 47(125), 48(23a, 125), 50(23a), *72*, *76*
Dodson, B., 85(27), 86(27), *164*, 234(294), *264*
Döge, G., 271(26, 27, 30), 273(30), 276 (107), 285(26, 30, 107), 286(26, 27), 286(30, 107), 288(30), 289(26, 27, 30, 118), 290(26, 27, 30, 107), 296(26, 30, 107), 297(26), 298(26, 27, 30, 118, 130), 299(26, 30), 300(135), 301(30, 135), 312 (26, 130), 313(26), 314(26, 135), 317 (107), 318(107), 319(107), 320(107), 321(107), 323(107), 324(107), *326*, *328*, *329*
Dominguez, J. A. G., 239(319), 240(319), *264*
Dondi, F., 186(140), *260*
Donyagina, V. F., 436(382), 438(382), 441(382), *456*
Door, F., 430(359), 433(359), 434(359), *456*
Drago, R. S., 196(174), 202(174), 207 (208), 234(174), *261*, *262*
Drifford, M., 274(39), *326*
Drinkwater, J. W., 176(40), *257*
Drucker, C., 231(280), *263*
Dubois, J. E., 367(181, 183, 184), 374 (183), 375(183), 393(183), *451*
Duerksen, W. K., 345(97), 355(97), 377 (198), 378(198), *449*, *451*
Duncan, F. T., 188(163), *261*
Dupuy, J. C., 392(257), *453*
Dwivedi, P. C., 332(17), 339(71), 355(17), 357(17), 365(17), 371(17), 379(17), 419 (17), 432(17), *447*, *448*
Dymond, J., 360(145), *450*

E

Eagles, T. E., 280(71, 72), 296(71, 72), *327*
Ebel, S., 182(120), *259*
Ebert, M., 398(272, 273), 399(273), 401 (282, 285), 402(285), *453*, *454*
Echiba, S., 419(344), *455*
Edrissi, M., 430(365), *456*
Edwards, R. L., 231(256), *263*
Efrima, S., 18(66c), *74*
Egawa, K., 15(65b), 61(65b), *74*
Ege, G., 99(75), *166*
Ehmke, B., 93(65), *165*
Eigen, M., 63(160), *77*
Eilbracht, P., 143(160), *168*
Eisenthal, K. B., 8(40, 41), 11(40, 56), 12(41), 14(56), 19(56), 26(56), 34(101), *73*, *75*
Ekstrom, L., 414(324), *455*
Eley, D. D., 139(148), 142(158), *168*, 377(195), 378(195), *451*
Ellison, M., 178(75), *258*
El-Sayed, M. A., 367(175), *451*
Elsken, J., van der, 275(49), *326*
Emerald, R. L., 115(113), 118(113), 121 (113), 123(113), 131(113), 133(113), *167*
Emslie, P. H., 346(101), *449*
Engler, E. M., 83(15), 84(21), 139(150, 149(174), *164*, *168*, *169*, 339(66), 352 (66), *448*
Eon, C., 191(167, 168), 192(167,168), 193(168), 203(183), 206(167, 168, 204), 215(167), *261*, *262*
Epstein, A. J., 84(23), *164*
Ermer, O., 367(176), *451*
Etique, P., 274(38), *326*
Ettre, L. S., 178(73), 179(97), *258*, *259*
Evans, D. F., 339(67), 358(67,128), 361 (67,128), 362(67, 128, 147), 368(67, 147), 371(128), 372(67, 128, 147), 377 (67, 128, 147), 378(147), 397(288), 403 (67, 288, 289, 291), 405(298), 408(291, 298), 410(288), 411(288, 323), 412 (288), 413(288, 298), 414(325), 431 (128), 432(128), 435(128), *448*, *450*, *454*, *455*
Evans, G. J., 284(99a, 100), 285(100), 306(99a), *328*
Evans, G. T., 385(248), *453*
Evans, M. W., 272(33), 275(33), 281(84), 282(84, 86, 87, 88, 89, 90, 91, 96), 283 (33, 87, 88, 89, 90), 284(87, 89, 90, 99a, 101), 306(84, 99a), 307(90), 308(90), *326*, *327*, *328*
Evans, R. G., 142(158), *168*

Everdell, M. H., 187(152), *260*
Everett, D. H., 179(93, 94, 95), 180(93, 99, 106), 255(344), *259*, *265*
Evert, G. V., 436(382), 438(382), 441 (382), *456*
Eyring, H., 63(159), *77*
Ezumi, K., 6(30), 25(30), 66(30), *72*

F

Factor, A., 141(156), *168*
Fairbrother, F., 355(120), *449*
Falconer, W. E., 188(163), *261*, 380(216), *452*
Farmer, M. F., 346(98), 348(98), 421(98, 353), 430(353), 433(98), 435(353), *449*, *445*
Farrell, P. G., 188(160), 189(160), *260*
Faulkner, L. R., 20(44), 21(44), 22(44), *73*
Faure, J., 392(257), *453*
Fauquembergue, R., 289(120, 121), 298 (120, 121), 324(163), 325(163), *328*, *329*
Fedotov, N. S., 436(382), 438(382), 441 (382), *456*
Feibush, B., 186(142), 196(175), 197(175), 202(142), *260*, *261*
Fenby, D. V., 339(65), 347(103), *448*, *449*
Feng, P. Y., 180(103), *259*
Ferguson, J., 4(25), *72*
Ferraris, J., 84(19), 139(149), *164*, *168*
Fesenko, T. N., 409(309), 411(309), *454*
Feuer, J., 93(68), *165*
Fielden, E. M., 398(272), *453*
Figgins, C. E., 239(323), *265*
Fini, G., 270(22), 273(22), 313(22), 314 (22, 144), 317(154), 323(154), *326*, *329*
Fischer, S. F., 285(108), 293(108), 296 (108), 297(108), 298(108), 318(108), *328*
Fisher, A. P., 84(23), *164*
Fisher, J. F., 289(122), 296(122), 297 (122), 298(122), 302(122), 303(122), *328*
Fixman, M., 385(248), *453*
Flatow, A., 90(57), *165*
Fletcher, A. N., 415(328), *455*
Flory, P. J., 182(126), *260*
Folland, D. F., 182(129), *260*
Foreman, M. I., 85(27), 86(27), *164*, 234 (294), *264*
Fornier, de Violet, P., 392(256, 258, 260), 398(256), 399(258), 402(256), *453*
Forss, D. A., 178(71), *258*
Förster, Th., 2(1, 3), 4(1), *71*, 337(43, 44), *448*
Foster, R., 80(2, 3, 4, 5), 81(2), 85(27), 86(27, 28), 93(2), *163*, *164*, 187(207), 207(207), 208(207), 234(294), *262*, *264*, 268(2), 277(2), 282(2), 310(2), *325*, 332 (3, 9, 10, 12), 333(3, 9), 338(3), 340(3, 73, 76, 77), 344(3, 73), 346(101), 348(3), 351(3), 369(3), 419(3), 435(9), *446*, *447*, *448*, *449*
Fox, M. F., 339(69, 70), *448*
Francis, J. M., 398(272), *453*
Franck, E. U., 323(162), *329*
Franck, J., 385(244), *453*
Franklin, J. L., 361(146), 366(146), 367 (146), 368(146), 369(146), 371(146), 372(146), 374(146), 376(146), 377(146), *450*
Franks, F., 230(289, 290), *264*
Freed, S., 365(153), 366(153), 371(153), 372(153), 374(153), *450*
Fredericks, E. M., 237(298), *264*
Freeguard, G. F., 180(100), *259*
Frenkel, D., 275(49), *326*
Friedheim, G., 377(190), *451*
Frilette, J. V., 178(64), *258*
Fritz, D., 182(121), *259*
Froix, M., 116(118), *167*
Fujita, T., 3(18a, 22a), 7(18a), 19(18a), 38(18a, 22a), 44(18a), 46(18a), 54(18a, 22a), *72*, 89(46), *175*
Fujiwara, H., 7(38), 53(38), *73*
Fujiyama, T., 285(112), 293 (112), 296 (112), 302(137), 308(137), 318(155), *328*, *329*
Fuke, K., 364(151), *450*
Futamura, K., 24(76), *74*
Fyfe, C. A., 340(77), 346(101), *448*, *449*

G

Gaoni, Y., 110(98), *166*
Garcia Vazquez, J. A., 379(206a), *452*
Gardner, H. C., 436(377, 378, 379), 437 (377, 378, 379), 438(377), 439(377, 378), 440(377), 441(377), *456*

Gardy, E. M., 70(187), *78*
Garg, S. K., 314(145), *329*
Garito, A. F., 84(19), 117(119), 137(119), 142(119), 148(171, 172), *164*, *167*, *168*
Garnier, F., 367(183, 184), 374(183), 275 (183), 393(183), *451*
Gebus, B., 105(86), *166*
Geier, H. J., 298(130), 312(130), *328*
Geissler, U., 102(82), *166*
Gerschel, A., 275(47), 284(99b), 306(99b), *326*, *328*
Gershon, N. D., 277(59), *327*
Gersmann, H. R., 366(168), *451*
Geseva, L. N., 38(106), *75*
Gesser, H. D., 178(65), *258*
Gevorkyan, B. Z., 365(154), 372(154), *450*
Gibson, R. E., 343(87a), 356(87a), *449*
Giddings, J. C., 172(15, 18), *257*
Gijzeman, O. L. J., 416(314), *454*
Gil-Av, E., 187(145, 147, 150), 188(150), *260*
Gilbert, C. W., 398(272), *453*
Gilbert, M., 274(39), *326*
Gill, W. D., 114(108), 115(114), 118(108), 123(108), 125(108), 129(108), 130(114), 131,(108), *167*
Gillson, J. L., 84(20), *164*
Gilson, T. R., 274(41), *326*
Giordini, M., 314(144), *329*
Giussani, Y., 269(6), 285(6), 286(6), 287 (6), 296(6), 297(6), *325*
Glasgow, L. C., 364(150), *450*
Glasstone, S., 63(159), *77*
Glavis, F. J., 446(392), *456*
Glenn, T. H., 178(78), *258*
Glew, D. N., 360(144), *450*
Gnatz, G., 424(349), *455*
Goates, J. R., 417(334), 419(346), 422 (334), 423(334), *455*
Goedde, A. O., 116(116, 118), 121(116), 124(116), *167*
Goedert, M., 176(51), 177(51), 183(51), *258*
Gold, H., 182(114), *259*
Goldberg, H. S., 298(132), 299(132), 302(132), 317(132), *329*
Golden, D. M., 349(110), *449*
Goldschmidt, C. R., 7(37), 28(88), 34 (37), 52(37), 59(147), 65(169), 68(169), 69(169), *73*, *74*, *76*, *77*
Goldshtein, I. P., 332(2), 333(2), 337(2), 342(2), 351(2), 353(2), 357(2), 432(2), *446*
Goldup, A., 255(343, 345), *265*
Golten, W. C., 379(205), *452*
Goodenow, J. M., 377(198), 378(198), *451*
Goodings, E. P., 83(14), 142(158), 149 (175), *164*, *168*, *169*
Goodman, L., 65(167), *77*
Gordon, M., 82(9), *164*, 337(47), *448*
Gordon, R. G., 269(10, 11), 278(10, 11, 63), 279(63), 280(66), 282(66), 283(63), 284(63), 296(66), 302(63), *325*, *327*
Gorton, J., 85(27), 86(27), *164*, 234(294), *264*
Gover, T. A., 388(250), 392(250), 393 (250), 398(250), 399(250), *453*
Grabowski, Z. R., 13(60), 47(60), 48 (126, 129, 130), *73*, *76*
Graf, P. E., 382(226), *452*
Grammatica, S., 116(117), 133(117), *167*
Gray, C. G., 279(65), 296(65), *327*
Greatbatch, W., 114(105), 161(105), *167*
Green, D. C., 84(20, 21), 147(169), 149 (174), *164*, *168*, *169*
Green, S. A., 176(39), *257*
Greene, E. F., 382(233), *452*
Gregory, N. W., 377(197, 199), 378(197, 199,), *451*
Grellmann, K. H., 3(14), 13(60), 47(60), 67(178, 179), 68(178, 179), *72*, *73*, *77*
Griffiths, J. E., 270(20), 285(104), 296 (104), 298(133, 134, 152), 299(152), 302(134), 309(134), 311(133), 312(104, 134), 317(133, 152), 323(133, 134, 152), *325*, *328*, *329*
Griffiths, J. H., 172(7), *256*
Grina, L. D., 410(306), *454*
Grosjean, D., 367(181), *451*
Grossweiner, L. I., 392(261), *453*
Grube, P. L., 135(140), 142(159c), *168*
Grundnes, J., 342(81, 83, 84), 343(88), 344(88), 350(111), 353(88, 115), 354 (88), 355(88), 361(88), 362(88), 364(88), 371(88), 372(88), 396(111), 442(111), *449*
Guggenheim, E., 339(68), 348(68), *448*
Guha, O. K., 186(141), *260*
Guillet, J. E., 83(12), 88(12), *164*, 217 (218), *262*

Guiochon, G., 173(29), 176(51), 177(51), 183,(51), 191(167), 192(167), 203(183), 206(167, 204), 215(167), *257*, *258*, *261*, *262*
Gump, B. H., 188(158), *260*
Günther, H. D., 298(130), 312(130), *328*
Gupta, P. L., 205(196), *261*
Gurdzhiyan, L. M., 409(309), 411(309). *454*
Gurr, M., 3(14), *72*
Gur'yanova, E. N., 332(2), 333(2), 337(2), 340(2), 351(2), 353(2), 357(2), 379 (206), 435(2), *446*, *452*
Gutman, D., 370(189), *451*
Gutmann, F., 118(122), 138(145), 139 (145), 147), 140(145), 161(200), *167*, *168*, *169*
Guttenplan, J. B., 29(93), 61(93), 62(157), *75*, *77*

H

Haack, R., 138(144), *167*, *168*
Haahti, E. O. A., 221(225), 238(225), *262*
Haberkorn, R., 71(188), *78*
Habgood, H. W., 177(59), *258*
Hackmann, W. K., 382(235), *452*
Hadden, R. C., 84(22), *164*
Hadek, V., 138(146), 139(151), 140(152), *168*
Haenel, M. W., 90(57), *165*
Haffmans, R., 282(95), 307(95), *328*
Haffner, H., 90(56), *165*
Haink, H. J., 96(73), *166*
Haley, N. F., 84(25), *164*
Halpern, A. M., 388(252), 389(252), 398 (252), 399(252), *453*
Ham, J., 360(139), 362(139), 366(139), 367(139), 372(139), *450*
Hamill, W. H., 400(278), 401(284), 402 (284, 287), *453*, *454*
Hamilton, C. H., 178(72), *258*
Hamilton, T. D. S., 410(321), *455*
Hammes, G., 63(161), *77*
Hammick, D. L., 340(76), *448*
Hammond, P. R., 342(80), 357(123, 124), 358,(135), 417(123, 124, 337, 338, 339, 340), 418(123, 341), 419(123, 135, 343), 420(339), 421(135, 347), 422(123), 423 (123), 424(337), 425(337, 338, 339), 426 (339, 341, 351), 427(339, 340, 351), 428 (340, 352), 429(340, 351), 434(123), 442 (80, 343, 352, 384, 384a), 443(80, 352, 384, *455*, *456*
Han, B. J., 366(162), 373(162), *450*
Hand, R. L., 149(175), *169*
Hanna, M. W., 93(67), *165*, 335(27, 28, 29), *447*
Harbison, M. W. P., 177(54), 183(54), 184(54), 185(54), 226(238, 239), 230 (238, 239, 239(238, 239), 243(238, 239), 245(54, 238), 246(238), 247(238), 248 (238), 251(54), *258*, *262*,
Harkins, W. D., 230(287), *264*
Harp, G. D., 269(9), 278(9), 283(98), *325* *328*
Harper, M. F., 188(160), 189(160), *260*
Harris, W. E., 177(59), *258*
Harrison, A. J., 383(238), *452*
Hartkopf, A., 173(37), *257*
Hartmann, H., 358(131), *450*
Hartzler, H. D., 144(163), *168*
Harvey, D., 184(135), *260*
Hasegawa, E., 112(100), *166*
Haselbach, E., 93(66), *165*
Hassel, O., 352(114), *449*
Hastings, S. H., 361(146), 366(146), 367(146), 368(146), 369(146), 371(146), 372(146), 374(146), 376(146), 377(146), *450*
Hatano, M., 137(143), 142(143), *168*, 418 (342), 419(342),421(342), 422(342), 434 (342), *455*
Hautala, R. R., 89(43), *165*
Hayashi, K., 60(150, 154), *77*
Hayashi, T., 5(28), 22(28), 23(72), 35(28, 104), 52(28, 72), *72*, *74*, *75*, *76*
Hayashi, Y., 112(101), 154(185), *166*,*169*
Hayduk, W., 223(236), *262*
Hayon, E., 29(95), *75*, 392(259, 262), 399 (259), 401(262), *453*
Heeger, A. J., 84(19), 117(119), 137(119), 142(119), 148(171, 172), 158(202), *164*, *167*, *168*, *169*
Heidt, L. J., 414(324), *455*
Heilbronner, E., 367(176), 369(187), 431 (370), *451*, *456*
Heinsohn, G. E., 141(156), *168*
Heller, C. A., 415(328), *455*
Hendra, P. J., 274(41), *326*
Henke, 90(57), *165*

Hepler, L. G., 180(107), *259*
Herling, J., 187(150), 188(150), *260*
Hermann, A. M., 114(107a, 107c, 107d, 107e), 124(107a, 107c, 107d, 107e), 134 (138), 138(144, 145), 139(145, 147), 140 (145, 154), 161(200), *167*, *168*, *169*
Herndon, W. C., 93(68), *165*
Herre, W., 34(101), *75*
Hertler, W. R., 146(167), 148(167), 154 (167), *168*
Hertz, J. J., 137(142), 142(142), *168*
Herz, C. P., 90(57), 92(62), *165*
Herzberg, G., 379(311), *452*
Herzfeld, K. F., 295(127), 297(127), 318 (127), *328*
Hess, D. W., 306(138), *329*
Heywood, A., 172(5), *256*
Higashimura, T., 90(55), *165*
Hildebrand, G. P., 221(231), 251(231), *262*
Hildebrand, J. H., 332(19), 340(19), 344 (19), 349(108, 109), 360(109, 144, 145), 366(19, 156), *447*, *449*, *450*
Hinkins, R. L., 239(318), *264*
Hino, T., 58(144), 62(144), 63(162), 64 (144, 165), *76*, *77*
Hippler, H., 383(241), 385(341, 342, 343), *452*, *453*
Hirayama, F., 5(27a), 35(27a), *72*
Hoare, D. E., 381(231), *452*
Hoare, M. R., 172(13), *257*
Hoegl, H., 123(127, 128, 130), *167*
Hofeldt, R. H., 47(124), *75*
Hoijtink, G. J., 403(292), 411(322), *454*, 455
Holder, D. D., 93(69), *166*
Holmes, T. J., 84(23), *164*
Homer, J., 187(152), *260*, 338(57), 344 (57), 430(362, 363), *448*, *456*
Hooker, D. M., 226(240), 230(240), 239 (240), 243(240), *262*
Hori, Y., 178(67), *285*
Horita, H., 87(31), *164*
Horman, I., 346(101), *449*
Horning, E. C., 221(225), 238(225), *262*
Houghton, L. E., 89(52), *165*
Hovel, H. J., 161(199), *169*
Hubbard, P. S., 280(76), 297(76), *327*
Huber, J. F. K., 254(341), 255(341), *265*
Huber, R. J., 96(73), *166*
Huck, P. J., 430(363), *456*
Hughes, H. W. D., 221(224), 237(224), *262*
Hughes, L. M., 205(190), *261*
Hui, M. H., 10(50), 11(50), *73*, 89(43), *165*
Hunter, T. F., 187(153), *260*, 339(70), 346(99), 348(99), *448*, *449*
Hurst, E. L., 142(159b), *168*
Husmann, H., 178(84,85), *259*
Hussey, C. L., 176(49), 185(49), *258*
Hutton, E., 2(2), *71*
Hyde, P., 82(7), *164*

I

Ichobanova, I., 100(77), *166*
Ide, R., 3(18a, 18b), 7(18a, 18b), 19(18a, 18b), 38(18a, 18b), 44(18a), 46(18a), 54(18a), *72*
Ilie, V. A., 200(177), *261*
Ilie, Z. E., 227(247), *263*
Imanishi, Y., 90(55), *165*
Inami, A., 112(101), 113(102), 154(185, 186), *166*, *169*
Inoue, A., 10(52), *73*
Inoue, H., 13(59a), *73*
Inukai, K., 105(87, 88), *166*
Ioffe, B. V., 187(148), *260*
Iogansen, A. V., 172(26), *257*
Irie, M., 60(150, 154), *76*, *77*
Irwin, R. S., 188(163), *261*
Isack, F. L., 377(195), 378(195), *451*
Ishibe, N., 365(155), 371(155), 372(155), *450*
Ishida, H., 357(126), 405(126), 411(126), 412(126), 413(126), 415(329a), *450*, *455*
Islam, A., 221(229), 238(229), *262*
Itaya, A., 99(76), 100(76), 103(76), 104 (76), 106(76), *166*
Ito, H., 100(80), 101(80), *166*
Ito, O., 418(342), 419(342), 421(342), 422(342), 423(342), *455*
Itoh, M., 3(19), 7(19), 13(19), 25(19, 75), 35(105), *72*, *74*, *75*, 87(35), 88(36, 37), *165*
Ives, D. J. G., 230(290), *264*
Ivin, K. J., 442(389), 445(389), *456*
Iwata, S., 29(96), 32(96), 33(96), 34(102), *75*
Iwatsuki, S., 100(78), 101(78), 105(78, 87, 88), *166*
Izmailov, R. I., 172(24), *257*

J

Jackson, C. J., 187(152), *260*
James, A. T., 172(3, 4), 237(3, 296), *256*, *264*
James, D. H., 172(6), 177(57), *256*, *258*
Janak, J., 173(30, 34), 176(50), 177(50), 179(50), 182(50), 183(50), 186(141), 239(324), *257*, *258*, *260*, *265*
Janik, A., 205(195), *261*
Janini, G. M., 205(188, 193), 222(235), 223(235), *261*, *262*
Janssen, E., 406(299), 409(299), 413(299), *454*
Jasny, J., 48(129), *76*
Jauquet, M., 338(58a), 344(58a), *448*
Jensen, R. J., 417(334), 422(334), 423 (334), *455*
Jepson, W. B., 359(138), *450*
Job, P., 417(335), *455*
Joesten, M. D., 357(127), 421(127), *459*
Johnson, B. M., 200(178), *261*
Johnson, C. S., 306(138), *329*
Johnson, J. F., 239(318), *264*
Jolley, K. W., 205(190), *261*
Jonas, J., 273(37), 280(77), 281(78, 80), 285(37), 286(37), 287(37), 289(122), 292(37), 295(37), 296(37, 122), 297 (37, 122), 298(122), 302(122), 303(122), 308 (141a, 141b), 309(141a, 141b), 311 (141a, 141b), 317(37), 318(37), 320 (37), 323(78), 324(78), *326*, *327*, *328*, *329*
Jones, D. R., 289(119), 298(119), 300 (119), 302(119), 303(119), 317(119), 323(119), 325(119), *328*
Jones, E. N., 430 (357), 431(357), 433 (357), *455*
Jones, R. N., 269(5), *325*
Jonker, K. M., 254(341), 255(341), *265*
Jonsson, J. A., 178(68), *258*
Jonsson, R., 194(170), 215(170), 216 (170), *261*
Jordan, J. H., 238(309), *264*
Jortner, J., 13(61), 48(61), *73*, 358(133), 403(133), 408(304), 410(133), 413(133), 414(133), 445(133), 446(133), *450*, *454*
Joussot-Dubien, J., 392(256), 258, 260), 398(256), 399(258), 402(256), *453*
Juchert, I., 93(65), *165*
Julien, L. M., 354(118), 362(118), 364 (118), 371(118), 372(118), *449*
Jurs, P. C., 239(322,323), *265*
Jurinski, N. B., 444(395), *456*
Juvet, R. S., Jr., 179(96), 186(139), 200 (180, 181), *259*, *260*, *261*

K

Kagarise, R. E., 444(397), *456*
Kaifu, Y., 3(14), 40(115, 116), *72*, *75*
Kaiser, R. E., 182,(116, 120), *259*
Kaiser, W., 285(105, 106, 116), 296(105, 106), 300(105), 309(106), *328*
Kajikawa, T., 398(275), 401(275), *453*
Kakimoto, M., 285(112), 293(112), 296 (112), 302(137), 308(137), 318(155), *328*, *329*
Kalinina, G. P., 378(202), *452*
Kaliya, O. L., 409(309), 411(309), *454*
Kambara, S., 137(143), 142(143), *168*
Kanchencko, Y. A., 182(128), *260*
Kaneta, K., 56(141), *76*
Kaplan, M. L., 84(22, 24), *164*
Kaplan, R. L., 172(1), 230(1), *256*
Kaplanova, B., 173(30), *257*
Kaptein, K., 70(184), *77*
Karaianev, S., 366(167), 373(167), *451*
Karger, B. L., 173(37, 38), 191(168), 192 (168), 193(168), 206(168), *257*, *261*
Karkchi, G. A., 172(26), *257*
Karnaukhov, A. P., 172(26), *257*
Karpathy, O. C., 221(227), 238(227), *262*
Karthaus, F., 187(149), 198(149), *260*
Kasper, K., 2(1), 4(1), *71*
Kasuya, T., 10(52), *73*
Kato, K., 135(139), *168*
Kato, M., 28(80b), 62(80b), *74*
Katsumata, S., 60(148b, 148c), *76*, 369 (188), *451*
Kaufman, F., 149(174), *169*, 416(314), *454*
Kaufman, F. B., 84(21), *164*
Kaufman, I., 254(340), *265*
Kawai, K., 60(151), *76*
Kawai, M., 55(140), 60(140), *76*
Kawasaki, Y., 3(14), *72*
Kayashi, K., 60(151), *76*
Kaye, J. A., 394(267), 395(267), 397(267), 400(267), *453*

Kearns, D. R., 416(316), *455*
Keefer, R. M., 332(5), 333(5), 344(93), 358(130), 366(93, 158, 159, 160, 169, 170, 171), 367(171), 368(185), 373(93, 158, 159), 375(171), 377(169), 378(179), 430(93), 438(383), 442(386), 444(170), 445(386), *447*, *449*, *450*, *451*, *456*
Keehn, P. M., 87(31, 32), *164*,*165*
Keene, J. P., 379(214), 398(272, 273), 399(273), *452*, *453*
Kellawi, H., 430(361), 433(361), 434 (361), *456*
Keller, R. A., 172(15), 221(230, 232), 238(230), 239(232), *257*, *262*
Kemula, W., 238(307), *264*
Keppler, J. G., 172(11), *257*
Keszthetlyi, C. P., 20(71), 22(71), *74*
Ketelaar, J. A. A., 353(116), 355(116), 366(116, 168, 172), 373(116), 375(172), *449*, *451*
Keulemans, A. I. M., 237(297), *264*
Keyanpoor-Rad, M., 101(81), *166*
Keyes, T., 277(55, 57), 296(57), *327*
Khalil, O. S., 47(124), *75*
Khan, M. A., 200(181), *261*
Khuen, A., 271(30), 273(30), 285(30), 286(30), 288(30), 289(30), 290(30), 296 (30), 298(30), 299(30), 301(30), *326*
Kieselbach, R., 178(89), *259*
Kihara, T., 381(230), *452*
Kikuchi. K., 28(81), *74*
Kilp, H., 314(145), *329*
Kim, E. R., 366(165), 373(165), *451*
Kim, S. K., 380(217), *452*
Kimura, K., 60(148a, 148b, 148c, 152, 153), *76*, 369(188), *451*
King, A. D., Jr., 403(294), *454*
King, J. W., 202(182), 205(182, 188), *261*
Kinoshita, M., 28(90), 65(90), *75*
Kira, M., 93(70), *166*, 436(375), 439(375), 440(375), *456*
Kirkwood, J. G., 277(58), *327*
Kiselev, A. V., 172(26), *257*
Kivelson, D., 272(32), 274(43), 277(55), 278(43,61), 280(68a), 281(43, 61, 83), 283(32), 296(68a), 297(68a), 311(68a), *326*, *327*
Kivelson, M., 278(61), 281(61), *327*
Klein, J., 217(219), 218(219), 221(219), *262*
Kleinberg, J., 359(136), *450*
Klöpffer, W., 2(6), *71*, 94(71), 96(71), *166*
Knapp, O., 177(60), *258*
Kneubühl. F., 274(38, 42), *326*
Knibbe, H., 6(29b), 10(53), 44(121, 122), 56(122, 142a, 142b), 57(142a, 142b), 58(122, 142a), 67(176), *72*, *73*, *75*, *76*, *77*
Knight, J. A., 176(43), *257*
Knipe, R. H., 342(80), 357(123), 417 (123), 418(123), 419(123), 422(123), 423(123), 434(123), 442(80), 443(80), *448*, *450*
Knobler, C. M., 180(108), *259*
Knoesel, R., 105(86), *166*
Knox, J. H., 177(58), *258*
Kobayashi, R., 172(19, 20), 178(67), 182 (115), *257*, *258*, *259*
Kobayashi, T., 7(36), 32(98), 65(166), *73*, *75*, *77*
Kochi, J. K., 436(377, 378, 379), 437 (377, 378, 379), 438(377), 439(377, 378), 440(377), 441(377), *456*
Koizumi, M., 28(81), 40(115, 116), 56 (141), *74*, *75*, *76*
Kokovin, G. A., 377(203), 378(203), *452*
Kokubun, H., 28(81), 56(141), *74*, *76*
Kolb, K. E., 365(152), 368(152), *450*
Kolesnikova, V. V., 400(279), 401(279), 402(279), *454*
Kolninov, O. V., 400(279), 401(279), 402(279), *454*
Komatsu, K., 84(18), *164*
Komers, R., 186(144), *260*
Konynenburg, van, P., 270(24), 273(34), 281(24), *326*
Koole, N. J., 199(176), 200(176), *261*
Kopecni, M. M., 227(246, 247), *263*
Kopple, K. D., 137(141, 142), 142(142), *168*
Korol, A. N., 172(25), *257*
Koros, E., 332(14), *447*
Kortüm, G., 355(121), 359(137), 377 (190), *449*, *450*, *451*
Kosower, E. M., 3(23a, 23b), 22(23a, 23b), 28(82), 29(23a, 23b), 35(105), 47 (125), 48(23a, 125, 132), 49(132), 50 (23a, 134, 135, 136), 51,(134), 52(132), *72*, *74*, *75*, *76*
Kostova, A., 182(123), *260*
Kots, C. E., 84(21), *164*
Kovats, E., sz, 182(121), 239(325), *259*

265
Kowalski, V. L., 410(320), *455*
Kraak, J. C., 254(341), 255(341), *265*
Kraitr, M., 186(144), *260*
Krauss, D. C., 285(110b), 296(110b), *328*
Krauss, H. L., 424(349), *455*
Kremser, M., 176(48), *258*
Kreysig, D., 93(65), *165*
Kroll, M., 187(151), *260*, 344(91), *449*
Krowczynski, A., 48(126, 130), *76*
Kryszewski, M., 122(125), 157(190, 191, 192), *167*, *169*
Kubo, R., 274(62), 278(62), 286(62), 287 (62), *327*
Kubota, M., 3(18a), 7(18a), 19(18a), 38(18a), 46(18a), 54(18a), *72*
Kubota, T., 2(5), 9(5), 28(5), *71*, 332(11), 333(11), 360(142), *447*, *450*
Kubota, Y., 367(176a), *451*
Kucera, P., 254(337), *265*
Kuhnle, W., 6(27c), 35(27c), 36(27c), 48(126), *72*, *76*
Kulevsky, N., 85(27), 86(27), *164*, 408 (306), 409(307, 308, 310, 311), 410(306, 307, 308), 413(310, 311), 414(311), *454*
Kurchal, R. K., 205(196), *261*
Kusabayashi, S., 99(76), 100(76), 103 (76), 104(76), 106(76), 135(139), *166*, *168*
Kusagawa, H., 154(187), *169*
Kusumoto, H., 365(155), 371(155), 372 (155), *450*
Kuzim, M. G., 38(106), *75*
Kwantes, A., 173(33), 237(297), 255(342), *257*, *264*, *265*
Kwon, S. J., 366(161), 373(161), *450*
Kwun, O. C., 358(131), *450*

L

Labes, M. M., 115(111), 122(111), 161 (111), *167*
LaBudde, R. A., 348(105), *449*
Laidler, K. J., 63(159), *77*
Lakatos, A. I., 123(131,132), *167*
Lake, R. R., 357(123), 417(123, 337, 338, 340), 418(123), 419(123, 343), 422(123), 423(123), 424(337), 425(337, 338), 427 (340), 428(340), 429(340), 434(123), 442(343), 444(343), *450*, *455*
Lambeth, P. F., 61(156), *77*
Land, E. J., 65(171), 66(171), *77*, 398(272, 273), 399(273), *453*
Landel, R. F., 140(154), *168*
Landman, U., 94(72), 95(72), 96(72), 99(72), 103(72), *166*
Lane, E. H., 344(92), 349(92, 107), *449*
Lang, F. T., 345(95, 96), 355(96), *449*
Lang, R. P., 357(125), 360(141), *450*
Langer, S. H., 186(138), 188(161), 194 (138), 200(178), *260*, *261*
Lantz, T. E., 400(280), *454*
Lardon, M., 123(129), *167*
Larkin, I. W., 282(93, 94, 95, 96), 307(93, 94, 95), *327*, *328*
Larsh, A. E., 379(212), *452*
Lassier, B., 282(92), 307(92), *327*
Laszlo, P., 338(58a), 339(66), 344(58a), 352(66), *448*
Laub, R. J., 172(14), 173(14), 176(53), 177(53, 54), 182(53, 127), 183(54), 184 (54), 185(53, 54), 186(14), 187(14), 188 (14), 206(201, 202, 203), 207(205, 206), 208(205, 206), 209(205, 206), 215(203), 216(14, 203), 219(221), 222(53), 223 (14), 224(237), 226(238, 239), 230(238, 239, 251), 231(251), 233(251), 234 (251), 235(251), 236(251), 239(238, 239), 241(329), 241(327), 242(327, 329), 243(238, 239), 245(54, 238), 246 (238), 247(238), 248(238), 249(221, 329, 330, 331), 250(332), 251(54, 333), 252(334), 253(330, 333, 334, 335), 254 (339), *257*, *258*, *260*, *261*, *262*, *263*, *265*
Laubereau, A., 285(105, 106, 108, 116), 293(108), 296(105, 106, 108), 297(108), 298(108), 300(105), 309(106), 318(108), *328*
Laurence, D. J. R., 50(133), *76*
Lautenberger, W. J., 430(357), 431(357), 433(357), *455*
Lawler, R. G., 70(186), *78*
Leary, J. J., 221(233), 239(233), *262*
Leathard, D. A., 178(91), *259*
Le Blanc, O. H., 114(109), *167*
Leckenby, R. E., 335(39), *447*
Ledwith, A., 82(7), 89(52), 94(72), 95(72), 96(72), 97(74), 98(74), 99(72), 101(81), 103(72, 84), 104(84), 106(74), *164*, *165* *166*
Lee, S. K., 15(64b), *73*, *74*

Lee, Y. T., 382(234), *452*
LeFévre, R. J. W., 335(35), *447*
Leitner, J. E., 177(61), 178(92), *258*, *259*
Lell-Doller, E., 123(129), *167*
Leonhardt, H., 3(8), 65(8), 67(8), *71*
Leroy, Y., 324(163), 325(163), *329*
Le Vanda, C., 143(161), *168*
Levanon, H., 415(327), *455*
Levi, G., 280(75), *327*
Levy, A., 178(62), *258*
Lewis, A., 89(49), *165*
Lewis, C., 410(318), 416(317, 318), *455*
Leyte, J. C., 271(29), 285(29, 109), 286 (29, 109), 289(29), 290(109), 296(29, 109), 297(109), 298(29, 109), 308(29), 312(29, 109), 314(109), *326*, *328*
Liang, Y. F., 146(165, 166), 148(165), *168*
Liao, H-L., 173(38), 188(156), 195(172), 196(172), 198(172), 205(172), 212(172), 213(156), *257*, *260*, *261*
Liberti, A., 178(81), *258*
Libman, J., 66(174), *77*
Lichnevskii, V. A., 367(182), 374(182), *451*
Ligny, C. L., de, 186(137), 187(149), 198(137, 149), 199(176), 200(176), *260* *261*
Lim, E. C., 337(46), 410(320), *448*, *455*
Limburg, W. W., 111(99), 116(116), 121 (116), 124(116), 154(188, 189), *166*, *167*, *169*
Linde, D., von der, 285(116), *328*
Lindqvist, L., 50(136), *76*
Linschitz, H., 29(92), *75*
Lippert, E., 13(58a, 58b), 22(58a), 40 (114), 44(114), 47(123), 51(58a), *73*, *75*
Lippert, J. L., 93(67), *165*, 335(27, 29), *447*
Liptay, W., 40(112), *75*, 338(51), 344(51), *448*
Litovitz, T. A., 270(14), 272(14), 274(14), 276(51), 281(82), 295(14, 51, 127, 150a, 150b), 296(150a, 150b), 297(127, 150a, 150b), 308(14), 317(14), 318(127), 323 (14), *325*, *326*, *327*, *328*,*329*
Litt, M. H., 102(83), 135(83), 136(83), *166*
Littlewood, A. B., 172(12), 238(314), *257* *264*
Livingston, R. C., 276(53), 279(53), 286 (53), 290(53), 308(53), 309(53), 311(53), *326*
Lochner, M., 177(60), *258*
Locke, D. C., 172(27), 181(112), 184(27), *257*, *259*
Lockmüller, C. H., 176(47), *258*
Lodge, J. P., 178(79), *258*
Loeffler, O. H., 343(87a), 356(87a) *449*
Loewenschuss, A., 270(21), 323(21, 160), *326*, *329*
Logan, S. R., 392(256), 398(256), 402 (256), *453*
Longuet-Higgins, H. C., 40(111), *75*
Longworth, J. W., 21(70), *74*
Lopata, V. J., 70(187), *78*
Lorenz, L. J., 178(77), *258*
Loufty, R. O., 62(157), *77*
Louwrier, P. W. F., 401(284), 402(284, 287), *454*
Luckhurst, G. R., 255(345), *265*
Lüder, W., 13(58b), 47(123), *73*, *75*
Luhowy, R., 87(32), *165*
Lukacovic, L., 238(304), *264*
Lumry, R., 3(10), 52(10), *71*
Lupinski, J. H., 137(141, 142), 142(142), *168*
Luther. K., 383(241), 385(241, 242, 243), *452*, *453*
Lyons, L. E., 118(122), *167*
Luyton, J. A., 182(118), *259*
Luzzati, V., 230(282), *263*
Lyden, E. F. X., 230(284), *263*
Lynch, D. F., 221(233), 239(233), *262*
Lynden-Bell, R. M., 273 (35, 114), 285 (113, 114), 287(117), 290(114), 292 (114), 296(113, 114), 297(114, 151), 312(151), 314(114), *326*, *328*, *329*

M

McAlonie, G. E., 376(192), 377(192), 378(192), *451*
McCarthy, R. L., 379(213), *452*
McClung, R. E. D., 280(68a, 68b, 69, 70, 71, 72, 73, 74, 75), 296(68a, 68b, 69, 70, 71, 72, 73, 74), 297(68a, 68b, 69), 298(129), 302(129), 308 (129), 309 (129), 311(68a, 68b), *327*, *328*
McConnell, H., 378(191), *451*
MacDiarmid, A. G., 158(202), *169*
McEwan, W. S., 417(339), 420(339),

425(339), 426(339), 427(339), *455*
McFadden, W. H., 221(223), 237(223), *262*
McGlashan, M. L., 180(101), *259*, 316 (147), *329*, 358(129), *450*
McGlynn, S. P., 4(26b), 28(90), 47(124), 65(90, 167), *72*, *75*, *77*, 332(13), 333(13), *447*
McKellar, J. F., 61(156), *77*
MacLachlan, A., 379(213), *452*
McLean, R. R., 424(350), 426(350), 427 (350), *453*
McRae, E. G., 40(110), *75*
McReynolds, W. O., 239(326), *265*
MacRury, T. B., 276(52), *326*
McWilliam, I. G., 178(90), *259*
Madden, P. A., 272(32), 283(32), 285 (113), 296(113), *326*, *328*
Madigosky, W. M., 295(150b), 296 (150b), 297(150b), *329*
Maeda, K., 406(312), 415(312), 416(312), *454*
Magdzinski, L. K., 62(157), *77*
Maier, H. J., 221(227), 238(227), *262*
Maine, M. M., de, 376(192), 377(192), 378(192), *451*
Maine, P. A. D., de, 376(192,193), 377 (192, 193, 194), 378(192, 193, 194), 442(388), 444(395), 445(388), 446(388), *451*, *456*
Mallik, K. L., 172(18, 28), 205(196), *257*, *261*
Manecke, G., 151(181), *169*
Mangelson, N. F., 417(334), 422(334), 423(334), *455*
Manager, C. L., 403(295), *454*
Mann, A., 382(235), *452*
Mantione, M., 335(30, 31), *447*
Marchetti, F., 394(265, 266), *453*
Marcus, R. A., 17(66a, 66b), *74*
Mardaeva, A. I., 302(136), *329*
Maréchal, E., 269(7), 270(7), 285(7), 286(7), 287(7), 296(7), 297(7), *325*
Marin, C. K., 109(96), *166*
Marsault, J. P., 280(75), *327*
Marsault-Herail, F., 280(75), *327*
Marsh, D. G., 94(72), 95(72), 96(72), 99(72), 103(72), *166*
Marshall, J., 84(24), *164*
Marshall, R., 379(212, *452*
Martin, A. J. P., 172(3), 237(3, 296), *256*, *264*
Martin, J. J., 173(35), *257*
Martin, R. L., 181(109), *259*
Martire, D. E., 172(17), 176(53), 177(53, 54), 181(111), 182(53, 122), 183(54), 184(54), 185(53, 54, 132), 188(111, 156), 194(122), 195(122), 195(171, 172, 173), 196(172), 198(172), 202(171, 173, 182, 184, 186), 204(187), 205(171, 172, 173, 182, 188, 193), 212(172), 213(156), 217(184), 222(53, 234, 235), 223(235), 226(238, 239), 230(238, 239), 239(238, 239, 321), 243(238, 239), 245(54, 238), 246(238), 247(238), 248(238), 251(54), *257*, *258*, *259*, *260*, *261*, *262*, *265*
Martynyuk, R. N., 220(222), *262*
Marvel, C. S., 446(392), *456*
Masaguer, J. R., 379(206a), *452*
Masaki, S., 3(18a, 22b), 7(18a), 19(18a, 22b), 38(18a, 22b), 44(18a, 22b), 46 (18a, 22b), 54(18a), *72*
Masclet, P., 367(181), *451*
Masuhara, H., 3(12, 21), 6(34, 35), 8(21), 12(21), 13(21), 15(12), 19(21), 28(80a, 80b, 83), 31(12, 34, 35), 32(97), 38(21), 39(21), 44(21), 54(21), 58(144), 60(149, 150), 61(12), 62(80a, 144), 63(162), 64(144, 165), 66(172a), *72*, *73*, *74*, *75*, *76*, *77*, 86(29, 30), 87(34), *164*, *165*
Masukawa, S., 182(115), *259*
Masuyama, Y., 144(164), 148(164), *168*
Mataga, N., 2(5), 3(9, 12, 14, 18a, 18b, 20a, 20b, 21, 22a, 22b), 5(28), 6(29a, 30, 34, 35), 7(18a, 18b, 38), 8(20a, 20b, 21), 9(5, 45), 10(45, 48, 51), 12(21,57), 13(21, 57, 59a, 59b, 63), 15(12, 48, 65a, 65b), 16(48), 17(68), 18(68), 19(18a, 18b, 20a, 20b, 21, 22b), 22(28), 23(72), 24(9, 74a, 74b), 25(30, 48, 74b), 27(9, 20a, 77), 28(5, 77, 80b, 83), 29(91), 31(12, 34, 35), 32(97), 35(28, 104), 38(18a, 18b, 20a, 20b, 21, 22a, 22b), 39(21, 57), 40(115, 116), 42(20a, 20b, 118), 43(118), 44(18a, 20, 21, 22b), 46 (18a, 20a, 22b), 47(59b), 52(28, 72), 53(38), 54(18a, 21, 22a, 57), 55(57, 63, 140), 56(118), 57(118), 58(143, 144), 59(143), 60(140, 149, 150, 151), 61(12, 65b), 62(80a, 80b, 144), 63(162), 64 (144, 165), 66(9, 20a, 30, 77, 140a, 172a, 172b), 67(77), 68(20b), *71*, *72*, *73*, *74*,

75, *76*, *77*, 86(29, 30), 87(34), 89(40, 46), *164*, *165*, 332(11), 333(11), *447*
Matheson, M. S., 392(261), *453*
Mathiasson, L., 194(170), 215(170), 216 (170), *261*
Matsen, F. A., 333(22), 361(146), 366 (146), 367 (146), 368(146), 369(146), 371(146), 372(146), 374(146), 376(146), 377(146), *447*, *450*
Matsuda, T., 221(226), *262*
Matsui, H., 10(51), *73*
Matsumoto, H., 10(51), *73*, 369(188), *451*
Matsumoto, S., 7(36), 34(102), *73*, *75*
Matsuyama, Y., 100(80), 101(80), 103 (85), 104(85), *166*
Matsuzaki, A., 3(14), *72*
Mayo, P., de, 337(47), *448*
Mazee, W. M., 415(329), *455*
Mead, R., 114(105), 161(105), *167*
Meen, D. L., 188(159), 190(159), 207 (205), 208(205), 209(205), *260*, *262*
Meier, H., 118(123), *167*
Melby, L. R., 144(163), *168*
Melnikov, A. S., 239(316, 320), 248 (316, 320), *264*, *265*
Meluish, W. H., 431(368), *456*
Melzer, M., 180(103), *259*
Menon, U., 27(78), *74*
Merrifield, R. E., 348(106), *449*
Merritt, V. Y., 161(199), *169*
Metcalf, W. S., 431(368), *456*
Michaelian, K. H., 93(64), *165*
Michel-Beyerle, M. E., 71(188), *78*
Migita, M., 55(140), 60(140), 66(140a), *76*
Mikawa, H., 60(151), *76*, 99(76), 100(76), 103(76), 104(76), 106(76), 115(115), 135(139), *166*, *167*, *168*, 332(4), 333(4), *446*
Mikes, F., 187(147), *260*
Mikkelsen, L., 177(55), *258*
Milinchuk, V. K., 400(279), 401(279), 402 (279), *454*
Miller, J. G., 339(64), 430(357), 431(357), 433(357), *448*, *455*
Miller, J. M., 176(44), *257*
Milonjic, S. K., 227(246, 247), *263*
Mimura, T., 3(19), 7(19), 13(19), 25(19, 75), *72*, *74*, 87(35), 88(36, 37), *165*
Mioshi, A., 29(91), *75*
Mirone, P., 270(22), 273(22), 313(22), 314 (22, 144), 317(154), 323(154), *326*, *329*
Mishima, M., 419(344), *455*
Mishra, S. P., 397(269), *453*
Misumi, S., 3(18a, 18b, 21, 22b), 5(28), 7(18a, 18b), 8(21), 12(21), 13(21), 19 (18a, 18b, 21, 22b), 22(28), 23(72), 35 (28, 104), 38(18a, 18b, 21, 22b), 39(21), 44(18a, 21, 22b), 46(18a. 22b), 52(28, 72), 54(18a, 21), 55(140), 60(140), *72*, *74*, *75*, *76*, 86(29, 30), 87(31), 89(40), *164*, *165*
Mitchinson, K. M., 187(153), *260*
Mitooka, M., 238(311, 312), *264*
Mittal, J. P., 400(278), *453*
Mittal, K. L., 230(293), *264*
Miyake, H., 238(312), *264*
Mobley, M. J., 93(64), *165*
Modaress, H., 430(365), *456*
Moede, J. A., 442(387), *456*
Molera, M. J., 239(319), 240(319), *264*
Monck, A. V., 403(290), 410(290), 414 (290), 415(290), *454*
Montillier, J. P., 100(79), 101(79), *166*
Montroll, E., 117(121), *167*
Moore, J. H., Jr., 403(295), *454*
Moore, P. T., 141(155), *168*
Moore, W. J., 343(87), *449*
Moreland, A. K., 176(47), *258*
Mori, H., 283(98), *328*
Mori, T., 27(77), 28(77), 66(77), 67(77), *74*
Morimoto, K., 112(101), 113(102), 154 (185, 186), *166*, *169*
Morita, H., 343(89), 344(89), 353(89), 368 (89), 369(89), 376(89), 378(89), 394(89), 395(89), 396(89), 397(89), *449*
Morita, M., 35(104), *75*
Morita, T., 29(91), *75*
Morokuma, K., 335(36), *447*
Morris, F., 188(159), 190(159), *260*
Morrow, R. M., 231(252, 253, 258, 259), *263*
Mort, J., 83(13), 115(113), 116(117), 118 (113), 121(113, 124), 123(113, 131, 132), 131(113), 133(113, 117), 134(137), *164*, *167*
Mottl, J., 367(180), *451*
Mouvier, G., 367(181), *451*
Mozumder, A., 62(158), 64(158), *77*
Muanda, M., Ma, 214(210), *262*
Mueller-Westerhoff, U. T., 143(160), *168*
Muhs, M. A., 188(162), 224(162), *261*

Mukherjee, T. K., 142(159a), *168*
Müller, A., 231(269), *263*
Müller, K., 274(38, 42), *326*
Mulliken, R. S., 28(86), *74*, 80(1), *163*, 187(155), 203(185), *260*, *261*, 332(7, 15, 16, 20, 21), 333(7, 15), 334(7, 20, 25), 335(7, 15), 336(7), 337(7), 338(7, 20, 48), 344(7, 48, 94), 345(7, 20, 90), 346 (7, 20), 351(94), 353(7), 358(132), 360 (7, 48), 366(20, 157), 369(7), 370(7), 378(7), 389(7), 391(7), 403(132), 404 (132), 405(132), 408(132), 411(132), 412(132), 413(132), 414(132), *447*, *448*, *449*, *450*
Munns, G. W., Jr., 178(64), *258*
Murakawa, M., 13(63), 55(63), *73*
Murao, K., 135(139), *168*
Murata, I., 91(58), *165*
Murata, S., 56(141), *76*
Murata, Y., 15(65a), *74*
Murawec, T., 215(212, 213, 214, 215), 238 (212, 213), *262*
Murrell, J. N., 4(26a), *72*, 334(26), 338 49, 50, 61), 346(61), 347(61), 404(49), 408(302), *447*, *448*, *454*
Mutai, K., 89(54), *165*
Muzerenko, Y. T., 15(64a), *73*
Myher, J. J., 417(336), 418(336), 423 (336), *455*
Mysak, A. Y., 182(128), *260*

N

Naarmann, H., 108(94), 151(94), 152 (94), *166*
Nafie, L. A., 270(18), 272(18), 274(18), *352*
Nagakura, S., 3(14, 15), 7(50), 10(52), 24(76), 29(96), 32(96, 98), 33(96), 34 (15, 102), 65(15, 166), *72*, *73*, *74*, *75*, *77*, 336(41), 337(41), 364(151), 369(188), *448*, *450*, *451*
Nagao, M., 134(138), *167*
Nagy, J. B., 214(210), *262*
Nagy, O. B., 214(210), *262*
Nakajima, A., 38(107), *75*
Nakamishi, K., 230(291), *264*
Nakamura, J., 34(102), *75*
Nakane, A., 409(312), 412(312), 416(312), *454*
Nakashima, N., 3(20b, 21), 7(38), 8(20b, 21), 9(45), 10(45, 48), 12(21), 13(21, 59a, 59b, 63), 15(48, 65b), 16(48), 19 (20b, 21), 25(48), 38(20b, 21), 39(21), 42(20b), 44(21), 47(59b), 53(38), 54 (21), 55(63), 61(65b), 68(20b), *72*, *73*, *74*
Nakatani, K., 149(173), *168*
Nakato, Y., 67(177), *77*
Nakayama, T., 367(180), *451*
Nakazawa, T., 91(58), *165*
Napier, K. H., 184(131), *260*
Narita, M., 146(165, 166), 148(165), *168*
Naskashima, N., 66(172b), *77*
Navon, G., 414(327), 415(327), *455*
Negita, H., 419(344), *455*
Nelson, H. D., 199(176), 200(176), *261*
Nemzek, T. L., 11(55), *73*
Neugebauer, W., 123(127, 130), *167*
Neusser, H. J., 71(188), *78*
Neuwald, K., 406(299), 409(299), 413 (299), *454*
Nickel, B., 71 (189), *78*
Nicol, M. F., 338(56), 344(56), *448*
Niederstrass, H., 217(217), 221(217), *262*
Nieudorp, G. H. E., 199(176), 200(176), *261*
Niimura, N., 33(99), *75*
Nikolov, R. N., 182(123, 125), *260*
Nikolski, A., 215(212, 213, 214), 238 (212, 213), *262*
Nishima, Y., 58(143), 59(143), 60(151), *76*
Nishimura, T., 55(140), 60(140), 66(140a, 172b), *76*, *77*
Nishizaki, S., 154(187), *169*
Niu, C., 409(308), 410(308), *454*
Noguchi, N., 138(146), 140(152), *168*
Nolting, F., 66(173), 67(173), *77*
Nomori, H., 137(143), 142(143), *168*
Norfolk, D. H., 346(99), 348(99), *449*
Norman, M. A., 273(36), 323(36), 325 (36), *326*
Norrish, R. G. W., 379(210), 383(238), *452*
Norton, D. A., 362(148), 371(148), 372 (148), *450*
Nosworthy, J. M., 398(272), *453*
Novak, J., 173(34), 176(50), 177(50), 179(50), 182(50), 183(50), *257*, *258*
Novros, J., 65(170), 66(170), 67(170), 68(170), 69(170), *77*

Noyes, R. M., 10(54), *73*, 377(201), 378(201), 385(245, 247, 249), *451*, *453*

O

Oberholtzer, J. E., 176(45), *257*)
O'Connor, J. G. 87(31), *164*
O'Donnell, S. E., 202(182), 205(182), *261*
Ogryzlo, E. A., 300(200), 378(200), *451*
Ohashi, Y., 33(99), *75*
Ohta, H., 89(42), *165*
Ohta, T., 88(37), *165*
Okada, T., 3(9, 18a, 18b, 21, 22a, 22b), 6(29a), 7(18a, 18b), 8(21), 10(51), 12(21, 57), 13(21, 57), 17(68), 18(68), 19(18a, 18b, 21, 22b), 24(9, 74b), 25 (74b), 27(9, 77), 28(77), 38(18a, 18b, 21, 22a, 22b), 39(21, 57), 42(118), 43 (118), 44(18a, 21, 22b), 46(18a, 22b), 54(18a, 21, 22a, 57), 55(57), 56(118), 57(118), 66(9, 77), 67(77), *71*, *72*, *73*, *74*, *75*, 89(40, 46), *165*
Okai, T., 414(326), 445(326), 446(326), *455*
Okamoto, K., 99(76), 100(76), 103(76), 104(76), 106(76), 135(139), *166*, *168*
Okamoto, T., 3(19), 7(19), 13(19), 25(19), *72*, 88(37), *165*
Okawara, M., 100(80), 101(80), 144(164), 148(164), *166*, *168*
Olechewski, J. R., 367(174), 374(174), *451*
Olson, R. D., 409(310), 413(310), *454*
Onsager, L., 40(113), 41(113), *75*
Oohari, H., 3(9), 10(51), 17(68), 18(68), 24(9), 27(9), 66(9), *71*, *73*, *74*
Ooshika, Y., 40(109), *75*
Oppenheim, I., 278(61), 281(61), *327*
Orbach, N., 3(23a), 22(23a), 29(23a), 35(100), 48(23a), 50(23a), 51(139), 53 (100, 139), 54(139), 55(139), 58(139), 59(139, 145), 64(100, 139, 145), 65(145, 170), 66(145, 170), 67(170), 68(145, 170, 180), 69(139, 145, 170, 180), 70(139, 145), 71(100, 145), *72*, *75*, *76*, *77*
Orgel, L. E., 93(63), *165*, 203(185), *261*, 344(94), 345(94), 351(94), *449*
Orlov, I. G., 84(16), 100(16), *164*
Orwoll, R. A., 182(126), *260*
Oseroff, A. R., 230(288), *264*
Oswal, S. L., 316(149), *329*
Ota, Y., 24(74a), *74*
Otsubo, T., 87(31), *164*
Ott, J. B., 417(334), 419(346), 422(334), 423(334), *455*
Ottolenghi, M., 3(23a), 6(33), 7(37), 22(23a), 28(88), 29(23a), 31(33), 34(16, 37, 101), 48(23a, 131), 50(23a), 51(139), 52(37), 53(139), 54(131, 139), 55(131, 139), 58(139), 59(139, 145, 146, 147), 60(146), 64(139, 145), 65(16, 145, 169, 170), 66(16, 145, 170), 67(170), 68(145, 169, 170, 180), 69(139, 145, 169, 170, 180), 70(139, 145), 71(145), *72*, *73*, *74*, *75*, *76*, *77*, 82(6), *164*, 337(45), 408(304), *448*, *454*
Owen, G., 149(175), *169*
Oxtoby, D. W., 285(110a), 295(110a), 296(110a), *328*
Ozeki, M., 99(76), 100(76), 103(76), 104(76), 106(76), *166*

P

Pai, D. M., 83(13), 123(126), 131(126), 151(179), 152(179, 182), *164*, *167*, *169*
Pakhomova, V. I., 219(220), 238(220), *262*
Palmer, R. C., 176(43), *257*
Palocsay, F. A., 221(233), 239(233), *262*
Pampallona, M., 162(201), *169*
Pantazoplos, G., 186(138), 194(138), *260*
Pantos, E., 410(321), *455*
Parcher, J. F., 173(32), 176(49), 185(49), 227(244), *257*, *258*, *263*
Park, J., 142(159a), *168*
Park, S. M., 8(43), 20(43), 21(43), 22(43), *73*
Parks, G. S., 231(257), *263*
Parola, A., 28(79), 29(79), 61(79), *74*
Parsons, G. H., Jr., 28(79), 29(79), 61(79), *74*
Paskal, L. P., 182(128), *260*
Passchier, A. A., 377(196, 197, 199), 377(196, 197, 199), *451*
Patel, V. V., 139(150), *168*
Patterson, D., 205(192), 227(242, 243), *261*, *263*
Patterson, G. D., 298(134), 302(134),

309(134), 312(134), 323(134), *329*
Pauschmann, H., 238(313), *264*
Pearson, J. M., 50(176), 83(13), 116(116), 121(116), 124(116), 150(177, 178), 153 (183), *164*, *167*, *169*
Pease, E. C.. 185(133), *260*
Pecora, R., 275(46), 277(54, 56, 60), 278 (54), 289(119), 298(119), 300(119), 302 (119), 303(119), 309(54), 310(54), 317 (119), 323(56, 119), 325(119), *326*, *327*, *328*
Pecsar, R. E., 173(35), *257*
Pecsok, R. L., 172(14), 173(14), 181(110, 111), 182(127), 186(14), 187(14), 188 (14, 110, 111, 158), 206(201, 202), 207(206), 208(206), 209(206), 216(14), 223(14), *257*, *259*, *260*, *261*, *262*
Pekkarinen, L., 29(92), *75*
Perano, J., 388(251, 253), 398(251, 253), *453*
Peredereeva, S. I., 84(16), 100(16), *164*
Perlstein, J. H., 84(19), 117(119), 137 (119), 139(149), 142(119), *164*, *167*, *168*
Pershon, P. S., 298(132), 299(132), 302 (132), 317(132), *329*
Person, W. B., 187(155), *260*, 332(7, 16), 333(7), 334(7), 335(7), 338(7), 340(78), 344(7), 345(7), 346(7), 348(78), 352(78), 353(7), 354(118), 360(7), 362(118), 364 (118), 369(7), 370(7), 371(118), 372 (118), 377(78), 378(7), 379(205), 389(7), 391(7), 430(355), 431(366), 434(355), 435(355), *447*, *448*, *449*, *452*, *455*, *456*
Peticolas, W. L., 270(18), 272(18), 274 (18), *325*
Petkov, V. H., 182(124), *260*
Petkovic, Dj. M., 227(248), *263*
Petsev, N. D., 182(123, 124, 125), *260*
Pfister, G., 116(117), 133(117), *167*
Phillipoff, W., 230(286), *264*
Phillips, C. S. G., 172(6, 7, 12), 177(57), *256*, *257*, *258*
Phillips, W. D., 88(38), *165*, 348(106), *449*
Pierotti, G. J., 172(9), *256*
Pilgrim, G. W., 221(232), 239(232), *262*
Piterskaya, I. V., 15(64a), *73*
Pithig, R., 142(158), *168*
Pitt, P., 178(76), *258*
Pittman, C. U., 135(140), 142(159a, 159b, 159c), 144(162), 146(165, 166), 147(168), 148(162, 165, 168), *168*
Platt, J. R., 430(356), *455*
Plucknett, W. K., 373(208), *452*
Plyler, E. K., 366(157), *450*
Poczynailo, A., 227(249), *263*
Pollara, L. Z., 172(17), *257*
Polle, E. G., 340(72), *448*
Pommier, C., 191(167), 192(167), 206 (167, 204), 215(167), *261*, *262*
Pople, J. A., 40(111), *75*
Popov, A. I., 375(205), *452*
Porter, G., 379(210), 380(218), 381(232), 382(228), 383(218, 228, 238), 385(228), 388(250), 392(250), 393(250), 398(250), 399(250), 416(314), *452*, *453*, *454*
Porter, P. E., 172(9, 10), 184(10), *256*, *257*
Porter, R. S., 239(318), *264*
Possanzini, M., 178(81, 82), *258*
Potashnik, R., 6(33), 7(37), 28(88), 31(33), 34(37, 101), 52(37), 59(147), 65(169), 68(169, 180), 69(169, 180), *72*, *73*, *74*, *75*, *76*, *77*
Potter, D. J. B., 180(101), *259*
Powles, J. G., 270(15), 271(15), *325*
Prausnitz, J. M., 349(109), 360(109), 430(360), 431(372), 433(373), 434(360), 435(360), 442(385), 444(385), 445(385), *449*, *456*
Premru, L., 176(48), *258*
Price, D. T., 172(12), *257*
Priesti, H. F., 417(330), *455*
Primavesi, G. R., 237(303), *264*
Prochorow, J., 89(46), 92(59, 60), *165*, 338(62), 445(62, 393), 446(62, 393), *448*, *456*
Prout, C. K., 89(47), *165*
Prue, J. E., 344(90), 346(90), 353(90), *449*
Pshezhetskii, S. Ya., 400(279), 401(279), 402(279), *454*
Purer, A., 172(1), 230(1), *256*
Purnell, J. H., 172(13, 16), 176(42, 53), 177(53, 54), 181(111, 112), 182(53), 183(54), 184(54), 185(53, 54), 186(139), 188(111, 157, 159, 161, 166), 190(159, 166), 201(166), 202(166), 204(166), 206(200, 203), 207(166), 207(205), 208 (166, 205), 209(205), 210(209), 211 (209), 213(209), 214(209), 215(203), 216(203, 209, 216), 217(216), 219(221), 222(53, 234), 224(237), 226(238, 239), 230(238, 239, 251), 231(251), 233(251), 234(251), 235(251), 236(251). 237(299),

239(238, 239, 299), 240(329), 241 (327), 242(327, 328, 329), 243(238, 239), 245(54, 238), 246(238), 247(238), 248 (238), 249(221, 329, 330, 331), 250 (332), 251(54, 333), 252(334), 253(330, 333, 334, 335), 254(339), *257*, *258*, *259*, *260*, *261*, *262*, *263*, *264*, *265*

Q

Queignec, R., 188(165), 202(165), 234 (165), *261*
Quentrec, B., 282(97), 283(97), *328*
Quinn, M. J., 70(187), *78*

R

Rabinowitch, E., 385(244, 246), *453*
Radford, D. V., 335(35), *447*
Rahaman, M. S., 354(119), 355(119), 361(119), 362(119), 364(119), 371(119), 372(119), 377(119), *449*
Rakov, A. V., 274(40), *326*
Ramakrishnan, V., 27(78), *74*
Ramamurthy, V., 206(202), *261*
Ramsay, D. A., 270(25), *326*, 379(211), *452*
Rand, S. J., 380(215), 391(255), 398(255), *452*, *453*
Randic, M., 334(26), *447*
Rao, C. N. R., 332(17), 333(23), 339(71), 354(23), 355(17, 23), 357(17), 362(149), 365(17, 23), 368(149), 371(17, 23, 149), 376(149), 379(17, 204), 419(17), 432 (17), *447*, *448*, *450*, *452*
Rao, V. R., 27(78), *74*
Rastogi, P. R., 316(147), *329*
Raupp, G., 237(302), *264*
Rawlins, F. I. G., 231(278), *263*
Ray, N. H., 172(8), *256*
Regensburger, P. J., 114(106), 120(106), 123(106), 131(106), *167*
Rehm, D., 6(31), 10(53), 17(67a, 67b), 18(67a, 67b), 19(67a, 67b), 28(67b), 56(142b, 142c), 57(142b, 142c), 67 (176), *72*, *73*, *74*, *76*, *77*
Reichardt, Chr., 51(137), *76*
Reilley, C. N., 221(231), 251(231), *262*
Reinbold, B. L., 239(322), *265*
Reiss-Husson, F., 230(282), *263*
Rembaum, A., 114(107a, 107c, 107d), 124(107a, 107c, 107d), 138(144, 145, 146), 139)145, 147, 151), 140(145, 152, 153, 154), 161(200), *167*, *168*, *169*
Rentzepis, P. M., 13(61), 48(61, 127, 128), *73*, *76*, 285(104), 296(104), 312 (104), *328*
Rest, A. J., 405(297), 406(297), 410(297), 411(297), 415(297), *454*
Reucroft, P. J., 160(197, 198), *169*
Reuther, K. H., 237(301), *264*
Rezl, V., 173(30), *257*
Reznikov, S. A., 205(197, 198, 199), *261*
Rhodes, M., 149(175), *169*
Ricci, A., 162(201), *169*
Rice, O. K., 335(33, 38), 338(38), 345(33), 346(33), 352(33), 353(33), 378(33), *447*
Rice, S. A., 285(110a), 295(110a), 296 (110a), *328*
Richards, H. L., 373(208), *452*
Richards, J. T., 65(171), 66(171), *77*
Richardson, M. F., 186(142), 202(142), *260*
Richter, H. P., 10(49), *73*
Rieckhoft, K. E., 93(64), *165*
Riedl, P., 182(122), 194(122), 195(122), *260*
Riedmann, M., 182(119), *259*
Riedo, F., 182(121), *259*
Rijks, J. A., 176(52), 177(52), 182(118), 239(324), *258*, *259*, *265*
Rijnders, G. W. A., 173(33), 255(342), *257*, *265*
Rios, J., 269(6), 285(6), 286(6), 287(6), 296(6), 297(6), *325*
Risby, T. H., 239(322, 323), *265*
Roach, S. R., 342(83), *449*
Robb, J. C., 403(293), 411(303), 415(293, 303), *454*
Robbin, P. W., 230(288), *264*
Robbins, E. J., 335(39), *447*
Rochester, C. H., 377(195), 378(195), *451*
Rochlitz, J., 128(136), *167*
Rodgers, M. A. J., 63(164), *77*
Rogers, L. B., 176(45, 46, 47), *257*, *258*
Rogers, M. T., 308(140), 309(140), *329*
Rogozinski, M., 254(340), *265*
Rohatgi, K. K., 431(369), *456*
Rohrschneider, L., 238(310), *264*
Rolinski, J., 231(261), *263*

Rollig, K., 56(142a), 57(142a), 58(142a), *76*
Romero, J., 379(206a), *452*
Romm, I. P., 332(2), 333(2), 337(2), 340(2), 351(2), 353(2), 357(2), 432(2), *446*
Roper, J. N., Jr., 176(41), *257*
Rosasco, G. J., 276(53), 279(53), 286(53), 290(53), 308(53), 309(53), 311(53), *326*
Rosch, E. J., 338(61), 346(61), 347(61), *448*
Rose, J., 332(6), 333(6), *447*
Rose, N. J., 207(208), *262*
Rosenthal, L. C., 309(142), 310(142), *329*
Ross, J., 380(217), *452*
Rosseinsky. D. R., 430(361), 433(361), 434(361), *456*
Rossi, M., 93(66), *165*
Rossi-Sonnichsen, I., 279(64), 308(139), 309(139), *327*, *329*
Rothschild, W. G., 271(28), 273(28), 276(53), 278(28), 279(53), 285(28, 103), 286(53), 287(28, 103), 288(28), 289(28), 290(53), 292(103), 293(103), 297(28, 103), 298(28), 308(28, 53, 103), 309(28, 53, 106), 311(53), 314(146), *326*, *328*, *329*
Rotkiewicz, K., 13(60), 47(60), 48(126, 129), *73*, *76*
Rowley, G. N., 187(153), *260*
Rowlinson, J. S., 227(241), *263*, 272(33), 275(33), 283(33), *326*, 359(138), *450*
Roy, J. K., 34(103), *75*
Ruoff, A., 308(139), 309(139), *329*
Russell, K. E., 382(225), 383(225), 417 (336), 418(336), 423(336), *452*, *455*

S

Saito, T., 12(57), 13(57), 39(57), 54(57), 55(57), *73*, 89(40), *165*
Saito, Y., 33(99), *75*
Sakata, T., 149(173), *168*, 414(326), 445 (326), 446(326), *455*
Sakata, Y., 3(18a, 18b, 21, 22b), 5(28), 7(18a, 18b), 8(21), 12(21), 13(21), 19(18a, 18b, 21, 22b), 22(28), 23(72), 35(28, 104), 38(18a, 18b, 21), 39(21), 44(18a, 21, 22b), 46(18a, 22b), 52(28, 72), 54(18a, 21), 55(140), 60(140), *72*, *74*, *75*, *76*, 86(29, 30), 87(31), 89(40), *164*, *165*
Sakharov, V. M., 172(26), 227(250), *257*, *263*
Sakodynskii, K. I., 172(26), *257*
Saksena, B. D., 444(397), *456*
Sakurai, H., 93(70), *166*, 436(375), 439 (375), 440(375), *456*
Salisbury, K., 405(297), 406(297), 410 (297), 411(297), 415(297), *454*
Sambhi, M. S., 335(37), *447*
Samperi, R., 253(336), *265*
Sancier, K. M., 365(153), 366(153), 371 (153), 372(153), 374(153), *450*
Sanctuary, B. C., 377(200), 378(200), *451*
Sandman, D. J., 84(19, 23), *164*
Sandros, K., 89(45), *165*
Sanioto, D. L., 342(79), *448*
Sargent, F. P., 70(187), *78*
Sasaki, Y., 142(159a, 159b, 159c), *168*
Satchell, D. P. N., 417(331), *455*
Satchell, R. S., 417(331), *455*
Sato, H., 357(126), 398(275), 401(275), 405(126), 411(126), 412(126), 413(126), *450*, *453*
Sato, K., 103(85), 104(85), *166*
Sawyer, D. T., 200(179), 253(179), *261*
Scatchard, G., 340(75), *448*
Schaad, L. J., 357(127), 421(127), *450*
Schafer, F. P., 56(142a), 57(142a), 58 (142a), *76*
Schäffer, A., 271(26), 286(26), 289(26), 290(26), 298(26), 299(26), 312(26), 313 (26), 314(26), *326*
Scheibe, D., 298(131), 312(131), 313(131), *328*
Scher, H., 117(121), 134(137), *167*
Schiebel, A. H., 89(42), *165*
Schiemann, V. H., 273(37), 285(37), 286(37), 287(37), 292(37), 295(37), 296 (37), 297(37), 308(141b), 309(141b), 311(141b), 317(37), 318(37), 320(37), *326*, *329*
Schiller, J. C., 361(146), 366(146), 367 (146), 368(146), 369(146), 371(146), 372(146), 374(146), 376(146), 377(146), *450*
Schlag, E. W., 71(188), *78*
Schnecko, H., 188(164), *261*
Schneider, A. A., 114(105), 161(105), *167*
Schneider, F., 13(58a), 22(58a), 51(58a), *73*

Schols, J. A., 172(11), *257*
Schomburg, G., 178(84, 85), *259*
Schomburg, H., 68(181), 71(181), *77*
Schreiber, H. P., 205(192), *261*
Schröder, H., 71(188), *78*
Schroeder, J., 273(37), 285(37), 286(37), 287(37), 292(37), 295(37), 296(37), 297 (37), 308(141b), 309(141b), 311(141b), 317(37), 318(37), 320(37), *326*, *329*
Schuchmann, H-P., 406(299), 409(299), 413(299), *454*
Schug, J. C., 335(34), *447*
Schulten, K., 71(189), *78*
Schulz, R. C., 102(82), 107(92), 111(92), 152(92, 182), *166*, *169*
Schumaker, R. R., 149(174), *169*
Schumb, W. C., 417(330), *455*
Schurig, V., 187(145, 146, 147), 196(175), 197 (175), *260*, *261*
Schuster, H., 34(101), *75*
Schwartz, M., 289(123), 298(123), 302 (123), *328*
Scibona, G., 227(249), *263*
Scott, B. A., 149(174), *169*
Scott, J. F., 403(290), 410(290), 414(290), 415(290), *454*
Scott, R. L., 340(74), 341(74), 347(103, 104), 349(104, 109), 360(109), *448*, *449*
Scott, R. P. W., 254(337), *265*
Scrosati, B., 162(201), *169*
Seanor, D. A., 111(99), 115(112), 154 (188), *166*, *167*, *169*
Searles, S., Jr., 360(140), 366(166), *450*, *451*
Seidlith, H., 71(188), *78*
Seki, H., 117(120), *167*
Selenkina, M. S., 238(308), *264*
Sergeev, G. B., 367(177, 178, 179), *451*
Serguchev, Yu. A., 367(179), *451*
Serteev, G. B., 378(202), *452*
Sevcik, J., 178(88), *259*
Shaffert, R. M., 114(104), 120(104), 125 (104), 158(104), *166*
Shapiro, S. M., 148(172), *168*
Sharko, P. T., 273(37), 285(37), 286(37), 287(37), 292(37), 295(37), 296(37), 297 (37), 317(37), 318(37), 320(37), *326*
Sharp, D. W. A., 424(350), 426(350) 427(350), *455*
Sharp, J. H., 114(110), 116(110), 159 (196), *167*, *169*
Shattuck, M. D., 158(194), *169*
Shaw, V. R., 200(181), *261*
Sheppard, W. A., 144(163), *168*
Sheridan, J. P., 185(132), 195(171, 172, 173), 196(172), 198(172), 202(171, 173, 182), 205(171, 172, 173, 182), 212(172), *260*, *261*
Shevchuk, I. M., 227(250), *263*
Shida, T., 60(151), *76*
Shimada, M., 60(149), *76*
Shirane, G., 148(172), *168*
Shiruta, Y., 60(151), *76*
Shizuka, H., 29(91), *75*
Shold, D. M., 89(43), *165*
Sicilio, F., 176(43), *257*
Sidorov, R. I., 205(197, 198, 199), *261*
Siemlarczuk, A., 48(130), *76*
Sievers, R. E., 186(142, 143), 200(143), 202(142), *260*
Silverman, B. D., 148(170), *168*
Simon, M. S., 141(155), *168*
Simons, J., 382(225), 383(225), *452*
Simons, J. P., 374(209), 375(209), 376 (209), 434(209), 435(209), *452*
Sinanoglu, O., 338(52), 344(52), *448*
Sinclair, T. J., 270(19), *325*
Singer, L. A., 89(44), *165*
Singh, A., 70(187), *78*
Singliar, M., 238(304), *264*
Sisido, M., 90(55), *165*
Sitters, R., 411(322), *455*
Sivaramakrishnan, K., 154(184), *169*
Skinner, E. W., 231(254, 258), *263*
Slifkin, M. A., 405(296), 410(296), 411 (296), 412(296), 413(296), 414(296), *454*
Slough, W., 142(157), *168*
Smalley, J. F., 369(186), 393(263), 399 (186), 400(186), 401(186), *451*, *453*
Smets, G., 107(91), *166*
Smirnov, V. V., 367(177), *451*
Smith, C. D., 436(380), 440(380), *456*
Smith, G. H., 237(296), *264*
Smith, J. A., 381(232), 382(228), 383 (228), 385(228), *452*
Smith, J. F., 182(113), *259*
Smith, K. C., 103(84), 104(84), *166*
Smith, M., 159(196), *169*
Smyth, C. P., 314(145), *329*
Sneeringer, P. V., 409(307, 308), 410 (306, 307, 308), *454*

Snyder, S. T., 109(97), *166*
Soczewinski, E., 238(305), *264*
Sodeau, J. R., 405(297), 406(297), 410 (297), 411(297), 415(297), *454*
Sogani, C. M., 231(262), *263*
Sojak, L., 239(324), *265*
Sokolov, U., 358(133), 403(133), 410 (133), 413(133), 414(133), 445(133), 446(133), *450*
Solaro, R., 97(74), 98(74), 106(74), *166*
Somersall, A. C., 83(12), 88(12), *164*
Somoano, R., 139(151), 140(153), *168*
Sonntag, C. von, 406(299), 409(299), 413(299), *454*
Soulignac, J-C., 392(257), *453*
Sousa-Alonso, A., 379(206a), *452*
Soussen-Jacob, J., 323(159), 324(159), *329*
Spangler, R. D., 231(266, 270), *263*
Spanner, K., 285(105), 296(105), 300 (105), *328*
Spencer, M. S., 237(299), 239(299), *264*
Spertell, R. B., 180(104), *259*
Springer, C. S., 186(142), 202(142), *260*
Springer, T., 270(16), *325*
Srivastava, O. P., 188(166), 190(166), 201(166), 202(166), 204(166), 207(166), 208(166), *261*
Staab, H. A., 90(56, 57), 92(62), 99(75), *165*, *166*
Staerk, H., 68(181), 71(181, 189), *77*, *78*
Steel, C., 29(92), *75*
Steele, W. A., 270(24), 273(34), 276(52), 281(34), *326*
Stefanova, A. D., 182(125), *260*
Steffons, E., 71(188), *78*
Stein, G., 408(304), *454*
Steinberg, V. I., 409(307, 308, 310, 311), 410(306, 307, 308), 413(310, 311), 414 (311), *454*
Stepanov, B. I., 436(382), 438(382), 441 (382), *456*
Stevens, B., 2(2), 28(87), *71*, *74*, 434(367), *456*
Stevenson, D. P., 430(358), 431(358), 433(358), *455*
Stewart, F. E., 138(145), 139(145), 140 (145), *168*
Stewart, G. H., 172(15), 221(230), 238 (230), *257*, *262*
Stewart, G. W., 231(252, 253, 254, 255, 256, 258, 260, 263, 264, 265, 266, 267, 268, 271, 272, 274, 276, 277, 279), *263*
Stiles, P. J., 335(35), *447*
Stillman, M., 187(153), *260*
Stock, R., 180(100), *259*
Stoddart, C. T. H., 179(93), 180(93), 255(344), *259*, *265*
Stoicheff, B. P., 270(23), *326*
Stokes, J. M., 180(107), *259*
Stokes, R. H., 180(107), *259*
Stolka, M., 113(103), *166*
Stolpe, C. van de, 366(168, 172, 173), 373(173), 375(172, 173), *451*
Strauss, H-L., 309(142), 310(142), *329*
Streiter, F. J., 419(345), 421(346), *455*
Stromme, K. O., 352(114), *449*
Strong, R. L., 345(96), 355(96), 369(186), 380(215), 382(226, 236), 384(236), 388 (251, 253), 391(255), 394(267), 395 (267, 268), 397(267, 268), 398(251, 253, 255, 271, 274), 399(186), 399(268), 400(186, 267), 401(186, 236, 274), *449*, *451*, *452*, *453*
Stross, F. H., 172(10), 184(10), *257*
Strukova, T. P., 187(148), *260*
Struve, W. S., 13(61), 48(61, 127, 128), *73*, *76*
Stubley, D., 358(129), *450*
Sullivan, R. J., 419(346), *455*
Sulzberg, T., 108(93), 151(93), 152(93), *166*
Summers, D. M., 219(221), 249(221), 251(333), 253(333), *262*, *265*
Summers, J. W., 102(83), 135(83), 136 (83), *166*
Sunder, S., 280(68b), 296(68b), 297(68b), 311(68b), *327*
Supina, W. R., 237(295), *264*
Suppan, P., 338(53), 344(53), *448*
Suprynowicz, Z., 238(305, 306), *264*
Suzuki, M., 239(317), *264*
Surynarayanan, B., 144(162), 148(162), *168*
Sus, O., 123(127), *167*
Suzuki, H., 42(119), *75*
Suzuki, T., 5(28), 22(28), 35(28), 52(28), *75*, 302(137), 308(137), *329*
Swaay, M. van, 178(63), *258*
Swallow, A. J., 393(264), 398(272, 273), 399(264, 273), *453*
Swanton, W. T., 255(345), *265*

Swift, S. M., 178(71), *258*
Swingle, R. S., 176(46, 47), *257*, *258*
Symons, M. C. R., 397(269), *453*
Szabo, Z. G., 380(218), 383(218), *452*
Szymanski, A., 122(125), *167*

T

Tabisz, G. C., 297(151), 312(151), *329*
Tabushi, I., 436(381), 438(381), 440(381), 441(381), *456*
Tachikawa, H., 20(71), 22(71), *74*
Tada, K., 60(151), *76*
Taglieber, V., 90(57), *165*
Takagi, H., 90(55), *165*
Takahashi, K., 160(197, 198), *169*
Tamir, M., 59(146), 60(146), *76*
Takahashi, H., 357(126), 405(126), 411 (126), 412(126), 413(126), *450*
Tamres, M., 187(154), 209(154), *260*, 333(24), 335(24), 338(24, 60), 339(24), 341(60), 342(81, 85), 343(85, 88, 89), 344(24, 88, 89), 345(97), 346(24), 348 (60, 105), 349(60), 350(24, 112), 351 (113), 352(24), 353(24, 88, 89, 117), 354(24, 88, 119), 355(24, 88, 99, 117, 119), 360(140), 361(88, 119), 362(24, 88, 119), 364(88, 119, 151), 366(113, 166), 368(24, 89), 369(89), 371(88, 119), 372(88, 119), 373(113), 376(89), 377 (198), 378(24, 89, 198), 394(89), 395 (89), 396(24, 89), 397(89), 446(390), *447*, *448*, *449*, *450*, *451*, *456*
Tanaka, F., 28(80b), 62(80b), *74*
Tanaka, H., 107(92), 111(92), 152(92, 182), *166*, *169*
Tanaka, J., 4(26a), 29(96), 32(96), 33 (96), 35(104), *72*, *75*
Tanaka, M., 89(48), *165*
Taniguchi, Y., 29(91), 58(143), 59(143), 60(151), *75*, *76*
Tanimoto, O., 17(68), 18(68), *74*
Tanizawa, K., 3(23a), 22(23a), 29(23a), 48(23a, 132), 49(132), 50(23a), 52(132), *72*, *76*
Tarjan, G., 182(121), *259*
Tatemitsu, H., 86(29, 30), *164*
Taylor, G. N., 89(42), *165*
Tazuke, S., 100(80), 101(80), 103(85), 104(85), *166*, 332(4), 333(4), *446*
Tebedev, N. N., 107(90), 152(90), *166*
Teck, R. J., 178(79), *258*
Teitelbaum, Z., 34(101), *75*
Templeton, D. H., 419(345), 421(346), *455*
Teo, B. K., 84(24), *164*
Tewari, Y. B., 185(132), 195(171), 202 (171), 205(171, 192), *260*, *261*
Thanh, N-V., 279(64), 308(139), 309 (139), *327*, *329*
Thomas, H. T., 3(17), 7(17), 37(17), 52(138), *72*, *76*
Thomas, J. K., 65(171), 66(171), *77*, 399(277), *453*
Thompson, C. C., 93(69), *166*, 335(32), *447*
Thorburn, S., 185(133), *260*
Thurman, R. G., 178(66), *258*
Timm, D., 372(207), 400(207), *452*
Tohgo, Y., 28(83), *74*
Toi, H., 412(313), 416(313), *454*
Tokuhiro, T., 285(103), 287(103), 292 (103), 293(103), 297(103), 308(103), 309(103), *328*
Tokura, N., 332(4), 333(4), *446*
Tomchuk, E., 316(148), 317(148), *329*
Tomimoto, S., 60(150, 151), *76*
Tomono, T., 84(17), 112(100), *164*, *166*
Torihashi, Y., 3(14), 24(74a), *72*, *74*
Tornheim, L., 239(318), *264*
Torrance, J. B., 148(170), *168*
Touchstone, J. C., 215(212, 213, 214, 215), 238(212, 213), *262*
Toukubo, K., 230(291), *264*
Townsend, M. G., 380(218), 383(218), *452*
Tramer, A., 338(62), 430(354), 434(354), 435(354), 445(62), 446(62), *448*, *453*
Traven, V. F., 436(374, 376, 382), 437 (374, 376), 438(382), 439(374, 376), 440(374, 376), 441(382), *456*
Traynham, J. G., 367(174), 374(174), *451*
Treinin, A., 29(95), *75*, 392(259, 262), 399(259), 401(262), *453*
Trestianu, S., 172(22), *257*
Trethewey, K. R., 89(41), *165*
Troe, J., 383(239, 240, 241), 385(241, 242, 243), *452*, *453*
Trotter, P. J., 93(67), *165*, 335(29), 338(63), *447*, *448*
Truong, K. D., 85(26), *164*

Tsang, W., 173(36), 188(36), *257*
Tschida, E., 84(17) *164*
Tse, H. C., 342(86), 351(86), 446(390), *449*, *456*
Tsubomura, H., 28(80b, 86), 60(151), 62(80b), 67(177), *74*, *76*, *77*, 149(173), *168*, 332(4), 333(4), 357(125, 126), 358(132), 398(275), 401(275), 403(132), 404(132), 405(126, 132, 297a), 406 (300), 408(132), 409(312), 410(132), 411(126, 132, 297a, 300), 412(126, 132, 312, 313), 413(126, 132), 414(132, 326), 415(329a), 416(312, 313), 417(332), 423 (332), 445(326), 446(326), *446*, *450*, *453*, *454*, *455*
Tsuchida, E., 112(100), *166*
Tsujino, N., 3(12), 6(35), 15(12), 31(12, 35), 61(12), 66(172a), *72*, *73*, *77*
Turkeltaub, N. M., 238(308), *264*
Turner, P. H., 61(156), *77*
Turner, S. R., 109(95), 113(103), 151 (179), 152(179, 182), *166*, *169*
Turoff, M. L. H., 254(338), *265*
Turro, N. J., 89(43), *165*

U

Uchida. T., 436(375), 439(375), 440(375), *456*
Ueno, Y., 144(164), 148(164), *168*
Ullal, H., 160(197, 198), *169*
Umemoto, T., 23(72), 52(72), *74*
Umeyama, H., 335(36), *447*
Ushio, F., 10(48), 15(48), 16(48), 25(48), *73*
Usui, H., 3(19), 7(19), 13(19), 25(19), *72*

V

Vahtra, U., 158(194), *169*
Vaidyanathan, S., 27(78), *74*
Valentin, P., 173(29), *257*
Valiev, K. A., 285(111), 293(111), 296 (111), *328*
Van den Bergh, H., 383(239, 240), *452*
Vandenheuvel, W. J. A., 221(225), 238 (225), *262*
van der Hart. D. L., 309(143), 311(143), *329*
Van der Weil, A., 415(329), *455*
Vargas de Andrade, J. M., 210(209), 211 (209), 213(209), 214(209), 216(209, 216), 217(216), *262*
Veber, E. R., 205(197), *261*
Velinov, G., 100(77), *166*
Venditti, F. J., Jr., 395(268), 397(268), 399(268), *453*
Verhoeven, J. W., 89(50, 51, 53), 92(61), *165*
Verlaat, T. van't, 187(149), 198(149), *260*
Versino, B., 182(117), *259*
Versmold, H., 280(73), 296(73), 323(153), *327*, *329*
Vigdergauz, M. S., 172(24), 219(220), 220(222), 238(220), *257*, *262*
Vincent, C. A., 162(201), *169*
Virzi, D. R., 366(166), *451*
Visco, R. E., 21(70), *74*
Vitenberg, A. G., 187(148), *260*
Vogel, E., 86(28), *164*
Vogel, W. M., 359(137), *450*
Vogler, H., 99(75), *166*
Voigt, E. M., 93(64), *165*, 360(143), 368 (143), *450*
Volino, F., 270(17), *325*
Volterra, V., 276(51), 295(51), *326*

W

Wachi, F. M., 200(180), *261*
Wade, R. L., 177(61), 178(80), *258*
Waksmundzki, A., 205(194), 238(305, 306), *261*, *264*
Walatka, V., 84(19), 139(149), *164*, *168*
Walker, L. L., 142(159b), *168*
Walker, M. S., 3(10), 52(10), *71*
Walker, S. M., 124(133), *167*
Walkley, J., 360(144), *450*
Walsh, A. D., 381(231), *452*
Walz, H., 355(121), *449*
Wang, C. H., 275(50), 287(50), 289(123), 298(123), 302(123), 317(50), 320(50), 323(50), *326*, *328*
Wang, C. T., 409(310, 311), 413(310, 311), 414(311), *454*
Ward, H. K., 231(275), *263*
Ward, H. R., 70(186), *78*
Wardley, A. A., 340(76), *448*
Ware, W. R., 8(39), 9(39, 46), 10(49, 50),

11(50, 55), 15(64b), *73*, *74*, 82(9), *164*, 337(47), 410(318), 416(317, 318), *448* 455
Warren, B. E., 231(281), *263*
Washington, E., 139(151), *168*
Wasik, S. P., 173(36), 186(139), 188(36), *257*, *260*
Wassermann, E., 380(216), *452*
Watanabe, K., 367(180), *451*
Watanabe, T., 239(317), *264*
Watari, H., 28(81), *74*
Watkins, A. R., 29(94), 67(178, 179), 68(178, 179), *75*, *77*
Watson, I. D., 205(190), *261*
Watts, H., 358(129), *450*
Webb, J. D., 421(348), 429(348), *455*
Weber, G., 50(133), *76*
Weeke, F., 178(84, 85), *259*
Wegdam, G. H., 275(49), *326*
Wei, K. S., 408(305), 411(305), *454*
Weigl, J. W., 123(129), *167*
Weimer, R. F., 430(360), 434(360), 435 (360), 442(385), 444(385), 445(385), *456*
Weiner, P. H., 173(38), 176(49), 185(49), *257*, *258*
Weiser, G., 125(134, 135), 131(134), 157(134), *167*
Weiss, F. T., 188(162), 224(162), *261*
Weiss, K., 388(252), 389(252), 398(252), 399(252), *453*
Welch, C. M., 109(97), *166*
Welke, F., 406(299), 413(299), *454*
Weller, A., 3(8, 11, 13, 14), 4(13), 6(29b, 31, 32), 7(37), 10(53), 17(67a, 67b), 18(67a, 67b), 19(67a, 67b), 20(69), 28(67b), 34(37), 42(13), 44(121), 52 (37), 56(142a, 142b, 142c), 57(142a, 142b, 142c), 58(142a), 65(8), 66(173), 67(8, 173, 176, 178, 179), 68(178, 179, 181), 71(181, 189), *71*, *72*, *73*, *74*, *75*, *76*, *77*, *78*, 82(8), 87(33), *164*, *165*
Wellington, C. A., 186(136), 187(136), 188(136), *260*
Wen, W. Y., 377(201), 378(201), *451*
Wenz, D. A., 207(208), *262*
Werner, H. J., 71(189), *78*
West, R., 84(18), *164*, 436(374, 376), 437(374, 376), 439(374, 376), 440(374, 376), *456*
Westaway, M. T., 179(95), *259*
Westlake, T. N., 173(32), 176(49), 185 (49), 227(244), *257*, *258*, *263*
Wheland, R. C., 84(20), *164*
Whitney, P. M., 187(152), *260*
Whitten, D. G., 34(103), *75*
Whittenberg, S. L., 275(50), 287(50), 317 (50), 320(50), 323(50), *326*
Wiberg, N., 443(394), *456*
Wicarova, O., 176(50), 177(50), 179(50), 182(50), 183(50), *258*
Widdecke, H., 217(219), 218(219), 221 (219), *262*
Wildman, R. P., 384(237), *452*
Willard, J. E., 364(150), 382(226), *450*, *452*
Williams, D. J., 94(72), 95(72), 96(72), 99(72), 103(72), 116(116, 118), 121 (116), 124(116), 159(195), *166*, *167*, *169*
Williams, D. R., 334(26), *447*
Williams, P. S., 177(54), 183(54), 184(54), 185(54), 226(238, 239), 230(238, 239), 239(238, 239), 243(238, 239), 245(54, 238), 246(238), 247(238), 248(238), 249(330, 331), 251(54, 333), 253(330, 333), *258*, *262*, *265*
Willis, M. R., 139(148), 142(158), *168*
Willmott, F. W., 238(314), *264*
Wilson, R. S., 285(110b), 296(110b), *328*
Windham, E. S., 238(315), *264*
Windsor, M. L., 180(98, 105, 108), 181 (98), 182(105), *259*
Winfield, J. M., 424(350), 426(350), 427 (350), *455*
Wiseman, J. R., 367(176), *451*
Wobschall, D. C., 362(148), 371(148), 372(148), *450*
Woerkom, P. C. M. van, 271(29), 285(29, 109), 286(29, 109), 289(29), 290(109), 296(29, 109), 297(109), 298(29, 109), 308(29), 312(29, 109), 314(109), *326*, *328*
Wojciechowski, P., 157(192), *169*
Wojtkowiak, B., 188(165), 202(165), 234 (165), *261*
Wolf, M. W., 89(44), *165*
Wong, W. H., 381(220, 221), 382(220, 221), *452*
Wood, W. C., 385(246), *453*
Wright, D. A., 308(140), 309(140), *329*
Wright, R. B., 289(123), 298(123), 302 (123), *328*

Wu, C-H., 215(213), 238(213), *262*
Wudl, F., 84(22, 24), *164*
Wyllie, G., 272(31), 274(31), 276(31), 282(31), 285(31), *326*

Y

Yager, W. A., 380(216), *452*
Yagishita, T., 412(313), 416(313), *454*
Yakovenko, E. I., 378(202), *452*
Yamabe, S., 335(36), *447*
Yamagishi, F. G., 84(19), *164*
Yamamoto, N., 6(29a), 42(118), 43(118), 56(118), 57(118), 60(151), 67(177), *72*, *75*, *76*, *77*, 398(275), 401(275), 406 (300), 411(300), *453*, *454*
Yamamoto, S., 28(81), *74*
Yamamoto, Y., 60(154), *77*
Yamamura, K., 436(381), 438(381), 440 (381), 441(381), *456*
Yamanaka, C., 9(45), 10(45, 48), 13(59a), 15(48, 65b), 16(48), 25(48), 61(65b), *73*, *74*
Yamato, Y., 239(317), *264*
Yamazaki, K., 381(230), *452*
Yang, N. C., 66(174), *77*, 89(43), 110(98), *165*, *166*
Yanus, J. F., 116(116), 121(116), 124 (116), 150(176, 177, 178), *167*, *169*
Yarwood, J., 268(1), 269(1), 275(44), 276(1, 107), 277(1), 280(1), 285(107), 286(107), 290(107), 296(107), 310(1), 317(107), 318(107), 319(107), 320(107), 321(107, 156, 157), 323(107, 158), 324 (107), *325*, *326*, *328*, *329*, 332(8), 350 (112), 435(8), *447*, *449*
Yashin, Y. I., 172(26), *257*
Yatsugi, H., 221(226), *262*
Yee, K. C., 158(203), *169*
Yellin, N., 270(21), 323(21, 160), *326*, *329*
Yen, S. P. S., 139(151), 140(153, 154), *168*
Yip, R. W., 62(157), *77*
Yllana, A. de, 181(110), 188(110), *259*
Yomosa, S., 42(120), *75*
Yoshida, M., 86(29, 30), *164*
Yoshida, Z., 365(155), 371(155), 372 (155), *450*
Yoshihara, K., 3(14), 10(52), 24(76), 32(98), *72*, *73*, *74*, *75*
Young, C. L., 172(23), 180(98, 105), 181(98), 182(105), 215(211), *257*, *259*, *262*
Young, H. D., 183(130), *260*
Young, R. P., 269(5), *325*

Z

Zaal, P., 237(297), *264*
Zachariasse, K. A., 6(27c), 8(42), 20(42, 69), 35(27c), 36(27c), 66(173), 67(173, 175), *72*, *73*, *74*, *77*
Zahn, C., 186(138), 194(138), *260*
Zhukhovitskii, A. A., 238(308), *264*
Zielinski, W. L., Jr., 239(321), *265*
Zlatkis, A., 187(146), 196(175), 197(175), 237(300), *260*, *261*, *264*
Zwaan, D. de, 281(80), *327*
Zwaan, J. de, 306(138), *329*
Zwart, M. de, 271(29), 285(29, 109), 286(29, 106), 289(29), 290(109), 296 (29, 109), 297(109), 298(29, 109), 308 (29), 312(29, 109), 314(109), *326*, *328*

Subject Index

A

Acceptor molecules, halogens as, 359
  polymers, 106
Acetates, 186
Acetonaphthone, 30
Acetone, 30, 406
Acetonitrile, 317
Acetylenes, 225
Acrylic acceptor polymer, 109
Activation, enthalpy, 309
  model, 311
  volume, 311, 323
Activity coefficient, 186, 191, 203
N-Acyl-polyethylenimines, 136
Additives, alkyl halides and cyanides, 199
  amines, 199
  ethers, 199
  ketones, 199
  sulphides, 199
Aggregation, 231
$AgNO_3$, 186
Alcohols, 186, 196, 442
  as donors, 392
Alicyclic hydrocarbons, 227
Alkanes, 222, 227
Alkane–iodine systems, 364
Alkenes, 224
Alkene–halogen interactions, 367
Alkyl iodide–iodine complexes, 393
  benzenes, 88
n-Alkyl halides, 230
Alkyl halide–iodine interactions, 368
Alkylnaphthalene, 87
α values, 251
Alkynes, 202
Amorphous complexes, 136
  molecular glasses, 115
Angular harmonic motion, 282
  momentum correlation time, 280
Anharmonicity, 270
Aniline, 188, 404, 407
Anisole, 407
Annulenes, 86
Anomalous fluorescence, 47
Anthracene, 10, 20, 21, 30, 34, 44, 56, 58, 60, 66, 109, 114, 157
(Anthracene)–$(CH_2)_n$–(*N*,*N*-dimethylaniline), 7
Anthracene–DEA, 12, 19, 26
Anthracene–DMA, 11, 25
Anthracenophanes, emission spectra of, 35
1-(1-Anthryl)-3-(4-*N*,*N*-dimethylaminophenylpropane), 25
1-(9-Anthryl)ethylmethacrylate homopolymer, 105
1-(9-Anthryl)ethyl pivalate, 105
Anti-Stokes scattering, incoherent, 300
Aromatic amine–iodine complexes, conductivities of, 124
Aromatic hydrocarbons, 17, 188, 227
Aromatic hydrocarbons, anions of, 20
Aromatic hydrocarbon–amine systems, 27
Aromatic hydrocarbon–halogen interactions, 366
6-*N*-Arylaminonaphthalene-2-sulphonate, 28, 48
Associated liquids, 312
Association constant, 24, 103, 188
  by glc, 202
  degree of, 339
Asymmetry in glc (A_S), 179
Atactic polymers, 142
Attractive interactions, 286
Autocorrelation function, 272 *et seq.*
Autoxidation of hydrocarbons, 408
Azulenophane, 87

B

Back-CT transitions, 34
Back transfer of an electron, 17
Ball-plane interactions, 342, 419
Band asymmetry, 270
  broadening effects, 285
  moments, 278
  profile of CHF_3, 306
  resolution procedure, 104
  shape, 270, 272
  splitting, 270
  spreading, 179
Benesi–Hildebrand plot, 85, 202, 209, 235, 340, 388, 417
Benzaldehyde, 312
Benzene, 63, 216, 229, 245, 312, 345, 404, 405, 407
Benzene–oxygen contacts, 356
Benzidine, 89
3,4-Benzophenanthrene, 21
Benzophenone, 21, 28, 61
Benzoquinones, 150
Benzotrifluoride, 216
B–H—see Benesi–Hildebrand
9,9′-Bianthryl, 13, 22, 51
Biferrocene CT complexes, 142
Binary collisions, collinear, 293
Biphenyl, 10, 20, 44, 66, 157
Biphotonic dissociation, 60
4,4′-Bipyridylium, 141
Birefringence properties, 134
Bisdicyanomethylene-1,3-dithietan, 84
2,5-Bis(2-hydroxyethoxy)-7,7,8,8-tetracyanoquinodimethane, 154
Bithiopyran, 84
Blue shift, 38, 342, 359, 363, 396
  in the iodine visible band, 352
Borrowing of intensity, 408
Bromine dopant, 158
Bromochloromethane, 214
Bromoform, 205
Bromotrichloromethane, 214
Brot–Larkin model, 283, 307
Br_4, CT studies, on, 378
n-Butanol, 214
s-Butanol, 214
t-Butanol, 214
Butenes, 186, 187

C

Cage recombination, 63
Capacity factors, 251
Carbazole, 28, 157
  chloranil complexes, 98
  -containing polymers, 94, 104
Carbon-black-filled conductive elastomers, 140
Carbon disulphide, 307
  tetrabromide, 11, 214
  tetrachloride, 214, 307
Carbonyl triplets, photoreduction of, 29
Cardiac pacemakers, 114, 161
Carrier drift mobilities, 122
CCT—see contact charge-transfer
Cell electrode, 114
  model, 296
Charge carriers, 114
  carrier mobilities, 121
Charge-transfer, binding energy, 80
  complexes, excitation of, 82
  energies, 389
  salts, 117
Charge-transfer-to-solvent spectra, 339
Charge transport, 114
Chemical reactions in polymer-based systems, 82
Chemically induced electron-spin polarization, 70
Chemically induced nuclear-spin polarization, 70
Chemiluminescence, 67
Chemiluminescence spectra, 20
Childs' law, 122
Chloranil, 94, 96, 103, 157
Chlorobenzene, 216, 405
Chlorodibromomethane, 214
Chloroform, 205, 214, 309
Chrysene, 20
Circular dichroism, measurements, 98
  spectra, 106
Clustering, 230, 273
Cobalt(II) compounds, complex formation by, 197
Collision model, 347
  times, 276
Collisional encounter complexes, 83
  interaction, 25, 403

Column liquid volume, 182
Column thermostats, construction of, 176
Combination bands, 270
Competitive equilibrium study, 268
Complex, definition of, 333
  dimensions of, 44
  strength, 391
Complexation constants, 202
Complexes, crystalline adducts, analysis of, 85
Complexing phases, 213
Conductive organic materials, 137
Conductivity, 114
Configuration of higher-order CT complexes, 86
Conformational effects in CT phenomena, 89
  factors, 153
Conformations, 94
Consolute temperature, 219
Constant-activity method, 342
Constant density, temperature-dependent experiments, 302
Contact-charge-transfer absorption spectra, 333
Contact CT complexes, 25, 332 *et seq.*
  interaction, 397, 403
  ion pair, 29, 31
"Contact pairs", 203
Continuous-variation method, 417
  plots, 419
Copolyurethanes, 156
Coriolis coupling, 274, 302
Correlation function, 283
  of n.m.r. and u.v. data, 235
  time, 271
Crystalline complexes, 136
Crystallinity of polymeric CT complexes, 142
Crystallographic data, 419
CT stabilization energy, 96
CTTS—see charge-transfer-to-solvent
Cumene, 405
1-Cyanoanthracene, 21
1-Cyanonaphthalene, 44
Cybotaxis, 230, 231
Cyclized conformations, of polysarcosine, 90
Cyclohexane, 216, 405, 407
Cyclooctene, 405
Cyclophane, three-layered, 86
Cyclophanes, 2
[2.2]Cyclophanes, 92
Cyclopropanes, interaction with iodine, 365

D

Damping effects, 282
Dark decay, 152
Dative-bond contribution to CT complexation, 397
  wavefunction, 353
Dative structure, 334
DEA—see *N*,*N*-diethylaniline
Deactivation processes, 157
"Dead" time, 174, 182
Decay curves, 9
Dember coefficients, 137
  voltage, 119
Dephasing, 293
  effects, 309
  rate ($1/\tau_{ph}^{-1}$), 295
  rates, for liquid acetonitrile, 320
  theories, 300
Depolarized Rayleigh spectra, 276
Detectors, in glc, 178
Deuterochloroform, 309
Diachor, algorithm, 252
  logic, 250
Diachoric solutions, 216, 222, 230
Dialkyl phthalates, 188, 190
Dianthrylethane, 23, 35
1,2-Di-(9-anthryl)ethane, 22
1,2-Di-(1-anthryl)ethane, fluorescence of, 5
1,2-Di-(9-anthryl)ethane, fluorescence of, 5
Dibromomethane, 214
Dialkyl ethers, complexes with iodine, 358
Di-n-butyl adipate, 188, 190, 207
Di-n-butyl esters, 201
  ether, 216
  maleate, 190
  phthalate, 235
  sebacate, 190, 191, 235
  succinate, 188, 190, 235
Di-n-butyl tetrachlorophthalate, 206
Dielectric continuum model, 45

2,3-Dichloro-5,6-dicyano benzoquinone (DDQ), 136
Dichloromethane, 214, 312
Dichroic absorption bands, 98
9,10-Dicyanoanthracene, 25
(9,10-Dicyanoanthracene)–$(CH_2)_3$–(naphthalene), 7
1,4-Dicyanobenzene, 3, 87
N,*N*-Di-(2-cyanoethyl)formamide, 254
Dicyanomethylene–nitrofluorenone polyesters, 151
N,*N*-Diethylacetamide, 202
N,*N*-Diethylaniline, 10, 44, 53, 56, 58, 188
Diethyl ether–iodine complexes, 353
Diffusion-controlled reaction, 10
Diffusional quenching, 15
  rotator, 281
Diglycerine, 238
1,1′-Diisocyanatoferrocene, 154
4,4′-Diisocyanatotetrathiafulvalene, 154
Dilution technique, 418
3,5-Dimethoxy-*N*,*N*-dimethylaniline, 71
Di-2-methoxyethyl adipate–di-2-ethylhexyl sebacate, 221
p-*N*,*N*-Dimethylaminobenzonitrile, 13, 47
4-Dimethylaminobenzonitrile, 52
4-Dimethylaminostyrene, 110
N,*N*-Dimethylaniline, 3, 10, 58, 66, 404
N,*N*-Dimethylaniline–oxygen contacts, 356
  complex, 397
9-(4-Dimethylanilino)anthracene, 48
9,10-Dimethylanthracene, 20, 21
2,6-Dimethylazulene, 87
2,2-Dimethylbutane, 405
Dimethyldichlorosilane, deactivation with, 181
2,3-Dimethylpentane, 405
2,4-Dimethylpentane, 405
1,2-Di(*N*-methyl-4-pyridinium)ethylene complex, 139
N,*N*-Dimethyltoluidine, 62
N,*N*-Dimethyl-*o*-toluidine, 404
N,*N*-Dimethyl-*p*-toluidine, 404
N,*N*-Dimethyl-2,6-xylidine, 404
Dinaphthylalkanes, 5
3,5-Dinitrobenzoyl cotton cellulose, 109
4,4-Dinitrobiphenyl, 89
2,4-Dinitrocumene, 107
Dinitrofluorenone dicarboxylic acid, 108
Dinonyl phthalate, 183, 206, 243, 245
Dinonyl phthalate–benzene, 229
Di-n-octyl ether, 195, 202, 205, 213
Di-n-octylmethylamine, 195, 205, 213
Di-n-octyl thioether, 195, 205, 213
Diol derivative of TCNQ, 152
Dioxan, 314, 404
Diperfluorohexyl ether, 362
N,*N*-Diphenyl-*p*-phenylene diamine, 29
Dipolar coupling, 324
Dipole moment, 38, 43, 46
Dipole moments of termolecular complexes, 86
Dipyrenylalkanes, 35
  fluorescence of, 6
Dispersion solubility, 203
DMA—see *N*,*N*-dimethylaniline
DMT—see *N*,*N*-dimethyltoluidine
Dodecyl laurate, 216
Donor polymer-acceptor systems, 136
  site, 409
  size, 391
Donor–iodine interactions, 354
Doped polyacetylenes, 158
Doping, 123, 161
DPPD—see *N*,*N*-diphenyl-*p*-phenylenediamine
Drift mobility, 120
3-D Trajectory/Monte Carlo calculation, 380
Dual luminescence, 46, 48
Durene, 157

E

Eclipsed arrangements of donor and acceptor units, 91
Eigen's equation, 63
Electrical anharmonicity, 291
  conductivity of CT complexes, 85
  properties of solid CT complexes, 114
Electroabsorption spectra, 126
Electrochemical luminescence, 21
Electrogenerated radical, 21
Electromedical devices, 162
Electron affinities, 104
  distribution, 268
  exchanges, 116
  mobilities, 115, 151

Electron-transfer quenching, 157
Electronic conduction in organic molecules, 118
Electronic transport in PVK, 125
Electrophotographic industry, 158
Electrophotography, 100, 114
Emission frequency, calculated, 41
Emission-limited current, 122
Emissive transition probability, 56
Encounter complexes, 28, 62, 83, 332
Energy distribution processes, 285
Energy-level diagram, for contacts, 336
Energy, relative, of CT transitions, 99
Energy relaxation, function ($\phi_E(t)$), 296
processes, 285, 295
Energy transfer, mechanism, 380
quencher, 416
Enthalpies of complexation, 202
Enthalpies of formation, 419
Enthalpy of association, 80
Environmental reorientation, 14
Equilibrium constant, 205, 344
Esr signal, 409
Esters, 187, 196
ET—see energy transfer
$E_T(3)$ values, 51
Ethanol, 404, 407
Ethanol solutes, β-substituted, 199
Ethers, 187, 196
Ethylbenzene, 190
N-Ethylcarbazole, 96, 157
Ethylcyclohexane, 216
Ethylene glycol, 219
2′-Ethylmethacrylyl 4,5,7-trinitrofluorenone-2-carboxylate, 150
Europium$(fod)_3$, 186, 200
Eutectic melts, 200
Exchange parameters, 205
Excimer, 2
Excimer interactions in polymers, 83
Excimers, geometrical requirements, 89
Excimer states, wavefunction of, 4
Exciplex absorption spectrum, effect of solvent polarity on, 53
Exciplex, binding energies, 9
formation, characterization of, 82
geometrical requirement, 89
interactions, 82
states, 69
Exciplexes, ultrashort-lived, 28
Excited state association, 416
Excited states of EDA complexes, 3
Exciton resonance interaction, 4
Extended diffusion model, 280
Extinction coefficients of charge-transfer bands, 332

F

Far-infra-red spectra, 276
"Fast" ISC, 66
Fast-pulsed excitation, 3
"Fast" triplet generation, 70
Ferrocene polymeric CT complexes, 142
Fick's law, 63
Field dependence of hole and electron mobilities, 129
Flash photodissociation of iodine, 395
photolysis, 379, 381, 393
spectrographic analyses, 386
Flory–Huggins theory, 192
Flory-type interaction parameters, 175
Flow meters, in glc, 177
Fluoranthene, 30
Fluorene, 107
Fluorenone, 30
Fluorenone-2,7-dicarboxylic acid, 108
Fluorescein, 30
Fluorescence, anomalous, 47
decay, 11
decay kinetics, 10
emission, 86
kinetics, 39
probes in biological systems, 49
quantum yields, 10
quenching, 17, 48, 416, 431
quenching by amines, 27
shifts, 15
yields, temperature dependence, 13
Fluorescent state, 32
Fluorobenzene, 216
Folded excimer, 23
Force constants, 268
Formation constants, 418, 419
Franck–Condon excited state, 32
Free-radical solution polymerization, 113
Frequency shift, 268, 294
Friction constants, 276
Fugacity, 175, 180, 191

Fulvalene CT complexes, 142
Functional-group contributions, 239

G

Gas chromatography, low- and high-temperature, 172
Gas compressibility, 174
Gas–liquid interfacial adsorption, 219
Gaussian period, 309
Geminate ion-pair, 61, 70
  recombination, 59
Geometrical anisotropy, 306
Geometrical changes, 8
Gil-Av–Herling method, limitations, 206
  relation, 188
Glc measurements, 205
Glycidyl 4,5,7-trinitrofluorenone-2-carboxylate, 150
Gordon M and J diffusion models, 280
Grazing encounter, 347

H

Hall technique, 119
  mobilities, 138
Halogen atom CT complexes, 390
Halogens as acceptor molecules, 359
Halogens as donor molecules, 378
Hard-core collisions, 307
Heats of complexation, 234, 418
Henry's law activity coefficient, 174
n-Heptadecane, 211
n-Heptane, 216, 405
cis and *trans*-Hept-2-ene, 216
Heteroexcimer, 3
Hexadecyl halides, 205
Hexamethylbenzene, 418, 430
  complex with TCNB, 34
  stoichiometry of complexes with, 85
n-Hexane, 245
  as a reference solvent, 361
Hexanediol, 108
n-Hexatriacontane, 222
Higher complexes, 419
Higher-order complexes, 88, 99, 103
High-performance liquid chromatography, 253
Hindered biphenyls, 442
  rotations, 13
HMO calculations, 95
Hole and electron transport, 116
  mobilities, 129
  transport, 116, 132, 149
HOMO, 91, 116, 133
Hopping, 116, 117, 133, 143, 147
"Hot" bands, 270, 317
Hydrocarbon–amine systems, 10
Hydrocarbon–iodine complexes, 360
Hydrocarbon solutes, fugacity correction, 180
Hydrogen atom transfer, 28
Hydrogen-bonded complexes, 3, 28, 268
Hydrogen-bonding, 195, 202
Hydrophobicity effect, 230

I

I_4, CT studies on, 378
IBC (binary collision) model, 298
Induced dipole fluctuations, 307
Inert solvent, 208, 442
Inertial effects, 282
Infinite dilution work, 173
Infrared analysis of polymeric complexes, 136
  spectra, 275
Inhomogeneous broadening, 285
Injectors, in glc, 178
Insertion reaction, 438
Insulator, 117, 137
Intensities of CT bands, orientation effects on, 92
Intensity changes, 268
Interaction parameter, 203
  terms, 294
Interfacial adsorption, 188, 227
Intermolecular electron transfer, 18
  forces, from band shape, 306
  interactions, theoretical analysis of, 40
  potential, 269, 279, 295
  torque, 269, 276, 279, 283, 306
Internuclear separation, 80
Interpretation of band shapes, 269
Intersystem crossing, 21, 65
Intrachain EDA complexes, 110
Intramolecular complexation, 154
  cyclophane system, 92
  heteroexcimers, 7
  heteroexcimer formation, 13
  polymeric CT complexes, 110

Inversion of states, 47
Iodine, 345
Iodine chloride, 268
Iodine dopant, 158
Ionenes, 138
Ionic character, 391
  photodissociation, 56
Ionization energies, 96, 104
  potentials, 416
Ion-radical pair, 82, 83, 137
  rate of dissociation, 63
  salts, 117
ISC—see intersystem crossing
Isobutanol, 214
Isooctane, 404
Isopiestic complexes, 353
Isopropanol, 214
N-Isopropylcarbazole, 114
Isosbestic point, 343
Isotactic polymers, 142
Isotope effect, 48
Isotopic dilution method, 298
Isotropic Raman band profile, 291
Itinerant-oscillator model, 282

J

J diffusion model, 280, 311
Jump angle, 309
  times, 276

K

Katharometer, 178
Kelvin contribution, 181
Ketones, 186, 187
Kinetic spectrophotometric analysis, 386
Kirkwood factors, 277
K_r values, MP-predicted, 246
Kubo model, 297, 318

L

^{1}L band, 24
Lanthanum(facam)$_3$, 186, 200
Laser flash spectroscopy, 6
  photoconductivity studies, 58
Lennard-Jones particles, 230
Level depopulation, 293
Librational harmonic motion, 282
Liquid crystalline materials, 134
Lithium nitrate–ethylene glycol, 198
Local excitation, 32, 369
Long-range forces, 281
Loose complexes, 25
Loss of symmetry, effect on complexation, 421
Low-temperature techniques, 367
LUMO, 91, 131

M

M diffusion model, 280
Macromolecular acceptors, 109
Macroscopic miscibility, 218
  viscosity, 280
Magnetic fields, effect of, 22
Manganese(II) compounds, complex formation by, 197
Mannich polymer, 112
Manostat devices, 177
Martire–Riedl theory, 203
Mass density analysis of PK–TNF films, 125
Matrix, oxygen, 405
Maximum-overlap principle, 93
Mechanical anharmonicity, 291
Mechanically blended packings, 221, 237, 249
Medical devices, 162
Memory functions, 283, 284, 308
Merocyanine dyes, 42
Mesitylene, 59, 345, 404, 417
Metal-like conduction, 117
Metallocenophane, 143
Metalloporphyrins, 34
Metal–semiconductor transition, 139
Metapyrenophane, 52
Methanol, 407
N-Methylacetamide, 186
9-Methylanthracene, 21
Methylbenzenes, complexes with iodine, 358
Methyl cyanide, 268
Methylcyclohexane, 216, 245, 405
Methyl iodide (d_3), 300
Methyl methacrylate, 105

Methylsilicone–polyethylene glycol, 221
Methyl-substituted benzenes, 31
Methyl-substituted naphthalenes, 31
N-Methylphenothiazine, 103
4-(Methylthio)anisole, 103
Methoxybiphenyl polymer, 104
Microscopic partition (MP) theory, 231
Microsecond flash photolysis, 392
Microviscosity correction, 311
Mixed liquids, 239
  phases in glc, 237
Modulation, rate, 320
  time τ_c, 287
Molecular oxygen, quenching by, 28, 48, 53, 64
  polarizability, 116
Mori formalism, 283, 306
Motional narrowing, 289, 318
MP model, 245
Mulliken potential-energy diagram, 334
  wavefunctions, 4, 334
Multiple complexes, 88
Multi-well potential, 282

N

$n = 3$ rule, 7, 35, 38
Nanosecond flash photolysis, 392
1-Naphthaldehyde, 30
Naphthalene, 3, 20, 24, 30, 44, 66, 157
β-Naphthol, 28
Naphthylalkylamines, 37
Naphthylamine, 28, 107
$NbCl_5$, 200
Negative charging, 159
Neutron spectroscopy, 270
  scattering, 271
Nickel(II) compounds, complex formation by, 197
Nitrated phthalic acid isomers, 108
  polymers, 154
Nitroaromatics, 34
Nitrofluorenone polyesters, 151
Nitromethane, 431
Nitrophenyl acrylate polymers, 107
NMR, 205
No-bond contribution to CT complexation, 397
  structure, 334
  wave function, 353
Non-fluorescent exciplexes, 26
Non-geminant recombination, 385
Non-interactive solutes, 206
Non-sandwich arrangements of donor and acceptor, 91

O

n-Octadecane, 222
Octafluorotoluene, 216
n-Octane, 245
Olefin, 187
Onsager's ion-recombination model, 62
  reaction-field model, 40
Opalescence phenomena, 218
Optically active models, 106
  polymers, 97
Organic metals, 137
Organic polymeric materials, 160
Organogermanium compounds, 436
Organosilicon compounds, 436
Orientation, 47
  of acceptor and donor, 93
  anisotropic nature of, 323
  of donor and acceptor, effect on CT absorption bands, 93
  effect on CT spectra, 90
Orientational isomers, 345
  moments, 278
Oscillator strength, 93, 337
Outer complexes, 43
Oxidative instability, 149

P

Pair correlation times, 276
[3,3]Paracyclophanes, 92
Paramagnetic ions, 408
Particle sizes, 181
Partition coefficients, 211, 216
  n-alkane/n-alkane, 185
  measurements of, 251
  liquid-gas, 173
Partitioning, 173
$PdCl_2$, 186
Peak asymmetry in glc, 179
Peak-broadening, 397
Pendant groups, 88, 156
Pentacene, 20
Peralkylmetals, 436

Perfect solutions, 214
Perfluoroheptane, 362
Permethylpolysilanes, 436
Person criterion, 352
Perylene, 3, 10, 24, 161
  complexes with, 85
Phase-change chromic behaviour, 357, 417
Phase coherence, 285
  memory, 288
Phase-relaxation function $[\phi_{pp}(t)]$, 296
  processes, 285
Phenanthrene, 20
Phenazine CT complexes, 142
Phenol, 268
Phenothiazine, 161
  polymer, 104
p-Phenylenebistetrathiafulvalene, 84
Phosphorescence, emission, 65
  intensity, 59
Photochemical reactions, 431
Photochemical reaction, between I_2 and alkenes, 367
Photoconducting materials, 83
Photoconductivity, 113
  of *N*-vinylcarbazole-*N*-vinylphthalimide copolymers, 154
Photocurrent, 61, 157
Photodimerization, 5
Photodischarge, field-dependent, 152
Photoexcitation, 380
Photogeneration, of charge carriers, 127, 157
  process, 159
Photoinduced discharge curves (PIDC), 121
  ionization, 60
Photo-oxidation, 408
Photoreduction, 61
Photovoltage, 119
Photovoltaic cell, 160
Physicochemical data acquisition, 173
PIDC—see photoinduced discharge curves
π*-acid, 432
π basicity, 86
π–π complexation, 209
π donors, 392
PMDA—see pyromellitic dianhydride
Polar excited state, 15
  exciplexes, 42
  excited molecular states, 47
Polarization, 205
Poly(acenaphthylene), nitrated, 112
Poly-(*p*-anisyliminodiethanol-bisphenol A) carbonate, 152
Poly-[bis-(2-hydroxyethyl)-5-nitroisophthalate bisphenol A]carbonate, 152
Polycarbonates, 133
Poly-(2,4-dinitrostyrene), 107
Polyesters, 111, 152
Polyethylene glycol, 238
Poly(ethynylferrocene) complexes, 143
Poly(hexane-1,6-diol 5-nitrosoisophthalate), 108
Polymer, chain conformation, 106
  chain effect, 105
  stationary phases, 217
  tacticity, 142
Polymeric binders, complexes in, 157
  complexes, esr measurements of, 124
  donor–acceptor, 85
  donor–polymeric acceptor complexes, 152
  matrices, 157
Poly(methylmethacrylate), 157
Poly(phenyliminodiethanol isophthalate), 108
Poly(propylene glycols), 140
Polyquinocycloalkanes, 84
Polysarcosines, 90
Polystyrene, 157
Polytransesterification, 146
Poly(2,4,7-trinitro-9-fluorenyl methacrylate), 109
Polyurethanes, 156
Poly(vinyl alcohol) acetals, CT complexes of, 102
Poly(*N*-vinylcarbazole), 97, 114, 118, 161
Poly(*N*-vinylcarbazole), charge-transfer complexes of, 100, 103
Poly(*N*-vinylcarbazole)-2,4,7-trinitrofluorenone complex, 114
Poly(vinylpyridine), 137, 161
Poly(2-vinylpyridine)–iodine complex, 114
Poly(2-vinylquinoline), 161
Positive charging, 159
Power spectrum, 307
Pressure controllers, in glc, 177

Primary cell, 161
Prompt triplet generation, 68
Prompt triplet yield, 70
n-Propanol, 214
Pulse radiolysis, 70, 379, 393, 394
Pulse radiolysis, generation of iodine atoms, 395
Pulsed photolysis, 64
PVK—see poly(*N*-vinylcarbazole)
PVK–acceptor complexes, 118
PVK films, 120
PVK–TNF films, 125
PVK–TNF complex, 158
P2VP—see poly(2-vinylpyridine)
P3VK complexes, 124
Pyrazine, 30
Pyrene, 2, 10, 20, 21, 24, 44, 53, 56, 58, 60, 62, 66, 71, 157
(Pyrene)-(CH_2)-(*N*,*N*-dimethylaniline), 7
Pyrene semiquinone radical, 27
Pyrene–DEA, 25, 34
Pyrene-*N*,*N*-dimethylaniline, 25, 43
Pyrene–TBA, 16
Pyrene–TCNE, 115
Pyrene–triethylamine, 16
m-Pyrenophane, 23
Pyridine, 28, 268, 406
Pyridinium phenol betaine, 51
Pyromellitic dianhydride, 59, 60
Pyrrole, 202, 404, 407

Q

Quadricyclane, 438
Quantum yield of dissociation, 385
Quasidimer, 380
Quenching, 11
  by amines, 27
  by inorganic ions, 29
  charge-transfer, 50
  processes, 20
  rates, 416
  rate constant *k*, 18
Quinones, 34
Quinone-containing polymers, 151

R

Radiationless deactivation, 26
Radiative transition probability, 58
Radical cation formation, 409
Radical ions, 20
Radical-ion recombination, 8
Radical-molecule (RMC) mechanism, 380
Radical-pair model, 70
Radical recombination processes, 20
Radicals, intramolecular interaction, 35
Raman band, anisotropic part, 302
  of benzaldehyde, 312
  variable-pressure measurements, 311
Raman scattering, spontaneous, 296
  spectra, spontaneous, 295
  spectroscopy, 270
Random copolymers, 105
  pair interactions, 346
Rapid measurement techniques, 367
Rayleigh spectra, 275
Reaction-field model, 40
Recombination rate constants, 388
  steps, 388
Red shift, 5, 15, 36, 51, 396
  of charge-transfer band, 339
  effect of polar molecules on, 52
Red-shifted bands, 395
  fluorescence, 2
Regular solution theory, 360
Relative retention, 205
Relaxed exciplex state, 60
Relaxation processes, 272
  rate, 297
  vibrational and reorientational, 306
Reorganization energy, 335
Reorientational band profiles, 276
Reorientational correlation time, of dioxan-d_8 in $CDCl_3$, 317
  functions, 270
  motion, 303, 309
Repulsive intermolecular potential, 292
  potential, 309
Residence times, 276
Resistivities, 114, 135
Resolution function, 273
Resonance energies, 391
  energy transfer, 289
  stabilization, 335
  vibrational energy transfer, 306
Resonant transfer of vibrational quanta, 309

Retention behaviour, 172
equations, 173
time, 174
Retentions, functional group contributions to, 239
Reverse CT transitions, 52
Rhodamine B, 30
Rhodium(II) acetate and benzoate, 186
Rigid media, 404
RMC—see radical-molecule
Rotational correlation in chloroform, 309
correlation functions, 306
diffusion, 275
motion, 13
Raman spectra, 276
translational degrees of freedom, 285
velocity correlation function (RVCF), 281

S

"Salt" effects, 225
Sandwich conformation, 89
structure, 5, 36, 86, 94
Sandwich-type exciplexes, 47
$SbCl_3$, 200
Scatchard method, 85
Scott modification, of Benesi–Hildebrand procedure, 341
Seebeck technique, 119, 137
Self-association stabilization, 88
Self-interaction, 314
Semiconducting materials, 83
polyester complexes, 152
Semiconductor, 117, 137
Shift theorem, 270
Short-range forces, 281
Silver ion, 187
nitrate, 225
nitrate–ethylene glycol, 187, 198, 211
Single-particle correlation times, 276
Singlet–singlet spectroscopy, 54
Singlet–triplet band, 406
enhancement, 408
"Slow" ISC, 66
Smoluchowski relation, 354
$SnCl_4$, 417
$S_n \leftarrow S_1$ spectra, 7, 31, 32
Sociation, 339, 348
Solute, activity coefficient, 175
partition coefficients, 188
retentions, 188
specific retention volume, 175
vapour pressure, 175
Solution viscosities of polymers, 108
Solvated dihalide ion, 395
Solvation effects, 40
shell, 83
Solvation-induced reversal of energy levels, 44
Solvent cage, 59
effects, 236, 357
fluidity, 356, 416
interaction, 43
model, 347
polarity effects, 6
polarity parameter, 22, 47, 50
relaxation, 15, 55
reorganization phenomena, 14
viscosity, effect of, 14
Sorbents, multicomponent, 237
Sorption–desorption processes, 180
Specific retention volume, 194, 239
Spectral broadening, 290
shifts, 442
Spectroscopic analysis of PVK–TNF films, 125
Spherical-top molecule, 279
Spin distribution, 116
Spin-forbidden singlet-triplet band, 406
Spin–lattice relaxation, 277
Spin–lattice relaxation time (T_1) of dioxan–d_8, 317
Spin–orbit interactions, 66
splitting in alkyl halides, 394
Spirocyclopropane-2,4,5,7-tetranitrofluorene, 111
Spirocyclopropane-tetranitrofluorene polymers, 107
Squalane, 183, 203, 216, 243, 245
Squalane–dinonyl phthalate, 227
Squaric acid based dyes, 161
Stability constants, 186, 188, 202, 204, 206, 214
Stable radical ions, 60
Stack type organic conductors, 137
Stacking axis interaction, 148
"Standard" solutes, 206
Stationary phases, silicone polymers, 215
Steric factors, 154
hindrance, 21

Steroid solutes, 215
"Sticking together" time, 343
Stilbene, 157
Stochastic parameters, 284
  perturbation, 286
Stoicheiometry of complexes, 85
Stokes shift, 15
Stokes–Einstein relationship, 280
Strained hydrocarbon, 438
"Strong" complexing agents, 206
Sulphides, 196
Superconducting materials, 83
Surfactants, 239
Swarming, 230
Symmetries of donor and acceptor orbitals, 95
Symmetry requirements of multiple CT transitions, 92

T

T → T absorption, 65
$TaCl_5$, 200
Tailing absorption, 403
Tandem column systems, 221, 237
TBA—see tri-n-butylamine
TCNB—see 1,2,4,5-tetracyanobenzene
TCNQ—see tetracyanoquinodimethane
TCPA—see tetrachlorophthalic anhydride, 60
Temperature dependence of hole and electron mobilities, 129
  effects in HPLC, 254
TENF—see 2,4,5,7-tetranitrofluorenone
Termolecular complexation, 234
Ternary complexes, 419
Tetracene, 20, 430
Tetrachloroethylene, 216
Tetrachlorophthalic anhydride, 60, 115
1,2,4,5-Tetracyanobenzene (TCNB), 2, 3, 15, 60 *et seq.*, 88
Tetracyanoethylene, 60, 87, 93, 136, 206, 404, 437
Tetracyanoquinodimethane, 85, 117, 136, 404
Tetracyanoquinoquinazolinoquinazoline, 84
Tetradecylamine, 205
Tetrafluoroethylene, 202
Tetrafulvalenes, 146
Tetrahalophthalate esters, 186, 200
Tetrahydrofuran, 186
N,N,N′,N′-Tetramethyl-*p*-phenylenediamine, 20, 59
2,4,5,7-Tetranitrofluorenone (TENF), 136
Tetranitrofluorenone–fluorene copolyester, 152
Tetranitromethane, 431
2,2′,6,6′-Tetraphenyldithiapyranylidene–TCNQ complex, 158
Tetraselenafulvalene, 144
Tetrathiafulvalene, 84, 146
Thermalized exciplexes, 61
Thermochromic behaviour, 357
Thermodynamic quantities from CT spectra, 339
Thiodipropionitrile, 188, 190
Third body, effect on halogen atom recombination, 382
  ionization potential, 383
Through-space interaction, 83
$TiBr_4$, 417
$TiCl_4$, 417
Time dependence of fluorescence, 9
Time-dependent rate constant, 11
Time-of-flight apparatus, 122
Time-resolved absorption spectrum, 55
  spectra, 15
$TlNO_3$, 187
TMPD—see *N,N,N′,N′*-tetramethyl-*p*-phenylenediamine
TNF—see trinitrofluorenone
Toluene, 62, 187, 190, 216, 245, 345, 405, 407
p-Toluidine, 66
Torque, 279
TPTA—see tri-*p*-tolylamine
Trajectory calculations, 3-D, 382
Transannular interaction, 23
Transient absorption, 392
  absorption band, 394
  spectra, 395
  CT absorbance, rate of disappearance of, 387
Transient-current apparatus, 122
Transient-current technique, 122
Transients, detection of, 386

Transit times of carriers, 122
measurements, 124
Transition-dipole interaction, 309
Trapping, 115
effects, 122
Tri-n-butylamine, 15
Tributyl phosphate, 219
1,1-Trichloroethane, 214
Trichloroethylene, 216
Tri(*p*-dimethylaminophenyl)amine, 21
Triethylamine, 28, 404
Triethylenediamine, 405
3-Trifluoroacetylcamphorates (tfacCam), 198
Trifluoromethane, 306
Tri-n-hexylamine, 195
Tri-isobutylene, 221
Tri-isobutylene-silver nitrate–ethylene glycol columns, 238
2,2,4-Trimethylpentane, 405
1,3,5-Trinitrobenzene, 87, 157, 206
1,3,5-Trinitrobenzene, stoicheiometry of complexes with, 85
2,4,7-Trinitrofluorenone, 114, 188, 201, 206, 235
2,4,7-Trinitrofluoreneone, radical anion, 128
Triphenylene, 20
Tri-*p*-tolylamine, 21
Tritolyl phosphate, 188
Triple complex, 88
Triplet generation path, 67
Triplet–triplet annihilation, 20
Tropylium ion, as an acceptor, 87
Tumbling motion, activation energy of, 309
Tunnelling, 116
"Two-way CT complex", 378

U

Ultraviolet maxima, 397
measurements, 205
spectra of iodine, vapour phase, 363
Unimolecular decay rate constants, 11
Unresolved spectra, 405
Unsaturated compounds, complexation of, 226

V

Valence angles, distortion of, 438
Vapour-phase formation constants, 389
Variable-pressure measurements of Raman bands, 311
Vertical electron affinity, 404
VF—see vinylferrocene, 135
Vibrational correlation functions, 270
energy, resonant transfer of, 306
excitations, 18
relaxation, 116, 272, 285, 292
relaxation function, 272, 296
relaxation in acetonitrile, 317
relaxation in *p*-dioxan, 314
relaxation rate, 297
relaxation rate (τ_V^{-1}), in methyl iodide, 298
second moment, $(M2)_v$, 297
spectra, 267
N-Vinylcarbazole, 111, 156
Vinylferrocene, 125
3-Vinyl-bis-(fulvalene)di-iron, polymer of, 144
1-Vinylnaphthalene, 142
N-Vinylphthalimide, 111
Vinylpyridines, 110
N-Vinyl-3-tricyanovinylcarbazole, 156
Viologen—see 4,4′-bipyridylium
Virial coefficients, 403
effects, 175, 227
Viscosity, 13
dependence, of reorientational correlation times, 278
effects, 227
Viscous solvents, 50
Volatile stationary phases, 173
$VOCl_3$, 417
Volterra equations, 283
VRF—see vibrational relaxation function, 298

W

Water, 407
Weak molecular complex, spectral changes on formation of, 269
Window diagrams, 241 *et seq*
Windows of separation, 241
Wyllie–Larkin model, 283

X

Xenon, CT complexes with metal fluorides, 421
Xerographic discharge, 119
process, 160
X-ray analysis of polymeric complexes, 89, 136
of TCNB–hexamethylbenzene, 33
X-ray crystallographic studies of EDA complexes, 89
p- Xylene,216, 345
Xylenes, 190

Z

Z Values, 50

QD 461.M599 v2
3 9358 00485830 1

Classification number
chem QD 461 M599 v2

Accession number
4 8 5 8 3 0

Date Due JAN 0 5 1995

SEP 24 1988

CHEM
QD461
M599
v.2

Molecular association : including molecular complexes / edited by R. Foster. -- London ; New York : Academic Press, 19-
v. : ill. ; 24 cm.

485830

QD 461.M599 v2
3 9358 00485830 1